Southern California Earthquake Center

ANNUAL MEETING 2018

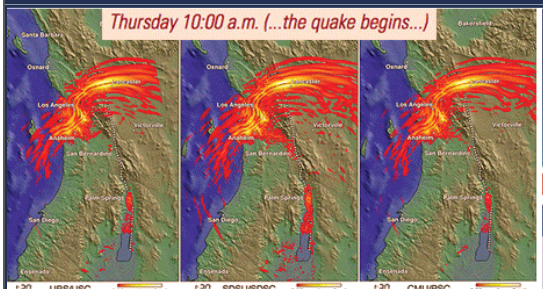

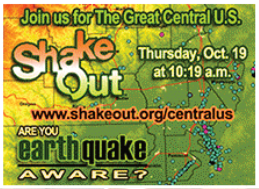

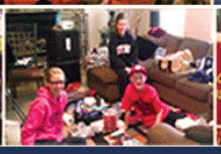

SCEC
AN NSF+USGS CENTER

PROCEEDINGS VOLUME XXVIII

September 8-12, 2018

Core Institutions and Board of Directors (BoD)

USC **John Vidale**, Chair	Harvard **John Shaw**, VC	Texas A&M **Patrick Fulton**	UC Santa Barbara **Toshiro Tanimoto**	USGS Menlo Park **R. Harris, S. Hickman**
Caltech **Jean-Phillippe Avouac**	MIT **Tom Herring**	UC Los Angeles **Peter Bird**	UC Santa Cruz **Emily Brodsky**	USGS Pasadena **Kate Scharer**
CGS **Tim Dawson**	SDSU **Tom Rockwell**	UC Riverside **David Oglesby**	UNR **Graham Kent**	At-Large Member **Rachel Abercrombie**
Columbia **Bruce Shaw**	Stanford **Paul Segall**	UC San Diego **Yuri Fialko**	USGS Golden **Nico Luco**	At-Large Member **Rowena Lohman**

Science Working Groups & Planning Committee (PC)

	Disciplinary Committee			
	Seismology	Tectonic Geodesy	EQ Geology	Computational Science
PC Chair **Greg Beroza***	**Yehuda Ben-Zion* Jamie Steidl**	**Gareth Funning* Manoo Shirzaei**	**Mike Oskin* Whitney Behr**	**Eric Dunham* Ricardo Taborda**
	Interdisciplinary Focus Groups / Working Groups			
PC Vice-Chair **Judi Chester***	FARM **Nadia Lapusta* Nick Beeler**	SDOT **Kaj Johnson* Bridget Smith-Konter**	EFP **Max Werner* Ned Field**	Ground Motions **Domniki Asimaki* Annemarie Baltay**
* PC Members	EEII **Jack Baker* Jon Stewart**	SAFS **Michele Cooke* Ramon Arrowsmith**	CXM **Liz Hearn* Scott Marshall**	Special Projects **Christine Goulet* Phil Maechling***

CEO Planning Committee (CEO PC)

* AC liaison ** Board liaison *** PC liaison	**Tim Sellnow**, Chair U Central Florida	**Kate Long** CalOES	**Danielle Sumy** IRIS
	Tim Dawson** CGS	**Sally McGill** CSUSB	**Ricardo Taborda***** Colombia EAFIT

Center Management

	Center Director **John Vidale***	Center Co- Director **Greg Beroza***	PC Vice-Chair **Judi Chester***	Board Vice-Chair **John Shaw***
Comm, Educ, Outreach Assoc Director **Mark Benthien***	Information Technology Assoc Director **Phil Maechling***	Special Projects Exec Sci Director **Christine Goulet***	Science Operations Assoc Director **Tran Huynh***	Administration Assoc Director **John McRaney***
Communications Mgr **Jason Ballmann**	Research Programmers **Scott Callaghan** **Bill Savran** **Fabio Silva** **Mei-Hui Su**	Research Programmer **Kevin Milner**	Business Ops Specialist **Deborah Gormley**	
Web Manager **John Marquis**			Research Programmer **Edric Pauk**	
ELCA Manager **Gaby Noriega**	Director of Comp Svc **John Yu**			
Asst Director of Strategic Partners **Sharon Sandow**				* Members on the Executive Committee of the Center

Advisory Council (AC)

Meghan Miller, Chair UNAVCO	**Louise Kellogg** UC Davis	**Tom O'Rourke** Cornell	**Tim Sellnow** U Central Florida
Rick Aster Colorado State	**Yann Klinger** IPGP/Paris	**Susan Owen** NASA JPL	**Heidi Tremayne** EERI
Susan Beck Univ of Arizona	**Warner Marzocchi** INGV Rome	**Ellen Rathje** Univ of Texas	

Table of Contents

State of SCEC, 2018

John E. Vidale, SCEC Director

Welcome to the 2018 Annual Meeting!

As we have since 1991, for the 28th year, the SCEC community is convening to share recent accomplishments and chart the future. 571 people have pre-registered for the meeting, similar to the last 5 years with the exception of the 700+ 2016 attendees. 314 poster abstracts have been submitted. The pre-registrants include more than 147 first-time attendees and 284 undergraduates, graduate students, and postdocs.

We have completed the leadership transition from Tom Jordan, who will now take a very well earned sabbatical year in Boston, New Zealand, and Italy. Greg Beroza and Judi Chester have stepped up, expertly and energetically guiding the Planning Committee, while I've been gaining immersive experience.

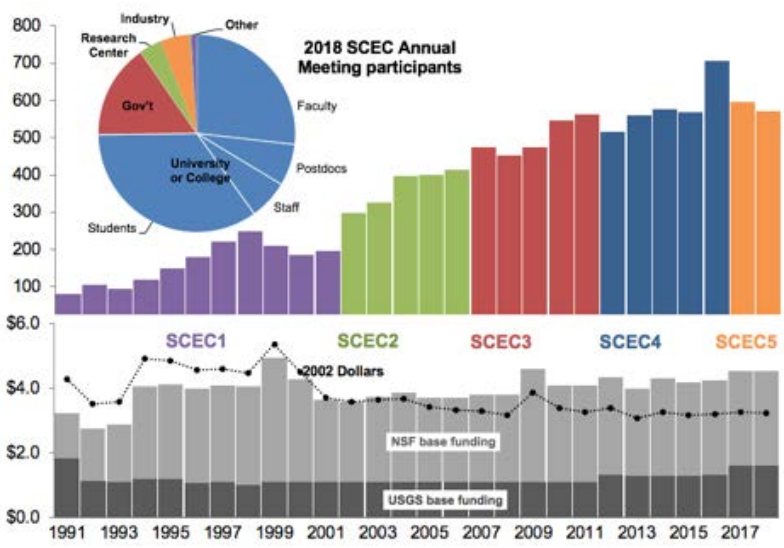

Upper bar chart shows registrants at SCEC Annual Meetings 1991-2018. Pie chart shows the demographic profile for 2018 pre-registrants (571 total). The lower bar chart is the history of SCEC base funding in as-spent millions of dollars; the connected dots are the base-funding totals in 2002 dollars.

Please note that we have implemented a SCEC Activities Code of Conduct, approved by the Board of Directors in June, 2018. Each registrant of the 2018 SCEC Annual Meeting was asked to accept and abide by the SCEC Activities Code of Conduct in order to complete registration. We at the Southern California Earthquake Center are committed to providing a safe, productive, and welcoming environment for all participants. The SCEC Annual Meeting is the keystone event of our collaboration each year. We bring together experts and early career researchers from all backgrounds and disciplines to improve our understanding of earthquake system science. We take pride in fostering a diverse and inclusive SCEC community. Information on the SCEC Activities Code of Conduct is available at https://www.scec.org/meetings/code-of-conduct.

We are in the 2nd year of SCEC5. SCEC5 has been authorized for another five years at a target funding level near $4.6 million per year, beginning in 2017, by its two principal sponsoring agencies—the National Science Foundation and U.S. Geological Survey.

The goal of this Annual Meeting is to review the progress of our collaborations, refine our draft science plan, and to develop ambitious research initiatives in new thematic areas. Concurrently, from the formal presentations and posters and from the informal discussions with our scientific colleagues, we'll deepen our basic understanding of earthquakes and the applied science of their mitigation.

The inspired and herculean SCEC Planning Committee has changed the channel from the Eagles to the Beatles, and arranged Saturday and Sunday workshops:

- SCEC Workshop on Predictive Skill Across Tectonic Settings and Planning CSEP 2.0
- SCEC Cajon Pass Earthquake Gate Area Initiative: Integrated Science Workshop and Field Trip
- SCEC Community Rheology Model Workshop on Loading of Southern California Faults: Bulk Lithospheric Deformation and/or Localized Ductile Shear Zone Strain

- SCEC Open-Source Software and Data Access Workshop
- SCEC Communications Workshop— Media Interview Theory and Practice, Through War and Peace

At 6pm Sunday evening, this year's Distinguished Speaker Jim Dieterich will kick off the main meeting with a plenary lecture on "Earthquake and Fault System Dynamics: Putting the Pieces Together." Over the next three days, the agenda will feature keynote speakers addressing fundamental problems, discussions of major science themes, poster sessions on research results, earthquake response exercises, technical demonstrations, education and outreach activities, and lively social gatherings.

The session titles indicate the range of the science we will discuss:

The State of SCEC,
How Do We Construct Effective and Synergistic Community Models?, and
What Needs to be Done to Increase the Impact of Dynamic Rupture Modeling? on **Monday**,
How Do We Assess Hazard and Risk from Distributed Deformation?,
How Do We Use and Further Improve Earthquake Simulators?, and
How Should SCEC Keep Up with Rapid Developments in Computational Science? on **Tuesday**, and
ShakeOut - What Has Shaken Out since 2008? and
SCEC Looking Forward on **Wednesday**.

The poster sessions scheduled between Sunday evening through Tuesday evening will span the spectrum of SCEC accomplishments. Posters will stay up for the entire meeting to facilitate the face-to-face interactions that power SCEC scientific research. Monday afternoon will feature lightning talks to provide a rapid overview.

Please participate as an active member of the SCEC community!

The SCEC5 Community Science Vision

The SCEC5 Science Plan is cast in five basic earthquake science questions. Recent SCEC progress, arranged in this framework, is summarized below in the Research Accomplishments section.

Basic Questions of Earthquake Science (SCEC5)

1. How are faults loaded across temporal and spatial scales?
2. What is the role of off-fault inelastic deformation on strain accumulation, dynamic rupture, and radiated seismic energy?
3. How do the evolving structure, composition and physical properties of fault zones and surrounding rock affect shear resistance to seismic and aseismic slip?
4. How do strong ground motions depend on the complexities and nonlinearities of dynamic earthquake systems?
5. In what ways can system-specific studies enhance our general understanding of earthquake predictability?

Science Plan

Research priorities have been developed to address the five basic questions above. Elucidating the priorities are fourteen science topics distributed across four main thematic areas.

Modeling the fault system: We seek to know more about the geometry of the San Andreas system as a complex network of faults, how stresses acting within this network drive the deformation that leads to fault rupture, and how this system evolves on time scales ranging from milliseconds to millions of years.

1. Stress and Deformation Over Time. We will build alternative models of the stress state and its evolution during seismic cycles, compare the models with observations, and assess their epistemic uncertainties, particularly in the representation of fault-system rheology and tectonic forcing.

2. Special Fault Study Areas: Focus on Earthquake Gates. “Earthquake gates” are regions of fault complexity conjectured to inhibit propagating ruptures, owing to dynamic conditions set up by proximal fault geometry, distributed deformation, and earthquake history. We will test the hypothesis that earthquake gates control the probability of large, multi-segment and multi-fault ruptures.

3. Community Models. We will enhance the accessibility of the SCEC Community Models, including the model uncertainties. Community thermal and rheological models will be developed.

4. Data Intensive Computing. We will develop methods for signal detection and identification that scale efficiently with data size, which we will apply to key problems of Earth structure and nanoseismic activity.

Understanding earthquake processes: Many important achievements in understanding fault-system stresses, fault ruptures, and seismic waves have been based on the elastic approximation, but new problems motivate us to move beyond elasticity in the investigation of earthquake processes.

5. Beyond Elasticity. We will test hypotheses about inelastic fault-system behavior against geologic, geodetic, and seismic data, refine them through dynamic modeling across a wide range of spatiotemporal scales, and assess their implications for seismic hazard analysis.

6. Modeling Earthquake Source Processes. We will combine co-seismic dynamic rupture models with inter-seismic earthquake simulators to achieve a multi-cycle simulation capability that can account for slip history, inertial effects, fault-zone complexity, realistic fault geometry, and realistic loading.

7. Ground Motion Simulation. We will validate ground-motion simulations, improve their accuracy by incorporating nonlinear rock and soil response, and integrate dynamic rupture models with wave-scattering and attenuation models. We seek simulation capabilities that span the main engineering band, 0.1-10 Hz.

8. Induced Seismicity. We will develop detection methods for low magnitude earthquakes, participate in the building of hydrological models for special study sites, and develop and test mechanistic and empirical models of anthropogenic earthquakes within Southern California.

Characterizing seismic hazards: We seek to characterize seismic hazards across a wide spectrum of anticipation and response times, with emphasis on the proper assessment of model uncertainties and the use of physics-based methods to lower those uncertainties.

9. Probabilistic Seismic Hazard Analysis. We will attempt to reduce the uncertainty in PSHA through physics-based earthquake rupture forecasts and ground-motion models. A special focus will be on reducing the epistemic uncertainty in shaking intensities due to 3D along-path structure.

10. Operational Earthquake Forecasting. We will conduct fundamental research on earthquake predictability, develop physics-based forecasting models in the new Collaboratory for Interseismic Simulation and Modeling, and coordinate the Working Group on California Earthquake Probabilities.

11. Earthquake Early Warning. We set no milestones for this topical element, which the USGS preferred to cover through other programs.

12. Post-Earthquake Rapid Response**.** We will improve the rapid scientific response to strong earthquakes in Southern California through the development of new methods for mobilizing and coordinating the core geoscience disciplines in the gathering and preservation of perishable earthquake data.

Reducing seismic risk: Through partnerships coordinated by SCEC’s Earthquake Engineering Implementation Interface, we will conduct research useful to motivating societal actions to reduce earthquake risk. Two topics investigated by these engineering partnerships will be:

13. Risk to Distributed Infrastructure**.** We will work with engineers and stakeholders to apply measures of distributed infrastructure impacts in assessing correlated damage from physics-based ground-motion simulations. An initial project will develop earthquake scenarios for the Los Angeles water supply.

14. Earthquake Physics of the Geotechnical Layer. In collaboration with geotechnical engineers, we will advance the understanding of site effects and soil-structure interactions by incorporating nonlinear rheological models of near-surface rock and soil layers into full-physics earthquake simulations. Since the SCEC5 proposal, this topic has been revised to "Velocity and Rheology of Basin Sediments" and referred as such in milestones and accomplishments documents.

The Planning Committee and Executive Committee of the Center have drafted the annual SCEC science plan (included in the Meeting Proceedings). Highlights of recent progress in the SCEC5 science plan is given in the Research Accomplishments of the Meeting Proceedings. At this annual meeting, we solicit input from the entire SCEC community on accomplishments and the details of the 2019 SCEC science plan. A final version of the science plan derived from this input will be posted in early October, soliciting proposals due November 15, 2018.

Communication, Education and Outreach Plan

The SCEC/CEO program is managing an expanding suite of successful activities within four CEO focus areas:

1. Knowledge Implementation connects SCEC scientists and research results with practicing engineers, government officials, business risk managers, and other professionals in order to improve application of earthquake science.

2. Public Education and Preparedness educates people of all ages about earthquakes, tsunamis, and other hazards, and motivates them to become prepared.

3. K-14 Earthquake Education Initiative improves Earth science education in multiple learning environments, overall science literacy, and earthquake safety in schools and museums.

4. Experiential Learning and Career Advancement provides research opportunities, networking, and other resources to encourage students and sustain careers in STEM fields.

Four long-term intended outcomes of the CEO program are: improved application of earthquake science in policy and practice; reduced loss of life, property, and recovery time; increased science literacy; and increased diversity, retention, and career success in the scientific workforce. SCEC's vigorous promotion of workforce diversity is being augmented by a new Transitions Program that will provide students and early-career scientists with mentoring and resources at major steps in their careers.

The CEO Planning Committee, comprises members representing the four CEO focus areas. They are chartered to provide guidance and support for the portfolio of SCEC/CEO activities and partnerships, review reports and evaluations, and identify synergies with other parts of SCEC and external organizations. The CEO-PC includes CEO partners and SCEC Community stakeholders, with some members drawn from the AC, Board, and Science Planning Committee. The Chair of the CEO-PC is Tim Sellnow (U. Central Florida), who is also on the AC. Sellnow represents the Public Education and Preparedness CEO focus area along with Kate Long (formerly CalOES, now with the Dr. Lucy Jones Center). Danielle Sumy (IRIS) represents the K-14 Earthquake Education Initiative. Sally McGill (CSU San Bernardino) represents the Experiential Learning and Career Advancement focus area. Tim Dawson (California Geological Survey) and Ricardo Taborda (Universidad EAFIT, Colombia) represents the Knowledge Implementation focus area. Dawson and Taborda are also the representatives of the SCEC Board and PC, respectively, on the CEO-PC.

Further details of the SCEC/CEO program may be found in the CEO section below, reported by the Associate Director for CEO, Mark Benthien. Highlights of CEO activities for the past year will also be presented in an oral summary on Monday morning. In addition to Mark, the entire SCEC CEO staff (webmaster John Marquis, communications manager Jason Ballmann, assistant director for strategic partnerships Sharon Sandow de Groot,

and manager for Experiential Learning and Career Advancement Dr. Gabriela Noriega) are eager to discuss their activities and new ideas.

Special Projects

The SCEC Special Projects are research partnerships in targeted earthquake research that heavily leverage the core program. Synergy between the special projects and the core program is ensured by a central SCEC policy, instituted by the Board of Directors in 2005: the science objectives of all SCEC special projects must be aligned with those of the SCEC core program and explicitly included as objectives in the SCEC Annual Science Plan. Under this policy, any SCEC participant can propose core-program research pertinent to a special project, enabling them to participate in that project.

Community Modeling Environment (CME). Traditionally, the Special Projects were heavily focused on tasks requiring extensive computations, such as the activities from the CME. The CME is SCEC's high-performance computing collaboratory for large-scale earthquake simulations. Major grants to support CME software engineering have come from the NSF/CISE Directorate and the NSF/EAR Geoinformatics program, as well as from the utility industry. SCEC competes for supercomputer allocations through the NSF XSEDE and PRAC programs and the DOE INCITE program. In 2018, SCEC was awarded allocations exceeding 450 million service units, primarily on the NCSA's Blue Waters, ALCF's Mira, and ORNL's Titan supercomputers. These resources have enabled SCEC to sustain its HPC usage at a high level of productivity. CME resources support five major SCEC computational platforms:

High-F Platform**:** The High-F platform comprises the AWP-ODC, Hercules, and other codes that SCEC researchers are using to push earthquake simulations to higher frequencies (> 1 Hz). Software under development will be capable of modeling the effects of fault roughness, near-fault plasticity, frequency-dependent attenuation, topography, small-scale near-surface heterogeneities, and near-surface nonlinearities. The High-F Platform will support ground-motion studies as part of the SCEC5 plans to move simulations Beyond Elasticity.

CyberShake Platform**:** The CyberShake Platform uses seismic reciprocity to generate large ensembles of simulations (> 10^8) that Monte-Carlo sample earthquake rupture forecasts and multiple crustal-structure models. Implementation of physics-based probabilistic seismic hazard modeling requires this capability. The platform was developed using the Los Angeles region as a test bed, and it has already produced PSHA models as candidates for the USGS Urban Seismic Hazard Mapping Project. Two years ago, CyberShake PSHA models have been developed for Central California as part of the Central California Seismic Project (see below). The expansion of CyberShake to the Bay Area is underway in partnership with the USGS. Because reciprocity derives from linear elasticity, a SCEC5 challenge will be the re-engineering of CyberShake to enable the efficient, large-ensemble simulation of nonlinear wave phenomena that lie Beyond Elasticity.

Broadband Platform**:** The open-source Broadband Platform (BBP) provides a verified, validated, and user-friendly computational environment for generating broadband (0-100 Hz) ground motions. In its validation mode, the BBP computes goodness-of-fit measures that quantify how well the synthetics match the observations. In its scenario mode, it calculates suites of synthetic seismograms from user-specified rupture sets, structural models, and station sets. In SCEC5, the BBP will be extended from 1D to 3D structural models, and it will support the development and validation of physics-based ground-motion models in projects and partnerships managed under the EEII.

Unified Community Velocity Model Platform**:** The UCVM platform provides an easy-to-use software framework for comparing and synthesizing 3D Earth models and delivering model products to users. This community software is an important component of the CME cyberinfrastructure: a standardized, high-speed query interface enables users to build very large simulation meshes very quickly, and its file utilities can export meshes in both eTree and NetCDF formats.

Uniform California Earthquake Rupture Forecast. UCERF is a joint project of SCEC, USGS, and CGS to build a California-wide, time-dependent, fault-based earthquake rupture forecast, managed through the Working Group on California Earthquake Probabilities. The latest (third) version comprises a time-independent model used in the 2014

release of the National Seismic Hazard Mapping Project (UCERF3-TI), a time-dependent model based on long-term Reid renewal statistics (UCERF3-TD), and a time-dependent model based on short-term ETAS statistics (UCERF3-ETAS). The latter has been developed as a candidate model for use in operational earthquake forecasting. A major SCEC5 initiative is to incorporate more physics into UCERF models through the use of physics-based earthquake simulators, such as RSQSim. A workshop on testing UCERF3 was held in February 2018 at the Powell Center, and there is CEA-funded ongoing work and an upcoming workshop to explore further testing and improvement of UCERF.

Collaboratory for the Study of Earthquake Predictability. CSEP provides an international cyberinfrastructure that sustains the prospective, blind testing of short- and medium-term earthquake forecasts on regional and global scales. CSEP testing centers (except Japan and China) run a common software stack that is developed and released by SCEC software engineers. CSEP operations at SCEC include the testing of California and global forecasting models in addition to the development and maintenance of the collaboratory software. SCEC is responsible for the registration of new models and the coding of new testing procedures; many of these innovations, such as the testing of geodetic anomaly detectors, have come from the SCEC core program. ~400 earthquake-forecasting models and their variations are currently under prospective CSEP testing. The registration and testing of external forecasting models is underway and is aiming to include USGS operational models. CSEP and its new sister collaboratory, CISM (see below), will be critical SCEC5 infrastructures for the development and evaluation of comprehensive earthquake forecasting models. The merit of the proposed earthquake-simulator effort is supported by the recent results of the CSEP Canterbury Retrospective Experiment, which suggests that models incorporating the physics of rate-state nucleation and Coulomb stress transfer can outperform purely statistical models such as ETAS.

CSEP was initiated in 2006 with support from the W. M. Keck Foundation and has been subsequently funded under grants and contracts from the USGS and Department of Homeland Security. Owing to CSEP's importance to SCEC core research, the SCEC5 proposal requested USGS funding of $200k/year to support collaboratory operations in California and USGS-relevant software development, and this budgetary increase was approved and implemented. Allocation of CSEP resources to specific projects is being guided as part of the core budgeting process by the Joint SCEC/USGS Planning Committee. The CSEP 2.0 workshop held prior to the Annual Meeting this year will explore future directions of the collaborations between SCEC, the USGS, and the international testing centers and their users. As the software is revamped, issues of completion of initial calculations, synthesis of existing results, archiving, back-compatibility of new software, and technical support for adaptation of the new software will be discussed.

Collaboratory for Interseismic Simulation and Modeling. In July, 2015, SCEC received a three-year, $2M grant from the W. M. Keck Foundation to construct a Collaboratory for Interseismic Simulation and Modeling. CISM provides a unique environment for developing large-scale numerical models that can simulate sequences of fault ruptures and the seismic shaking they produce. The goal of CISM is to equip earthquake scientists with HPC-enabled infrastructure for creating a new generation of comprehensive, physics-based earthquake forecasts using California as the primary test bed. CISM provides a computational framework for combining earthquake simulations that account for the physics of earthquake nucleation and stress transfer with ground-motion simulations. RSQSim was selected as the main earthquake simulation code to move forward with the CISM research activities. Recent advances included the porting of RSQSim ruptures into the Broadband Platform to generate simulated seismograms and the computation of proof-of-concept hazard curves with CyberShake, using the RSQSim ruptures. This year the successful implementation of physics-based ERFs from RSQSim into the CyberShake Platform has shown that this approach has great promise for generating more realistic hazard estimates.

PG&E Projects on Seismic Hazard. The SCEC collaboration with Pacific Gas & Electric Company is going strong. Although the collaboration supports a wide range of projects related to seismic hazard, one key aspect is to assess the effectiveness of seismic wavefield modeling in reducing the epistemic uncertainties in site and path effects that control hazard estimates at low exceedance probabilities. We are recasting the activities with PG&E with a broader context that advances SCEC's non-ergodic ground motion modeling. SCEC started working on the evaluation of epistemic uncertainties using its most recent CyberShake study (Study 17.3 for Central California) and has made substantial progress this year. The first step required the development of statistical computation tools to compute

partitioned residuals relative to ground motion prediction equations (GMPEs) regression. The quantification of uncertainties in terms that are understood by engineers and hazard analysts is critical to their acceptance results; addressing partitioned residuals relative to GMPEs serves that purpose. Our plans for the next year is to continue with the development of computational tools in close collaboration with the PG&E team.

Mining Seismic Wavefields Project. In May, 2016, a SCEC working group led by PI Greg Beroza (Stanford) and co-PIs: Zhigang Peng (Georgia Tech), Egill Hauksson (Caltech), Yehuda Ben-Zion (USC), Phil Maechling (USC), and Tom Jordan (USC), received a two-year grant from the NSF geoinformatics program to develop and deploy cyberinfrastructure for mining seismic wavefields through data intensive computing techniques to extend similarity searches for earthquake detection to massive data sets. Similarity searches have been used to understand the mechanics of tectonic tremor, transform our understanding of the depth-dependence of faulting, illuminate diffusion within aftershock seismicity, and reveal new insights into induced earthquakes. These results were achieved with modest data volumes – from ~10 seismic stations spanning ~10 km – yet they increased the number of detected earthquakes by a factor of 10 to 100. This geoinformatics project is developing the cyberinfrastructure required to enable high-sensitivity studies of earthquake processes through the discovery of previously undetected seismic events within both long duration (large-T) and instrumentally dense (large-N) data sets.

This effort has resulted in fundamentally new methods of rapidly searching for small events, distribution of new template matching codes, and applications of these methods to a range of scientific questions. This project received an additional year of bridge funding in April 2018 based on exemplary results, covering the interval when the geoinformatics program had a 1-year hiatus.

New initiatives. New initiatives are being pursued by the Executive Science Director for Special Projects (ESDSP), Christine Goulet. The first involves engagement with USC Corporate Relations to develop new partnerships with corporations. This has led to a productive meeting with a transportation corporation, who is interested in SCEC's BBP capabilities. Current discussions involve a small financial involvement to initiate the development of this new partnership. The second initiative pursued by the ESDP is the development a new research program to be funded by a state agency. The initial plans are for a three-year proposal to be developed in the Fall of 2018 involving simulations with CyberShake and non-ergodic modeling of ground motions. Initial funding discussed is on par with PG&E's support annually. Additional partnerships are being built with several engineering departments in CA with SCEC as the leading the seismic hazard partner. Finally, the ESDSP is working with the SCEC Director on the development of a collaboration plan with NASA and JPL.

Leadership and Administration

SCEC has developed an effective management structure for coordinating earthquake research and educational activities. The Center's strength in facilitating collaborative, investigator-driven research has been repeatedly proven by its diverse accomplishments. Participation in SCEC is rising despite flat funding, and its national and international partnerships are flourishing. In its annual reports, the SCEC External Advisory Council has repeatedly documented the enthusiasm among SCEC participants and endorsed their high levels of satisfaction with the Center's leadership and administration.

SCEC5 operates under a similar set of bylaws as its predecessor SCEC4. The University of Southern California (USC) continues as the managing institution. However, the by-laws now designate the responsibilities of a Center Co-Director, Greg Beroza of Stanford University, who is Co-PI on the SCEC5 proposal. Establishment of a co-directorship and several other augmentations to the SCEC leadership structure enabled last year's SCEC leadership transition. The SCEC by-laws were revised this year to allow Christine Goulet (USC) to serve as principal investigator on SCEC proposals where her special expertise applied.

Recent Director Transition. John Vidale, who signed up in April 2017, started at USC in August 2017, took over as SCEC Director in September 2017. Tom Jordan, the SCEC5 proposal PI, had been the Center Director since 2002, and remains at USC and deeply engaged, but will be out of town on sabbatical this next year.

Core and Participating Institutions. SCEC is an institution-based center, governed by a Board of Directors who represent its members. The Center currently involves more than 1000 scientists and other experts in active SCEC

projects, making it one of the largest formal collaborations in geoscience. It will continue to operate as an open consortium, available to all qualified individuals and institutions seeking to collaborate on earthquake science in Southern California, and its membership will no doubt continue to evolve. The institutional membership currently stands at 76, which includes 18 core institutions and 58 participating institutions, which are listed on the inside back cover of the meeting program. As you can see from the list, SCEC institutions are not limited to universities, nor to U.S. organizations. The three USGS offices in Menlo Park, Pasadena, and Golden and the California Geological Survey are core institutions, and AECOM Corporation is a participating institution. 14 foreign institutions are currently recognized as partners with SCEC through a set of international cooperative agreements.

Board of Directors. The SCEC5 board comprises 17 core and at-large voting members, plus four USGS members, who serve in non-voting liaison capacity. The Board is the primary decision-making body of SCEC; it meets three times per year (typically in February, June, and September) to approve the Annual Collaboration Plan and budget and deal with major business items. Ex officio members include the Co-Director; the PC Vice-Chair; the Associate Director for Science Operations (serving as Executive Secretary); the Associate Director for CEO; the Associate Director for IT; and the Executive Science Director for Special Projects.

The complete SCEC5 Board of Directors is listed on the inside front cover of the meeting program. The Board is chaired by Center Director John Vidale and John Shaw serves as Vice-Chair. Each of the 18 core institutions appoints one member to the SCEC5 Board of Directors. Rachel Abercrombie and Rowena Lohman joined the Board this year, representing the participating institutions. Kate Scharer from the Pasadena office of the USGS joined the Board this year, replacing Rob Graves.

Executive Committee. An Executive Committee of the Center handles daily decision-making responsibilities. It comprises of the Center Director (John Vidale), the Co-Director (Greg Beroza), the Board Vice-Chair (John Shaw), the PC Vice-Chair (Judi Chester), the Executive Director for Special Projects (Christine Goulet), the Associate Directors for CEO (Mark Benthien), Information Technology (Philip Maechling), Administration (John McRaney), and Science Operations (Tran Huynh). John McRaney will retire early in 2019, and new hiring will precede the retirement to assure continuity and maintain operational capacity of the SCEC headquarters.

Planning Committee. The chair of the Planning Committee (PC) is the SCEC Co-Director, Greg Beroza of Stanford, and its Vice-Chair is Judi Chester of Texas A&M. The PC comprises the leaders of the SCEC science working groups—disciplinary committees, focus groups, and special project groups—who, together with the working group co-leaders, guide SCEC's research program. The PC is responsible for formulating the Center's science plan, conducting proposal reviews, and recommending projects to the Board for SCEC support. Its members play key roles in implementing the SCEC5 science plan. We urge you to communicate your thoughts about SCEC research plans to them as well as Director Vidale at the Annual Meeting and elsewhere.

The PC members and their science expertise are listed inside the front cover of the Meeting Program. Gareth Funning and Michele Cooke stepped up to lead their working groups, and Ramon Arrowsmith and Manoochehr Shirzaei have joined the PC as co-leaders of San Andreas Fault System focus group and Tectonic Geodesy disciplinary committee, respectively. We greatly appreciate the accomplishments of Kate Scharer and Dave Sandwell, who rotated off from these groups.

The SCEC science planning organization comprises a number of disciplinary committees, focus groups, special project teams, and technical activity groups (see figure below). These working groups have been our engines of success, and many of the discussions at this meeting will feed into their plans. The leaders of the disciplinary committees and focus groups form the membership of the planning committee.

The Center supports disciplinary science through **disciplinary committees** in Seismology, Tectonic Geodesy, Earthquake Geology, and Computational Science. These groups are responsible for disciplinary activities relevant to the SCEC Science Plan, and they make recommendations to the Planning Committee from the perspective of disciplinary research and infrastructure.

SCEC coordinates earthquake system science through **interdisciplinary focus groups**. The importance and scale of effort involved with community models led us to request funding for a Community Models Developer in the SCEC5

proposal. The requested budget increase was not granted, but we were able to readjust funding enough to hire Mei-Hui Su in this role a year ago.

A **technical activity group** (TAG) is self-organized to develop and test critical methodologies for solving specific problems. TAGs have formed, for example, to verify the complex computer calculations needed for wave propagation and dynamic rupture problems, to assess the accuracy and resolving power of source inversions, and to develop geodetic transient detectors and earthquake simulators. TAGs share a modus operandi: the posing of well-defined "standard problems", solution of these problems by different researchers using alternative algorithms or codes, a common cyberspace for comparing solutions, and meetings to discuss discrepancies and potential improvements.

SCEC5 science planning organization chart, consisting of Disciplinary Committees (green boxes), Interdisciplinary Focus Groups (yellow boxes), and Technical Activity Groups (ellipses) coordinated by Working Group leaders in Special Projects, San Andreas Fault System, SCEC Community Models, and the Earthquake Engineering Implementation Interface.

External Advisory Council. The external Advisory Council (AC) is charged with developing an overview of SCEC operations, identifying strengths, opportunities, and vulnerabilities, and advising the Director and the Board. Since the inception of SCEC in 1991, the AC has provided perspective to maintain the vitality of the SCEC and help its leadership chart new directions. The Center has always provided its sponsoring agencies and participants with a complete copy of the yearly AC report. The full 2017 AC report is included in this volume. The current AC membership can be found inside the front cover of the meeting program.

The AC was reconstituted as part of the SCEC5 transition. Meghan Miller, the president of UNAVCO, is the current AC Chair. She has served on the AC since 2012 and is well known for her acumen, organizational skills and scientific leadership. The new AC members are Ellen Rathje (University of Texas, Austin), Louise Kellogg (UC Davis). Continuing members are Warner Marzocchi (INGV, Rome), Rick Aster (Colorado State U), Susan Beck (U Arizona), Yann Klinger (IPGP/Paris), Tom O'Rourke (Cornell), Susan Owen (JPL), Heidi Tremayne (EERI), and Tim Sellnow (U. Central Florida). Rotating off the AC this past year are Donna Eberhart-Phillips (UC Davis) and Roger Bilham (U. Colorado), who served the SCEC AC with alacrity and vision.

Center Budget and Project Funding

The Southern California Earthquake Center is funded by the NSF and USGS through cooperative agreements with the University of Southern California (USC). Additional funding for the annual SCEC research program may be provided by the Pacific Gas & Electric Company, the Keck Foundation, the California Earthquake Authority, geodesy royalty funds, and potentially other external sources. Funding to SCEC supports earthquake research in Southern California that engages an interdisciplinary community of over 1,000 active participants. Funding from external sources have constraints on how they can be spent. For example, SCEC receives funding from PG&E for studies in rupture dynamics, development and maintenance of the broadband ground motion simulation platform, and ground motion prediction studies in Central California, mainly with CyberShake.

The SCEC core program has been level-funded by NSF and USGS since 2002. About 69% of the NSF and USGS core funding is spent on science and infrastructure; other budget lines include management (11%), the education and outreach programs (12%), meetings (6%), and a Director's reserve fund (2%). Augmented USC support of the Center

allows SCEC to maintain administrative costs at very low levels while increasing the professional staff at SCEC headquarters.

In 2018, NSF cut base funding again by about $76K (from the $3,000,000 per year SCEC5 authorized level) to $2,923,365. The USGS fully funded SCEC at the authorized level of $1,602,965 in 2018. Building the 2018 SCEC budget was again challenging due to vagaries of federal funding, approvals, and cash flow. The SCEC5 year 2 budget was not finalized until May 2018. For the 2018 funding cycle, SCEC received 152 proposals (by 188 distinct investigators) requesting a total of $4,895,422. The allocated funding for these 2018 science proposals is $3,010,800. Augmenting the base funding from NSF and USGS is an additional $400K from Pacific Gas & Electric Company, the Keck Foundation, and geodesy royalties.

The annual budget cycle begins with a SCEC Leadership Meeting in early June, where the Board, Planning Committee (PC), Executive Committee of the Center, and agency representatives discuss SCEC research priorities. Based on these discussions, the PC drafts an annual SCEC Science Plan, which is presented to the SCEC community at the Annual Meeting in early September. The PC uses the feedback received at the meeting to finalize the Annual Science Plan, and a project solicitation released in October. SCEC participants submit proposals in response to this solicitation in November. All proposals are independently reviewed by the Director, the Co-Director, Vice-Chair of the PC, and the leaders of at least three relevant science working groups. Reviews are assigned to avoid conflicts of interest.

The PC meets in January to review all proposals and construct an Annual Collaboration Plan. The plan's objective is a coherent science program, consistent with SCEC's basic mission, institutional composition, and budget that achieves the Center's short-term objectives and long-term goals, as expressed in the Annual Science Plan. The PC Chair submits the recommended Annual Collaboration Plan to the Board of Directors for approval. The annual budget approved by the Board and the Center Director is submitted to the sponsoring agencies for final approval and funding. Upon approval by the agencies, notifications are sent out to the investigators.

To construct the Annual Collaboration Plan, proposals submitted in response to the annual solicitation are evaluated based on: (a) scientific merit of the proposed research; (b) competence, diversity, career level, and performance of the investigators; (c) priority of the proposed project for short-term SCEC objectives; (d) promise of the proposed project for contributing to long-term SCEC goals; (e) commitment of the principal investigator and institution to the SCEC mission; (f) value of the proposed research relative to its cost; and (g) the need to achieve a balanced budget while maintaining a reasonable level of scientific continuity given funding limitations. With respect to criterion (b), improving the diversity of the SCEC community and supporting early-career scientists is a major goal of the Center. It is important to note that a proposal that receives a low rating or no funding does not necessarily imply it is scientifically inferior. Rather, these proposals may be downgraded because they may not meet other criteria noted above.

Thanks and Acknowledgements

It is a great honor and privilege to be entrusted with the SCEC enterprise. The broad vista of science and the exposure to earthquake destruction and disruption in southern California requires the kind of teamwork and forward thinking embodied by the Earthquake Center. We have been successful because of the collaborative efforts of many people over many years, and of course the foundational grounding by former Center directors Kei Aki, Tom Henyey, Dave Jackson, Bernard Minster, and Tom Jordan.

Especially critical this first year has been the Science Planning Committee, with dedicated Chair Greg Beroza and Co-Chair Judi Chester, who form and implement the annual science plan, evaluate proposals, plot the annual meeting, and set out milestones for the next steps with the help of their colleagues on the PC.

I have been immeasurably helped with SCEC science and engineering goals by the energetic expertise of Christine Goulet and Phil Maechling. Together they manage many SCEC projects and oversee our team of talented software developers and computer scientists. Mei Su has taken the reigns to tame the community models. Scott Callaghan and Kevin Milner deftly create large and intricate meshes, feed them into cavernous computers, and crunch out trillions of important numbers and intuit their meaning in the form of intelligible stories. Fabio Silva keeps the

computer tool shed sharp and rust-free, John Yu supplies the hardwire, wires it together, and tells us weekly what we've done wrong and which passwords we've lost and forgotten. Bill Savran, our latest acquisition, is laying the groundwork to move into the next stage of earthquake forecasting science.

Tran Huynh's coordination and operational prowess and good sense hold the Center together. The day-to-day business and financial operations of SCEC are supported superbly by Deborah Gormley, while Edric Pauk deftly manages the many diverse aspects of SCEC'S community information systems that supports our collaboration.

Mark Benthien and his larger than life CEO team spread the word of SCEC across the globe. Gaby Noriega leads the intern programs with aplomb and calm, creating an especially successful program this past summer sorting through the impacts of the worst earthquake nightmares facing Los Angeles. Jason Ballmann manages SCEC media relations and all aspects of ShakeOut communications, and feeds the social media with verve and subtlety, bringing the instagram, Facebook, and twitter SCEC presence to life. Our collaborations across statewide and foundation support are prospering under Sharon Sandow, and John Marquis holds together the diverse web resources of CEO.

A very special thanks to John McRaney, who will retire after 40 years, to whom we will give thanks and celebrate at the Monday night banquet. He still retains all SCEC memories, corporate and other, and is still fixer nonpareil. His results with Excel rival what the rest of us strive to gain on Blue Waters. Most of us wish we could remember and recount stories as accurately and well as the Chaplain—many of us hope he'll write the definitive history of earthquake science, scientists, policy, and history in southern California.

Please do not hesitate to contact any member of the SCEC team if you have questions, comments, or suggestions about our meeting activities and future plans.

Let the 27th Annual SCEC meeting begin!

2017 Report of the Advisory Council

M. Meghan Miller, SCEC Advisory Council Chair

Introduction

The SCEC Advisory Committee (AC) convened at the SCEC Annual meeting in Palm Springs from September 10 to 13, 2017, reviewing SCEC activities in order to offer advice to the SCEC leadership. The SCEC AC comprises the following members, all of whom were present at the meeting, except where noted:

M. Meghan Miller, Chair, UNAVCO
Rick Aster, Colorado State U.
Susan Beck, U. Arizona
Roger Bilham, U. Colorado
Donna Eberhart-Phillips, U. California, Davis
Yann Klinger, IPGP/Paris
Warner Marzocchi, INGV, Rome
Tom O'Rourke, Cornell U. (not present)
Susan Owen, JPL
Tim Sellnow, U. Central Florida (not present)
Heidi Tremayne, EERI

Advisory Committee members were given a 140-page briefing book on September 6. The AC met initially on September 9 and was briefed by SCEC leadership and by USGS and NSF representatives. Director Tom Jordan and incoming Director John Vidale provided the AC with a summary of the state of SCEC and provided a list of issues on which they sought AC feedback. Following the leadership briefing, the AC attended scientific sessions and solicited feedback from attendees. The AC also met three additional times during the meeting to discuss observations and findings. AC Chair Miller presented a summary of AC observations on Wednesday morning of the meeting, and this written report is intended to provide more detail. All committee members reviewed this report.

This report addresses the various questions and topics posed by the SCEC leadership, and offers additional observations.

Overview

At this critical transition to SCEC5 and a new SCEC Director, the Advisory Committee commends the exceptional achievements of SCEC and its globally significant contributions to earthquake and Earth system science. In spite of funding limitations and other external challenges, the AC sees a healthy organization with excellent future prospects and a coherent and ambitious 5-year plan.

AC Membership

0. Are new AC members needed?

An Engineering Seismologist or Geotechnical Engineer would be an appropriate addition to the AC to expand the committee expertise at the interface between engineering and seismology. Heidi Tremayne can help to identify possible candidates, if desired.

SCEC5 Science and Applications

1. Are the SCEC5 milestones appropriate?

The milestones are appropriate with enough detail to assure a structure to evaluate progress. The workshop provides useful points to engage current and new researchers in SCEC5 components and milestones that include a useful mixture of developmental research, quantitative products and consensus building aspects.

2. The Earthquake Gates Area Initiative represents a sustained commitment. How should they evolve, and should more be seeded?

The Earthquake Gates initiative looks very promising with some exciting early results. Understanding the controls on the probability of an earthquake rupturing multiple segments is key because it may control the ultimate size of the earthquake rupture. Hence, we view the Earthquake Gates initiative as an important activity for SCEC. We agree with the SCEC plan to use community input to identify one or more focus sites. Some issues, however, might not be possible to tackle at the chosen EG site and SCEC should stay open to investigation outside EG site proper, elsewhere in the US or abroad, as long as the study area remains clearly relevant to SCEC EG activities. Starting with a small number of focus sites and then expanding as resources allow may be the best approach. It will be important to identify criteria to define the success of the Earthquake Gates initiative.

3. SCEC Community Models are in various stages of completion and improving at various rates. Are the levels of effort and accomplishment appropriate?

The SCEC community models, with their wide and integrated application, are a highlight achievement. The articulated goals going forward are appropriate (and appropriately ambitious). The goal of going to higher frequency and more accurately reflecting near-surface structure and effects, as well as fault geometries, will require even more massive data collection, assimilation, and validation.

The levels of effort and accomplishment are appropriate. The development of unified ways to represent detail will make the results more useful and facilitate addressing research questions that flow from integrating the various CXM. The systematic study of velocity and rheology of basin sediment will provide necessary parameters for inferring near-surface effects on ground motion. At the meeting, it has been good to see the work done so far on the rheology component, including even some implementation. It appears that the CRM will also eventually improve the CVM, and the groups will develop new understanding, as the rheology users may define deeper crustal features for determining viscoelastic response.

4. How can we make better progress on the reduction of risk to distributed infrastructure? What would be good ways to interact with the relevant engineering community?

Regional oil and gas pipeline operators have not planned for the possibility of multiple simultaneous lesions during a major earthquake, nor the consequences of unstemmed leaks into State Parks, highways and wildlife preserves. A cost-benefit analysis of cleanup costs following an earthquake that causes multiple or major pipe ruptures (as a counterexample, the averted Alaska Oil Spill after Denali Earthquake) might provide an incentive for future interactions between pipeline operators and SCEC. Although state legislation may ultimately be necessary to ensure implementation, a cost-benefit analysis of a catastrophic multiple failure event may persuade operators of the urgency of pipeline resilience or inform state action.

A useful direction might be to contact and connect with the existing LA lifelines council, National and State Parks, Wildlife organisations, to encourage California legislation to mitigate fault-crossing pipe damage.

In his presentation Jack Baker showed clearly the importance of the spatial correlation of ground shaking in its effects on loss estimation, in particular when the target is a spatially distributed system (e.g. highways). This effect cannot be accounted for through the usual PSHA and GMPEs models, because the models are targeted only on single sites. The procedure described by Jack, although at a preliminary stage, appears very promising and immediately applicable. This motivates higher frequency (temporal and spatial) CyberShake-type ground motion modeling and its use in this type of analysis.

Regarding enhanced partnerships with the engineering community, promoting collaboration on PSHA is an excellent opportunity to shape a common language and to understand what engineers need and what seismologists can provide.

SCEC should also continue knowledge transfer activities to the engineering community that reach engineers in locations where they normally gather. Expanding collaboration with engineering research centers and organizations would facilitate this task. One suggestion is to design more sessions, presentations and workshops at related

engineering conferences/events that seek feedback on SCEC products, similar to SCEC's work for the 11th National Conference on Earthquake Engineering in Los Angeles in June 2018 including a partnership with the Earthquake Engineering Research Institute (EERI). Other engineering groups of interest for technical collaboration and feedback include Natural Hazards Engineering Research Infrastructure (NHERI) SimCenter and DesignSafe, Pacific Earthquake Engineering Research (PEER), American Society of Civil Engineers (ASCE) Geo-Institute, and Structural Engineers Association of California (SEAOC).

Communication, Education, and Outreach

5. Does the draft SCEC5 CEO Evaluation Framework and its related logic model, metrics, and milestones provide an appropriate level of assessment?

The scope and scale of CEO activities continues to impress the Advisory Committee. The CEO is successful as a means of educating the public about earthquakes, and as an inspiration for what the public might do to mitigate their effects. Efforts to train and transition students (especially from underrepresented groups) to early career researchers and practitioners is also admirable.

The CEO group has actively responded to the 2015 evaluation recommendations by strategically selecting key indicators and metrics. This work is applauded and should be extended by identifying effective assessment tools or procedures to gather data for metrics that don't have simple quantitative metrics. Because long-term outcomes can be difficult to quantify and the number of outcomes in the logic model are numerous, the CEO group (with limited staff time and funding for assessment) may want to consider focusing more targeted, detailed, or nuanced assessments for some activities or specific outcomes, while more straightforward statistics collection/numerical metrics/reporting for other outcomes may be sufficient to track their progress. Such assessment should be incorporated as the logic model evolves in the first year of application, taking into account how the logic model should influence and inform an evaluation plan.

Some discussion centered on metrics to track ShakeOut success that had been generated in the CEO Planning Meeting, and to work with USGS and social scientists to identify how to add or modify 1-2 questions on the "Did You Feel It" survey to reflect (1) if the citizen reporting providing feedback actually dropped, covered, and held on, or took other protective actions, and (2) if they have participated in ShakeOut drills that influenced this action. This discussion included the caveat that any modification of questions should be carefully reviewed and validated by social scientists.

6. The proposed Transitions Program was favorably reviewed and is a priority for NSF, yet with reduced funding its activities will be limited…. What other cost efficient concepts should we consider to increase retention and diversity into geoscience careers?

We applaud SCEC for the focused breakfast meetings with students and early career scientists at the SCEC meeting. Similar events could be undertaken jointly with UNAVCO and IRIS (or other organizations) at the AGU meeting. A website for early career scientists where they can share information and resources would also be of value. The summer internship programs have been very successful and should be continued. We agree that partnering with SCEC institutions to identify external intern opportunities is important.

One cost efficient concept for increasing diversity and retention in geoscience careers would be to plan for a presentation, workshop, or session at future SCEC annual meetings, one that explores implicit bias and strategies for reducing its influence. AGU (with others) is leading a national and international conversation on implicit bias and its role in limiting diversity. SCEC could consider reaching out to AGU or AWG for speaker suggestions on implicit bias and strategies to avoid it. University programs that succeed in broadening participation in geosciences or other STEM fields (e.g., the Harvey Mudd program to increase female students participation in computer science) could also be a source for inspirational speakers or workshop leaders.

7. The AC has strongly encouraged SCEC to provide risk communication training/discussion at the SCEC Annual Meeting. For the second year CEO has organized a communications workshop on Sunday for interested attendees. Is this sufficient or should there be a plenary session presentation as well?

The Public Communications workshop included an informative talk on how to interact with the public with a hands-on practice; it was commended for engaging participants. The SCEC Distinguished Speaker also did a nice job of elevating the topic of risk communication to all participants in a plenary setting Sunday evening. And the Temblor demonstration provided a useful tool to enable individual conversations between SCEC participants and non-specialists.

The committee further noted the usefulness of skills development for communicating science results to lay-people (as well as communicating risk). Few researchers are likely to participate in a press conference, but many of us have wished we knew how to prepare and perform better in common media situations. SCEC should consider expanding specific training to include the more basic topic of a media interview (live tv, radio, other interviews or written contributions).

8. SCEC annual meeting size challenges SCEC resources and may hinder function — should we strive to limit attendance to ~500, and if so, how?

Optimized meeting size is one broad measure of SCEC's success. The large number of early career attendees, for example, is a positive factor for the community at large and for long-term advancement of SCEC goals; thus their integration is highly desirable. The 2017 meeting hit this right, and corrected for the open floodgates of 2016.
More broadly, limiting strategies should be motivated by clear and prioritized overall meeting goals and letting these goals drive decisions regarding recruitment, with appropriate incentives and disincentives to optimize attendance. The 2017 emphasis on communication, reflected in the Sunday workshop and Distinguished Speaker topic, well served the advancement of SCEC's broader influence and ultimate value to society, while engaging scientists in critical communications, an area where many aspire to do better.

Large plenary sessions can make discussion difficult, and can be intimidating for early career participants. Some organizations are experimenting with ways for attendees to provide questions/comments via tools like Google Docs that moderators and session chairs can use to seed questions and stimulate discussions. Texting could also provide a mechanism that doesn't encourage broad use of laptops in plenaries. That said, the discussions following plenary sessions were much improved over previous years on two counts: colleagues kept each other in check and younger participants were more forthcoming. While they may have been postdocs rather than grad students, this is still good progress. The online strategies could further this progress for 2018, and potentially expand participation.

Recommendations for action - opportunities and threats

9. How can we better recruit excellent high performance computing (HPC) talent and maintain connections to the HPC world?

One strategy to consider for recruiting HPC talent is to reach out to those who have interests in the broader scientific and societal problems to be addressed with the application of their HPC expertise and talent. These individuals can be recruited and retained through broader engagement in the mission, publications, and exposure to Earth science, combined with a concerted focus on mentorship. Emphasizing the scientific mission of SCEC, plus the altruistic appeal and societal impact of careers in earthquake science, could make SCEC positions more desirable to millennials and other early career prospects. SCEC should also expect and plan for the inevitable turnover in its own staff (given national trends for younger professionals) by ensuring overlap in knowledge, tasks, and skills.

10. What additional strategies should we pursue for funding CEO activities?

NSF's Division of Education and Human Resources offers a changing landscape of award opportunities, a landscape that SCEC leadership is aware of. Visit program officers in their new digs in Alexandria, monitor EHR program solicitations for focus areas that align with SCEC goals, and cultivate a spectrum of community-embedded capabilities and expertise (pedagogy, assessment) to draw on for new initiatives. Some of these might be accessed (and are being accessed) in the community geophysics facilities as well; partnerships could provide further synergies.
Mitigation strategies might include: Diversification of the SCEC portfolio and sponsorship, but this can be very time consuming to cultivate and unreliable over time. Choosing what not to do is another mitigation. There is no substitute for sponsorship that has wholesale ownership of the mission and structure of the organization. That said, in the

current mix, SCEC should continue to develop projects that cultivate new capabilities and sponsorship including the broader public sector or private interests - power, water, transportation, municipalities.

11. Changes in leadership at PG&E: Norm Abrahamson is leaving, PG&E budget was cut from $1.6M to ~$1M late in the year, and planning the future of PG&E funding is in flux. We proactively discussing with PG&E management on future research priorities.

The committee recognizes the potential impact of losing this key relationship, and encourages the new leadership to commit time to developing new relationships (or strengthening other existing relationships) at PG&E. PG&E's interest is well aligned with SCEC. Find the PG&E new kid in town and cultivate common interests.

12. NSF has postponed announcement of the next solicitation of Geoinformatics and SI2 proposals, two mainstays of SCEC Special Project efforts. How do we plan for continuation of efforts supported by these programs?

Continued engagement with NSF leadership on the importance of specific solicitations to the community, or partnering with other groups affected by the delay in solicitations to communicate en masse, might help shine light on the costs to NSF in lost productivity. NSF programs are expected to evolve, and recipients are expected to evolve as well - so engagement with NSF program managers on future directions could help ensure that NSF is evolving in alignment with SCEC community needs. NSF uses unmet priorities in the investigator community to shape solicitations. The new director would be well served to interact with program officers in a variety of roles and directorates.

Other wisdom from the committee includes guidance (1) to develop a plan that consistently pursues a diverse set of funding sources, to increase stability when programs change and (2) develop a funding 'succession plan' by reviewing other information technology programs within NSF (e.g., EarthCube or whatever succeeds it) and outside of NSF (e.g., NASA).

13. A byproduct of the extensive SCEC5 NSF risk assessment has been outlawing the overhead waiver on subcontracts (e.g., subawards). Heroic efforts by John McRaney, Tran Huynh, and Deborah Gormley have adjusted SCEC arrangements so this change does not affect finances, at a cost of increased complication in administration of budgets. Does this somewhat convoluted arrangement require further corrective adjustments?

Heroic efforts are duly noted and highly commended! The subaward rule is long-standing, while NSF's attention to and application of award rules is increasingly comprehensive and rigid, creating significant new administrative burden. It is not clear if or when the pendulum will swing back. Until a sea change comes, recipient award administrators might benefit from taking a more proactive stance. Participation by the USC award administrator in structured NSF events like the Large Facilities Workshop (or similar professional development) can build understanding on both sides, expose model practices for coming constraints, and help anticipate or even shape change. Such participation develops communication pathways to directly convey the impact of the administrative burden on awardees. This is important to make visible at NSF.

14. The SCEC5 NSF risk assessment and subsequent overhead negotiations have resulted in separate start dates for NSF (May) and USGS (February) cooperative agreements. How do we bring the NSF date back to February, in sync with USGS and internal planning and funding cycles, and obviating the problematic budgetary gyrations necessitated by multiple start and end dates?

Alignment of the dates may simply not be achievable, even at the cost of one quarter of funding. Greg Anderson has demonstrated creativity and effectiveness in finding solutions to odd administrative problems at NSF in cases where a solution could be found. If Maggie and Greg cannot explore and devise a technical fix for this problem, NSF options will likely have been exhausted. At that point, it might be time to seek the serenity to accept the things that cannot change and work to minimize impact on staff and workload, which the committee recognizes will be significant. This might include a reporting schedule based on a defined project year that makes sense for SCEC, but cannot match the various fiscal years of different sponsors, if sponsor agreement can be secured.

15. Future steps for UCERF? We just submitted a 1-year, $370K proposal to CEA for understanding uncertainties in UCERF3 and simplifying calculations (logic tree trimming).

Quantifying uncertainties and simplifying calculations are positive new directions. Ongoing refinement of UCERF is foundational to SCEC's mission, and for planning and prioritization. The risk information coming out from UCERF3-ETAS may be of interest to reinsurance and insurance companies.

16. There are potential opportunities for SCEC funding through DOE and NASA. Ben Phillips, the lead for NASA's Earth Surface and Interior Focus Area, has been invited to the past two SCEC meetings, and he has indicated that a SCEC proposal to the NASA Research Opportunities in Space and Earth Sciences (ROSES) program would be appropriate. Funding from DOE is more problematic, because earthquake science is not well represented in the RFP for their Scientific Discovery through Advanced Computing (SciDAC) program. AC advice on how to approach these agencies is welcome.

The AC encourages SCEC leadership to first consider goal alignment between NASA and DOE goals - e.g., does integrating SCEC better with the NASA ESI community make sense and provide benefit to both SCEC and NASA? With NASA launching a SAR mission in 2021, there is potential for significant overlap in research goals related to earthquake science.

As for any sponsor, spend the time to develop new relationships to explore common interests and goals and to explore and understand the agency award mechanisms. Proactive development of the relationship could lead to inclusion of SCEC-aligned NASA priorities in a specific announcement of opportunity, if the groundwork has been done in advance.

There are also institutional structural limitations for researchers at NASA centers to receive funding to participate in research projects and community working groups. SCEC could discuss with Ben Phillips potential avenues for better integration of NASA scientists into the SCEC community through NASA funding of NASA participants in SCEC research projects - effectively enlarging the funding pool for small research awards.

Earthquake Response Planning

17. Post-earthquake response planning is timely and there is growing consensus that we should get more organized: how do we form a southern California response plan and how do we sustain SCEC effort at an operational level?

Revisiting the scope and objectives of SCEC's earthquake response plan and its engagement platform response.scec.org is timely.

Post-Earthquake Response is a cross-cutting topic amongst many areas and many SCEC partnerships. SCEC leadership should define the SCEC vision and strategy in this landscape before working with external partners and finalizing a plan.

After internal alignment of goals and priorities, SCEC should ensure that the leadership successfully engages and strategizes with other partners and agencies who are working in the area of post-earthquake response (e.g., California Earthquake Clearinghouse, GEER, EERI, USGS, CGS, CalOES, IRIS, UNAVCO, universities), and align their plans accordingly. Goals might include filling gaps, avoiding duplication, and capitalizing on SCEC strengths and mission. Several specific recommendations came out of discussions during the meeting that should be explored for feasibility and alignment with other SCEC efforts:

(A) Provide training or resources to support scientists' awareness about mental health impacts when responding to earthquakes, including how to be sensitive to people who have experienced losses. These resources may also be helpful in times of stress unrelated to earthquakes.
(B) Continue to strategize SCEC's involvement and role in the California Earthquake Clearinghouse. One way would be to raise awareness of data sharing and available tools, as an option in addition to SCEC's response.scec.org website.

(C) Conduct an Earthquake Response Workshop at every SCEC Annual Meeting using the California Earthquake Clearinghouse Training module that could be customized for SCEC. This workshop would include a Disaster Service Worker certification.
(D) Explore provision of GIS support (possibly via an ArcGIS Online interface) during the earthquake response phase to collate and visualize data gathered by SCEC researchers, establishing base layers of background data helpful for field studies, or analysis of existing data.

Other comments

18. Notes on the Leadership Transition

The SCEC leadership transition was very well executed. Tom Jordan is commended for his dedication to ensuring the success of the transition, both by continuing his service until a successor was identified and recruited, enabling Greg Beroza's elevated role, and by graciously handing over the reins while remaining available and engaged with SCEC's success.

John Vidale is poised to succeed in this new role and brings breadth, leadership, and a history of work with broader constituencies at PNSN to the leadership position at SCEC. The Committee looks forward to a productive future in working with SCEC Leadership.

The dedication and professionalism of SCEC staff across the organization is also highly commended. Leadership transitions are difficult times, and staff members have clearly engaged in ensuring SCEC's future through staying the course, supporting the transition, and continuing to provide a signature level of extraordinary support for the organization and the SCEC Community. Well done!

19. SCEC5 as a Framework for Augmentation

The committee noted that the scientific, cyber, and observational infrastructure of SCEC could provide leverage and synergies to broader efforts or emerging opportunities:

Improved understanding of intermediate period fault behavior likely requires greater knowledge of hydrogeology, aqueous geochemistry, fluid pressure effects, and fluid sources. Work in this area may benefit from new and/or smaller-scale simulations of fault-fluid interactions and studies of induced seismicity outside of southern California.
There may be valuable unrealized opportunities for SCEC programmatic involvement in induced seismicity research and/or possible upcoming in-situ earthquake experiments being considered elsewhere in the seismological community.

Dense portable seismic arrays have clear benefits for high-resolution modeling of near-surface structures, fault structures, and response, as well as for post-earthquake studies. Such studies could benefit site characterization.
Coordinate with existing facilities and institutions that support instrumentation and data acquisition to ensure SCEC's unique strengths benefit broader data collection efforts.

20. Annual Meeting Logistics

Additional coffee stations are needed for a meeting of this size. The 15-minute break is simply too short to move 500 people in and out of the large plenary room. The unstructured time to interact with colleagues is very useful in stimulating interaction.

The meeting increasingly relies on posters for expanded participation, and some adjustments are needed to ensure effectiveness. (1) If there is to continue to be no dinner on Tuesday, provide snacks to support poster attendance; this is a key time for interaction between student/early career investigators and senior scientists. (2) There are a number of technical problems with the poster room. A larger room or acoustic absorption props could reduce the decibel level and permit conversations to be undertaken without participants shouting at each other. The illumination cross lighting of the past several years hinders viewing of posters beneath the spotlights. Consider more elevated lighting.

It was further noted that the restrooms really need to be moved to the plenary meeting floor, with little hope that this is within SCEC's span of influence.

21. Improving Clarity and Ease of SCEC and SCEC AC interactions

It would be useful to the AC if SCEC provided a secure discussion list-serve or email list that does not include SCEC staff to freely air, peer-educate, reconcile and integrate disparate perspectives and misconceptions while including off-site committee members, before finalizing the report. We believe that this will provide a more informed report.
Establishing a set of staggered terms for Committee Members is an important step forward. It would be useful for SCEC leadership to communicate the term for each committee member in an appointment letter or email at the time of appointment.

Communication, Education, and Outreach Report

Mark Benthien, SCEC Associate Director for CEO

Overview

SCEC's Communication, Education, and Outreach (CEO) program addresses the final element of SCEC's mission: Communicate understanding to end-users and society at large as useful knowledge for reducing earthquake risk and improving community resilience. Our strong and effective regional, national and global collaborations anticipate many years of joint activity of research and educational products that improve the preparedness of the general public, government agencies, businesses, research and practicing engineers, educators, students, and the media—locally in California as well as in other states and countries. Thus, the theme of the CEO program in SCEC5 is Partner Globally, Prepare Locally; preparing not only for local hazards, but also preparing students and the public with enhanced science literacy to make informed decisions (split-second as well as long-term) to reduce their risk, and preparing the next generation of scientists via research opportunities and support through career transitions.

CEO is an evidence-based program built on education and social science research. Strategies for motivating particular actions are continuously adapted from successful efforts in community building, education, marketing, environmental change, organizational culture change, and other disciplines. These principles are implemented within four CEO focus areas (Figure 1). Knowledge Implementation connects SCEC scientists and research results with practicing engineers and other professionals who apply earthquake science, as well as with public and private decision makers. Public Education and Preparedness educates people of all ages about earthquakes, tsunamis, and other hazards, and motivates preparedness. K-14 Earthquake Education Initiative improves Earth science education in multiple learning environments, overall science literacy, and earthquake safety in schools and museums. Experiential Learning and Career Advancement provides research opportunities, networking, and other resources to encourage and sustain careers in STEM fields. Each of these areas build on improved earthquake science understanding.

Figure 1. SCEC CEO Focus Areas and Programs

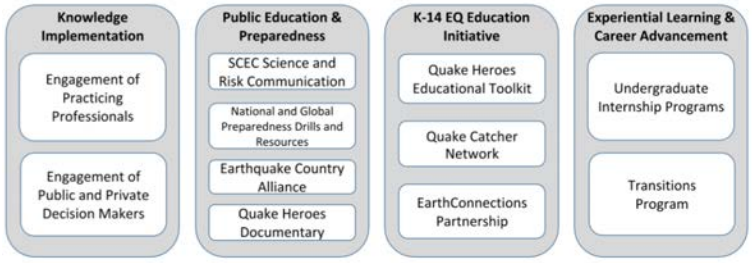

Associate Director for CEO Mark Benthien leads an accomplished team of staff and consultants (Figure 2), each managing portfolios that span the CEO focus areas. CEO staff are John Marquis (CEO web manager), Jason Ballmann (communications manager), Sharon Sandow de Groot (assistant director for strategic partnerships), and Dr. Gabriela Noriega (manager for Experiential Learning and Career Advancement). CEO consultants include Jozi Pearson (UseIT supervisor), and Dr. Michele Wood (CSU Fullerton) who supports CEO evaluation activities.

Figure 2. SCEC CEO Staff and Consultants

The CEO Planning Committee (CEO-PC, Figure 3) provides guidance and support for CEO activities and partnerships, review reports and evaluations, and identifies synergies across SCEC and with external organizations. It is comprised of SCEC stakeholders selected to represent the four CEO focus areas, with some members drawn from the SCEC Advisory Council, Board, and Science Planning Committee. The Chair of the CEO-PC is Tim Sellnow (U. Central Florida), who is also on the AC. Sellnow represents the Public Education and Preparedness CEO focus area along with Kate Long (Dr. Lucy Jones Center). Danielle Sumy (IRIS) represents the K-14 Earthquake Education Initiative. Sally McGill (CSU San Bernardino) represents the Experiential Learning and Career Advancement focus

Figure 3. SCEC CEO Planning Committee

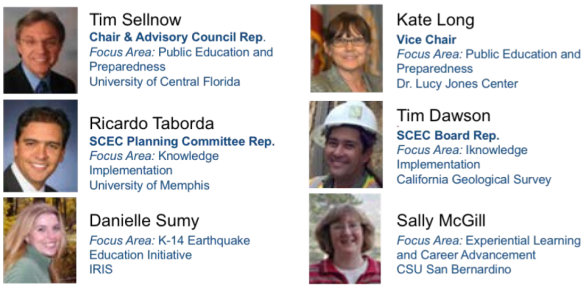

area. Tim Dawson (California Geological Survey) and Ricardo Taborda (Universidad EAFIT, Colombia) represents the Knowledge Implementation focus area. Dawson and Taborda are also the representative of the SCEC Board and PC, respectively, on the CEO-PC.

SCEC/CEO has been very successful in leveraging its base funding with additional support. For example, since 2010, FEMA has provided SCEC more than $2 million to coordinate the Earthquake Country Alliance in California (at the request of the California Office of Emergency Services, CalOES) and for national ShakeOut coordination. ShakeOut regions in the U.S. and internationally have also provided funding, and the California Earthquake Authority (CEA) has spent nearly $20 million dollars on television, radio, and print advertising that features ShakeOut each year. SCEC's intern programs have been supported with more than $1.6 million in additional funding from several NSF programs and a private donor. NOAA (via CalOES) now provides funding to SCEC for developing the TsunamiZone.org website. In addition, CEO receives sponsorship support from AAA, State Farm, and other partners.

Evaluation

The CEO program in SCEC5 is organized for extensive evaluation, including the annual review by SCEC's external Advisory Council; annual reporting of milestones and metrics to funding agencies; evaluations of individual activities (post-ShakeOut surveys, teacher workshop evaluations, post-internship discussions, etc.); and as part of the proposal review process. The CEO Planning Committee works with CEO staff to plan and review these evaluation activities, along with the support of Dr. Michele Wood, an experienced program evaluator who reviewed the CEO program and its evaluation structures [Wood, 2015] and provided many evaluation recommendations that are being implemented in SCEC5. This includes a new comprehensive logic model that relates all CEO activities to the accomplishment of four long-term intended outcomes:

- Improved application of earthquake science in policy and practice
- Reduced loss of life, property, and recovery time
- Increased science literacy
- Increased diversity, retention, and career success in the scientific workforce

The CEO logic model provides the theoretical basis for identifying appropriate measures for assessing progress towards achieving these outcomes. CEO metrics are selected process measures (program outputs and short-term outcomes) that most inform program management, that represent progress along the logic model, and that can be assessed within limited program resources. CEO milestones include major accomplishments planned for activities and also progress towards achieving and reporting medium- and long-term outcomes. The full logic model is within the SCEC5 CEO Evaluation Framework along with annual milestones through the end of SCEC5. This Framework is the basis for the charts below which list the outcomes for each focus area and current metrics for each program. Year 2 milestones for each focus area are also discussed, along with expected activities and milestones for Year 3.

Knowledge Implementation (KI)

SCEC's Implementation Interface working group provides the organizational structure for connecting SCEC scientists and research results with research engineers and key partners (such as PG&E) to improve application of earthquake science. The CEO Knowledge Implementation focus area extends these connections to practicing engineers, government officials, business risk managers, and other professionals. SCEC CEO has partnered for many years with city, county, and state agencies who need earthquake information, organizes workshops and other trainings (including those provided by the Earthquake Country Alliance and GeoHazards Messaging Collaboratory), and held activities with the EERI Southern California Chapter and the Structural Engineers Association of Southern California.

A key aspect of this focus area is to expand these activities and also improve the articulation of science process and results by the SCEC Community, both internally and with external audiences, in order to increase the adoption of

SCEC science and products in the development of improved building codes, updated insurance rates, and more realistic emergency management planning scenarios. Example products include the Maximum Considered Earthquake response spectra (MCE_R) data access tool produced by the SCEC Committee for Utilization of Ground Motion Simulations (or "UGMS Committee"), SCEC simulations (High-F, Broadband, CyberShake), UCERF (Uniform California Earthquake Rupture Forecast), and OEF (Operational Earthquake Forecasting). More examples are available under the “Characterizing Seismic Hazard” and “Reducing Seismic Risk” sections of the Research Accomplishments.

Knowledge Implementation spans two programs: Engagement of Practicing Professionals and Engagement with Public and Private Decision Makers. Each has a set of activities with short-term outcomes, leading to mid-term outcomes for the KI focus area that will indicate progress towards the long-term outcomes of 1) improving application of earthquake science in policy and practice, and 2) reducing loss of life, property, and recovery time. (Table 1).

Table 1. Knowledge Implementation Focus Area Outcomes

Programs	Short-Term Program Outcomes	Mid-Term Focus Area Outcomes	Long-Term CEO Outcomes
Engagement of Practicing Professionals	• Increased knowledge and use of SCEC science among technical audiences	• Documented examples of increased life safety and resilience (policies enacted, improved buildings or infrastructure, etc.) • Expanded partnerships, additional activities/resources, and "next level" policies/plans	• Improved application of earthquake science in policy and practice • Reduced loss of life, property, and recovery time
Engagement with Public and Private Decision Makers	• Awareness increased (EQ issues in general, and of SCEC science) • Legislation or other actions (i.e., cities and organizations develop/ revise resilience plans)		

KI-1: Engagement of Practicing Professionals

This program seeks to increase the knowledge and use of SCEC science among technical audiences that directly implement earthquake science and engineering research products. Examples include practicing structural and civil engineers, geotechnical consultants, building officials and others involved in designing structures to withstand levels of shaking determined from the USGS National Seismic Hazard Maps, or insurers who us the Uniform California Earthquake Rupture Forecast to set rates. The strategy is to interact with these audiences through meetings and webinars of professional associations (SEAOSC, ATC, CGS, CALBO, ASCE, AEG, etc.) and to invite their participation in SCEC activities, including the annual meeting, technical workshops and outreach partnerships such as Earthquake Country Alliance regional alliances and statewide committees.

11NCEE. Perhaps the best example of this type of engagement was the 11th National Conference on Earthquake Engineering held in Los Angeles on June 25-29, 2018 (Figure 4), for which SCEC and EERI were co-organizers. As the co-program chair, SCEC’s Executive Science Director for Special Projects Christine Goulet developed the conference technical program entitled “Integrating Earthquake Science, Engineering, and Policy” with the goal of increasing visibility of SCEC research products for earthquake engineering researchers and practitioners. This included a pre-conference Ground Motion Simulations and Engineering Applications Workshop featuring SCEC scientists and seismic hazard products. SCEC CEO’s Mark Benthien and Jason Ballmann supported publicity for the conference, which resulted in articles highlighting SCEC research and products, including in the New York Times. Ballmann also led a pre-conference workshop on Media Interview and Press Conference Techniques and Practice, and Gabriela Noriega coordinated

Figure 4. 11NCEE.org website

a visit by the SCEC undergraduate interns to observe the Undergraduate Seismic Design Competition held during the Conference.

Evaluation. Tracking the activities of this program is just getting started in Year 2 with the completion of the SCEC Logic Model and selection of program metrics, as shown in Table 2. The activity coordinated in Y2 is the 11NCEE conference workshop and the MCE_R tool is the initial resource listed. Determining how to track citations of SCEC research or resources is a Y2 goal.

Table 2: KI-1 Metrics	Y1	Y2
Activities coordinated	n/a	1
Participants in activities	n/a	80
Resources created/distributed	n/a	1
Citations of SCEC research/resources	n/a	TBD

KI-2: Engagement with Public and Private Decision Makers

This KI program builds connections between SCEC and those who make decisions based on an understanding of earthquake hazards and risk, including elected officials, emergency managers, business leaders, building owners, financial institutions, and insurers. SCEC is increasing its involvement with professional associations and regional government groups such as the Building Owners and Managers Association (BOMA), Association of Contingency Planners (ACP), California Emergency Services Association (CESA), Southern California Association of Governments (SCAG) and Association of Bay Area Governments (ABAG), and the International Association of Emergency Managers (IAEM). This audience is also being engaged through the Earthquake Country Alliance. An example is the annual Structural Engineers Association of Southern California “Strengthening Our Cities” Summits, which SCEC and ECA have supported since 2011, that seeks to inform government officials and others of the latest approaches to managing earthquake risk. SCEC/ECA also helped create the “Earthquake 2014 Business Preparedness Summit” with FLASH, Safe-T-Proof, Simpson Strong Tie, and several other partners, which launched the FEMA QuakeSmart recognition program for businesses that demonstrate mitigation they have implemented; this program is now offered in many locations nationwide each year.

Evaluating Risk and Building Resilience: Preparing LA for the Big One. SCEC CEO’s Sharon Sandow de Groot has been coordinating with Price School of Public Policy, Dornsife Alumni Relations, and Real Estate Affinity Network through Alumni Affinity Programs to develop this special event to be held on September 26 at the Intercontinental Hotel in Los Angeles. It will feature a keynote address from SCEC Director John Vidale as well as a panel discussion about the vulnerability of Los Angeles (focusing on high rise buildings as well as overall infrastructure). The panel will be moderated by Ryan Arba of the California Governor’s Office of Emergency Services. The panel will feature Christine Goulet from SCEC, Jennifer McElyea from Watt Investment Companies, and Marissa Aho, the Chief Resilience Officer of the City of Los Angeles, and will explore the implications of the vulnerability of Los Angeles on policy makers, real estate developers, and the community at large.

Annual Meeting ShakeOut Session. Marissa Aho is also speaking at the 2018 Annual Meeting in the Wednesday morning session highlighting the 10th Anniversary of the ShakeOut Scenario and drills. She will comment on how the ShakeOut Scenario inspired the Resilience By Design project led by Dr. Lucy Jones which resulted in new retrofitting ordinances for “Tuck Under Parking” apartment buildings and Non-Ductile Concrete Buildings.

Evaluation. Tracking the activities of this program is just getting started in Y2 with the completion of the SCEC Logic Model and selection of program metrics, as shown in Table 3. The activity coordinated in Y2 is the September 26, 2018 event described above. Determining how best to track citations or use of SCEC research or resources is a Y2 goal.

Table 3: KI-2 Metrics	Y1	Y2
Activities coordinated	n/a	1
Participants in activities	n/a	TBD
Resources created/distributed	n/a	TBD
Citations/use of SCEC research/resources	n/a	TBD

KI Focus Area Year 2 Milestones

Among the four CEO focus areas, Knowledge Implementation clearly has the greatest need for development of programmatic activities. A key Y2 CEO milestone is to form a SCEC KI Working Group to identify needed resources and potential activities in line with these outcomes. Developing protocols for assessing medium-term outcomes is another Y2 milestone.

KI Focus Area Year 3 Activities and Milestones

Looking forward to Year 3, we expect to expand our partnerships with professional organizations and offer training webinars and participate in or host meetings and workshops to foster the understanding and use of SCEC research. The KI Working Group established in Y2 will be instrumental in identifying opportunities for coordinating these activities, and recommending science products of use for risk reduction. Y3 milestones include delivering these products to KI audiences and assessing progress towards accomplishing KI mid-term outcomes.

Public Education and Preparedness (PEP)

The activities and products in this focus area are intended to educate people of all ages about earthquakes, tsunamis, and related hazards, and motivate them to improve resilience and personal preparedness. PEP's four major programs each organize activities with short-term outcomes, leading to mid-term outcomes for the focus area that indicate progress towards SCEC5 CEO long-term outcomes of: 1) reducing loss of life, property, and recovery time; and 2) increasing science literacy. In addition to these major programs, SCEC staff also participate in local government, non-profit, and business meetings throughout the year.

Table 4. Public Education and Preparedness Focus Area Outcomes

Programs	Short-Term Program Outcomes	Mid-Term Focus Area Outcomes	Long-Term CEO Outcomes
National and Global Preparedness Drills/Resources	• Increased knowledge of EQ hazard/risk/safety • Increased participation in safety drills • Global adoption of consensus messaging • Sharing of best practices	• Expanded drill participation, school safety, and community resilience worldwide • Improved household, school, workplace and community planning, preparedness, and mitigation in California • Increased knowledge/visibility of SCEC as credible and trusted partner/resource (among public, decisionmakers, partners, reporters, etc.) • Increased knowledge of earthquake science (general concepts, local hazards/risk, etc.)	• Reduced loss of life, property, and recovery time • Increased science literacy
Earthquake Country Alliance	• Increased coordination with key stakeholders • Increased use of ECA messaging and resources • Increased knowledge of EQ hazard/risk/safety • Sharing of best practices		
SCEC Science and Risk Communication	• Increased awareness of SCEC and EQ science • Improved SCEC Community media skills • SCEC known as valued media resource		
Quake Heroes Documentary	• Increased knowledge of EQ hazard/risk/safety • Increased participation in CERT • Increased household/community preparedness		

PEP-1: National and Global Preparedness Drills and Resources

Great ShakeOut Earthquake Drills. SCEC worked with the USGS and Earthquake Country Alliance leaders to create the first multi-sector "Great ShakeOut" earthquake safety drill in 2008, which involved 5.4 million southern Californians. SCEC/CEO webmaster John Marquis created and maintains the ShakeOut.org website and registration portal for California (with NEHRP funding through CalOES), and SCEC/CEO has expanded its use by coordinating ShakeOut's expansion across the U.S. (with NEHRP support directly from FEMA) and around the world (57+ million people participated in 2017) across 26 Official ShakeOut Regions and independently in more than 70 countries (Figure 5). In 2018 New Zealand switched from participation every three years to holding its national ShakeOut annually, and interest from school officials in China is rapidly expanding (a group from Sichuan province will observe ShakeOut activities in Los Angeles in October, 2018). While K-12 and college students and staff comprise the largest number of participants, ShakeOut has also recruited businesses, nonprofits, government agencies, neighborhoods groups, and individuals. Annual surveys show that ShakeOut participation increases overall preparedness and planning, and that

Figure 5. ShakeOut websites managed by SCEC

ShakeOut websites are now online in English, Spanish, French, Italian, and Japanese.

ShakeOut participants actively encourage their peers to also participate [Wood, 2015].

ShakeOut has become a global infrastructure for providing earthquake information to the public and involving them in community resiliency. New countries are being actively recruited to join the ShakeOut movement, which serves to coordinate earthquake messaging internationally. Participants receive monthly ShakeOut newsletters and more frequent content via social media. Millions more learn about ShakeOut via broad news media coverage that encourages dialogue about earthquake preparedness. In the near future, ShakeOut will be utilized for educating West Coast residents about Earthquake Early Warning, with yearly tests to be held on ShakeOut day.

Figure 6. New resources for grades K-3 developed with guidance from SCEC (RocketRules.org)

In 2017 SCEC worked with the local Hero in You Foundation non-profit to create earthquake science and preparedness materials for grades K-3 (Figure 6). This growing partnership has led to the "2018 Great ShakeOut Rocket Rules Challenge" (ShakeOut.org/rocketrules) in which all Los Angeles Unified School District second grade classrooms can complete simple safety lessons and film a "flash mob" style dance that demonstrates earthquake safety. Six winning schools will be chosen from the submitted entries, with every participating classroom, school and student receiving educational and safety resources.

As we mark the 10th Anniversary of ShakeOut, we also are looking to its future by adapting the Collective Impact Framework for planning and assessing all aspects of the initiative. This is an approach which CEO has discovered as part of participation in the EarthConnections initiative (see K14-3 below). Collective Impact has five key elements:

1. Common Agenda for change including a shared understanding of the problem and a joint approach
2. Mutually Reinforcing Activities via a plan of action that outlines roles and leverages expertise
3. Common Progress Measures across all participants that ensure alignment and accountability.
4. Continuous Communication that builds trust, assures mutual objectives, and creates common motivation.
5. Backbone Organization(s) that coordinates participating organizations and agencies.

SCEC/CEO is the Backbone Organization of ShakeOut, and we are increasing the visibility of this role in SCEC5. Activities include: creating and distributing customized monthly update emails for all Shakeout regions; contacting organizations to renew participation each year; posting frequent social media messaging (ShakeOut.org/messaging), new drill guidance resources and educational content; training ShakeOut Regional Coordinators and developing tools for their use (such as the new ShakeOut Coordinators Portal which allows state or local coordinators to access their participant data in order to increase participation and improve networking); and coordinating Evaluation (via Michele Wood, CSU Fullerton). SCEC/CEO's Jason Ballmann oversees most of these efforts with web and database support from CEO webmaster John Marquis. A major activity of Y2 will be to plan and implement a major update of all U.S. ShakeOut websites by combining most content into a national site and creating state/regional subpages, which will greatly improve the ability to keep information updated, provide better access via smartphones, and simplify overall management. SCEC is also revising ShakeOut healthcare materials to show how ShakeOut can count towards new training requirements of all healthcare facilities nationwide by the Centers for Medicare and Medicaid Services.

TsunamiZone. As a result of its leadership of ShakeOut, SCEC now also receives NOAA funding provided through the California Office of Emergency Services to create and manage TsunamiZone.org (Figure 7). This international site adapts the ShakeOut registration system to assess participation in Tsunami activities, whether as part of their ShakeOut activities or during local tsunami preparedness weeks or months. Participation in 2018 so far has exceeded 500,000 people, primarily in California and more than 40 countries in the Caribbean and surrounding areas that participated in the "Caribe Wave" regional exercise. Jason Ballmann has become a leader within the National Tsunami Hazard Mapping Program community, and redeveloped tsunami

Figure 7. TsunamiZone.org website

educational graphics (TsunamiZone.org/graphics) that are now being used worldwide. In 2019, Oregon, Washington, Alaska and Hawaii will expand their use of the TsunamiZone website.

Evaluation. The activities coordinated by the PEP-1 program have greatly exceeded expectations in terms of adoption worldwide and continued interest in improved resources, new levels of participation, and new partnerships. Metrics shown in Table 5 are for all of Y1 and through the midpoint of Y2. Data combines statistics for both ShakeOut and TsunamiZone websites, registrations, and resources. Some statistics are newly tracked in Y2, such as TsunamiZone website visits. Improved ways of tracking distribution of resources are being developed as we know the number is far higher than currently listed (website downloads only).

ShakeOut is also evaluated through annual participant surveys each year. In 2016 the survey of all participants was greatly simplified, and a more detailed questionnaire is being developed to assess participation of more statistically-representative sample of the many types of organizations involved. Talks and posters about ShakeOut data analysis were presented at several conferences in 2017 and 2018, and papers are now being written for publication.

Table 5: PEP-1 Metrics	Y1	Y2
Visitors to websites	489,729	101,684
Participants (CA, National, Global)	10.5M; 20M; 58M	6.2M; 10.6M; 11.6M
Resources distributed	28,197	3,985
Media citations about ShakeOut	1,580	77
Social media followers	~23,000	25,000

PEP-2: Earthquake Country Alliance

In 2003, SCEC created the Earthquake Country Alliance (ECA) with partner organizations in southern California that provide earthquake information and services. The initial purpose was to organize activities for the 10-year anniversary of the Northridge earthquake. Since then, ECA has become a statewide public-private-grassroots organization with:

- Regional Alliances which organize local activities (Figure 8)
- Sector-based committees which develop resources and programs for statewide audiences (and beyond)
- Outreach Bureaus which manage recruitment for ShakeOut and Tsunami Week, provide speakers and booths for events, and coordinate media relations.

Financial support for ECA is provided to SCEC by the California Governor's Office of Emergency Services (CalOES) and FEMA. SCEC manages annual budgets for each regional alliance, coordinates 6-8 workshops each year, manages more than 40 conference call meetings annually across all ECA groups, creates messaging documents and graphics with input from these groups, distributes ECA materials, maintains ECA's EarthquakeCountry.org (English) and Terremotos.org (Spanish) websites, and manages ECA social media channels (facebook.com/earthquakecountryalliance and twitter.com/eca). Mark Benthien serves as ECA's Executive Director.

Regional Alliances. ECA expanded statewide along with ShakeOut in 2009, at the suggestion of leaders from the San Francisco Bay Area who saw value in connecting efforts and many requests from organizations throughout northern California for ShakeOut to be a statewide event. In addition to a new Bay Area alliance, the Redwood Coast Tsunami Work Group (which was organized in the early 1990s) also joined the statewide effort. ECA Central Coast is now being established in coordination with local champions. Each Regional Alliance has three co-chairs, who collectively comprise the Steering Committee of ECA which meets quarterly to share activities and set priorities.

Figure 8. ECA Regional Alliances

ECA Southern California: This regional alliance is the largest both geographically as well as by population. The alliance is led by a Coordinating Committee chaired by Connie Lackey (Providence Health) Heidi Rosofsky (Global Vision), Margaret Vinci (Caltech Earthquake Programs) and is supported by SCEC's Gabriela Noriega. This group holds bimonthly teleconferences to coordinate regional activities, with reports from committee members who manage regional workshops, membership, communications, events bureau activities, and other efforts.

ECA SoCal organizes 3-4 workshops each year, held in various locations throughout the region in order to build local participation (so far in Y2 these have been held at the Hyperion Water Treatment Plant, at the Rancho Cucamonga Fire Training Facility, and at Angel Stadium in Anaheim). Topics include new ECA resources, opportunities to participate, local mitigation efforts, science updates, ShakeOut recruitment strategies, a feedback screening of the Quake Heroes film, and announce the availability of 8-10 “mini awards” of $500 each provided each year to support member efforts to improve preparedness and resilience.

ECA SoCal coordinates a Primary Media Event on ShakeOut day each year, with an earthquake simulator and displays for news media beginning at 4 a.m. at a Shakeout drill location. In 2017 the event was at the Los Angeles County Natural History Museum, and in 2018 it will be at Los Angeles City Hall. A major event is also being planned by ECA SoCal to commemorate the 10th Anniversary of ShakeOut, on November 1 at the new Los Angeles County Fire Museum in Bellflower. This morning breakfast event will include a variety of displays and presentations highlighting how the ShakeOut scenario has led to many upgrades to utility systems and new retrofitting ordinances, as well as how the ShakeOut drill has improved planning and preparedness.

ECA Bay Area: This regional alliance has been revitalized over the past two years with the support of SCEC’s Sharon Sandow de Groot, working with a local Coordinating Committee chaired by Daniel Homsey (City of San Francisco Neighborhood Empowerment Network (NEN), Jennifer Lazo (City of Berkeley), and Bob Beecher (Cisco, San Jose). The group has the same committee structure as ECA SoCal and similar activities. ECA Bay Area workshops in Y2 have been at Cisco Headquarters in San Jose and at Alameda County Emergency Services in Dublin. Topics have included new ECA resources, HayWired Scenario overviews, local earthquake hazards, ShakeOut recruitment strategies, etc. ECA Bay Area also provides $500 “mini awards” each year, and its Primary Media Event on ShakeOut day will be held at Berkeley’s Civic Center Plaza in 2018.

Figure 9. Community Resilience Summit Flyer

In May 2018, ECA Bay Area partnered with the Neighborhood Empowerment Network to host the “2018 Bay Area Regional Community Resilience Summit” at City Hall in San Francisco. More than 150 community leaders from around the Bay Area attended the summit, which addressed the importance of applying a community-centered planning approach for creating culturally competent disaster resilience strategies that emphasize equity and ensure the health and well-being of all residents (Figure 9). The summit began with the “Run Your Resilientville” tabletop exercise which challenges participants to build teams at the community level to meet the care and shelter needs of residents.. This was followed by a series of briefings and discussions:

- An overview of the Haywired Initiative (Dale Cox, USGS)
- A briefing on the Empowered Communities Program (Daniel Homsey, NEN)
- A keynote address on The Essential Role of Social Cohesion in Creating Resilient Communities (Prof. Daniel Aldrich, Northeastern University)
- A panel on Advancing Equity in Our Pursuit of Resilience facilitated by community leader Felisia Thibodeaux
- A presentation on the work of the Earthquake Country Alliance (Mark Benthien, SCEC)

The Summit also announced the planned expansion of the Neighborhood Empowerment Networks’ Neighborfest project, which organizes more than 40 neighborhood block parties throughout San Francisco each summer and Fall featuring tabletop discussions on local vulnerabilities and resources, vendors and community groups, fun activities, and food. ECA is working with NEN and Ready America on a plan to expand the Neighborfest concept throughout the Bay Area (and eventually statewide). A “Neighborfest Plus” event on Sunday, September 16, 2018 is in the works for

the Fruitvale community of Oakland, which will engage this historically challenged area in resilience conversations and feature the “Quake Cottage” earthquake simulator.

ECA Bay Area has also been active in the rollout of the USGS’ HayWired Scenario. ECA leaders participate in the HayWired Coalition, which is now coordinated via biweekly calls led by SCEC’s Mark Benthien. The initial release of the scenario (a final volume is still being reviewed) was held on April 18, 2018 with a press conference at Berkeley Stadium and in Central Park in Hayward. Benthien is also organizing HayWired messaging products; a messaging workshop held on August 30, 2018 at ABAG/MTC in San Francisco prioritized topics for a series of 1-2 page documents for key audiences.

Redwood Coast Tsunami Work Group: This group coordinates earthquake and tsunami education resources and activities for the northernmost counties of California’s coastline. This region has unique hazards and risk due to the proximity to the Cascadia Subduction Zone. For many years the RCTWG has coordinated the region’s participation in Tsunami Preparedness Week with “live-code” drills of tsunami warnings, hosted an “Earthquake and Tsunami Room” educational center at county fairs each summer (which SCEC’s Jason Ballmann helped staff in 2018), and since 2009 promoted ShakeOut registration each October. SCEC provides ECA funding as part of our NEHRP support for these activities, and worked with RCTWG leaders to update the tsunami safety imagery shown in FIgure 10. In 2018, RCTWG is splitting their tsunami drills such that far-source tsunamigenic earthquakes are the scenario for Tsunami Preparedness Week in March (including the live-code test as this scenario is when official warnings will be the basis of response), while during ShakeOut a near-source Cascadia event will be the scenario (when the natural warning of the shaking will prompt coastal residents to Drop, Cover, and Hold On, and then evacuate. ECA steering committee representatives of RCTWG chairs Kerry Sherin (Humboldt State University) and Ryan Aylward (National Weather Service), along with Charlie Helms (Crescent City Harbor Master). Sandow de Groot is the SCEC liaison.

Figure 10. Tsunami Safety Guidance

Sector-Based Committees. ECA’s sector-based committees develop resources and organize activities for many audiences. SCEC’s Sandow de Groot took over coordination of the committees in 2017 and is increasing participation, frequency of meetings, and development of products. Committee membership includes leaders from each sector, primarily within California but because the committees develop resources promoted via ShakeOut across the country (and beyond), some participants are from other regions. Sectors served include Businesses, the Public Sector, Non-Profits & Faith-Based Organizations, Healthcare, K-12 Schools, and Higher Education. ECA’s EPIcenter Network of Museums, Parks, and Libraries is being reorganized with the same structures of other sector-based committees, and a new multi-cultural committee will focus on ECA’s outreach to the many language/cultural communities of California. Figure 11 shows a very popular product developed by the ECA Seniors and People With Disabilities Committee. The committee also coordinated the filming of a ShakeOut Earthquake Safety Video Series segment on how people with disabilities can protect themselves during earthquakes.

Figure 11. Earthquake Safety Guidance

Each committee has a set of tasks to accomplish each year:

1. Engage leaders/groups from within the sector
2. Hold bimonthly committee meetings (online)
3. Review and update existing ECA materials
4. Develop new sector-based materials
5. Represent ECA at a workshop or other event
6. Develop/host a webinar

Outreach Bureaus. The newest organizational structure of the ECA are its three bureaus, which coordinate campaign outreach in support of ECA's Regional Alliances and Committees.

Participation Bureau: While all ECA members and groups work together to promote the Great California ShakeOut and Tsunami Preparedness Week each year, this Bureau led by SCEC/CEO's Jason Ballmann is building a network of County Coordinators who conduct direct outreach to their constituents to maintain and build ShakeOut and Tsunami Preparedness Week participation. Each Coordinator has access to the ShakeOut Coordinator Portal, through which they can call registrants who have not renewed their organization's participation for the current year; identify groups that have never participated; build connections with people responsible for preparedness and safety for their organizations, and develop multi-organization drills. This structure is being first established in southern California led by chairs Ken Kondo (Los Angeles County Emergency Management) and Jenny Novak (CalOES).

Media Bureau: Ballmann also oversees ECA's statewide media coordination, through this Bureau that meets monthly throughout the year with representatives of the regional alliances, partnering organizations, and local/state/federal agencies. The lead up to ShakeOut is when the group has been most active in past years, but in 2018 Ballmann successfully expanded activity year-round, including Tsunami Preparedness Week coordination and long-term discussions on post-earthquake messaging and coordination efforts.

Events Bureau: In 2018, the former Speakers and Events Bureaus have been combined into a single group that coordinates requests for ECA representatives at events organized by community groups, businesses, and other organizations. This includes speaking invitations as well as requests for information tables at preparedness fairs. A new request form has been created at EarthquakeCountry.org/events and a series of presentations are being developed for ECA speakers to have available. Presentation trainings will be coordinated occasionally as part of ECA regional workshops or via teleconference, and booth supplies have been purchased including 43" monitors with carrying cases, easels for signage, luggage carts for transporting materials and even sandbags (for stabilizing signage in windy outdoor locations). SCEC/CEO's Benthien coordinates the Bureau which is led by volunteer chairs Lance Webster and John Hammett from Southern California.

ECA products. SCEC's Putting Down Roots in Earthquake Country handbook (Figure 12) has provided earthquake science and preparedness information to southern Californians since 1995. The 2004 update coordinated by ECA introduced the Seven Steps to Earthquake Safety (FIgure 12), which has continued to be the main organizing structure for preparedness messaging of SCEC, ECA, CEA, and (as a result of ShakeOut) a growing number of other partners, states, and national organizations (including FEMA). In 2014 the California Earthquake Authority, California Office of Emergency Services, and ECA created a simpler booklet, Staying Safe Where the Earth Shakes, with customized versions for 10 regions of the state and multiple language editions (Spanish and Chinese to start).

Figure 12. ECA Booklets

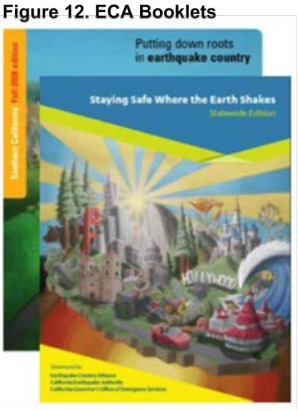

Additional resources developed by SCEC and ECA Associates include earthquake safety materials and ShakeOut guidelines for seniors and people with disabilities, higher education, government agencies, businesses, and healthcare facilities. Each year new materials are developed by ECA Sector-based Committees and made available through ECA's websites, social media channels, and ShakeOut websites, emails, and social media messaging worldwide. SCEC also has developed as series of short videos in its "Earthquake Safety Video Series" which can be viewed at Youtube.com/greatshakeout.

Evaluation. The Earthquake Country Alliance marks its 15th Anniversary in 2018, and is stronger than ever. Coordinating Committee structures for ECA SoCal and ECA Bay Area have provided more opportunity for local leaders to be involved in this success. In 2018 ECA's website was updated with responsive design aspects for better use via smartphones, and a new online-membership system will feature new

Table 6: PEP-2 Metrics	Y1	Y2
Visitors to websites	150,585	112,530
ECA members & leaders	~500; ~40	~550; ~50
Participants in ECA events & meetings	~500	600
Resources distributed	50,000+	20,000+
Social Media followers	4,500	5,000

membership levels and features that will greatly increase and improve ECA participation. As with ShakeOut, we are developing better ways or tracking all ECA activities (Table 6), including distribution of resources online, via shipping of materials, and at in-person events.

PEP-3: SCEC Science and Risk Communication

This program led by SCEC's Communications Manager Jason Ballmann focuses on communicating SCEC research findings as well as about the SCEC Community, as well as coordinating activities that improve risk communication both internally and externally of SCEC. This includes the distribution of press releases, management of interviews and media events, developing articles for the SCEC website, oversight of SCEC's social media presence (Twitter.com/scec, Facebook.com/scec, Youtube/com/scecmovies, and Instagram.com/SCECinsta, and coordination via all these aspects for post-event messaging and media requests.

SCEC Media Trainings. SCEC partners with several organizations to offer programs that train (1) the media on how to report earthquake science and (2) the SCEC community on how to communicate diverse and highly technical research to the public and media. For the latter, communications workshops are held at each SCEC Annual meeting, and a similar workshop was held at the 11NCEE (see KI-1 above) in July, 2018.

GeoHazards Messaging Collaboratory (GMC). Ballmann worked with partners at IRIS (Wendy Bohon) and UNAVCO (Beth Bartel) to create this multi-organization messaging group, which now includes representatives of USGS (Lisa Wald) and NOAA (Cindi Preller). The GMC offers webinars for media and scientists, special outreach campaigns, and conference workshops, all focused on the value of messaging consistency and resource leveraging. Post-earthquake messaging coordination has been an active aspect of the GMC, allowing each organization to share or amplify key findings or messaging in order to reach more people with the information they need.

Evaluation. This program has grown rapidly in SCEC5 with several new structures and partnerships now in place to improve SCEC's capacity for risk communication. Table 7 shows the status of metrics for this program in August, 2018.

Table 7: PEP-3 Metrics	Y1	Y2
Visitors to scec.org	112,021	60,694
Participants in media trainings	30	30-40
SCEC-related media citations	n/a	300
Social Media followers	9,000	11,000

PEP-4: Quake Heroes Documentary

Quake Heroes, a 50-minute documentary based on interviews of people who experienced the Northridge earthquake, has been in development for several years by SCEC and Blue Tavern Productions (established by Mark Romano, a former SCEC intern), and is about to be completed after a year of feedback screenings which have helped refine the messaging and identify needed elements. Primary funding was provided by FEMA; additional sponsors include Simpson Strong Tie, State Farm, the Structural Engineers Association of Southern California, the Hero in You Foundation, Safe-T-Proof, and More Prepared.

Figure 13. A scene from *Quake Heroes*

The film portrays stories of people who took action to help their neighbors, along with a description of the science of the earthquake by SCEC and USGS scientists, engineering aspects by a structural engineer, and several others. Recent interview footage is shown with archival news footage, as well as live-action reenactments filmed with actors portraying our main characters at the time of the earthquake and realistic sets built for the filming. The Seven Steps to Earthquake Safety and ShakeOut are featured with the goal of prompting viewers to take action.

The film will be made available via a variety of settings and approaches. A classroom toolkit with science and engineering lesson plans is described in the next section as it will be a new program of the K-14 Education Initiative. Quake Heroes Special Events will be organized (many have already been requested) to screen the film and then have a Seven Steps to Earthquake Safety event where attendees can buy furniture straps, disaster supplies, learn about earthquake insurance, register for CERT and other trainings, and much more (all these activities will provide assessment of our success of motivating preparedness behaviors). The Quake Heroes website will let viewers (and

anyone) share their own earthquake stories, expanding on the personal stories showcased in the film. It is also hoped that the film will be of interest to cable television or streaming services.

Evaluation. This is one of SCEC's most readily measurable activities. Four feedback screenings attended by more than 600 people over the past year (see Table 8) have all used a paper survey to gather ratings of the film and comments which have been overwhelmingly positive (as well as provided very useful suggestions and corrections). With the film's completion in 2018, the requests for Quake Heroes Special Events are likely to greatly expand which will have many evaluation components, especially in terms of actions taken as a result of viewing the film.

Table 8: PEP-4 Metrics	Y1	Y2
# Screenings and # of Attendees	1; 50	3; 600
Actions taken (CERT registrations, etc.)	0	TBD
Visitors to website	n/a	TBD
Stories shared	n/a	TBD

PEP Focus Area Year 2 Milestones

Major milestones for Y2 are: the coordination of 10th Anniversary ShakeOut activities with major events and participation increases in California, including HayWired scenario integration in the Bay Area; the combination of U.S. ShakeOut websites in a simpler, unified and modern web framework, the completion of the Quake Heroes documentary, and the development of protocols for assessing mid-term PEP outcomes. The ShakeOut website update is a huge project and we have identified a consultant to support the effort.

PEP Focus Area Year 3 Activities and Milestones

Most of the activities described within each program above will continue into Y3. New activities include the rollout of the new Shakeout website, the inclusion of Earthquake Early Warning messaging in all of our efforts for the West Coast, media trainings with CalOES and other partners, and the development of the Quake Heroes Special Events concept. Milestones identified include the expansion of the Neighborfest program statewide (based upon results in the Bay Area) and an assessment of progress towards PEP mid-term outcomes.

K-14 Earthquake Education Initiative (K14)

This CEO focus area aims to improve earth science education in multiple learning environments, overall science literacy, and earthquake safety in schools and museums via three programs as shown in Table 9. Each has a set of activities with short-term outcomes, leading to mid-term outcomes for the K-14 focus area that will indicate progress towards achieving CEO long-term outcomes of: 1) increasing science literacy; and 2) increasing diversity, retention, and career success in the scientific workforce.

In addition to these primary programs, SCEC also supports earth science education (primarily focused on earthquake topics) via booths at the California Science Teachers Association (CSTA) annual conference each year, joint with the California Geological Survey with more than ~2000 attendees each year. SCEC also hosted a booth at the 2016 National Science Teachers Association conference held in Los Angeles. Earthquake science resources such as SCEC's very popular Plate Tectonics Puzzle Map are distributed, SCEC internship programs and other opportunities are shared, and and all attendees are encouraged to participate in Great ShakeOut Earthquake Drills.

Table 9. K-14 Education Initiative Focus Area Outcomes

Programs	Short-Term Program Outcomes	Mid-Term Focus Area Outcomes	Long-Term CEO Outcomes
Quake Heroes Educational Toolkit	• Increased awareness of geoscience and engineering degrees/careers • Increased knowledge of EQ hazard/risk/safety • Increased participation in Teen CERT	• Increased knowledge of key earthquake science concepts and engineering among participants • Participants improve preparedness in their school/household/ community • Participants pursue geoscience or STEM majors at higher rates • Improved retention of geoscience majors, including women and underrepresented minorities	• Increased science literacy • Increased diversity, retention, and career success in the scientific workforce.
Quake Catcher Network	• Increased knowledge/use of seismic concepts and data in classrooms/ museums • Expanded collection of seismic data		
EarthCon-nections Partnership (INCLUDES, etc.)	• Increased knowledge of EQ hazard/risk/ safety • Increased awareness of geoscience and engineering degrees/careers • Increase family/community support for students interested in geoscience careers		

K14-1: Quake Heroes Educational Toolkit

Figure 14. Quake Heroes Toolkit Cover

This program is a counterpart of PEP-4, Quake Heroes Documentary. The film has been designed to deliver basic earthquake science and engineering concepts, in addition to raising awareness of what can happen in a major earthquake (which relatively few Americans have experienced, especially those that were born since the mid 1990s). To improve the ability for Quake Heroes to be shown in high-school classes, a toolkit has been developed that features several simple earthquake science and engineering lessons and activities that correlate with each act of the film (allowing the film to be shown over several days, with a lesson delivered each day). The toolkit will also include household and community preparedness guidance, and encourage schools to organize a Teen CERT (Community Emergency Response Teams) club at their school.

State Farm has provided sponsorship support of this program for bringing the toolkits to Los Angeles Unified School District high schools, which will be among the first to receive the toolkits. We hope to expand such sponsorships to deliver more free kits to schools, however they also will be available for sale.

Evaluation. As the toolkits have not yet been released at the time of this report, no metrics as listed in Table 10 were available in Y1, but will begin to be assessed this Fall. We are very hopeful that the toolkit is popular among schools and inspires more youth to become trained, prepared their families, and lead their communities.

Table 10: K14-1 Metrics	Y1	Y2
Toolkits distributed	n/a	TBD
Teen CERT clubs established	n/a	TBD
Actions by students to improve home/school safety	n/a	TBD
Stories shared by students	n/a	TBD

K14-2: Quake Catcher Network (QCN)

Over the past 10 years SCEC has built on QCN's citizen science concept by installing the network's low cost seismometers at over 26 museum locations in California and Oregon, and at more than 100 schools in each west coast state including Alaska. The goal has been to establish several K-12 sensor stations around a local museum hub as a means to build long-term educational partnerships around the ShakeOut, citizen science, and enrich K-12 STEM curriculum. In 2015 a new partnership was established between SCEC, IRIS, and USGS to continue the expansion and development of QCN worldwide, beginning with installations in 14 schools and museums in the

Table 11: K14-2 Metrics	Y1	Y2
Active QCN stations	n/a	TBD
School/Museum participants	~100	~130
Event recordings	n/a	TBD
Uses of curricula	n/a	TBD

Central U.S, and in several Coachella Valley school districts (along the San Andreas fault) in 2016, which in 2018 developed into a partnership with schools in Anchorage area in Alaska who also had QCN sensors installed.

Evaluation. Over the past year, a major upgrade of the software and programming that enable QCN's data collection has been underway by a contractor paid jointly by SCEC and IRIS. The effort has been successful and the consultant is now assisting with other improvements to the user experience, and will allow better tracking of the metrics listed in Table 11. Still, SCEC and IRIS have decided to focus on school and museum installations as QCN's primary audience. Language on the QCN website (QuakeCatcher.net) inviting anyone to host a QCN site is being changed to reflect this focus, and may redirect interested people to other initiatives such as OSOP's Raspberry Shake or Berkeley's MyShake app for smartphones.

K14-3: EarthConnections

SCEC is a founding national partner (along with InTeGrate, UNAVCO, and IRIS) of EarthConnections, an NSF INCLUDES project linking three regional projects (one of which is centered in San Bernardino with CSU San Bernardino Prof. Sally McGill) to increase diversity in the geosciences, managed by SCEC/CEO's Gabriela Noriega. The program develops pathways for high school, community college, and university students to explore and achieve career opportunities, including geology club joint activities, field trips, and meetings with geotechnical professionals and research scientists. Educator workshops have also been offered.

Figure 15. San Bernardino Pathway Model

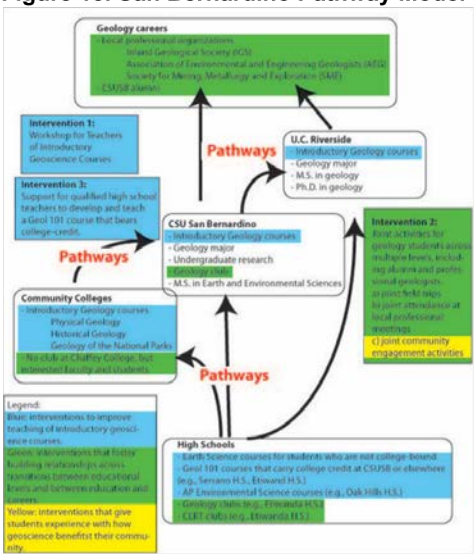

The program builds on SCEC's long-term partnership with Prof. McGill in support of summer GPS data collection by teachers and students as part of the NASA-funded InSight Vital Signs of the Planet (VSP) Professional Development Program which involved more than 30 teachers and students in real-world research along with lesson plan development and presentation of posters at the SCEC Annual Meeting.

Evaluation. The metrics as shown in Table 12 are incomplete as of the writing of this report; data will be requested to complete the table for both Y1 and Y2. A proposal to the NSF GEOPATHS solicitation will be submitted in Fall, 2018, to expand this partnership with more participating schools (high school, community college, and universities), further connection with SCEC's internship programs, ShakeOut, QCN, Quake Heroes, and other initiatives, and expanded funding for SCEC staff.

Table 12: K14-3 Metrics	Y1	Y2
Schools involved (HS, 2yr, 4yr)	3	5
Educators involved	~30	~40
Students involved	~40	~40
Underrepresented students	TBD	TBD
Participants in activities	TBD	TBD
New geology majors	n/a	TBD

K14 Focus Area Year 2 Milestones

Major milestones for Y2 are the initial distribution of Quake Heroes Toolkits; completion of the upgrade of the QCN Server and expanded installations; continued distribution of SCEC's educational products and activities, and development of protocols for assessing medium term K-14 outcomes. All these activities are on track for completion.

K14 Focus Area Year 3 Activities and Milestones

The rollout of the Quake Heroes Toolkit will be in full swing in Y3, and we are hopeful that a successful GEOPATHS proposal will allow the continued development of our EarthConnections Alliance activities, with possible expansion beyond San Bernardino. A Y3 milestone will be to assess progress towards K-14 medium-term outcomes.

Experiential Learning and Career Advancement (ELCA)

This focus area works to increase diversity, retention, and career success in the scientific workforce and improve the application of earthquake science in policy and practice. SCEC/CEO's manager of ELCA, Gabriela Noriega, coordinates two programs: undergraduate internship programs and the Transition Program launched in SCEC5 which offers resources and mentoring for students and early career scientists at key transitions (into graduate school, into industry, etc.). Each has a set of activities with short-term outcomes, leading to mid-term outcomes for the ELCA focus area. CEO long-term outcomes for the ELCA focus area are 1) increasing diversity, retention, and career success in the scientific workforce; and 2) improving application of earthquake science in policy and practice.

Table 13. Experiential Learning and Career Advancement Logic Model

Programs	Short-Term Program Outcomes	Mid-Term Focus Area Outcomes	Long-Term CEO Outcomes
Undergraduate Internship Programs	• Increased knowledge of EQ & computer science • Increased interest in pursuing geoscience or other STEM graduate degrees and careers • Development of software applications for the SCEC Community and others	• Increased retention of women and underrepresented minorities (and others) in geoscience education and careers • Continued development of pathways to increase participation • Long-term SCEC participation among participants • Improved software applications for SCEC Community	• Increased diversity, retention, and career success in the scientific workforce • Improved application of earthquake science in policy and practice
Transitions Program	• Improved relationships with partner institutions to increase recruitment and resource capacities • Improved support for SCEC students across transitions (undergrad->grad, grad->career) • Increased readiness for career advancement at all points of career		

Undergraduate Internship Programs

The SCEC Experiential Learning and Career Advancement (ELCA) program enhances the competency and diversity of the STEM workforce by engaging students in research experiences at each stage of their academic careers and by providing leadership opportunities to students and early career scientists that engage them in the SCEC Community. ELCA manages two undergraduate internship programs that involve over 30 students each summer. Since 2002, over 1600 eligible applications have been submitted to the SCEC internship programs (at scec.org/internships).

Undergraduate Studies in Earthquake Information Technology (UseIT). This flagship SCEC CEO program brings together students from across the country to an NSF Research Experience for Undergraduates Site at USC. The eight-week program develops programming skills while teaching the critical importance of collaboration for successful learning, scientific research and product development. Since 2002, 261 students have participated from more than 40 colleges and universities, including 24 in 2018 (Figure 16). The program is managed by Dr. Noriega with full-time in-lab supervisor Jozi Pearson and the support of intern program alumni. Many of SCEC's computational science staff as well as other SCEC researchers actively participate in the program as mentors to the 4-5 teams that are formed each summer.

Figure 16. 2018 UseIT Interns

UseIT interns tackle a scientific "Grand Challenge" developed each year by Prof. Thomas Jordan that involves developing software and resources for use by

earthquake scientists or outreach professionals. The 2018 Grand Challenge was to: 1) develop a computational system for probabilistic forecasting of earthquake sequences in Southern California; 2) apply the system to initial-event scenarios and compare the simulator-based probabilities against official data of large aftershocks from Uniform California Earthquake Rupture Forecast version 3 (UCERF3); and 4) illustrate the hazards and risks of multi-event scenarios that could threaten the Los Angeles with sequence-specific maps of expected ground motions, economic losses, and human casualties.

Several new aspects were introduced to the UseIT program in 2018:

- Presentations to recruit interns by Dr. Noriega at East Los Angeles College and Pasadena City College;
- Connections were developed with CSU Los Angeles, CSU Long Beach, and LA Harbor Community College;
- A pre-summer workshop to support community college interns;
- In addition to the UseIT Symposium held on the final day of the program, interns also presented at the AGU Virtual Symposium, SoCal CISE REU Workshop, and USC Undergrad Symposium;
- A machine learning component was included for the first time;
- Students to be engaged year-round with webinars and research symposiums.

Intern program alumni report that their internship made lasting impacts on their course of study and career plans, often influencing them to pursue or continue to pursue earthquake science degrees and careers. By observing and participating in the daily activities of earth science research, interns reported having an increased knowledge about working in research and education, which coupled with networking at the SCEC annual meeting, gave them the confidence to pursue earth science and career options within the field.

Summer Undergraduate Research Experience (SURE). This program places undergraduate students with SCEC scientists around the country to conduct primary research. More than 270 interns have participated since 1994, with research projects spanning earthquake science, engineering, and education.

In advance of the 2018 intern application process, a few changes were made to the funding and selection process to address complications of the SCEC funding cycle. SURE internships were awarded outside of SCEC's funding cycle, with intern support fully paid by SCEC and not dependent on whether SCEC scientists' proposals were successfully funded. This previously delayed timing of notifications meant many qualified students had already accepted another internship by the time SCEC offers arrived. For 2018, mentors were willing to host interns regardless of the status of their SCEC funding. The new SURE recruitment process is as follows:

1. SURE applications are received and reviewed;
2. SCEC proposals are reviewed for any that indicate intern opportunities and list requirements;
3. SCEC researchers are contacted for potential projects and requirements;
4. intern applicants who meet requirements are identified and asked to rate their interest in proposed projects;
5. Mentors rank candidates who are interested in their research; and
6. Final mentor/intern pairings are completed.

The SCEC5 base budget enables 3-4 students to participate in the SURE program each year. In 2017, the delayed start of the SCEC5 NSF award resulted in insufficient time to pair funded SCEC researchers with students for summer projects. This allowed five SURE internships to be awarded in 2018, with students working with SCEC mentors from UC Riverside, UC Irvine, UC San Diego, and Occidental College.

Evaluation. UseIT is an ongoing success and many new structures are being developed under the leadership of Dr. Noriega, who is also reorganizing how SURE is managed. All interns complete extensive pre- and post- internship surveys, and are tracked longitudinally to see how participation increases the likelihood of SCEC interns attending graduate school and/or remaining in STEM fields. Much of the success in increasing diversity has come from increased efforts to recruit students from southern California community colleges, so recruitment efforts for

Table 13: ELCA-1 Metrics	Y1	Y2
Applicants	251	170
Undergraduate interns (UseIT; SURE)	22; 0	24; 5
Female interns	12; 0	10; 3
Underrepresented minority interns	11; 0	10; 1
Mentors	8; 0	9; 5

2018 were focused more locally. This accounts for the drop in the number of applicants in Y2 shown in Table 13.

Transitions Program

SCEC launched the Transitions Program in 2017 to provide junior members of the SCEC community with resources and mentoring across key career transitions, directing efforts to encourage and sustain careers in the geosciences and other STEM fields. At the 2017 SCEC Annual Meeting, ELCA hosted two breakfasts to connect early career attendees with peers and mentors to share experiences and develop strategies for navigating the transition from undergraduate to graduate school and from graduate school to professional career (within and outside of academia), and these breakfasts will be held again at the 2018 SCEC Annual Meeting. Through the 2018 SCEC Science Plan, the Transitions Program solicits proposals from researchers to expand awareness of professional advancement opportunities and pathways, as well as improve competency in earthquake research tools and techniques for students of the SCEC community.

Figure 17. Transitions Breakfast

New initiatives planned include:

- Mentors Workshop: A one day meeting at USC to help redefine the Transitions Program vision, mission, and objectives. Outcomes of the workshop will include targets for upcoming years and facilitating buy-in from SCEC community. A Transitions Program Planning Group will convened to coordinate the workshop, which will include potential mentors who participated in the SCEC Annual Meeting breakfasts.
- Careers in STEM Workshops and Webinars: CEO will partner with SCEC institutions to host a workshop on their campus, or online, to reach geoscience students who cannot attend the SCEC Annual Meeting.
- Summer "Bridge" Program: This will help prospective and new students transition into graduate school by providing stipends to initiate research summer projects or training with researchers at SCEC institutions before the actual start of graduate school.

Evaluation. This new program is a very important priority for SCEC. Activities are still being developed, along with how the metrics shown in Table 14 (and other aspects) will be assessed.

Table 14: ELCA-2 Metrics	Y1	Y2
Students supported (funding, application assistance)	0	TBD
Institutions involved	TBD	TBD
Networking events	2	2+
Participants in events	~120	100+

ELCA Focus Area Year 2 Milestones

Major milestones for Y2 are to expand partnerships with new and existing institutions to increase mentor, recruitment, and resource capacities; to update longitudinal tracking processes that show impact of ELCA programs; to assess how SCEC's learning and career pathways are advancing diversity in geoscience education and careers, and develop protocols for assessing medium-term ELCA outcomes.

ELCA Focus Area Year 3 Activities and Milestones

In Y3 the new initiatives developed in Y2 will be continued and expanded. Intern recruitment will expand to more community colleges and local universities. A new proposal for UseIT will be submitted to support another three years of activities. The Transitions Program will provide Summer Bridge support for the first time, and offer workshops and other meetings throughout the year. A new Y3 milestone will be to assess progress towards ELCA mid-term outcomes.

Research Accomplishments

Gregory C. Beroza, SCEC Science Planning Committee Chair
Judith S. Chester, SCEC Science Planning Committee Vice-Chair

Introduction

The SCEC5 Science Plan comprises 14 topical elements, organized into four themes (see State of SCEC). Research priorities within each topical element are guided by a progressive set of science milestones, used by SCEC and its sponsoring agencies as indicators of research progress along conceptual pathways. The milestones are more explicit in the early years than the out-years of SCEC5 owing to the evolving and unpredictable nature of basic research. This section summarizes the science accomplishments under each topical element.

Theme A: Modeling the Fault System

1. Stress and Deformation Over Time

We are making progress developing models of the stress state and its evolution during seismic cycles, comparing those models with observations, and assessing their uncertainties, particularly in the representation of fault-system rheology and tectonic forcing. The construction of the Community Thermal Model and the Community Rheology Model builds on this effort (see "Community Models" section below).

An important contribution to deformation over time is characterizing the non-secular, transient deformation associated with earthquake cycle (milestone 1c). Devries and Meade have made an important contribution to computing efficiently the transient deformation due to viscoelastic flow in the mantle. They trained neural networks to approximate the solutions of the viscoelastic mantle response to fault slip with accurate approximations of the predicted motions (mean absolute errors were ~2e-6 mm) for a range of input parameters with a computational run time reduction of 500x.

We continue to develop and populate the Community Stress Model with borehole constraints (milestone 1d). Persaud and colleagues have compiled industry borehole breakout data to constrain the direction of maximum horizontal compressive stress (SH) at Long Beach and Inglewood at depths less than 2 km. They find a rather heterogeneous stress state with significant variations in SH (45-90 degrees) over spatial scales less than 1 km. Abolfathian and Ben-Zion have conducted stress inversions using dense focal mechanism data sets in the Crafton Hills

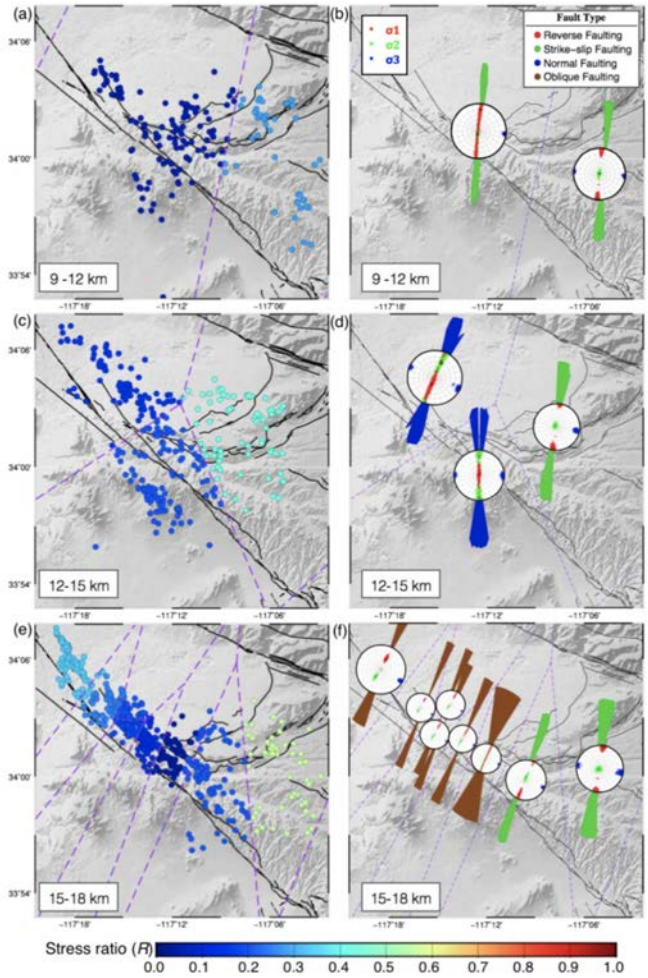

Figure 1. Variations in SH max directions, faulting types, and stress ratio R with depth in the Crafton Hills region of the San Jacinto fault zone near Riverside. From Abolfathian et al. (2018).

region of the San Jacinto fault zone near Riverside (Figure 1). They too find remarkable variation in stress with depth, over small intervals (a few km) and short spatial scales (5-10 km). These studies highlight an important observation that while stress state in southern California appears to be relatively homogeneous or smoothly varying over large wavelengths (100 km), strong heterogeneity may occur also at shorter spatial scales near faults.

Cooke and Beyer contributed to efforts to map the partitioning between seismic and aseismic deformation along major faults using geodetic and seismic data along the San Jacinto fault and San Bernardino Basin (milestone 1f). They find that focal mechanisms show enigmatic normal slip below 7.5 km that would not be expected during interseismic loading of the San Bernardino basin; however, they show with mechanical models that off-fault normal slip distributed through the crust is consistent with interseismic fault creep on the San Andreas and San Jacinto Faults below 10 km depth. This suggests that local, off-fault stress state does not necessarily reflect the far-field loading on faults.

Smith-Konter and colleagues made important contributions to ongoing efforts to develop physics-based fault system models that capture possible variations in elastic material properties (milestone 1h). They compared computed moment accumulation rate on faults in California using homogeneous and heterogeneous elastic models and found systematic biases in the homogeneous calculations (Figure 2). In the southern portion of the fault system (near the Salton Trough), there is a significantly lower seismic moment accumulation rate with heterogeneous models. In contrast, along the Mojave segment of the SAFS, heterogeneous models imply systematically higher moment accumulation rate on the fault.

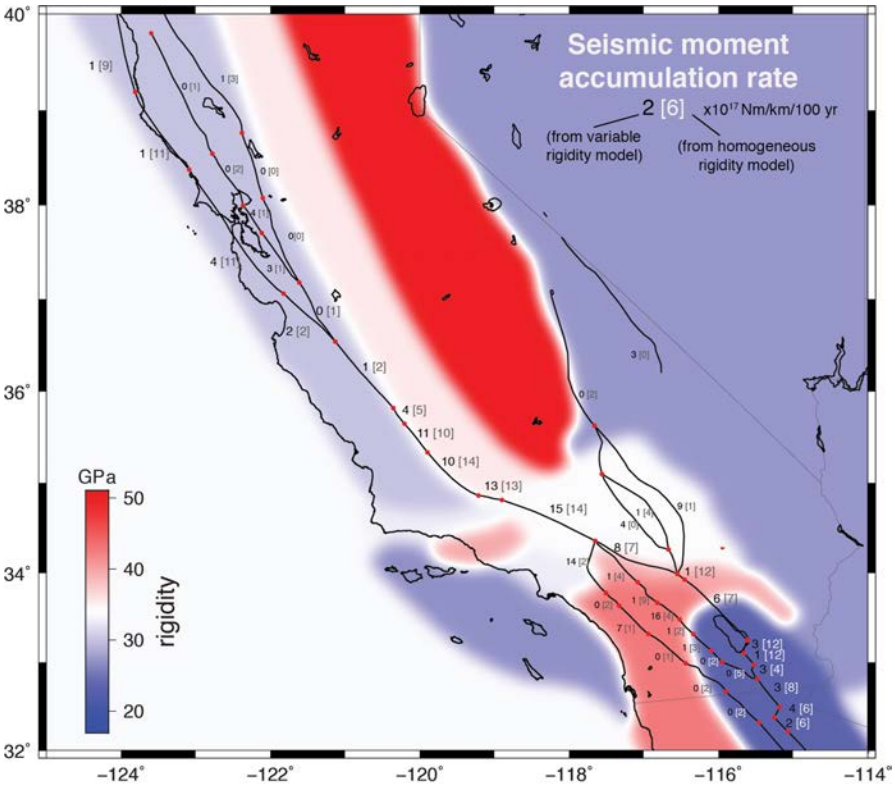

Figure 2. Crustal rigidity and computed seismic moment accumulation rates from both the homogeneous (bracketed value on the right) and variable crustal rigidity (value on the left) models of the SAFS. The background map indicates the prescribed crustal rigidity variations.

Milestone		Y1	Y2	Y3	Y4	Y5
a	Compare GPS-based stressing rates with focal mechanism-based stressing rates.		x	x	x	
b	Collect and analyze campaign GPS data in areas of sparse GPS coverage and poor InSAR correlation.	x	x	x		
c	Assess level and impact of non-secular deformation in SCEC region from the combined CGM inputs				x	
d	Populate the CSM below the upper crust with depth-dependent modeled stresses. Release updated versions of the CSM based on additional borehole constraints and geodynamic modeling.		x	x		
e	Update high-precision earthquake catalogs, including detection of small events, improved locations, and focal mechanisms, to help inform the CSM.	x	x	x	x	x

f	Map the partitioning between seismic and aseismic components of deformation along the major faults using geodetic and seismic data.		x	x	x	
g	Refine the geologic slip rates on faults in Southern California, including offshore faults, and optimally combine the geologic data with geodetic measurements to constrain fault-based deformation models, accounting for observational and modeling uncertainties.				x	
h	Develop physics-based fault system models that capture possible variations in elastic material properties, and permanent/inelastic deformation processes in the crust.			x	x	x

2. Special Fault Study Areas – Focus on Earthquake Gates

Earthquake Gate Areas (EGAs) are regions of fault complexity that may control the propagation of large earthquakes. This was the first year of proposal solicitation for the Cajon Pass EGA, and several projects are now underway. Work proposed for the Cajon pass addresses each of milestones 2d, 2e, 2f and 2h. The Cajon Pass EGA will have a one-day field trip and ½ day workshop before the 2018 SCEC annual meeting (milestones 2b and 2c). These activities will present on-going research in the region and highlight knowledge gaps to investigate within the next few years (milestone 2c). The SCEC Planning Committee decided not to designate a second earthquake gate area but encourages investigators to submit proposals related to conditional termination of rupture outside of Cajon Pass through the 2019 science planning process.

Several recently published papers (Barrett et al., 2018; Rockwell, et al., 2018) have refined the slip history of the San Andreas Fault system (milestones 2g and 2h).

On-going analysis by Arrowsmith, Alana Williams, Grant-Ludwig, and Akciz of paleoseismic events along the Cholame segment shows correlation of five slip events with previously document events on the SAF (milestone 2h). Guns, Bennett and Blisniuk are collecting data to investigate geologic and geodetic evidence for activity along the Blue Cut fault (milestone 2h). In studies of the Agua Blanca fault, Behr, Rockwell, Fletcher, Owen and Gold found that the paleoseismic, slip-per-event and slip rate measurements over the past ~1.6-1.4 kyr are mutually consistent and suggest that, whether or not displacement is regular or variable, the Agua Blanca fault is likely near the middle of an earthquake cycle and thus is unlikely to produce a strong earthquake in the immediate future (milestone 2h, Figure 3).

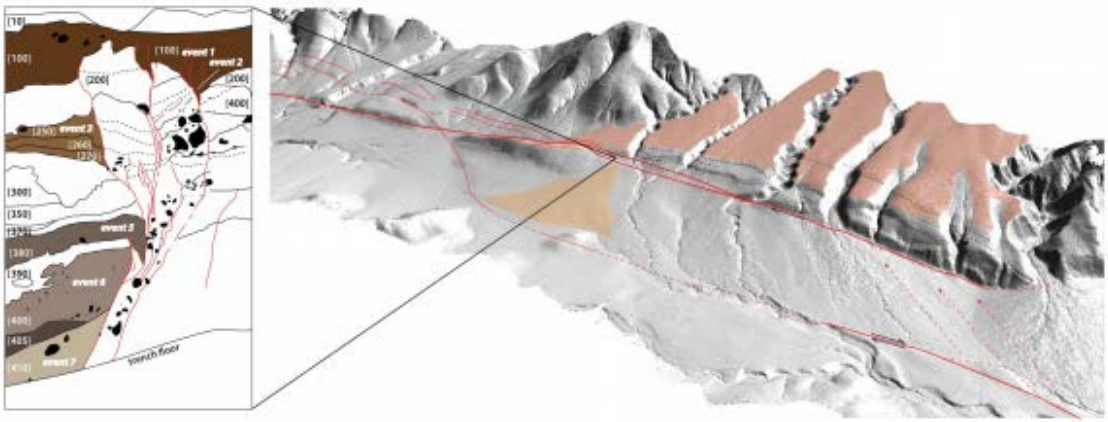

Figure 3. Valle Agua Blanca Lidar Perspective Map.

Preliminary mapping of sediment provenance and landford dating by Blisniuk, Fosdick and Moon (and students Waco and Emmons) show evidence of recent slip along the Mission Creek fault in a region previously interpreted as inactive (milestone 2h). The paleoseismic event database is under development by Biasi and Rockwell (milestone 2g).

Milestone		Y1	Y2	Y3	Y4	Y5
a	Hold incubator workshop to develop a research strategy and candidate locations or topics for the Earthquake Gates initiative.	x				
b	Decide on at least one target for the Earthquake Gates initiative and hold an inaugural workshop.		x			
c	Hold joint workshop on multi-disciplinary research on Earthquake Gates focus area(s). Assess scope of Earthquake Gates projects, solicit work as needed.		x	x		
d	Collect and synthesize earthquake recurrence, slip-rate, interseismic deformation and fault geometry information within Earthquake Gate Area(s).	x	x	x	x	
e	Develop multi-cycle rupture and deformation models within the Earthquake Gate focus area(s).	x	x	x	x	
f	Calibrate the model results from the Earthquake Gate area(s) with geologic and geophysical data from within the EGA(s). Incorporate understanding developed under this initiative to improve earthquake rupture forecasts.			x	x	x
g	Develop a paleoseismic event database that includes event ages and quality ranking not limited to Earthquake Gate Area(s).	x	x	x	x	
h	Determine how model-based hypotheses about fault interactions through zones of complexity can be tested by observations of accumulated slip and paleoseismic chronologies.			x	x	x

3. Community Models

A portal website (www.scec.org/research/cxm) to facilitate access to individual community model products has been created, together with a template for standardization of individual CXM websites (milestone 3c). The Community Fault Model (CFM) website is the first to be updated making use of the new template (milestone 3i), and work on similarly updating and linking the Community Stress Model (CSM) website is underway. New borehole stress constraints (milestone 3aa) and modeled stresses for the CSM will be added to the CSM once the new website is live. The Unified Community Velocity Model (UCVM), a collection of software tools and application programming interfaces designed for standardized access to the multiple seismic velocity models used in SCEC research, is also linked to the portal website. A paper describing the UCVM software framework was published in September 2017. During 2018, new seismic velocity models representing central and northern California have been incorporated into the UCVM, bringing SCEC closer to completing a state-wide seismic velocity model (milestone 3m). Detailed seismic velocity models of the Central Valley and the Santa Maria Basin, based on extensive new well log datasets, are embedded in the new central California velocity model, CS173-H (milestone 3k). A Community Rheology Model (CRM) workshop held in September 2017 (milestone 3a) resulted in a prioritized list of research tasks to move the CRM toward a draft product by 2019 (www.scec.org/proposal/report/17206). During the remainder of 2018, progress continued on defining and reviewing the geologic framework (milestone 3n), as well as flow laws for rocks and shear zones (milestone 3o). SCEC-supported passive seismic imaging of the central Mojave region will address key problems in understanding tectonic layering and underplating in this region that may affect strain accumulation within the Eastern California Shear Zone. A preliminary Community Thermal Model (milestone 3e) is complete and under refinement in preparation for distribution.

Following a September, 2017 workshop, the CFM group released CFM 5.2, which includes geometrical refinements based on the latest earthquake catalogs and surface trace maps; a new metadata spreadsheet featuring fault hierarchies and other supporting information; regular-gridded representations of the CFM 5.2 fault surfaces; and linkages of CFM faults to UCERF3 slip rates (milestones 3i and 3j). A website featuring downloadable versions of recent CFM's in a consistent format was developed (milestone 3i) and linked to the CXM web portal page. 2018 saw a torrent of activity in the Community Geodetic Model (CGM) group and significant progress toward its SCEC5 milestones. A workshop was held March, 2018, in addition to several virtual meetings for GPS and InSAR specialists. One focus of the workshop (Figure 4) was comparing 3D cGPS time series for southern California by six individual research groups and addressing how to combine them with campaign GPS data into a consensus GPS velocity field

(milestones 3t and 3r). Another was comparing interferograms and LOS time series for a test problem, to understand differences in results from different processing methods and identify best practices (milestone 3u). Strategies for combining GPS and InSAR datasets, and for delivering consensus InSAR LOS datasets to SCEC, were also addressed in the workshop and the virtual meetings (milestones 3u and 3v).

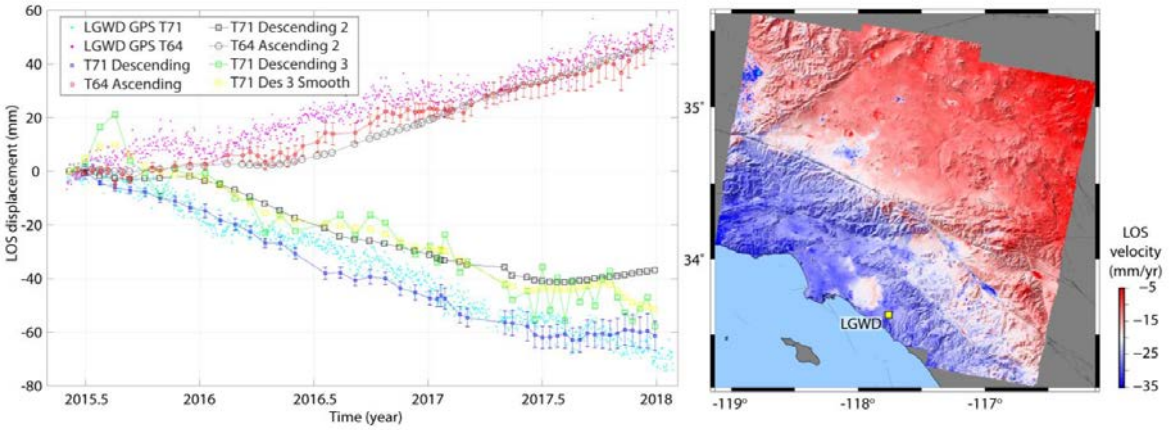

Figure 4. Left – Comparison of GPS daily solutions provided by UNAVCO for station LGWD and InSAR time series derived using different software for location of LGWD. Cyan and magenta dots are GPS daily solutions projected to satellite LOS. Blue and red curves represent descending and ascending solutions (Xu, 2017) using GMTSAR. Black and grey curves show the descending and ascending solutions by Zhen Liu using ISCE and framework developed by H. Fattahi. Green and yellow curves show descending solutions (Neely et al., 2017) using GMTSAR, with different degrees of smoothing applied. All curves are referenced to zero initial displacement. Right – LOS velocity map from descending track T71 with constraints from GPS ITRF08 velocity field (Xu, 2017). Location of GPS station LGWD marked by yellow square. Figure courtesy of Xiaohua Xu.

Milestone		Y1	Y2	Y3	Y4	Y5
a	Convene a workshop focused on guiding community model development towards self-consistent and well-integrated community models.		x			
b	Organize TAGs for community models, as appropriate, including a TAG to develop a geologic framework for the Community Rheology Model (CRM).	x				
c	Develop a strategy for a unified approach to data integration, manipulation and querying of community models (CXMs), and identify common or sharable data structures between different CXMs.		x			
d	Develop standards to represent smaller scale features in the CXMs, such as stochastic variations in elastic properties, attenuation, stress, temperature, rheology, fluid transport properties, and fault orientation.				X	
e	Deliver a preliminary Community Thermal Model (CTM) that provides crustal temperatures throughout southern California based on 1D conductive heat flow and a simplified 3D distribution of thermal properties.	x				
f	Update the CTM from 1D to 3D so that it is consistent with CRM lithologies and field data. Improve surface heat flow maps. Search for additional heat flow and thermal property data in areas with poor coverage.		x	x		
g	Add a CTM branch that quantifies advective heat transport, and evaluate the need for anisotropic thermal properties. Provide error ranges for modeled temperatures and alternative models where there are significant disagreements.				x	x
h	Conduct peer review of the Community Fault Model (CFM) 5.1 through a virtual workshop; release a revised version with preferred fault representations.	x				

i	Implement a portable, user-friendly interface to access CFM model versions, components, and metadata, incorporating a new fault naming and number system compatible with the USGS Fault and Fold database.		x	x		
j	Refine CFM representations of the linkages among major fault systems.				x	x
k	Improve the resolution of the Community Velocity Models (CVM-S and CVM-H) in the shallow crust, by adopting products developed or results obtained through the research activities defined for D.14 (physics of the geotechnical layer) and validate against observations.			x		
l	Define and implement a protocol to introduce alternative representations into existing CVMs, leveraging the seismic studies of various geographic regions (e.g., San Jacinto, Salton Sea).			x		
m	Develop a statewide CVM, and validate against independent ambient seismic field measurements.				x	
n	Construct a provisional 3D geologic framework of southern California, as a first step towards developing a CRM. Convene a workshop on how to characterize the brittle, ductile, plastic, and viscoelastic rheologies of the southern California lithosphere, including shear zones.		x			
o	Implement mixing laws for polymineralic rocks of the CRM. Release CRM version 1.0 that includes 3D geologic framework and constitutive models consistent with the CTM.				x	
p	Unify representation of SCEC community models, including refined CFM and CVM structures and prototypes of the CTM and CRM, and enhance their interoperability. Release a CRM that incorporates the rheologies of shear zones.					x
q	Define and implement standards for the periodic evaluation (verification and validation) of different CXMs through direct (e.g., exploration or experimental) and indirect (modeling and simulation) methods, as applicable.	x	x	x		
r	Produce a consensus combined campaign/continuous GPS time series product.	x	x			
s	Develop grids of horizontal velocity and strain rate derived from consensus GPS time series. Upload to CGM v. 1.0 website.	x	x			
t	Develop consensus vertical time series from continuous GPS sites.		x	x		
u	Identify and develop best practices for producing and updating LOS time series from the new data streams provided by Sentinel-1A and 1B, and ALOS-2.		x	x		
v	Produce a consensus secular velocity InSAR product using the full archive of SAR data (ERS, Envisat, ALOS-1, Sentinel) for the SCEC region.	x	x	x	x	
w	Conduct peer review of initial CGM products through a virtual workshop.			x		
x	Develop methods for integrating full vector GPS time series with LOS InSAR time series from multiple platforms to construct 1 km spatial resolution grids of horizontal and vertical time series.				x	x
y	Populate the CSM below the upper crust with depth-dependent modeled stresses. Release updated versions of the CSM based on additional borehole constraints and geodynamic modeling.		x	x		
z	Populate CSM at all depths with stresses (amplitudes) from static deformation models that account for upper crustal rheology as well as ductile rheologies from the CRM			x	x	x
aa	Extend the Community Stress Model (CSM) to incorporate borehole stress data.		x	x		
bb	Deliver a deformation model based on the Community Geodetic Model (CGM) to the CSM.			x		

4. Data-Intensive Computing

Continuous seismic waveform data is accumulating rapidly at the Southern California Earthquake Data Center (SCEDC) and growing at an accelerating rate both due to the development of a denser seismic network for earthquake early warning and due to the increasing trend for dense seismic deployments (Figure 5).

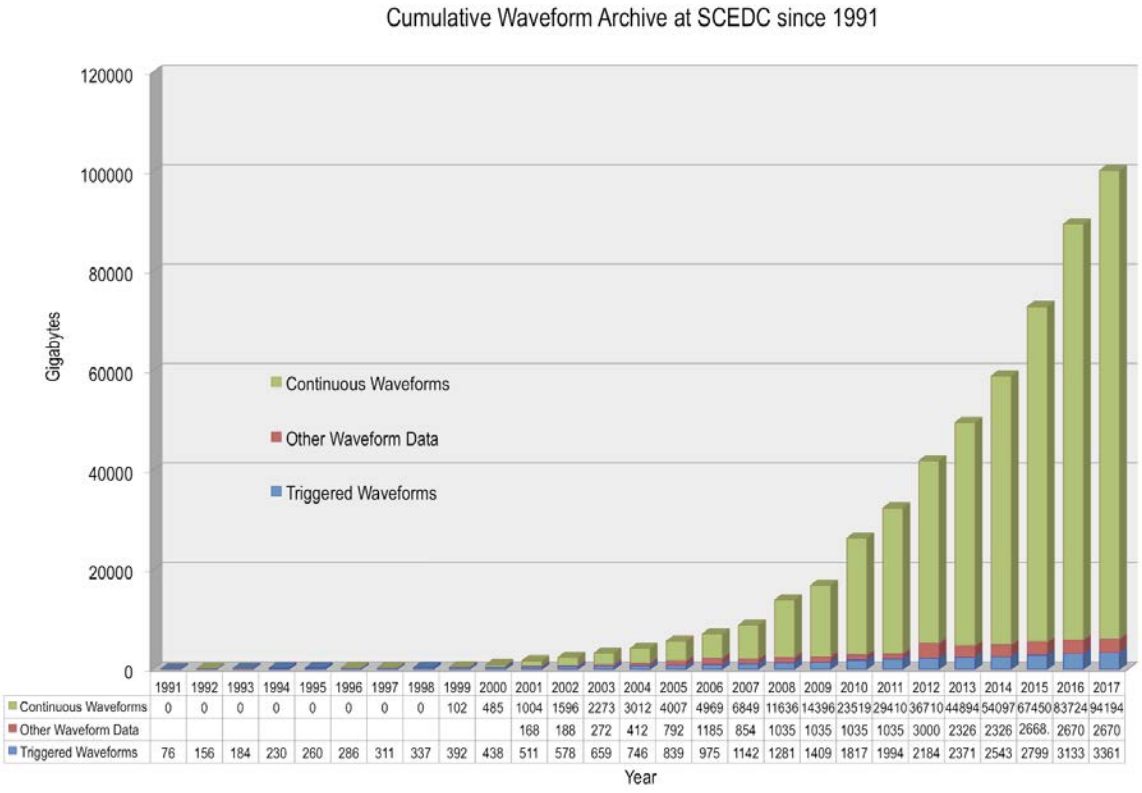

	1991	1992	1993	1994	1995	1996	1997	1998	1999	2000	2001	2002	2003	2004	2005	2006	2007	2008	2009	2010	2011	2012	2013	2014	2015	2016	2017
Continuous Waveforms	0	0	0	0	0	0	0	0	102	485	1004	1596	2273	3012	4007	4969	6849	11636	14396	23519	29410	36710	44894	54097	67450	83724	94194
Other Waveform Data											168	188	272	412	792	1185	854	1035	1035	1035	1035	3000	2326	2326	2668.	2670	2670
Triggered Waveforms	76	156	184	230	260	286	311	337	392	438	511	578	659	746	839	975	1142	1281	1409	1817	1994	2184	2371	2543	2799	3133	3361

Figure 5. Data volumes stored at the SCEDC for seismological research. Note the rapid acceleration in continuous data holdings over the past decade.

With these larger data sets comes a need for novel approaches that can extract as much useful information as possible from them, which is a need recognized by the Computational Science disciplinary focus group. As an example of this approach, we have developed methods for signal detection and identification that scale efficiently to very large data volumes, which we are applying to key problems in Earth structure and seismicity. The initial “Mining Seismic Wavefields” NSF geoinformatics grant and a follow-on bridge grant from NSF has allowed SCEC to sustain this work. Participants in this proposal, and others at SCEC, are aggressively adopting machine learning for a variety of purposes that advance earthquake science, including supervised and semi-supervised machine learning for ground motion prediction (Figure 6). These efforts address milestones 6a-6d.

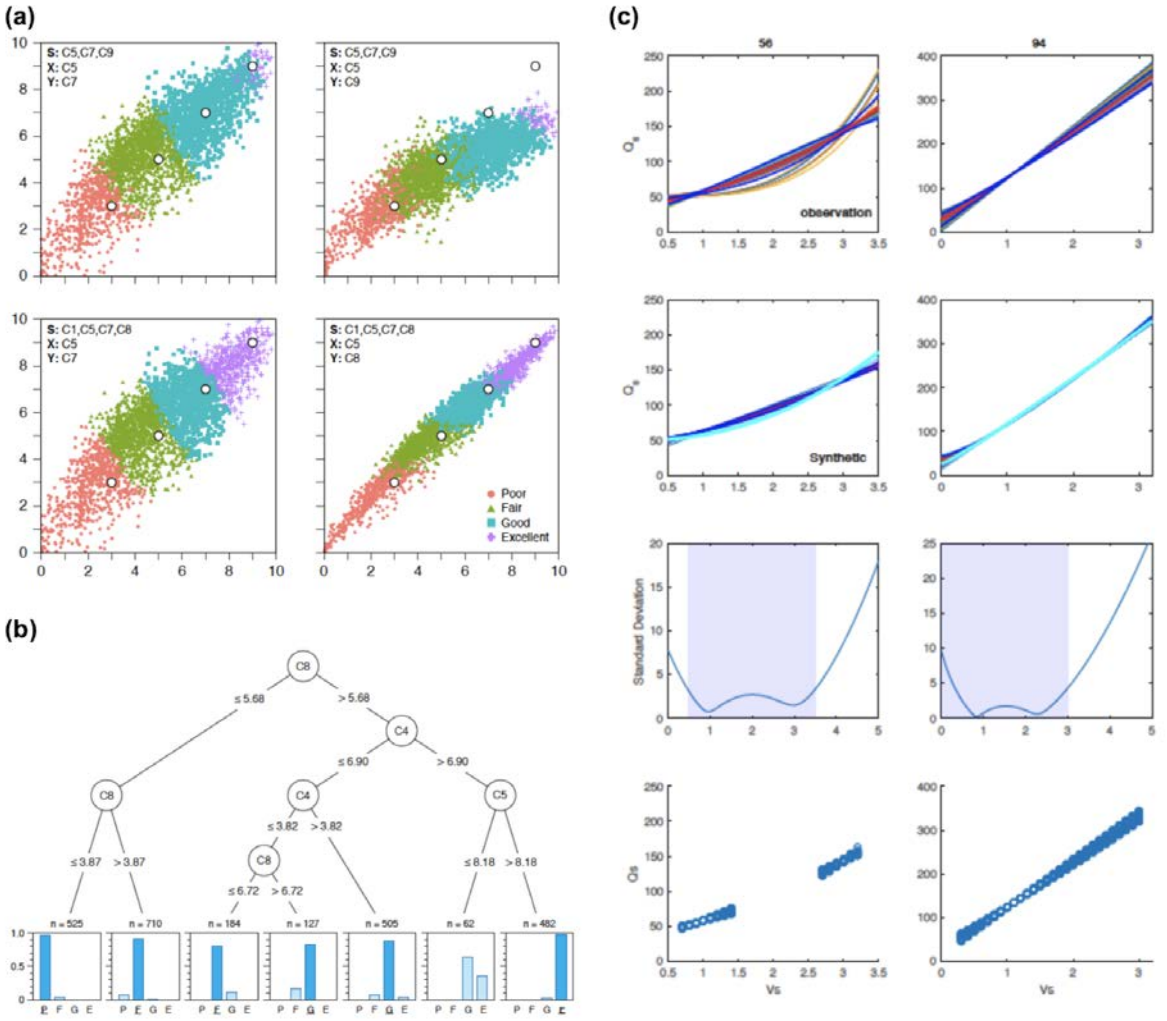

Figure 6. Clustering analysis carried out on a large dataset of results from a ground motion simulation validation process comparing the relationships that exist in a multidimensional space of goodness-of-fit metrics. (b) Topology of a decision tree reducing the validation of ground motion simulations to a comparison of only three goodness-of-fit metrics (C4, C5, C8) after having identified the thresholds needed to discretize the validation scores into for different categories (poor, fair, good, and excellent). (c) Optimization process to identify Qs-Vs relationships when comparing synthetic results from surrogate simulators with observations (from Khoshnevis, N. and Taborda, R., 2018).

Milestone		Y1	Y2	Y3	Y4	Y5
a	Develop a distribution pathway (e.g., via GitHub or CIG) for SCEC community software.	x				
b	Distribute efficient earthquake detection software for community use.		x	x	x	x
c	Develop computing tools to handle large datasets from geodesy, lidar and structure-from-motion, 3D tomography, ambient seismic field measurements, and other signal processing techniques used, for example, to search for tectonic tremor and repeating events.		x	x	x	x
d	Develop tools and algorithms for uncertainty quantification in large-scale inversion and forward-modeling studies, for managing I/O, data repositories, workflow, advanced seismic data format, visualization, and end-to-end approaches.		x	x	x	x

Theme B: Understanding Earthquake Processes

5. Beyond Elasticity

SCEC is engaged in multiple efforts to examine the interplay of fault roughness and plasticity from an observational point of view, as it may explain the apparent deficit of shallow slip in earthquakes, as it affects numerical models of rupture and ground motion, and as it affects long-term fault behavior. Among the ongoing work are sensitivity studies of differing forms of plastic response, and modeling advances where off-fault distributed deformation can be non-continuum (milestones 5d, and 5e). Off-fault plasticity was introduced into rate-and-state earthquake cycle simulations, and for certain parameter choices up to 10% of the tectonic displacement in the shallow crust was accommodated by distributed deformation extending a few hundred meters from the fault (Erickson et al., 2017, Figure 7). This addresses milestones 5d and 5f. Effort commenced to build a paleoseismic event database to better characterize natural earthquake recurrence behavior and potential system-wide super-cycles. This addresses several milestones: 2g, 5i, 9d, 9e, and 9g.

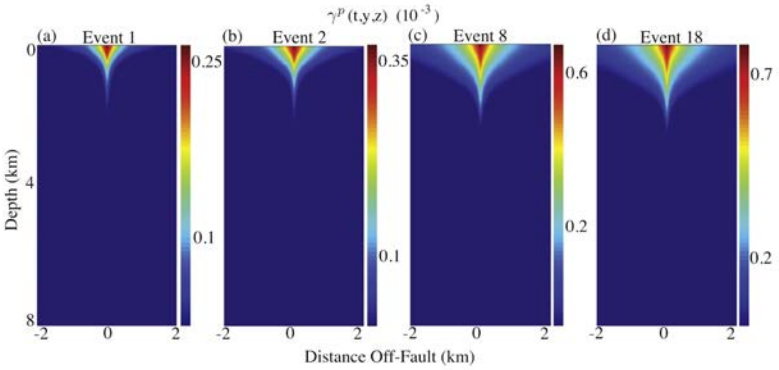

Figure 7. Panels show off-fault equivalent plastic strain after the first, second, eighth and eighteenth rupture events. For this choice of parameters the magnitude and off-fault extent of plastic strain increases at a decreasing rate with successive ruptures. After 18 events, it has begun to saturate near 2 km. (from Erickson et al., 2017).

Milestone		Y1	Y2	Y3	Y4	Y5
a	Hold an interdisciplinary workshop focused on the topic of Beyond Elasticity.	x				
b	Identify existing modeling capabilities for inelastic rheology, how these are compatible with each other, and establish a framework for verification as presently done for linear anelastic problems.	x	x			
c	Develop inelastic wave propagation codes that can be ported to HPC architectures.	x				
d	Develop strategies to quantify the contribution of inelastic off-fault deformation to geodetic estimates of strain accumulation.		x	x		
e	Apply inelastic crustal deformation models to estimate fault slip rates and assess results through comparison to geologic slip rates.				x	
f	Develop strategies to identify the potential of near-surface distributed deformation and its effect on ground motion prediction, with emphasis on forward wave propagation simulation, to develop multi-step strategies to account for inelastic behavior.		x	x	x	
g	Develop and quantify the uncertainty of prototype approaches to represent the effects of non-linearity that would allow the continued use of linear wave propagation as an effective approximation.		x	x	x	
h	Identify key material parameters that will be necessary to characterize inelastic behavior of geomaterials in the upper crust and near-surface deposits, and define strategies to add these data to community models (e.g., CVM, CRM) for use in forward and inverse modeling.		x	x	x	
i	Assess the evidence for earthquake supercycles in southern California, and identify future data needs.		x	x		
j	Constrain alternative forms of fault-zone and distributed inelasticity , as well as the factors that influence it, such as cohesion and pore fluid pressure.			x		

k	Quantify the differences between full 3D nonlinear and simpler approximations (developed under milestone 5h) and linear anelastic simulations; and their effects on ground motion prediction, intensity measures, and hazard estimation.			x	x	x

6. Modeling Earthquake Source Processes

Among the accomplishments for 2018 has been a first-of-its-kind experiment to image flash-heated contacts formed during sliding of rock surfaces at seismic slip rates in the laboratory (milestone 6d). This has the potential to provide key insights into earthquake source processes, particularly when paired with recent developments in SCEC that document localized heating with fault-zone petrology. Uncovering the physics of the earthquake source and its evolution with time requires rigorous modeling of seismic and aseismic slip and their interaction (milestone 6f). We have made several advancements on that front. We have initiated an exercise of comparing simulations of Earthquake Sequences and Aseismic Slip (SEAS) among groups with different methodologies that will not only ensure that the problems are properly treated computationally, but also determine best practices in this challenging field, facilitating the associated scientific studies. Also on this topic, we have been developing increasingly realistic multi-cycle earthquake simulations that include coupled thermal-mechanical effects (milestone 6d), using the SEAS simulations to investigate the correspondence between on-fault and seismologically inferred properties of the earthquake sources (milestone 6e), and implementing a new source inversion validation plan that is initially focused on stress-drop validation. Several numerical studies have considered the factors that allow ruptures to propagate through geometric complexities (milestone 6c; Figure 8). Finally, Meng et al. (2018) developed a novel eGf deconvolution method that greatly increases the number of events that can be analyzed, and that improves the number of apparent duration measurements sufficiently to resolve forward and backward directivity effects in both the P and S-wave derived measurements (milestone 6e).

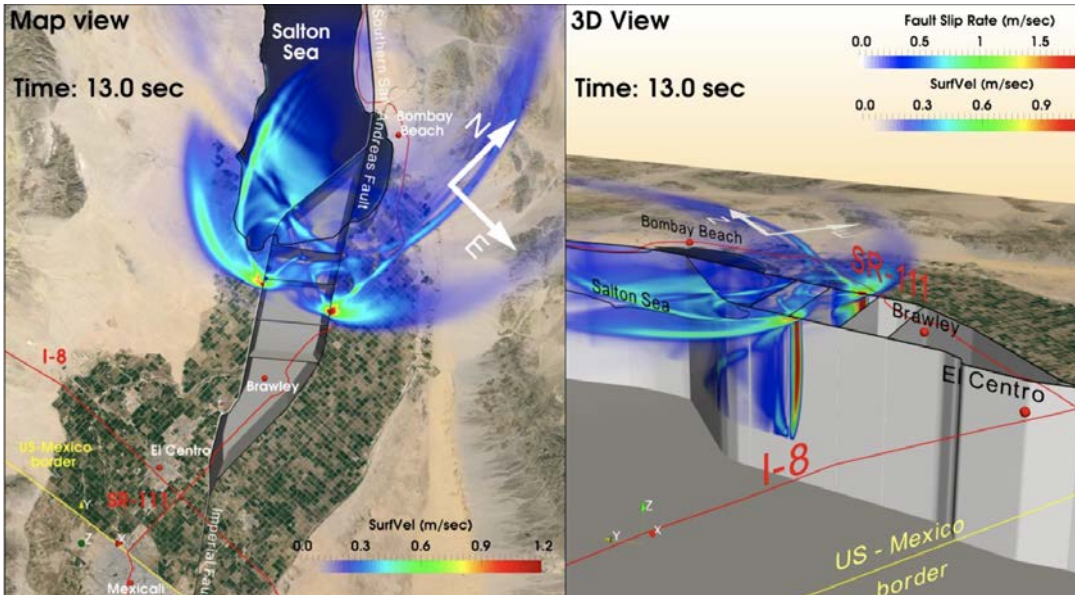

Figure 8. Dynamic rupture model of through-going rupture in the Brawley Seismic Zone (Kyriakopoulos, annual report). Nucleation location is on the SSAF (North to South propagation). Note rupture propagates through an area of fault complexity and where cross-faults intersect the main segments. Interstate 8 and SR-111 are marked with red lines. Yellow line shows US-Mexico border. Black line represents Salton Sea shoreline. The dynamic rupture code used for this simulation is FaultMod (Barall, 2009).

Milestone		Y1	Y2	Y3	Y4	Y5
a	Understand and quantify how different levels of complexity and variability in source models influence advances in other areas such as broadband and deterministic ground motion simulation.	x	x	x		
b	Understand how inelastic strain associated with fault roughness and discontinuities influences seismic radiation and scaling of earthquake source parameters, and quantify their effects on ground motion.		x	x	x	
c	Describe how fault complexity, fluid pressure and inelastic deformation interact to determine the probability of rupture propagation through structural complexities.			x		
d	Assess how shear resistance and energy dissipation depend on the maturity and hydrogeological state of the fault system, and how these are expressed geologically.				x	
e	Determine how earthquake source properties such as stress drop estimated from seismic observations based on simplified models correspond to properties of physically realistic sources.		x	x		
f	Study how seismic and aseismic deformation processes interact, and how that interaction affects long-term fault behavior, by exploring how slow slip and microseismicity redistributes stress for the following large events and how large events interact with deeper fault extensions.	x	x	x	x	x
g	Use numerical models to investigate which fault constitutive laws and parameter ranges are compatible with paleoseismic findings, including average recurrence, slip rate, coefficient of variation of earthquake recurrence, and the possibility of earthquake supercycles; determine whether such behavior can be compatible with the currently observed statistics of smaller-magnitude events.					x

7. Ground Motion Simulation

SCEC has built a broad range of ground motion simulation tools that include the effects of topography, fault roughness, and plasticity—both near that fault and remote from it; as well as improved velocity models, including refined shallow geotechnical layers and with stochastic representation (milestone 7b) of crustal properties (Shi and Asimaki, 2018). In 2018, we further improved the one-dimensional (1D) depth-dependent stochastic model for the shallow crust of the Los Angeles basin sediments, previously referred to as Geotechnical Layer (or GTL). We also performed preliminary tests to extend the model to 3D by coupling the depth-dependent statistical properties with stochastic representation of high resolution array inversions in Southern California; we plan to implement the 3D stochastic model in UCVM and validate shortly thereafter the formulation and correlation structure by comparison against strong ground motion records and scattering attenuation properties. The stochastic sediment model realization along a cross-section of the Los Angeles basin is compared to the realization of the same cross section using GTL in Figure 9.

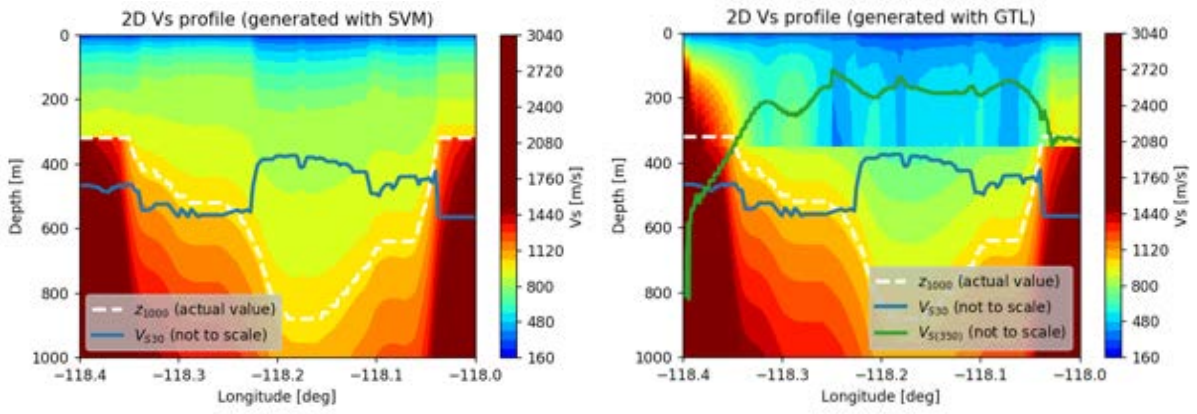

Figure 9. Example of 2D realization of the stochastic sediment model relative to the previous version (GTL).

We also developed improved imaging products to map the shallow crust using scattered waves or fiber optic cables spanning the highly populated urban centers of the Los Angeles basin (milestone 7d). We further expanded many of these modeling efforts into Central California with the benefit of additional support from PG&E. Examples include the imaging of the Diablo Canyon subsurface using dense arrays.

During Year 2, we continued the development and implementation of several inelastic realistic constitutive models to represent the inelastic behavior of rock and deposit materials (soils) in 3D deterministic and 2D broadband ground motion simulations (milestone 7e). These include an enhanced Drucker-Prager plasticity model that uses a multi-surface parallel-series type Iwan model; and a J2 bounding surface plasticity model with a vanishing elastic region, called multi-axial cyclic plasticity model for cyclic clay behavior. To coordinate research and dissemination of work on the velocity model and nonlinear laws governing the shallow crustal sediments, members of the SCEC community have formed a Technical Activity Group that will convene at the 2018 Annual Meeting.

On the broadband platform, we have extended modules to capture multi-segment kinematic ruptures (milestone 7a), inter-period correlations of ground motions (milestone 7j), and more realistic duration simulations. We have also been developing two families of nonlinear Fourier-based amplification factors: one based on empirical Fourier amplitudes from the PEER NGA West2 database (Bayless et al., SCEC Annual Report 17148); and one based on simulated ground motions coupled to a rigorous nonlinear soil model developed during SCEC4. We expect both families to be tested, validated and implemented on the platform by Year 3 (milestone 7e).

Under the guidance of the Committee for the Utilization of Ground Motion Simulations (UGMS), we finished development the web-based data access tool for MCER ground motions and released it in May 2018 (milestone 7k). The MCER response spectra cover greater Los Angeles, providing a resource for cities and counties in the region. The UGMS also continued to validate CyberShake using data from the 1994 Northridge earthquake, and the committee examined differences between long-period response spectra from the UCERF2 model used in the CyberShake simulations and the UCERF3 model used by the USGS to develop the 2014 national MCER maps. A webinar, organized by the Structural Engineers Association of Southern California (SEAOSC), was given on October, 2017 by UGMS chair, C.B. Crouse, who reported the availability of the tool and illustrated its use. Crouse then gave a similar presentation at the COSMOS seminar on November, 2017 and at the 11th National Conference on Earthquake Engineering in Los Angeles in June, 2018. Other validation exercises consist of the continuation of the Ground Motion Simulation Validation (GMSV) TAG for SCEC5 led by Rezaeian and Stewart (SCEC Annual Report 17185), and specific projects coordinated therein.

Milestone		Y1	Y2	Y3	Y4	Y5
a	Incorporate and validate multi-segment rupture, non-linear amplification factors, and inter-period correlations in the Broadband Platform.	x	x			
b	Derive and implement stochastic models for the representation of the heterogeneous, anisotropic near-surface velocity structure for CVMs.	x	x	x		
c	Implement standardized approaches and develop software tools to analyze recorded data and synthetic seismograms, and facilitate streamlined verification and validation of broadband and deterministic simulations.	x	x			
d	Gather and develop novel data sets (e.g., small earthquakes, tremor/low-frequency earthquakes, ambient noise) and new instrumentation (e.g., cell-phone accelerometers, strainmeter data, dense arrays) to develop and validate ground motion predictions.	x	x	x		
e	Develop, validate and incorporate appropriate and realistic constitutive models to represent the inelastic behavior of rock and deposit materials (soils) in 3D deterministic and 2D broadband ground motion simulations.		x	x	x	x
f	Investigate ground motion intensity proxies to automate the selection of scenarios that will integrate nonlinear effects in Cybershake via forward nonlinear 3D simulations.			x	x	x
g	Quantify the relative roles of fault geometry, heterogeneous frictional resistance, wavefield scattering, intrinsic attenuation, and near-surface heterogeneities and nonlinearities in controlling ground motion and its variability.		x	x	x	

h	Quantify the relative importance of nonlinearities near the fault, along the path, and in near surface soft-material deposits, and their susceptibility to subsurface topography (i.e., 3D basin and site effects).			x	x	x
i	Develop and implement methods for computing, storing, and serving 3D Green's functions.				x	
j	Evaluate the spatio-temporal correlation of ground motions at regional scales from recordings and using CyberShake data. Compare and validate pertinent CyberShake results against empirical correlations.			x	x	x
k	Develop programs and activities to advance the use of 3D deterministic and broadband ground motion simulation products, and results in engineering design, seismic hazard assessment and mitigation.	x	x	x	x	x

8. Induced Seismicity

The USGS Earthquake Hazards Program has a well-developed program to investigate induced seismicity nationwide, and SCEC has been asked to coordinate activities in this area with the USGS program through FARM leader Nick Beeler. Relevant to this work is the development of methods for detecting small earthquakes under the Mining Seismic Wavefields NSF geoinformatics grant. We have used these methods to develop an understanding of the signature of non-earthquake sources, including planes and helicopters (Figure 10), and to detect induced earthquakes (milestone 8c).

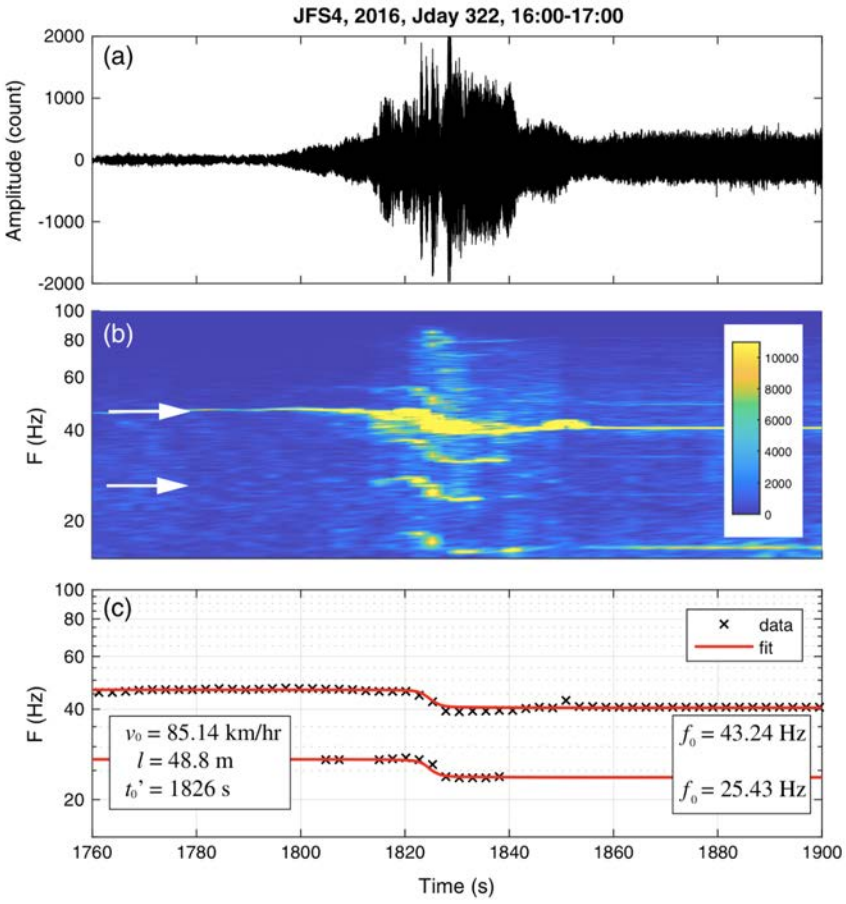

Figure 10. a) A raw vertical component waveform for a known helicopter event flying over seismic station JFS4. (b) Corresponding spectrogram with vertical axis in log scale. Arrows denote two strong overtones picked for analysis. (c) Time and frequency data (black crosses) for two overtones picked in the spectrogram in (b) and line fit to the data based on equation (1) (red curves). Inferred parameters for the helicopter are indicated in the box. (from Meng and Ben-Zion, 2018)

Milestone		Y1	Y2	Y3	Y4	Y5
a	Assemble appropriate fluid flow data to assess the relationship to earthquakes.		x			
b	Determine the degree to which ground motion from induced seismicity is similar, or different, than that from natural tectonic seismicity.			x		

c	Develop and apply approaches for improved detection and improved characterization, e.g., microseismic detection using fingerprinting and matched-filter approaches to suspected induced seismicity in California.				x	

Theme C. Characterizing Seismic Hazards

9. Probabilistic Seismic Hazard Analysis

We are continuing to develop physics-based earthquake rupture forecasts and ground-motion models within the CyberShake PSHA framework (milestones 9f,9h). We simulated ground motions for ~40,000 ruptures of moment magnitude M ≥ 6 in Southern California from the Uniform California Earthquake Rupture Forecast, UCERF2, generating ~440,000 pairs of horizontal component time histories for 336 sites. This ensemble is large enough to sample aleatory variability of the rupture process, including hypocenter and slip variations. The time histories were computed using the high-resolution 3-D crustal model CVM-4.26 (Figure 11).

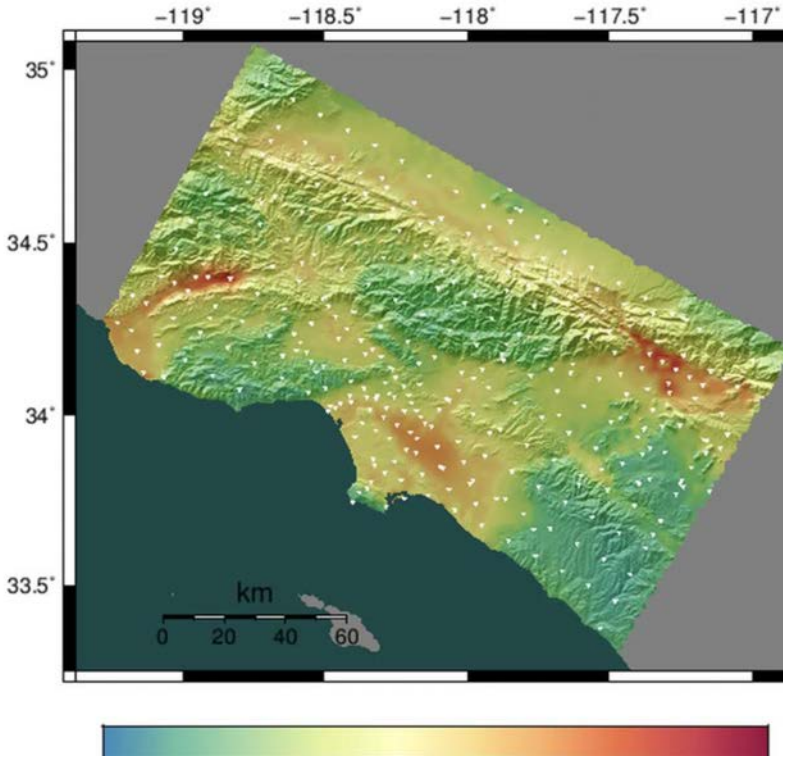

We are increasingly focused on fully characterizing faults, velocity models, and recurrence in order to reduce systematically the epistemic uncertainty in shaking intensities for hazard maps. We continue to verify and validate CyberShake to higher frequencies - now up to 1 Hz - and expand the areal coverage - most recently into Central California. As a proof of concept for evaluating long-term earthquake forecasts on faults, we evaluated the 1988 WGCEP rupture forecast (milestone 9a). The evaluation required a degree of subjectivity, underlining the importance of building testability into the forecast model development.

Figure 11. Regional MCER spectral acceleration map for 5-sec period (milestone 9h). The 336 CyberShake sites shown by solid inverted white triangles. Acceleration scale in g. (From Crouse et al., 2018)

Milestone		Y1	Y2	Y3	Y4	Y5
a	Develop methods for evaluating forecasts of finite-size earthquake ruptures against observations. Identify and characterize suitable datasets for retrospective tests of finite-rupture forecasts.		x	x		
b	Identify pathways for using information from physics-based simulators in PSHA and OEF.		x			
c	Carry out targeted experiments to validate ground motion effects identified through simulations of wave propagation in the CVMs.	x	x	x	x	
d	Assess predictive capability of long-term earthquake rupture forecasts by combining patterns of earthquake occurrence and strain accumulation with neotectonic and paleoseismic observations of the last millennium.			x		

e	Place geologic bounds on the character and frequency of multi-segment and multi-fault ruptures of extreme magnitude.				x	
f	Develop a statewide Cybershake-based hazard model.					x
g	Develop earthquake cycle models consistent with paleoseismic chronologies (slip estimates and event dates) that investigate stress accumulation and stress drop sequences over multiple earthquake cycles. Test the hypothesis that seismic supercycles seen in earthquake simulators actually exist in nature and explore the implications for earthquake predictability.					x
h	In coordination with the USGS, communicate improvements in physics-based seismic hazard analysis to the earthquake engineers, emergency responders, and general public.	x	x	x	x	x

10. Operational Earthquake Forecasting

We held the third Workshop on Operational Earthquake Forecasting (OEF) in April, 2017, and published a full OEF model for California (UCERF3-ETAS). Potential early adopters attended this meeting and articulated and compiled potential use cases and their value. One goal of this meeting was to provide guidance to the USGS on what level of effort should be put into developing these capabilities (milestones 9b,9h,10a). The importance of accounting for faults in time-dependent hazard calculations is demonstrated in Figure 12.

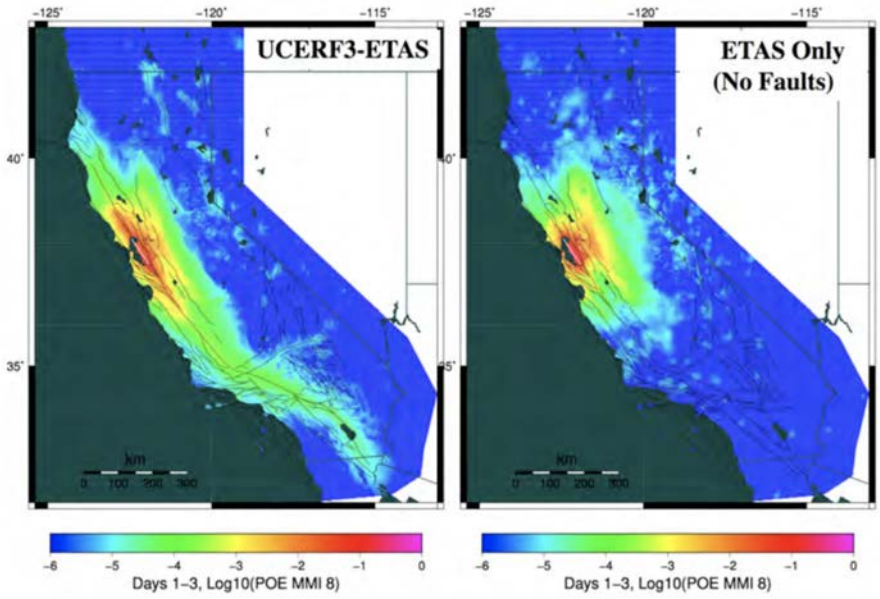

Figure 12. Average hazard maps following the M 7.1 Hayward Fault "Haywired" scenario earthquake, with panels on the left showing UCERF3-ETAS results and those on the right showing results for a pure (no faults) ETAS model. Maps show the probability of exceeding MMI 8 over the first 3 days, for which the influence of faults is profound (from Field and Jordan, SCEC Annual Report 17091).

We continue to make progress towards earthquake-simulator-based forecasting through the Collaboratory for Interseismic Simulation Modeling (CISM) project (milestone 9b).

The Collaboratory for the Study of Earthquake Predictability (CSEP) published a Focus Section in the Seismological Research Letters in July 2018, containing nine articles that present new CSEP evaluations of forecast models from around the globe, many relevant as OEF candidate models. We found that the Coulomb hypothesis, when described with appropriate uncertainty, could compete with (but not yet surpass) statistical ETAS clustering models during the 2010-12 Canterbury, New Zealand, earthquake sequence. Another, global, study found support for merging strain-rate data into smoothed seismicity models for improved forecasting skill.

Milestone		Y1	Y2	Y3	Y4	Y5
a	Develop methods for validating UCERF3-ETAS model forecasts utilizing CSEP or other tools.		x			
b	Formulate approaches for validating physics-based earthquake simulators against observations, and for using them to help constrain existing uncertainties in statistically based OEF models (e.g. UCERF3-ETAS).			x		

c	Assess the predictive power of the Coulomb stress hypothesis by testing physics-based clustering models against multiple earthquake sequences across various tectonic settings.				x	
d	Integrate ensemble modeling techniques within CSEP to enable ensemble forecasting.			x		
e	Assess the importance of visco-elastic post-seismic response for earthquake cycle models.				x	
f	Develop earthquake simulators that can resolve fault processes across the range of scales required to investigate stress-mediated fault interaction, including those caused by dynamic wave propagation or that combine coseismic dynamic rupture and multi-cycle simulators; generate synthetic seismicity catalogs; and assess the viability of earthquake rupture forecasts.				x	
g	Develop approaches for incorporating real-time data products into OEF candidate models.				x	
h	Develop methods for prospectively testing UCERF3-ETAS.				x	
i	Extend CSEP capability to evaluate real-time OEF models.					x

11. Earthquake Early Warning

We set no milestones for this topical element, which the USGS is covering well under research programs outside of SCEC.

12. Post-Earthquake Rapid Response

We continue to improve the rapid scientific response capability for future earthquakes in Southern California through development of new methods and protocols for mobilizing and coordinating the core geoscience disciplines, and gathering and preservation of perishable earthquake data. In March of 2018, SCEC participated in a USGS-led exercise to improve coordination of public communication and event-response activities. A workshop will be held in fall, 2018 to continue these discussions and update the SCEC response plan and knowledge base of available resources for scientific response (milestones 12a,12c,12d,12e,12f).

During this project period, Shaw, Plesch, Hauksson, and Meier developed a new, statistically robust way to identify the fault (or sets of faults) in the Community Fault Model (CFM) that generated an earthquake using information typically provided soon after an event occurs. This effort is important to rapid response, and it bridges the information provided by increasingly sophisticated near real-time seismograph networks, and the capabilities they enable, with comprehensive 3D CFM's developed by SCEC (Figure 13)

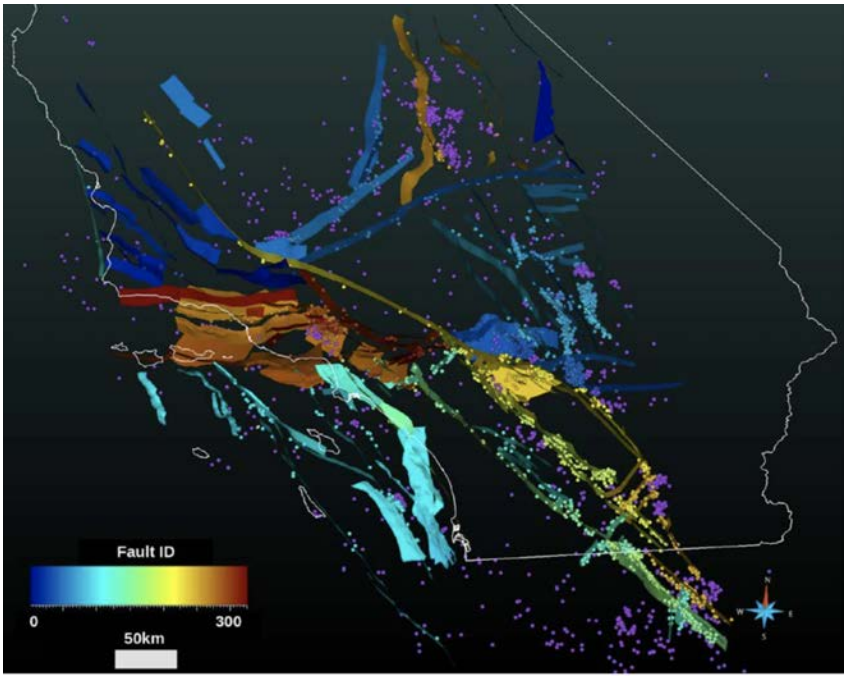

Figure 13. Catalog of M > 3 earthquakes, associated with CFM 5.1 faults. Colors for both earthquakes and faults represent a fault identification number. Thus, colors of events are shared with the fault that has the highest probability of association. Purple color for events indicates the lack of primary fault association.

Milestone		Y1	Y2	Y3	Y4	Y5
a	Hold an annual scientific earthquake response exercise.	x	x	x	x	x
b	Update earthquake response plans, including satellite communication and data exchange capabilities.	x				
c	Coordinate response plans annually with the USGS and the California Earthquake Clearinghouse.	x	x	x	x	x
d	Work with partners (e.g., IRIS, UNAVCO, USGS) to improve instrumental availability for rapid response.		x			
e	Identify and develop opportunities for linking high-resolution postseismic deformation to geological observations (UAVSAR, lidar, SfM).		x			
f	Improve post-event communication between SCEC and other agencies through sharing of information portals, datasets, etc.		x	x	x	x

Theme D. Reducing Seismic Risk

13. Risk to Distributed Infrastructure

The spatial correlation of strong ground motion is critical to quantifying the risk to spatially extensive infrastructure. Baker and Chen (SCEC Annual report 17058) have evaluated spatial correlation in ground motion residuals using CyberShake simulations (milestone 13c). The results show general agreement between the distance decay of correlations relative to empirical recordings. The simulations also show strong period dependence in correlations – perhaps stronger than empirical recordings indicate (Figure 14). It will be important to validate/calibrate this correlation structure of simulations against data.

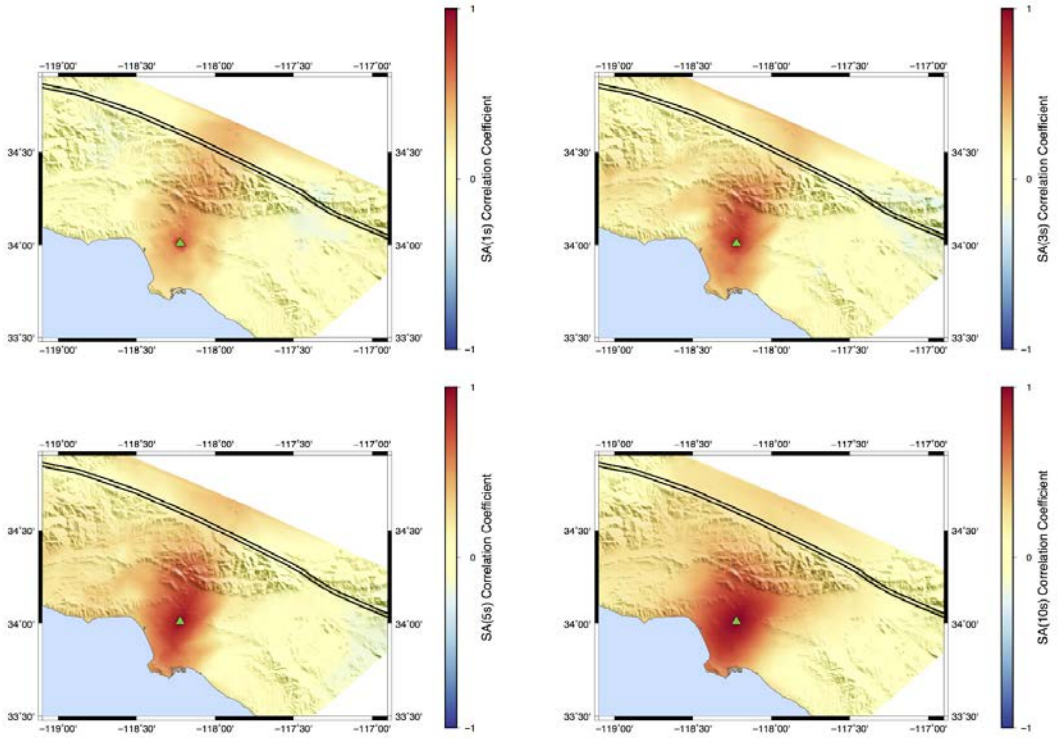

Figure 14. Correlation coefficients for spectral acceleration at T=1s, 3s, 5s, and 10s. A reference site is indicated by a triangle, and correlation coefficients between this site and all other sites in the region are indicated by colored shading.

Work is progressing rapidly on the dissemination of ground motion simulation data to engineers responsible for design and assessment of both individual buildings and distributed infrastructure. An engineering-centric tool for accessing CyberShake ground motion predictions in Los Angeles is now active. A recent special session on ground motion simulations at the 10th National Conference on Earthquake Engineering was attended by over 100 research and practicing engineers.

We are working with engineers and stakeholders to apply measures of distributed infrastructure impacts in assessing correlated damage from physics-based ground-motion simulations (milestones 13a,13b,13d). These provide ground motion predictions at densities that existing seismic data cannot. Due to the scale of effort required, we expect that research on this topic will likely be funded under Special Projects rather than the base funding from NSF and USGS. We submitted a proposal to NIST entitled “Development of Science-Based Tools and Framework for Seismic Resilience Assessment of Regional Lifeline Systems,” which included several of the California water agencies as partners. Unfortunately, despite very good reviews, this proposal was not funded, but we continue to engage public utilities and the California Department of Water and Power on this topic and pursue funding opportunities.

Milestone		Y1	Y2	Y3	Y4	Y5
a	Identify engineering needs for integrated (multi-step or end-to-end) earthquake simulation. Convene an interdisciplinary workshop bringing together ground motion modelers and earthquake engineers to define a reduced number of scenarios and case-studies that can be used to concentrate subsequent research activities (e.g., LA water supply).	x	x			
b	Develop computational tools to facilitate integrated earthquake modeling and site-city interaction effects. These tools should allow multi-step or end-to-end simulation and analysis of ground motion and infrastructure (buildings or distributed systems such as buried pipelines) response.		x	x	x	
c	Investigate the implications of ground motion simulations (including amplitude and spatial variability) by integrating observed and simulated ground motions with engineering-based building and distributed infrastructure systems response models. Validate the results by comparison to observed response of instrumented building and distributed infrastructure systems.			x	x	x
d	Develop methods for estimating fault displacements, including distributed deformation and large-scale tilts, for the evaluation of risk to large distributed infrastructures.		x	x	x	
e	Assess the performance of distributed infrastructure systems using simulated ground motions. Evaluate the potential impact of basin effects, rupture directivity, spatial distribution of ground motion, or other phenomena on risk to infrastructure systems.				x	x

14. Velocity and Rheology of Basin Sediments

In this effort, which focuses on what is sometimes called the geotechnical layer, we are drawing from the extensive geotechnical engineering literature to advance the implementation of site effects by incorporating nonlinear rheological models of near-surface rock and soil layers into full-physics earthquake simulations. A Workshop on Nonlinear Shallow Crust Effects was held September, 2017. Progress towards milestones 14b, 14d, and 14e, are reported under

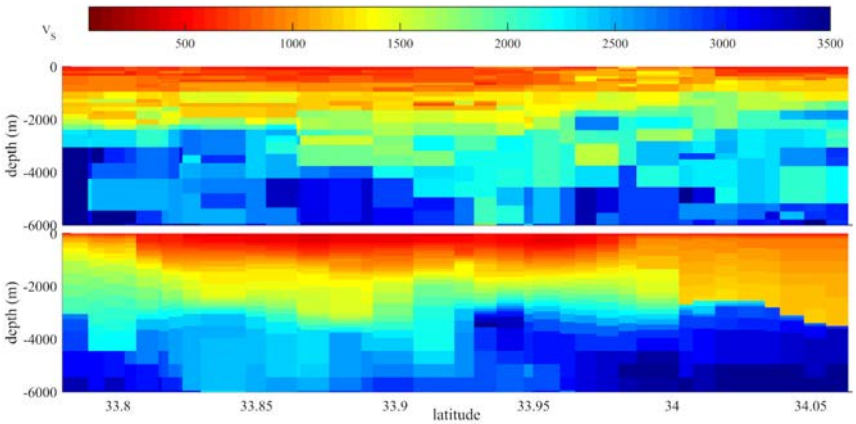

Figure 15. Top shows results of joint inversion for S-wave velocity across the LA Basin using fundamental mode Love wave and fundamental and first-higher mode Rayleigh wave dispersion, together with HVSR measurements of the ambient field along the LASSIE line. Lower panel shows SCEC CVM-H. (from Spica et al., 2018).

the closely related topical element of ground motion prediction in section 7. A longer-term goal of effort in this area is to develop accurate, efficient methods to characterize nonlinear effects to implement in SCEC simulation platforms (Broadband, CyberShake, High-F). Several groups developed improved techniques to image the Los Angeles and other basins in southern California. SCEC research also analyzed differences between classical site amplification effects in basin associated with vertically-incident body waves from these generated by surface waves. We continue to use ambient-seismic-field measurements to constrain shallow basin structure. The efforts are important for reducing epistemic uncertainties in ground motion prediction. In the current year we have begun to use the HVSR method to characterize basin structure along the LASSIE profile (Figure 15). This helps to address milestone 14c.

Milestone		**Y1**	**Y2**	**Y3**	**Y4**	**Y5**
a	Create a Sediment Velocity and Rheology Model (SVRM) TAG to foster collaborations between geotechnical engineers and ground motion modelers to advance modeling and simulation of the physics and effects of the geotechnical layer on ground motion prediction.	x				
b	Develop and validate 3D constitutive models to capture nonlinear phenomena such as near-surface plasticity, permanent ground deformation and earthquake triggered ground failure, for implementation into physics-based simulations.	x	x	x		
c	Develop new velocity parameterizations of the near-surface sediments, based on available site characterization data from past invasive and non-invasive methods, and constrained by the deeper CVM basement structure, and implement these in CVM applications (i.e., UCVM) to facilitate their evaluation through validation exercises.	x	x			
d	Use borehole measurements, near-surface material stiffness proxies (e.g., Vs30, topography), and empirical correlations to estimate input parameters necessary for nonlinear ground motion modeling in both physics-based simulations and empirical models .		x			
e	Develop empirical correlations between measured near-surface sediment properties and the rheology model parameters of these sediments, also drawing information from the velocity and rheology CXMs, to facilitate incorporation of nonlinear response and effects of permanent ground deformation.into regional-scale ground motion simulations.		x	x	x	
f	Populate the CRM with rheology models (velocity, anelastic attenuation, nonlinear properties) of the rock and soil layers of the crust to capture nonlinear phenomena such as off-fault plasticity, permanent ground deformation and earthquake triggered ground failure phenomena in physics-based simulation.			x		
g	Quantify epistemic uncertainties of the velocity variability and nonlinear constitutive laws and parameters derived and implemented for the response of the soft sediments.		x	x	x	x

Draft 2019 Science Plan

SCEC Science Planning Committee, September 2018

1. New This Year

The SCEC Science Plan (aka RFP) reflects the research priorities articulated in the SCEC5 proposal, and the project plan approved by the National Science Foundation and the U.S. Geological Survey. The SCEC Science Plan detailed in this document is provisional pending final SCEC5 Year 2 budget authorization. Substantial changes have been made to the RFP since last year, so we strongly encourage researchers to read carefully the RFP in its entirety.

- The time-period for SCEC funded projects will reset to the dates SCEC has traditionally used: February 1 as the start date, and January 31 as the end date.
- The Science Planning Committee (PC) was reconfigured for SCEC5. The current composition includes four disciplinary committees (Seismology, Tectonic Geodesy, Earthquake Geology, and Computational Science), and five interdisciplinary focus groups (FARM, SDOT, EFP, GM, SAFS, CXM and EEII), each with individual representation in the PC. The PC also includes two members representing the Special Projects.
- A new focus area, called “Earthquake Gates” was started in the first year of SCEC5. This initiative is designed to foster multidisciplinary studies of the factors that permit earthquakes to start or stop (as at a gate). To organize this initiative the SCEC community held an incubator workshop in March 2017 and solicited proposals to establish Earthquake Gate Areas. The Cajon Pass Region has been selected as the first and only Earthquake Gate of SCEC5. We do not plan to initialize any new Earthquake Gate Area in years 3-5 of SCEC5. Refer to section 5.5 SAFS for more information on the Earthquake Gates Initiative and the Cajon Pass Earthquake Gate Integrated Science Plan.
- If identical or closely related work is also proposed to another institution (e.g., National Science Foundation), an explanation of the relationship of such work to this proposal should be provided.
- Investigators that anticipate extensive use of computational resources should consider consulting with the relevant SCEC Special Projects leadership to develop a strategy to acquire or support such resources.
- Investigators interested in undergraduate summer interns should include an "intern project" description in their proposal. The undergraduate intern will be recruited by the SCEC CEO Program staff. Selected intern projects will be awarded as supplemental funds on the proposal award. Funds used for summer stipends and travel support to the SCEC annual meeting for the selected undergraduate students will be managed at and dispersed from USC. The number of intern projects awarded each year will depend on available funding in the SCEC annual budget and the pool of interested applicants.
- A new SCEC Transitions Program has been launched for SCEC5. This program will provide students and early-career scientists with resources and mentoring, particularly at major transitions in their educational and professional careers. In doing so, the Transitions Program aims to encourage and sustain careers in the geosciences and other STEM fields. The SCEC Transitions Program welcomes proposals that expand awareness of professional advancement opportunities and pathways, as well as improve competency in earthquake research tools and techniques of the junior members of the SCEC community.
- The geochronology infrastructure supports Accelerator Mass Spectrometer analysis of ^{14}C, ^{10}Be, ^{26}Al, and 36Cl through collaboration with Lawrence Livermore National Laboratory and the University of California, Irvine (^{14}C only). Luminescence dating (OSL, pIR-IRSL) will be supported through regular proposal budgets, through arrangement with a luminescence laboratory (see Earthquake Geology section for suggestions).
- SCEC no longer supports proposals solely for annual meeting participation. Funding for travel to participate in the SCEC Annual Meeting will be considered only in the context of a research proposal in response to the

current Science Plan. International travel funding for a co-investigator to participate in the SCEC Annual Meeting will be considered, provided the proposal clearly states (a) how the investigators are critical to the project and (b) a plan for how the international participant's institution will cost-share the anticipated travel expenses.

2. Overview

The Southern California Earthquake Center (SCEC) was founded as a Science & Technology Center on February 1, 1991, with joint funding by the National Science Foundation (NSF) and the U. S. Geological Survey (USGS). Since 2002, SCEC has been sustained as a stand-alone center under cooperative agreements with both agencies in three consecutive, five-year phases (SCEC2–SCEC4). The Center was extended for another 5-year period, effective 1 February 2017 to 31 January 2022 (USGS SCEC5) and 1 May 2017 to 30 April 2022 (NSF SCEC5). SCEC coordinates fundamental research on earthquake processes using Southern California as its main natural laboratory. Currently, over 1000 earthquake professionals participate in SCEC projects. This research program is investigator-driven and supports core research and education in seismology, tectonic geodesy, earthquake geology, and computational science. The SCEC community advances earthquake system science by gathering information from seismic and geodetic sensors, geologic field observations, and laboratory experiments; synthesizing knowledge of earthquake phenomena through system-level, physics-based modeling; and communicating understanding of seismic hazards to reduce earthquake risk and promote community resilience.

2.1 The SCEC5 Research Vision

Earthquakes are emergent phenomena of active fault systems, confoundingly simple in their gross statistical features but amazingly complex as individual events. SCEC's long-range science vision is to develop dynamical models of earthquake processes that are comprehensive, integrative, verified, predictive, and validated against observations. The science goal of the SCEC5 core program is to provide new concepts that can improve the predictability of the earthquake system models, new data for testing the models, and a better understanding of model uncertainties.

The validation of model-based predictions against data is a key SCEC activity, because empirical testing is the most powerful guide for assessing model uncertainties and moving models towards better representations of reality. SCEC validation efforts tightly couple basic earthquake research to the practical needs of probabilistic seismic hazard analysis, operational earthquake forecasting, earthquake early warning, and rapid earthquake response. Moreover, the risk-reduction problem—which requires actions motivated by useful information—strongly couples SCEC science to earthquake engineering. SCEC collaborations with engineering organizations are directed towards end-to-end, physics-based modeling capabilities that span system processes from the earthquake source to infrastructure performance and risk.

SCEC connects to the social sciences through its mission to convey authoritative information to stakeholders in ways that result in lowered risk and enhanced resilience. SCEC's vision is to engage end-users and the public at large in on-going, community-centric conversations about how to manage particular risks by taking specific actions. The SCEC Communication, Education, and Outreach (CEO) program seeks to promote this dialog on many levels, through many different channels, and inform the conversations with authoritative earthquake information. Towards this goal, the SCEC5 CEO program continues to build networks of organizational partners that can act in concert to prepare millions of people of all ages and socioeconomic levels for inevitable earthquake disasters.

2.2 The SCEC5 Science Plan

The SCEC5 Science Plan was developed by the non-USGS members of the SCEC Planning Committee and Board of Directors with extensive input from issue-oriented "tiger teams" and the community at large. The strategic framework for the SCEC5 Science Plan is cast in the form of five basic questions of earthquake science:

(1) How are faults loaded on different temporal and spatial scales?

(2) What is the role of off-fault inelastic deformation on strain accumulation, dynamic rupture, and radiated seismic energy?

(3) How do the evolving structure, composition and physical properties of fault zones and surrounding rock affect shear resistance to seismic and aseismic slip?

(4) How do strong ground motions depend on the complexities and nonlinearities of dynamic earthquake systems?

(5) In what ways can system-specific studies enhance the general understanding of earthquake predictability?

These questions cover the key issues driving earthquake research in California, and they provide a basis for gauging the intellectual merit of proposed SCEC5 research activities.

Research priorities have been developed to address these five basic questions. Tied to the priorities are fourteen science topics distributed across four main thematic areas (described in section 2.2.2).

2.2.1 Basic Questions of Earthquake Science

Q1. How are faults loaded across temporal and spatial scales?

Problem Statement: Fault systems are externally loaded, primarily by the relatively steady forces of plate tectonics, but also by mass transfers at the surface due to long-term interactions of the solid Earth with its fluid envelopes (climate forcing) and by short-term gravitational interactions (tidal forcing). Much is yet to be learned about the stress states acting on active faults and how these stress states evolve through external loading and the internal transfer of stress during continuous deformation and discontinuous faulting.

In SCEC4, we initiated research on a Community Stress Model (CSM) to describe our current knowledge about the stress state of the San Andreas fault system. The ensemble of stress and stress-rate models comprised by the current CSM is a quantitative representation of how well we have been able to answer Q1. Empirical models have been developed for stress orientations in the upper crust based on abundant focal mechanisms and more limited in-situ data, as well as 3D dynamic models of stress; e.g., from finite-element simulations of long-term tectonics, including nonlinear laboratory rheologies. A new approach builds 3D stress models as sums of analytic solutions that satisfy momentum conservation everywhere, while approximating the previous stress-direction and stress-amplitude models in a least-squares sense. Though we are encouraged by our recent progress, understanding stress is a long-term proposition.

Research Priorities:

P1.a. Refine the geologic slip rates on faults in Southern California, including offshore faults, and optimally combine the geologic data with geodetic measurements to constrain fault-based deformation models, accounting for observational and modeling uncertainties. (Geology, Geodesy, SDOT, SAFS)

P1.b. Determine the spatial scales at which tectonic block models (compared to continuum models) provide descriptions of fault-system deformation that are useful for earthquake forecasting. (SDOT, Geodesy, EFP, CXM)

P1.c. Constrain how absolute stress and stressing rate vary laterally and with depth on faults, quantifying model sensitivity, e.g., to rheology, with inverse approaches. (SDOT, CXM, Geology)

P1.d. Quantify stress heterogeneity on faults at different spatial scales, correlate the stress concentrations with asperities and geometric complexities, and model their influence on rupture initiation, propagation, and arrest. (Seismology, SDOT, FARM, Geology)

P1.e. Evaluate how the stress transfer among fault segments depends on time, at which levels it can be approximated by quasi-static and dynamic elastic mechanisms, and to what degree inelastic processes contribute to stress evolution. (SDOT, Geodesy, Seismology, FARM, CS)

Q2. What is the role of off-fault inelastic deformation on strain accumulation, dynamic rupture, and radiated seismic energy?

Problem Statement: In the brittle upper crust, observations of low-velocity zones associated with active seismogenic faults, together with time-dependent evolution of seismic velocities following stress perturbations suggest intrinsic relationships between damage, healing, and effective elastic moduli of rocks in a fault zone. Such relationships are only poorly understood, but they can elucidate the development and evolution of fault zones in space and time, as well as the interplay between damage accumulated over multiple earthquake cycles and rupture dynamics. Current dynamic rupture models show that the assumption of elastic deformation of the host rocks is often violated; e.g., in regions of high stress concentration near the propagating rupture front, particularly when stress is further concentrated by geometrically complex fault surfaces. This raises important questions about the effect of inelasticity and damage on the nucleation, propagation, and arrest of rupture. Neglecting inelastic response may systematically bias inversions of seismic and geodetic data for slip distribution and rupture geometry, affect measurements of coseismic slip at the surface, and inferences of long-term slip rates from the geologic record.

The SCEC community is at the forefront of research on inelastic material response associated with earthquake faulting and its effects on dynamic rupture propagation and seismic ground motion. The SCEC focus on extreme ground motion for the Yucca Mountain Project drew attention to the physical limits that realistic, inelastic material response places on strong shaking. Recent simulations of earthquakes in the Los Angeles region have demonstrated how yielding near the fault and in sedimentary basins substantially reduces predicted ground motions relative to purely elastic simulations. Accounting for inelasticity brings the model predictions more in line with empirical constraints on strong shaking.

Research Priorities:

P2.a. Determine how much off fault deformation contributes to geodetic estimates of strain accumulation and what fraction of seismic-moment accumulation is relaxed by aseismic processes. (FARM, Geodesy, CS)

P2.b. Explore approaches to represent the effects of nonlinearity that would allow the continued use of linear wave propagation as an effective approximation. (GM, CS, Seismology)

P2.c Constrain the form of fault-zone and distributed nonlinearity, as well as the material properties and factors, such as cohesion and pore fluid pressure, that are likely to influence it. (FARM, CS, GM, Seismology)

P2.d. Understand how inelastic strain associated with fault roughness and discontinuities influences rupture propagation, seismic radiation, and scaling of earthquake source parameters. (CS, FARM, Seismology)

P2.e Describe how fault geometry and inelastic deformation interact to determine the probability of rupture propagation through structural complexities, and determine how model-based hypotheses about these interactions can be tested by the observations of accumulated slip and paleoseismic chronologies. (EFP, FARM, CS, Geology, SAFS)

Q3. How do the evolving structure, composition and physical properties of fault zones and surrounding rock affect shear resistance to seismic and aseismic slip?

Problem Statement: Fault systems show complexities that range from the macroscale of plate tectonics to the microscale of asperity contacts on a fault surface in highly damaged rocks that are fluid-filled and chemically reactive. Many questions about the evolving, multi-scale dynamics of these complex systems remain unanswered. The inferred values of heat outflow from mature faults, such as the San Andreas, Taiwan's Chelungpu Fault, and the Japan Trench megathrust, imply that shear stress acting during sliding is an order of magnitude lower than estimates from Byerlee's law and typical static friction measurements—an inconsistency famously known as the "heat-flow paradox." Low values for shear stress acting on major faults are also supported by the steep angles between the principal stress direction and fault trace, slip-vector rake rotations during faulting, and significant rotations of principal stresses after large earthquakes. In addition, multi-fault earthquake simulations show that observed propagation onto unfavorably oriented structures appears to be more likely to occur if the faults are subject to low tectonic stress.

These and other observations motivate the continued investigation of the structure, composition, and physical properties of fault zones that host earthquake sources. One important question is which faults are susceptible to coseismic weakening mechanisms, such as flash heating, thermal pressurization of pore fluids, partial or full melting

of the shearing zone, silica-gel formation, and thermal decomposition of sheared materials into friction-reducing byproducts. Coseismic weakening may lead to large unexpected slip in creeping fault regions, including deeper fault extensions below the seismogenic layer, a phenomenon compatible with some recent observations. Fluids play a key role in several of the weakening processes, potentially dominating coseismic resistance to slip. In fact, fluids can lead to extreme localization of the shearing layer, promoting coseismic weakening. Conversely, fluids can also provide a stabilizing factor, for example due to inelastic shear-induced dilatancy of the pore space, and the resulting reduction of pore pressure and hence increase of the effective normal stress.

Research Priorities:

P3.a. Refine the geometry of active faults across the full range of seismogenic depths, including structures that link and transfer deformation between faults. (CXM, Seismology, Geodesy, Geology, SAFS)

P3.b. Constrain the active geometry and rheology of the ductile roots of fault zones. (CXM, SDOT, FARM, Geology)

P3.c. Assess how shear resistance and energy dissipation depend on the maturity of the fault system, and how these are expressed geologically. (FARM, SDOT, Geology)

P3.d. Determine how damage zones, crack healing and cementation, fault zone mineralogy, and off-fault plasticity govern the degree of strain localization, the state and stability of slip (e.g., creeping vs. locked, seismic vs aseismic), interseismic strength recovery, and rupture propagation. (FARM, Geology, CS)

P3.e Constrain the extent of permanent, off-fault deformation, and its contribution to geologic and geodetic fault slip-rate estimates. (Geology, SAFS, Geodesy, EFP)

P3.f. Study the mechanical and chemical effects of fluid flows, both natural and anthropogenic, on faulting and earthquake occurrence, and how they vary throughout the earthquake cycle. (FARM, Geology, EFP)

P3.g. Assess the importance of the mechanical properties of the near-surface in reconciling geodetic and seismological estimates of fault slip at depth with fault offset at the surface. (Seismology, Geodesy, Geology, GM, FARM)

Q4. How do strong ground motions depend on the complexities and nonlinearities of dynamic earthquake systems?

Problem Statement: Realistic physics-based predictions of strong ground motions are among the highest long-term priorities of SCEC; comparing them with data is essential to testing our understanding of source and wave dynamics, and they connect the basic science of earthquakes to the practical applications of seismic hazard analysis. Ground-motion simulations have become useful in performance-based engineering (for nonlinear building response analyses, for example), in operational earthquake forecasting, and in earthquake early warning. Validated numerical simulations that yield predictions adapted to local geologic conditions, such as sedimentary basins, structural boundaries, and steep topography, can provide meaningful ground-motion estimates for conditions poorly represented in the empirical database.

An appropriate baseline for measuring future progress in ground-motion modeling is the recent CyberShake 15.4 study, which produced hazard curves for the Los Angeles region from a stochastically complete set of UCERF2 ruptures using the CVM-S4.26 crustal structure. The resulting hazard model has several notable limitations: (i) the sources were prescribed by a pseudo-dynamic (kinematic), rather than fully dynamic, rupture model; (ii) the wavefield calculations were computed to an upper cutoff frequency of 1 Hz, compared to engineering needs that can exceed 10 Hz; and (iii) the principle of seismic reciprocity was used to compute the requisite ensemble of seismograms.

To preserve reciprocity and its associated computational benefits, Cybershake hazard computations would be constrained to perfectly linearly elastic media; near-fault inelasticity would have to be built into the rupture model as a source effect, and near-surface inelasticity would have to be built into the wave propagation simulations as a shallow-crust path effect

In SCEC5, we are moving away from the classical trichotomy of source, path, and site effects as decoupled processes by a new paradigm. Under this new paradigm, in which the surface ground motions are modeled as the nonlinear response of a dynamical system, these effects are coupled and can't be modeled separately. As the CyberShake example above indicates, identifying approaches that preserve the computational efficiency enabled by reciprocity and superposition, but approximate the inelastic response of rocks and soils from source to surface will be a major challenge. Our plan will be guided by four priorities that recognize the practical potential of this paradigm shift.

Research Priorities:

P4.a. Determine the relative roles of fault geometry, heterogeneous frictional resistance, crustal material heterogeneities, intrinsic attenuation, shallow crust nonlinearities and ground surface topography in controlling and bounding ground motions. (GM, Seismology, EEII)

P4.b. Construct methods for validating ground-motion predictions that account for the paucity of recordings in the near field, where the motions are expected to be strong and inelastic effects large. (GM, EEII)

P4.c. Develop ground-motion simulations for anticipated large events that are suitable for probabilistic seismic hazard and risk analysis. (CS, GM, EEII)

P4.d. Communicate improvements in physics-based seismic hazard analysis to the earthquake engineers, emergency responders, and general public. (EEII, GM)

Q5. In what ways can system-specific studies enhance the general understanding of earthquake predictability?

Problem Statement: Earthquake prediction is one of the great unsolved problems of physical science. We distinguish intrinsic predictability (the degree to which a future earthquake behavior is encoded in the precursory behavior of an active fault system) from a specific prediction (a testable hypothesis, usually stated in probabilistic terms, of the location, time, and magnitude of an earthquake). A key objective of the SCEC5 core program is to improve our understanding of earthquake predictability as the basis for advancing useful forecasting models. We propose to take a broad view of the earthquake predictability problem. For example, many interesting conditional predictions can be posed as physics questions in a system-specific context: What will be the shaking intensity in the Los Angeles basin from a magnitude 7.8 earthquake on the southern San Andreas Fault? By how much will the strong shaking be amplified by the coupling of source directivity to basin effects? Will deep injection of waste fluids cause felt earthquakes near a newly drilled well in the San Joaquin Valley? How intense will the shaking be during the next minute of an ongoing earthquake in Los Angeles?

Earthquake system science offers a "brick-by-brick" approach to improving our understanding earthquake predictability. In SCEC5, we propose to build system-specific models of rupture recurrence, stress evolution, and triggering within a probabilistic framework that can assimilate a wide variety of geologic, geodetic, and seismic observations. Five research priorities will guide this plan.

Research Priorities:

P5.a. Develop earthquake simulators, which are earthquake rupture simulation codes that allow the development of long-term earthquake catalogs based on approximations to rupture physics and earthquake interaction, and encode the current understanding of earthquake predictability. (EFP, CS, FARM)

P5.b. Place useful geologic bounds on the character and frequency of multi-segment and multi-fault ruptures of extreme magnitude. (SAFS, Geology, EFP)

P5.c. Assess the limitations of long-term earthquake rupture forecasts by combining patterns of earthquake occurrence and strain accumulation with neotectonic and paleoseismic observations of the last millennium. (EFP, SAFS, Geology)

P5.d. Test the hypothesis that “seismic supercycles, seen in earthquake simulators actually exist in nature and explore the implications for earthquake predictability. (EFP, SAFS, Geology)

P5.e. Exploit anthropogenic (induced) seismicity as experiments in earthquake predictability. (FARM, EFP)

2.2.2 SCEC5 Thematic Areas and Topical Elements

The basic science questions reflect the core issues currently driving earthquake research. SCEC5 will address these questions through an interdisciplinary program comprising 14 topics in four main thematic areas. While these are not the only research activities to be undertaken in SCEC5, they constitute a cogent plan for making progress on the core scientific issues.

1. Modeling the fault system: We seek to know more about the geometry of the San Andreas system as a complex network of faults, how stresses acting within this network drive the deformation that leads to fault rupture, and how this system evolves on time scales ranging from milliseconds to millions of years.

- Stress and Deformation Over Time. We will build alternative models of the stress state and its evolution during seismic cycles, compare the models with observations, and assess their epistemic uncertainties, particularly in the representation of fault-system rheology and tectonic forcing.
- Earthquake Gates. Earthquake gates are regions of fault complexity conjectured to inhibit propagating ruptures, owing to dynamic conditions set up by proximal fault geometry, distributed deformation, and earthquake history. We will test the hypothesis that earthquake gates control the probability of large, multi-segment and multi-fault ruptures.
- Community Models. We will enhance the accessibility of the SCEC Community Models, including the model uncertainties. Community thermal and rheological models will be developed.
- Data Intensive Computing. We will develop methods for signal detection and identification that scale efficiently with data size, which we will apply to key problems of Earth structure and nanoseismic activity.

2. Understanding earthquake processes: Many important achievements in understanding fault-system stresses, fault ruptures, and seismic waves have been based on the elastic approximation, but new problems motivate us to move beyond elasticity in the investigation of earthquake processes.

- Beyond Elasticity. We will test hypotheses about inelastic fault-system behavior against geologic, geodetic, and seismic data, refine them through dynamic modeling across a wide range of spatiotemporal scales, and assess their implications for seismic hazard analysis.
- Modeling Earthquake Source Processes. We will combine coseismic dynamic rupture models with inter-seismic earthquake simulators to achieve a multi-cycle simulation capability that can account for slip history, inertial effects, fault-zone complexity, realistic fault geometry, and realistic loading.
- Ground Motion Simulation. We will validate ground-motion simulations, improve their accuracy by incorporating nonlinear rock and soil response in the shallow crust, and integrate dynamic rupture models with wave-scattering and attenuation models. We will expand our simulation capabilities to capture the frequency band of engineering interest, 0.1-10 Hz. In collaboration with geotechnical engineers and engineering geologists, we will develop or implement nonlinear rheological models of near-surface rock and soil layers tailored to the computational constraints and parameter scarcity of full-physics earthquake simulations.
- Induced Seismicity. We will develop detection methods for low magnitude earthquakes, participate in the building of hydrological models for special study sites, and develop and test mechanistic and empirical models of anthropogenic earthquakes within Southern California.

3. Characterizing seismic hazards: We seek to characterize seismic hazards across a wide spectrum of anticipation and response times, with emphasis on the proper assessment of model uncertainties and the use of physics-based methods to lower those uncertainties.

- Probabilistic Seismic Hazard Analysis. We will attempt to reduce the uncertainty in PSHA through physics-based earthquake rupture forecasts and ground-motion models. A special focus will be on reducing the epistemic uncertainty in shaking intensities due to 3D along-path structure.
- Operational Earthquake Forecasting. We will conduct fundamental research on earthquake predictability, develop physics-based forecasting models in the new Collaboratory for Interseismic Simulation and Modeling, and coordinate the Working Group on California Earthquake Probabilities.
- Post-Earthquake Rapid Response. We will improve the rapid scientific response to strong earthquakes in Southern California through the development of new methods for mobilizing and coordinating the core geoscience disciplines in the gathering and preservation of perishable earthquake data.

4. Reducing seismic risk: Through partnerships coordinated by SCEC's Earthquake Engineering Implementation Interface, we will conduct research useful in motivating societal actions to reduce earthquake risk. Two topics investigated by these engineering partnerships will be:

- Risk to Distributed Infrastructure. We will work with engineers and stakeholders to apply measures of distributed infrastructure impacts in assessing correlated damage from physics-based ground-motion simulations. An initial project will develop earthquake scenarios for the Los Angeles water supply.

2.3 Management of the SCEC Research Program

The SCEC Science Planning Committee (PC) is responsible for developing the SCEC Annual Science Plan, which describes the Center's research interests and priorities, and the SCEC Annual Collaboration Plan, which details how resources will be allocated to projects. The PC is chaired by the SCEC Co-Director (Greg Beroza), who is assisted by a PC Vice-Chair (Judi Chester). The PC comprises the leaders of the SCEC science working groups—disciplinary committees, focus groups, and special project groups—who, together with the working group co-leaders, guide SCEC's research program. The Executive Director for Special Projects (Christine Goulet) manages science activities in the externally funded SCEC Special Projects and coordinates these activities with the PC and the SCEC Associate Director for Information Technology (Philip Maechling), who has oversight of SCEC Information Technology, including the software standards for data structures and model interfaces. The Center Director (John Vidale) and the Associate Directors for Science Operations (Tran Huynh), Administration (John McRaney) and CEO (Mark Benthien) serve as ex officio members. The PC is responsible for formulating the Center's science plan, conducting proposal reviews, and recommending projects to the Board of Directors for SCEC support. Its members play key roles in implementing the SCEC5 science plan.

3. Annual SCEC Science Plan

The SCEC Science Plan solicits proposals from individuals and groups to participate in the SCEC research program on an annual basis. Typical grants awarded under the SCEC Science Plan fall in the range of $10,000 to $35,000. This is not intended to limit SCEC to a fixed award amount, nor to a specified number of awards, but rather to calibrate expectations for proposals submitted to SCEC. Field investigations outside southern California may be considered, provided the proposed research demonstrates direct relevance to SCEC5 goals that are not achievable within the southern California natural laboratory.

3.1 Investigator Eligibility and Responsibilities

3.1.1 Who May Submit Proposals

Any person eligible to serve as a Principal Investigator (PI) at a U.S. academic institution or private corporation based in the U.S. may submit a proposal to SCEC.

Collaborative proposals involving non-U.S. participants will be considered provided the proposal (1) clearly states how the investigator from the non-U.S. institution is critical to the project and (2) the requested budget for the international participant only includes direct costs (e.g. travel support). The funding for research requested on such projects should only be for the U.S. portion of the collaborative effort.

Collaborative proposals with investigators from the U.S. Geological Survey are encouraged. USGS employees should submit requests for support through USGS channels.

Any person with an overdue project report (for prior SCEC-funded awards) at the time of the proposal deadline will not be allowed to submit a new or continuation proposal as a PI or co-PI.

3.1.2 Investigator Responsibilities

By submitting a proposal to SCEC, investigators agree to all three conditions listed below. Investigators who fail to meet these conditions may (a) not receive funding until conditions are satisfied, and/or (b) become ineligible to submit a future proposal to SCEC.

1. Community Participation. Principal investigators will interact with other SCEC scientists on a regular basis and contribute data, results, and models to the appropriate SCEC resource.

    SCEC Annual Meeting. The PI will attend the annual meeting and present results of SCEC-funded research in the poster sessions, workshops and/or working group meetings.

    Data Sharing. Funded investigators are required to contribute data and results to the appropriate SCEC resource (e.g., Southern California Earthquake Data Center, database, community model).

2. Project Reporting. Principal investigators will submit a project report by the due date listed below.

    Workshop Awards. A report on results and recommendations of the workshop funded by SCEC is due no later than 30 days following the completion of the workshop. The report will be posted on the SCEC website as soon as possible after review by SCEC leadership.

    All Other Awards. Investigators funded by SCEC must submit a project report no later than March 15 (5:00 pm PST) in the year after the funding was received. Reports should be a maximum of 5 pages (including text and figures). Reports must include references to all SCEC publications during the past year (including papers submitted and in review) with their SCEC contribution number (see 3 below).

3. Registration of Publications. Principal investigators will register publications resulting entirely or partially from SCEC funding in the SCEC Publications System (www.scec.org/publications) to receive a SCEC contribution number. Publications resulting from SCEC funding should acknowledge SCEC and include the SCEC contribution number.

3.2 Proposal Categories

3.2.1 Research Proposals

A. Data Gathering and Products. SCEC coordinates an interdisciplinary and multi-institutional study of earthquakes in Southern California, which requires data and derived products pertinent to the region. Proposals in this category should address the collection, archiving, and distribution of data, including the production of SCEC community models that are online, maintained, and documented resources for making data and data products available to the scientific community.

B. Integration and Theory. SCEC supports and coordinates interpretive and theoretical investigations on earthquake problems related to the Center's mission. Proposals in this category should be for the integration of data or data products from category A, or for general or theoretical studies. Proposals in categories A and B should address one or more of the basic questions of earthquake science (see Questions), and may include a brief description (<200 words) as to how the proposed research and/or its results might be used in a special initiative (see Special Projects) or in education and/or outreach (see CEO).

3.2.2. Collaborative Proposals and Technical Activity Groups

A. Collaborative Proposals involving multiple investigators and/or institutions are strongly encouraged. The lead investigator should submit only one proposal for the collaborative project. Information on all investigators requesting SCEC funding (including budgets, complete and up-to-date current and pending

support statements) must be included in the proposal submission. Note that funding for Collaborative Proposals may be delayed or denied if any of the investigators listed on the proposal has overdue project report(s) for a prior SCEC award.

B. Technical Activity Groups (TAGs) self-organize to develop and test critical methodologies for solving specific problems. In the past, TAGs have formed to verify the complex computer calculations needed for wave propagation and dynamic rupture problems, to assess the accuracy and resolving power of source inversions, and to develop geodetic transient detectors and earthquake simulators. TAGs share a modus operandi: the posing of well-defined “standard problems”, solution of these problems by different researchers using alternative algorithms or codes, a common cyberspace for comparing solutions, and meetings to discuss discrepancies and potential improvements. TAG proposals typically involve a workshop and should include a research coordination plan that sets a timetable for successful completion of TAG activities no later than the end of SCEC5.

3.2.3 Participant Support Proposals

A. Workshops. SCEC participants who wish to convene a workshop between May 1, 2018 and April 31, 2019 should submit a proposal for the workshop in response to this Science Plan. The proposed lead convener of the workshop must contact Tran Huynh (scecmeet@usc.edu) for guidance in planning the scope, budget and scheduling of the proposed workshop before completing the proposal submission. Note that workshops scheduled in conjunction with the SCEC Leadership Retreat (June) or SCEC Annual Meeting (September) are limited in number and may have further constraints due to space and time availability.

B. SCEC/SURE Intern Project Supplement. SCEC coordinates a Summer Undergraduate Research Experience (SURE) Program that enables undergraduate students to work alongside SCEC scientists on a variety of research projects during the summer. Investigators interested in mentoring an undergraduate student over the summer should include an "intern project" description in their proposal that aligns with the overall proposed project plan. Undergraduate interns will be recruited by SCEC Communication, Education, and Outreach (CEO) Program staff in coordination with potential mentors. Selected intern projects will be awarded as supplemental funds to the proposal award. The supplemental funds will provide (1) a summer stipend up to $6,500 for the selected undergraduate student and (2) travel support for the student to participate in the all intern field trip and to present his/her summer research at the SCEC annual meeting. The number of intern projects awarded each year will depend on available funding in the SCEC annual budget and the available student applicant (interest) pool. The funds will be disbursed and managed at USC. Questions about the SCEC/SURE Program should be directed to Gabriela Noriega (213-821-1117; gnoriega@usc.edu).

C. SCEC Transitions Program. In order to accomplish the long-term outcome of increasing diversity, retention, and career success in the scientific workforce, the CEO is launching a new Transitions Program in SCEC5. This program will provide students and early-career scientists with resources and mentoring, particularly at major transitions in their educational and professional careers. In doing so, the Transitions Program aims to encourage and sustain careers in the geosciences and other STEM fields. The SCEC Transitions Program welcomes proposals that expand awareness of professional advancement opportunities and pathways, as well as improve competency in earthquake research tools and techniques of the junior members of the SCEC community.

3.3 Guidelines for Proposal Submission

3.3.1 Proposal Due Date

The deadline date is November 15, 2018 (5:00pm Pacific Time). Late proposals will not be accepted.

3.3.2 How to Submit Proposals

Every investigator listed on the proposal must have a registered account on www.SCEC.org, with current contact information and profile information updated. Proposals must be submitted through the SCEC Proposal System, accessible via www.scec.org/scienceplan.

Proposals do not need to be formally signed by institutional representatives.

3.3.3 Project Duration

The proposed project period should be 1-year duration (starting February 1, 2019 and ending January 31, 2020).

3.3.4 Proposal Contents

Every proposal submitted must include all of the contents listed below. Proposals must be received through the online system by the due date, with all required information, to be considered complete. Incomplete proposals may be rejected and returned without comment.

1. Cover Page. The proposal cover page should include all the following information, which will be required when submitting the proposal online:

- Project Title, Principal Investigator(s), and Institutional Affiliation(s)
- Total Amount of Request on Proposal, Amount of Request per Investigator
- Proposal Category (see Section 3)
- Three SCEC science priorities, listed in ranked order, that the proposal addresses (e.g. P4.c, P3.d and P2.a; see Section 2).

2. Project Plan. In 5 pages maximum (including figures), describe the proposed project and how it relates to SCEC5 objectives and priorities (see Section 2). References are excluded from the 5-page limit.

- Previous Support or Multiple Proposals. All proposals should include a section reporting on the PI(s) research results from projects previously-funded by SCEC, and/or howconcurrent proposal submissions complement each other, if applicable. This section should emphasize how such efforts relate to, or distinguished themselves from, the current proposal. This section counts toward the 5-page limit.
- Continuation Projects. If the proposed project is a continuation of a prior SCEC award, the project plan must include a 1-page summary of the research results obtained from that SCEC funding. This summary is counted towards the 5-page limit. Continuation proposals must have a section outlining how the proposed research relates to the SCEC5 science objectives.
- Collaborative Proposals. The project plan may include one extra page per investigator to report recent results from previously-funded, related research.
- Technical Activity Proposals. TAG proposals should include a research coordination plan that sets a timetable for successful completion of TAG activities no later than the end of SCEC5. The research coordination plan is counted towards the 5-page limit.
- Workshop Proposals. Workshop proposals that include travel support for international participants must clearly state how such participants are critical to the workshop.
- SURE Intern Project Supplement. The project must include an “intern project” description (1 page maximum) if requesting support for a summer undergraduate intern. In the description briefly describe the project, location(s) where research will take place, the role of the intern in the project, the time span the intern will work on the project, and any specific skills or educational background required. The project description submitted will be used to recruit students and posted on the SCEC Internship website. This description is not included in the 5-page limit.
- Transitions Program Proposals. The SCEC Transitions Program provides students and early-career scientists with resources and mentoring, particularly at major transitions in their educational and professional careers. The project plan should clearly articulate how the proposed activities will expand awareness of

professional advancement opportunities and pathways and/or improve competency in earthquake research tools and techniques of the junior members of the SCEC community.

3. Budget and Budget Justification. Every proposal must include a budget table and budget justification for each institution requesting funding. The budgets should be constructed using NSF categories.

- Budget Guidance. Typical SCEC awards range from $10,000 to $35,000. This is not intended to limit SCEC to a fixed award amount, nor to a specified number of awards, but rather to calibrate expectations for proposals written by SCEC investigators.
- Field Research. Field investigations outside southern California may be considered, provided the proposed research demonstrates direct relevance to SCEC5 goals that are not achievable within the southern California natural laboratory.
- Salary Support. An investigator can receive no more than 1 month of summer salary support in any given year from all combined SCEC funded awards in that year.
- SCEC IT Support. Investigators on proposals that anticipate use of SCEC computational resources and/or help from SCEC software developers should consult with SCEC Special Projects leadership for budget time support estimates and coordination planning.
- International Travel Funding Support. Funding for international travel to participate in the SCEC activities will be considered, provided the proposal clearly states (a) how the investigators are critical to the project and (b) a plan for how the international participant's institution will cost-share the anticipated travel expenses. The requested international funding support should not exceed $1,500 per person in the proposed budget.
- Unallowable Direct Expenses. Under guidelines of the SCEC Cooperative Agreements and A-81 regulations, secretarial support and office supplies are not allowable as direct expenses.
- For each organization requesting funding, the budget information must be entered through the online submission system. This information should also be included in the PDF uploaded at the time of proposal submission.

4. Current and Pending Support. Accurate and up-to-date statements of current and pending support must be included for each Principal Investigator requesting funding on the proposal, following NSF guidelines. If identical or closely related work is also proposed to another institution (e.g., National Science Foundation), an explanation of the relationship of such work to this proposal should be provided. Proposals without a complete current and pending support statement may be rejected and returned without review.

- Each investigator requesting funding must enter his/her current and pending support information through the online submission system. **This information must also be included in the PDF uploaded at the time of proposal submission**.
- Workshop Proposals. Current and pending support information is not required from investigators submitting workshop proposals.

3.4 Proposal Review Process

The annual budget cycle begins with a SCEC Leadership Meeting in early June, where the Board, Planning Committee (PC), Executive Committee of the Center, and agency representatives discuss SCEC research priorities. Based on these discussions, the PC drafts an annual SCEC Science Plan, which is presented to the SCEC community at the Annual Meeting in early September. The PC uses the feedback received at the meeting to finalize the Annual Science Plan, and a project solicitation released in October. SCEC participants submit proposals in response to this solicitation in November. All proposals are independently reviewed by the Director, the Co-Director, Vice-Chair of the PC, and the leaders of at least three relevant science working groups. Reviews are assigned to avoid conflicts of interest.

The PC meets in January to review all proposals and construct an Annual Collaboration Plan. The plan's objective is a coherent science program, consistent with SCEC's basic mission, institutional composition, and budget that achieves the Center's short-term objectives and long-term goals, as expressed in the Annual Science Plan. The PC Chair submits the recommended Annual Collaboration Plan to the Board of Directors for approval. The annual budget

approved by the Board and the Center Director is submitted to the sponsoring agencies for final approval and funding. Upon approval by the agencies, notifications are sent out to the investigators.

To construct the Annual Collaboration Plan, proposals submitted in response to the annual solicitation are evaluated based on: (a) scientific merit of the proposed research; (b) competence, diversity, career level, and performance of the investigators; (c) priority of the proposed project for short-term SCEC objectives; (d) promise of the proposed project for contributing to long-term SCEC goals; (e) commitment of the principal investigator and institution to the SCEC mission; (f) value of the proposed research relative to its cost; and (g) the need to achieve a balanced budget while maintaining a reasonable level of scientific continuity given funding limitations. With respect to criterion (b), improving the diversity of the SCEC community and supporting early-career scientists is a major goal of the Center. It is important to note that a proposal that receives a low rating or no funding does not necessarily imply it is scientifically inferior. Rather, these proposals may be downgraded because they may not meet other criteria noted above.

It should be also noted that SCEC maintains close alignment with the USGS Earthquake Hazards Program through three mechanisms: (1) reporting and accountability required by USGS funding of SCEC, (2) liaison memberships on the Board of Directors by the three USGS offices now enrolled as SCEC core institutions, and (3) a Joint SCEC/USGS Planning Committee (JPC). The JPC augments the SCEC Planning Committee with a group of program leaders designated by the USGS who participate in the construction of the Annual Collaboration Plan. If requested, the PC chair will continue to sit on the Southern California Proposal Review Panel for the USGS External Research Program.

3.5 Award Procedure

The Southern California Earthquake Center is funded by the NSF and USGS through cooperative agreements with the University of Southern California (USC). Additional funding for the annual SCEC research program may be provided by the Pacific Gas & Electric Company, the Keck Foundation, the California Earthquake Authority, geodesy royalty funds, and potentially other external sources. Funding to SCEC supports earthquake research in Southern California that engages an interdisciplinary community of over 1,000 active participants. Funding from external sources have constraints on how they can be spent.

The SCEC research program supports over 100 projects each year. Science funding includes (a) smaller grants for individual scientists working in Center focus areas and collaborations, (b) larger grants for scientists and collaborative teams collecting new data on major Center projects or performing data integration and advanced modeling, and (c) workshops that bring all interested scientists together to focus on specific research initiatives.

Funding received from all sources is combined for the purposes of building the overall Annual Collaboration Plan. Each research award is funded via a cost-reimbursable subcontract between USC and the Investigators' institution. Multiple awards from the same funding source at the same institution might be included in a single contract. Multiple awards at the same institution might be set up from different funding sources as separate contracts. When SCEC funding becomes available to investigators depends on (1) how soon SCEC/USC receives Center funding from the NSF and USGS and other external sources, and (2) how quickly contracts are negotiated between USC and institution to receive funding. Participant support (workshops, intern project supplement, and travel) award expenditures are managed through the master SCEC account at USC. For investigators at USC, the project expenses are also charged directly to the master SCEC account.

For project proposals approved for funding, the investigators submit formal requests for a subaward through their research offices with a final statement of work (SOW), final budget, and budget justification. The formal requests are carefully reviewed at SCEC to ensure that the SOW and budget reflect the approved research. Historically, most budgets include salary funds for the investigator, post-docs, and students (including tuition), materials and supplies to accomplish the research objectives, and travel to the SCEC annual meeting to present research results. SCEC very rarely funds requests for equipment. Budget formats are comparable to normal NSF proposal submission and verified by the submitting organization that they reflect current salaries and costs for other items. Before the final subaward

can be established, the formal request and the original informal submission is submitted to NSF or USGS for approval.

Once a subaward is made, the SCEC Planning Committee and working group leaders monitor the scientific and technical progress of SCEC-funded projects through (1) investigator presentations at the SCEC Annual Meeting, workshops, working group meetings, and/or other national meetings; (2) written project reports submitted to SCEC (www.scec.org/reports/projects); and registration of publications to the SCEC database (www.scec.org/reports/publications). Funded investigators are also required to contribute data and results to the appropriate SCEC resource (e.g., Southern California Earthquake Data Center, database, community model). This information feeds into the annual review of the SCEC program, and allows SCEC to drive and change the direction of research as needed to meet the Center's goals, milestones, and metrics. The Annual Science Plan will be adapted based on the progress by the SCEC community of researchers.

With respect to financial monitoring on the subawards, the SCEC administration team reviews every invoice (a) to ensure expenses are within the approved scope of work, (b) to determine funds spent are reasonable and expensed in a timely manner, and (d) to track who is receiving funds and their level of effort. Any change in scope or major change in budget categories requires approval by the SCEC Director. Detailed documentation will be requested from the investigators when an invoice significantly deviates from the approved budget. The summary financial report submitted by investigators at the end of the budget period also provides critical information for the Center's budget planning for following budget years.

If an investigator submits a successful proposal to SCEC the following year, his/her subcontract is usually amended to add on the new year of funding. Alternatively, investigators may not be funded in consecutive years if (1) they do not submit a proposal or (2) their submitted proposal is unsuccessful. This process means that the roster of participating investigators changes each year as new people and institutions become involved in the SCEC research collaboration. This annual review of the SCEC program (and associated subawards) allows SCEC to drive and change the direction of research as needed to meet the Center's goals, milestones, and metrics. The fact that this is done on an annual basis with so many people and institutions involved is a unique characteristic of SCEC, and very different from how other research centers typically operate.

3.6 SCEC / USGS-EHP Research Coordination

Earthquake research in Southern California is supported both by SCEC and by the USGS Earthquake Hazards Program (EHP). EHP's mission is to provide the scientific information and knowledge necessary to reduce deaths, injuries, and economic losses from earthquakes. Products of this program include timely notifications of earthquake locations, size, and potential damage, regional and national assessments of earthquakes hazards, and increased understanding of the cause of earthquakes and their effects. EHP funds research via its External Research Program, as well as work by USGS staff in its Pasadena (California), Menlo Park (California), Vancouver (Washington), Seattle (Washington), and Golden (Colorado) offices. The EHP also directly supports SCEC.

SCEC and EHP coordinate research activities through formal means, including USGS membership on the SCEC Board of Directors, a SCEC/USGS Joint Planning Committee, appointment of a SCEC representative (usually the PC Chair) to the USGS external research proposal review panel for Southern California, and through a variety of less formal means. Interested researchers are invited to contact Dr. Rob Graves, EHP coordinator for Southern California, or other SCEC and EHP staff to discuss opportunities for coordinated research.

The USGS EHP supports a competitive, peer-reviewed, external program of research grants that enlists the talents and expertise of the academic community, state and local governments, and the private sector. The investigations and activities supported through the external program are coordinated with and complement the internal USGS program efforts. This program is divided into six geographical/topical 'regions', including one specifically aimed at Southern California earthquake research and others aimed at earthquake physics and effects and at probabilistic seismic hazard assessment (PSHA). The Program invites proposals that assist in achieving EHP goals.

The EHP web page, http://earthquake.usgs.gov/research/external, describes program priorities, projects currently funded, results from past work, and instructions for submitting proposals. The annual EHP external funding cycle has

different timing than SCEC's, with the USGS RFP due out in February and proposals due in May. Interested PIs are encouraged to contact the USGS regional or topical coordinators for Southern California, Earthquake Physics and Effects, and/or National (PSHA) research, as listed under the "Contact Us" tab. The USGS internal earthquake research program is summarized at http://earthquake.usgs.gov/research/topics.php.

4. Research by Disciplinary Committees

The Center supports disciplinary science through standing committees in Seismology, Tectonic Geodesy, Earthquake Geology, and Computational Science. They are responsible for disciplinary activities relevant to the SCEC Science Plan, and they make recommendations to the Science Planning Committee regarding the support of disciplinary research and infrastructure.

4.1 Seismology

4.1.1 Research Objectives

The Seismology disciplinary group gathers data on the range of seismic phenomena observed in southern California, develops improved techniques for extracting detailed and robust information from the data, and integrates the results into models of velocity structures, source properties and seismic hazard. We solicit proposals that foster innovations in network deployments and data collection, especially those that fill important observational gaps, real-time research tools, and data processing. Proposals to develop community products that support one or more SCEC5 goals or include collaboration with network operators in southern California are especially encouraged. Proposers should consider the SCEC resources available including (a) the Southern California Earthquake Data Center (SCEDC) that provides extensive data on southern California earthquakes, as well as crustal and fault structure; (b) the network of SCEC funded borehole instruments that record high quality reference ground motions; and (c) the pool of portable instruments operated in support of targeted deployments or aftershock response.

4.1.2. Research Strategies

- Enhance and continue operation of the SCEDC and other existing SCEC facilities, particularly the near-real-time availability of earthquake data and automated access.
- Process network data in real-time to improve estimation of source parameters in relation to faults, short-term evolution of earthquake sequences, and real-time stress perturbations on major fault segments. Understand and reduce the variability and uncertainty of source parameters, and work to resolve discrepancies reported between various methods of estimation, particularly through collaborative, community based research.
- Enhance and continue to develop earthquake catalogs that include smaller events. Develop improved catalogs of focal mechanisms and other source properties. Improve locations of important historical earthquakes.
- Advance practical strategies for densification of seismic instrumentation in Southern California, including borehole instrumentation, and develop innovative algorithms to utilize data from these networks. Develop metadata, archival and distribution models for these semi-mobile networks.
- Develop innovative methods to search for unusual signals using combined seismic, GPS, and borehole strainmeter data; Encourage collaborations with EarthScope or other network operators.
- Investigate near-fault crustal properties, evaluate fault structural complexity, and develop constraints on crustal structures and state of stress.
- Enhance collaborations, for instance with ANSS, that would augment existing and planned network stations with downhole and surface instrumentation to assess site response, nonlinear effects, and the ground coupling of built structures.
- By preliminary design and data collection, seed future passive and active experiments such as dense array measurements of basin structure, fault zones and large earthquake properties, OBS deployments, and deep basement borehole studies.

- Investigate whether earthquake properties in southern California have systematic dependencies on properties of faults, the crust, and anthropogenic activities, which may be used to extract more detailed information from recorded seismic data.

4.1.3 Research Priorities

- Low-cost seismic network data utilization and archiving. New seismic networks utilizing low-cost MEMS accelerometers are currently being developed. We seek proposals on innovative algorithms to utilize data from these networks, develop metadata and archiving models, and make the data and products available to the user community.
- The shallow crust**.** Seismic properties in top few kilometers of the crust have strong effects on ground motion, but are generally not well understood or constrained. Deriving detailed regional images of seismic velocities and attenuation coefficients , that expand the SCEC community models (CXM) to the inelastic material response regime of the shallow crust, is among the research priorities of the Seismology group.
- Tremor and related signals. Tremor has been observed on several faults in California. Although we will continue to consider proposals aiming to detect and analyze tremor in southern California, and to distinguish tremor from other sources that may produce similar signals, such proposals should be mindful of the limited success of similar endeavors to date.
- Earthquake directivity. Rupture directivity can have strong influence on ground motion, but it is not clear if earthquake directivity on given fault sections is systematic or random. We seek proposals on robust estimations of rupture directivities of a large population of earthquakes in relation to the major faults in southern California, and demonstration of applicability to ground motion estimation.
- Seismic coupling. The partitioning between seismic and aseismic deformations strongly affects the seismic potential of faults, but is generally not well known. We seek proposals that develop and implement improved techniques for estimating the seismic coupling of different fault sections, and for constraining the depth-extent of seismic faulting in large earthquakes.
- Short-term earthquake predictability. We seek proposals that develop new methods in earthquake statistics or analyze seismicity catalogs to develop methods for determining short-term (hours to days) earthquake probability gain.
- Processes and properties **in special areas.** We seek proposals that use seismic data to improve the knowledge of structural properties and seismotectonics in southern California, especially those identified as “Earthquake Gates” (see SAFS for definition).

4.2 Tectonic Geodesy

4.2.1 Research Objectives

The Tectonic Geodesy disciplinary group uses geodetic measurements of crustal deformation to understand the interseismic, coseismic, postseismic, and hydrologic processes associated with the earthquake cycle along the complex fault network of the Southern San Andreas system. This activity supports several of the SCEC5 science questions including: How are faults loaded across temporal and spatial scales? What is the role of off-fault inelastic deformation on strain accumulation, dynamic rupture, and radiated seismic energy? The Tectonic Geodesy group also plays a role in earthquake monitoring and response, from tracking surface deformation changes that may precede or accompany induced seismicity, to measuring coseismic displacements and postseismic transients, either in near-real time as part of earthquake early warning, or as part of a coordinated post-earthquake rapid response.

In addition, the group is tasked with developing a Community Geodetic Model (CGM) for use by the SCEC community in system-level analyses of earthquake processes over the full range of length and timescales. The CGM is built on the complementary strengths of temporally dense GPS data and spatially dense InSAR data. Much of the SCEC4 activity was focused on the assembly and testing of GPS and InSAR data sets for measuring secular motions and comparing geodetically inferred fault slip rates with geological rates based on paleoseismic studies (e.g., UCERF3). The quality and quantity of both GPS and InSAR data is rapidly improving to enable a breakthrough in the spatial and temporal resolution of the CGM. In particular, reprocessing of long GPS time series has provided high

accuracy vertical measurements that reveal a wide range of new hydrologic and tectonic signals. In addition, two new C-band InSAR satellites (Sentinel-1A and B) are providing highly accurate systematic coverage of the entire SCEC region every 12 days from two look directions. Developing methods to integrate and update these dense spatio-temporal datasets will be a major task in SCEC5.

4.2.2. Research Strategies

These advances motivate the following strategies:

- Develop vector time series of crustal deformation at ~1 km spatial resolution and better than seasonal temporal resolution.
- Increase vertical precision of multi-decadal GPS time series.
- Develop methods to estimate robustly spatial and temporal uncertainties in GPS/InSAR/combined time series.
- Provide derived geodetic data products such as strain rate maps, displacement fields, common mode signals, seasonal signals, and noise assessments.
- Develop methods to constrain the extent of permanent, off-fault deformation, and its contribution to geodetic fault slip-rate estimates.
- Improve methods for characterizing transient deformation, including episodic aseismic creep, the effects of surface hydrology and anthropogenic activity, and both short- and long-term postseismic deformation transients, and for decomposing geodetic time series into secular and transient components.
- Develop and test mechanistic models of the crustal deformation associated with hydrology and/or anthropogenic activities, with a view to gaining insight into the processes associated with induced seismicity.
- Improve techniques for inferring fault rupture parameters from time-limited geodetic data.
- Develop block models and earthquake cycle models that contribute to and utilize the emerging Community Rheology Model (CRM) to understand the importance of spatial variations in rheology on geodetic inversions for fault slip and crustal strain.
- Use these data in combination with other SCEC Community Models, as well as physical models, to address the major SCEC science questions.

4.2.3 Research Priorities

The major research priorities this year are:

- Community Geodetic Model (CGM) secular velocities. Produce a consensus secular velocity InSAR product using the full archive of SAR data (ERS, Envisat, ALOS-1) for southern California. Coordination between participating groups in this effort is encouraged. Continue to develop methods to improve error characterization and/or reduction in secular geodetic velocity estimates, e.g. by refined analysis of campaign GPS data in combination with large-area InSAR analyses, by developing improved noise models, or by improving methods for mitigating temporally or spatially correlated noise.
- Community Geodetic Model (CGM) time series. Produce a consensus time series GPS product integrating both continuous and campaign data. Coordination between participating groups in this effort is encouraged. Develop methods for processing, updating and integrating InSAR time series in near-real time, using the latest generation of SAR satellites (e.g. Sentinel-1, ALOS-2). Continue to develop methods for GPS/InSAR time series integration for southern California, including methods that combine multiple InSAR data sets with different viewing geometries and temporal sampling rates.
- Off-fault deformation. Develop methods for constraining the proportion of the southern California deformation budget that is not accommodated by the major faults, and its uncertainty.
- Research pertaining to other community models. Foster the development of models that include spatial variations in crustal rheology, including 4D models of the earthquake cycle, and models of contemporary crustal strain and/or fault slip rates, to motivate development of the Community Rheology Model. Work with other SCEC scientists to develop the Community Stress Model as well as an improved understanding of how stress varies from the earthquake cycle timescale to the mountain building timescale (see SDOT).

- GPS data collection and preparation for earthquake rapid response. Collect campaign GPS data in areas of sparse GPS coverage and poor InSAR correlation. Develop a coordinated rapid response GPS capability, including updating GPS site coordinates in the vicinity of major faults, in preparation for a major event.
- Community Outreach. Work with the SCEC Communication, Education & Outreach group to highlight the importance of geodetic measurements for improving earthquake forecasting.

4.3 Earthquake Geology

4.3.1 Research Objectives

The Earthquake Geology disciplinary group promotes studies of the geologic record of the Southern California natural laboratory that advance SCEC science. Its primary focus is on the Late Quaternary record of faulting and ground motion, including data gathering in response to major earthquakes. Earthquake Geology also fosters research activities motivated by outstanding seismic hazard issues, understanding of the structural framework and earthquake history of faults in southern California, and contributes significant information to the statewide Unified Structural Representation and the Community Rheology Model (CRM). Collaborative proposals that cut across disciplinary boundaries are encouraged.

4.3.2. Research Strategies

- Paleoseismic documentation of earthquake ages and displacements, with emphasis on long paleoseismic histories, coordinated slip-per-event and incremental slip-rates, and system-level behavior (e.g. seismic supercycles, fault evolution or slip rate variability).
- Gathering well-constrained slip-rates on the southern California fault system, with emphasis on major structures, along-strike variations, quantification of uncertainties, and comparison with geodetic observations and fault-loading models.
- Mapping and analysis of fault-zone geometries, mechanical properties, compositions, and fluid histories in regions where the seismogenic zone, the brittle-ductile transition or the ductile roots of major fault zones have been exhumed.
- Quantifying variations in fault roughness, complexity, strain localization, and damage in relation to the rupture propagation processes, including the extent, magnitude, and mechanisms of off-fault deformation and potential indicators of paleoseismic rupture direction.
- Improving the statewide community fault model in areas of inadequate fault representations or where new data is available, such as using high-resolution topographic data sets to better define fault traces, spatial uncertainty, and stochastic heterogeneity of fault geometry, and the addition of new fault geometries based on geophysical data.
- Validating ground motion prediction through analysis and dating of precariously balanced rocks and other fragile geomorphic features.
- Developing a geologic framework for the Community Rheology Model (CRM) that is consistent with existing and emerging geologic and geophysical observations, and the tectonic history of southern California.

4.3.3 Research Priorities

- Development of a paleoseismic event model to facilitate regional correlation with paleoclimate and other proxy records, document record completeness, and to enhance comparison of event history with the outcomes of earthquake simulations.
- Link fault representations within the statewide community fault model to slip rate information used to develop the Uniform California Earthquake Rupture Forecast, and alternative sources, where appropriate, in order to enhance utility of the model for simulations.
- Data synthesis and new data gathering targeted at understanding fault behavior through the Cajon Pass Earthquake Gate Area (see SAFS for definition).

- Improve constraints on fault-rupture hazard (magnitude-displacement scaling) specific to the California plate boundary fault system.
- Develop methods or models for estimating fault displacements at the surface and at depth for the evaluation of risk to infrastructure (as relevant for EEII). Consider primary fault displacement (main fault trace), secondary fault displacement (distributed deformation zones in the near-field are around faults) as well as vertical tectonic motion.
- Data synthesis and new data gathering aimed at developing and refining 3D long-wavelength geologic models of the lithotectonic provinces defined for the CRM.

4.3.4 Geochronology Infrastructure

The shared geochronology infrastructure supports C-14 and cosmogenic dating for SCEC-sponsored research. The purpose of shared geochronology infrastructure is to allow flexibility in the number and type of dates applied to each SCEC funded project as investigations proceed. Investigators requesting geochronology support should clearly state in their proposal an estimate of the number and type of dates required. For C-14, specify if sample preparation will take place at a location other than the designated laboratory. For cosmogenic dating, investigators are required to arrange for sample preparation and include these costs in the proposal budget. Investigators are encouraged to contact the investigators at the collaborating laboratories prior to proposal submission. Currently, SCEC geochronology has established relationships with the laboratories listed in table below for C-14 and cosmogenic dating.

Investigators may request support for geochronology outside of the infrastructure program for methods not listed here or if justified on a cost-basis. These requests must be included in the individual proposal budget, and will normally involve a collaborative proposal with the participating geochronologist. This includes OSL, pIR-IRSL and U-series dating, each of which are techniques that require that the geochronologist work closely with the project PI. Several investigators and laboratories, listed below, are available for collaboration on SCEC projects.

	Method	Laboratory	Contact	Email
Geochron-ology Infra-structure	C-14	University of California at Irvine	John Southon	jsouthon@uci.edu
		Lawrence Livermore National Lab	Tom Guilderson	tguilderson@llnl.gov
	Cosmo-genic	Lawrence Livermore National Lab	Susan Zimmerman	zimmerman17@llnl.gov
Individual Collab-orative Proposals	OSL / pIR-IRSL	University of Cincinnati	Lewis Owen	lewis.owen@uc.edu
		Utah State University	Tammy Rittenour	tammy.rittenour@usu.edu
		Desert Research Institute	Amanda Keen-Zebert	akz@dri.edu
	U-Series	Berkeley Geochronology Laboratory	Warren Sharp	wsharp@bgc.org

Student participation in lab analysis is strongly encouraged by SCEC and by all participating geochronology laboratories. Please direct questions regarding geochronology infrastructure to the Earthquake Geology group leader, Mike Oskin (meoskin@ucdavis.edu).

Data Reporting Requirements. Funded investigators are required to provide full reporting of metadata for their geochronology samples, including sample preparation , and geographic/stratigraphic/geomorphic context (what was dated?) before samples are submitted for analysis. Contact the Earthquake Geology group leader, Mike Oskin (meoskin@ucdavis.edu), to arrange for analysis and a link and spreadsheet for metadata submission.

4.4 Computational Science (CS)

4.4.1 Research Objectives

The Computational Science disciplinary group promotes the use of advanced numerical modeling techniques, data intensive (big-data) computing, and high performance computing (HPC) to address the emerging needs of SCEC users and the scientific community on a variety of computer systems, including HPC platforms. The group works with SCEC scientists across a wide range of topics to take advantage of rapidly changing computer architectures and

algorithms. We engage and coordinate with national HPC labs, centers, and service providers in crosscutting efforts to enable large-scale and data-intensive computing milestones. The group encourages research using national supercomputing resources, and supports students from both geoscience and computer science backgrounds to develop their skills in the area. Projects listing Computational Science as their primary area should involve significant software-based processing, big-data synthesis, or HPC in some way. Proposed research with the potential to be transferred to data intensive and HPC applications should make this explicit and include Computational Science as a secondary focus area. Research utilizing standard desktop computing should list the most relevant non-Computational Science working group as the primary area.

Computational Requirements. If your proposed research requires substantial computing resources or allocations we suggest that you could benefit from coordinating your computing needs with the SCEC IT Architect and/or Special Projects Leaders. Investigators on proposals that anticipate use of SCEC computational resources and/or help from SCEC software developers should consult with SCEC Special Projects leadership for budget time support estimates and coordination planning.

Note that researchers may request startup allocations from NSF's Extreme Science and Engineering Discovery Environment (XSEDE) at https://www.xsede.org/allocations, before coordinating with SCEC special projects, as a way to determine whether XSEDE computing resources will be useful to their research.

4.4.2. Research Strategies

- Reengineer and optimize existing HPC codes for CPU-based, GPU-based, and manycore-based (e.g. Xeon Phi) supercomputers; or adapt existing or develop new HPC codes using emerging supercomputer hardware architectures; with emphasis on issues such as performance, portability, interoperability, power efficiency, and reliability; and focusing on software elements that can contribute to reaching SCEC research goals.
- Develop software tools needed to support large-scale simulations, such as software tools for building simulations meshes, data management tools for distributing simulation results, or visualization tools for improving analysis and presentation of large-scale simulation results.
- Develop novel algorithms and implementation of more realistic models for earthquake simulation, particularly those that improve efficiency and accuracy or expand the class of problems that can be solved (see SCEC5 Thematic Areas).
- Optimize earthquake cycle simulators that can resolve fault processes across the range of scales required to investigate stress-mediated fault interaction, including those caused by dynamic wave propagation, or that combine coseismic dynamic rupture and multi-cycle simulators; generate synthetic seismicity catalogs; and assess the viability of earthquake rupture forecasts.
- Develop tools and algorithms for uncertainty quantification in large-scale inversion and forward-modeling studies, for managing I/O, data repositories, workflows, advanced seismic data format, visualization, and end-to-end approaches.
- Develop data-intensive computing tools, including but not limited to, InSAR and geodesy, lidar and structure-from-motion, 3D tomography, cross-correlation algorithms used in ambient noise seismology, and other signal processing techniques used, for example, to search for tectonic tremor and repeating events.
- Develop new or adapt existing software architectures and application programming interfaces (APIs) that can contribute to building new, or integrating existing SCEC community models (CXMs), and how these can be used with HPC applications for modeling and simulation; with emphasis in software development for accelerating model creation, data synthesis, manipulation and integration, and model building (meshing and gridding) and visualization, (see also SCEC Community Models Research Priorities).

4.4.3 Research Priorities

- Community Models (CXMs)
    - Develop tools that can accelerate community building of new (or existing) community models. These may include but are not limited to the design of versatile data-structures and application

libraries (software elements) for data manipulation and integration, meshing and gridding, and visualization of community models.
    - Develop tools that can help integrate different community models between themselves and/or with simulation software. These may include but are not limited to the design software interfaces capable of connecting in efficient manners HPC simulation codes with community models.
- Seismic wave propagation
    - Develop tools and implement procedures to validate SCEC community fault and seismic velocity models as applied in inverse and forward problems.
    - Develop and improve existing software tools and algorithms with application to HPC that accelerates and advances high-frequency simulation methods, while contributing to solve standing research problems as stated in the Ground Motions interdisciplinary group priorities.
    - Develop software tools and algorithms to incorporate more realistic constitutive material models and material model representation with application in wave propagation HPC codes. Examples include, but are not limited to, developing efficient tools and algorithms for modeling inelastic deformation, scattering by small-scale heterogeneities, and topography.
- Tomography
    - Develop new or adapt existing forward modeling software to solve full 3D tomography (F3DT) problems using HPC resources. Computational Science research in this area should help diversify current dependency on existing software and provide alternatives for SGT and F3DT verification, as done in dynamic rupture and forward ground motion simulation.
    - Develop efficient and sustainable computational procedures to facilitate the assimilation of regional waveform data in the SCEC community velocity models (CVMs); and integrate F3DT and inversion results into existing CVMs.
- Rupture dynamics
    - Develop computational codes that incorporate more sophisticated and realistic descriptions of fault weakening processes, complex fault geometry, and material heterogeneity and inelastic response in large-scale earthquake simulations, ideally with minimal impact on computational efficiency. This might require novel numerical approaches like adaptive mesh refinement.
    - Develop computational codes that merge single event rupture models with earthquake cycle models.
- Scenario earthquake modeling
    - Develop software processing tools such as workflows that can facilitate modeling a suite of scenario ruptures, incorporating material properties and fault geometries from SCEC community models, and investigate the sensitivity of simulations to models and modeling parameters.
    - Develop alternative methods using machine learning techniques that could potentially accelerate or optimize use of HPC resources in physics-based earthquake hazard calculations.
    - Isolate causes of amplified ground motion using adjoint-based sensitivity methods.
- Data-intensive computing
    - Develop computational tools for advanced signal processing algorithms, such as those used in ambient noise seismology and tomography as well as InSAR and other forms of geodesy.
    - Integrate Big Data analytics techniques involving software stacks such as Hadoop/Spark, fault recovery, data format, generation, partitioning, abstraction, and mining.
    - Evaluate alternative computational methods to determine the tradeoffs between the scientific effectiveness and the computational costs of these alternatives.
- Engineering applications
    - Develop computational tools to investigate the implications of ground motion simulation results by integrating observed and simulated ground motions with engineering-based building response models; and to validate the results by comparison to observed building responses.

- Develop and advance existing computational platforms that will facilitate end-to-end modeling capabilities that can help transform earthquake risk management into a cyberinfrastructure science and engineering discipline.

5. Research by Interdisciplinary Working Groups

SCEC coordinates earthquake system science through interdisciplinary working groups including: Fault and Rupture Mechanics (FARM), Stress and Deformation Over Time (SDOT), Earthquake Forecasting and Predictability (EFP), and Ground Motions (GM). The Southern San Andreas Fault Evaluation (SoSAFE) group has evolved into the San Andreas Fault System (SAFS) working group for SCEC5. This group coordinates research on the San Andreas and the San Jacinto master faults. Also new in SCEC5 is the SCEC Community Models (CXM) working group, focused on developing, refining and integrating community models that describe a wide range of features of the southern California lithosphere and asthenosphere. Seismic hazard and risk analysis research continues to be coordinated by the Earthquake Engineering Implementation Interface working group. Their activities include educational as well as research partnerships with practicing engineers, geotechnical consultants, building officials, emergency managers, financial institutions, and insurers.

5.1 Fault and Rupture Mechanics (FARM)

5.1.1 Research Objectives

The Fault and Rupture Mechanics (FARM) interdisciplinary working group develops (1) constraints on the properties, conditions and physical processes that control faulting in the lithosphere over the entire range of pre-, co-, and post-seismic periods using field, laboratory, and theoretical studies; and (2) physics-based fault models applicable to various spatial and temporal scales, such as nucleation, propagation and arrest of dynamic rupture or long-term earthquake sequence simulations. This fundamental research aims to develop physics-based understanding of earthquakes in the Southern California fault system and contribute to SCEC hazards estimates such as the Uniform California Earthquake Rupture Forecast (UCERF) and physics-based ground motion predictions.

5.1.2. Research Strategies

Observational constraints on earthquake physics come from a range of sources, including seismology, geodesy, field geology, borehole geophysics, heat flow, hydrology, and gravity. Insights into earthquake physics are obtained by targeted laboratory fault and rock mechanics experiments and theoretical studies. Numerical modeling is used for understanding, analyzing, and relating theories, laboratory findings, and observations as well as exploring the implications of the findings. FARM supports fundamental research using these and related approaches. FARM research strategies include:

- Field, laboratory, and theoretical studies to determine spatial (including depth-dependent) and temporal variations in evolving fault strength and the effect of various relevant factors such as temperature, composition, pore pressure, degree of shear localization, and damage, including the variations and heterogeneity of relevant fault and rock properties.
- Theoretical and laboratory studies of nucleation, propagation, and arrest of seismic and aseismic fault slip.
- Seismological, geodetic, geophysical, laboratory and theoretical determinations of earthquake triggering, including triggering by static and dynamic stressing, fluid injection (induced earthquakes), and aseismic deformation.
- Geologic descriptions of fault complexity and shear zone structure, their relation to fault-scale and system-scale structural complexity, and representations suitable for inclusion in physics-based models.
- Characterization of fault damage zones and their evolution over both seismic and interseismic periods using seismological, geodetic, geologic, laboratory, and numerical experiments.
- Inferences and measurements of fault zone pore pressure, fluid flow, and their temporal and spatial variation.
- Development of improved numerical approaches to interrogate various temporal and spatial scales of faulting, including long-terms simulations of fault slip that incorporate inertial effects during earthquakes and

geologic/fault system scale earthquake simulations (simulators) for the next generation of seismic hazard estimates ('beyond PSHA').

5.1.3 Research Priorities

- Constrain how absolute stress, fault strength and rheology vary with depth on faults.
- Determine the mechanisms dominant in coseismic (dynamic) fault resistance, including the relative importance of various potential dynamic weakening mechanisms and off-fault processes, and their compatibility with observational constraints such as stress drops and temperature measurements.
- Determination of the scaling with magnitude of seismic source parameters, such as radiated energy or stress drop. Understanding and reducing the variability and uncertainty of these parameters, and working to resolve discrepancies reported between various methods of estimation, so that these source parameters can be accurately incorporated into ground motion studies and numerical and rheological models. In particular, we encourage collaborative, community based work on this topic.
- Investigate the effect of fine-scale processes on the nucleation and dynamic rupture of large earthquakes and the resulting ground shaking, including whether fine-scale processes can be suitably coarse-grained at the system scale.
- Investigate the relation between material, geometrical, and dynamic (deformation-induced) on- and off-fault heterogeneity, its effect on rupture initiation, propagation, and arrest, and implications for radiated energy, slip and rupture speed distributions, their scaling, and ground motion.
- Investigate how inelastic strain associated with fault roughness and discontinuities influences rupture propagation, seismic radiation, and scaling of earthquake source parameters.
- Determine how damage zones, crack healing and cementation, fault zone mineralogy, and off-fault yielding govern strain localization, slip stability, interseismic strength recovery, and rupture propagation.
- Determine how much off-fault inelasticity contributes to strain accumulation and what fraction of strain is relaxed by aseismic processes.
- Describe how fault complexity and inelastic deformation interact to determine the probability of rupture propagation through structural complexities.
- Assess how shear resistance and energy dissipation depend on the maturity of the fault system, and how these are expressed geologically.
- Constrain the active geometry, degree of localization and rheology of the vicinity of brittle-ductile transition - including frictional sliding stability transition zone - and ductile roots of fault zones, and determine their implications for depth limits of large earthquakes, overlap of seismic and aseismic slip, geodetic estimates of fault locking, and transition from frictional sliding to visco-plastic flow.
- Study the mechanical and chemical effects of fluid flow, both natural and anthropogenic, on faulting and earthquake occurrence, and how they vary throughout the earthquake cycle.
- Determine how seismic and aseismic deformation processes interact, and how that interaction affects long-term fault behavior, by conducting laboratory experiments at the appropriate temperatures and stress conditions, and by developing numerical simulations that incorporate both seismic and interseismic periods and a combination of relevant physical factors, e.g., establishing the long-term effect of off-fault damage during earthquakes and off-fault healing during the interseismic periods, exploring how slow slip and microseismicity redistributes stress for the following large events, and determining how large events can rupture into interseismically stable fault regions due to coseismic weakening.
- Study the implications of earthquake physics findings on earthquake hazard by developing physics-based long-term simulations of earthquake sequences on fault systems (earthquake simulators).
- Use numerical models to investigate which fault properties are compatible with paleoseismic findings, including average recurrence, slip rate, coefficient of variation of earthquake recurrence, and the possibility of system-wide “supercycles,” e.g. periods of several large earthquakes followed by periods of their absence; determine whether such behavior can be compatible with the currently observed statistics of smaller-magnitude events.

- Exploit anthropogenic (induced) seismicity as experiments in earthquake physics and earthquake predictability.

5.2 Stress and Deformation Over Time (SDOT)

5.2.1 Research Objectives

The focus of Stress and Deformation Over Time (SDOT) interdisciplinary working group is to improve our understanding of how faults in the crust are loaded in the context of the wider lithospheric system. SDOT studies lithospheric processes on timescales from tens of millions of years to tens of years using the structure, geological history, and physical state of the southern California lithosphere as a natural laboratory. One objective is to characterize the present-day state of stress and deformation on crustal-scale faults and the lithosphere as a whole, and to tie this stress state to the long-term evolution of the lithospheric architecture through geodynamic modeling. Another central goal is to contribute to the development of a physics-based, probabilistic seismic hazard analysis for southern California by developing and applying system-wide deformation models.

5.2.2. Research Strategies

Addressing the SDOT research objectives requires a better understanding of fundamental quantities including lithospheric driving forces, the relevant rock rheology for processes acting over a wide range of time scales, fault constitutive laws, and the spatial distribution of absolute deviatoric stress. Tied in with this is a quest for better structural constraints, such as on density, rock type, Moho depths, thickness of the seismogenic layer, the geometry of lithosphere-asthenosphere boundary, as well as basin depths, rock type, temperature, water content, and seismic velocity and anisotropy. These quantities are constrained by a wide range of observables from disciplines including geodesy, geology, and geophysics.

Specific SDOT strategies include:

- Seismological imaging of the crust, lithosphere and upper mantle using interface and transmission methods.
- Examinations of geologic inheritance and evolution, on faults and off, and its relation to the three-dimensional (3D) structure and physical properties of the present-day crust and lithosphere.
- Development of models of interseismic, earthquake cycle, and long-term deformation
- Development of models using approaches that may include analytical or semi-analytical methods, spectral approaches, boundary, finite, or distinct element methods.

5.2.3 Research Priorities

- Characterize the 3D distribution of isotropic and anisotropic wave speed variations. Assemble 3D lithological models of the crust, lithosphere, and mantle based on active- and passive-source seismic data, potential field data, and surface geology.
- Contribute to the development of the geologic framework for the Community Rheology Model (CRM).
- Advance research into averaging, simplification, and coarse-graining approaches in numerical models across spatio-temporal scales, addressing questions such as the appropriate scale for capturing fault interactions, the adequate representation of frictional behavior and dynamic processes in long-term interaction models, fault roughness, structure, complexity and uncertainty.
- Develop models to estimate slip rates on southern California faults, fault geometries at depth, and spatial distribution of slip or moment deficits on faults. Incorporate rheological and geometric complexities in such models and explore mechanical averaging properties. Assess potential discrepancies of models based on geodetic, geologic, and seismic data. Provide informative slip rates for fault representations defined by the Community Fault Model (CFM) for usage in earthquake simulator activities.
- Develop deformation models (fault slip rates and locking depths, off-fault deformation rates) in support of earthquake rupture forecasting.
- Develop improved estimates of spatio-temporal variations of stress based on inversions of earthquake focal mechanisms.

- Determine the spatial scales at which tectonic block models (compared to continuum models) provide descriptions of fault system deformation that are useful for earthquake forecasting.
- Develop interseismic and long-term deformation models that incorporate inelastic deformation. Develop models that can predict the relative proportions of elastic, recoverable strain associated with the earthquake cycle and permanent, distributed strain in the crust.
- Develop more comprehensive models for understanding the role of fluids on 3D and time-dependent deformation; improve our usage and application of geodetic data that are heavily influenced by hydrologic processes within the crust..
- Apply stress and deformation measurements at various time scales for hypothesis testing of issues pertaining to postseismic deformation, fault friction, rheology of the lithosphere, seismic efficiency, the heat flow paradox, stress and strain transients, stress complexities at earthquake gates and fault system evolution. Improved constraints on the active geometry and rheology of ductile roots of fault zones.
- Contribute to the Community Stress Model (CSM). Development of spatio-temporal (4D) representations of the stress tensor in the southern California lithosphere using diverse stress constraints (e.g. from borehole or anisotropy measurements) and geodynamic models of stress.
- Contribute to the Community Thermal Model (CTM) and Community Rheology Model (CRM) (see Community Models Research Priorities). Test provisional rheology models with numerical models and geodetic, seismic, and geologic data. Assess sensitivity of stress and deformation patterns to parameter variations to facilitate determining what level of detail is needed in the CRM and CTM.
- Develop vertical deformation models (interseismic and multi-earthquake cycle) that incorporate improved vertical constraints from the Community Geodetic Model (CGM). Improve analyses of model sensitivity to non-tectonic vertical motion signals.
- Develop earthquake cycle stress models consistent with paleoseismic chronologies (slip estimates and event dates) that investigate stress accumulation and stress drop sequences over multiple earthquake cycles.

5.3 Earthquake Forecasting and Predictability (EFP)

5.3.1 Research Objectives

The Earthquake Forecasting and Predictability (EFP) interdisciplinary working group coordinates five broad types of research projects: (1) the development of earthquake forecast methods, (2) the development of methods for evaluating the performance of earthquake forecasts, (3) expanding fundamental physical or statistical knowledge of earthquake processes relevant for forecasting, (4) the development and use of earthquake simulators to understand predictability in complex fault networks, and (5) fundamental understanding of the limits of earthquake predictability.

5.3.2. Research Strategies

We seek proposals that will increase our understanding of how earthquakes might be forecasted, to what extent and precision earthquakes are predictable, and what is the physical basis for earthquake predictability. Proposals of any type that can assist in this goal will be considered. To increase the amount of analyzed data and reduce the amount of time required to learn about predictability, proposals are welcome that deal with global data sets and/or include international collaborations.

We encourage researchers to consider how their proposals may further the objectives of special project working groups focussing on earthquake predictability and forecasting: the Collaboratory for Interseismic Simulation and Modelling (CISM, section 6.4), the Collaboratory for the Study of Earthquake Predictability (CSEP, section 6.2), and the Working Group on California Earthquake Probabilities (WGCEP, section 6.1).

5.3.3 Research Priorities

- Enhance methodology for evaluating forecasts of finite-size earthquake ruptures against past and/or future observations, including geological, geodetic, and seismological data.

- Enhance statistical methods of analyzing spatio-temporal patterns of seismicity, including cluster identification and declustering methods, in connection with understanding the physical basis of earthquake predictability.
- Assess the limitations of long-term earthquake rupture forecasts by combining patterns of earthquake occurrence and strain accumulation with neotectonic and paleoseismic observations of the last millennium.
- Place useful geologic bounds on the character and frequency of multi-segment and multi-fault ruptures of extreme magnitude.
- Determine the spatial scales at which tectonic block models (compared to continuum models) provide descriptions of fault-system deformation that are useful for earthquake forecasting.
- Develop earthquake simulators that encode the current understanding of earthquake physics for elucidating predictability.
- Test the hypothesis that “seismic supercycles’’ seen in earthquake simulators actually exist in nature and explore the implications for earthquake predictability.
- Describe how fault complexity and inelastic deformation interact to determine the probability of rupture propagation through structural complexities, and determine how model-based hypotheses about these interactions can be tested by the observations of accumulated slip and paleoseismic chronologies.
- Constrain the extent of permanent, off-fault deformation, and its contribution to geologic and geodetic fault slip-rate estimates.
- Evaluate how the stress transfer among fault segments depends on time, at which levels it can be approximated by quasi-static and dynamic elastic mechanisms, and to what degree inelastic processes contribute to stress evolution.
- Assess the predictive power of the Coulomb stress hypothesis by testing physics-based clustering models against multiple earthquake sequences across various tectonic settings.
- Exploit anthropogenic (induced) seismicity as experiments in earthquake predictability. Proposals that align with USGS priorities are particularly welcome (see, e.g., p. 40-43 of the Open File Report on “Incorporating Induced Seismicity into the US National Seismic Hazard Model”, http://pubs.usgs.gov/of/2015/1070/pdf/ofr2015-1070.pdf).
- Study the mechanical and chemical effects of fluid flows, both natural and anthropogenic, on faulting and earthquake occurrence, and how they vary throughout the earthquake cycle.
- Strengthen testing methodology that accounts for epistemic uncertainties, dependence and observational errors in seismicity and rupture forecasts.
- Support government agencies in their efforts to deploy Operational Earthquake Forecasting (OEF) systems by developing real-time forecasting tools and protocols, including estimates of real-time data uncertainty and ensemble modelling techniques.
- Connect earthquake early warning algorithms with short-term earthquake forecast models to produce ground motion forecasts that span a range of timescales.

5.4 Ground Motions (GM)

5.4.1 Research Objectives

The primary goal of the Ground Motions (GM) interdisciplinary working group is to study the characteristics of ground motion data; understand and model the complex wave propagation mechanisms that give rise to these characteristics (e.g., nonlinearity, scattering effects); implement these models in physics-based ground motion simulation methodologies to predict strong-motion broadband waveforms and their effects (e.g., constitutive models for off-fault plasticity and permanent ground deformation); and validate the simulated time-series using ground motion data and their statistics.

Both source and path characterization play a vital role in ground-motion prediction and are important areas of research for this group. An important focus for SCEC5 is the development of methodologies for validation of ground-motion simulations against observed data, and the implementation and testing of these methodologies. Another important focus of SCEC5 is to investigate the role of nonlinear material deformation and material failure on

simulated ground motions. The GM focus group seeks to understand and simulate the conditions under which nonlinear effects reduce the ground surface shaking; the conditions which cause amplification due to impedance contrasts between stiff and soft crustal layers accentuated by material yielding; and the more dramatic effects of ground failure such as liquefaction and landslides. The overarching goal is to produce simulated ground motions that are valid across a range of magnitudes, distances, and frequency bands, but especially for large magnitudes at close distances.

Given the emphasis of SCEC5 on nonlinear phenomena, which manifest in the vicinity of the fault as well as in the near-surface, the shallow crust (soils and rocks, previously known as the Geotechnical Layer or GTL) is a constituent of the path. In turn, to incorporate near-surface nonlinear effects in physics-based simulations, the GM focus group seeks proposals that develop and implement rheological models for the materials that comprise the shallow crust. These models should account for the computational and modeling challenges of large-scale simulations as outlined by the Computational Science (CS) Working Group and by the SCEC Community Models (CXM) Focus Group (see pertinent sections). These shallow crust inelastic models should lastly enable predictions of phenomena that govern the risk of infrastructure systems, as outlined research priorities of the Earthquake Engineering Implementation Interface (EEII) Focus Group and of some of the Special Projects.

5.4.2. Research Strategies

- Analyze ground motion data and develop models that capture the observed characteristics of recorded data, such as how the frequency content, amplitude, duration and their spatio-temporal variability scale with magnitude and distance.
- Develop 3D rheology models (velocity, anelastic attenuation, nonlinear properties) of rock and soil materials of the shallow crust, for integration in physics-based nonlinear wave propagation simulations.
- Validate ground motion simulations through development and testing of algorithms that trace the predictability and uncertainties of the simulated ground motions across frequency ranges.
- Continue development of the SCEC Broadband Platform.
- Coordinate efforts across the working groups, possibly via the formation of Technical Activity Groups (TAGs). Example of a TAG that would benefit the GM group would focus on the modeling, integration and simulation of nonlinear phenomena in the near-surface soft sediments (effort cuts across CS, EEII, CXM and GM).

5.4.3 Research Priorities

- Gather and develop novel data sets to be used as ground motion data for application to any of the research priorities. This may include, but certainly not limited to different sources (i.e., small magnitude earthquakes, tremor/low-frequency earthquakes, ambient noise), new instrumentation types (cell-phone accelerometers, strainmeter data, etc), or large data sets.
- Use observed ground-motion data to infer physical understanding of the controls on ground motion, to aid in the development of ground-motion simulations. Determine the relative roles of fault geometry, heterogeneous frictional resistance, directivity, wavefield scattering, intrinsic attenuation, and near-surface nonlinearities in controlling ground motions.
- Determination of the scaling with magnitude of seismic source parameters, such as radiated energy or stress drop. Understanding and reducing the variability and uncertainty of these parameters, and working to resolve discrepancies reported between various methods of estimation, so that these parameters can be accurately incorporated as source information into ground motion studies. In particular, we encourage collaborative, community based work on this topic.
- Develop three-dimensional constitutive models to capture nonlinear phenomena such as off-fault plasticity, permanent ground deformation and earthquake triggered ground failure in physics-based simulations, especially in the near-field, where there is paucity of recorded data.
- Contribute to the development of a community rheology model for the shallow crust (including anelastic attenuation,nonlinear properties, heterogeneity, etc.) to capture nonlinear phenomena such as off-fault plasticity, permanent ground deformation and earthquake triggered ground failure phenomena in physics-based simulation (especially in the near-field, where there is paucity of recorded data). Use

available borehole measurements, near-surface material stiffness proxies (e.g., Vs30, topography) and/or empirical correlations to estimate input parameters necessary for the physics-based nonlinear ground motion simulations. This effort should be coordinated with the research priorities and activities of the SCEC Community Models (CXM), to ensure that the sedimentary models are properly constrained by the rheological properties of the deeper Community Velocity Model structure (including the 3D geometry of sedimentary basins), and avoid spurious reflections from fictitious impedance contrasts that could emerge from improper integration of the sedimentary layers with the underlying rock basement.

- Quantify the epistemic and parametric uncertainties of these models; and develop protocols on how to map material proxies (such as Vs30, or velocity profiles where available) and empirical estimates of the nonlinear soil and rock parameters (e.g., friction angle as a function of confining pressure) on the input parameters. Coordinate with research priorities and activities of the SCEC Community Models (CXM) (especially the velocity and rheology models); of the Fault and Rupture Mechanics (FARM) group with respect to the development and implementation of consistent material models for fault-zone and off-fault plasticity of rocks; and of the Computational Science (CS) group for the integration of these models in large-scale simulations.
- Develop statistical models of the sedimentary layers for stochastic media realizations, intended to capture scattering attenuation for the SCEC Broadband Platform (BBP) and for 3D physics-based simulations (see Community Models Research Priorities). Consider anisotropy in mapping the differences between lateral and vertical heterogeneities. Compare simulated ground motions from rough faults propagating through realistic heterogeneous media to simulated ground motions representing scattering via anelastic frequency dependent attenuation and to historical data.
- Conduct systematic verification (comparison against theoretical predictions) of the simulation methodologies with the objective to develop robust and transparent simulation capabilities that incorporate consistent and accurate representations of the earthquake source and three-dimensional velocity structure.
- Conduct systematic validation of ground-motion simulation methodologies to appropriate observed historical ground-motion data. Trace the modeling and parametric uncertainties of the simulated ground motions. Conduct validation across frequency ranges (each representative of the scale of the model input parameters and source models). Compare synthetic ground motions from deterministic and stochastic approaches to data for overlapping bandwidths. Validate specific elements, such as source, path or site components, of the complex physics-based simulation models to identify topics where improvement is necessary. Coordinate with Earthquake Engineering Implementation Interface (EEII), to work on validation for engineering applications.
- Incorporate new effects and features in the SCEC Broadband Platform such as multi-segment rupture; nonlinear amplification factors; spatial variability of crustal properties; 3D basins and their on ensemble averaged long-period ground motions (e.g., by comparing ensemble averages of long-period (<~1Hz) ground motions computed in 1D and 3D crustal models for events included in the GMSV). Develop and implement methods for computing and storing 3D Green's functions, both source- and site-based, (see CXM section for related efforts).

5.5 San Andreas Fault System (SAFS)

5.5.1 Research Objectives

The San Andreas Fault System (SAFS) interdisciplinary working group will develop projects within SCEC that are focused on the occurrence of large earthquakes on the San Andreas Fault system, seeking (1) projects that collect and analyze data on the timing and size of large earthquakes on the SAFS and (2) projects that investigate the features of the fault system that may halt or permit continued rupture. This second class of projects falls under a new SCEC5 initiative called “Earthquake Gates” for multidisciplinary study of conditional earthquake rupture. The Cajon Pass region has been selected as an earthquake gate area for SCEC5. Research proposals to study conditional rupture in other regions or settings within southern California are welcome.

5.5.2. Research Strategies

A. Research on the timing and size of large earthquakes on the San Andreas Fault System are encouraged that utilize
   - High-resolution imaging of ground deformation (in trenches or preserved in topography)
   - Data collection and analysis of vertical deformation associated with coseismic land-level changes on reverse faults and coastal faults
   - Modern geochronologic techniques, or exploration of uncertainties in paleoearthquake or geomorphic event dating

B. The Earthquake Gates initiative is designed to bring together groups of collaborators across multiple disciplines to investigate the features that promote or arrest large earthquakes on the San Andreas Fault System. The goal is to study features that may conditionally arrest ruptures so that at some times the gate is 'closed' while at other times the gate is 'open' in order to better forecast earthquake behavior. The Cajon Pass Region has been selected as an Earthquake Gate for SCEC5 and has a specific Integrated Science Plan (www.scec.org/research/ega).

5.5.3 Research Priorities

- Basic research on the occurrence of large earthquakes on the San Andreas Fault System. This includes study of the factors that lead to occurrence and preservation of ground rupture and offsets, as well as improved dating and correlation techniques for development of fault rupture histories.
- Cajon Pass Earthquake Gate Area
    - Gather data to characterize evidence of earthquake deformation and related ground shaking using methods such as LiDAR, photogrammetry, geologic mapping, paleoseismology, InSAR/GPS, precariously balanced rocks and well data.
    - Gather geophysical, seismological and well data to characterize subsurface conditions related to geology, material properties (e.g. crustal velocities and fault strength), material interfaces as well as stress state and style of faulting. Material properties and stress state information will interface with Community Model (CRM and CSM) efforts.
    - Evaluate and improve the Community Fault Model 3D fault representations in the Cajon Pass area using improved 3D velocity models, relocated seismicity, geophysical constraints and insights from kinematic and mechanical models. For example, a passive portable seismic array, refraction microtremor and ambient noise studies may yield critical insights on fault structure, how and where major faults intersect, or the characteristics of other important interfaces at depth.
    - Develop more realistic 3D representations of subsurface conditions within the Cajon Pass that include complexities, such as active secondary faults and important material interfaces, and incorporate these representations into forward crustal deformation models, geodetic inversions and dynamic rupture models that are consistent with independent datasets.
- Additional EGAs will not be considered for SCEC5; however PIs interested in conditional earthquake rupture outside of Cajon Pass are encouraged to coordinate their efforts and propose related research.

5.6 SCEC Community Models (CXM)

5.6.1 Research Objectives

The SCEC CXM working group develops, refines and integrates community models describing a wide range of features of the southern California lithosphere and asthenosphere. These features include: elastic and attenuation properties (Community Velocity Model, CVM), temperature (Community Thermal Model, CTM), rheology (Community Rheology Model, CRM), stress and stressing rate (Community Stress Model, CSM), deformation rate (Community Geodetic Model, CGM), and fault geometry (Community Fault Model, CFM). The goal of the CXM working group is to provide an internally consistent suite of models that can be used to simulate seismic phenomena in southern California.

SCEC5 research goals involve continued refinement of existing community models (CFM, CVM, CSM, CGM), continuing development of newer community models (CTM and CRM), and integration of the models into a self-consistent suite. Objectives also include quantification of uncertainties and development of techniques for propagating uncertainties from observations through community model development to simulation predictions.

5.6.2. Research Strategies

- Develop and apply inversion techniques to populate and refine the community models.
- Collect additional observations to improve resolution of a community model and/or resolve discrepancies among competing models.
- Develop viable alternative community models that facilitate representation of the epistemic uncertainty.
- Develop methods to characterize uncertainty in each of the community models.
- Validate individual community models and verify consistency across multiple community models (e.g., consistency of stress predictions from the CTM and CRM with the CSM).
- Use community models in simulations to forecast behavior, including estimates of the uncertainties in predicted values.
- Expand community participation in model development, validation, and application through workshops, tutorials, and participation in and/or collaboration with related efforts (e.g., EarthCube).

5.6.3 Research Priorities

- Science integration. Convene a workshop focused on guiding community model development towards self-consistent and well-integrated community models.
- Information technology integration. In collaboration with the Community Modeling Environment (CME) and the CXM developer- and user-communities, develop detailed documentation defining standard user-interface(s) and storage formats for the community models. Design goals include: ease of use, computational efficiency, and common interfaces and storage for each class of model (e.g., grid-based or object-based). The documentation should include complete specification of user-interfaces as well as appropriate use cases for each community model. Emphasis is on defining long-lasting, effective standards.
- Training. Provide virtual or in-person hands-on training in how to use the existing community models in research applications. Training should target user needs (e.g., from surveys of the community). Training should be archived for on-demand access.
- Small scale features. Develop methods to represent smaller scale features in the CXMs, such as stochastic variations in elastic properties, attenuation, stress, temperature, rheology, and fault strike and dip.
- Validation. Develop and apply procedures (i.e., goodness-of-fit measures) for evaluating updated CXMs against observations (e.g., seismic waveforms, gravity, etc) to discriminate among alternatives and quantify model uncertainties.
- Community Fault Model (CFM)
    - Improve and evaluate the CFM, placing emphasis on defining the geometry of major faults that are incompletely, or inaccurately, represented in the current model, and on faults of particular concern, such as those that are located close to critical facilities.
    - Refine representations of the linkages among major fault systems.
    - Generate maps of geologic surfaces compatible with the CFM that may serve as strain markers in crustal deformation modeling and/or property boundaries in future iterations.
    - Collaborate with developers of related data products to improve consistency in the organization and naming scheme (e.g., USGS Fault and Fold database).
- Community Velocity Model (CVM)
    - Integrate new data (especially the Salton Sea Imaging Project) into the existing CVMs with validation of improvements in the CVMs for ground-motion prediction.
    - Quantify uncertainty in the CVM structure and its impact on simulated ground motions.
    - Develop efficient and sustainable computational procedures to facilitate the assimilation of regional waveform data into the CVMs (see Computational Science Research Priorities).

- Community Stress Model (CSM)
    - Assess sensitivity of stress and deformation patterns to parameter variations to facilitate determining what level of detail is needed in the CRM and CTM.
    - Compile diverse constraints on stress (e.g. from borehole or anisotropy measurements) and evaluate the accuracy of the CSM (see Stress and Deformation Over Time Research Priorities).
- Community Geodetic Model (CGM)
    - See Tectonic Geodesy Research Priorities.
- Community Thermal Model (CTM)
    - Deliver a preliminary CTM that provides temperatures throughout the southern California lithosphere and asthenosphere consistent with radiogenic heat production.
    - Improve/interpolate surface heat flow maps. Search for additional heat flow and thermal property data in areas with poor coverage.
- Community Rheology Model (CRM)
    - Develop a preliminary geologic framework for remaining domains based on geological consensus, and identify reasonable ductile flow laws for pertinent rock types. Compare predicted seismic velocities with the SCEC CVM.
    - Characterize sensitivity of rock rheology to composition, water content, strain rate and temperature to assess the relative importance of these factors.
    - Compare brittle-ductile transition and crustal strength distribution inferred from the CRM with the distribution of seismicity with depth.
    - Evaluate candidate/provisional CRM's against postseismic deformation models, with focus on the Mojave and Salton Trough regions.
    - Add provisional representations of shear zones (rheology and width) to the CRM based on simulations and natural examples at all available exposure levels, and test these for consistency with depth of rupture propagation, post-seismic deformation, and geodetic and seismically inferred locking depth.
    - Assess the relative importance of basal tractions, and appropriate boundary conditions for plate-boundary scale deformation models.
    - Investigate the importance of rheological anisotropy (from distributed fabric or localized shear zones) to the dynamics of the regional deformation
    - Hold workshops addressing high-priority topics suggested by 2017 CRM workshop attendees: shear zones, upper crustal rheologies, the brittle-ductile transition, and/or the Salton Trough region.

5.7 Earthquake Engineering Implementation Interface (EEII)

5.7.1 Research Objectives

The purpose of the Earthquake Engineering Implementation Interface (EEII) is to create and maintain collaborations with research and practicing engineers. These activities may include ground motion simulation validation, as well as the end-to-end analysis of structures and infrastructure systems. Our goal of impacting engineering practice and large-scale risk assessments requires partnerships with the engineering and risk-modeling communities, which motivates the following activities.

5.7.2. Research Strategies

Example strategies to achieve these objectives include:

- Perform engineering and risk analysis using SCEC research products related to hazards and ground motions, in order to determine the impact of research insights on engineering decisions, and sensitivity of engineering-related result to parameters in the science models.
- Develop tools and approaches that facilitate the transfer of SCEC science products to the research community.

- Form groups to reach consensus on methods to validate and utilize simulated ground motions, simulation-based hazard maps, and other SCEC science products of relevance to engineers and risk analysts.

5.7.3 Research Priorities

Ground motion simulation validation and utilization

- Develop, coordinate and vet methods for validating simulations of ground motions for engineering use.
- Demonstrate ground motion simulation validation methodologies with existing simulated ground motions.
- Develop methodologies to validate and use SCEC CyberShake and high-frequency ground motion simulations for developing probabilistic and deterministic hazard maps for building codes and other engineering applications. Investigations of observed versus simulated region-specific path effects for small-magnitude earthquakes in southern California are encouraged.
- Develop data, products or tools that enable physics-based hazard calculations or ground motions to be utilized by engineers and risk modelers.
- Identify or demonstrate links between ground motion metrics or structural response parameters and ground motion simulation features, so that simulation models and/or algorithms might be improved to better represent ground motion features of interest.
- Quantify and evaluate spatial variation in amplitudes from regional ground motion simulations, for the purpose of validating simulations versus observations from empirical networks, and for quantifying the role of geological features in the observed variation.

Collaboration in engineering and risk analysis

- Assess the performance of distributed infrastructure systems using simulated ground motions. Evaluate the potential impact of basin effects, rupture directivity, spatial distribution of ground motion, or other phenomena on risk to infrastructure systems.
- Enhance the reliability of simulations of long period ground motions in the Los Angeles region using refinements in source characterization and seismic velocity models, and evaluate the impacts of these ground motions on tall buildings and other long-period structures (e.g., bridges, waterfront structures).
- Identify the sensitivity of structural response to ground motion parameters and structural parameters through end-to-end simulation. Buildings of particular interest include non-ductile concrete frame buildings.
- Perform detailed assessments of the results of ground motion simulation scenarios, as they relate to the relationship between ground motion characteristics and structural response and damage.
- Develop improved site/facility-specific and portfolio/regional risk analysis (or loss estimation) techniques and tools, and implement them in software tools.
- Identify earthquake source and ground motion characteristics that control damage and financial loss estimates.
- Evaluate the spatio-temporal correlation of ground motions at regional scales from recordings and using CyberShake data. Compare and validate CyberShake results with empirical correlations.
- Develop methods or models for estimating fault displacements at the surface and at depth for the evaluation of risk to large distributed infrastructures. Consider primary fault displacement (main fault trace), secondary fault displacement (distributed deformation zones in the near-field are around faults) as well as vertical tectonic shift which would cause tilt in distributed infrastructure.

Proposals for other innovative projects that would further implement SCEC information and techniques in seismic hazard, earthquake engineering, risk analysis, and ultimately loss mitigation, are encouraged.

6. Research by Special Projects Working Groups

Special Projects are organized around large-scale projects funded through special grants outside of the NSF-USGS cooperative agreements that support the SCEC base program, but have synergistic goals and are aligned with the overall SCEC research program priorities. The current Special Projects teams include Working Group on California

Earthquake Probabilities (WGCEP), the Collaboratory for the Study of Earthquake Predictability (CSEP), the Community Modeling Environment (CME), the Collaboratory for Interseismic Simulation and Modeling (CISM), and Mining Seismic Wavefields.

6.1 Working Group on California Earthquake Probabilities (WGCEP)

The Working Group on California Earthquake Probabilities (WGCEP) is a collaboration between SCEC, the U.S. Geological Survey, and California Geological Survey aimed at developing official earthquake-rupture-forecast models for California. The project is closely coordinated with the USGS National Seismic Hazard Mapping Program, and has received financial support from the California Earthquake Authority (CEA). The WGCEP has now completed all three main UCERF3 models: the long-term, time-independent model (UCERF3-TI, which relaxes segmentation and includes multi-fault ruptures); the long-term, time-dependent model (UCERF3-TD, which includes elastic-rebound effects); and the complete model (UCERF3-ETAS, which includes spatiotemporal clustering to account for the fact that triggered events can be large and damaging). The latter (UCERF3-ETAS) is now being evaluated as potential basis for operational earthquake forecasting (OEF). Information on all models is available at http://wgcep.org/ucerf3. We are also starting to plan for UCERF4, which we anticipate will utilize physics-based simulators to a greater degree (see last bullet below).

The following research activities would contribute to WGCEP goals:

- Evaluate fault models in terms of the overall fault connectivity at depth (important for understanding the likelihood of multi-fault ruptures) and the extent to which faults represent a well-defined surface versus a proxy for a braided deformation zone.
- Evaluate existing deformation models, or develop new ones, in terms of applicability of GPS constraints, categorical slip-rate assignments (based on “similar” faults), applicability of back-slip methods, and other assumptions. Of particular interest is the extent to which slip rates taper at the ends of faults and at fault connections.
- Evaluate the UCERF3 finding that 30% to 60% of off-fault deformation may be aseismic.
- Help determine the average along-strike slip distribution of large earthquakes, especially where multiple faults are involved (e.g., is there reduced slip at fault connections?).
- Assess the average down-dip slip distribution of large earthquakes, which may be the ultimate source of existing discrepancies in magnitude-area relationships. Are surface slip measurements biased in estimating slip at depth?
- Develop a better understanding of the distribution of creeping processes and their influence on rupture dimension and seismogenic slip rate.
- Contribute to the compilation and interpretation of mean recurrence-interval estimates (including uncertainties) from paleoseismic data and/or develop site-specific models for the probability of undetected events at paleoseismic sites.
- Develop ways to constrain the spatial distribution of maximum magnitude for background seismicity (for earthquakes occurring off of the explicitly modeled faults).
- Address the question of whether small volumes of space exhibit a Gutenberg Richter distribution of nucleations, both on and off faults.
- Develop improved estimates (including uncertainties) of the total long-term rates of observed earthquakes for different sized volumes of space.
- Refine our magnitude completeness estimates (as a function of time, space, and magnitude). Develop such models for use in real-time applications such as operational earthquake forecasting.
- Develop methods for quantifying elastic-rebound based probabilities in un-segmented fault models.
- Help quantify the amount of slip in the last event, and/or average slip over multiple events, on any major faults in California (including variations along strike).
- Develop models for fault-to-fault rupture probabilities, especially given uncertainties in fault endpoints.

- Determine the extent to which seismicity rates vary over the course of historical and instrumental observations (the so-called Empirical Model of previous WGCEPs), and the extent to which this is explained by decaying aftershock sequences.
- Determine the applicability of higher-resolution smoothed-seismicity maps for predicting the location of larger, more damaging events.
- Explore the UCERF3 “Grand Inversion” with respect to: possible plausibility filters, relaxing the UCERF2 constraints, not over-fitting data, alternative equation-set weights, applying a characteristic-slip model, and applicability of the Gutenberg Richter hypothesis on faults (see report at www.WGCEP.org).
- Develop methods for combining spatiotemporal clustering with long-term forecast models.
- Are sequence-specific parameters for aftershock sequences warranted?
- Determine if there is a physical difference between a multi-fault rupture and a separate event that was triggered quickly.
- Develop more objective ways of setting logic-tree branch weights, especially where there are either known or unknown correlations between branches.
- Develop easily computable hazard or loss metrics that can be used to evaluate and perhaps trim logic- tree branches.
- Develop techniques for down-sampling event sets to enable more efficient hazard and loss calculations.
- Because all models will be wrong at some level, develop valuation metrics that allow one to quantify the benefit of potential model improvements in the context of specific uses.
- Develop novel ways of testing UCERF3, especially ones that can be integrated with CSEP. For example, UCERF3-ETAS could be tested against historic ruptures that have occurred in the state.
- Address the extent to which large triggered events can or cannot nucleate from within the rupture area of a main shock (the answer has an important influence on UCERF3-ETAS results).
- Help constrain the distance decay of triggered earthquakes, especially in light of a finite seismogenic thickness and a depth-dependent rate of earthquake nucleation.
- Compile global datasets of large-event triggering, and compare with the more robust statistics available for smaller events. Also try to quantify the extent of spatial overlap between large main shocks and large triggered events (an important metric that could be used to tune models like UCERF3).
- Study and test the behavior of computational earthquake-cycle simulators, envisioning that they could become essential ingredients in future UCERF projects and a cornerstone of SCEC5. The goal is to develop the capability of simulators to be able to contribute meaningfully to hazard estimates. Important tasks include:
    - Study and test, using code verification exercises and more than one code, the sensitivity of simulator results to input details including fault-system geometry, stress-drop values, tapering of slip, methods of encouraging rupture jumps from fault to fault, cell size, etc.
    - Develop physically realistic ways of simulating off-fault seismicity.
    - Add additional physics into simulators, for example, the inclusion of high-speed frictional weakening and of off-fault viscoelastic and heterogeneous elastic properties.
    - Develop alternate methods of driving fault slip besides “back-slip”.
    - Make access to existing simulators easy for new users, including adequate documentation and version numbers, examples of input and output files for initial testing, and access to analysis tools. Publicize availability.
    - Develop new approaches to designing simulators and/or of making them more computationally efficient, including the use of better algorithms, point source Green’s functions, and GPUs.
    - Develop validation tools for simulators, utilize existing UCERF data comparison tools with them, and develop capabilities for simulators to interact with UCERF infrastructure.
    - Develop the capability of simulators to deal with UCERF and SCEC CFM fault geometries, both for rectangular and triangular cell representations.

- Create statewide synthetic earthquake catalogs spanning 100 My using as many different simulators as possible, in order to generate statistically significant behavior on even slow-slipping faults. Use small time-steps to permit evaluation of short-term clustering.
- Use these catalogs as synthetic laboratories for CSEP testing as described under CSEP.
- Data-mine these catalogs for statistically significant patterns of behavior. Evaluate whether much-shorter observed catalogs are statistically distinguishable from simulated catalogs. Consider and explore what revisions in simulators would make simulated catalogs indistinguishable from observed catalogs.
- Develop and test a variety of statistical methods for determining the predictability of earthquakes in these simulated catalogs, especially with respect to large triggered earthquakes.
- Compute other data types such as gravity changes, surface deformation, InSAR images, in order to allow additional comparisons between simulated results and observations.

Further suggestions and details can be found at http://www.WGCEP.org, or by contacting the project leader (Ned Field: field@usgs.gov; (626) 644-6435).

6.2 Collaboratory for the Study of Earthquake Predictability (CSEP)

CSEP is developing a virtual, distributed laboratory—a collaboratory—that supports a wide range of scientific prediction experiments in multiple regional or global natural laboratories. This earthquake system science approach seeks to provide answers to the questions: (1) How should scientific prediction experiments be conducted and evaluated? and (2) What is the intrinsic predictability of the earthquake rupture process?

A major focus of CSEP is to develop international collaborations between the regional testing centers and to accommodate a wide-ranging set of predictability experiments involving geographically distributed fault systems in different tectonic environments.

6.2.1. Priorities for CSEP

- Develop retrospective and prospective tests of UCERF3-ETAS**.** This new WGCEP model combines fault-based long-term time-dependence with short-term earthquake clustering and specifies forecasts as a set of simulated catalogs. New strategies for retrospective and prospective testing are required to evaluate the model.
- **Develop forensic tools** for understanding what aspects of a model dominate CSEP results.
- Evaluate the Coulomb stress hypothesis. Assess the predictive skill of forecast models based on Coulomb stress through retrospective and prospective experiments on multiple earthquake sequences. For example, build on the retrospective evaluation of physics-based and statistical forecasting models during the 2010-12 Canterbury, New Zealand, earthquake sequence by applying these models to other earthquake sequences in different tectonic settings.
- Global experiments. Develop and test global high-resolution models that (i) encode fundamental hypotheses about earthquake occurrence at a global scale for faster evaluation, and (ii) elucidate differences in the predictability of earthquakes across tectonic settings.
- Strengthening evaluation methodologies. Develop computationally efficient performance metrics of forecasts and predictions that can account for epistemic uncertainties and evaluate forecasts specified as sets of simulated catalogs (e.g., simulation-based ETAS models or UCERF3-ETAS).
- Supporting Operational Earthquake Forecasting (OEF). (i) Developing forecasting methods that address real-time data deficiencies, (ii) update forecasts on an event basis and evaluating forecasts with overlapping time-windows or on an event basis, (iii) improve short-term forecasting models, (iv) develop prospective and retrospective experiments to evaluate OEF candidate models.
- Earthquake rupture simulators. Develop experiments to evaluate the predictive skills of earthquake rupture simulators, against both synthetic (simulated) and observed data (see also the WGCEP and CISM sections), with specific focus on how to automate the identification of a large earthquake with a modeled fault.

- External Forecasts and Predictions. Develop and refine experiments to evaluate forecasts and predictions generated outside of CSEP, including operational forecasts by official agencies and prediction algorithms based on seismic and electromagnetic data;
- Induced seismicity. Develop models and experiments to test forecasts of induced seismicity, e.g. in California or Oklahoma. Proposals that align with USGS priorities are particularly welcome (see, e.g., p. 40-43 of the Open File Report on "Incorporating Induced Seismicity into the US National Seismic Hazard Model", http://pubs.usgs.gov/of/2015/1070/pdf/ofr2015-1070.pdf).
- Hybrid/ensemble modeling. Develop methods for forming optimal hybrid and ensemble models from multiple probability-based or alarm-based forecasting models;
- Evaluating hazard models. Develop methodologies for prospectively evaluating seismic hazard models and their components (e.g., ground motion models).
- Forecasting focal mechanisms. Develop methodology to forecast focal mechanisms and evaluating the skill of such forecasts.
- Paleo-based forecasts. Develop experiments to test the fault rupture and earthquake probabilities implied by paleoseismic investigations of California faults (e.g., testing probabilities of future ruptures at paleoseismic sites where numerous ruptures have been documented, the relative effectiveness of proposed fault segment boundaries at stopping ruptures, and the relative frequency of on-fault and off-fault ruptures in California) (see also the WGCEP and SoSafe sections).

6.2.2 General Contributions

- Establish rigorous procedures in controlled environments (testing centers) for registering prediction procedures, which include the delivery and maintenance of versioned, documented code for making and evaluating forecasts including intercomparisons to evaluate predictive skills.
- Construct community-endorsed standards for testing and evaluating probability-based, alarm-based, fault-based, and event-based predictions.
- Develop hardware facilities and software support to allow individual researchers and groups to participate in prediction experiments.
- Design and develop programmatic interfaces that provide access to earthquake forecasts and forecast evaluations.
- Provide prediction experiments with access to data sets and monitoring products, authorized by the agencies that produce them, for use in calibrating and testing algorithms.
- Characterize the influence of limitations and uncertainties of such data sets (e.g., completeness magnitudes, source parameters, real-time vs post-processed data uncertainties).
- Conduct workshops to facilitate international collaboratories.

6.3 Community Modeling Environment (CME)

The Community Modeling Environment (CME) is a SCEC special project that develops improved ground motion forecasts by integrating physics-based earthquake simulation software, observational data, and earth structural models using advanced computational techniques including high performance computing (HPC). CME researchers develop methods that improve physics-based ground motion forecasts using an iterative process involving four computational pathways which include (1) use of GMPEs, (2) use of deterministic wave propagation simulations, (3) use of dynamic ruptures, and (4) use of full 3D tomography. CME research makes use of the structural and computational models developed by other SCEC research groups including SCEC CFMs, CVMs, earthquake rupture forecasts, GMPEs, deterministic wave propagation methods, dynamic rupture methods, and tomographic methods. The simulation tools used in CME activities include rupture generators (dynamic and kinematic), wave propagation models (low and high frequency), nonlinear site response modules, and validation capabilities (including assembled observational strong motion data sets and waveform-matching goodness-of-fit algorithms and information displays).

6.3.1 SCEC Computational Platforms

The SCEC community can contribute research activities to CME by providing scientific or computational capability that can improve ground motion forecasts for any of the activities described below.

OpenSHA Platform. The OpenSHA Platform provides an open-source probabilistic seismic hazard analysis software platform, including the reference implementations the UCERF2 and UCERF3. The OpenSHA platform makes use of SCEC community models, including the CFM, and it provides input parameters used in CyberShake hazard model calculations, and is used to analyze and evaluate CyberShake hazard model results.

Broadband Platform. The open-source Broadband Platform (BBP) provides a verified, validated, and user-friendly computational environment for generating broadband (0-100Hz) ground motions. The BBP includes a suite of kinematic source models, wave propagation codes and site response modules to calculate suites of synthetic seismograms from user-specified rupture sets, structural models, and station sets.

High-F Platform. The High-F platform comprises source and wave propagation codes (kinematic ruptures with the AWP-ODC wave propagation code and Hercules for both) used by SCEC researchers to push earthquake simulations to higher frequencies (> 1Hz). High-F activities aim at including more realistic physics while improving the upper frequency limits of physics-based ground motions. Physics models currently tested in the High-F platform include those for fault roughness, near-fault plasticity, frequency-dependent attenuation, topography, small-scale near-surface heterogeneities, and near-surface nonlinearities.

CyberShake Platform. The CyberShake Platform provides physics-based probabilistic seismic hazard curves and maps using seismic reciprocity to generate large ensembles of ground motion simulations (> 10^8). CyberShake combines an earthquake rupture forecast (currently UCERF2) with a kinematic source generator (Graves and Pitarka) and a wave propagation code (AWP-ODC) to provide rates of exceedance of ground motions.

F3DT Platform. This platform integrates the software needed for full-3D waveform tomography using the adjoint-wavefield and scattering-integral formulations of the structural inverse problem. F3DT can invert both earthquake waveforms and ambient-field correlograms for high-resolution crustal models, and it can refine the centroid moment tensors of earthquakes by matching observed waveforms with 3D synthetics.

Unified Community Velocity Model Platform. The UCVM platform provides an easy-to-use software framework for comparing and synthesizing 3D Earth models and delivering model products to users. UCVM is used as a repository and delivery system for Community Velocity Models (CVMs) developed by SCEC researchers. UCVM allows the generation of large simulation meshes which can be used for High-F and CyberShake simulations.

6.3.2 Research Priorities

In addition to specific priorities described in the Ground Motions section, the CME group is seeking proposals to:

- Develop codes to be included in an upcoming dynamic rupture platform, DynaShake. DynaShake is intended to operate in a fashion similar to the BBP, where independent codes can input standardized input parameters, and calculate standardized output results, that can be evaluated using agreed upon validation methods for realistic hazard-scale ruptures. Dynamic rupture code developers must be willing to work under an open source license. Preference will be given to codes that have been verified under the Dynamic Rupture Code Verification Technical Activity Group and to codes that have been parallelized or are in the process of being parallelized to run on multiple core systems (clusters and HPC).
- Improve and integrate models for source generation, wave propagation, and site effects into any of CME's simulation platforms. This can include the development of scientific software that simulates one or more physical processes from the source to the surface.
- Improve our ability to extend ground motion simulations to higher frequencies and to improve the accuracy of such models through the integration of better physics. Proposals can be targeted to any of the ground motion simulations platforms, but are most relevant in the context of High-F.

- Develop the computational and integration frameworks to extend 3D structural modeling capabilities to the BBP.
- Develop or improve ground motion simulation validation computational and organizational tools. Research in this area would contribute to the efforts under the ground motion simulation validation (GMSV) technical activity group and the EEII. Validation of ground motions and models is important for any and all of the simulation platforms under CME.
- Improve the accuracy of community velocity models (CVMs), through the development of techniques that may involve, for example, the development of 3D tomography codes as well as the integration of geology constraints into CVMs. Proposals are also sought to improve the methodologies used for integration of models from different sources and scales within UCVM.
- Develop tools for decimating the UCERF3 model for use within CyberShake for specific regions (Southern and Central California) and accounting for the loss of precision and accuracy from the simplified model.
- Evaluate the spatio-temporal correlation of ground motions at regional scales from recordings and using CyberShake data. Compare and validate CyberShake results with empirical correlations.
- Continue development and provide improved capabilities of codes (current and/or prospective) used by the SCEC community. An important aspect of this priority is to support the porting of codes to the evolving pool of HPC systems and to improve code performance.

We also encourage proposals that address the implementation and propose solutions to the data management tasks included in the SCEC5 Data Management Plan.

6.4 Collaboratory for Interseismic Simulation and Modeling (CISM)

The Collaboratory for Interseismic Simulation and Modeling (CISM) is an effort to forge physics-based models into comprehensive earthquake forecasts using California as its primary test bed. Short-term forecasts of seismic sequences, in combination with consistent long-term forecasts, are critical for reducing risks and enhancing preparedness. CISM involves multiple specialties and groups, including those from WGCEP and CSEP and those involved with earthquake simulators. The Planning Committee is welcoming proposals that support CISM in its mission to improve predictability by combining rupture simulators that account for the physics of rupture nucleation and stress transfer with ground-motion simulators that account for wave excitation and propagation. CISM forecasting models will be tested against observed earthquake behaviors within the existing CSEP. Detailed research priorities associated with CISM include the use and calibration of earthquake simulators and priorities listed under the WGCEP and CSEP sections.

7. Communication, Education, and Outreach Activities

SCEC's Communication, Education, and Outreach (CEO) program facilitates learning, teaching, and application of earthquake research. In addition, SCEC/CEO has a global public safety role in line with the third element of SCEC's mission: "Communicate understanding of earthquake phenomena to end-users and society at large as useful knowledge for reducing earthquake risk and improving community resilience." The theme of the CEO program in SCEC5 is Partner Globally, Prepare Locally. Our partnerships foster new research opportunities and ensure the delivery of research and educational products that improve the preparedness of the general public, government agencies, businesses, research and practicing engineers, educators, students, and the media—locally in California as well as in other states and countries. Prepare Locally not only refers to improved resiliency to local hazards, but also to preparing students and the public for the future with the enhanced science literacy to make informed decisions to reduce their risk, and to preparing future scientists via research opportunities and support through career transitions. In SCEC5, the CEO program will manage and expand activities within four CEO focus areas:

1. Knowledge Implementation connects SCEC scientists and research results with practicing engineers, government officials, business risk managers, and other professionals active in the application of earthquake science.
2. The Public Education and Preparedness focus area will educate people of all ages about earthquakes, tsunamis, and other hazards, and motivate them to become prepared.

3. The K-14 Earthquake Education Initiative will improve Earth science education in multiple learning environments, overall science literacy, and earthquake safety in schools and museums.
4. Finally, the Experiential Learning and Career Advancement program will provide research opportunities, networking, and other resources to encourage and sustain careers in STEM fields. See the next section for a description about SCEC's new Transitions Program.

The long-term outcomes of these focus areas are to: improve application of earthquake system science in policy and practice; reduce loss of life, property, and recovery time; increase science literacy; and increase diversity, retention, and career success in the scientific workforce.

Investigators interested in contributing to CEO activities are strongly advised to contact Mark Benthien (213-740-0323; benthien@usc.edu) before submitting a proposal since alternative approaches may be more appropriate.

7.1 Transitions Program

7.1.1. Program Objectives

In order to accomplish the long-term outcome of increasing diversity, retention, and career success in the scientific workforce, CEO is launching a new Transitions Program in SCEC5. This program will provide students and early-career scientists with resources and mentoring, particularly at major transitions in their educational and professional careers. In doing so, the Transitions Program aims to encourage and sustain careers in the geosciences and other STEM fields.

7.1.2. Program Strategies

The SCEC Transitions Program welcomes proposals that expand awareness of professional advancement opportunities and pathways, as well as improve competency in earthquake research tools and techniques for students of the SCEC community.

Major priorities for this year are activities that support:

- Career Development. Workshops, seminars, or webinars that provide opportunities for students to (1) learn about career pathways; (2) develop networking techniques; and (3) gain insight on navigating STEM [science, technology, engineering, and mathematics] careers.
- Specialized Research Skills Development. Student training opportunities that develop or improve knowledge and skills in earthquake science research, particularly those relevant to SCEC5 priorities. Activities could include web-based trainings, in-person short courses (with travel support) that provide hands-on experiences, or a combination of these approaches.

Investigators interested in contributing to the Transitions Program priorities described above should contact Gabriela Noriega (213-821-1117; gnoriega@usc.edu) before submitting a proposal.

Saturday, September 8

09:00 - 17:00 **Workshop: Predictive Skill across Tectonic Settings and Planning CSEP2.0,** Maximilian Werner, Thomas Jordan, Warner Marzocchi, Andy Michael, David Rhoades, and Hiroshi Tsuruoka (https://www.scec.org/workshops/2018/csep)

09:00 - 17:00 **Workshop: Toward a SCEC Community Rheology Model (CRM) Workshop,** Wayne Thatcher, Whitney Behr, Elizabeth Hearn, Greg Hirth and Michael Oskin (https://www.scec.org/workshops/2018/crm)

09:00 - 17:00 **Fieldtrip: Cajon Pass Earthquake Gate Area,** Julian Lozos, Nate Onderdonk, and Craig Nicholson (https://www.scec.org/workshops/2018/cajon)

09:00 - 17:00 **Training: SCEC Software Products,** Philip Maechling, Christine Goulet, and Tran Huynh (https://www.scec.org/workshops/2018/software)

Sunday, September 9

07:00 - 17:00 **SCEC Annual Meeting Registration & Check-In,** Hilton Lobby

09:00 - 22:30 **SCECmeetUP Space Available,** Tapestry Room

To facilitate informal, small group discussions at the SCEC Annual Meeting, the Tapestry Room is available for anyone to use without reservations at the designated times. Meeting rooms for groups up to 24 people are also available with reservations for 2-hour blocks. See the sign-up sheet in the Hilton Lobby to reserve a room for your group.

09:00 - 12:00 **SCEC Special Projects Planning Meeting,** Christine Goulet

13:30 - 17:00 **Workshop: Media Interview Theory and Practice, Through War and Peace,** Jason Ballmann, Mark Benthien, and Zachary Hall (https://www.scec.org/workshops/2018/communications)

13:00 - 17:00 **Workshop: Integrated Science for the Cajon Pass Earthquake Gate Area,** Julian Lozos, Nate Onderdonk, and Craig Nicholson (https://www.scec.org/workshops/2018/cajon)

15:00 - 17:00 **Poster Set-Up,** Plaza Ballroom

17:00 - 18:00 **Welcome Social,** Hilton Lobby and Plaza Ballroom

18:00 - 19:00 **Distinguished Speaker Presentation,** Horizon Ballroom

Earthquake and Fault System Dynamics: Putting the Pieces Together, Jim Dieterich

In nature earthquakes do not occur as independent events on faults that are isolated in time and space. Rather they occur as emergent phenomena from the system dynamics of geometrically complex fault networks. Earthquake simulations that integrate fault system geometry, evolving stress conditions from interactions among earthquakes, and rate- and state-dependent fault constitutive properties capture well-established system-level characteristics of earthquakes including scaling statistics and Omori-type space-time clustering. In addition, long simulations with the California fault system and Cascadia models point to some relationships that would not be particularly obvious in the short historical record of earthquake observations. Among the relationships of possible significance to short- and long-term forecasts are 1) repeating slip patterns in large earthquakes whose characteristics are tied to the local fault system geometry and loading conditions; 2) the important role of structural complexities in both limiting through-going ruptures and enhancing earthquake clustering; and 3) the dependence of clustering rates on local stress conditions, which affect the probabilities of foreshock/mainshock sequences. Looking ahead, there is much room for further development of fault and earthquake system simulations. Of particular interest is the coupling of fault system simulations and background seismicity occurring off of the major modeled faults. One-way coupling of the background seismicity rates to stress changes from slip on the modeled system faults is doable in the short-term. A proof-of-concept implementation of full coupling appears to be quite promising.

James H. Dieterich's research interests have to do with the mechanics of deformation processes, particularly as they relate to earthquake and volcanic phenomena. Areas of emphasis include development of governing relations for earthquake nucleation and earthquake occurrence; estimation of earthquake probabilities; fault constitutive properties; and coupled interactions between magmatic activity, faulting, and earthquakes. Current research includes 1) numerical simulation of earthquakes processes in interacting fault systems, 2) origins of earthquake clustering including foreshocks and aftershocks, 3) application of seismicity rate changes to infer stress changes in volcanic and tectonic environments, 4) laboratory investigation of fault constitutive properties and surface contact process.

19:00 - 21:00 **Welcome Dinner,** Hilton Poolside

19:00 - 21:00 **Leadership Meeting: SCEC Advisory Council,** Palm Canyon Room

21:00 - 22:30 **Poster Session,** Plaza Ballroom

Monday, September 10

07:00 - 08:30 **SCEC Annual Meeting Registration & Check-In,** Hilton Lobby

07:00 - 08:30 Breakfast, Hilton Poolside

07:00 - 08:30 **SCEC Transitions Program Breakfast,** Tapestry Room

The Office of Experiential Learning and Career Advancement (ELCA) launched the SCEC Transitions Program to provide junior members of the SCEC community with resources and mentoring across key career transitions. At the 2018 SCEC Annual Meeting, ELCA will host its second Breakfast Club Meetup. The goal of these meetups is to provide a platform for early career attendees to connect with peers and mentors for the purpose of discussing pathways in earthquake science careers. These networking opportunities are intended for anyone starting, pursuing, building, or transitioning into a earthquake science career. (www.scec.org/workshops/2018/transitions)

08:30 - 10:10 **Plenary Session 1:** "The Long and Winding Road" **The State of SCEC,** Horizon Ballroom
Moderators: John Vidale, Greg Beroza

08:30 Welcome and State of the Center (John Vidale)

08:40 Remarks from the National Science Foundation (Maggie Benoit)

08:50 Remarks from the U.S. Geological Survey (Bill Leith)

09:00 Remarks from the Pacific Gas & Electric Company (Katie Wooddell)

09:05 Remarks from the Federal Emergency Management Agency (David Javier)

09:10 SCEC Communication, Education, & Outreach Highlights (Mark Benthien)

09:25 SCEC Science Accomplishments (Greg Beroza and Christine Goulet)

10:00 Lightning Talks: Workshop Summaries

10:10 - 10:30 Break

10:30 - 12:00 **Plenary Session 2:** "All Together Now" **How Do We Construct Effective and Synergistic Community Models?** Horizon Ballroom Moderators: Liz Hearn, Scott Marshall

10:30 **Heat Flow Data and Seismic Imaging Reveal Both Transient and Steady-State Thermo-Mechanical Processes at Work Beneath Southern California,** Wayne R. Thatcher and David S. Chapman

Analysis of heat flow and seismic data provides glimpses of the dynamical processes shaping the thermal evolution of southern California. The present day thermal field bears an imprint of long-lived subduction prior to 30 Ma and subsequent growth of a continental transform boundary. Post 30 Ma processes include (1) a continental analog of seafloor spreading beneath the Salton Trough, (2) thermal pulses due to slab window effects, (3) mantle lithosphere detachment and sinking beneath late Cretaceous batholiths, and (4) extension and formation of metamorphic core complexes (MCC) in the offshore Inner Borderland.

Over 200 high quality surface heat flow (SHF) measurements define 14 distinct southern California heat flow regions (HFRs) where SHF is relatively constant. Assuming seismic estimates of lithosphere-asthenosphere boundary depth (sLAB) coincide with thermal LAB, two remarkable features are revealed. First, for 11 HFRs with SHF 40-83 mW/m2, sLAB depth is a surprisingly constant 70 ± 5 km. These data points naturally separate into 2 clusters, the first with average SHF of 40-58 mW/m2 (Cluster 1), the second with SHF of 68-83 mW/m2 (Cluster 2).

Simple 1D steady-state thermal conduction models can match the six Cluster 2 HFRs. P/T constraints from mantle xenoliths and erupted lavas considerably narrow the range of acceptable geotherms, with Moho at 700˚- 800˚C and LAB 1200˚- 1300˚C. However, such simple models are inconsistent with the low SHF of Cluster 1. In each of these 5 HFRs there is geologic and/or seismic evidence for Late Cenozoic detachment and sinking of mantle lithosphere. A transient 1D conduction model is used that includes an initially 30 to 50 km thick lithosphere exposed to hot asthenosphere 3-10 Ma BP conductively cooled and thickened by mafic underplating. Current temperatures are warm in the lower crust, ~850˚C at the Moho, and ~1200˚C at the LAB.

Salton Trough has the highest SHF (100-140 mW/m2) and thinnest lithosphere (45-55 km) in southern California. A model with steady state crustal thickness of 24 km, constant rates of stretching and

sedimentation into the Trough and basaltic under-plating at the Moho matches the data, with a hot lower crust and ~1400˚C asthenosphere at the Moho.

Finally, the Inner Borderland HFR has an unusually thin lithosphere of 49±6 km and SHF of 77±6 mW/m2, consistent with its origin as a Miocene MCC subsequently unroofed and depleted of its upper crustal heat producing elements.

11:00 **On the Role of Temperature and Rheology in Seismicity in Convergent Margins,** Ylona van Dinther, Luca Dal Zilio, Mario D'Aquisto, Robert Herrendörfer, & Taras Gerya

Earthquake nucleation, propagation and arrest are governed by fault stress and strength. Thus understanding how these are regulated by long-term processes involving temperature, rheology and tectonic forcing - in combination with short-term earthquake interactions - is important. To decipher and extend our too limited and indirect observational record, we developed the first quantitative model able to simulate the dynamics governing both tectonic processes over millions of years and the family of fault slip processes down to milliseconds. We utilize this seismo-thermo-mechanical modeling framework to show how stress evolution, temperature, and crustal and lithospheric rheology interact to shape convergent margins, seismic cycle observations and seismicity behavior. Through quantifying their feedback in a self-consistent manner, we establish how convergence rate across continental collision zones affects temperature and viscosity distribution. This determines stress and strength distributions, which govern earthquake maximum magnitude, recurrence patterns, and Gutenberg-Richter statistics. In a more observationally constrained approach, temperature, geometry and forcing can be predefined using geological and geophysical constraints to improve our understanding of seismicity in particular regions. Such tectonically realistic models of the Nepal Himalaya demonstrate the Main Himalayan Thrust geometry facilitates a bi-modal seismicity regime with M>=8 surface ruptures following a series of deeper, ~M7 megathrust earthquakes. In the Northern Apennines (Italy), such models show that slab delamination and retreat along with a high temperatures and a ductile lower crustal rheology are necessary to match both long- and short-term observations. These self-consistent and regionally-constrained examples illustrate the importance of thermal and rheological models for understanding seismicity.

11:30 Group Discussion

12:00 - 13:30 Lunch, Hilton Restaurant, Tapestry Room, and Poolside

13:00 - 17:00 **SCEC Annual Meeting Registration & Check-In,** Hilton Lobby

13:30 - 15:00 **Plenary Session 3:** "Getting Better" **What Needs to be Done to Increase the Impact of Dynamic Rupture Modeling?** Horizon Ballroom Moderators: Eric Dunham, David Oglesby

13:30 **Moving Earthquake Science Forward - Earthquake Simulation Codes and the SCEC-USGS Dynamic Rupture Group,** Ruth A. Harris

Computational simulations of earthquake rupture provide clues for deciphering earthquake behavior. In a perfect world, we would have a complete set of observations at Earth's surface and at depth that would allow us to forgo simulations, but in reality, this is never the case and additional tools are required to fill the gaps in our knowledge about how earthquakes work. Dynamic earthquake rupture simulation is one of the tools that is being used. This type of computational simulation is powerful, but it is also complex, so additional steps are required to ensure that it is working as expected. The SCEC-USGS Dynamic Rupture Group has provided a solution. We developed an extensive suite of benchmark exercises that are used to test computer codes aiming to simulate dynamic earthquake rupture and the resulting nearby ground shaking. To date, more than a dozen codes have performed the exercises, demonstrating that they reliably produce similar results for fault rupture behavior and ground motions, when they use the same assumptions about fault geometry, initial stresses, crustal properties, and friction. Our website, scecdata.usc.edu/cvws, provides the details of our benchmark exercises and other information about our group's work. As part of our investigations we have examined cutting-edge earthquake hazards problems, from a study of the effect of fault geometry on future large earthquakes near a power plant to examinations of off-fault yielding's effects on earthquake progress and near-field ground shaking. Our group has also set an example for how a long-running open and welcoming collaboration can move forward with interesting science discoveries while mentoring the next generation of scientists in our field.

14:00 **Advancing Simulations of Sequences of Earthquakes and Aseismic Slip [SEAS],** Junle Jiang and Brittany A. Erickson

Robust predictive models of earthquake source processes have fundamental importance in earthquake science. Numerical simulations of dynamic earthquake ruptures have excelled in reproducing detailed processes during individual events. To bridge the shorter and longer time scales, it is important to consider

earthquake source processes that interact with slow tectonic deformation, through the simulation of Sequences of Earthquakes and Aseismic Slip (SEAS). In SEAS models, the interplay of aseismic periods and dynamic events gives rise to a wide range of geophysical observables such as aseismic deformation, microseismicity, and ground shaking during dynamic ruptures, providing an avenue to connect earthquake behavior to geological, paleoseismic, and geodetic observations from a fault zone. SEAS modeling can also determine which physics at what scales dominates the resulting fault behavior, aiding the interpretation of long-term seismicity patterns in large-scale models of fault systems that require various simplifications.

Understanding how earthquakes nucleate, propagate, and terminate necessitates the development of SEAS models capable of simulating pre-, inter- and postseismic slip and loading between earthquakes. Multiscale faulting processes and multiple physical factors involved lead to the complexity of SEAS models, posing significant challenges for numerical simulations. This reality requires collaborations of researchers to compare and verify simulation results. Over the past year we have initiated a community code-verification effort, with the goals to further advance our computational capabilities, promote robust and reproducible earthquake science, and develop best practices and tools for the broader community. During the first SEAS workshop this spring, we brought together ~20 modelers to participate in our first benchmark problem, a 2D quasi-dynamic crustal faulting problem that serves as the first step to ensuring that different methodologies can produce closely matching results. The initial success of this benchmark prepares us to consider models with further complexities, including irregular earthquake patterns, nonvertical faults, 3D problems, and additional physics such as inelasticity and full dynamic effects, as we move forward. This community exercise will foster the development of a new generation of accurate SEAS models, towards a long-term goal to validate and integrate these models with geophysical observations.

14:30 Group Discussion

14:00 - 22:00 **SCECmeetUP Space Available,** Tapestry Room

To facilitate informal, small group discussions at the SCEC Annual Meeting, the Tapestry Room is available for anyone to use without reservations at the designated times. Meeting rooms for groups up to 24 people are also available with reservations for 2-hour blocks. See the sign-up sheet in the Hilton Lobby to reserve a room for your group.

15:00 - 17:00 **Poster Session**

15:00 **Lightning Talks** (series of presentations from SCEC Community), Horizon Ballroom

15:30 **Poster Viewing,** Plaza Ballroom

15:00 - 18:00 **Leadership Meeting: SCEC CEO Planning Committee,** Palm Canyon Room

19:00 - 22:00 **SCEC Honors Banquet:** "In My Life" **Tribute to SCEC Associate Director John McRaney,** Grand Ballroom at Hotel Zoso

Tuesday, September 11

07:00 - 08:30 Breakfast, Hilton Poolside

07:00 - 08:30 **SCEC Transitions Program Breakfast,** Tapestry Room

The Office of Experiential Learning and Career Advancement (ELCA) launched the SCEC Transitions Program to provide junior members of the SCEC community with resources and mentoring across key career transitions. At the 2018 SCEC Annual Meeting, ELCA will host its second Breakfast Club Meetup. The goal of these meetups is to provide a platform for early career attendees to connect with peers and mentors for the purpose of discussing pathways in earthquake science careers. These networking opportunities are intended for anyone starting, pursuing, building, or transitioning into a earthquake science career. (www.scec.org/workshops/2018/transitions)

08:30 - 10:00 **Plenary Session 4:** "Fixing a Hole" **How Do We Assess Hazard and Risk from Distributed Deformation?** Horizon Ballroom Moderators: Jack Baker, Domniki Asimaki

08:30 **On the possibility of earthquake rupture through clay-rich faults,** Daniel Faulkner, Marieke Rempe, John Bedford, C Sanchez-Roa, C Boulton, & S den Hartog

Many mature, large-displacement fault zones exhibit a clay-rich fault core. This low porosity, low permeability material inhibits the migration of fluid and consequently small changes in porosity produce pore pressure transients that take significant time to dissipate. Despite most clay-rich fault gouges displaying velocity strengthening frictional characteristics, variations in pore-fluid pressure can result in a wide range of behaviour including apparent velocity weakening leading to possibility of these rocks hosting instabilities. We present laboratory constraints of the frictional properties of clay-rich fault gouge both at low slip velocity, commensurate with earthquake nucleation and at higher slip velocity, equivalent to that during rupture

propagation. We show that small amounts of compaction can result in large strength changes and apparent velocity weakening behaviour at slow slip velocity. At higher slip velocity, experimental results suggest thermal pressurization in clay-rich fault gouge is an efficient process that produces weakening over small slip displacements. Accounting for pore-fluid pressure effects during slip predicts a wide variety of behaviour including enhanced fault creep, slip transients, and even the possibility of rupture propagation on clay-rich fault zones.

09:00 **Assessing Surface Fault Rupture Deformation,** Jonathan Bray

Surface fault rupture can produce localized or distributed deformation. In addressing the surface fault rupture hazard, the potential patterns of ground deformation should be developed through the use of a comprehensive site investigation including detailed mapping. Measured patterns of surface fault-induced ground deformation from similar types of faulting from past events offer useful insights to complement site-specific studies. Mitigation can be achieved in those cases when avoidance is not possible or practical. Engineers can design structures to accommodate fault-induced ground movements. Building strong, ductile structural foundation elements that can accommodate some level of ground deformation and isolating the superstructure from much of the underlying ground movement are effective design measures. Structures should not be tied into the ground with piles or piers. Other mitigation measures include establishing non-arbitrary setbacks based on fault geometry and displacement, and the overlying soil; constructing reinforced earth fills to spread out the underlying ground movements; and using slip layers to decouple ground movements from foundation elements.

09:30 Group Discussion

10:00 - 10:30 Break

10:30 - 12:00 **Plenary Session 5:** "Act Naturally" **How Do We Use and Further Improve Earthquake Simulators?**
Horizon Ballroom Moderators: Ned Field, Jacqui Gilchrist

10:30 **Earthquake Simulators are Ready for Prime Time,** Bruce E. Shaw

A major leap has been made in the last year where earthquake simulators have been shown to replicate seismic hazard statistics across California, matching remarkably well the results from UCERF3. What this means, how to take advantage of it, why it has worked, and where we are pushing further forward will all be discussed. This application of earthquake simulators will also be deployed as an example to address the more general question of how to use, and how not to use simulators, and the importance of robustness.

11:00 **On the present and future of physics-based earthquake source modeling,** Nadia Lapusta

Accelerating streams of field observations, lab studies, and numerical modeling have significantly improved our understanding of earthquakes and physical factors that affect them. The main suspects have been known for a while. Tectonic loading, static and wave-mediated stress transfers, aseismic slip, rate-and-state friction, fault geometry and roughness, visco-plastic deformation at depth, shear heating during rapid slip, variations in pore fluid pressure, and off-fault damage/healing have all been shown to significantly affect, and in some cases dominate, the stress/strength evolution on faults and hence the earthquake patterns that result. Through combined field, lab, and numerical studies, our research community is well on the way to systematically quantifying the physical factors and evaluating their relative importance for different faults/phenomena/scales. A number of earthquake source models are being developed, focusing on different combinations of the physical factors and scales, to aggregate the available knowledge and identify crucial gaps. Together, the modeling efforts are advancing towards interpreting field observations in terms of tractable models with physically meaningful fault and bulk properties that can be evaluated, at least in principle, through lab, field, and smaller-scale numerical studies.

Earthquake simulators have taken on a necessary and formidable task of investigating earthquake patterns on realistic fault networks, which is presently tractable only with simplifications and omissions of the other physical factors. They have been successful in finding sets of parameters, some physical and some ad-hoc, that allow the models to match known statistical properties of regional earthquake sequences. The simulators are valuable research tools for studying fault system dynamics. However, their simplifications necessitate careful considerations about which conclusions they allow us to draw. For example, why would we expect the simulators to provide realistic probabilities of jumps over step-overs if they ignore the potentially dominating physics - dynamic stress changes brought by seismic waves? Including the simulators in hazard assessment requires clear communication of their limitations, verification through comparisons with smaller-scale models that more accurately capture relevant physics, and community consensus of what criteria and observations the models need to satisfy. We are not there yet, but we are on the right track.

11:30 Group Discussion

12:20 - 13:30 Lunch, Hilton Restaurant, Tapestry Room, and Poolside

13:30 - 15:00 **Plenary Session 6: "**We Can Work It Out" **How Should SCEC Keep Up with Rapid Developments in Computational Science?** Horizon Ballroom Moderators: Ricardo Taborda, Phil Maechling

13:30 **Deep learning for aftershock location patterns and the earthquake cycle,** Phoebe DeVries, Thomas B. Thompson, Martin Wattenberg, Fernanda Viegas, and Brendan J. Meade

Over the past few years, deep learning has led to rapid advances in applied computer science, from machine vision to natural language processing. These methods are now accessible to scientists across all disciplines due to the availability of easy-to-use APIs and affordable GPU acceleration. We demonstrate two specific applications of deep learning within earthquake science. In the first, we train a deep neural network to learn computationally efficient representations of viscoelastic solutions, across large ranges of times, locations, and rheological structures. Once found, these efficient neural network representations may accelerate computationally intensive viscoelastic calculations by more than 50,000%. In the second, we focus on aftershock location patterns and find that a fully connected neural network trained on 131,000+ mainshock-aftershock pairs can explain aftershock locations in an independent testing data set of 30,000+ mainshock-aftershock pairs more accurately (AUC = 0.849) than static elastic Coulomb failure stress change (AUC = 0.583). In contrast to the common assertion that deep learning produces "black box" results, in both applications, the trained neural networks can provide unique physical insights.

14:00 **Detecting millions of earthquakes in southern California with template matching,** Zachary E. Ross, Egill Hauksson, Daniel T. Trugman, and Peter M. Shearer

Over the last twenty years, earthquake detection rates in southern California have improved dramatically, resulting in the minimum magnitude of completeness decreasing from M~2.5 to M~1.5 today. It is believed, however, that these events still constitute less than 10% of all activity that is being recorded by the seismic network on a regular basis. To address these shortcomings, we applied a matched filter (template matching) algorithm to the entire continuous waveform archive of the Southern California Seismic Network using the seismograms of ~300,000 past events as templates. This GPU supercomputing effort resulted in a catalog of ~2.4 million earthquakes for the period 2008-2017, which is ~13 times as many events as the standard regional catalog, and has a completeness magnitude of ~0.5. The recent double-difference GrowClust algorithm was applied to the entire dataset and its 1.3 billion differential times, resulting in state-of-the-art hypocenter precision for the whole of southern California. I will first discuss basic summary information about the catalog and new regional-scale observations. Then, I will focus on the most active sequences that occurred during the period and use the seismicity to investigate connections between properties of fault zones and the earthquake rupture process. The unprecedented level of detail in this next-generation seismicity catalog is expected to facilitate important new analyses of earthquakes and faults in southern California.

14:30 Discussion

14:00 - 22:00 **SCECmeetUP Space Available,** Tapestry Room

To facilitate informal, small group discussions at the SCEC Annual Meeting, the Tapestry Room is available for anyone to use without reservations at the designated times. Meeting rooms for groups up to 24 people are also available with reservations for 2-hour blocks. See the sign-up sheet in the Hilton Lobby to reserve a room for your group.

15:00 - 17:00 **Poster Session**

15:00 **Lightning Talks** (series of presentations from SCEC Community), Horizon Ballroom

15:30 **Poster Viewing,** Plaza Ballroom

19:00 - 21:00 **Group Dinner,** Poolside

21:00 - 22:30 **Poster Session,** Plaza Ballroom

Wednesday, September 12

07:00 - 08:30 Breakfast, Hilton Poolside

08:30 - 10:00 **Plenary Session 7:** "With a Little Help from My Friends" **ShakeOut—What Has Shaken Out Since 2008?** Horizon Ballroom Moderators: Mark Benthien, Ken Hudnut

08:30 **Earth Science Research Needs for Improving Earthquake Scenarios,** Brad T. Aagaard

Earthquake scenarios provide important opportunities to showcase the effectiveness of integrating science from across the spectrum of earthquake hazards research. These scenarios complement probabilistic hazard assessments by examining specific realizations of large, potential earthquakes and their consequences to improve our resilience to natural disasters. They also raise the profile of our research with national media coverage. Consequently, it is especially important to leverage knowledge from earthquake geology, tectonic geodesy, and seismology to create the most realistic earthquake scenarios possible.

The 2008 ShakeOut scenario brought together more than 300 contributors to quantify the hazards and risks associated with a magnitude 7.8 occurring on the southern San Andreas fault. This effort set new expectations for how we develop sophisticated earthquake scenarios. In 2008 the USGS also led a collaborative effort to develop a suite of earthquake ground-motion scenarios for the Hayward fault, one of which is being used as the basis for the more comprehensive HayWired earthquake scenario. Since these scenarios were developed 10 years ago, our science has continued to advance but many open questions persist.

Creating realistic earthquake ruptures remains one of the major challenges. How to select rupture end points, the depth extent of coseismic slip, and multi-fault ruptures are basic issues. Additional research is necessary to constrain rupture details, such as the spatial variability of slip, the potential hypocenter relative to geologic features and microseismicity, and the speed and direction of rupture propagation. Furthermore, we have a limited understanding of when and where we should expect significant afterslip, which impacts infrastructure response planning.

In computing scenario ground motions, research is needed to further develop techniques for incorporating sophisticated, shallow, anelastic behavior into 3D simulations and constraining the anelastic properties at regional scales. Additional work is also necessary to develop regional-scale analysis techniques for estimating the extent and severity of ground failure. Aftershock forecasts can be improved with regional parameters for clustering and fault locations.

Pursuing these research directions will lead to more accurate estimates of the anticipated consequences of large earthquakes and help support better decision-making in urban planning and disaster preparedness.

09:00 **Where We Have Been, Where We Are Going… And How We Can Work Together,** Marissa Aho

More than 10 years after the 2008 ShakeOut scenario, the Mayor's Office of Resilience is still working with many of the original authors and other partners to advance the region's seismic resilience. ShakeOut and other related efforts have had a major impact on seismic policy in the City of Los Angeles, including the formation of the Mayor's Seismic Safety Task Force, the advancement of DWP's water resilience program, the partnership with U.S. Geological Survey that enabled Dr. Lucy Jones to serve as Mayor Garcetti's Science Advisor, and the release of the Mayor's Resilience by Design report in December 2014. Resilience by Design focused on strengthening LA's most vulnerable buildings, fortifying LA's water system, and enhancing reliable telecommunications. Now approaching its 4-year anniversary, I will discuss the status of many of the recommendations in Resilience by Design that have been implemented.

Resilience by Design is undoubtedly the cornerstone of Los Angeles' resilience-building. As inaugural members of 100 Resilient Cities pioneered by the Rockefeller Foundation, the City of Los Angeles worked with hundreds of partners during 2016-2017 to develop Resilient Los Angeles. Resilient Los Angeles was released by Mayor Garcetti in March of 2018 as a strategy that addresses Disaster Preparedness and Recovery, Climate Adaptation, Infrastructure Modernization, Economic Security and Leadership and Engagement. A number of the 96 Actions in Resilient Los Angeles advance the City's seismic resilient efforts. I will highlight some of them and talk about how we can work together to continue to advance seismic resilience together.

09:30 Group Discussion

10:00 - 10:30 Break

10:30 - 12:00	**Plenary Session 8:** "I Want to Hold Your Hand" **SCEC Looking Forward,** Horizon Ballroom Moderators: John Vidale, Greg Beroza
10:30	Report from the Advisory Council (Meghan Miller)
10:50	2019 Science Plan and Request for Proposals (Greg Beroza)
11:50	Director's Closing Remarks (John Vidale)
12:00	2018 SCEC Annual Meeting Adjourns
12:30 - 14:30	**Leadership Meeting: SCEC Planning Committee,** Palm Canyon Room
12:30 - 14:30	**Leadership Meeting: SCEC Board of Directors,** Tapestry Room

Poster Sessions

View full abstracts at www.scec.org/meetings/2018/am

Sunday, September 9, 2018

15:00 – 17:00 Poster Set-Up

21:00 – 22:30 Poster Session 1

Monday, September 10, 2018

15:00 – 17:00 Poster Session 2

Tuesday, September 11, 2018

15:00 – 17:00 Poster Session 3

21:00 – 22:30 Poster Session 4

Ground Motions / Earthquake Engineering Implementation Interface

Posters 001-028, 298-305

001 Long Shaking Durations within the Los Angeles Basin from Shallow Earthquakes, Voon Hui Lai, Zhongwen Zhan, Robert W Graves, and Donald V Helmberger

002 Effect of source rupture directivity on the ground shaking from strike-slip earthquakes and its implication for directivity models, Junju Xie, Paolo Zimmaro, Xiaojun Li, and Zengping Wen

003 Evaluating and Improving Ground Motion Predictions for Scenario Earthquakes in The San Francisco East Bay by Integrating Earthquake Ground-Motion Simulations and Noise-Derived Empirical Green's Functions, Taka'aki Taira, and Arthur J Rodgers

004 Broadband Ground Motion and Variability from 3D Dynamic Rupture Simulations along the Wasatch Fault, Utah, incorporating both Stochastic Fault Roughness and Deterministic Long-wavelength Geometry, Kyle B Withers, Morgan P Moschetti, and Kenneth Duru

005 Nonlinear Modeling of High-Rise Buildings Subject to Long-Period Ground Motion, Lauren M Santullo, Ahmed E Elbanna, and Setare Hajarolasvadi

006 Evaluation of CyberShake ground motions for engineering practice, Ganyu Teng, and Jack W Baker

007 Spatial correlations in CyberShake physics-based ground motion simulations, Yilin Chen, and Jack W Baker

008 Cybershake NZ v18.6: New Zealand simulation-based probabilistic seismic hazard analysis, Brendon A Bradley, Karim Tarbali, Robin L Lee, Jonney Huang, D Lagrava, V Polak, J Motha, and Sung Bae

009 Strong ground motions simulations for Dunedin city, New Zealand: First steps using the SCEC Broadband Simulation Platform, Mark W Stirling

010 Implementing Inter-Frequency Correlations into the SDSU Broadband Ground Motion Method, Nan Wang, Rumi Takedatsu, Kim B Olsen, and Steven M Day

011 Implementing Inter-Period Correlations into SCEC BBP Simulations, Jeff R Bayless, and Norman A Abrahamson

012 Nonlinear Fourier-based Amplification Factors for the SCEC Broadband Platform, Domniki Asimaki, and Jian Shi

013 Sampling Parametric Rupture Variability using Broadband Ground Motion Simulations, Robert W Graves

014 Simulated ground motions for induced seismicity at a 12-story structure in Oklahoma using the SCEC Broadband Platform, Jessie K Saunders, Frankie Martinez, Jennifer S Haase, and Mohamed Soliman

015 The SCEC Broadband Platform: Open-Source Software for Strong Ground Motion Simulation and Validation, Fabio Silva, Philip J Maechling, Christine A Goulet, and John E Vidale

016 Toward Hybrid Broadband Ground Motion Simulation Validation for Mw>3.5 New Zealand Earthquakes, Robin L Lee, Brendon A Bradley, and Xavier Bellagamba

017 Kinematic rupture simulations of earthquakes on multi-segment faults, Jorge G Crempien, and Ralph J Archuleta

018 Kinematic Source Models for Earthquake Simulations with Fault-zone Plasticity, Zhifeng Hu, Daniel Roten, Kim B Olsen, and Steven M Day

019 Implementation of Iwan-type Plasticity Model in AWP-ODC, Daniel Roten, Kim B Olsen, Steven M Day, and Yifeng Cui

020 Modeling shallow crustal nonlinearity in physics-based earthquake simulations: Beyond perfect plasticity, Elnaz Esmaeilzadeh Seylabi, Doriam Restrepo, Domniki Asimaki, and Ricardo Taborda

021 An Updated Compilation of VS30 in the United States, Alan Yong, Devin McPhillips, Julie Herrick, and Jessica Dozal

022 A Proposed Seismic Velocity Profile Database Model, Sean K Ahdi, Shamsher Sadiq, Okan Ilhan, Yousef Bozorgnia, Youssef Hashash, Dong Youp Kwak, Duhee Park, Alan Yong, and Jonathan P Stewart

023 Dense mapping of shallow velocity structure in the Raymond Basin using the Pasadena Distributed Acoustic Sensing Array, Ethan F Williams, Zhongwen Zhan, Martin Karrenbach, Steve Cole, and Lisa LaFlame

024 Preliminary Results on Fully Nonergodic Ground Motion Models in Central California Using NGA-West2 and SCEC CyberShake Datasets, Xiaofeng Meng, Christine A Goulet, Kevin R Milner, and Scott Callaghan

025 Probabilistic Seismic Hazard Analysis in California Using Non-Ergodic Ground-Motion Prediction Equations, Nicolas M Kuehn, Norman A Abrahamson, and Melanie Walling

026 GMPE specific average velocity profiles for developing spatially-varying path coefficients, Kathryn E Wooddell, Linda Al Atik, and Norman A Abrahamson

027 Probabilistic Seismic Hazard Analysis for Harrat Madinah, Saudi Arabia Using Regional Ground Motion Prediction Equations, Ryota Kiuchi, Walter D Mooney, and Hani M Zahran

028 Constraining epistemic uncertainties on hazard models in the Marmara region using SHERIFS (Seismic Hazard and Earthquake Rates in Fault Systems), Thomas Chartier, Oona Scotti, and Hélène Lyon-Caen

298 Characterization of high-wavenumber subsurface random heterogeneity using a very dense array at Diablo Canyon, California, Nori Nakata

299 Multi-scale study of ground motion coherence in Piñon Flats Observatory, Lei Qin, Christopher W Johnson, Frank L Vernon, and Yehuda Ben-Zion

300 Zoning Verification in Mexico City using strong motions of the M7.1 M7.1 Puebla-Morelos earthquake of September 19, 2017, Mehmet Celebi, Valerie J Sahakian, Diego Melgar, and Luis Quintanar

301 Investigating the Ground Motion Characteristics of the 2016 Mw 5.5 Gyeongju, South Korea, Earthquake Using the SCEC Broadband Platform, Seok Goo Song, Kwan-Hee Yun, and Sangmin Kwak

302 The 1933 Long Beach, California, Earthquake, Susan E Hough, and Robert W Graves

303 Sensitivities and Uncertainties in Probabilistic Fault Displacement Hazard Analysis in Southern California, Hong Kie Thio, and Jeff R Bayless

304 Towards Structural Imaging Using Scattering Artifacts Detected in Ambient Field Correlations, Lise Retailleau, and Gregory C Beroza

305 Characteristics of ground motion generated by interaction of wind gusts with trees, structures and other obstacles above the surface, Christopher W Johnson, Haoran Meng, Frank L Vernon, Nori Nakata, and Yehuda Ben-Zion

Earthquake Forecasting and Predictability — Posters 030-053

030 Development of monitoring and forecasting methods for crustal activity utilizing large-scale high-fidelity finite element simulations with 3D heterogeneous medium, Takane Hori, Tsuyoshi Ichimura, Kohei Fujita, Takuma Yamaguchi, Takeshi Iinuma, and Ryoichiro Agata

031 Probabilities of Earthquakes in the San Andreas Fault System: Estimations from RSQSim Simulations, Jacquelyn J Gilchrist, Thomas H Jordan, and Kevin R Milner

032 Fully physics-based PSHA: coupling RSQSim with deterministic ground motion simulations, Kevin R Milner, Bruce E Shaw, Thomas H Jordan, Scott Callaghan, and Christine A Goulet

033 The Collaboratory for the Study of Earthquake Predictability version 2.0 (CSEP2.0): New Capabilities in Earthquake Forecasting and Testing, William H Savran, Philip J Maechling, Maximilian J Werner, Thomas H Jordan, Danijel Schorlemmer, David A Rhoades, Warner Marzocchi, John Yu, and John E Vidale

034 Nowcasting Induced Seismicity at the Groningen gas field in the Netherlands, Molly Luginbuhl, John B Rundle, and Donald L Turcotte

035 Induced Earthquake Forecasting in Oklahoma Using Models of Fluid Diffusion and Earthquake Nucleation, Guang Zhai, and Manoochehr Shirzaei

036 3D models of seismicity beneath the Greater Tokyo Area, Yosihiko Ogata, Koichi Katsura, Hiroshi Tsuruoka, and Naoshi Hirata

037 Statistics of seismicity associated with a sequence of explosive eruptions at Kilauea, Hawaii, Rebecca A Fildes, Louise H Kellogg, Donald L Turcotte, and John B Rundle

038 Forecasting earthquake behavior on the Alpine Fault, New Zealand, Nicolas C Barth, Jamie Howarth, Keith B Richards-Dinger, Sean Fitzsimons, and Glenn P Biasi

039 Emergent failure process of a M4.2 earthquake offshore Istanbul observed from GONAF downhole recordings, Marco Bohnhoff, Peter E Malin, Murat Nurlu, and Felix Bluemle

041 How Much Farther? Estimating Rupture Length Probabilities After a Rupture Has Started, Steven G Wesnousky, and Glenn P Biasi

042 Sequential Data Assimilation for Seismicity: Probabilistic Estimation and Forecasting of Fault Stresses, Ylona van Dinther, Hans Rudolf Künsch, and Andreas Fichtner

043 Are we still seeing aftershocks from the M6.8 1872 Central Washington Earthquake? Thomas M Brocher

044 Faulty Intuition about b-values and Aftershock Productivity within a Fault Network, Morgan T Page, and Nicholas J van der Elst

045 New software for computing time dependent seismic hazard during aftershock sequences using the OpenSHA platform, Nicholas J van der Elst, Kevin R Milner, Edward H Field, Sara K McBride, and Morgan T Page

046 Why do strike-slip earthquakes produce fewer aftershocks? Kelian Dascher-Cousineau, Emily E Brodsky, and Thorne Lay

047 Updated California Aftershock Parameters, Jeanne L Hardebeck, Andrea L Llenos, Andrew J Michael, Morgan T Page, and Nicholas J van der Elst

048 Aftershock Matters, Nicole S Gage, David J Wald, and Kristin D Marano

049 Uncertainties in Probabilistic Seismic Hazard Analysis for a Poisson Earthquake Occurrence Model, Yuehua Zeng, and Mark D Petersen

050 Improved medium-term earthquake forecasting: Compensating for incomplete contributions of precursory earthquakes, David A Rhoades, and Annemarie Christophersen

051 The earthquake rates they are a-changin': Improving forecasts during earthquake swarms, Andrea L Llenos, Andrew J Michael, Morgan T Page, Nicholas J van der Elst, and Sara K McBride

052 Building Earthquake Early Warning Networks With Low Cost, Off-the-Shelf Components, Ryan Logsdon, Robert L Walker, and Sean Gibbons

053 ShakeAlert v. 2.0 Testing and Certification, Deborah E Smith, Monica D Kohler, Jennifer R Andrews, Angela I Chung, Renate Hartog, Ivan Henson, Douglas D Given, and Stephen Guiwit

Seismology

Posters 054-112, 283-286

054 Detailed seismic catalog for the San Jacinto fault zone region (2008-2016) from automated processing of raw waveform data, Malcolm C White, Yehuda Ben-Zion, and Frank L Vernon

055 Checking Data Quality of Co-located Broadband and Strong-motion Sensors in Southern California Seismic Network, Zefeng Li, Egill Hauksson, Thomas H Heaton, Luis Rivera, and Jennifer R Andrews

056 Absolute and relative focal depth determination of moderate-sized earthquakes: An example from the 2010 El Mayor-Cucapah earthquake sequence, Chunquan Yu, Egill Hauksson, Zhongwen Zhan, Elizabeth S Cochran, and Donald V Helmberger

057 Cloud Computing and Big Data – Using the Southern California Earthquake Data Center (SCEDC) and the Southern California Seismic Network (SCSN) Products and Services for Earthquake Research, Ellen Yu, Prabha Acharya, Aparna Bhaskaran, Shang-Lin Chen, Jennifer R Andrews, Valerie Thomas, Egill Hauksson, and Robert W Clayton

058 Earthquake catalog reconstruction from analog seismograms: Application to the Rangely Experiment microfilms, Kaiwen Wang, William L Ellsworth, Gregory C Beroza, Gordon Williams, Miao Zhang, Dustin Schroeder, and Justin L Rubinstein

059 Tracking thousands of microearthquakes for a month in northern Oklahoma: What a large-N array can reveal about induced seismicity, Sara L Dougherty, Elizabeth S Cochran, Rebecca M Harrington, and Zachary E Ross

060 Matched-filter Detection of Microseismicity Around the Eruption of the 2018 Kilauea Volcano, Hawaii, Hui Huang, and Lingsen Meng

061 Machine Learning in detecting Low-frequency Earthquakes in Shikoku, Japan, Huiyun Guo, Hui Huang, Tian Feng, and Lingsen Meng

062 Illuminating faulting complexity of the 2017 Yellowstone (Maple Creek) earthquake swarm, David R Shelly, and Jeanne L Hardebeck

063 The Similarity Matrix Profile, an efficient method for detecting both low and high signal to noise ratio seismic events in very long time series, Nader Shakibay Senobari, Gareth Funning, Zachary Zimmerman, Yan Zhu, and Eamonn Keogh

064 Reliable Real-Time Signal/Noise Discrimination with Deep and Shallow Machine Learning Classifiers, Men-Andrin Meier, Zachary E Ross, Anshul Ramachandran, Ashwin Balakrishna, Peter Kundzicz, Suraj Nair, Zefeng Li, Egill Hauksson, and Thomas H Heaton

065 Envelope-Based Early Warning Algorithm Using Nested Grid Search, Becky Roh, Thomas H Heaton, and Zachary E Ross

066 Spatial variations of rock damage production by earthquakes in southern California, Yehuda Ben-Zion, and Ilya Zaliapin

067 Crustal seismogenic layer at active faults inferred by background seismicity and temperature data in Japan, Makoto Matsubara, and Tomoko E Yano

068 Two Moho-Depth Earthquake Swarms along the Sierra Microplate Basin and Range Boundary Region, Emily L Maher, Ken D Smith, Rachel L Hatch, Kent M Graham, Neal W Driscoll, and Noah Conway

069 Sudden Surges of Seismicity within Natural Slow Growing and Long Duration Seismicity Swarms near Cahuilla Valley in the Central Peninsular Ranges, Southern California, Egill Hauksson, Zachary E Ross, and Elizabeth S Cochran

070 Delayed Triggering of small Local Earthquakes near the San Jacinto Fault after the 2014 Mw 7.2 Papanoa Earthquake, Bo Li, and Abhijit Ghosh

071 Comprehensive Study on Reservoir-induced Seismicity in the Xiaowan Reservoir, Yunnan Province, China, Wei Hua, Naichen Ke, and YAQIONG DAI

072 Towards Quasi-Automated Estimates of Source Properties of Small to Moderate Southern California Earthquakes with Second Seismic Moments, Haoran Meng, Jeff J McGuire, and Yehuda Ben-Zion

073 Investigating microearthquake finite source attributes with IRIS Community Wavefield Demonstration Experiment in Oklahoma, Wenyuan Fan, and Jeff J McGuire

074 Fast moment acceleration in the development phase of an earthquake derived from a large catalog of Source Time Functions, Julien Renou, and Martin Vallée

075 Testing and Reconciling EGF Methods for Estimating Corner Frequency and Stress Drop from P-wave Spectra, Peter M Shearer, Rachel E Abercrombie, Daniel T Trugman, and Wei Wang

076 Characteristics of Three Small (Mw < 4.5) Urban Area Sequences in the Walker Lane: Earthquake Interaction, Fault Structure, and Source Properties, Rachel L Hatch, Rachel E Abercrombie, Christine J Ruhl, and Ken D Smith

077 Characteristics of earthquake source complexity in the San Jacinto Fault Zone, Qimin Wu, and Xiaowei Chen

078 Source parameter variability of intraslab earthquakes as determined from the empirical Green's function method, Shanna Chu, Gregory C Beroza, and William L Ellsworth

079 Effective stress drop and aseismic deformation, Tomas Fischer, and Sebastian Hainzl

080 Revisiting historical earthquakes in our backyard: 1925 Santa Barbara and 1952 Kern County, Scott J Condon

081 Applying improved spectral analysis to an induced earthquake sequence in Oklahoma and implications on earthquake triggering, Xiaowei Chen, and Rachel E Abercrombie

082 Comparison of Brune-type Stress Drops Estimated from Direct P, S, and Coda Waves, Wei Wang, and Peter M Shearer

083 Relating teleseismic backprojection images to earthquake kinematics, Jiuxun Yin, and Marine A Denolle

084 Mitigating Spatial Bias of Back-projections with the Slowness Enhanced Back Projection, Han Bao, and Lingsen Meng

085 Using Kinematic models to Evaluate the Back Projection Results, Baoning Wu, Bo Li, David D Oglesby, and Abhijit Ghosh

086 Combining back-projection and matched filter in detecting offshore seismicity: Application to NE Japan subduction zone, Tian Feng, and Lingsen Meng

087 Exploration of Prompt Elastogravity Signal for the 2004 M9.0 Sumatra and 2010 M8.8 Maule Earthquakes, Xinyu Jiang, and Lingsen Meng

088 Rupture Model of the 2016 M5.8 Pawnee Induced Earthquake, Morgan P Moschetti, Stephen Hartzell, and Robert B Herrmann

089 Rapid induced seismicity mitigation and its impact on aftershock productivity in Oklahoma, Thomas H Goebel, Zach Rosson, Emily E Brodsky, and Jake I Walter

090 Characterizing seismogenic fault structures in Oklahoma, Rob Skoumal, and J. Ole Kaven

091 2017 Mw 5.4 Pohang earthquake, South Korea and poroelastic stress change associated with fluid injection, YoungHee Kim, Hobin Lim, Kai Deng, Jin-Han Ree, and Teh-Ru Song

092 Capturing Frictional Asperities along the Complex Structure of the Main Himalayan Thrust in Nepal after the 2015 Mw 7.8 Gorkha Earthquake, Manuel M Mendoza, Bo Li, Abhijit Ghosh, Marianne S Karplus, John Nabelek, Soma N Sapkota, Lok B Adhikari, Simon L Klemperer, and Aaron A Velasco

093 Towards Seismic Inverse Problems Using Deep Learning, Jared T Bryan, Alexander N Breuer, and Yifeng Cui

094 Machine learning-based surface wave tomography of Long Beach, CA, USA, Michael J Bianco, Kim B Olsen, Peter Gerstoft, and Fan-Chi Lin

095 First-arrival traveltime tomography at Long Beach California using ambient seismic noise and the adjoint-state method, Jorge A Castillo Castellanos, and Robert W Clayton

096 New techniques in point cloud analysis of high-density seismic array data to determine three dimensional fault and crustal structures in the Long Beach Basin, Andrew Allevato, Robert W Clayton, and Dayanthie S Weeraratne

097 A Proposal for an Industry-Scale Seismic Survey in the Los Angeles Basin, Daniel D Hollis, and Robert W Clayton

098 Shallow Velocity Structure of Los Angeles Basin from ambient noise correlations with dense seismic arrays, Zhe Jia, Robert W Clayton, and Jorge A Castillo Castellanos

099 Basin Amplification Seismic INvestigation: tracking the propagation of waves from the San Andreas Fault to Los Angeles, Robert W Clayton, Marine A Denolle, Kim B Olsen, Patricia Persaud, and Jascha Polet

100 Eikonal Tomography of the Southern California Plate Boundary Region, Hongrui Qiu, Yehuda Ben-Zion, and Fan-Chi Lin

101 Seismic imaging of the Southern California plate boundary around the South-Central Transverse Ranges using double-difference tomography and fault zone head waves, Pieter-Ewald Share, Hao Guo, Clifford H Thurber, Haijiang Zhang, and Yehuda Ben-Zion

102 Mapping Near-Surface Rigidity Structure using Co-located Pressure and Seismic Sensors from the EarthScope Transportable Array, Jiong Wang, and Toshiro Tanimoto

103 3-D upper crustal velocity structure of the Coachella Valley, Southern California: results from the salton seismic imaging project, Rasheed Ajala, Patricia Persaud, Joann M Stock, Gary S Fuis, John A Hole, Mark R Goldman, and Daniel S Scheirer

104 Modeling Crust of Columbia River Basalts Using Ambient Noise Recordings, Mackenzie R Wooten, Jorge A Castillo Castellanos, and Robert W Clayton

105 Geometric and Level Set Tomography for Interface Detection in the Near Surface, Jack B Muir, and Victor C Tsai

106 Full waveform ambient noise inversion, Korbinian Sager, Christian Boehm, Laura Ermert, Lion Krischer, and Andreas Fichtner

107 Testing the Amplitude of Ambient-field Green's Function by Simulated Scattered Waves in a 3D Sedimentary Basin, Shiying Nie, and Shuo Ma

108 Finite Frequency Sensitivity Kernel for the Correlation of Ambient Noise Correlations: Theory and Numerical Tests, Xin Liu, and Gregory C Beroza

109 Detecting the Earth's Interior Structure Using Reverse-Time Migration Based on Wavefield Normalized Cross-Correlation Imaging Condition, Lei Yang, Gregory C Beroza, and Liang Zhao

110 Shear wave velocity structure of a remnant slab beneath the western Transverse Ranges offshore southern California, Dayanthie S Weeraratne, Kaitlyn Amodeo, Sampath Rathnayaka, Escobar Lennin, Carlos D Gomez, and Monica D Kohler

111 Preliminary Site Response Results across the San Gabriel and San Bernardino Basins Utilizing the Ambient Noise Spectral Ratio Method, Anisha D Tyagi, Margaret Grenier, Rachel Kreuziger, Jacob S Kays, and Jascha Polet

112 Enhancing 0.4-1.0 Hz seismic signals in Green's functions through judicious selection of time intervals, Ian Vandevert, Aaron K Anderson, Taro Okamoto, and Toshiro Tanimoto

283 Preliminary evidence for localized lithospheric deformation in the western Basin and Range and Walker Lane from Ps receiver function analysis, Heather A Ford

284 Fault Continuity and Rupture Branching of the 2014 Mw 6.0 South Napa Earthquake Viewed by Fault-Zone Trapped Waves, Yong-Gang Li

285 The rupture process of 2018 Mw 7.0 Kalapana, Hawaii earthquake and relation with the 1975 event, Jinlai Hao, Wenze Deng, and Chen Ji

286 Magma movement from Nāpau down to Leilani Triggered the 4th May 2018 Mw 7.0 Hawaii earthquake, Kejie Chen, Jonathan D. Smith, Jean-Philippe Avouac, Zhen Liu, and Song Y. Tony

Tectonic Geodesy

Posters 113-142

113 Surface Creep Rate of the Southern San Andreas Fault Modulated by Stress Perturbations from Nearby Large Events, Xiaohua Xu, Lauren Ward, Junle Jiang, Bridget R Smith-Konter, Ekaterina Tymofyeyeva, Eric O Lindsey, Arthur G Sylvester, and David T Sandwell

114 Geodetic and geologic observations of creep on the Southern San Andreas Fault triggered by the 2017 Chiapas (Mexico) earthquake, Ekaterina Tymofyeyeva, Yuri Fialko, Junle Jiang, Roger Bilham, David T Sandwell, Thomas K Rockwell, Chelsea M Blanton, and Allen M Gontz

115 Using a dense GPS array as a strain meter on the Anza section of the San Jacinto fault, Margaret Grenier, and Yuri Fialko

116 Creep Along the Central San Andreas Fault Measured from Surface Cracks, 3D Topographic Differencing, and UAVSAR imagery, Chelsea P Scott, Nathan A Toke, Michael Bunds, and Manoochehr Shirzaei

117 Monitoring Fault Creep on the Hayward Fault using Structure from Motion, Jerlyn L Swiatlowski, and Gareth J Funning

118 Slow Slip Events: Earthquakes in Slow Motion, Jean-Philippe Avouac, Sylvain G Michel, and Adriano Gualandi

119 Periodic Slow Slip Events and Their Interactions with Megathrust Earthquakes on Northeast Japan Subduction Zone, Mostafa Khoshmanesh, Jennifer M Weston, Manoochehr Shirzaei, and Naoki Uchida

120 Stress accumulation rate on source faults around the junction of Ryukyu and Southwest Japan arcs using finite element model, Akinori Hashima, Hiroshi Sato, Tatsuya Ishiyama, Andrew Freed, and Thorsten W Becker

121 Present day interseismic slip rates of the Xianshuihe Fault observed by InSAR, Yuexin Li, and Roland Bürgmann

122 Pre-seismic and Co-seismic Deformations in the Seismogenic zone of the Lushan MS7.0 earthquake, Yanqiang Wu

123 3D surface deformation in the 2016 MW 7.8 Kaikōura, New Zealand earthquake from optical image correlation: Implications for strain localization and tectonic evolution of the Pacific-Australian plate boundary, Robert Zinke, James Hollingsworth, James F Dolan, and Russ J Van Dissen

124 Earthquake damage patterns resolve complex rupture processes. The 2016 M7.8 Kaikoura earthquake, Yann Klinger, Kurama Okubo, Amaury Vallage, Johann Champenois, Arthur Delorme, Esteban Rougier, Zhei Lei, Earl Knight, Antonio Munjiza, Claudio Satriano, Stephane Baize, Robert M Langridge, and Harsha S Bhat

125 Co-seismic Vertical Offset Retrieval From High-Resolution, Stereogrammetric DEMs: Examples from the 2013 Baluchistan, Pakistan Earthquake, William D Barnhart, Hannah Shea, Katherine Peterson, Ryan D Gold, Rich Briggs, and David J Harbor

126 Probing fault frictional properties during afterslip up- and down-dip of the 2017 Mw 7.3 Iran-Iraq earthquake, Kang Wang, and Roland Bürgmann

127 Pre-seismic and co-seismic deformation of the 2017 Mw 6.5 Jiuzhaigou, eastern Tibet earthquake constrained by GPS and InSAR data, Guojie Meng, Xiaoning Su, Shunying Hong, Xin Zhou, Yanfang Dong, and Chengtao Li

128 Post-seismic deformation mechanism of the Mw 9.0 Tohoku-Oki earthquake detected by GPS and GRACE observations, Wuxing Wang, Xiaodong Zhang, Ming Liang, and Jing Zhang

129 Lower-crustal rheology and thermal gradient in the Taiwan orogenic belt illuminated by the 1999 Chi-Chi earthquake, Chi-Hsien Tang, Ya-Ju Hsu, Sylvain D Barbot, James Moore, and Wu-Lung Chang

130 Can we hide an active fault within a geodetic network? Yes, we can., Maria Beatrice Magnani

131 Optimal GNSS observations in Southern California, Eileen L Evans, and Sarah E Minson

132 Decadal variation of crustal deformation in California inferred from EDM and GPS and its implication to seismic hazard, Zheng-Kang Shen, and Yuehua Zeng

133 The Network of the Americas (NOTA) GNSS Network in California - Providing Reliable Data Streams for Early Warning Applications, Christian Walls, Doerte Mann, Ryan C Turner, Shawn Lawrence, Ken Austin, Glen S Mattioli, Tim Dittman, and Karl Feaux

134 A long-term-average estimate of earthquake likelihoods and the largest earthquake in central Los Angeles, Chris Rollins, and Jean-Philippe Avouac

135 Seasonal and long-term crustal stress modulation due to aquifer compaction and groundwater unloading during the 2007-2010 drought in California, Grace Carlson, Manoochehr Shirzaei, Chandrakanta Ojha, and Susanna Werth

136 Recent spatiotemporal evolution of deformation in the Los Angeles Basin and southern Central Valley of California in the context of anthropogenic activity, Kyle D Murray, and Rowena B Lohman

137 Updating GPS site positions and velocities and improving GPS coverage in southern California for the Community Geodetic Model, Eneas Torres Andrade, Gareth Funning, and Jerlyn L Swiatlowski

138 InSAR/GPS time series deformation of the 2018 Kilauea event: Preparation for a large Southern California event, Bridget R Smith-Konter, Xiaohua Xu, Lauren Ward, Liliane Burkhard, and David T Sandwell

139 Measurements of 3-component, time-dependent deformation using Sentinel-1 SAR interferometry and continuous GPS data, Yuri Fialko, and Ekaterina Tymofyeyeva

140 Quantifying the bias introduced by vegetation in InSAR studies of ground deformation and surface processes, Paula Burgi, and Rowena B Lohman

141 Soil moisture effects on InSAR time series in arid regions, Rowena B Lohman, Teresa Jordan, and Junle Jiang

142 Salton Trough Deformation in GeoGateway Tools, UAVSAR and GeoFEST, Jay W Parker, Gregory A Lyzenga, Andrea Donnellan, Margaret T Glasscoe, Marlon E Pierce, Jun Wang, Magali Barba, and Kristy F Tiampo

SCEC Community Models (CXM) — Posters 143-152

143 Estimates of Shallow Crustal Stress Heterogeneity Length Scale from Borehole Breakouts and Local Earthquake Focal Mechanism Inversions in the Los Angeles Basin, Karen M Luttrell, and Jeanne L Hardebeck

144 SCFM 3.1: Updates, maps and modeling support, Andreas Plesch, John H Shaw, . SCFM Working Group, and Craig Nicholson

145 Enhancements, Updates, and Improved Access to the Community Fault Model, Craig Nicholson, Andreas Plesch, John H Shaw, and Scott T Marshall

146 Assessing the Deep Geometry of the Los Angeles Basin Using Full H/V Spectral Ratio and Multimode Surface Waves, Zack Spica, Mathieu Perton, Robert W Clayton, and Gregory C Beroza

147 Optimization of Data Functionals for Full-3D Tomography, Alan Juarez, and Thomas H Jordan

148 Inferring crustal viscosity from seismic velocity: Application to the lower crust of Southern California, William Shinevar, Mark Behn, Greg Hirth, and Oliver Jagoutz

149 Modal mineralogy of the continental crust and implications for fault-zone rheology: Data mining the Southern Sierra Nevada exhumed crustal section, Alex E Morelan, and Michael E Oskin

150 RHEOL_GUI: A Matlab-based graphical user interface for the interactive investigation of strength profiles, Laurent G Montesi, and William Leete

151 Offshore Geology Framework for the Community Rheology Model, Mark R Legg, and Michael E Oskin

152 Progress toward a Community Rheology Model of Southern California, Elizabeth H Hearn, Michael E Oskin, Wayne R Thatcher, Greg Hirth, Whitney M Behr, and Mark R Legg

Stress and Deformation Over Time (SDOT) — Posters 153-168

153 New Constraints on Stress Heterogeneity along High Risk Fault Systems in the Santa Barbara Channel, California from Borehole Breakouts, Edward H Pritchard, Patricia Persaud, and Joann M Stock

154 Borehole Breakout Determined Stress Regime in the Southern Los Angeles Basin, California, Justin O Kain, Patricia Persaud, and Edward H Pritchard

155 Numerical simulations of stress variations with depth in a model for the San Jacinto fault zone, Niloufar Abolfathian, Christopher W Johnson, and Yehuda Ben-Zion

156 Monitoring Seasonally-Driven Stress Changes on Faults within the Plate Boundary Zone in California using cGPS Observations, Jeonghyeop Kim, Alireza Bahadori, and William E Holt

157 Orientation of faults, fault roots, rock fabric, stress, and deformation in Southern California: Geographical comparisons and field and numerical experiments, Thorsten W Becker, Vera Schulte-Pelkum, Whitney M Behr, Robert Porritt, and Meghan S Miller

158 Assessing off-fault damage during development of a dismembered flower structure, Emma J Vierra, Bonnie A Flynn, Mario S Bermudez, Heather N Webb, Gary H Girty, and Thomas K Rockwell

159 Dipping fault structures near the brittle-ductile transition and deep foliation fabric in southern California, Vera Schulte-Pelkum, Zachary E Ross, Karl J Mueller, and Yehuda Ben-Zion

160 Seafloor scarps, stepover geometry, and kinematics of the Newport-Inglewood fault zone offshore Oceanside, California, James Conrad, Daniel S Brothers, Maureen L Walton, Ray W Sliter, and Peter Dartnell

161 Shear heating and the brittle-ductile transition: thermomechanical earthquake cycle simulations on continental strike-slip faults, Kali L Allison, and Eric M Dunham

162 Lithosphere Viscosity Variations in Southern California, William E Holt, Laurent G Montesi, and Alireza Bahadori

163 The role of rheological evolution on active deformation of Southwestern North America within the Pacific-North America Plate Boundary Zone since the Oligocene, Alireza Bahadori, William E Holt, Jeonghyeop Kim, Troy Rasbury, Weisen Shen, and Julia Grossman

165 Assessing kinematic compatibility of fault geometry and slip rates along the southern San Andreas fault system in the San Gorgonio Pass region, Jennifer L Hatch, and Michele L Cooke

166 Fault linkage through the Imperial Valley, California is required to match current slip rate estimates, Scott T Marshall, Elizabeth H Madden, Jacob H Dorsett, and Michele L Cooke

167 Deformation in the Yuha Desert from the 2010 M7.2 El Mayor – Cucapah Earthquake, Andrea Donnellan, Jay W Parker, Michael B Heflin, John B Rundle, Lisa Grant Ludwig, and Gregory A Lyzenga

168 Afterslip and Viscoelastic Processes and Their Relation with Seismic Activity: An Example from the Study of the Mw 7.2 El Mayor-Cucapah Earthquake (Mexico), Adriano Gualandi, and Zhen Liu

Fault and Rupture Mechanics (FARM) — Posters 169-216, 279-281

169 The composition and structure of shallow portions of the San Andreas and San Gabriel Faults, James P Evans, Rebekah Reimann, Caroline Studnicky, and Kelly K Bradbury

170 Detailed mapping of normal fault array geometry using dm-scale high resolution topographic imagery from the Volcanic Tablelands, Bishop, California, Tyler R Scott, Ramon Arrowsmith, Chelsea P Scott, and Daniel Lao Davila

171 Gouge Development in the San Andreas Fault from Lake Elizabeth core samples, Heather M Savage, Randolph Williams, and Christie D Rowe

172 Fluid-enhanced grain boundary sliding in pseudotachylyte survivor clasts: does creep cavitation lead to earthquake rupture? Elena Miranda, and Alberto Perez-Huerta

173 Nanoscale evidence for transient rheology during an earthquake, Alexis K Ault, Jordan L Jensen, and Robert G McDermott

174 Evolution of frictional shear resistance in response to rapid variations of normal stress, Yuval Tal, Vito Rubino, Nadia Lapusta, and Ares J Rosakis

175 Seismic Radiation During Slip Along a Bimaterial Fault: An Experimental Investigation, Tanner Shadoan, Brett M Carpenter, Ze'ev Reches, Xiaofeng Chen, and Simon Zu

176 Preliminary data on detecting asperity flash heating on hematite faults with laboratory experiments and hematite (U-Th)/He thermochronometry, Gabriele V Calzolari, Alexis K Ault, and Greg Hirth

177 Progress Report 2 on Addition of a High-Speed Drive to High-Pressure, Rotary-Shear Apparatus, Terry E Tullis

178 Mechanics of Fault-Tip Deformation in Brittle and Ductile Faults: Laboratory Test of Off-Fault Yield Models & Fracture Energy Budget, Taka Kanaya, and Greg Hirth

179 The effect of grain size and gouge microstructure on fault slip behavior, John Bedford, and Daniel Faulkner

180 Does effective stress have reduced sensitivity to pore pressure at seismogenic depths? Patrick M Fulton, Szu-Ting Kuo, Hiroko Kitajima, and Xiaoda Liu

181 Thermal pressurization evolution with total slip, Nir Z Badt, Terry E Tullis, and Greg Hirth

182 Effect of fault architecture and permeability evolution on response to fluid injection, Zhuo Yang, Alissar Yehya, and James R Rice

183 The spatial footprint of injection wells in a global compilation of induced earthquake sequences, Emily E Brodsky, and Thomas H Goebel

184 Understanding Injection-induced Seismicity Effects on Fault Damage Zones: Beyond Poroelastic Models, Robert L Walker, Mahshad Samnejad, and Fred Aminzadeh

185 Fluid-induced aseismic slip can outpace pore-fluid migration – evidence from in situ data, Pathikrit Bhattacharya, and Robert C Viesca

186 Numerical Modeling of a Fluid-Induced Aseismic-Seismic Slip Sequence on a Rate-and-State Fault, Stacy Larochelle, Nadia Lapusta, Jean-Paul Ampuero, and Frederic Cappa

187 Nucleation and propagation of slow slip pulses on rate-strengthening faults, Elias R Heimisson, Eric M Dunham, and Martin Almquist

188 Probing mechanisms of unsteady shallow creep on major crustal faults, Junle Jiang, and Yuri Fialko

189 The slow slip of viscous faults, Robert C Viesca, and Pierre Dublanchet

190 Crack models of repeating earthquakes predict observed moment-recurrence scaling, Camilla Cattania, and Paul Segall

191 Modeling low-frequency earthquakes on a rate-and-state fault, Zhichao Shen, and Nadia Lapusta

192 The Community Code Verification Exercise for Simulating Sequences of Earthquakes and Aseismic Slip (SEAS): Initial Benchmarks and Future Directions, Brittany A Erickson, Junle Jiang, Michael Barall, Nadia Lapusta, Eric M Dunham, Ruth A Harris, Lauren Abrahams, Kali L Allison, Jean-Paul Ampuero, Sylvain D Barbot, Camilla Cattania, Ahmed E Elbanna, Yuri Fialko, Benjamin Idini Zabala, Jeremy E Kozdon, Valere R Lambert, Yajing Liu, Yingdi Luo, Xiao Ma, Paul Segall, Pengcheng Shi, and Meng Wei

193 Investigation of Adaptive Time-Stepping Algorithms for Simulating Sequences of Earthquakes and Aseismic Slip (SEAS), Yanke Song, Valere R Lambert, and Nadia Lapusta

194 Earthquake Sequences in Rate-and-State Fault Models with Thermal Pressurization, Valere R Lambert, Stephen M Perry, and Nadia Lapusta

195 Coupled interactions of fluid-pressure and earthquake cycles: Numerical simulations of fault-valve behaviour, Weiqiang Zhu, Kali L Allison, and Eric M Dunham

196 Persistent effects of low-velocity fault zones on earthquake rupture after multiple earthquake cycles, Benjamin Idini, and Jean-Paul Ampuero

197 3D Ruptures Simulations Across Stepping Faults; Comparing the Slip Weakening and Rate-State Friction, Kayla A Kroll, James H Dieterich, Keith B Richards-Dinger, and David D Oglesby

198 A novel hybrid numerical finite element-spectral boundary integral scheme for modeling earthquake cycles, Mohamed Abdelmeguid, Xiao Ma, and Ahmed E Elbanna

199 Modeling Earthquake Mechanics with High Resolution Fault Zone Physics: New Computational Tools for Addressing The Conundrum of Scales, Ahmed E Elbanna, Setare Hajarolasvadi, Xiao Ma, Mohamed Abdelmeguid, David Kammer, Gabriele Albertini, Bob Haber, and Amit Madhukar

200 Modeling Dynamic Ruptures with High Resolution Fault Zone Physics, Xiao Ma, and Ahmed E Elbanna

201 Modeling damage evolution in the near-fault region as a result of rupture on complex fault, Khurram Aslam, and Eric G Daub

202 Rupture Dynamics at the Interface Between a Thin Compliant Layer and Stiffer Underlying Half-Space, Lauren S Abrahams, Kali L Allison, and Eric M Dunham

203 Investigating and validating surface rupture characteristics with rupture dynamics on faults with shallow complexities, Sebastien Hok, Rihab Sassi, and Yann Klinger

204 Multi-physical couplings and microstructure size effects on the localization of deformation in a fault core, Hadrien Rattez, Ioannis Stefanou, Jean Sulem, Manolis Veveakis, and Thomas Poulet

205 A Dynamic Earthquake Simulator for Geometrically Complex Faults Governed by Rate- and State-Friction, Dunyu Liu, Benchun Duan, and Bin Luo

206 Dynamic rupture and cross-fault activation: the effect of high pre-stress contrast, David D Oglesby, Christodoulos Kyriakopoulos, Thomas K Rockwell, Aron J Meltzner, Michael Barall, and Jon Fletcher

207 The Effect of Along-Strike Variation in Dip on Rupture Propagation on Strike-Slip Faults, Julian C Lozos

208 Effects of Fault Geometry and Pre-Stress Loading for Scenarios of Earthquakes on the Eastern San Gorgonio Pass Region in CA using Dynamic Rupture Simulations, Roby Douilly, David D Oglesby, Michele L Cooke, and Jennifer L Beyer

209 Dynamic rupture modeling to investigate the role of fault geometry in jumping rupture between parallel-trace thrust faults, Paul L Peshette, Julian C Lozos, Doug Yule, and Eileen L Evans

210 Surface Displacement and Ground Motion from Dynamic Rupture Models of Thrust Faults with Variable Dip Angles and Burial Depths, Sirena Ulloa, and Julian C Lozos

211 Landers 1992 "reloaded": an integrative dynamic earthquake rupture model, Stephanie Wollherr, Alice-Agnes Gabriel, and Paul M Mai

212 Searching for Spot-Fire Earthquakes Triggered During the 2004 Parkfield Mainshock, Norman H Sleep

213 Earthquake behaviors in Source Time functions: energetic onset of earthquakes and biases from over-simplifying the source pulse, Marine A Denolle, and Philippe J Danré

214 Earthquake sub-event scaling: new perspective for rupture determinism, Philippe J Danré, Jiuxun Yin, Bradley P Lipovsky, and Marine A Denolle

215 Compressional branching during the 2012 Mw 8.6 Off-Sumatra Earthquake: Implications from Earthquake Cycle Simulations, Yuqing Xie, and Lingsen Meng

216 A Physical Interpretation for Anomalous Source Spectra with a Deficit at Intermediate Frequencies, Yongfei Wang, Steven M Day, and Peter M Shearer

279 Tsunami Source Inversions Using Adjoint-state Methods, Lingsen Meng, Tong Zhou, Xie Yuqing, and Jiayuan Han

280 Inelastic Wedge Failure and Along-Strike Variations of Tsunami Generation in the Shallow Subduction Zone, Shuo Ma, and Shiying Nie

281 Stress-glut representation by orthogonal moment-tensor fields, Thomas H Jordan, and Alan Juarez

Earthquake Geology / San Andreas Fault System (SAFS) — Posters 217-278

217 A 6000-Year-Long Paleoseismologic Record of Earthquakes along the Xorkoli Section of the Altyn Tagh Fault, China, Jing Liu, Zhaode Yuan, Wei Wang, Ray J Weldon, Michael E Oskin, and Yanxiu Shao

218 Paleoseismology of the northern San Jacinto fault, San Bernardino County, Katherine J Kendrick, and Thomas E Fumal

219 Sequence of cascading earthquakes on the Newport-Inglewood-Rose Canyon Fault zone from paleoseismic observations, Drake M Singleton, Thomas K Rockwell, and Jillian M Maloney

220 Re-evaluation of the late-Pleistocene slip rate of the Haiyuan fault near Songshan, Gansu province, China, WENQIAN YAO, Jing Liu, Michael E Oskin, Veronica B Prush, Wei Wang, and Zhanfei LI

221 Paleoearthquake record of the Conway segment of the Hope fault: Implications for patterns of earthquake occurrence in northern South Island and southern North Island, New Zealand, Alexandra E Hatem, James F Dolan, Robert M Langridge, Robert W Zinke, Russ J Van Dissen, Christopher P McGuire, and Ed J Rhodes

222 Preliminary geologic slip rates along Andes fastest slipping crustal fault, the Liquiñe-Ofqui Fault Zone (LOFZ), Patagonia, Chile, Gregory P De Pascale, Melanie Froude, Ivanna Penna, Reginald Hermanns, Daniel Moncada, Sergio Sepulveda, Mario Persico, David Petley, Gabriel Vargas, William Murphy, and Sebastian Pairoa

223 The Thousand Lake Fault: Earthquake Geology of a Long Recurrence Normal Fault at the Eastern Edge of the Basin and Range, Nathan A Toke, David W Marchetti, Christopher M Bailey, Robert Biek, Joseph Phillips, Hanna Bartram, and Clayton Forster

224 Using relative structural complexity of fault segment barriers to model prehistoric earthquake rupture histories, Christopher B DuRoss, Ryan D Gold, Rich W Briggs, and Scott E Bennett

225 Contemporary and Paleoliquefaction Induced Lateral Spreading in Christchurch New Zealand, Jeffrey L Bachhuber, Gregory P De Pascale, Ellen Rathje, michael Little, Peter Almond, Christian Ruegg, and Michael Finnemore

226 Analysis of Offset Stream Channels – Deconstructing Creep and Coseismic Slip Components Using Very High Resolution SfM Imagery, Southern San Andreas Fault, Coachella Valley, California, Chelsea M Blanton, Thomas K Rockwell, Allen Gontz, and Josh Kelly

227 Are offset channels accurate representations of strike-slip fault displacement? Implications from landscape evolution modeling, Nadine Reitman, Karl J Mueller, Gregory E Tucker, and Katherine R Barnhart

228 High Resolution Geodetic Measurements of Co-seismic Fault-zone Deformation for Probabilistic Fault Displacement Hazard Assesment and Confidence Intervals on Geologic Slip Rates, Chris W Milliner, and Andrea Donnellan

229 Geologic and Structural Characterization of The Rock Volume Imaged by the Dense Nodal Seismic Array Along the San Jacinto Fault at Sage Brush Flat, Southern California, Adam Wade

230 Seismic and aseismic fault slip revealed by luminescence bleaching depth profiles of the bedrock normal fault scarp, Jie Chen, Ming Luo, Jintang Qin, Jinhui Yin, Lewis A Owen, Haoran Wang, Huili Yang, Jinfeng Liu, and Boxuan Zhang

231 Dear Prudence: how many surface clasts are required to yield an accurate exposure date? Veronica B Prush, and Michael E Oskin

232 Earthquake hazard assessment evaluated by fragile geologic features in coastal Central California, Anna H Caklais, Dylan H Rood, Mark W Stirling, Christopher M Madugo, Norman A Abrahamson, Klaus Wilcken, Tania Gonzalez, Albert R Kottke, and Alexander C Whittaker

233 Precariously Balanced Rocks in northern Utah: are Wasatch Fault earthquakes worse than expected? Amir A Allam, Austin Sorscher, Alysha Armstrong, Cole Richards, Austin McKell, and Sam Clairmont

234 Dating of Offset Geomorphic Features Along the Garlock Fault, Mojave Desert, California: Testing a Proposed Earthquake Supercycle Model, James E Burns, Sally F McGill, Ed J Rhodes, James F Dolan, and Nathan D Brown

235 Complex faulting structures in Eureka Valley, Death Valley National Park, CA, Michael J Lawson, Steven G Okubo, Tyanna M Schlom, Ed J Rhodes, Jeff Knott, and An Yin

236 Tectonic and geometric constraints for the Wind Canyon fault block on the western Garlock fault: an apatite fission track analysis, Iris Smith

237 Distributed fault slip in the Eastern California shear zone: adding a piece to the puzzle, Elizabeth K Haddon, David M Miller, Victoria E Langenheim, Tanzhuo Liu, Elmira Wan, and Laura C Walkup

238 Investigating strain transfer along faults in Joshua Tree National Park, CA, with possible implications for along strike variations in southern San Andreas Fault slip rate, Katherine A Guns, Richard A Bennett, Kimberly D Blisniuk, and Sally F McGill

239 Paleoseismology of the central Garlock Fault in Searles Valley, California., Kyle Peña, Sally F McGill, Ed J Rhodes, James F Dolan, Robert Zinke, Alexandra E Hatem, and Nathan D Brown

240 Paleoseismology and Neotectonics of the Southern Sierra El Mayor, Baja California, Mexico, Keene W Karlsson, Thomas K Rockwell, John M Fletcher, Allen M Gontz, Paula M Figueiredo, and Lewis A Owen

241 The Hidden Past of the Alai Valley: Understanding the Seismic History and Behavior of the Central Pamir Frontal Thrust System through Paleoseismology., Magda Patyniak, Angela Landgraf, Ramon Arrowsmith, Atyrgul Dzhumabaeva, Alana M Williams, Kanatbek Abdrakhmatov, and Manfred Strecker

242 Coral microatolls as a tool for subduction zone paleoseismology: Identifying rare events along the Sunda megathrust and the Manila trench, Aron J Meltzner

243 Active Tectonics across the Indo-Burma Range, Patcharaporn Maneerat

244 Deducing Crustal-scale Reverse-Fault Slip Distribution from Folded River Terraces, Qilian Shan, China, Yiran Wang, Michael E Oskin, and Youli Li

245 Characterizing the 3D geometry of the Ventura-Pitas Point fault system and its implications for earthquake hazards in southern California, Jessica Don, Andreas Plesch, Mattie M Newman, and John H Shaw

246 Shallow fault mapping in the Sacramento-San Joaquin Delta, Shannon A Klotsko, Jillian M Maloney, and Janet Watt

247 Late Quaternary Deformation in the Inverted Santa Maria Basin, CA: Documenting and Quantifying Active Folding from Syn-Tectonic Deposits, Ian McGregor, and Nate W Onderdonk

248 3D insights into active deformation, stratigraphic architecture, and submarine slope failure in the Santa Barbara Channel, southern California, Jared W Kluesner, Daniel S Brothers, Alexis Wright, and Samuel Johnson

249 Towards characterizing the geometry and potential fault system connectivity at the southern termination of the Palos Verdes fault, offshore southern California, Dan Boyd, and Jayne M Bormann

250 The Wilmington Blind-Thrust Fault: An active, concealed earthquake source beneath Los Angeles, CA, Franklin D Wolfe, John H Shaw, Andreas Plesch, Daniel J Ponti, James F Dolan, and Mark R Legg

251 Rupture scenarios for the San Diego Trough and San Pedro Basin fault systems, offshore Southern California, Jayne M Bormann, Graham M Kent, and Neal W Driscoll

252 Structural Architecture of the Western Transverse Ranges and Potential for Large Earthquakes - New Results of Trishear Forward Models, Yuval Levy, Thomas K Rockwell, John H Shaw, Andreas Plesch, Neal W Driscoll, and Hector Parea

253 Geomorphic evidence for the geometry and slip rate of the Southern San Cayetano fault: Implications for hazard assessment and fault interaction in complex tectonic environments, Alex Hughes, Dylan H Rood, Alexander Whittaker, Rebecca Bell, Thomas K Rockwell, Yuval Levy, Klaus Wilcken, Lee Corbett, Paul Bierman, Duane E DeVecchio, Scott T Marshall, Larry D Gurrola, and Craig Nicholson

254 Quaternary Slip History of the Central Sierra Madre Fault, Southern California, Reed J Burgette, Katherine M Scharer, Nathaniel Lifton, Austin Hanson, Devin McPhillips, and Tammy M Rittenour

255 Quantifying uncertainty in cumulative surface slip along the Cucamonga Fault, a crustal thrust fault in southern California, Devin McPhillips, and Katherine M Scharer

256 Quaternary slip history of the Santa Susana fault, western Transverse Ranges: Insights from U-Pb detrital zircon geochronology, Jonathan Ingram, Reed J Burgette, and Brian A Hampton

257 Geomorphic and structural mapping in pursuit of a slip rate for the Santa Susana Fault, Southern California, Michael P Reed, Reed J Burgette, Katherine M Scharer, Nathaniel Lifton, and Devin McPhillips

258 Using GeoGateway Data to Explore Deformation in the Cajon Pass Region, Megan A Mirkhanian, Lisa Grant Ludwig, Andrea Donnellan, Jay W Parker, and Robert A Granat

259 Multicomponent Model of Crustal Stress at Cajon Pass with Implications for Stress Field Heterogeneity, Elliott C Helgans, Karen M Luttrell, and Bridget R Smith-Konter

260 Strain rate dependence on crustal rheology for the Cajon Pass, California, Lauren Ward, Bridget R Smith-Konter, Xiaohua Xu, and David Sandwell

261 Revisiting the Cajon Pass Quaternary Terraces with Geochronology dating– implications for the long term slip rates of the San Jacinto and San Andreas systems, Paula M Figueiredo, Ray J Weldon, and Lewis A Owen

262 Earthquake cycle stress accumulation disparities of the Cajon Pass region, Liliane Burkhard, Bridget R Smith-Konter, Lauren Ward, Katherine M Scharer, and David T Sandwell

263 Paleoearthquakes within 100 km and 1000 years of modern Cajon Pass, California, Katherine M Scharer

264 The Current Unlikely Earthquake Hiatus at California's Transform Boundary Paleoseismic Sites, Glenn P Biasi, and Katherine M Scharer

265 When do San Andreas Fault ruptures diverge on to other faults? Gordon G Seitz, and David P Schwartz

266 Late Holocene Rupture History of the South-Central San Andreas Fault at the Van Matre Ranch site, Carrizo Plain, California, Nick J Inserra, and Sinan O Akciz

267 Refining the earthquake chronology of the last millennium along the Cholame segment of the San Andreas fault, Alana M Williams

268 Preliminary ages of prehistoric earthquakes on the Banning Strand of the San Andreas Fault, near North Palm Springs, California, Bryan A Castillo, Sally F McGill, Katherine M Scharer, Doug Yule, Devin McPhillips, James C McNeil, and Alan Pace

269 Holocene slip rates along the Mojave Section of the San Andreas fault, Elaine K Young, Eric S Cowgill, and Katherine M Scharer

270 In search of earthquakes, a biomarker thermal maturity investigation into the seismic potential of the central San Andreas Fault, Genevieve L Coffey

271 Contrasts in integrated crustal strength drive the asymmetric distribution of topography and deformation within restraining bends, Curtis W Baden, and George E Hilley

272 Gravity and aeromagnetic maps of the San Gorgonio Pass region, California: Potential insights from potential-field data on fault and basin geometry in a restraining bend, Victoria E Langenheim, and Jonathan C Matti

273 Characterization of Faulting at the San Andreas Oasis in the Dos Palmas Preserve Using Ground-based Magnetics, VLF and DC Resistivity, Drew Faherty, Stacey R Petrashek, Raul Contreras, and Nathan W Pulver

274 Unraveling a tectonic knot: structural domains, voluminous fault zones, creep, and dispersed strain between the San Andreas Fault and Brawley Seismic Zone, Clara Thomann, Susanne U Jänecke, Daniel Markowski, James P Evans, and Robert Quinn

275 Focal mechanisms and seismicity of LFEs on Parkfield, Miki Aso, Naofumi Aso, and Satoshi Ide

276 Urban Nodal Array Maps Structure of the Northern Los Angeles Basins with Teleseismic Receiver Functions, Patricia Persaud, Guibao Liu, and Robert W Clayton

277 A Moving Mud Pot Threatening Railroad Tracks and a Highway, Imperial County, California, David K Lynch, Travis Deane, Carolina Zamora, Dean G Francuch, James S Bailey, Christopher W Allen, Justin D Rogers, and Cassandra Gouger

278 Looking Ahead by Looking Down – Potential Applications of Very High Resolution Drone-Based Imagery for Tectonic Geomorphology, Allen M Gontz, Chelsea M Blanton, Thomas K Rockwell, and Joshua T Kelly

Computational Science / Community Modeling Environment (CME) — Posters 287-297

287 The New Zealand Velocity Model (NZVM) Version 2.0 and ground motion simulations of Hope Fault earthquakes, Ethan M Thomson, Brendon A Bradley, and Robin L Lee

288 California Transverse Mercator projection (CATM) for Building Gridded Seismic Velocity Volumes for Seismic Wave Propagation Simulations, David A Okaya, Yao-Yi Chiang, Philip J Maechling, and Mei-Hui Su

289 Fused Earthquake Simulations on Deep Learning Hardware, Alexander N Breuer, Alexander Heinecke, and Yifeng Cui

291 An Efficient Numerical Method for the Simulation of Earthquake Cycles in Complex Geometries, Jeremy E Kozdon, and Brittany A Erickson

292 Unraveling earthquake dynamics through large-scale multi-physics simulations, Alice-Agnes Gabriel, Stephanie Wollherr, Thomas Ulrich, Elizabeth H Madden, Kenneth Duru, and Duo Li

293 Towards topography in AWP-ODC, Ossian O'Reilly, Alexander N Breuer, Yifeng Cui, Christine A Goulet, and Kim B Olsen

294 Unified and Continuous Software Development for AWP-ODC-OS, Yifeng Cui, Alexander N Breuer, Rajdeep Konwar, and David Lenz

295 A SCEC CyberShake Physics-Based Probabilistic Seismic Hazard Model for Northern California, Scott Callaghan, Philip J Maechling, Christine A Goulet, Kevin R Milner, Mei-Hui Su, Robert W Graves, Kim B Olsen, Brad T Aagaard, Kathryn E Wooddell, Albert R Kottke, Thomas H Jordan, and John E Vidale

296 The SCEC Software Ecosystem for Earthquake System Science Research, Philip J Maechling, Jacobo Bielak, Scott Callaghan, Yifeng Cui, Edward H Field, Christine A Goulet, Robert W Graves, Thomas H Jordan, Kevin R Milner, Kim B Olsen, Daniel Roten, William H Savran, Fabio Silva, Mei-Hui Su, Ricardo Taborda, and John E Vidale

297 Developing Software to Support SCEC Research Collaborations and Data Dissemination: A Case Study of the Committee for the Utilization of Ground Motion Simulations (UGMS) Project, Edric Pauk, Tran T Huynh, Kevin R Milner, Scott Callaghan, David Gill, Christine A Goulet, and C.B. Crouse

Communication, Education, and Outreach (CEO) — Posters 311-320

311 2018 USEIT: Using Machine Learning to Forecast Earthquakes, Anthony A Guerra, Brandon T Ho, Varduhi Kababjyan, Ramon Mei, Tomoe Mizutani, Tiffany Streitenberger, Shalani Weerasooriya, Jordan Wolz, Guillermo Beas, Shengyu Wang, Abhijit Kashyap, and Jacquelyn J Gilchrist

312 Simulating Millions of Years of Earthquakes in California using HPC, Varduhi Kababjyan, Shril P Panchigar, Anthony G Lopez, Tomoe Mizutani, Anthony A Guerra, Scott Callaghan, Jacquelyn J Gilchrist, Jozi K Pearson, Gabriela R Noriega, and Thomas H Jordan

313 Predictive Skill: Using the Bayesian Inference to Study RSQSim and UCERF3, Jordan Cortez, Guillermo Beas, Shengyu Wang, Cynthia Tong, Sebastien D Rossouw, and Katia Ascencio

314 The Development of 3-D Software to Assist the Visualization of Large and Concurrent Earthquake Data, Brandon T Ho, Shalani R Weerasooriya, Alejandro G Narvaez-Colon, Tiffany Streitenberger, Dian Zhu, Trent L Jones, Bill Addo, John Yu, Kevin R Milner, Gabriela R Noriega, Jozi K Pearson, and Thomas H Jordan

315 Visualization of Hazards Associated with Simulated Earthquakes in Southern California, Ashlee Trotter, Ramon Mei, Paige R Given, Christina Polcino, Elvis Carrillo, Jordan Wolz, Resherle Verna, Jozi K Pearson, Gabriela R Noriega, and Thomas H Jordan

316 Combining 3D printing and virtual reality goggles in outreach and communication events, Christodoulos Kyriakopoulos, and David D Oglesby

317 Causes of deaths and injuries in the 2015 Gorkha (Nepal) earthquake, Marla A Petal

318 Communicating Seismological Uncertainty to the Public: A Case Study in Oklahoma, Georgia Halkia, and Lisa Grant Ludwig

319 Lab Talk with Laura: STEM research meets comedy on the radio, Laura A Fattaruso

320 Preliminary Results of a Study to Identify Archaeological Artifacts from San Salvador in Colton, CA, Using Ground Penetrating Radar, Chloe S Sutkowski, Oscar Prado, Veronica Hernandez, and Jascha Polet

Meeting Abstracts

Earth Science Research Needs for Improving Earthquake Scenarios, Brad T Aagaard (Oral Presentation Wed 08:30)

Earthquake scenarios provide important opportunities to showcase the effectiveness of integrating science from across the spectrum of earthquake hazards research. These scenarios complement probabilistic hazard assessments by examining specific realizations of large, potential earthquakes and their consequences to improve our resilience to natural disasters. They also raise the profile of our research with national media coverage. Consequently, it is especially important to leverage knowledge from earthquake geology, tectonic geodesy, and seismology to create the most realistic earthquake scenarios possible.

The 2008 ShakeOut scenario brought together more than 300 contributors to quantify the hazards and risks associated with a magnitude 7.8 occurring on the southern San Andreas fault. This effort set new expectations for how we develop sophisticated earthquake scenarios. In 2008 the USGS also led a collaborative effort to develop a suite of earthquake ground-motion scenarios for the Hayward fault, one of which is being used as the basis for the more comprehensive HayWired earthquake scenario. Since these scenarios were developed 10 years ago, our science has continued to advance but many open questions persist.

Creating realistic earthquake ruptures remains one of the major challenges. How to select rupture end points, the depth extent of coseismic slip, and multi-fault ruptures are basic issues. Additional research is necessary to constrain rupture details, such as the spatial variability of slip, the potential hypocenter relative to geologic features and microseismicity, and the speed and direction of rupture propagation. Furthermore, we have a limited understanding of when and where we should expect significant afterslip, which impacts infrastructure response planning.

In computing scenario ground motions, research is needed to further develop techniques for incorporating sophisticated, shallow, anelastic behavior into 3D simulations and constraining the anelastic properties at regional scales. Additional work is also necessary to develop regional-scale analysis techniques for estimating the extent and severity of ground failure. Aftershock forecasts can be improved with regional parameters for clustering and fault locations.

Pursuing these research directions will lead to more accurate estimates of the anticipated consequences of large earthquakes and help support better decision-making in urban planning and disaster preparedness.

A novel hybrid numerical finite element-spectral boundary integral scheme for modeling earthquake cycles, Mohamed Abdelmeguid, Xiao Ma, and Ahmed E Elbanna (Poster Presentation 198)

Modeling earthquake ruptures is a complex challenge due to the eclectic sources of nonlinearities, such as friction law, plasticity, and material damage. In addition to the nonlinearities, another challenging aspect of earthquake dynamic is the multiscale nature of the problem, both spatially and temporally. Spatially, principle slip surfaces can be several orders of magnitude smaller than the fault rupture. Temporally, stress accumulation and instability initiations occur on a much larger time scale than the sudden energy release of a rupture episode. Accordingly, novel numerical approaches are required to resolve both temporal and spatial scales, as well as account for the nonlinearities accurately.

Here, we present a hybrid scheme that combines finite element method (FEM) and spectral boundary integral method (SBIM) to simulate earthquake cycles with rate and state fault subjected to slow tectonic loading processes of long duration intermitted by episodes of dynamic fracture in the presence of near-field heterogeneities or nonlinearity. On a spatial level, regions of small-scale heterogeneities and complex fault geometry are handled using a FEM approach, while the linearly elastic bulk with a known Green's function is modelled using SBIM. Accordingly, we benefit from the flexibility of FEM in handling nonlinear problems, while retaining the superior performance and accuracy of SBIM. We handle the intricacies associated with this time evolution using an alternating explicit-implicit scheme, such that during dynamic rupture an explicit time integration is utilized for computational efficiency, with the implicit time integration being specific only to inter-seismic periods where larger time steps are required. The presented approach is validated using a benchmark problem from the Southern California Earthquake Center's dynamic rupture simulation validation exercises. We further demonstrate the capabilities of this computationally- efficient scheme by modeling earthquake cycles for a 2D in plane problem with different parameters and settings. Finally, we discuss the potential of our approach in modelling a wide class of problems in geophysics and engineering.

Numerical simulations of stress variations with depth in a model for the San Jacinto fault zone, Niloufar Abolfathian, Christopher W Johnson, and Yehuda Ben-Zion (Poster Presentation 155)

Depth dependent crustal stress orientations produced in strike-slip faulting environments are explored using quasi-static numerical simulations with variations to the geometry and rheology of the layered substrate to test model conditions that support or reject focal mechanism stress inversion from the San Jacinto fault zone. We attempt to understand observed rotations up to ~30˚ of the principal stress axes below 10 km depth in this region. The simulations employ the finite element software package PyLith for solving the partial differential equations describing the tectonic deformation. The basic model consists of a vertical right-lateral frictional fault in horizontal crustal layers with constant tectonic loading and gravitational forces. The model design incorporates three different scenarios with a fault in an elastic upper layer atop a viscoelastic transition zone which can be adapted to simulate a widening viscoelastic region at the base of the fault. Preliminary results indicate that the stress evolution shows similar pattern in cases with different rheological parameters. The continuing work will focus on effects of spatial variations of background stress related to topography and variations of geometrical features of faults and the crust on changes of the stress tensor with depth.

Rupture Dynamics at the Interface Between a Thin Compliant Layer and Stiffer Underlying Half-Space, Lauren S Abrahams, Kali L Allison, and Eric M Dunham (Poster Presentation 202)

In this study we examined the sliding dynamics of a frictional interface between elastic solids. Sliding dynamics is well understood for two identical or dissimilar half-spaces (e.g., Rice et al, 2001; Aldam et al., 2017). Sliding between a thin layer over a half-space has also been studied, but to a lesser extent (Ranjith, 2009; Aldam et al., 2016; Lipovsky & Dunham, 2017). The thin layer over half

space problem arises in many contexts, ranging from shallowing dipping subduction zones to ice streams (in particular, the Whillans Ice Plain (WIP), which advances via twice-daily Mw 7 slow slip events). Our objective is to quantify sliding stability and rupture styles for this geometry with rate-and-state friction. Specifically, we study the influence of layer thickness (H) on conditions for steady sliding vs. slow slip cycles vs. fast slip cycles, using both linear stability analysis and earthquake cycle simulations on a 2D anti-plane shear sliding of a thin compliant layer over a stiffer half-space.

Steady sliding with velocity-weakening rate-and-state friction is linearly unstable above a critical wavelength (Lc). For thin layers, such as the WIP, Lc is proportional to the square-root of H. But, as H is increased, Lc becomes independent of H and approaches to the well-known solution for sliding between two half-spaces.

The stability analysis provides insight into more complex situations, such as the nonlinear earthquake cycle dynamics of a nominally velocity-strengthening interface containing a velocity-weakening patch of width W. For small W, the patch slides steadily with the rest of the interface, and for large W the patch fails in fast earthquakes. Between these two limits, the patch exhibits slow slip events. We use our cycle simulations to map sliding style as a function of H and W, finding a trend that is consistent with the stability analysis. Overall this study demonstrates how the decreasing elastic stiffness associated with small layer thickness reduces the critical wavelength for instability, with important implications for rupture dynamics in thin layer geometries.

A Proposed Seismic Velocity Profile Database Model, Sean K Ahdi, Shamsher Sadiq, Okan Ilhan, Yousef Bozorgnia, Youssef Hashash, Dong Youp Kwak, Duhee Park, Alan Yong, and Jonathan P Stewart (Poster Presentation 022)

We describe the data model currently in use in a publicly available velocity profile database under development for the United States. The initial implementation of the database contains data primarily from California, but also currently includes various sites around the U.S. Our data model consists of JavaScript Object Notation (JSON) format files for storing metadata and data. For a site to be included in the database, the minimum metadata requirements are accurate geodetic coordinates, and the minimum data requirement is a shear-wave velocity profile. The JSON files are structured in a hierarchal manner to store metadata and data using a nested structure consisting of location, velocity profiles, dispersion curve data (for surface-wave methods), geotechnical data, and horizontal-to-vertical spectral ratios (HVSR). At the present stage of the project, we are populating the database using the schema described herein. However, the schema and JSON file structure are flexible, and as we continue to develop the data model and populate the database with various data sources, we have the ability to include other relevant data, as well as evaluate other file formats to increase the efficiency of data storage and querying. In the current data model, location information includes site geodetic values (latitude, longitude, and elevation) and various site descriptors related to surface geology, geomorphic terrain category, and topographic slope gradient, among other site-level metadata. Velocity data include the geophysical method(s) used to obtain the shear-wave velocity profile, modeled primary- and shear-wave velocity (VP and VS, respectively) and its uncertainty as a function of depth, modeled profile maximum depth, and the computed time-averaged VS to the maximum profile depth. VS30, the time-averaged VS to 30 m depth, is computed and included if the maximum profile depth reaches 30 m. In the case of surface-wave based data, dispersion curve data can be recorded in the data structure as phase velocity versus either wavelength or frequency. Geotechnical data includes boring logs, standard penetration resistance, cone penetration test sounding logs, and laboratory index test results. HVSR plots are given as a function of frequency. The database to date contains digitized velocity profiles at over 1000 sites, and we eventually anticipate to include an estimated 4500 total profiles in the U.S., with nearly 2000 profiles in California alone.

Where We Have Been, Where We Are Going… And How We Can Work Together, Marissa Aho (Oral Presentation Wed 09:00)

More than 10 years after the 2008 ShakeOut scenario, the Mayor's Office of Resilience is still working with many of the original authors and other partners to advance the region's seismic resilience. ShakeOut and other related efforts have had a major impact on seismic policy in the City of Los Angeles, including the formation of the Mayor's Seismic Safety Task Force, the advancement of DWP's water resilience program, the partnership with U.S. Geological Survey that enabled Dr. Lucy Jones to serve as Mayor Garcetti's Science Advisor, and the release of the Mayor's Resilience by Design report in December 2014. Resilience by Design focused on strengthening LA's most vulnerable buildings, fortifying LA's water system, and enhancing reliable telecommunications. Now approaching its 4-year anniversary, I will discuss the status of many of the recommendations in Resilience by Design that have been implemented.

Resilience by Design is undoubtedly the cornerstone of Los Angeles' resilience-building. As inaugural members of 100 Resilient Cities pioneered by the Rockefeller Foundation, the City of Los Angeles worked with hundreds of partners during 2016-2017 to develop Resilient Los Angeles. Resilient Los Angeles was released by Mayor Garcetti in March of 2018 as a strategy that addresses Disaster Preparedness and Recovery, Climate Adaptation, Infrastructure Modernization, Economic Security and Leadership and Engagement. A number of the 96 Actions in Resilient Los Angeles advance the City's seismic resilient efforts. I will highlight some of them and talk about how we can work together to continue to advance seismic resilience together.

3-D upper crustal velocity structure of the Coachella Valley, Southern California: results from the salton seismic imaging project, Rasheed Ajala, Patricia Persaud, Joann M Stock, Gary S Fuis, John A Hole, Mark R Goldman, and Daniel S Scheirer (Poster Presentation 103)

The Coachella Valley is host to the southernmost section of the San Andreas fault (SAF), which is generally considered to be overdue for a large magnitude (M≥7) earthquake. To improve seismic risk assessments in this region, accurate knowledge of the Coachella Valley sedimentary basin structure and fault structure is required. We inverted first P-wave arrival times from local seismicity (39,998 events) and shots (251 land/sea explosions) from the 2011 Salton Seismic Imaging Project to produce a 3-D Vp model of the Coachella Valley and the surrounding mountain ranges. Several inversion and resolution tests were performed to ensure that the best parameters were used in the modeling procedure and that the final model is representative of a smooth version of the actual structure. Our model has a grid spacing of 0.5 km with good resolution (~50 rays/cubic km) to 9 km depth. The top ~3 km of the model conforms with the surface geology. Sediment thickness in the valley ranges from a maximum of ~4 km at the northern end of Salton Sea and thins to ~2 km at the northern end of the valley. The basin asymmetry is evident from the

persistence of low velocities on the eastern side of the valley compared to the western side. Estimated basement depths in the Coachella Valley using a 4.5 km/s isovelocity surface reveal multiple sub-basins related to upward steps in basement toward the NW. Lateral velocity contrasts subparallel to and offset from mapped surface faults provide fault geometry information, including evidence supporting a northeast-dipping SAF. Basement in the valley is highly heterogeneous and comprises high velocity (≥6.4 km/s) regions that we interpret to be mylonitic and schistose rocks from the Peninsular Ranges and Eastern Transverse Ranges, respectively.

Precariously Balanced Rocks in northern Utah: are Wasatch Fault earthquakes worse than expected?, Amir A Allam, Austin Sorscher, Alysha Armstrong, Cole Richards, Austin McKell, and Sam Clairmont (Poster Presentation 233)

Where they persist in seismically active regions, precariously balanced rock [PBR] formations can be used to provide constraint on the strongest co-seismic ground motions which occurred during the largest prehistoric earthquakes. The Wasatch Fault system in Northern Utah consists of at least ten active segments each capable of producing M>7.0 earthquakes with recurrence intervals on the order of 500-1000 years based on paleoseismic trenching, active-source seismic, Lidar, and a variety of other geological data. This fault system is among the most hazardous in North America based on probabilistic hazard assessment and deterministic ground motion simulations, the latter of which show acceleration of 1g in the most densely-populated valley regions of Utah. To provide quantitative data for direct comparison to such simulations we identify, map, and model PBRs in the vicinity of the Wasatch Fault zone. We ultimately measure the force required to topple each formation by comparing these observations to previous work and through ongoing drone-based photogrammetry and multiphysics modeling, from which we infer the maximum possible co-seismic ground motion at each site. By identifying the geological units and geomorphological conditions that lead to PBR formation, we also map regions where we would expect but fail to find any PBRs. Based on extensive field mapping in which we've located 27 PBRs, we observe a systematic pattern: we find no PBRs at all within 15km of the Wasatch fault, a few semi-precarious rocks (<0.7g toppling force) from 15km to 30km distance, with true PBRs (<0.4g) only at distances greater than 30km. These combined results suggest that the ground motion simulations are underestimating the regional extent or amplitude of co-seismic shaking due to Wasatch fault earthquakes.

New techniques in point cloud analysis of high-density seismic array data to determine three dimensional fault and crustal structures in the Long Beach Basin, Andrew Allevato, Robert W Clayton, and Dayanthie S Weeraratne (Poster Presentation 096)

The lack of knowledge of crustal structure and fault surface behavior at depth can adversley affect earthquake hazard analysis in highly populated areas. Interactions between faults and crustal layers at depth may also be important. Using passive seismic data recorded in Long Beach, California from 2011 to 2012, we propose a new method to find crustal layer discontinuities utilizing point cloud methods. This is a high-density study using 7,781 geophones within a 98 square km area, which allows for excellent resolution of detailed structures at crustal depths. The development of this new methodology may prove to be cost-effective, while also providing a way for seismologists and companies to check hypotheses using passive seismic data before fully deploying an active source experiment. We first create a 3D model of the autocorrelated passive data. We then locate clear planes or surfaces within the 3D seismic data set. We isolate each structural plane separately and connect each point in the point cloud to another point forming small triangles. Each of the trianglar surfaces are filled in using Delaunay triangulation. The three dimensional structure of the northwest-southeast trending Newport-Inglewood Fault is identified from point cloud analysis. We observe that the Moho is dipping inland at a 25-degree angle from horizontal. Major crustal boundaries, such as the upper crust, lower crust, and several minor layers in between, are also identified. These results can be used in hazard analysis of the Long Beach area, while also giving us a better understanding of the Long Beach Basin in general.

Shear heating and the brittle-ductile transition: thermomechanical earthquake cycle simulations on continental strike-slip faults, Kali L Allison, and Eric M Dunham (Poster Presentation 161)

We investigate interactions between coseismic slip in the seismogenic zone, deeper interseismic fault creep, and off-fault viscous flow in the context of earthquake cycle simulations on a strike-slip fault in continental crust, like the San Andreas. We focus on the effects of shear heating, which creates a thermal anomaly (i.e., temperature difference from a 1D background geotherm) around the fault and its viscous root. This reduces the effective viscosity near the fault, and therefore changes the depths of the brittle-ductile transition (BDT), earthquake nucleation, and the down-dip limit of coseismic slip. To investigate these issues, we have developed a finite-difference code for simulating earthquake cycles with rate-and-state friction and power-law viscoelasticity coupled to the heat equation.

We use flow laws for dislocation creep for feldspar in the crust and olivine in the mantle. We consider a range of background geotherms, parameterized by the lithosphere-asthenosphere boundary depth, degree of fluid overpressure, and frictional shear zone width w. We find that frictional and viscous shear heating contribute roughly equally to the thermal anomaly. Also, frictional shear heating produces a transient temperature rise, which for small w can reach hundreds of degrees, but its limited lifespan and spatial extent means that most cycle results are insensitive to this transient thermal anomaly. Instead, features like the cycle-averaged temperature distribution and the BDT are well-characterized by a steady-state approximation to the system with constant slip velocity and viscous strain rates (in which, as in our cycle simulations, the transition from frictional sliding to viscous flow is not imposed a priori but determined as part of the solution). We also find that the models without shear heating predict a BDT near or below the Moho, permitting interseismic fault creep below the Moho. In contrast, the thermomechanical models predict a BDT in the mid-crust, and many predict a 1-2 km wide zone in which coseismic slip and viscous flow both occur. Thus, we find that the simulations with shear heating are consistent with observations of faults which root in viscous shear zones in the lower crust, and observations of zones in which both viscous flow and coseismic slip occur, unlike simulations without shear heating.

Nonlinear Fourier-based Amplification Factors for the SCEC Broadband Platform, Domniki Asimaki, and Jian Shi (Poster Presentation 012)

We use nonlinear site response simulations to calculate Fourier-basad site amplification factors for California. The amplification factors are designed to correct Broadband Platform simulated time-series on reference site conditions, thus integrating site

response for engineering structural design applications. Our amplification factors are conditioned to two site-specific parameters: Vs30 (representing site stratigraphy) and z1000 (representing basin depth); and are derived using the Stochastic Sediment Model for the shallow crust, and the BBP for source and path realizations. We also compute response-spectra based site amplification factors using our simulated data and compare results to the NGA-West2 GMPEs site amplification terms. Our factors best compare with those of BSSA14.

Modeling damage evolution in the near-fault region as a result of rupture on complex fault , Khurram Aslam, and Eric G Daub (Poster Presentation 201)

We couple short-term (i.e. the co-seismic) and long-term (i.e. the inter-seismic) phase of an earthquake, in order to investigate how induced static stress changes during the co-seismic phase of an earthquake cycle influence the dynamics of strain accumulation during the inter-seismic phase. We perform dynamic rupture simulations on complex strike slip faults in 2D, incorporating off-fault plastic failure and strong dynamic weakening on the fault governed by the slip weakening law. Our strike slip fault has a self-similar fractal profile with RMS height taken from observational studies. Our dynamic rupture simulation results show that the stresses in the region surrounding the fault are highly complex and heterogeneous. This heterogeneity in stresses is mainly related to roughness of fault profile and at distances where fault roughness effects are not dominant, the stresses are mostly uniform. We extract these complex stresses together with the plastic deformation from the dynamic model and use them as the input to run the long-term tectonic model (LTM). This provides us insight into the dynamics of off-fault plastic deformation in the loading phase of an earthquake. Our LTM results show that most of the shear zones (i.e. new features e.g. fractures and faults) develop and grow at oblique angles to the main fault while considerable amount of damage keeps accumulating along the immediate sides of the fault profile. The development and growth of these new features occurs in the locations where geometrical bends in the fault profile has caused the deformation in the dynamic phase to be localized. This localized deformation due to fault roughness acts as a seed for the development of new features. We conclude that the complex damage pattern in the fault damage zones (observed in observational studies) is mainly due to the fault surface roughness effects. During the co-seismic phase, the stresses concentrate near the fault bends due to rough fault profile. During the inter-seismic phase, these locations are favored for the development of new features during the inter-seismic phase the earthquake.

Focal mechanisms and seismicity of LFEs on Parkfield, Miki Aso, Naofumi Aso, and Satoshi Ide (Poster Presentation 275)

Tectonic LFEs have been found at plate boundaries worldwide and considered to be associated with regional slow deformation. Therefore, it is natural that the focal mechanisms of LFEs have been determined as low-angle thrust in subduction zones, such as southwest Japan, Mexico, and Cascadia [Ide et al., 2007; Royer and Bostock, 2014; Frank et al., 2013], and strike-slip along the Alpine Fault, New Zealand [Baratin et al., 2018]. However, despite numerous detections of LFE along the San Andreas faults, their focal mechanisms are yet unknown, mainly due to poor S/N ratio of seismic waveforms. Here we try to determine the focal mechanisms of LFEs at Parkfield, CA, by improving the S/N ratio with a stacking method to keep amplitude information of each LFE. We use seismic waveforms of LFEs categorized into 88 families [Shelly, 2017], recorded at 131 stations in five networks near Parkfield, HRSN, NCSN, SCSN, BDSN, and PBOBSN. The quality of seismograms in five networks is not homogeneous in space and time, with some stations eliminated, replaced, and installed during the study period from April 2001 to January 2018. To minimize the effect of the inhomogeneous observation, we adopt a stacking method explained as follows. For each family and each station, we prepare normalized stacked waveforms, by simply stacking all available waveforms normalized by its maximum amplitude. The dot product of the normalized stacked waveform and an event waveform is regarded as the amplitude of each event measured at each station. These amplitude values are inverted into relative magnitude of ~10,000 events and path-site terms at ~100 stations, by solving a least-squares problem. Some stacked waveforms show P and S phases with recognizable polarities, which are mostly consistent with right-lateral strike slip expected along the San Andreas Fault. Nevertheless, there is the non-negligible number of inconsistent observations, and we need further careful investigation.

Nanoscale evidence for transient rheology during an earthquake, Alexis K Ault, Jordan L Jensen, and Robert G McDermott (Poster Presentation 173)

Nanoscale textures record the evolution of fault rock rheology and strength during the earthquake cycle. Earthquakes occur on thin fault surfaces and require a dramatic reduction in fault friction, potentially aided by a concomitant spike in fault temperature. Here, we apply novel nano-imaging and nano-chemistry tools to reveal evidence for transient rheological changes on a hematite fault mirror or high gloss, light reflective fault surface. We target a fault that crosscuts megacrystic specularite with minor quartz in the Pleistocene El Laco Fe-ore deposit, northern Chile. Scanning and transmission electron microscopy methods, including electron backscattered diffraction (EBSD) of the natural fault surface, indicate the mirror comprises a 50 micron zone of nanoscale, sintered polygonal hematite grains (<2 micron in diameter) with no shape or crystallographic preferred orientation, rhombohedral twins and misoriented magnetite nanoparticles in some hematite crystals intersecting the slip surface, and decreasing grain size away from the fault mirror. Locally, amorphous interstitial silica connects sub-5 nm silica films detected by electron energy loss spectroscopy that encase hematite grains. A network of topographic ridges defining a polygonal pattern transects the polygonal hematite crystals on the mirror. These ridges are hematite that impinges or protrudes into the polygonal grain boundaries of material on opposing side of the fault that is no-longer preserved. We suggest friction-generated heat from a dense network of geometric asperities resulted in amorphization of hematite and quartz and observed high-temperature reduction of Fe at the fault surface, a process that is aided by crystal comminution and the increased surface area of the nanoparticles created during incipient earthquake propagation. Following dynamic weakening, hematite crystals regrow and interlock across the slip surface, aiding in strength recovery post-earthquake. These results imply the interplay between transient heat and evolving fault rock rheology – even at the nano-scale – controls fault strength and may promote stick-slip behavior.

Slow Slip Events: Earthquakes in Slow Motion, Jean-Philippe Avouac, Sylvain G Michel, and Adriano Gualandi (Poster Presentation 118)

Faults can slip episodically during earthquakes, but also during transient aseismic slip events, commonly called Slow Slip Events (SSEs). The mechanisms at the origin of SSEs might be investigated based on their scaling properties. Previous compilation of SSE characteristics from various area suggested their moment, M0, is proportional to their duration, T, suggesting a different physics from regular earthquakes which obey M_0♥T^3. Thanks to a new catalog of SSEs on the Cascadia megathrust consisting of 65 events between 2008 and 2018, we find that SSEs actually follow the same scaling laws as regular earthquakes: M_0♥T^3, M_0♥A^(3/2), where A is the rupture area, , and the Gutenberg-Richter frequency-magnitude relationship, with a b-value of ~0.8. These scaling properties are to expected if slow slip events, like regular earthquakes, are frictional instabilities on faults embedded in a elastic medium, though with much lower stress drop that we estimated to ~1 kPa. SSE might therefore be considered as earthquakes in slow motion.

Contemporary and Paleoliquefaction Induced Lateral Spreading in Christchurch New Zealand, Jeffrey L Bachhuber, Gregory P De Pascale, Ellen Rathje, michael Little, Peter Almond, Christian Ruegg, and Michael Finnemore (Poster Presentation 225)

Earthquake triggered liquefaction and lateral spreading was widespread in Cantebury New Zealand during the 2010 to 2012 Cantebury earthquake sequence (CEF) and lead to $20 billion NZ dollars damage. Although the causes and timing of liquefaction during the CEF are well known, the geologic controls on lateral spreading are more poorly understood. We undertook a multi-disciplinary investigation funded by the National Science Foundation (NSF)and explored lateral spreading in Christchurch using image-differencing displacement maps, shear wave velocity profiles, boreholes and cone penetration soundings (CPT), and paleoseismic trenching combined with radiocarbon dating. Preliminary results suggest that cumulative displacements are less than those observed in the trench by downdropped blocks within the lateral spread and index beds in the subsurface which when combined with clear paleoliquefaction at the site (e.g. faulted pre-CES sandboils) suggest at least one major pre-CES lateral spreading event here. We feel this can be a powerful screening and mapping tool for identifying locations susceptible to lateral spreading to combine with typical geotechnical engineering methods.

Contrasts in integrated crustal strength drive the asymmetric distribution of topography and deformation within restraining bends, Curtis W Baden, and George E Hilley (Poster Presentation 271)

Restraining bends in the San Andreas Fault (SAF) generate zones of regional plate convergence along the Pacific-North American plate boundary. This causes uplift near them, and generates seismic activity as crust deforms. Interestingly, topography and deformation occur asymmetrically about these features along the SAF, which is not predicted by idealized elastic and plastic numerical models of deformation around these features. We propose that contrasts in crustal strength drive the localization of plastic deformation and uplift surrounding these bends, which ultimately generates the asymmetric topography observed. We test this idea using the finite element software Abaqus to simulate the impact of contrasts in material properties and boundary conditions on deformation and uplift around restraining bends. Specifically, we vary parameters of an elastoplastic rheology that yields according to a Drucker Prager or Mohr Coulomb constitutive model, and basal and horizontal boundary conditions, to determine each's effect on modeled long-term deformations. These models are tailored after the Santa Cruz Mountains restraining bend, where previous work quantifies deformation using geodetic, geomorphic, thermochronologic, and geologic methods. These data provide a framework through which we assess the agreement of our models with existing measurements and observations.

odel results show that, under certain constitutive rules and boundary conditions, crust may be asymmetrically advected and uplifted along the modeled restraining bend, consistent with thermochronologic, topographic, and geomorphic observations within the Santa Cruz Mountains. We contrast these patterns of long-term deformation with those expected over geodetic time-scales by calculating velocities for a purely elastic medium at the end of each model simulation. We find that, in addition to producing asymmetric distributions of topography and deformation, irrecoverable off-fault failure may be essential in reconciling fault zone behavior observed over geodetic and geologic timescales.

Thermal pressurization evolution with total slip, Nir Z Badt, Terry E Tullis, and Greg Hirth (Poster Presentation 181)

Dynamic weakening by thermal pressurization is studied on nominally flat surfaces of Frederick Diabase with a rotary-shear apparatus. Experiments are performed at a normal stress of 50 MPa, confining pressure of 45 MPa and pore fluid pressure of 25 MPa. Two types of surfaces are tested: (1) surfaces that underwent little initial displacement (<20 mm, low displacement - LD) and (2) surfaces that underwent large initial displacement (>1 m, high displacement - HD). While both types of surfaces display dynamic weakening at a slip rate of 2.5 mm/s (differing from their dry behavior – velocity strengthening), their frictional behavior differs significantly. LD surfaces exhibit dramatic weakening at the initial stages of fast-slip (40% drop in shear stress over the first ~3 mm of slip), followed by a healing stage, whereas HD surfaces weaken moderately over longer distances (34% drop in shear stress over ~60 mm of slip). The experimental data is compared to a thermal pressurization model (Rice, 2006), where the LD surfaces fit the model for only the initial stages of fast slip and exhibit decay distance of L*=12 mm, and HD surfaces better fit the model with L*=327 mm. Differences that arise between the data and the model lead us to explore a numerical solution to the thermal pressurization problem using spatially and temporarily variable hydraulic parameters, e.g. permeability, to supplement and compare to the model by Rice (2006) which solves for constant hydraulic parameters. Because the hydraulic properties depend on the effective stress which varies in space and time, this type of solution may be more realistic than that of Rice (2006).

The role of rheological evolution on active deformation of Southwestern North America within the Pacific-North America Plate Boundary Zone since the Oligocene, Alireza Bahadori, William E Holt, Jeonghyeop Kim, Troy Rasbury, Weisen Shen, and Julia Grossman (Poster Presentation 163)

Through a subduction to a transform dominated margin transition in western North America, highlands and thick crustal welts were dramatically altered to Basin and Range style topography and thin crustal structure. We incorporate the finite strain, paleotopography and crustal thickness models of Bahadori et al. (2018) to quantify vertically averaged deviatoric stress fields in

relation to body forces that drove deformation. We recover the laterally varying viscosity with respect to velocity and associated strain rates to provide associated deviatoric stresses. We calculate the average present-day upper mantle temperature using constraints from seismic shear velocities. We use NAVDAT database to calculate temperature variations at 100 km depth from present-day to 36 Ma. With these parameters we solve for effective water content variation within the lithosphere through time. Based on our results, as the East Pacific Rise contacts and evolves along the trench margin, and slab rollback progresses, boundary-sourced compressional stresses drop significantly within Nevada and Arizona, and gravitational potential energy associated stresses dominate in driving the extensional collapse of topography. Our results indicate that fluids must have had a central control on the effective viscosity of the lithosphere and weakening mechanisms for middle or lower crustal zones in dictating the timing of the gravitational collapse of topography (Nevadaplano and Mogollon highlands). Our inference on the role of fluids arises from several lines of evidence: (1) We observe a strong correlation between fluorine (F) concentrations in geothermal springs within the Great Basin and present-day transtensional strain rates. These high F concentrations also correlate with high He-3/He-4 ratios in geothermal fluids, indicating that F may be a powerful proxy for mantle fluid input. (2) Our time-dependent estimates of relative fluid content in our dynamic models correlate in space and time with the collapse of topography and active volcanism. (3)Position reconstructions of fluorite deposits within the southwestern Cordillera place them along linear belts that align with the paleotopography positions at 36 Ma, which subsequently experienced gravitational collapse. U-Pb dating of fluorite samples from these localities holds promise for testing the hypothesis that the timing of crustal weakening, and gravitational collapse of topography, resulted from significant volumes of crustal fluid input.

Mitigating Spatial Bias of Back-projections with the Slowness Enhanced Back Projection, Han Bao, and Lingsen Meng (Poster Presentation 084)

Benefiting from recently development of regional seismic arrays, the back-projection (BP) method images the dynamic rupture process and resolve their geometrical complexities with unprecedented details. Unlike source inversion methods, BP tracks high frequency radiators based on coherent phases of seismic traces without any prior assumptions of fault parametrization or regularization. However, the spatial accuracy of BP suffers from the travel-time errors when using 1D reference velocity model to approximate the real 3D Earth structures. For large earthquakes of hundreds of kilometers in rupture length, the static travel-time correction based on hypocenter alignment (Ishii et al., 2005) is only valid at the vicinity of hypocenters. Empirical interpolations of travel-time correction based on aftershock measurements have been employed to reduce the time errors for BPs of large earthquakes. However, such non-parametric interpolation requires dense and uniform distribution of large aftershocks. Meng et al (2016) proposed a parametric time correction based on the slowness error in the source area. This approach proves to significantly reduce spatial bias of BP using only a couple of large aftershocks. Here we perform the Slowness-Enhanced Back-Projection (SEBP) to image kinematic rupture process of the 2004 M 9.0 Sumatra, 2010 M8.8 Maule, 2011 M9.0 Tohoku-Oki, 2015 M8.3 Illapel, and 2017 M8.1 Mexico earthquakes. The effectiveness of SEBP can be firstly shown by th

Co-seismic Vertical Offset Retrieval From High-Resolution, Stereogrammetric DEMs: Examples from the 2013 Baluchistan, Pakistan Earthquake, William D Barnhart, Hannah Shea, Katherine Peterson, Ryan D Gold, Rich Briggs, and David J Harbor (Poster Presentation 125)

We highlight recent advances in the quantification of vertical offsets generated by earthquakes from time series of high-resolution stereogrammetric DEMs, with a focus on the 2013 Mw7.7 Baluchistan, Pakistan strike-slip earthquake. Topographic data sets, such as digital elevation models (DEMs) and LiDAR point clouds, are invaluable resources in the Earth science community that provide a base data set for numerous applications, including hydrological modeling, geomorphic and structural mapping, landscape evolution analysis, and orthorectification of remotely sensed imagery. In the field of active tectonics, topographic data sets allow for the characterization of regional elevation patterns, identification and quantification of discrete fault offsets, modeling of localized and regional fluvial responses to lateral and vertical fault displacements, and mapping of active fault traces, among other applications. The growing availability of sub-meter resolution satellite imagery further enhances and expands the applications of these data sets by allowing for both unprecedented spatial resolution and the generation of topographic time series. In this talk, we first present a suite of pre- and post-event 2-m resolution DEMs derived from commercial optical imagery and open source stereogrammetric tools that span the 2013 earthquake rupture. We highlight how various differencing schemes may introduce biases into the derived vertical offset field. Using the Iterative Closest Point (ICP) approach, we then provide a spatially dense vertical offset field for the 2013 earthquake and compare our results to previous vertical measurements made by manual mapping of post-event DEMs. Last, we provide an assessment of the shortcomings of our approach and means to overcome these issues, and future directions and applications of differential topography in the study of the earthquake cycle.

Forecasting earthquake behavior on the Alpine Fault, New Zealand, Nicolas C Barth, Jamie Howarth, Keith B Richards-Dinger, Sean Fitzsimons, and Glenn P Biasi (Poster Presentation 038)

New Zealand's Alpine Fault is perhaps the world's best example of a relatively simple, hypermature, active continental plate boundary transform. A 4000-year paleo-earthquake record from the Alpine Fault reveals the extent of the last 19 surface rupturing earthquakes along 300 km of the Central and South Westland sections of the fault; this record illuminates the most periodic earthquake recurrence behavior yet observed on a natural fault (coefficient of variation of 0.23 for the Central section), while also indicating these past earthquakes exhibit a range of rupture lengths and magnitudes. Importantly, the Central-South Westland section boundary (defined by a change in fault geometry and slip rake) behaves as an earthquake gate: about half (48%) of the recorded earthquakes rupture through the boundary as ~Mw 8 multi-section earthquakes and half (52%) terminate against the section boundary as ~Mw 7.5 single-section earthquakes with these two earthquake modes clustering in time. In other words, the central Alpine Fault exhibits a strong time dependence to earthquake return but the event magnitude and distribution may depend more strongly on the sequence of past earthquakes. We utilized the best constraints on fault geometry (fault strikes, fault dips, seismogenic depths) and fault kinematics (geological slip rates, slip rakes) along the full ~880 km length of the Alpine Fault to simulate 100,000 years of Alpine Fault earthquake behavior using the quasi-dynamic earthquake simulation code RSQSim. We find remarkable agreement in earthquake recurrence interval, recurrence interval coefficient of variation, single event displacement, and

the pattern of rupture between the paleo and synthetic earthquake records, which builds confidence that our data-rich simulations can be used to enhance earthquake forecasting. The last three earthquakes on the Alpine Fault have been ~Mw 8 multi-section events, a mode that our 100 kyr simulation shows is followed by another Mw 8 multi-section event 82 (+13/-18) % of the time. We use simulation-based extension of the recent rupture history of the Alpine Fault to produce three complementary time and mode dependent probabilities concerning rupture of the Alpine Fault's Central section in the next 50 years: (1) a 7 (+5/-5) % probability that no earthquake Mw > 7 occurs, (2) a 17 (+2.7/-3.7) % probability of a major (~Mw 7.5) earthquake occurring, and (3) a 76 (+12/-17) % probability of a multi-section great (Mw ~8) earthquake.

Implementing Inter-Period Correlations into SCEC BBP Simulations, Jeff R Bayless, and Norman A Abrahamson (Poster Presentation 011)

Methods for implementing the inter-period correlation of epsilon into two SCEC BBP simulation methods are explored. For Exsim (Atkinson and Assatourians, 2015), the correlated epsilons are introduced in the frequency domain and the Goulet et al. (2015) set of validation simulations are repeated. We compare the Exsim results in the form of waveforms, response spectral goodness of fit and variability, and correlation between frequencies. For GP (Graves and Pitarka, 2015), we evaluate the long-period correlations of the method in it's current form, and test the sensitivity of the correlations to various source methods: GP unmodified, SONG (Song, 2015) which uses GP wave propagation but a modified source representation, with simulations from Arben Pitarka, which use an asperity-based source along with GP wave propagation. Based on these results, we conclude that modifications to the source can have impactful effects on the between-event and within-event components of the correlation.

Orientation of faults, fault roots, rock fabric, stress, and deformation in Southern California: Geographical comparisons and field and numerical experiments, Thorsten W Becker, Vera Schulte-Pelkum, Whitney M Behr, Robert Porritt, and Meghan S Miller (Poster Presentation 157)

How do faults root into the ductile deep crust? Do pre-existing faults and shear zones affect present-day faulting and deformation? Here, we discuss constraints from existing datasets across Southern California and introduce a new seismic experiment in the Mojave designed to advance our understanding of lithospheric shear zone structure.

The spatial alignment between geological and geophysical indicators of deformation can provide interesting clues. Here, we comprehensively compare mapped fault traces, stress and strain patterns derived from different methods, estimates for seismic anisotropy from a range of depths from the upper crust to the mantle, and constraints from geological history. The results suggest reorientation of stress near major fault traces as well as faulting at non-optimal angles to stress. Anisotropic rock fabric appears pervasive across the region, and may explain some of the mismatch between deformation patterns and anisotropic "fast axes" within the crust. This has potential implications for mechanical anisotropy and stress transmission on faults from tectonic loading.

A closer look at the downward continuation of crustal faults into lithospheric shear zones is possible with dense temporary seismic deployments. Past deployments often cross faults where near-surface structure changes across the fault (usually crossing into a sedimentary basin on one side), making it difficult to disentangle near-surface effects on seismic waveforms from deeper structure. We report on a new 19-station, partially SCEC-funded deployment crossing several fault strands in the Mojave that is designed to place all stations on bedrock to reduce bias from near-surface effects. Separately funded work on crustal and mantle xenoliths erupted nearby provides ground truth constraints on seismically inferred rock fabric. Stations were installed in Spring 2018.

The effect of grain size and gouge microstructure on fault slip behavior, John Bedford, and Daniel Faulkner (Poster Presentation 179)

Conceptually, brittle fault zones are envisaged to be comprised of a localized fault core, or strands of multiple fault cores, surrounded by a distributed fractured damage zone. The core of fault zones, where the majority of slip is accommodated, generally consist of a granular gouge material formed progressively by cataclasis. Strain within these gouge layers may be highly localized onto discreet slip surfaces and experimental observations have shown that shear localization is a prerequisite for stick-slip instability. Here we investigate the effect of gouge grain size on structural evolution within experimental fault zones and also its effect on the stability of frictional sliding. Different grain size (5, 15 and 30 μm) synthetic quartz gouges are used, a material that is inherently unstable after a small amount of shear strain and characterised by velocity-weakening behaviour thereafter. It is found that the onset of instability in quartz gouge is a function of initial grain size, normal stress and shear strain. For a given grain size, a greater amount of shear strain is required to initiate unstable sliding at lower normal stresses. At a given normal stress, the onset of instability occurs at a lower shear strain for fine-grained gouges. The results show that grain size reduction must occur within the gouge in order to localize deformation and initiate unstable sliding. Initially fine-grained gouges have to undergo less grain size reduction in order to promote the formation of localized slip surfaces than coarse-grained gouges. These results are confirmed by microstructural observations, whereby throughgoing Y-shear planes, which are associated with instability, develop earlier within fine-grained gouge.

Spatial variations of rock damage production by earthquakes in southern California, Yehuda Ben-Zion, and Ilya Zaliapin (Poster Presentation 066)

We perform a comparative spatial analysis of earthquake production of rupture area and volume in southern California using observed seismicity and basic scaling relations from earthquake phenomenology and fracture mechanics. The analysis employs the catalog of Hauksson et al. (2012; extended to later years) for the period 1981-2017. We use only background events in the magnitude range [2-4] from a declustered version of the catalog to get temporally stable results representing typical activity during an inter-seismic period on all faults. The derived estimates can help separating rock damage and composition in models of seismic velocities and attenuation coefficients for the region. The analysis also highlights seismic zones that are active persistently beyond fluctuations associated with the large events. The results exhibit the following features. Regions of relative high inter-seismic damage production include the SJF, South Central Transverse Range (SCTR) especially near fault junctions (CP, SGP), Eastern CA Shear Zone (ECSZ) and Brawly seismic zone (BSZ) - Salton Sea area. The zones with high damage production are not necessarily associated with large earthquakes; there are M5 events outside these zones and very active damage areas with no large events in

the last 30 years. The Imperial fault, BSZ, so. SAF and ECSZ form a quasi-linear zone with ongoing damage production. The regions around the 1992 Joshua Tree and Landers earthquakes are active before 1990 and outline the ruptures of the future events. The seismically active crust becomes shallower to the NE from the peninsular ranges to the Mojave, north of the SCTR, and to the SE along the SJF and Elsinore fault, in agreement with Moho depth variations. The seismicity and damage zone are generally patchy, but more pronounced and continuous along-strike of main faults below 7.5 km than in the shallower crust.

Fluid-induced aseismic slip can outpace pore-fluid migration – evidence from in situ data, Pathikrit Bhattacharya, and Robert C Viesca (Poster Presentation 185)

Earthquake swarms attributed to subsurface fluid-injection are usually assumed to occur on faults destabilized by elevated pore-fluid pressures. But theory suggests that fluid-injection could also activate aseismic slip which might ultimately outpace pore-fluid migration and transmit earthquake triggering stresses beyond the fluid-pressurized region. We test this prediction by comparing numerical models of fluid-induced aseismic slip against in-situ data derived from fluid-injection experiments that activated and measured slow, aseismic slip on pre-existing, shallow faults (Guglielmi et al., 2015).

In our model, we couple axi-symmetric pore-pressure diffusion away from the borehole (within a permeable and compliant fault damage zone) to the slip response of a quasi-circular, planar, shear rupture governed by a frictional strength criterion. We use this model within a Bayesian inference framework to compare the numerical predictions to the in-situ pore-pressure and slip observations of Guglielimi et al., (2015). The inferred model provides direct in-situ constraints on the joint evolution of the hydrological and mechanical properties of the fault and its surrounding medium with active slip and the ambient state of stress.

We find evidence for permeability enhancement of about 60% with accumulating pore-pressure and slip -- the resultant model captures the pore-pressure evolution well with hydrological parameters that are consistent with laboratory-derived values. We further find that the modeled aseismic slip, induced by the pore-pressure diffusion model that best explains the hydrological data, fails to fit the observed acceleration in aseismic slip when prescribed a constant frictional strength. This accelerating slip is, instead, captured well by the model when friction is allowed to weaken linearly with slip. Remarkably, the joint observational constraints on both the modeled pore-fluid migration and the rupture front require that aseismic slip indeed outpace pore-pressure diffusion during late stages of injection. This suggests that aseismic slip mediated stress transfer could represent a plausible mechanism for trigerring induced-seismicity even on faults that are located outside the subsurface volume pressurized by pore-fluid migration. We also discuss preliminary results on the response of such large, spatially-extended, regions of aseismic slip to injection shut-off at the borehole and how such models might explain observations of continued induced-seismicity after the termination of injection.

Machine learning-based surface wave tomography of Long Beach, CA, USA, Michael J Bianco, Kim B Olsen, Peter Gerstoft, and Fan-Chi Lin (Poster Presentation 094)

We use a machine learning-based tomography method to obtain high-resolution subsurface geophysical structure in Long Beach, CA, from seismic noise processing on a "large-N" array. This locally sparse travel time tomography (LST) method exploits the dense sampling obtained from large arrays by learning a dictionary of local, or small-scale, geophysical features directly from the data. These local features are represented as small rectangular groups of pixels, called patches, from the overall phase-speed image. This local model is combined with the overall phase speed map, called the global model, via an averaging procedure. The global model constrains larger scale features using least squares regularization. Using data recorded from the Long Beach array in 2011, we perform high-resolution surface wave tomography of Long Beach region in the 1 Hz Rayleigh wave band. Among the geophysical features visible in the phase speed map, there is a prominent high-speed anomaly corresponding to the important aquifer Silverado aquifer, which has not been isolated in previous surface wave tomography studies. This anomaly is likely caused by the higher density of the Silverado relative to other geological units. Our results show promise for the use of LST in resolving high resolution geophysical structure in travel time tomography studies.

The Current Unlikely Earthquake Hiatus at California's Transform Boundary Paleoseismic Sites, Glenn P Biasi, and Katherine M Scharer (Poster Presentation 264)

Paleoseismic and historic earthquake records provide data used to quantify earthquake recurrence rates for seismic hazard estimation. Earthquake recurrence rates are equally useful to test the likelihood of seismically quiescent periods. At principal paleoseismic sites in California on the San Andreas, San Jacinto and Hayward Faults, no ground rupturing earthquake has occurred in the last 100 years, or about three times the average inter-earthquake time for the ensemble of sites. We examine long paleoseismic records from those faults, as they carry most of the transform fault slip on the plate boundary, to see if the hiatus has any precedent in the last 1000 years. The selection of sites is designed to sample fault sections unlikely to have ruptured together, so their conditional probabilities of a hiatus can be combined as independent events. The current 100-year hiatus is not predicted by common time-dependent or time-independent recurrence models. Paleoearthquake dating uncertainties can allow long open intervals at individual sites or subsets of sites, but do not explain the observed gap in the ensemble. After approximately removing redundancies in the full paleoearthquake record, the time-independent probability of the current 100-year gap is of order 0.3%. This raises several questions. Do we live in a statistically exceptional time? Or does some wide-scale effect modulate earthquake occurrence among sites over longer timescales? Finally, how should we understand seismic hazard estimates in California if the recurrence models on which they rely seem, at least, incomplete? Whether or not some longer-term modulation of earthquakes on the transform fault ensemble we investigate is operating in California, the results emphasize that the last century has been exceptional.

Analysis of Offset Stream Channels – Deconstructing Creep and Coseismic Slip Components Using Very High Resolution SfM Imagery, Southern San Andreas Fault, Coachella Valley, California , Chelsea M Blanton, Thomas K Rockwell, Allen Gontz, and Josh Kelly (Poster Presentation 226)

The southern segment of the San Andreas fault (SAF) has historically been the subject of geologic and geodetic slip rate and creep studies. Our investigation expands this research by focusing on small-scale offsets potentially related to creep since the last

earthquake and larger offsets due to paleoearthquakes which ruptured the Coachella Valley section of the SAF. Previous studies have utilized Structure from Motion (SfM) methodologies and achieved sub-meter to decimeter resolution (Javernick et al., 2014, Westoby et al., 2012, etc.), whereas this study has acquired sub-centimeter resolution, allowing for the examination of decimeter to meter scale offsets. We conducted drone surveys using a DJI Phantom 4 Pro at several sites along the southernmost SAF at altitudes of 25 to 60 m. We collected approximately 370,000 m2 of aerial imagery along five sections of fault for a total of 3 km of the fault over an 85 to 150 m width. Imagery was processed using Agisoft PhotoScan SfM software, resulting in DEMs and orthomosaics from base imagery with a maximum resolution of 7.5 mm/px. Geomorphic offsets were measured in the field using standard techniques, and field measurements were compared with measurements extracted from digital imagery with ArcGIS and MATLAB GUI LaDiCaoz v2.1 (Zielke et al., 2010). This section of the SAF last ruptured in 1726 ± 7 years (Rockwell et al., 2018). Related studies have demonstrated a local creep rate of 2-4 mm/yr (Lindsey et al., 2014), thus we would expect that any offset less than about a meter should be related to creep. Offsets observed in the DEMs range from approximately 50 cm to 100 m and reflect creep and multiple rupture events along this segment of the SAF. All offsets likely represent minimum values of slip for displacement in past earthquakes because multiple fault strands are present along much of the southern SAF, whereas discrete offsets are typically measured across a single strand. Forthcoming work will evaluate the long-term creep rate along with slip per event for the last several earthquakes, allowing for an assessment of paleoearthquake behavior along this segment of the SAF.

Emergent failure process of a M4.2 earthquake offshore Istanbul observed from GONAF downhole recordings, Marco Bohnhoff, Peter E Malin, Murat Nurlu, and Felix Bluemle (Poster Presentation 039)

The main branch of the North Anatolian Fault Zone below the Sea of Marmara is facing a high probability for a M>7 earthquake. Recently implemented monitoring efforts such as the downhole GONAF observatory nor allow for detecting low-magnitude seismicity along the eastern Marmara section offshore of Istanbul. The June25, 2016, M4.2 earthquake off the Armutlu peninsula was the largest local earthquake in years. Low-noise recordings from the closest vertical seismic GONAF array allowed to detect a series of earthquakes preceding and following the mainshock down to M~0. In the 64 hours before the M4.2 event, a total of 18 M>0 earthquakes with S-P times within 0.1 sec of the M4.2's S-P time took place. They reflect a type of self-organization and preparatory phase of the mainshock. In the subsequent 48 hours at least 3 to 4 times as many similar size-and-S-P time events were also detected. The relative magnitudes of the detected events span from the detection limit of the array at M~0 to M~3.5 as measured on the same scale as the M4.2. Based on their close hypocenter locations the entire series of detected events appear to fill a local seismic gap, whose dimensions are on the same order as the M4.2 rupture. A large fraction of the preceding and following events have similar waveforms. Average cross-correlation coefficients of foreshocks show a clear increase during the ten hours before that mainshock possibly reflecting a preparation process in direct vicinity to the mainshock hypocenter. If processed in near-real time this might support approaches in earthquake forecasting.

Rupture scenarios for the San Diego Trough and San Pedro Basin fault systems, offshore Southern California, Jayne M Bormann, Graham M Kent, and Neal W Driscoll (Poster Presentation 251)

The hazard posed by offshore faults for coastal populations in Southern California is poorly characterized and may be considerable, especially when these communities are located near long faults that have the ability to produce large earthquakes. Recent marine geophysical surveys along the San Diego Trough and the San Pedro Basin faults demonstrate that the mapped traces of these northwest striking, right-lateral faults are separated by a gap of <5 km, a distance which may allow ruptures to propagate between fault systems. The combined length of the two systems is ~330 km, and empirical scaling relationships indicate that an end-to-end rupture of both faults has the potential to produce a M 7.7-7.9 event.

Here, we present new observations from CHIRP and multichannel seismic reflection sub-bottom profiles, multibeam bathymetric data, and coring surveys to characterize the recency of deformation on the San Diego Trough and San Pedro Basin fault systems and evaluate the potential for ruptures that span both systems. Seismic reflection data collected in 2013 image the San Diego Trough fault offsetting young sediments at the seafloor for ~130 km between the US/Mexico border and Avalon Knoll; however a 30-km data gap exists between observations of seafloor offset in high-resolution MCS surveys on the San Diego Trough fault and seafloor offsets along the northern San Pedro Basin fault in legacy seismic reflection data. In June 2018, we collected ~400-line-km of high-resolution multichannel seismic reflection data in the San Pedro Basin to fill this data gap. The new profiles image offsets along the southern San Pedro Basin fault at depth, however we find no evidence of offset in the uppermost sedimentary packages in the San Pedro Basin. The thickness of the unfaulted packages is ~70 m in the center of the basin, and the sediments thin as they onlap the basin shoulders. The presence of the unfaulted sediments constrains the timing of the most recent slip on the San Pedro Basin fault to be prior to package deposition, however we lack absolute age constraints on the unfaulted sediments at this time. Our preliminary interpretation is that the southern San Pedro Basin fault is inactive, which minimizes the likelihood of an end-to-end rupture of the San Diego Trough and San Pedro Basin fault systems. This example highlights the importance of considering the recency of deformation on offshore structures when proposing fault models for seismic hazard evaluation.

Towards characterizing the geometry and potential fault system connectivity at the southern termination of the Palos Verdes fault, offshore southern California, Dan Boyd, and Jayne M Bormann (Poster Presentation 249)

The Palos Verdes fault (PVF) is a northwest-striking, strike-slip fault that cuts young marine and terrestrial sediments in the Los Angeles area from Santa Monica Bay in the north, across the Palos Verdes Peninsula, across the San Pedro Shelf and Slope to its southern terminus near Lasuen Knoll. The 95-km long fault is an active component of the Inner California Borderlands offshore strike-slip fault system that collectively accommodates ~6-8 mm/yr of Pacific-North American plate boundary shear. Slip rate estimates for the PVF range from ~1.5-3 mm/yr, and magnitude-length scaling relationships indicate the fault may be capable of producing a M7.3 event.

Despite posing significant hazard for coastal communities in Southern California, the geometry of the northern and southern ends of the PVF is poorly constrained. In recent years, several models of fault termination and connection have been proposed for the southern PVF. These models include: a through-going connection between the PVF and Coronado Bank fault to the southeast, PVF

slip transferred to the Newport-Inglewood fault along faults northeast of Lasuen Knoll, the PVF as terminating in a horsetail-splay southwest of Lasuen Knoll, termination of the fault at Lasuen Knoll, or a left step between the PVF and Carlsbad Ridge fault at Lasuen Knoll.

Here, we focus on distinguishing between proposed models of PVF termination to reduce uncertainty due to unknown fault geometry in regional seismic models. We use a focused high-resolution multichannel seismic (MCS) reflection dataset collected over Lasuen Knoll in combination with legacy industry and USGS seismic reflection data to produce a detailed map of deformational structures at Lasuen Knoll. Preliminary mapping indicates that high relief at Lasuen Knoll is the result of southward-verging, east-west trending, compressional structures east of Palos Verdes fault. We find no evidence that Lasuen Knoll results from oblique compressional slip on a low-angle, eastward dipping segment of the PVF. Accepted models of PVF termination and kinematics should be consistent observations of east-west trending compression at Lasuen Knoll. Future work includes sequence stratigraphic interpretation to determine the relative timing of deformation on structures at Lasuen Knoll and an evaluation for potential rupture connectivity with neighboring fault systems.

Cybershake NZ v18.6: New Zealand simulation-based probabilistic seismic hazard analysis, Brendon A Bradley, Karim Tarbali, Robin L Lee, Jonney Huang, D Lagrava, V Polak, J Motha, and Sung Bae (Poster Presentation 008)

This poster presents the computational workflow and results of the June 2018 version (v18.6) of probabilistic seismic hazard analysis (PSHA) in New Zealand based on physics-based ground motion simulations (`Cybershake NZ'). A total of ~12,000 finite fault simulations are undertaken and seismic hazard results computed on a spatially-variable grid of ~19,000 stations, with distributed seismicity sources considered via conventional empirical ground motion models.

In the current work completed to date, the Graves and Pitarka (2010, 2015) hybrid broadband ground motion simulation approach is utilized considering a transition frequency of 0.25 Hz, a detailed crustal model with a grid spacing of 0.4 km, and an empirically-calibrated local site response model. Additional simulations at finer computational scales are in preparation for faults with significant contribution to the hazard. A Monte Carlo scheme is used to sample variability in the seismic source parametrization (e.g. hypocenter location and slip distribution), with the total number of ruptures for each fault being a function of the rupture magnitude. We adopt a 'forward' simulation approach (as opposed to using reciprocity) because: (i) of the large number of stations relative to rupture realizations considered (i.e., 12,000 ruptures vs. 19,000 stations); (ii) a computational grid that is determined on a rupture-specific basis to optimize the domain size for a targeted minimum ground motion amplitude; and (iii) our near-term intention to include plasticity. As a result of (i) and (ii), there is not appreciable benefits to using reciprocity. Furthermore, the use of a dense grid of ~19,000 points at which seismic hazard is computed enables truly site-specific seismic hazard analysis and subsequent use of simulated ground motions in response history analysis of structural and geotechnical systems. Intensity measures for sample scenario ruptures and subsequently generated hazard curves and uniform hazard map across the country are presented. Treatment of uncertainty in the context of simulation-based PSHA, and improvements for future versions of the ongoing effort are discussed.

Assessing Surface Fault Rupture Deformation , Jonathan Bray (Oral Presentation Tue 09:00)

Surface fault rupture can produce localized or distributed deformation. In addressing the surface fault rupture hazard, the potential patterns of ground deformation should be developed through the use of a comprehensive site investigation including detailed mapping. Measured patterns of surface fault-induced ground deformation from similar types of faulting from past events offer useful insights to complement site-specific studies. Mitigation can be achieved in those cases when avoidance is not possible or practical. Engineers can design structures to accommodate fault-induced ground movements. Building strong, ductile structural foundation elements that can accommodate some level of ground deformation and isolating the superstructure from much of the underlying ground movement are effective design measures. Structures should not be tied into the ground with piles or piers. Other mitigation measures include establishing non-arbitrary setbacks based on fault geometry and displacement, and the overlying soil; constructing reinforced earth fills to spread out the underlying ground movements; and using slip layers to decouple ground movements from foundation elements.

Fused Earthquake Simulations on Deep Learning Hardware, Alexander N Breuer, Alexander Heinecke, and Yifeng Cui (Poster Presentation 289)

We present the status of recent and ongoing extensions to the Extreme-scale Discontinuous Galerkin Environment (EDGE) for seismic wave propagation. EDGE uses the Discontinuous Galerkin (DG-) Finite Element Method (FEM) to solve hyperbolic partial differential equations. Our software targets seismic models with high geometric complexity and extreme-scale ensemble simulations, using beyond 500,000 computer cores. The exploitation of inter-simulation parallelism allows the software to reach significantly higher simulation throughput over traditional, isolated approaches.

First, we present, that we are able to reduce EDGE's precision from double to single precision without loosing accuracy in established seismic wave propagation benchmarks. Through kernel-optimizations, we are able to harvest the single precision performance of the Intel Xeon Phi for Deep Learning (Knights Mill) in ground motion simulations, a traditional HPC application. In combination, our verification study and kernel optimizations increase the element-throughput of the solver by 4.2x, when comparing EDGE's single precision and fifth order performance to the solver SeisSol.

In the second part of the presentation, we show ongoing work, which targets two demanding inverse problems: 1) Seismic source inversion, and 2) the description of subsurface features in the seismic velocity model. Our model setups for both problems cover a realistic, two-dimensional layered velocity model and mountain topography in vicinity of the San Andreas Fault's Parkfield section. We train convolutional neural networks to invert for 1) the propagation of the rupture front, and 2) for the structure of the layered velocity model. By only using the raw and synthetic velocity components of surface receivers, our trained models are able to capture the respective model variations. Here, EDGE's parallelization over the seismic sources is crucial for fast generation of synthetic training data.

EDGE is available from http://dial3343.org.

Are we still seeing aftershocks from the M6.8 1872 Central Washington Earthquake?, Thomas M Brocher (Poster Presentation 043)

I investigate spatial and temporal relations between an ongoing and prolific seismicity cluster in central Washington state, near Entiat, and the December 14, 1872 Entiat earthquake, the largest historic crustal earthquake in Washington. A fault scarp produced by the 1872 earthquake lies within the Entiat cluster, and the locations and areas of both the cluster and the estimated 1872 rupture surface are comparable. Seismic intensities and the 1 to 2 m of coseismic displacement suggest a magnitude range between 6.5 and 7.0 for the 1872 earthquake. Aftershock forecast models for (1) the first several hours following the 1872 earthquake, (2) the largest felt earthquakes from 1900 to 1974, and (3) the seismicity within the Entiat cluster from 1976 through 2016 are also consistent with this magnitude range. Based on this aftershock modeling, most of the current seismicity in the Entiat cluster could represent aftershocks of the 1872 earthquake. Other earthquakes, especially those having long recurrence intervals, have long-lived aftershock sequences, including the Mw 7.5 1891 Nobi earthquake in Japan, with aftershocks continuing 100 years after the mainshock. Although I do not rule out ongoing tectonic deformation in this region, a long-lived aftershock sequence can account for these observations.

The spatial footprint of injection wells in a global compilation of induced earthquake sequences, Emily E Brodsky, and Thomas H Goebel (Poster Presentation 183)

Fluid injection induced seismicity is commonly modeled by assuming purely fluid-pressure driven earthquakes. However, this assumption is challenged by induced sequences with observed far-field triggering. To unravel triggering mechanisms of injection-induced earthquakes, we examine the spatial decay and space-time migration of ~20 induced seismicity cases. We limit our analysis to point source, single well injectors in the context of scientific, geothermal and wastewater injection. We perform an initial quality assessment, excluding datasets that cannot be distinguished from random Gaussian location uncertainty and uniform background seismicity. The spatial decay of the remaining cases is determined from the areal density of surface distances between wells and earthquakes. All sequences show a spatial gap between well locations and the location of highest seismicity density. Moreover, we observe two different types of spatial decay: 1) sequences with a near-well density plateau and rapid spatial decay and 2) sequences with steady decay, that extend to distances of more than ~10 km in some cases. Induced sequences with abrupt decay are dominated by square-root space-time migration, a characteristic of pressure diffusion. Sequences with steady spatial decay are dominated by linear migration or the absence of migration. The steady decay can be described by a power-law with an exponent of 1.8, which is significantly smaller (i.e. more gradual) than the spatial decay of aftershocks. This power-law behavior may be indicative of poroelastically induced earthquakes which lack the commonly expected rapid spatial decay and gradual spatial-temporal expansion of fluid-pressure-driven induced seismicity sequences. Far-reaching poroelastic stresses can lead to inflated hydraulic diffusivity estimates and a strongly underestimated spatial reach of injection wells.

Towards Seismic Inverse Problems Using Deep Learning, Jared T Bryan, Alexander N Breuer, and Yifeng Cui (Poster Presentation 093)

Understanding the behavior and state of fault systems is necessary to make thorough seismic hazard assessments, as well as to realistically model the evolution of earthquake ruptures. Estimation of the evolution of earthquake ruptures is a challenging inverse problem that traditionally requires heavy input of domain experts. We target this problem using deep convolutional neural networks (CNNs) and recurrent neural networks (RNNs), methods whereby the time consuming process of extracting rupture characteristics using traditional inverse methods can be exchanged for the one-time computational cost of training a deep neural network. In order to train a network for the inverse problem, we exploit the well-understood forward problem to generate synthetic seismic data in a realistic two-dimensional domain. The network then learns the mapping from a set of unmigrated seismic records to a description of the rupture front in space and time.

We phrase the inversion first as an image feature extraction, allowing us to use CNNs to map the unmigrated seismic traces to a spatially-discretized fault. In a second experiment, we phrase the inversion as a sequence mapping from unmigrated seismic traces to rupture start and end times for each subfault on a spatially-discretized fault. To train our networks, we took advantage of developments in forward seismic simulations by including a realistic velocity model and complex topography, and exploiting inter-simulation parallelism of the forward solvers. We then utilized parallel, high-throughput GPU computations to train our network.

Our method's computational costs are accrued entirely up front, after which the model can be applied to unknown data with very little computational power. For our subfault rupture localization and rupture front velocity regression problems, we tested two main network architectures: a deep CNN based on Inception-ResNet-V2 (IRNV2), and a simpler 9-layer CNN. For all tests, we iterate 50 times over 50,000 unique rupture patterns, 70% of which are used for training. IRNV2 performs best on both problems, albeit by a slim margin and at much higher computational cost than the 9-layer CNN. For our subfault rupture initiation and cessation problem, our RNN is able to combine the two problems addressed with CNNs with only slightly decreased accuracy. Further, the application of all three networks to a single dataset provides several independent estimations of the behavior of the earthquake rupture.

Quaternary Slip History of the Central Sierra Madre Fault, Southern California, Reed J Burgette, Katherine M Scharer, Nathaniel Lifton, Austin Hanson, Devin McPhillips, and Tammy M Rittenour (Poster Presentation 254)

The Central Sierra Madre thrust fault (CSMF) accommodates uplift of the San Gabriel Mountains along the northern Los Angeles metropolitan area. A suite of Quaternary terrace and fan surfaces are preserved near Arroyo Seco and offset across strands of the CSMF. We estimate fault slip (with uncertainty) from offset late Quaternary alluvial fan surfaces by analyzing swath profiles from lidar and a range of fault dips from published maps and trench studies. We determined the surface ages of the offset fan terraces combining 10Be depth profile dating and IRSL dating. Two of the most prominent late Quaternary geomorphic surfaces along the CSMF have modeled ages of ~55 and ~35 ka and are offset by ~28 and ~14 m, respectively. A thick, red, argillic soil developed on the oldest terrace surface is vertically separated across the fault ~260 m, based on surface and well data. Two sets of quartz-rich

cobbles were collected for 10Be/26Al isochron burial dating from ca. 8 m below the terrace and analyzed for cosmogenic nuclide abundance, but failed to yield robust isochrons due to uniformly low nuclide concentrations. Using the muon production dominant at the sampled depths and the lowest consistent 10Be concentrations from the two sites, we derived a mean exposure age estimate of ~170 ka.

In the Arroyo Seco area the calculated CSMF slip rate is ~1 mm/yr since ~55 ka and the time-averaged rate since ~170 ka is ~2 mm/yr, although the rates at the 95% confidence interval are considered equivalent. Fault dip is the dominant factor in slip rate uncertainty, and to make the slip rate constant would require that the fault dip has shallowed over time, for which we have no evidence. Given the multiple earthquake cycles over which the slower latest Quaternary rate is averaged, transfer of strain rate southward to other structures in the Los Angeles basin appears likely. The Quaternary rates provide spatial context for comparison with geodetic slip rates and late Cenozoic exhumation of the San Gabriel Mountains. The late Quaternary change in slip rate provides evidence of the ongoing evolution of plate boundary deformation.

Quantifying the bias introduced by vegetation in InSAR studies of ground deformation and surface processes, Paula Burgi, and Rowena B Lohman (Poster Presentation 140)

With the advent of more frequently acquired SAR data, regions with significant vegetative cover are now easier to study. We explore the sensitivity of InSAR to vegetation and land cover variations, which can bias InSAR-based interpretations of deformation histories. We analyze ALOS-1 data from Cascadia and Sumatra, where clearcutting is prevalent. SAR interferograms are sensitive to the vegetation structure, with the radar signal interacting with the canopy at a height that depends on radar wavelength and vegetation type. Similarly, Digital Elevation Models(DEMs) used in InSAR processing do not always represent the bare-earth surface, and are affected by the vegetation structure that existed at the time of their acquisition.Our target regions have experienced ongoing clearing since the time of the SRTM DEM acquisition (2000) and throughout the timespan of ALOS-1 SAR data acquisition (2007-2011). In this study, we explore methods to address these DEM- and vegetation-related issues, and assess their impact on InSAR time series analysis. We make use of independent remote sensing datasets such as Landsat to identify cleared areas, and apply a baseline-dependent, localized phase correction to each interferogram during time periods where the vegetation characteristics of that pixel did not change. We compare our corrected time series to a time series generated using more standard approaches. Globally, many fault systems are in highly vegetated regions, making it important to understand the contribution of vegetation to InSAR deformation time series. This work constrains the bias introduced by changes in vegetation, allowing for finer scale resolution of deformation on fault systems globally.

Earthquake cycle stress accumulation disparities of the Cajon Pass region, Liliane Burkhard, Bridget R Smith-Konter, Lauren Ward, Katherine M Scharer, and David T Sandwell (Poster Presentation 262)

As the San Andreas Fault System is known to participate in multi-segmented ruptures, it is important to understand how both fault segment properties and regional rheology can influence earthquake cycle stress accumulation. Here, we investigate stress accumulation rates as a function of depth for the Cajon Pass in southern California, representing a critical junction for possible past and future through-going ruptures. Using a new 4D viscoelastic earthquake cycle model that incorporates heterogeneous rheological constraints of the southern California lithosphere, we estimate stress rate disparities caused by spatial variations in crustal rigidity. We adopt a simplified representation of crustal rigidity derived from provisional heat flow estimates and seismically imaged lithosphere-asthenosphere boundary (LAB) depths. Preliminary estimates of crustal rigidity are slightly higher (~35-40 GPa) than CA average south of the Cajon Pass, due to a combined effect of slightly lower heat flow rates and thicker LAB depths. If these rigidity contrasts are real, they suggest reduced stress accumulation rates (by ~2-5 kPa/yr) south of the Mojave segment (i.e., on the San Bernardino (San Andreas) and Claremont (San Jacinto) segments), in a region that already hosts lower stress rates due to fault strain accommodated over the multiple paralleling segments. Over 100-200 year earthquake cycle time scales, accumulated stress could be reduced by at least 1 MPa on these segments, making the occurrence of major through-going ruptures less frequent at this earthquake gate junction. Moreover, longer earthquake recurrence times are needed to accumulate several MPa of stress along these segments south of the Cajon Pass, and may be a natural response of crustal rigidity variations in southern California.

Dating of Offset Geomorphic Features Along the Garlock Fault, Mojave Desert, California: Testing a Proposed Earthquake Supercycle Model, James E Burns, Sally F McGill, Ed J Rhodes, James F Dolan, and Nathan D Brown (Poster Presentation 234)

Recent investigations into the Garlock Fault at the northern edge of the Mojave Desert point to a strongly irregular pattern of earthquake recurrence, which may be related to temporal variations in slip-rate on the fault. These previously published investigations suggest a rapid slip rate coinciding with a succession of four closely spaced earthquakes within the past 2 ka, preceded by a 3000-year lull with no earthquakes evident in a paleoseismic trench near El Paso Peaks. This period of relative quiescence, followed by a period of more frequent large earthquakes suggests the possibly of an earthquake “Super-cycle”. To further investigate variations in slip rate and the possibility of an earthquake “super-cycle” on the Garlock fault, we are constructing a detailed slip history of the Garlock fault. We are in the process of using post-IR50-IRSL225 to date a number of geomorphic features that have been offset in the past 1-5 earthquakes on the Garlock fault in the El Paso Mountains and Pilot Knob Valley areas. The ages of these offset features will be compared to the published ages of prehistoric earthquakes from paleoseismic trenches at El Paso Peaks, Christmas Canyon and Echo Playa to determine the amount of slip in each of these past events. In the El Paso Mountains, we have sampled a 14-m offset channel and an 18-m offset alluvial fan, for which IRSL ages are pending. The 14-m offset is interpreted to represent the slip in the past two earthquakes combined, and the 18-m offset is interpreted to represent the slip in the past three earthquakes combined. We also intend to sample a 7-m offset channel, which is inferred to represent the slip in the most recent earthquake. Comparison of the ages of these features with published dates from the El Paso Peaks trench will either confirm or modify the number of earthquakes we have tentatively inferred for each offset feature. In Pilot Knob Valley, we intend to sample geomorphic features offset ~ 3 m, ~5-6 m, ~ 8 m, ~12 m and ~15 m. These ages will be compared to dates of prehistoric earthquakes in paleoseismic trenches at Echo Playa and Christmas Canyon in order to estimate the amount of slip in

each of past ~5 earthquakes. These results will constrain the late Holocene slip history for the Garlock fault at El Paso Mountains and Pilot Knob Valley, allowing us to examine changes in slip rate and recurrence interval over time and along strike.

Earthquake hazard assessment evaluated by fragile geologic features in coastal Central California, Anna H Caklais, Dylan H Rood, Mark W Stirling, Christopher M Madugo, Norman A Abrahamson, Klaus Wilcken, Tania Gonzalez, Albert R Kottke, and Alexander C Whittaker (Poster Presentation 232)

Probabilistic seismic hazard (PSH) models typically provide estimates of ground motions for return periods that exceed historical observations. It is therefore important to develop methods to evaluate ground motion estimates for long return periods, especially in proximity to major earthquake sources where estimates can be very high. Here we provide constraints over 10,000s years on ground motions from onshore and offshore seismic sources in central California using the distribution, age and fragility (threshold ground motion for toppling) of fragile geologic features.

Fragilities are estimated for seven precariously balanced rocks (PBRs) formed on uplifted marine terrace paleo-seastacks. The site is <10 km from the Hosgri Fault, a major offshore fault considered part of the San Andreas Fault system. PBR 3D models were constructed using photogrammetry to estimate unexceeded PGA ground motions of ~0.2-0.6 g, which are consistent with Newmark analysis of a slid block. We additionally quantify the probability of toppling of the PBRs, using empirical relationships, as a vector ground motion (PGV/PGA).

We obtain fragility ages (time that each PBR achieved its current geometry) using Be-10 cosmogenic surface exposure dating. Extremely low Be-10 concentrations (~5000 at/g) in modern high-stand samples demonstrates minimal inheritance and reliability of chert age estimates. Additionally, the volume of colluvium surrounding the paleo-seastack outcrops, determined from LiDAR, combined with alluvial fan surface dating (using Be-10 and soil profile development indices) indicates low erosion rates (~10 mm/ky) and long-term stability. Exposure ages that bound the fragility age by approximating the removal of surrounding blocks range ~17-95 ky. The age distributions for the suite of features suggests that all PBRs share a common evolution, and we interpret ~21 ka as the most defensible fragility age estimate of all seven PBRs. Despite the lack of constraints on the recurrence behavior of the Hosgri Fault, the slip rate is such that the PBRs have almost certainly experienced multiple large-magnitude, near-field earthquakes, and therefore provide rare constraints on low frequency ground motions.

Ongoing work includes a rigorous probabilistic comparison of unexceeded ground motions to the site's PSH model. We are developing methods to help reduce seismic hazard uncertainty for critical infrastructure, by the rejection of PSH logic tree branches inconsistent with the PBR observations.

A SCEC CyberShake Physics-Based Probabilistic Seismic Hazard Model for Northern California, Scott Callaghan, Philip J Maechling, Christine A Goulet, Kevin R Milner, Mei-Hui Su, Robert W Graves, Kim B Olsen, Brad T Aagaard, Kathryn E Wooddell, Albert R Kottke, Thomas H Jordan, and John E Vidale (Poster Presentation 295)

The Southern California Earthquake Center (SCEC) has developed CyberShake, a simulation platform that performs physics-based probabilistic seismic hazard analysis (PSHA) using 3D deterministic wave propagation simulations. The CyberShake PSHA calculations begin by simulating time- and space-varying Strain Green Tensors. An earthquake rupture forecast (ERF) is then extended by varying hypocenters and slips on finite faults, generating hundreds of thousands of events per site of interest. Seismic reciprocity is used to calculate synthetic seismograms for each event at each site, which are processed to obtain intensity measures (IMs) such as RotD50 spectral acceleration. These IMs are combined with ERF probabilities to produce hazard curves. PSHA results from hundreds of locations across a region are interpolated to produce hazard maps.

In 2018 SCEC initiated CyberShake Study 18.8, whose goals is to produce a physics-based PSHA hazard model for a large Northern California region that includes the San Francisco Bay Area. PSHA calculations up to 1 Hz for 869 locations in Central and Northern California were performed on the NCSA Blue Waters and ORNL Titan supercomputers. To support simulation volumes that included most of California, we tiled three separate 3D community velocity models (SCEC-CCA-06, USGS Bay Area 08.3.0, and SCEC-CVM-S4.26.M01) into a composite statewide model and applied smoothing around interfaces to minimize unrealistic reflections and refractions. To improve representation of near-surface velocity structure in the tomographically-derived models, we inserted a geotechnical layer (GTL) in the top 500 meters by applying the Ely (2010) method, assuming Vs30 values from the Wills (2015) map.

This computational effort enabled the calculation of a continuous physics-based PSHA map for a large portion of California, obtained by combining results from multiple CyberShake studies. We will present our new hazard results for a variety of sites and discuss the impacts of including a GTL and background seismicity on the overall hazard estimates.

Preliminary data on detecting asperity flash heating on hematite faults with laboratory experiments and hematite (U-Th)/He thermochronometry, Gabriele V Calzolari, Alexis K Ault, and Greg Hirth (Poster Presentation 176)

Friction-generated heat is a primary by-product of seismic slip on faults and can activate various mechanisms that lead to low coseismic strength. Hematite mineralization is ubiquitous in fault zones as striated or "mirrored" (high gloss, light reflective) hematite-coated slip surfaces. These faults archive important components of the thermal, physical, and chemical conditions of faulting. Hematite is amenable to (U-Th)/He analysis and has a closure temperature range of ~50-250 °C, which is a function of the hematite crystal size. Thermally-activated volume diffusion of He in hematite, responds to short duration, high temperature thermal pulses. To evaluate the role of heat in development of thin hematite slip surfaces, we integrate hematite rotary-shear experiments and (U-Th)/He thermochronometry to quantify temperature, friction, microstructure, and He loss evolution over variable slip displacements and rates. Our workflow requires textural and (U-Th)/He characterization of hematite starting material, deformation experiments, and comparative microscopy and (U-Th)/He dating of experimental products. Scanning electron microscopy (SEM) shows undeformed hematite comprises specularite plates (~2-80 μm-thick). Hematite (U-Th)/He dates from individual crystals (41-77 μm-thick) are ~207-284 Ma, positively correlate with plate thickness, and have a sufficient He budget to document He loss during slip. Deformation experiments were conducted using an Instron apparatus at 5 MPa normal stress, 0.01-340 mm/s sliding

velocity, and 35-2000 mm slip distance. Experiments reveal hematite is weak, with a low coefficient of friction from ~0.4-0.2 over a range of slip velocities, and exhibits dynamic weakening behavior. Experimentally-produced textures include a 20-100 μm-thick band of micron-scale, angular clasts and subrounded 0.5-0.2 μm particles. Low- and high-slip velocity runs yield mm-wide, high-gloss, light-reflective patches analogous to natural hematite fault mirrors. Preliminary SEM imaging of high speed runs shows some of these zones comprise sintered nanoparticles with polygonal grain boundaries, previously interpreted to represent recrystallization from transient, high temperatures. On-going nano-characterization and (U-Th)/He dating of experimental products will allow us to quantify friction-generated heat at subseismic to seismic slip rates, identify operative dynamic weakening mechanisms, and link experimental and natural hematite slip surface observables.

Seasonal and long-term crustal stress modulation due to aquifer compaction and groundwater unloading during the 2007-2010 drought in California, Grace Carlson, Manoochehr Shirzaei, Chandrakanta Ojha, and Susanna Werth (Poster Presentation 135)

Fluctuations in terrestrial water storage (TWS) cause deformation of Earth's crust. In regions with large seasonal TWS oscillations, subsidence is observed in the wet seasons and uplift in the dry, as the lithosphere responds elastically to changes in load. In California's Central Valley, groundwater storage maintains natural seasonal fluctuations, but also experiences long-term loss that is exacerbated by periods of intense drought. This loss has resulted in compaction of aquifer grains, causing permanent reductions in storage and hazardous ground fissures. In contrast to the regional elastic response, the local poroelastic response to changes in groundwater storage shows uplift when the aquifer is experiencing recharge and subsidence when storage is reduced. Here, we use vertical land motion measurements obtained through multitemporal interferometric processing of large datasets of SAR images acquired by the ALOS L-Band satellite over the Central Valley during 2007-2010 drought to study both the regional elastic loading response and local volumetric strain caused by groundwater storage change both seasonally and over the long-term. Using a first order 1D poroelastic model, we relate the observed vertical land motion to the volume of annual groundwater loss. Next, the groundwater volume loss is used in an elastic loading model to calculate corresponding vertical displacement at the locations of GPS stations and are compared to true vertical GPS displacements. We find that at most sites, groundwater unloading contributes less than 20 percent of vertical displacement, indicating GPS-based TWS estimates likely lack part of the groundwater component. We also examine the impact of aquifer compaction and elastic groundwater unloading on the stress field at the surface and at seismogenic depth. We find that the combined elastic and hydrodynamic response to groundwater loss on Coulomb stress has an effect on both seasonal and long-term stressing rates along faults in California. Comparing the tensile stress obtained from aquifer compaction modeling with the rock tensile strength, we also identify areas susceptible to surface fissures. This study highlights the importance of large-scale, high-resolution vertical land motion measurements in evaluating aquifer system dynamics and hazards associated with overdraft and how we can use these tools to better understand the influence of non-tectonic deformation on seasonal stress change and long-term stressing rates.

First-arrival traveltime tomography at Long Beach California using ambient seismic noise and the adjoint-state method, Jorge A Castillo Castellanos, and Robert W Clayton (Poster Presentation 095)

Knowledge of the fine-scale velocity structure of the subsurface is crucial for predicting ground motion and, thus, hazard assessment. In a recent study, Lin et al. (2013) showed that ambient noise surface wave correlations from a high-density oil-company survey could be used to produce a detailed 3D shear-wave velocity model for the top 800 m of Long Beach, CA. In this study, we extend their analysis and use the P-wave portion of the Green's function to generate multiple refraction profiles within Long Beach and determine the velocity structure to a depth of about 3 km. To overcome the inherent challenge of extracting body waves from ambient noise, we divide the Long Beach network into small-aperture subarrays and apply a double beamforming technique between all group of stations to isolate P waves from surface waves. The resulting beamed traces allow us to identify prominent direct and weak scattered arrivals traveling between all subarray pairs. To produce the final velocity profiles, we use a stacked seismic section to derive an initial 1D model and the adjoint-state method to construct the gradients of the misfit functional without the necessity of calculating and saving sensitivities (Fréchet derivatives). The inverted velocity profiles show velocity variations of the order of 0.3 km/s and strong lateral discontinuities caused by the presence of sharp structures such as the Newport Inglewood Fault. These profiles also provide us with a set of static corrections that will be applied to a follow on reflection analysis, which will in turn allow us to generate an even more detailed image of the subsurface.

Preliminary ages of prehistoric earthquakes on the Banning Strand of the San Andreas Fault, near North Palm Springs, California, Bryan A Castillo, Sally F McGill, Katherine M Scharer, Doug Yule, Devin McPhillips, James C McNeil, and Alan Pace (Poster Presentation 268)

The southernmost section of the San Andreas Fault (SAF) is the only section of the fault that has not ruptured in the last 200 years. It is not known whether this long quiescent period reflects a long average recurrence interval for this portion of the fault, or whether the current interseismic interval is longer than average. Near Indio, the SAF splits into 3 strands; limited paleoseismic work has been conducted on the Mission Creek and Garnet Hill strands and the Banning strand has no available age control for any surface-rupturing, prehistoric earthquakes. We studied a paleoseismic trench that was excavated across the Banning strand by Petra Geosciences (33.9172°, -116.538°). The trench exposed a ~30 m wide fault zone in interbedded alluvial sand and gravel, coarse-grained debris flow deposits, and clay/silt deposits. We documented evidence for eight prehistoric earthquakes, and we note that evidence for the events higher in the section is stronger than the evidence for those that are deeper in the section. Based on the age of two charcoal samples that bracket the most recent event (MRE), it occurred sometime between 560 and 960 cal. BP. We interpret that three earthquakes have occurred since ~1.8 ka, four earthquakes since ~2.7 ka, and five earthquakes have likely occurred since 5.0 ka. These event rates assume the stratigraphic section is complete and there are no missed events. Three charcoal samples located at the base of the trench have calibrated ages of 10.7 to 11.8 ka. All dated samples are detrital charcoal, so we use the youngest dated sample to estimate the age of each layer. Dates from luminescence samples are pending and will help to address the degree of inherited charcoal and place additional age constraints on individual events. Using our existing radiocarbon ages, we calculate a maximum average interval of 720 yrs based on three complete earthquake cycles between

earthquakes 1 and 4 or a minimum average interval of 330 yrs based on limiting ages for earthquakes 1 and 5. This makes the average interval equivalent to or less than the elapsed time since the MRE on the Banning strand. The average recurrence interval for the Banning section of the SAF appears to be intermediate between that for the San Gorgonio Pass thrust fault (~1000 years) and that for the Mission Creek and Coachella sections (~215 and ~220 years, respectively).

Crack models of repeating earthquakes predict observed moment-recurrence scaling, Camilla Cattania, and Paul Segall (Poster Presentation 190)

Small repeating earthquakes are highly periodic events, and they are thought to occur on velocity weakening (stick-slip) asperities embedded in a velocity strengthening (creeping) fault. In contrast, intermediate and large earthquakes (above ~ M4) do not exhibit such periodicity and characteristic ruptures. A puzzling observation is the scaling between the recurrence interval of small repeaters and seismic moment: a classical argument assuming constant stress drop and no interseismic slip on the asperity predicts Tr~ M0^(1/3), while the observed scaling is Tr~ M0^(1/6).

Here we use numerical simulations of rate-state faults and fracture mechanics concepts to understand how the seismic behaviour of isolated asperities loaded by creep varies depending on their dimension. We derive analytical expressions for the recurrence interval, which predict the Tr~ M0^(1/6) scaling over the entire range of R considered; however, the physical mechanism varies depending on the ratio of the asperity dimension to the critical nucleation radius Rc.

After a seismic rupture, creep penetrates inwards from the asperity boundary. We use an energy balance criterion to derive an equation of motion for the creep front and the time to nucleation, and identify two regimes: for R<2Rc, creep penetrates to the center of the asperity, where ruptures nucleate; the recurrence interval scales as Tr~ R, however the stress drop is not constant, due to the scale-dependence introduced by the finite nucleation radius. For 2Rc<R~<7Rc, simulations show simple cycles of ruptures nucleating near the edge and propagating laterally; stress drops are constant, and the Tr~ M0^(1/6) scaling is predicted by how the propagation of the creep front depends on R, which results in Tr~ R^(1/2).

Finally, larger asperities exhibit a mixture of partial and full ruptures; we estimate the recurrence interval for full ruptures from the requirement that the energy release rate everywhere on the asperity at least equals the fracture energy. We show that this criterion results in the scaling Tr~ M0^(1/6). Our results explain the behavior of repeaters over a wide magnitude range, and predict potentially observable changes in the rupture style and seismic cycle of isolated asperities depending on R/Rc.

Zoning Verification in Mexico City using strong motions of the M7.1 M7.1 Puebla-Morelos earthquake of September 19, 2017, Mehmet Celebi, Valerie J Sahakian, Diego Melgar, and Luis Quintanar (Poster Presentation 300)

Spectral ratios computed from accelerations recorded by strong-motion stations in Mexico City during the mainshock of the September 19, 2017, M7.1 Puebla-Morelos earthquake reveal predominate periods consistent with those mapped in the 2004 Mexican Seismic Design Code. Furthermore, the predominant periods thus computed validate those studies using mainshock and aftershock recordings of the handful strong motion stations that recorded the 19 September 1985 M8.1 Michoacán earthquake. 2017 data from stations in Zones I, II and IIIa,b,c,d allow confirmation of site frequencies (periods) attributable to the specific zones (particularly those in Zone IIIa,b,c,d. Spectral ratios are computed from (1) ratio of smoothed amplitude spectra of a horizontal channel in direction X of a station w.r.t the horizontal channel in the same X direction of a reference stiff soil (or rock) station, and (2) H/V ratio (or also known as the Nakamura's method), of both horizontal and vertical channels of the same station. Identified frequencies (periods) derived by both methods are in good agreement with those indicated in the zoning maps of Mexico City in the 2004 Seismic Design Code.

Constraining epistemic uncertainties on hazard models in the Marmara region using SHERIFS (Seismic Hazard and Earthquake Rates in Fault Systems), Thomas Chartier, Oona Scotti, and Hélène Lyon-Caen (Poster Presentation 028)

Modelling the seismic potential of active faults and the associated epistemic uncertainty is a fundamental step of probabilistic seismic hazard assessment (PSHA). SHERIFS (Seismic Hazard and Earthquake Rate In Fault Systems) is an open-source code allowing to build hazard models including earthquake ruptures involving several faults (or Fault-to-Fault FtF ruptures) while exploring epistemic uncertainties. Following the findings of UCERF3, SHERIFS considers a system level approach but doesn't rely on an inversion and instead applies an iterative approach following three rules: (1) the FtF ruptures allowed in the fault system are defined as input by the user, (2) the slip-rate budget attributed to each fault section is preserved in the calculation, and (3) the magnitude frequency distribution (MFD) of the modeled seismicity in the fault system must follow an imposed shape. SHERIFS is built to be as user-friendly and versatile as possible for an easy exploration of epistemic uncertainties on a wide range of tectonic settings. The SHERIFS methodology is applied to the North Anatolian fault (NAF) system exploring uncertainties concerning the creep condition of the fault, the maximum size of rupture in the system and the target shape of the MFD. SHERIFS contains a number of visualization tools that allows to compare the modeled earthquake rates for each branch of the logic tree to the rate calculated from the earthquake catalog and to the ratio of aseismic slip that was needed to be considered in order to respect the three rules. The comparison with the data allows discussing both the fundamental input hy

Seismic and aseismic fault slip revealed by luminescence bleaching depth profiles of the bedrock normal fault scarp, Jie Chen, Ming Luo, Jintang Qin, Jinhui Yin, Lewis A Owen, Haoran Wang, Huili Yang, Jinfeng Liu, and Boxuan Zhang (Poster Presentation 230)

Understanding the partitioning of seismic and aseismic fault slip is critical to seismotectonics as it ultimately determines the seismic potential of faults. Recent advances in tectonic geodesy and remote sensing make it possible to develop kinematic models of the spatiotemporal evolution of slip over the seismic cycle and to determine the budget of seismic and aseismic slip in subduction zones and continental faults in past two decades (eg. Avouac, 2015; Harris, 2017). However, it is still difficult to distinguish and estimate seismic and aseismic slip in geological time scale. Bedrock fault scarps are one of the best archives of past fault slip. They are

clearly associated with a particular fault, record whole slip history (Zreda and Noller, 1998). However, their reconstructions are limited because they often lack precise temporal constraint.

Recently, a new method dating for rock surfaces pioneered by Sohbati et al. (2011, 2012), is based on optically stimulated luminescence (OSL) bleaching profiles. If a rock surface continuously exposed to daylight, the luminescence resetting will penetrate deeper into the surface with time (the rock "bleaches"). Therefore, measuring the extent of bleaching in a sample can provide a measure of how long the sample has been exposed to daylight. Here, several models for luminescence bleaching depth profiles of bedrock normal fault scarps are proposed. The infra-red stimulated luminescence (IRSL) signals from rock slices exhibit increasingly deep bleaching profiles with altitude along the fault surface, which is consistent with episodic seismic or progressive aseismic fault slip. We demonstrate a case study of a bedrock normal fault surface at Langshan in north China, and show that rock luminescence bleaching profiles can be used to distinguish and estimate seismic and aseismic slip and is a promising tool for high-resolution reconstruction of fault slip, both in space and time, especially for events up to few hundreds or thousand years old.

Magma movement from Nāpau down to Leilani Triggered the 4th May 2018 Mw 7.0 Hawaii earthquake, Kejie Chen, Jonathan D. Smith, Jean-Philippe Avouac, Zhen Liu, and Song Y. Tony (Poster Presentation 286)

On 4th May 2018, a Mw 7.0 earthquake struck the south flank of Kīlauea, Hawaii, where volcanic activities have aggravated since late April. To investigate the possible cause-and-effect relationship between the magma movement and this earthquake, we have determined a co-seismic slip model based on geodetic, seismic and tsunami records and explored its relationship to the preceding stress evolution determined from modeling GPS time series from June 2012 to 20th April 2018. The Kilauea and Mauna Loa summits inflated at ~0.01 km3/yr, ~0.005 km3/yr, respectively, over that time period forcing ~25 cm/yr of seaward creep on the basal decollement beneath the southern flank of Mauna Loa. GPS and InSAR measurements from 20th April to 4th May 2018 imply opening by about 1 m of a 45 km long dyke. The dyke extends from Nāpau Crater, where it lies at depth between ~4 km and 8 km, to Leilani Estates, where it surfaces and where the eruption commenced. The magmatic inflation, dyking and creep on the decollement resulted in a U-shaped zone of stress unloading, fringed by a zone of stress build up which guided the rupture during the Mw 7.0 earthquake.

Applying improved spectral analysis to an induced earthquake sequence in Oklahoma and implications on earthquake triggering, Xiaowei Chen, and Rachel E Abercrombie (Poster Presentation 081)

Earthquake stress drop is an important parameter in ground motion prediction and earthquake source physics. However, it is notoriously known for its uncertainty. We develop an improved spectral analysis based on stacking. This method solves for an empirical correction spectrum (ECS) with stacked spectra across multiple magnitude bins. It is similar to the stacking method in Shearer et al. (2006) and Trugman and Shearer (2016), but it does not make any assumptions about the intrinsic scaling relationship of stress drop. Carefully designed synthetic test suggests that this method significantly improves the stability and reduces uncertainty of stress drop estimates with a small dataset. We apply this method to a well-recorded earthquake sequence in Oklahoma near Guthrie with over 700 earthquakes from M2 to M4, and carefully examine the influence of wave-type (P wave, S wave, and S-wave with coda), signal-to-noise ratio, number of stations recording each earthquake, and frequency band used for spectral fitting. P-wave produces the most significant scaling relationship, while S-wave and S-wave (coda) only result with minor scaling factor. Spectral fitting with wider frequency range significantly reduces the standard deviation of stress drops. We then compare with spectral ratio analysis based on individual event pairs. The results suggest that data quality control during spectral ratio analysis has strong impact on the resulted stress drop estimates. We further evaluate the role of spectral complexity (i.e., deviation from Brune-type source model) on the consistency in stress drop measurement. The improved results suggest that this induced earthquake sequence initiates with lower stress drop near structural bend, and large earthquakes tend to occur within high stress drop patches. The spatial pattern implies that fault strength variations influence the spatiotemporal evolution of earthquake sequence.

Spatial correlations in CyberShake physics-based ground motion simulations, Yilin Chen, and Jack W Baker (Poster Presentation 007)

This poster reports the results from quantifying spatial correlations in the intensity of ground shaking using physics-based simulations from the CyberShake platform. Currently, spatial ground motion variations in future earthquakes are predicted empirically, and calibrated using ground motion observations from densely recorded earthquakes. While useful, that calibration process requires strong assumptions about stationarity and isotropy of correlations due to the lack of repetitive ground motion intensity records at the same site. This project conducts non-stationary and anisotropic spatial variation estimation using CyberShake simulations. The results show that the method of Pearson's correlation coefficient is able to show the non-stationary and anisotropic behavior of spatial correlation. The results suggest that the geological condition and directivity of earthquake propagation have significant impact on spatial correlations. The role of between-event residual and within-event residual in spatial correlation are also be examined. Additionally, the spatial correlations observed in CyberShake simulations are compared to the empirical models from past earthquakes under stationarity and isotropy assumptions. The results show that the relationship between within-event correlation coefficient versus distance in CyberShake simulations is similar to the empirical models.

Source parameter variability of intraslab earthquakes as determined from the empirical Green's function method, Shanna Chu, Gregory C Beroza, and William L Ellsworth (Poster Presentation 078)

The mechanism of intraslab earthquakes are still incompletely understood. In particular, the relative importance of dehydration embrittlement, thermal shear runaway, hybrid dehydration-induced stress transfer, or some combination, and how these influences might vary in different subduction zones is unclear. To understand the contribution from these mechanisms, we investigate earthquake source parameters from data in the two subduction zones in Japan: the older and colder Pacific Plate east of Hokkaido, and the younger and warmer Philippine Plate south of Kyushu.

We estimate stress drops, radiated energies, and radiated efficiencies of earthquakes greater than M3.6 over a 12-year period using the method of empirical Green's functions (eGfs). Because intraslab earthquakes produce few aftershocks and because the signal-to-noise-ratio is low for small events, special attention must be given to eGf selection. We also consider the variation in high frequency fall-off rate between different events, noting that the standard omega-2 models used in such studies may be inappropriate for intraslab events. The methods we use are generally applicable to datasets of earthquakes in all settings for the common situation of low signal to noise ratio and/or insufficient data.

We find, in addition to the generally agreed-upon results of a higher stress drop and lower radiated efficiency for intraslab earthquakes, that there appears to be a break in self-similarity in the source parameters for the Hokkaido region, which suggests that different mechanisms may be important in the two subduction zones.

Basin Amplification Seismic INvestigation: tracking the propagation of waves from the San Andreas Fault to Los Angeles, Robert W Clayton, Marine A Denolle, Kim B Olsen, Patricia Persaud, and Jascha Polet (Poster Presentation 099)

Seismic amplification in sedimentary basins naturally arise from the contrast in elastic wave speeds between soft sediments and hard bedrock. Connectivity in sedimentary basins can thus act as seismic waveguides. The Basin Amplification Seismic INvestigation project aims to establish the presence of a coupling effect between the amplification due to seismic waveguides and that due to source directivity, which can enhance shaking intensity in sedimentary basins. The natural laboratory is the northern basins of the greater Los Angeles area (San Bernardino, Chino, San Gabriel) that may funnel long-period seismic waves from a San Andreas Earthquake to downtown Los Angeles. The BASIN project involves a multi-phase deployment of broadband seismometers and nodes between 2017 and 2018. Results from ambient noise spectral ratio analysis show clear long period (2-5 sec) peaks related to basin resonance, with significant variation in resonance frequencies and amplification factors across both the San Gabriel and San Bernardino Basins. Receiver functions show the Moho discontinuity, bottom of the basin, and intermediary sedimentary layers. Autocorrelation functions with nodes in the area exhibit reflectivity response that corresponds to transition between upper-lower crust and Moho. Preliminary ambient-noise cross correlations between permanent stations located on the San Andreas Fault and nodes contain anticausal Rayleigh waves with signal in the period range 2 – 10s.

In search of earthquakes, a biomarker thermal maturity investigation into the seismic potential of the central San Andreas Fault , Genevieve L Coffey (Poster Presentation 270)

Understanding the seismogenic potential of a fault is important in the assessment of seismic hazard in a region. We know that faults can exhibit a range of seismic behaviors from slow aseismic creep to fast earthquake slip. While earthquakes are not thought to nucleate in creeping regions, it is not well understood whether an earthquake nucleating elsewhere, with sufficient momentum, can propagate through one of these stable regions. This problem is of particular relevance to the San Andreas Fault, where the style of deformation varies from locked and seismogenic in the northern and southern sections, to active aseismic creep in the central section. Determining whether earthquakes can rupture through the stable, central San Andreas fault has significant implications to earthquake hazard in California, as the maximum magnitude event possible on the fault is markedly higher if the whole fault can rupture during a single event versus when rupture is restricted to the northern and southern sections.

We address this by searching for evidence of coseismic heating within material collected from the central San Andreas Fault. During coseismic slip, frictional heating along a fault can lead to the generation of very high temperatures, which means we can use evidence of temperature rise to identify where coseismic slip has occurred and also to extract earthquake properties like shear stress and displacement. Biomarkers (organic molecules produced by living organisms) are useful paleothermometers as their structure is systematically during heating to achieve more stable configurations with increasing temperature. Here we present preliminary biomarker thermal maturity results from the San Andreas Fault Observatory at Depth (SAFOD). These show that a 3 m wide region of high thermal maturity occurs along the fault (3193 – 3196 m), adjacent to the southern deforming zone. We apply these thermal maturity results to model temperature rise across the fault, which is a function of shear stress, displacement, and earthquake duration and is modulated by thickness of the slipping layer. Because earthquakes are known to localize along very narrow layers, our heating signal likely represents multiple earthquakes that have ruptured the creeping section at SAFOD.

Revisiting historical earthquakes in our backyard: 1925 Santa Barbara and 1952 Kern County, Scott J Condon (Poster Presentation 080)

We revisit the historic 1925 Santa Barbara and 1952 Kern County earthquakes using available seismic and geodetic data. As these two events occurred before the establishment of the World-Wide Standard Seismographic Network, our knowledge is very limited. For the 1925 Santa Barbara earthquake, we have digitized analog Bosch-Omori seismic records from the Berkeley Seismology Lab (BRK) using Teseo, a specialized digitization tool, and corrected for distortion caused by the instrument's mechanical arm. Our preliminary analysis, which treats this earthquake as a point source and the 2013 Mw 4.8 Isla Vista earthquake as an Empirical Greens Function (EGF), leads to a magnitude estimate of 6.4. For the 1952 Kern County Earthquake, our preliminary analysis reveals that the earthquake initiated on a thrust-dominant fault, dipping ~45°, and then migrated to a more energetic rupture with a different focal mechanism, after ~3 seconds. In view of the fact that the available bandlimited strong motion seismic data alone fails to constrain the source process, we are collecting geodetic observations to conduct a joint inversion with the goal of developing a slip model consistent with previous studies.

Seafloor scarps, stepover geometry, and kinematics of the Newport-Inglewood fault zone offshore Oceanside, California, James Conrad, Daniel S Brothers, Maureen L Walton, Ray W Sliter, and Peter Dartnell (Poster Presentation 160)

High-resolution Chirp sub-bottom data were collected in 2018 off the southern California coast between San Mateo Point and Carlsbad to image the right-lateral Newport-Inglewood (NI) fault zone and related faults on the outer shelf and upper slope. The data show two main strands of the NI fault (the Dana Point and Oceanside strands) separated by a ~3-km left step (the San Onofre stepover) northwest of Oceanside. Seafloor scarps showing apparent vertical offsets of 1-2 m have been imaged along both main

strands of the NI fault, providing clear evidence of post-transgressive (i.e., Holocene) offset. Sediment wedges deposited along both of these scarps have been cored and sampled for future radiometric dating.

Our new Chirp profiles, along with existing deeper-penetrating seismic reflection data, help to constrain deformation along the left-step in the NI fault offshore of the San Mateo Point-Oceanside coastline. Between the main NI fault strands, the stepover zone emplaces folded Miocene strata against younger flat-lying shelf sediments. This transpressional pop-up structure is bounded to the NE by an arcuate, SW-dipping reverse fault (imaged in deeper-penetrating industry seismic data) that up-warps adjacent young shelf sediments, linking the two main strands of the NI fault.

About 5-8 km NW of the NI stepover zone, the San Onofre (SO) fault, which trends obliquely up the slope from the south, appears to meet the NI fault at an angle of about 20°. Seafloor deformation apparent in bathymetric data reveals right-lateral offset of the slope along the SO fault. New Chirp profiles collected over this fault indicates offset of the Holocene drape layer. These results suggest that right-lateral slip is actively transferring onto the NI fault from the SO fault offshore San Mateo Point.

Predictive Skill: Using the Bayesian Inference to Study RSQSim and UCERF3, Jordan Cortez, Guillermo Beas, Shengyu Wang, Cynthia Tong, Sebastien D Rossouw, and Katia Ascencio (Poster Presentation 313)

The undergraduate studies in earthquake information technology (USEIT) probabilistic forecasting team at the Southern California Earthquake Center (SCEC) worked closely with the High Performance Computing (HPC) team to calibrate parameters within the Rate State earthQuake Simulator (RSQSim), a physics-based multi-cycle earthquake simulator. The parameters varied included normal stress, earthquake slip rate, and rate- and state-friction coefficients. Java code was written to analyze a battery of catalogs generated from distinct variations of these parameters to calculate rates of earthquakes of specified magnitudes and regions. These rates were then compared to those of the statistics-based Uniform California Earthquake Rupture Forecast version 3 (UCERF3) in order to find the catalog (and set of parameters) most closely resembling the best understanding of seismic activity in California. The team then established a probabilistic framework for analyzing larger catalogs being generated with the chosen parameters. For a set of 9 fault sections on major faults in Southern California, we computed transition probabilities (defined here as the probability of any combination of the 9 fault sections rupturing within a fixed time window) directly from RSQSim catalogs by counting. While RSQSim catalogs often show strong coupling of neighboring faults, catalogs with finite lengths cannot fully sample this probability space. Even with long (1 million year) synthetic catalogs, event counts for many permutations of the 9 considered faults were low or zero. To address this and provide more robust probabilistic estimates, we also computed marginal probabilities assuming independence of each fault section. We then took a Bayesian approach using Laplace smoothing with marginal probabilities as our prior, and transition counts from RSQSim catalogs as data. The Laplace smoothing alpha parameter (α0) controls the relative weight assigned to transition and marginal probabilities. We found optimal values for α0 through log-likelihood testing using probabilities computed from one catalog to predict another. Finally, we compared the skill of UCERF3 with the forecasts from RSQSim data. From our statistical analysis, we provide a framework for analyzing the strengths of each forecasting system and evaluating physics-based earthquake models. This process improves our understanding of earthquake behavior, thus contributing to earthquake hazard and risk awareness.

Kinematic rupture simulations of earthquakes on multi-segment faults , Jorge G Crempien, and Ralph J Archuleta (Poster Presentation 017)

The presence of bends or multiple faults in the earthquake rupture process significantly affects the spatial seismic-moment distribution per segment and the time evolution of the rupture front. Because of this, it is clear that multi-segment rupture complexity will greatly affect the spatial radiation of ground motion in the vicinity of the faults. Using the UCSB method for computing broadband synthetics (Schmedes et al., 2013; Crempien and Archuleta, 2015), we compare synthetic and recorded ground motion from several earthquakes (1992 Landers, 1999 Hector Mine, 1999 Chi-Chi) that ruptured on multiple faults. We use acceleration response spectra at several periods of engineering interest to compare observed and synthetic ground motions. We also compare the ground motion variability obtained by Crempien and Archuleta (2017) to the multi-segment ground motion simulations. Preliminary results show a slight increase of both between-events and within-events standard deviations for multi-segment faults.

Unified and Continuous Software Development for AWP-ODC-OS, Yifeng Cui, Alexander N Breuer, Rajdeep Konwar, and David Lenz (Poster Presentation 294)

State-of-the-art software development and engineering techniques are in high demand for increased code quality and usability. Important best practices include sound licensing, unified software development, version control for software and data, as well as Continuous Integration (CI) and Continuous Delivery (CD) solutions. Our poster showcases the application of best practices in software development and software engineering to AWP-ODC-OS, a highly scalable finite difference solver for seismic wave propagation. The final goal of our fully integrated software and data infrastructure is 1) a clear and transparent license structure for software and data, 2) well-documented and continuously tested examples and benchmarks, and 3) a significant reduction of development time through fast and automated status reports on the software's health.

The first part of the poster illustrates our newly introduced structure for related software and data. We showcase the layout of the respective repositories and provide insights on the technical aspects of the implementation. Further, we motivate and explain our newly introduced licenses, as well as required institutional steps for this open source release. We use the established BSD3 license for all software products and waivers (CC0) for all data products. This practice provides solid structure for inter-institutional collaboration, also extending to the commercial sector.

The second part of our poster showcases our CI and CD pipelines, using the open-source continuous delivery server GoCD (Apache License 2.0). Our GoCD server schedules work to agents, running on remote resources. For example, these resources could be hosted in terms of a local department-clusters, or in compute clouds, e.g., Amazon's AWS EC2. This setup overcomes computational limitations of commercial solutions for CI/CD, typically running a single CPU core. In addition, we interpret selected agents as interfaces to supercomputing infrastructure, e.g., TACC's Stampede or SDSC's Comet. By using the low-level workflow

tool SAGA-Python, our agents are able to automatically communicate with diverse job submission system. In summary, our final CI/CD pipelines will automatically analyze AWP-ODC-OS from simple sanity checks, e.g., memory debugging, towards continuous verification on supercomputing infrastructure.

Earthquake sub-event scaling: new perspective for rupture determinism, Philippe J Danré, Jiuxun Yin, Bradley P Lipovsky, and Marine A Denolle (Poster Presentation 214)

Strong ground motions during earthquake come from either a complex source time function or a complex wave propagation. We take advantage of global databases of source time functions (SCARDEC, Vallee et al. 2011, over 2,500 events and USGS, Hayes 2017, over 180 events) to explore earthquake source complexity. We use a sub-event detection method in each source time function to decompose the earthquake into sub-events that each carry a seismic moment and a duration. The strike slip earthquakes are systematically composed of more sub-events that other earthquake types. The number, the size, and the duration of sub-events grow with the earthquake magnitude. We construct a scaling of the sub-event moment Ma with the moment of the main event M0 and find that Ma ~ M0^(0.8). This allows us to estimate the earthquake magnitude using only the first few sub-events of the STF. Therefore, a magnitude estimate of earthquakes can be done with a good precision (Moment magnitude uncertainty is 0.28 at 10% of the rupture duration) before the rupture ends. We use quasi-static modeling of earthquake to explain our observations and constraint the fault strength parameter space. Our results demonstrate the importance of earthquake sub-events as the building blocks of larger ruptures.

Why do strike-slip earthquakes produce fewer aftershocks?, Kelian Dascher-Cousineau, Emily E Brodsky, and Thorne Lay (Poster Presentation 046)

The number of aftershocks generated by an earthquake is generally related to the size of the mainshock. However, aftershock sequences can have significant excursions from a simple magnitude-dependent productivity law. This variability is particularly concerning for great earthquakes where the number of damaging aftershocks can vary by factors of 40 for mainshocks of equivalent magnitude. We capitalize on the recent finding that strike-slip earthquakes produce fewer aftershocks at a given magnitude than dip-slip earthquakes to determine mainshock characteristics that govern productivity variations. Is the paucity of aftershocks for strike-slip earthquakes an effect of the typical tectonic stress regime for these earthquakes or does it reflect either the influence of the dynamics or geometry of the rupture itself? We use the Global CMT catalog and space-time windowing to measure productivity and examine its variations in the context of its tectonic setting, rupture properties, and source geometry. The data show that focal mechanism solutions separate the productivity data in generally convergent, divergent or transform plate boundaries. We proceed to build a catalog of earthquake source parameters based on the finite fault source inversions released by Hayes et al. [2017] for the great-sized earthquakes from 1990 to 2017. We tabulate new stress drop measurements, source dimensions, and seismic energy, as well as new metrics to characterize source geometry and heterogeneity. The compilation highlights that particularly long and narrow ruptures confined to the brittle crust, have markedly lower productivity. Additionally, building upon recent findings, we interpret the larger stress drops characteristic of strike-slip earthquakes to contribute to smaller ruptures, smaller activated volumes, and, therefore, fewer aftershocks. Neither the tectonic setting nor the released seismic energy appear to directly determine the paucity of aftershocks for strike-slip earthquakes; instead, it seems that source geometry plays a key role in their aftershock triggering

Preliminary geologic slip rates along Andes fastest slipping crustal fault, the Liquiñe-Ofqui Fault Zone (LOFZ), Patagonia, Chile , Gregory P De Pascale, Melanie Froude, Ivanna Penna, Reginald Hermanns, Daniel Moncada, Sergio Sepulveda, Mario Persico, David Petley, Gabriel Vargas, William Murphy, and Sebastian Pairoa (Poster Presentation 222)

Chile´s building code is designed for subduction zone events, and not for higher intensity strong-ground motions generated when crustal faults slip. Fault slip rates are therefore important imputs for these models. In Chile, crustal fault contribution to seismic hazard is poorly characterised (with unknown geologic slip-rates) including along the Andes longest fault, ~1200-km-long Liquiñe-Ofqui fault zone (LOFZ). We studied the southern ~500 km of the LOFZ using remote sensing, field mapping, and light detection and ranging data and document for the first time document field observations regarding style of faulting and fault displacements. Importantly we are able to evaluate long term (Miocene to present) to recent (Late-Quaternary) neotectonics along the LOFZ. Our new mapping changes the location of the LOFZ from previous mapping which was validated in the field through the presence of fault rocks coincident with the geomorphic surface traces. Preliminary results suggest Late Cenozoic to Quaternary LOFZ slip rates (~5 to 19 mm/yr (geologic) and 12 to 25 mm/yr (geomorphic)). These new Geologic and Geomorphic data imply that the LOFZ is the Andes fastest slipping crustal fault with high associated seismic hazard. We prefer the Quaternary rates due to less uncertainty than the longer term Miocene to present rates. Because our Quaternary rates are less than GPS rates (at least 7 mm/yr from a limited campaign) suggesting perhaps the LOFZ is perhaps late in its seismic cycle and one of the major crustal faults on Earth.

Earthquake behaviors in Source Time functions: energetic onset of earthquakes and biases from over-simplifying the source pulse, Marine A Denolle, and Philippe J Danré (Poster Presentation 213)

Global databases of earthquake source time functions (STFs) provide tremendous opportunities to explore the temporal evolution of the source. We use two such databases (SCARDEC Vallee 2011,2016 and USGS Hayes 2017), to extract information about earthquake behaviors from the shape of the STF. First, it is common to focus on the amplitude Fourier spectrum, provided an accurate and/or empirical treatment of wave propagation, and to simplify the source spectrum through smooth spectral shapes (Brune-like, Boatwright-like, Haskell-like). In particular, the attribution of a best-fit corner frequency to a source duration is usually qualitative and assumed magnitude-independent. Here, we show that the complexity in spectral shapes, which grows with earthquake magnitude (Danre et al 2018), biases the estimate of a corner frequency such that the relation between true pulse duration and modeled corner frequency depends on earthquake magnitude. This suggests that the interpretation of corner frequency in terms of earthquake stress drop may introduce a scaling bias. Second, we explore the temporal evolution of the moment-rate functions, the seismic power that we derive from moment accelerations, and the temporal evolution of the ratio of both that is a

time-dependent scaled energy. We find that earthquake onset contains most of the seismic radiation and that radiation productivity is mostly contained within 10% of the total duration of the source. This suggests that earthquake development is more energetic and abrupt than earthquake arrest

Deep learning for aftershock location patterns and the earthquake cycle, Phoebe DeVries, Thomas B Thompson, Martin Wattenberg, Fernanda Viegas, and Brendan J Meade (Oral Presentation Tue 13:30)

Over the past few years, deep learning has led to rapid advances in applied computer science, from machine vision to natural language processing. These methods are now accessible to scientists across all disciplines due to the availability of easy-to-use APIs and affordable GPU acceleration. We demonstrate two specific applications of deep learning within earthquake science. In the first, we train a deep neural network to learn computationally efficient representations of viscoelastic solutions, across large ranges of times, locations, and rheological structures. Once found, these efficient neural network representations may accelerate computationally intensive viscoelastic calculations by more than 50,000%. In the second, we focus on aftershock location patterns and find that a fully connected neural network trained on 131,000+ mainshock-aftershock pairs can explain aftershock locations in an independent testing data set of 30,000+ mainshock-aftershock pairs more accurately (AUC = 0.849) than static elastic Coulomb failure stress change (AUC = 0.583). In contrast to the common assertion that deep learning produces “black box” results, in both applications, the trained neural networks can provide unique physical insights

Earthquake and fault system dynamics – Putting the pieces together, James H Dieterich (Oral Presentation Sun 18:00)

In nature earthquakes do not occur as independent events on faults that are isolated in time and space. Rather they occur as emergent phenomena from the system dynamics of geometrically complex fault networks. Earthquake simulations that integrate fault system geometry, evolving stress conditions from interactions among earthquakes, and rate- and state-dependent fault constitutive properties capture well-established system-level characteristics of earthquakes including scaling statistics and Omori-type space-time clustering. In addition, long simulations with the California fault system and Cascadia models point to some relationships that would not be particularly obvious in the short historical record of earthquake observations. Among the relationships of possible significance to short- and long-term forecasts are 1) repeating slip patterns in large earthquakes whose characteristics are tied to the local fault system geometry and loading conditions; 2) the important role of structural complexities in both limiting through-going ruptures and enhancing earthquake clustering; and 3) the dependence of clustering rates on local stress conditions, which affect the probabilities of foreshock/mainshock sequences. Looking ahead, there is much room for further development of fault and earthquake system simulations. Of particular interest is the coupling of fault system simulations and background seismicity occurring off of the major modeled faults. One-way coupling of the background seismicity rates to stress changes from slip on the modeled system faults is doable in the short-term. A proof-of-concept implementation of full coupling appears to be quite promising.

Characterizing the 3D geometry of the Ventura-Pitas Point fault system and its implications for earthquake hazards in southern California, Jessica Don, Andreas Plesch, Mattie M Newman, and John H Shaw (Poster Presentation 245)

The Ventura-Pitas Point fault system, located in the western Transverse Ranges, is one of the largest earthquake sources in southern California with Holocene marine terraces suggesting that deformation occurs in discrete 7-9 meter uplift events (Rockwell et al., 1988; Hubbard et al., 2014; McAuliffe et al., 2015). Deformation of this scale is caused by large magnitude events that rupture multiple faults and pose significant ground shaking and tsunami hazards in southern California (McAuliffe et al., 2015, Ryan et al., 2015; Marshall et al., 2017). Recent studies have shown that the Ventura fault has a unique non-planar ramp-flat-ramp geometry that links at depth with several of the largest, fastest slipping faults in the area (Hubbard et al., 2014; Marshall et al., 2017; Levy et al., 2017).

We aim to characterize the geometry of the Pitas Point fault system, the direct offshore extension of the Ventura thrust in the Santa Barbara Channel, to further define the potential for large, multi-segment earthquakes. Previous studies have represented the Pitas Point fault with a planar geometry (e.g. Sorlien et al., 2000; 2015) which would limit its connection with other faults in the Santa Barbara Channel. In this study, we use 3D industry seismic reflection data from the Pitas Point and Dos Cuadras oil fields to directly constrain the fault geometry at depth. 2D seismic reflection data are used to extend our interpretations regionally to include the Oakridge and Blue Bottle trends. Extensive well control, including logs, horizon tops, and dipmeter, further constrain our interpretation.

We create a series of balanced cross sections using fault-related folding techniques and restoration modeling. These cross sections show that the Pitas Point fault system has a similar ramp-flat-ramp geometry to that of the onshore Ventura fault. This suggests that the Pitas Point fault also has linkages with other large faults at depth in the area. This improved fault geometry further supports the prospect for large, multi-segment ruptures and has implications for the associated hazards (such as ground motion and tsunamis) as well as geodetic strain and loading patterns.

Deformation in the Yuha Desert from the 2010 M7.2 El Mayor – Cucapah Earthquake , Andrea Donnellan, Jay W Parker, Michael B Heflin, John B Rundle, Lisa Grant Ludwig, and Gregory A Lyzenga (Poster Presentation 167)

UAVSAR and GPS measurements were collected north of the US Mexico border spanning the 2010 M7.2 El Mayor – Cucapah earthquake from 6 months before to 7 years following the event. The area includes the Yuha Desert, Ocotillo area, and Salton Trough. The area northwest of the north end of the rupture in the Yuha Desert and Ocotillo area shows extensive surface fracturing of the crust in a network on conjugate faults with little broad scale deformation. The Salton Trough northeast of the rupture shows little surface fracturing but a large gradient of deformation. The asymmetric deformation can be explained by a contrast in lithology between the compliant Salton Trough and rigid Peninsular Ranges. Postseismic motions in the Yuha Desert can be fit with a rate strengthening logarithmic decay from afterslip on the El Mayor – Cucapah rupture. Deformation from the M5.7 Ocotillo aftershock was observed with UAVSAR and the deformation matches the focal mechanism for the depth, geometry, and slip of the event. Afterslip continued for several years on the Ocotillo aftershock section and the Yuha fault and can be explained by stress decay from

afterslip on the mainshock rupture. While deformation in this area can be explained by rate and state friction laws, migration of fluid in the Salton Trough is likely to have occurred there.

Tracking thousands of microearthquakes for a month in northern Oklahoma: What a large-N array can reveal about induced seismicity, Sara L Dougherty, Elizabeth S Cochran, Rebecca M Harrington, and Zachary E Ross (Poster Presentation 059)

The substantial increase in earthquake rate observed in Oklahoma during the last decade has largely been attributed to the disposal of wastewater from energy production activities. While existing sparse regional networks are able to capture the occurrence of most M≥3 earthquakes and some smaller magnitude events, micro to minor earthquakes typically cannot be detected. To enable the detection of microseismicity, we deployed a temporary array of 1,833 vertical-component nodal seismometers in northern Oklahoma. The LArge-n Seismic Survey in Oklahoma (LASSO) array operated for approximately one month in spring 2016, covering a 25-km-by-32-km region with a nominal station spacing of ~400 m. We develop a local earthquake catalog from data recorded by the LASSO array, which allows us to investigate sequences of induced seismicity in this region of active wastewater injection with unprecedented clarity. A two-stage earthquake detection method utilizing standard short-term average/long-term average and waveform-correlation-based template matching techniques identifies more than 15,000 earthquakes recorded by the array, a factor of ~160 increase over the regional earthquake catalog. Estimated duration magnitudes for the detected events are as small as -0.4. Initial hypocentral locations indicate some instances of very small-scale (~0.5-1.5 km) lateral and vertical spatiotemporal migration of seismicity. Several dense clusters of seismicity that were active throughout the deployment are also observed. We use the catalog of local earthquakes recorded by the LASSO array to explore frequency-magnitude relationships and the spatiotemporal evolution of seismicity along individual fault segments. We also determine focal mechanisms for M≥2 earthquakes to constrain the sense of motion along these faults and potentially make inferences regarding the stress state of the shallow crust. The locations and orientations of active faults may provide insights into interactions between small-scale fault structures as well as potential locations of future induced earthquakes.

Effects of Fault Geometry and Pre-Stress Loading for Scenarios of Earthquakes on the Eastern San Gorgonio Pass Region in CA using Dynamic Rupture Simulations, Roby Douilly, David D Oglesby, Michele L Cooke, and Jennifer L Beyer (Poster Presentation 208)

Compilations of geologic data have illustrated that the right-lateral Coachella segment of the southern San Andreas Fault is past its average recurrence time period. On its western edge, this fault segment is split into two branches: the Mission Creek strand, and the Banning fault strand, of the San Andreas Fault. Depending on how rupture propagates through this region, there is the possibility of a through-going rupture that could lead to the channeling of damaging seismic energy into the Los Angeles Basin. The fault structures and rupture scenarios on these two strands are potentially very different, so it is important to determine which strand provides a more likely rupture path, and the circumstances that control the rupture path. In this study, we focus on the effect of different assumptions about fault geometry and initial stress pattern on the rupture process to test those scenarios and thus investigate the most likely path of a rupture that starts on the Coachella segment. We consider three types of fault geometry based on the Southern Community Fault Model (SCEC) and the Third Uniform California Earthquake Rupture Forecast (UCERF3), and we create a 3D finite element mesh for each. These three meshes are then incorporated into the finite element method code FaultMod to compute a physical model for the rupture dynamics. We use a slip-weakening friction law, and consider different assumptions of background stress, such as constant tractions and regional stress regimes with different orientations. Both the constant and regional stress distributions show that it is more likely for the rupture to branch from the Coachella segment to the Mission Creek compared to the Banning fault segment, even if the closest connectivity is between the Coachella and Banning. For the regional stress distribution, we encounter cases of super-shear rupture for the SCEC fault geometry with the northeast dipping Coachella segment, and sub-shear rupture for the other two geometries. The fault connectivity at this branch system seems to have a significant impact on whether a through-going rupture is more likely to occur or not.

Using relative structural complexity of fault segment barriers to model prehistoric earthquake rupture histories, Christopher B DuRoss, Ryan D Gold, Rich W Briggs, and Scott E Bennett (Poster Presentation 224)

Geometrically complex structures along faults, such as fault steps and bends, commonly limit the lateral extent of surface-rupturing earthquakes. However, reconstructions of prehistoric fault ruptures often treat these structures as binary limits to rupture. We hypothesize that for normal faults, the degree of structural complexity can inform the likelihood of throughgoing ruptures at proposed rupture barriers. That is, complex barriers are more likely to impede ruptures than simple barriers. Using a 100-km-long section of the 350-km-long Wasatch fault zone (WFZ) in Utah, we combine measures of fault structural complexity with earthquake-timing probability density function (PDF) data from fault trench studies to evaluate alternative earthquake correlations along strike. For six geometric structures along the Salt Lake City and Provo segments of the WFZ, we calculate values of relative structural complexity based on kilometer-scale fault geometry (e.g., fault steps, bends, and changes in orientation relative to a regional slip vector). We then compare the overlap of Holocene earthquake PDFs across these structures to both the relative structural complexity values and the timing uncertainty of the constituent PDFs to identify the most probable along-strike earthquake correlations. Our method yields a best-fit prehistoric rupture model that leverages all available structural and paleoseismic data. For the WFZ, our results suggest a complex history of rupture on the Salt Lake City and Provo segments, including rupture at and likely across the proposed Traverse Mountains structural barrier between them. These ruptures yield a cumulative fault displacement curve that closely resembles that from published point observations of Holocene fault-scarp offset. Our approach can be used to limit the range of possible rupture models and help define the epistemic uncertainty in rupture length for seismic-hazard analyses.

Modeling Earthquake Mechanics with High Resolution Fault Zone Physics: New Computational Tools for Addressing The Conundrum of Scales, Ahmed E Elbanna, Setare Hajarolasvadi, Xiao Ma, Mohamed Abdelmeguid, David Kammer, Gabriele Albertini, Bob Haber, and Amit Madhukar (Poster Presentation 199)

Modeling earthquake ruptures is a complex challenge due to the wide range of spatio-temporal scales contributing to the dynamic instability, ensuing propagation, and slow inter-seismic deformation. New numerical schemes based on efficient domain decomposition, or adaptive mesh refinement, are thus required to address this conundrum of scales and resolve the correct physics.

Here, I will present two recent developments in computational earthquake dynamics that my group has been working on to address the spatio-temporal complexity of earthquake slip. In the first half of this presentation, I will describe our progress in developing a hybrid numerical technique that couples domain-based methods with spectral boundary integral equations through the consistent exchange of displacement and traction boundary conditions, thereby benefiting from the flexibility of domain-based discretization techniques in handling problems with nonlinearities or small-scale heterogeneities and from the superior performance and accuracy of Spectral Boundary Integral (SBI) method. Our current computational infrastructure includes coupling finite element and finite difference methods with SBI in 2D in-plane and anti-plane settings as well as in 3D geometries using both explicit and implicit integration schemes and adaptive time stepping. We have validated the method using several benchmark problems and demonstrated its unique capabilities in modeling earthquake ruptures with high resolution fault zone physics. I will also demonstrate our preliminary results for modeling earthquake cycles with inelastic rheology and heterogeneous bulk.

In the second half of this presentation, I will briefly describe a recent collaborative effort in applying a novel space-time asynchronous Discontinuous Galerkin method (aSDG) for modeling exascale problems in earthquake dynamics. The method enables extreme dynamic adaptivity in space-time, over several decades of scales, and superior accuracy in resolving the process zone and high frequency radiation. I will demonstrate the potential of the method in modeling large scale dynamic rupture with laboratory-based friction parameters. These novel developments in computational dynamic fracture open new opportunities for multiscale modeling of earthquake physics for next generation seismic hazard models.

The Community Code Verification Exercise for Simulating Sequences of Earthquakes and Aseismic Slip (SEAS): Initial Benchmarks and Future Directions, Brittany A Erickson, Junle Jiang, Michael Barall, Nadia Lapusta, Eric M Dunham, Ruth A Harris, Lauren Abrahams, Kali L Allison, Jean-Paul Ampuero, Sylvain D Barbot, Camilla Cattania, Ahmed E Elbanna, Yuri Fialko, Benjamin Idini Zabala, Jeremy E Kozdon, Valere R Lambert, Yajing Liu, Yingdi Luo, Xiao Ma, Paul Segall, Pengcheng Shi, and Meng Wei (Poster Presentation 192)

Numerical simulations of Sequences of Earthquakes and Aseismic Slip (SEAS) have made great progress over the past decades to address important questions in earthquake physics and fault mechanics. Significant challenges in SEAS modeling remain in resolving multiscale interactions between aseismic fault slip, earthquake nucleation, and dynamic rupture; and understanding physical factors controlling observables such as seismicity and ground deformation. The increasing capability and complexity of SEAS modeling calls for extensive efforts to verify and advance these simulations with rigor, reproducibility, and broadened impact. Over the past year, we have initiated a community code-verification exercise for SEAS simulations, supported by SCEC (the Southern California Earthquake Center). Through this exercise, we aim to develop best practices, and code-verification and simulation tools for SEAS modeling that would benefit a larger community.

Here we present code comparison results from our first benchmark, designed to test the capabilities of different computational methods in correctly solving a mathematically well-defined, basic problem in crustal faulting. This benchmark is a 2D antiplane problem, with a 1D planar vertical strike-slip fault obeying rate-and-state friction, embedded in a 2D homogeneous, linear elastic half-space. The fault has a shallow seismogenic region with velocity-weakening friction and a deeper velocity-strengthening region, below which a relative plate motion rate is imposed. A periodic sequence of spontaneous, quasi-dynamic earthquakes and slow slip are simulated in the model. We have established an online platform (http://scecdata.usc.edu/cvws/seas/) for modelers to upload and compare simulation results. The comparison of ~20 models from 11 groups using different numerical methods (FDM/FEM/BEM) show excellent general agreements. We found that domain truncation and boundary conditions strongly influence interseismic fault stressing, earthquake recurrence, and coseismic rupture speed, and that agreement between models is only achieved with sufficiently large domain sizes. Building on this initial success, we are working toward more complex scenarios involving variable event sizes, a dipping fault, and a 3D problem in our upcoming benchmarks.

Modeling shallow crustal nonlinearity in physics-based earthquake simulations: Beyond perfect plasticity, Elnaz Esmaeilzadeh Seylabi, Doriam Restrepo, Domniki Asimaki, and Ricardo Taborda (Poster Presentation 020)

We implement and verify a multi-axial constitutive soil model in Hercules, one of SCEC's three-dimensional wave propagation codes for regional scale earthquake simulations. Our overarching goal is to compute the effects of shallow crust nonlinearities in broadband earthquake simulations using a realistic plasticity model to capture inelastic soil deformation. We specifically implement a total stress, bounding surface plasticity model with a vanishing elastic region. The model's hardening modulus within the bounding surface is defined by a simple mapping rule, and thus requires very few free parameters to be fully calibrated for a given shear modulus reduction curve. This feature, in turn, makes the model suitable for regional scale earthquake simulations, where geotechnical data in the shallow crust are scarce. To verify the implementation of the model in Hercules, we compiled a catalog of numerical experiments, which are also conducted using OpenSees---an open-source finite element code for earthquake engineering simulations. We specifically verify the model for the following canonical problems: (1) one dimensional linear and nonlinear site response; (2) standard material point-like pseudo-static analyses; and (3) elastic wave propagation in a heterogeneous half-space using an embedded point source. These efforts showcase the difficulties involved in nonlinear earthquake ground motion simulations but also the benefits that lie beyond perfect plasticity.

Optimal GNSS observations in Southern California, Eileen L Evans, and Sarah E Minson (Poster Presentation 131)

We evaluate the current Global Navigation Satellite Systems (GNSS) observation network in southern California to 1) quantify the relative information provided by expanding the network to include seafloor observations, and 2) to identify optimal locations for future GNSS observations. These goals require considering potential locations both onshore and offshore, while considering multiple scientific objectives: optimal locations for observing an earthquake rupture (requiring observations within 1-3 locking depths of active faults) will differ from optimal locations for estimating long-term fault slip rates (which may require observations farther away).

Furthermore, the high cost of seafloor geodesy limits the number of stations that may be deployed and monitored offshore. Therefore, it is essential that additional onshore and/or offshore stations are selected and positioned in such a way to provide the most informative data for resolving fault slip rates. To identify optimal locations for future geodetic observations, we use the theory of information entropy, a measure of the amount of missing information about parameters whose values are uncertain. In the case of southern California interseismic deformation, the primary uncertain parameters are fault slip rates and tectonic block motions within a kinematic block model. In the case of coseismic deformation, the uncertain parameters are fault slip. Ultimately relative financial costs of seafloor geodetic technology may be compared in terms of information gain per dollar, and will enable well-informed decisions about expanding current geodetic networks, both onshore and off.

The composition and structure of shallow portions of the San Andreas and San Gabriel Faults, James P Evans, Rebekah Reimann, Caroline Studnicky, and Kelly K Bradbury (Poster Presentation 169)

We investigate the composition and structure of the upper 2 km of strike-slip faults by examining core from two geotechnical investigations in the San Andreas (SAF) and San Gabriel Fault (SGF) zones. Seven steeply north inclined cores from Lake Elizabeth intersect steep south-dipping SAF zones up to 30 m thick of fault-related rocks, narrow slip surfaces, and wide zones of alteration to a depth of 140 m. We also examine a core acquired in a steeply plunging borehole across the steep north- dipping San Gabriel Fault in the western San Gabriel Mountains to a depth of ~ 500 m. The SGF zone is up to 100 m wide here.

Standard optical petrographic study of the SAF samples reveals a range of brittle deformation processes and evidence for syntectonic hydrothermal alteration. Narrow slip surfaces lie within bands of cataclasite and ‘gouge’ zones that consist of fractured and altered granitic rocks subsequently sheared. Mineralogy of the deformed rocks includes a host of alteration produces from the protolith gneiss, including epidote, chlorite, zeolites (laumontite, nontronite), clay minerals, and palygorskite. Brecciated epidote in veins document brittle overprint on higher temperature mineralization. Core from the SGF consists of granodiorite gneiss that contains indurated foliated cataclasite, narrow slip surfaces, and sheared and brecciated chlorite+zeolite zones, and injection related breccia. We used a 60 cm section of the Lake Elizabeth core to develop a new analytical method to map the geochemistry of the fault related rocks. We examined the core with macroscopic X-ray Fluorescence Spectrometry mapping to document fine-scale alteration patterns over a relatively large region of core at the SSRL, Stanford. Rapid elemental mapping of the core documents the mobility of alteration-related elements K, Na, Mg, and the concentration of less mobile Cr, Ni, and Mn.

The patterns observed in the core support a model of syntectonic hydrothermal alteration in the fault zone that represent either 1) the fault –related rocks we observe formed at depths > than 1.5 km and the fault zone was exhumed, or 2) elevated thermal gradients produce alteration in the shallow portion of the faults. The distributed deformation and alteration in these shallow levels may help explain how slip is diffused in the upper several km of a fault zone, and in part explains the shallow slip deficits observed in seismogenic faults.

Characterization of Faulting at the San Andreas Oasis in the Dos Palmas Preserve Using Ground-based Magnetics, VLF and DC Resistivity, Drew Faherty, Stacey R Petrashek, Raul Contreras, and Nathan W Pulver (Poster Presentation 273)

The San Andreas Oasis is located on the northeast side of the Salton Sea, within the Dos Palmas Preserve at the base of the Orocopia Mountains. This Oasis, among other oases and springs in the Preserve, are associated with the Hidden Springs Fault (HSF) and Powerline Fault. Because the water level at these locations has been on the decline in recent years, recharge basins were constructed 4 km northeast near the recently lined Coachella Canal. Unfortunately, little of this water appears to be reaching the San Andreas Oasis and limited knowledge of the subsurface structure makes it difficult to isolate the cause of this decline in water level. The HSF fault is located west of the oasis, while several other faults are hypothesized to exist east of the Oasis. These unmapped faults may relate to the origin of the oasis and affect groundwater flow from the recharge basins toward the Oasis. The right-lateral HSF trends northwest, bounding the Oasis to the west and continuing south for 1 km until it steps east towards what was mapped as the Powerline Fault by Babcock (1969). This feature was interpreted more recently by Clark (1984) as a left step in the HSF, which may continue south.

To investigate the extent and structure of the mapped and unmapped faults in our 2 km2 study area around the San Andreas Oasis, we use several geophysical surveying techniques including ground-based magnetic, Very Low Frequency (VLF), and Direct Current (DC) resistivity surveys. Total magnetic intensity data was collected with a GEM proton precession magnetometer with a VLF attachment and used to create a map of total magnetic field intensity. Anomalies appear to correlate with the known trace of the HSF and suggest the existence of another fault bounding the eastern portion of the San Andreas Oasis. Data for our VLF profiles exhibit high amplitude anomalies at their intersections with both the HSF and the hypothesized fault trace east of the San Andreas Oasis. An IRIS Syscal Kid with 24 electrodes at 5 m spacing was used to collect DC resistivity data near the traces of the HSF and unmapped faults. The resulting resistivity profiles show a conductive, vertically oriented feature suggesting clay-rich or saturated fault gouge at the mapped trace of the HSF. We plan to continue collecting magnetic, VLF, and DC resistivity data to determine whether the hypothesized fault trace continues south, and to investigate the possible stepover in the HSF about 1 km south of the San Andreas Oasis.

Investigating microearthquake finite source attributes with IRIS Community Wavefield Demonstration Experiment in Oklahoma, Wenyuan Fan, and Jeff J McGuire (Poster Presentation 073)

An earthquake rupture process can be kinematically described by rupture velocity, duration and spatial extent. These key kinematic source parameters provide important constraints on earthquake physics and rupture dynamics. In particular, core questions in earthquake science can be addressed once these properties of small earthquakes are well resolved. However, these parameters of small earthquakes are poorly understood, often limited by available data sets and methodologies. The Incorporated Research Institutions for Seismology Community Wavefield Experiment in Oklahoma deployed ζ350 three-component nodal stations within 40 km2 for a month, offering an unprecedented opportunity to test new methodologies for resolving small earthquake finite source properties in high resolution. In this study, we demonstrate the power of the nodal data set to resolve the variations in the seismic wavefield over the focal sphere due to the finite source attributes of an M2 earthquake within the array. The dense coverage allows

us to tightly constrain rupture area using the second moment method even for such a small earthquake. The M2 earthquake was a strike-slip event and unilaterally propagated towards the surface at 90 per cent local S-wave speed (2.93 km s−1). The earthquake lasted ζ0.019 s and ruptured Lc ζ70 m and Wc ζ45 m. With the resolved rupture area, the stress-drop of the earthquake is estimated as 7.3 MPa for Mw 2.3. We demonstrate that the maximum and minimum bounds on rupture area are within a factor of two, much lower than typical stress-drop uncertainty, despite a suboptimal station distribution. The rupture properties suggest that there is little difference between the M2 Oklahoma earthquake and typical large earthquakes. The new three-component nodal systems have great potential for improving the resolution of studies of earthquake source properties.

Lab Talk with Laura: STEM research meets comedy on the radio, Laura A Fattaruso (Poster Presentation 319)

In January 2018 I started producing a weekly STEM-themed radio show, Lab Talk with Laura, on the UMass Amherst radio station WMUA. The show is also distributed as a podcast on iTunes and Soundcloud, and promoted via Facebook and Twitter. I host each episode and have two or more researchers as guests on each episode, along with a rotating cast of comedians as co-hosts to bring humor and a non-science perspective to the dialogue. Researchers interviewed on the show include undergraduates, graduate students, postdocs, and professors at a variety of career stages. A wide range of STEM fields from Chemical Engineering and Computer Science to Food Science and Molecular Biology have been represented on the show. Topics discussed on the show have included wearable photovoltaic technologies, genetic engineering of food crops to enhance nutrition, climate science from a range of perspectives including ecology, paleoclimate, and forecast modeling, and biomechatronic manipulation of sea slug brains, just to name a few. I plan to record interviews at the 2018 annual SCEC meeting to make an earthquake science themed show.

Each episode is an hour long and features long-form open discussion of topics that arise from conversations about individual's research. Each episode ends with a game called GTA: Guess That Acronym to acknowledge and break down the communication barriers created by scientific jargon. Researchers from a variety of backgrounds have been interviewed on the show including people who are first-generation scientists, POC, foreign-born, and LGBTQ, to highlight the wide range of people who contribute to STEM fields. The show aims to humanize scientists and the research process, and make complex research accessible to a broad audience. I faced challenges in meeting some of my initial goals for the show, such as transcribing each episode so it would be accessible to deaf and hard of hearing communities, or promoting the show effectively to wider audiences. These are challenges that could be accounted for in the planning stages of future communication work. The show has also been successful in many of its goals: providing an outlet for scientists to share their research in their own voice, humanizing scientific research, and reaching a non-science audience.

On the possibility of earthquake rupture through clay-rich faults, Daniel Faulkner, Marieke Rempe, John Bedford, C Sanchez-Roa, C Boulton, and S den Hartog (Oral Presentation Tue 08:30)

Many mature, large-displacement fault zones exhibit a clay-rich fault core. This low porosity, low permeability material inhibits the migration of fluid and consequently small changes in porosity produce pore pressure transients that take significant time to dissipate. Despite most clay-rich fault gouges displaying velocity strengthening frictional characteristics, variations in pore-fluid pressure can result in a wide range of behaviour including apparent velocity weakening leading to possibility of these rocks hosting instabilities. We present laboratory constraints of the frictional properties of clay-rich fault gouge both at low slip velocity, commensurate with earthquake nucleation and at higher slip velocity, equivalent to that during rupture propagation. We show that small amounts of compaction can result in large strength changes and apparent velocity weakening behaviour at slow slip velocity. At higher slip velocity, experimental results suggest thermal pressurization in clay-rich fault gouge is an efficient process that produces weakening over small slip displacements. Accounting for pore-fluid pressure effects during slip predicts a wide variety of behaviour including enhanced fault creep, slip transients, and even the possibility of rupture propagation on clay-rich fault zones.

Combining back-projection and matched filter in detecting offshore seismicity: Application to NE Japan subduction zone, Tian Feng, and Lingsen Meng (Poster Presentation 086)

In this project, we combine the Back Projection (BP) imaging and match-filter detection (MF) techniques to improve the capability of detecting offshore events. The MF method searches for similar patterns by cross-correlating waveforms of known template events with continuous seismic records. However, the MF method is heavily relying on known earthquake templates, which are obtained from the routine catalogs that lack events in the offshore region. By including BP-detected events as additional templates in the MF detection, we can potentially improve the picture of offshore seismicity. We studied the 2011 M 9.0 Tohoku-Oki earthquake by performing BP imaging one week following the mainshock first. Comparing with JMA catalog, we detected 710 undocumented new events. We then take them as MF templates and find additional 49924 new events within 60 days after the mainshock. It shows a significant amount of newly detected seismicity outer rise the trench, consistent with positive static Coulomb stress changes induced by mainshock rupture. Also, we are extending the analysis to the two foreshock migration sequences starting ~1 month before the mainshock.

Measurements of 3-component, time-dependent deformation using Sentinel-1 SAR interferometry and continuous GPS data, Yuri Fialko, and Ekaterina Tymofyeyeva (Poster Presentation 139)

Interferometric Synthetic Aperture Radar (InSAR) data are increasingly used to image deformation due to active faults. Frequent InSAR acquisitions are expected to provide an improved signal to noise ratio for low-amplitude deformation signals. However, we find that increasing number of radar interferograms used in the analysis of surface deformation results in the accumulation of high-frequency spatial noise, which is introduced in the time series analysis due to filtering of the radar phase prior to unwrapping. We propose a method for "unfiltering" the filtered unwrapped radar phase. We demonstrate the feasibility of the proposed method using Sentinel-1 InSAR and Global Positioning System (GPS) data. We combine data collected by Sentinel-1 between 2014-2018 with continuous GPS measurements to calculate the three components of the surface velocity field over the southern San Andreas and San Jacinto fault zones at the resolution of InSAR data (~100 m). We obtain the 3 orthogonal components of surface motion using overlapping InSAR tracks with different look geometries, together with an additional constraint provided by GPS measurements of the local azimuth of the horizontal velocity vector. We estimate both secular velocities and displacement time

series. The latter are calculated by combining InSAR time series from different lines of sight with time-dependent azimuths computed using continuous GPS time series at every InSAR epoch. We use CANDIS method [Tymofyeyeva and Fialko, 2015], a technique based on iterative common point stacking, to correct the InSAR data for tropospheric and ionospheric artifacts when calculating secular velocities and time series, and to isolate low-amplitude deformation signals in our study region. This three-component, time-dependent description of surface deformation from a combination of geodetic data sets can be used as part of the SCEC Community Geodetic Model.

Revisiting the Cajon Pass Quaternary Terraces with Geochronology dating– implications for the long term slip rates of the San Jacinto and San Andreas systems, Paula M Figueiredo, Ray J Weldon, and Lewis A Owen (Poster Presentation 261)

The San Andreas (SA) and the San Jacinto (SJ) Faults are the two major active fault systems in Southern California, accommodating 50-70 % of the 52 mm/yr North America–Pacific plate boundary motion. At the Cajon Pass (CP) area, both fault systems converge and became parallel, displacing a terrace sequence younger than 700 ka (post-dating Noble's Old Alluvium unit). Since the inception of SJ, both systems have been evolving and interacting at different rates and time, and their long-term tectonic interaction is not sufficiently understood, particularly at the CP area. This poses limitations for the understanding of their structural evolution but also for the regional seismic hazard analysis. SA slip-rates decrease from N of CP (Palette Creek, 35±5 mm/yr, for Holocene and ~ 400 ka) to CP area (Holocene, 24.5 mm/yr) and south of it (Plunge Creek, 6.3-18.5 mm/yr). This decrease of about 5-10 mm/yr from Palette Creek to CP, most likely indicates transfer to other structures like Lytle Creek fault (2.5 mm/yr), or the Glen Helen fault, or the main geologic strand of the SJ. South of CP, a significant amount of slip seems to have been transferred to the northern SJ during late Pleistocene, while Holocene slip-rates indicate a similar or slightly higher rate for SJ. The terrace sequence at the CP displaced by SA and SJ is crucial to access slip-rates and tectonic interactions between these fault systems through time. The upper deposits, Qoa-e (500±200 ka), Qoa-d (55±12 ka), and Qoa-c correspond to significant alluvial fill deposits, over 50 m thickness widely present that can be correlated throughout the basin. The chronology of the sequence was established through a soil chronosequence: while the younger sequence (<35 ka) was dated and its soil chronosequence calibrated, the older sequence, namely the Qoa-e and the Qoa-d were never dated with absolute dating techniques. Aiming to refine ages for the older terraces and improve long term slip-rates for SA and SJ and understand their interaction during Pleistocene, we sampled depth profiles for TCN 10Be in the Qoa-e at 3 locations: Summit area (displaced by SA and Cleghorn F.), Texas Hill (displaced by Lytle Creek F.) and Cucamonga (displaced by Cucamonga T.). Samples are presently being measured at the Prime Lab Accelerator Mass Spectrometer and we will present preliminary results for the surface ages of the Qoa-e terrace as well as discuss further locations to sample and constrain the age of other terraces.

Statistics of seismicity associated with a sequence of explosive eruptions at Kilauea, Hawaii, Rebecca A Fildes, Louise H Kellogg, Donald L Turcotte, and John B Rundle (Poster Presentation 037)

Beginning about June 4, 2018, a remarkable quasi-periodic sequence of explosive eruptions began at Kilauea volcano, Hawaii. Explosive summit eruptions began after the M=6.9 earthquake on May 4, 2018 and the decay of its aftershock sequence. These eruptions, typically releasing the energy equivalent of a M = 5.3 earthquake, were associated with the drainage of magma from beneath the summit to the East Rift where surface eruptions occurred. The mean inter-eruption time at the summit was 1.30 +/- 0.32 days and the mean earthquake occurrence during each of these inter-event periods was 603 +/- 204 earthquakes. We consider only earthquakes with M ≥ 2. In the magnitude range 2.5 - 4.0 this seismicity has a good correlation with Gutenberg-Richter scaling, but with a somewhat high b = 1.6. Between each pair of eruptions there was a similar pattern of seismicity. Following an explosive eruption, there was a relatively quiescent period typically lasting 0.41 +/- 0.14 days, with no indication of aftershocks. Following the quiescent period, there was a sudden onset of seismicity at a nearly constant rate of 677 +/- 84 earthquakes per day. These active periods lasted 0.89 +/- 0.32 days. We show that the time series of inter-eruption times is strongly anti-persistent. To illustrate this behavior, we consider three consecutive inter-event periods. In the first period, there were 607 earthquakes with an active period of 0.80 days at a rate of 751 events per day. In the next period, 982 earthquakes occurred with the active period lasting 1.43 days at a rate of 679 events per day. In the third period, there were 604 earthquakes and an active period of 0.94 days at a rate of 641 events per day. Future studies of this remarkable volcanic and seismic sequence should provide important insights into both the physics of volcanic eruptions and their associated earthquakes.

Effective stress drop and aseismic deformation, Tomas Fischer, and Sebastian Hainzl (Poster Presentation 079)

The concept of effective stress drop of a seismic sequence is based on the cumulative seismic moment and area activated by seismic ruptures. The analysis of end-member cases of clustered seismicity shows that the estimated effective stress drop of a cluster is only in agreement with the stress drop of a single event rupturing the same area if no aseismic deformation takes place and rerupturing of asperities occurs during the sequence. The evolution of the cumulative seismic moment release as function of the cluster radius can be used to discriminate different processes: the exponent of seismic moment scaling with radius indicates if the ruptured area is uniformly loaded or whether external loading takes place.

Our analysis of 13 sequences ranging from injection-induced activity to natural swarm and aftershock activity shows standard cubic scaling of the total seismic moment in most cases. Slightly higher exponents in the case of injection-induced sequences are indicative of the ongoing local forcing related to the massive fluid injections during the cluster evolution, while lower exponents down to 1 in the case of creeping events might be related to a decreasing/fractal asperity density.

Three seismicity groups can be distinguished: a normal-stress-drop group of geothermal injections, swarms and mainshock-aftershock sequences, a low-stress-drop group of shale and gas fracking, and the very low-stress-drop case of creeping events. The small effective stress drop can be interpreted by small shear modulus of the rocks, or alternatively, by a large portion of creep in the total slip. Then the seismic events with normal static stress drop would account only for a small portion of deformation. This is probably the case of hydraulic fracturing. Considering the rigidity of sands and shales is of the same order as of other types of rocks, it appears that during hydraulic fracturing of these formations a high portion of strain is released aseismically.

Preliminary evidence for localized lithospheric deformation in the western Basin and Range and Walker Lane from Ps receiver function analysis, Heather A Ford (Poster Presentation 283)

Cenozoic-aged extension within portions of the Basin and Range has been estimated to be as large as 250 km, however others put estimates lower. A question that remains today is how strain is accommodated within the lithosphere beneath the Basin and Range. Vertically uniform deformation within the crust would produce large lateral variations in Moho topography, which is not observed. This is cited as evidence of viscous flow in the lower crust. Others have hypothesized that the lower crust is strong and that extension currently occurs along a mega-detachment at the base of the crust. Anisotropic receiver function analysis from six long-running stations within the greater Basin and Range province (Schnorr and Ford, 2016) found evidence for well-defined, layered anisotropy within the lowermost crust and uppermost mantle at stations located along the western margin of the Basin and Range (WVOR, TPNV, and MNV) but not in other locations (BMN, ELK and NEE). Such variability suggests that either strain or mineralogy differ locally.

In this study, additional anisotropic receiver function analysis has been performed on 16 stations located within the western Basin and Range and Walker Lane regions. 10 stations operated for ~1.5-2 years as part of Earthscope's Transportable Array. The remainder are long-running stations from the CI network and are confined to a geographic region including Owens Valley, Death Valley and the immediate surrounding areas. Preliminary results show a positive phase at most stations, interpreted to be the Moho, at approximately 3.5-4.5 seconds, although significantly more complicated behavior is observed at some stations (e.g., MLAC, GRA, N07B). Importantly, preliminary results indicate the presence of anisotropic structure within the lower crust and upper mantle (~30-60 km). While strong evidence for anisotropy exists, it exhibits significant complexity at individual stations with multiple layers possible at some locations (e.g., SLA, TIN, FUR). Additionally, there is little coherence among stations across the region, suggesting that lower crustal mineralogy may play an important role in the observed seismic anisotropy (i.e., Brownlee, 2017; Erdmann, 2013). Further work is still needed to better constrain the geometry of the anisotropic structure at individual stations, and to determine how the structure might be related to deformation within the western Basin and Range and Walker Lane regions.

Does effective stress have reduced sensitivity to pore pressure at seismogenic depths?, Patrick M Fulton, Szu-Ting Kuo, Hiroko Kitajima, and Xiaoda Liu (Poster Presentation 180)

The importance of fluids in fault mechanics is well-recognized. Pore pressure is known to affect elastic deformation and brittle failure through its control on effective stress, where Effective Stress = Stress – alpha * Pore Pressure.

However, the sensitivity of effective stress to pore pressure, controlled by the term alpha, may be less than the commonly assumed value of 1. Here we present an analysis of data from new rock deformation experiments conducted within the John W. Handin Laboratory for Experimental Rock Deformation at Texas A&M and a reanalysis of extant data to evaluate the pore pressure sensitivity of rocks under conditions representative of the brittle seismogenic zone.

Three key observations result from our analysis:

1. When considering the influence of effective stress on elastic deformation, we find that alpha is less than one for a variety of sandstones and for granite. In addition, this alpha for elastic deformation exhibits a stress dependence; it decreases with increasing confining pressure, consistent with theoretical considerations.

2. We also find alpha values less than one for the influence of effective stress on brittle failure. Similar to the effect on elastic deformation, we also find suggestions of a stress dependence on alpha for brittle failure.

3. Lastly, alpha increases as a result of rock damage. In other words, the same rock becomes more sensitive to pore pressure after it is damaged.

Together these results can help provide insight into properties and processes affecting the stress state on faults within Southern California and how they may respond to sudden transients.

Unraveling earthquake dynamics through large-scale multi-physics simulations, Alice-Agnes Gabriel, Stephanie Wollherr, Thomas Ulrich, Elizabeth H Madden, Kenneth Duru, and Duo Li (Poster Presentation 292)

Earthquakes are highly non-linear multiscale problems, encapsulating the geometry and rheology of propagating shear fractures that render the Earth's crust and emanate destructive seismic waves.
Using physics-based earthquake scenarios, modern numerical methods and hardware specific optimizations sheds light on the dynamics, and severity, of earthquake behaviour. This is enabled by the open-source software SeisSol (www.seissol.org) that couples seismic wave propagation of high-order accuracy in space and time (minimal dispersion errors) with frictional fault failure, off-fault inelasticity and visco-elastic attenuation. SeisSol exploits unstructured tetrahedral meshes to account for complex geometries, e.g. high resolution topography and bathymetry, 3D subsurface structure, and complex fault networks. The achieved degree of realism and accuracy is enabled by recent computational optimizations targeting strong scalability on many-core CPUs and a ten-fold speedup owing to an efficient local time-stepping algorithm (Uphoff, C., Rettenberger, S., Bader, M., Madden, E.H., Ulrich, T., Wollherr, S., and A.-A. Gabriel, SC'17).

The potential of in-scale earthquake rupture simulations for augmenting earthquake source observations is demonstrated in two recent examples: i) The 2016 M_w7.8 Kaikoura, New Zealand earthquake, considered the most complex rupture observed to date and causing surface rupture of at least 21 segments of the Marlborough fault system. High resolution dynamic rupture modeling unravels the event's riddles in a physics-based manner (Ulrich, T., A.-A. Gabriel, J.-P. Ampuero and W. Xu, https://eartharxiv.org/aed4b/); ii) The 2004 Mw 9.1-9.3 Great Sumatra-Andaman Earthquake challenged from a lack of near-source observations. We account for complex megathrust-splay fault geometries in the largest-scale dynamic earthquake rupture simulation

to date. The interplay of complex fault geometry and simple pre-stress yields good agreement of ground-deformation and long-period teleseismic data.

Lastly, we will discuss future directions for exploiting expected exascale computing infrastructure with the ExaHyPE high-performance engine for hyperbolic systems of PDEs (www.exahype.eu). Specifically, we aim to represent complex geometries with novel geometric transformations and diffuse interfaces on adaptive cartesian meshes (Duru et al., arXiv:1802.06380; Tavelli et al., arXiv:1804.09491), thus avoiding manual meshing.

Aftershock Matters, Nicole S Gage, David J Wald, and Kristin D Marano (Poster Presentation 048)

Aftershocks can be inconsequential, or they can cause more extensive damage and more human casualties than their associated mainshocks. Most studies of aftershocks focus on characterizing statistical properties such as their likelihood, frequency, size, and spatial distribution. However, an understanding of the impacts of aftershocks is important for operational aftershock forecasting, response protocols, and loss modeling efforts. The definition of “aftershock” has always been and remains open for interpretation. We acknowledge the ambiguous nature of aftershocks and as such, we consider only a practical definition. The events immediately following an earthquake of societal significance are of importance to scientists, responders, infrastructure managers and financers, among others. The goal of this study is to improve loss calculations for future earthquake sequences. In addition to the emotional toll often experienced by inhabitants, a typical result of an earthquake mainshock includes the reduction of human exposure to hazards during ensuing aftershocks (evacuation, sheltering, casualties), and changes to both the value and vulnerability of the building stock. To this end, we study the scope of effects from aftershocks by creating an inventory of losses for 20 California mainshock/aftershock sequences. Overall, few significant historic aftershock sequences caused extensive damage or fatalities. Though many of the 20 earthquake sequences studied generated aftershocks that caused additional damage, only the aftershocks of the 1952 Kern County and the 1987 Whittier Narrows earthquakes produced additional documented fatalities. Damage and possible fatalities resulting from aftershocks of the 1933 Long Beach and the 1906 Great San Francisco earthquakes are difficult to discern, though some commentary implies that they were important. Contemporary accounts of two of the mainshock/aftershock sequences studied (1940 Imperial Valley and 1992 Cape Mendocino) suggest that aftershocks may have produced greater damage than the mainshocks. We envision that analysis of the California aftershock data collected will support the development of strategies that can be applied operationally during an aftershock sequence to more accurately project losses. We expect that any such strategies will be regionally dependent, reflecting variable aftershock statistics and building vulnerabilities.

Probabilities of Earthquakes in the San Andreas Fault System: Estimations from RSQSim Simulations, Jacquelyn J Gilchrist, Thomas H Jordan, and Kevin R Milner (Poster Presentation 031)

The RSQSim model of Dieterich & Richards-Dinger (2010) is now capable of simulating very long (> 10^6 yrs) catalogs of M ≥ 5 earthquakes using the same fault geometry and slip rates as UCERF3 (Field et al., 2014), the latest seismic hazard model for California. Time-independent hazard maps derived from RSQSim and UCERF3 using NGA ground motion prediction equations are surprisingly similar (Shaw et al., 2018). The potential for incorporating information from RSQSim simulations into probabilistic forecasting models motivates us to address how it might be done in practice. We consider the time-independent forecasting of events composed of M binary subevents, where the mth subevent is failure/no-failure of the mth fault section. The M marginal distributions can be well estimated by simulation, but a complete forecast must specify the frequencies of N = 2^M composite events, many of which are rare and poorly sampled, even at long simulation times. We consider a Bayesian scheme in which the prior on the forecast probabilities is a Dirichlet distribution of order N. The mean values are specified either by a prior forecast, such as UCERF3, or as the product of the M marginals (i.e., assuming subevents independence). The relative uncertainty in the prior is specified by a pseudo-count. We take the likelihood function for the event counts to be the multinomial distribution, which is conjugate to the Dirichlet prior; therefore, the posterior can be calculated analytically, allowing M to be fairly large. We apply this forecasting method to the southern San Andreas fault system, focusing on the probabilities of composite events involving faults that interact in the El Cajon Pass and San Gorgonio Pass regions. We are particularly interested in how these regions of fault complexity act as earthquake gates, governing the propagation of ruptures from one fault to another. The subevents in our models include ruptures on sections of the San Andreas, San Jacinto, and major thrust faults in the eastern Transverse Ranges. In the restricted world of the current RSQSim model, rupture propagation through the San Gorgonio Knot is extremely rare. Propagation between the San Andreas and San Jacinto is also rare and tends to be mediated by ruptures on nearby thrust faults.

Rapid induced seismicity mitigation and its impact on aftershock productivity in Oklahoma, Thomas H Goebel, Zach Rosson, Emily E Brodsky, and Jake I Walter (Poster Presentation 089)

Induced earthquakes provide a rare opportunity to study the connection between stress perturbations and resulting seismic activity. Fluid-injection can directly trigger seismic events, leading to elevated background rates, but may also result in main-aftershock sequences and event clustering similar to tectonic sequences. We examine the influence of targeted injection rate reductions after notable earthquakes on ensuing aftershock sequences in Oklahoma. We identify aftershock sequences by separating the population of clustered from background events within a space-time-magnitude domain. In comparing aftershock productivity between California and Oklahoma up to magnitude ~6, we find similar power-law scaling between mainshock magnitude and average number of aftershocks with an exponent close to 1. However, several events above M4.4 in Oklahoma appear significantly deficient in number of aftershocks compared to the overall trend. Sequences with fewer aftershocks experienced rapid mitigation and reduced injection rates, whereas two events with M4.8 and M5 without mitigation exhibit normal aftershock productivity. The timing of when aftershock activity is reduced or ceases correlates with drops in injection rates within about a week. We quantify the expected poroelastic stress perturbations due to injection rate changes within a layered axisymmetric model and find stresses to be lowered by 10s to 100s kPa within the injection zone. The reduction in induced stresses is about an order of magnitude smaller at the depth of the earthquakes. The observations and modeling results suggest that targeted injection-rate-decrease can lower fault stresses below triggering stresses from preceding mainshocks. Induced seismicity mitigation may explain rapid drops in seismicity rates and low-productivity aftershock sequences.

Looking Ahead by Looking Down – Potential Applications of Very High Resolution Drone-Based Imagery for Tectonic Geomorphology, Allen M Gontz, Chelsea M Blanton, Thomas K Rockwell, and Joshua T Kelly (Poster Presentation 278)

Geomorphic analyses have relied on various methods throughout the recent past. In the 1940's, aerial imagery changed the way we look at the surface of the Earth. The 1980's brought Landsat and new capacity to image the surface of the Earth. In the past few years, Planet Lab made daily 3 meter resolution satellite imagery available. Arguably, the most impactful tool in recent years is the explosion of small, easy to fly and cheap remotely controlled aerial systems… also known as DRONES. Today's low-cost drones feature high-resolution cameras for still and video, GPS positioning, automated flight path planning and the ability to change cameras. We used a small commercially available drone, the DJI Phantom 4 Professional, to image sections of the southern San Andreas Fault. Flying at altitudes below 60 m and often as low as 25 m, we were able to acquire base imagery with a ground sample distance in the sub-centimeter range. The images were analyzed using structure from motion for creation of DEMs as well as orthophoto mosaics for sections along the southernmost San Andreas fault. Effective resolution of the data products is in the range of 1-10 cm, depending on the processing algorithm selected and altitude of imagery acquisition. Once a DEM is created, additional products, including hillshade models, surface curvature and slope-aspect maps can be created to facilitate identification of landscape features at various scales. One of the greatest potentials for very high-resolution drone-based imagery products is the speed at which data can be acquired. This approach facilitates rapid response to isolated events, such as earthquakes, and development of baselines for time series analyses. Time series data with centimeter-scale resolution has the potential to constrain slow-moving processes, such as creep, over reasonable time scales such as five years. We present examples of data products created from the imagery and use feature identification techniques that highlight offset geomorphic features that can be tied back to the earthquake record for this important fault.

Sampling Parametric Rupture Variability using Broadband Ground Motion Simulations, Robert W Graves (Poster Presentation 013)

Observations from past earthquakes show the rupture process can be complex, exhibiting spatial variations in rupture speed, slip and slip rate, as well as geometric roughness of the faulting surface. Incorporating these features within kinematic ground motion simulations is challenging due to uncertainty in the expected ranges and inter-correlations of the required parameters. Here, I calculate suites of broadband ground motion simulations for seven large (Mw 6.0 – 7.3) California earthquakes to help constrain appropriate ranges for key rupture parameters. Simulations are computed using the Graves and Pitarka (2010) method and are compared with recorded motions using the goodness-of-fit criteria of Goulet et al (2015). Typically, stations out to a distance of one fault length were included in the analysis with the fewest being 23 sites for North Palm Springs and the most 63 for Northridge. A total of 256 rupture scenarios are examined for each earthquake, with individual scenarios consisting of random realizations generated using the approach of Graves and Pitarka (2016). In addition to spatial variability in slip and fault roughness, each realization randomly samples from uniform distributions of average rupture speed (expressed as fraction of local shear wave velocity, Vr/Vs), down-dip fault width (Fwid) and seismic moment (Mo). For each earthquake, median values of Mo and Fwid are taken from published results, and these are allowed to vary by 25% and 15%, respectively, across the random realizations. The range of Vr/Vs is set at 0.725 to 0.875. For most events, the smallest misfits occur for a limited subset of parameter combinations. In general, the results are most sensitive to average rupture speed, followed by seismic moment and then fault width. The strike-slip and oblique events are modeled best with relatively low average rupture speed (~0.75) whereas the reverse events are modeled better with a relatively high average rupture speed (~0.85). No clear trends were seen for seismic moment and fault width when looking across all events. There were also cases for individual events where different combinations of parameters across the specified ranges produced equally good fits to the observations, highlighting the non-uniqueness of this approach. This reinforces the importance of adequately sampling ranges of rupture parameters when performing validations with past earthquakes, as well as when simulating ground motions for future events.

Using a dense GPS array as a strain meter on the Anza section of the San Jacinto fault , Margaret Grenier, and Yuri Fialko (Poster Presentation 115)

The San Jacinto fault is the most actively seismic fault in Southern California and has produced a series of moderately (M>6) sized earthquakes in the last 120 years. Within the main strand of the San Jacinto fault there is a ~20 km long locked section that has not ruptured in over 200 years and is bounded by fault segments with high seismicity rates (Sanders & Kanamori, 1984). This quiescent portion of the San Jacinto fault has been termed the Anza Seismic Gap. Previous geodetic studies have shown a high strain rate of ~0.4 microradians per year due to enhanced deformation within the few km wide fault zone (Lindsey et al., 2014). This high strain rate could be attributed to multiple factors such as a low rigidity fault zone, distributed elastic deformation within the fault zone, or an abnormally shallow locking depth. Understanding the details of strain accumulation within the Anza Seismic Gap can give rise to a better understanding of the fault zone architecture and improve seismic hazard estimates.

We investigate the local interseismic deformation within the fault zone by analyzing GPS data from 21 monuments comprising a ~400 m long alignment array at Anza. The data was collected in three GPS campaigns in 2013, 2015, and 2018. Analysis of the data was done using the GAMIT/GLOBK software package (Herring et al., 2018). We calculated precise baselines between all monuments of the array and used them to calculate velocities of each site. Given the right lateral motion of the San Jacinto fault interseismic deformation should result in an apparent rotation of the linear alignment array. Our result for the 5-year data set show an unexpected dilation signal with average velocities on the order of a few mm/year across the array. Our observations also confirm the lack of measurable localized creep in agreement with previous results that compare the total station observations and GPS data. The apparent fault zone dilation may be due to seasonal variability or residual noise. Further observations will provide more accurate constraints on the deformation style across the fault zone on the San Jacinto fault at Anza.

Afterslip and Viscoelastic Processes and Their Relation with Seismic Activity: An Example from the Study of the Mw 7.2 El Mayor-Cucapah Earthquake (Mexico), Adriano Gualandi, and Zhen Liu (Poster Presentation 168)

Different aseismic deformation processes perturb the stress field in the brittle crust, and consequently influence the seismic activity. Afterslip and viscoelastic relaxation are usually invoked to explain the observed displacements after a major earthquake. Discriminating between the two is challenging though. We achieve this result by applying a variational Bayesian Independent Component Analysis to the position time series from 125 GPS stations following the Mw 7.2 El Mayor-Cucapah earthquake, 2010 (Mexico). Among the retrieved Independent Components, two are clearly related to post-seismic activity: one is characterized by long relaxation time and broad spatial signature, while the other is concentrated in space and time near the mainshock and largest aftershock events. This separation can help to resolve the modeling tradeoff between these contributions. A comparison with the seismic activity that followed the mainshock shows that weak long-range interactions are likely mediated by viscoelastic relaxation while clustered earthquakes are controlled by afterslip.

2018 USEIT: Using Machine Learning to Forecast Earthquakes, Anthony A Guerra, Brandon T Ho, Varduhi Kababjyan, Ramon Mei, Tomoe Mizutani, Tiffany Streitenberger, Shalani Weerasooriya, Jordan Wolz, Guillermo Beas, Shengyu Wang, Abhijit Kashyap, and Jacquelyn J Gilchrist (Poster Presentation 311)

As part of the 2018 Undergraduate Studies in Earthquake Information Technology (UseIT) internship program, the Machine Learning (ML) team was challenged to investigate how ML might be used to derive statistical earthquake forecasts from deterministic earthquake simulations. The Rate-State Earthquake Simulator (RSQSim) is a physics-based faults system model that generates earthquake catalogs. The team filtered a one million year California statewide catalog produced by RSQSim using the Uniform California Earthquake Rupture Forecast version 3 (UCERF3) fault model for M≥7 events, which were then binned into in ten year intervals on four selected fault sections: Cholame, Carrizo, San Bernardino North, and Mojave South. Various ML algorithms were tested on this data to forecast ruptures, including a recurrent neural network, classification algorithms, and regression. Using a recurrent neural network we took into account the temporal and cyclic nature of earthquake ruptures, considering a series of time internal snapshots as one input. For the classification method, we took the rupture time intervals and classified them based on whether a rupture occurred, applying several algorithms including: logistic regression, decision trees, linear discriminant analysis, K-nearest neighbors, naive Bayes classifier, and then compared their accuracies and reliabilities in predicting the occurrence of ruptures. Further, we compared the fault rupture probabilities between RSQSim and the (UCERF3) transition probabilities that were obtained through regression on 4 different fault sections. We created a risk gradient fault labeling system based on recurrence intervals, which improved the R-squared scores for our classification algorithms. Future work should investigate adjustments to algorithms and rupture data processing, continuing to build on the potential for machine learning in the realm of earthquake rupture forecast in the future. With this increase we conclude that with more data, machine learning techniques are efficient tools that can help forecast earthquake activity by detecting patterns in data that humans are unable to recognize.

Investigating strain transfer along faults in Joshua Tree National Park, CA, with possible implications for along strike variations in southern San Andreas Fault slip rate, Katherine A Guns, Richard A Bennett, Kimberly D Blisniuk, and Sally F McGill (Poster Presentation 238)

The pattern of and relationship between elastic and permanent strain accumulation adjacent to the southern San Andreas Fault (SSAF) zone in the Eastern Transverse Ranges Province (ETR) are currently only poorly understood, hampering assessments of earthquake potential and associated hazards to southern California. To address this issue, we are integrating geodetic and tectonic geomorphologic methods to investigate how plate boundary strain is accommodated within the ETR, which lies between the SSAF and the Eastern California Shear Zone (ECSZ). We focus our studies on the five east-trending, left-lateral strike slip faults of the ETR within Joshua Tree National Park (JTNP). These faults each have measured cumulative offsets ranging between 1 km to 20 km. If active, these faults could be facilitating contemporary rotation of crustal blocks in the ETR, with implications for along strike variation of SSAF slip rate and the kinematics of strain transfer between the SSAF and ECSZ. Existing block models present a variety of slip rate estimates for these faults, from as low as zero to as high as 7 mm/yr, suggesting a gap in our understanding of what role they play in the larger system. To determine whether present-day block rotation along these faults contributes to strain accumulation in the region, we apply 10Be surface exposure dating methods to observed offset channel and alluvial fan deposits in order to estimate fault slip rates along two faults in the ETR. We employed detailed geomorphic mapping, LiDAR data analysis, and clast count studies to identify and quantify Quaternary (at least latest Pleistocene) offsets at 3 sites along the Blue Cut Fault and 1 site along the Smoke Tree Wash Fault. Initial dating (N=7) at one of the sites, indicates a preliminary fault slip rate of 0.5 1.75 mm/yr for the Hexie Mountains section of the Blue Cut Fault, though further 10Be dat

Machine Learning in detecting Low-frequency Earthquakes in Shikoku, Japan, Huiyun Guo, Hui Huang, Tian Feng, and Lingsen Meng (Poster Presentation 061)

Low-frequency earthquakes (LFEs) occur largely during slow slip events at subduction interfaces. Their actions affect the stress state of the seismogenic zone and potentially link to larger ordinary earthquakes. Detecting and analyzing low-frequency earthquakes is crucial for a better understanding of the subduction process. As LFEs lack distinct, impulsive body waves, it is challenging to detect them using classical techniques. The most common method for identifying low-frequency earthquakes involves autocorrelation or template matching techniques that often have low computational efficiencies and therefore difficult to be applied to large dataset. Fortunately, a rapid transformation has occurred in the field of computer vision in recent years due to the emergence of convolutional neural network (CNN). These CNNs are powerful variants of supervised machine learning which significantly improve the computational detecting similar waves in seismology. In this paper, we attempt to detecting low-frequency earthquakes 2018 in Shikoku, Japan using a highly scalable CNN developed by Perol et.al, 2018. We adopt the continuous waveforms from April, 2004 to March, 2011 recorded by five Hi-net stations, KWBH, YNDH, TBEH, OOZH and HIYH in central Shikoku. Based on the LFE catalog from Ohta et.al, 2017, we obtain 1222 events for the training set and 195 events for the testing set. Our preliminary results show that we detect 7251 of tremors in the testing period. These newly detected LFEs are confirmed with visual inspections and

anticorrelation tests. Our initial attempt demonstrate that CNN is effective in detecting LFEs. We plan to expand our effort to detect the LFEs across western Japan and Cascadia.

Distributed fault slip in the Eastern California shear zone: adding a piece to the puzzle, Elizabeth K Haddon, David M Miller, Victoria E Langenheim, Tanzhuo Liu, Elmira Wan, and Laura C Walkup (Poster Presentation 237)

The Lockhart (LF) and Mt. General (MGF) faults are two primary structures accommodating dextral shear across the northern portion of the Eastern California shear zone. Early mapping infers simple fault traces branching NW of the Lenwood fault and anticline, which underlies the city of Barstow. We leverage Structure-from-Motion topography (18–23 cm grid), gravity data, field observations, and geochronology to map geometrically complex fault traces along the margins of southern Hinkley Valley and reconstruct late Pleistocene and Holocene fault slip. Three distinct traces of the MGF deform the fan piedmont on the linear SW flank of Mt. General. Scarps on Holocene alluvial fans are SW-facing and up to ~1.5 m in height, with larger magnitude, down-on-the-SW displacement of Pleistocene surfaces and Tertiary bedrock. Apparent dextral offsets of bars, channels, and levees in Holocene deposits average ~4 m with corresponding vertical offset of ~0.6 m. Regional dating indicates deposition of Holocene alluvium at ~8–13 ka and suggests a Holocene slip rate on the MGF of ~0.3–0.4 mm/yr. Summing cumulative dextral offsets for subparallel fault traces cutting bedrock ridges and late Pleistocene surfaces (~160–170 ka) implies at least ~21–44 m of net dextral slip. Our longer-term dextral slip rate estimate on the MGF is ~0.1–0.3 mm/yr, which lags relative to the Holocene rate. Anastomosing traces of the ~1–2 km-wide LF zone deform a relict braid plain of middle Pleistocene sand and gravel deposited by the ancestral Mojave River between ~200–550 ka, based on tephra identified as 631 ka Lava Creek B ash and varnish microstratigraphy for overlying rockfall. Apparent offsets of inverted bar and channel deposits with subtle ridge-and-swale topography show distributed right-lateral and right-reverse oblique slip with an overall down-on-the-NE component. Cumulatively, fault strands yield ~110–180 m of dextral offset and suggest a long-term dextral slip rate of ~0.2–0.9 mm/yr. Dextral offset between ~8 and 10 m of a Holocene fluvial terrace riser and levee, related to the modern incised Mojave River and likely abandoned by ~8–13 ka, yields a similarly fast Holocene slip rate at ~0.6–1.3 mm/yr. Our preferred late Pleistocene dextral slip budget for the combined MGF and LF (~0.8 mm/yr) compares well with reported rates for the Lenwood fault (~0.8–1 mm/yr) and favors structural connectivity among spatially distributed faults of the MGF and Lenwood–Lockhart fault systems.

Communicating Seismological Uncertainty to the Public: A Case Study in Oklahoma, Georgia Halkia, and Lisa Grant Ludwig (Poster Presentation 318)

Over the past decade, seismicity in Oklahoma has increased dramatically. Communication research shows that people receive information from various channels and, based on their values and perceived risks, will decide if preparing for a disaster is worthwhile. Newspapers play an important role in society by informing the public about what is happening. We analyzed newspaper coverage of Oklahoma seismicity to understand how newspaper coverage and interviews with seismologists affected preparedness efforts. We performed a qualitative content analysis of newspaper articles utilizing Lexis Nexis Academic search engine. The date parameters were selected to capture a period of increasing rate of induced seismicity. The articles consisted mainly of news, editorials, and opinion pieces (N=314). We followed a grounded theory approach to develop themes, and utilized risk communication theory to gain a deeper understanding of the meaning of the written messages. The major themes identified were uncertainty over cause and risk, and non-consensus over regulating the oil industry. There were several key scientists and experts that were identified through this analysis and played an important role in communicating their knowledge to the people of Oklahoma through newspaper media coverage. Most of the articles captured conflicting views of stakeholders, in addition to lack of certainty from the experts. Risk communication research suggests delivery of uncertainty and conflicting messages deteriorates trust between experts and community members and minimizes their risk perception. The relatively low level of earthquake preparedness in Oklahoma suggests that the seismological information communicated did not persuade the people to take or demand action.

The rupture process of 2018 Mw 7.0 Kalapana, Hawaii earthquake and relation with the 1975 event, Jinlai Hao, Wenze Deng, and Chen Ji (Poster Presentation 285)

The Mw 7.0 2018 Kalapana, Hawaii earthquake struck the south flank of Kilauea volcano, Hawaii Island, on May 4th 2018, a day after the starting of the 2018 Lower Puna eruption. Its epicenter was a few km away from the epicenter of 1975 Mw 7.7 earthquake, outside the southeast coast of Hawaii island. The relations with previous event and new eruption drew our attention. Here we constrain the rupture process of the Kalapana earthquake by joint inverting the GPS static displacements, waveforms of local strong motion, teleseismic P and SH waves, and long period surface waveforms. Our preliminary study reveals that the rupture occurred on a low angle fault plane dipping 9 degree north-northwest, and broke a fault patch 35 km along strike and 20 km downdip, with an average slip of 1.2 m. The inverted rupture duration time and total moment of our preferred model are 22.4 s and 4.3x10**19 Nm (Mw 7.0), respectively. The centroid was located at about 7.2 km southwest of the hypocenter in a depth of 6.6 km. The rupture propagation is about 1.2 km/s along strike but much slower downdip. We will compare the rupture characterizations of 1975 and 2018 Kalapana earthquakes and investigate the impact of this earthquake to the 2018 Lower Puna eruption.

Updated California Aftershock Parameters, Jeanne L Hardebeck, Andrea L Llenos, Andrew J Michael, Morgan T Page, and Nicholas J van der Elst (Poster Presentation 047)

Reasenberg and Jones (Science, 1989) introduced a statistical model for aftershock rate following a mainshock, along with estimates of "generic" California parameter values based on past aftershock sequences. The Reasenberg and Jones (1989) model has been used for decades to issue aftershock forecasts following M≥5 mainshocks in California. Here we update the "generic" parameters for California through a fit to the aftershock sequences of M≥5 mainshocks occurring since 1980. We find aftershock productivity values that are lower on average than the generic productivity reported by Reasenberg and Jones (1989), likely because low-productivity sequences were omitted from their analysis. We confirm the observation of Llenos and Michael (SRL, 2017) that southern California sequences are more productive on average than northern California sequences. The Mendocino area is much less productive, while the hydrothermal areas in Long Valley, Coso, and the Salton Sea, in contrast, are much more productive. We also quantify the variability of the Reasenberg and Jones (1989) productivity parameter a between sequences with

a normal distribution. This distribution of a-values can be used to compute aftershock forecasts that include epistemic uncertainty, and can be used as the prior for Bayesian updating of the a-value as a sequence progresses (e.g. Page et al., BSSA, 2016).

Moving Earthquake Science Forward - Earthquake Simulation Codes and the SCEC-USGS Dynamic Rupture Group, Ruth A Harris (Oral Presentation Mon 13:30)

Computational simulations of earthquake rupture provide clues for deciphering earthquake behavior. In a perfect world, we would have a complete set of observations at Earth's surface and at depth that would allow us to forgo simulations, but in reality, this is never the case and additional tools are required to fill the gaps in our knowledge about how earthquakes work. Dynamic earthquake rupture simulation is one of the tools that is being used. This type of computational simulation is powerful, but it is also complex, so additional steps are required to ensure that it is working as expected. The SCEC-USGS Dynamic Rupture Group has provided a solution. We developed an extensive suite of benchmark exercises that are used to test computer codes aiming to simulate dynamic earthquake rupture and the resulting nearby ground shaking. To date, more than a dozen codes have performed the exercises, demonstrating that they reliably produce similar results for fault rupture behavior and ground motions, when they use the same assumptions about fault geometry, initial stresses, crustal properties, and friction. Our website, scecdata.usc.edu/cvws, provides the details of our benchmark exercises and other information about our group's work. As part of our investigations we have examined cutting-edge earthquake hazards problems, from a study of the effect of fault geometry on future large earthquakes near a power plant to examinations of off-fault yielding's effects on earthquake progress and near-field ground shaking. Our group has also set an example for how a long-running open and welcoming collaboration can move forward with interesting science discoveries while mentoring the next generation of scientists in our field.

Please see our new paper:

Harris, R.A., M. Barall, B. Aagaard, S. Ma, D. Roten, K. Olsen, B. Duan, D. Liu, B. Luo, K. Bai, J.-P. Ampuero, Y. Kaneko, A.-A. Gabriel, K. Duru, T. Ulrich, S. Wollherr, Z. Shi, E. Dunham, S. Bydlon, Z. Zhang, X. Chen, S.N. Somala, C. Pelties, J. Tago, V.M. Cruz-Atienza, J. Kozdon, E. Daub, K. Aslam, Y. Kase, K. Withers, and L. Dalguer (2018), A suite of exercises for verifying dynamic earthquake rupture codes, Seism. Res. Lett., 89(3), 1146–1162, doi:10.1785/0220170222.

Stress accumulation rate on source faults around the junction of Ryukyu and Southwest Japan arcs using finite element model, Akinori Hashima, Hiroshi Sato, Tatsuya Ishiyama, Andrew Freed, and Thorsten W Becker (Poster Presentation 120)

The Kyushu island of Japan is located at the hinge of the Ryukyu and the Southwest Japan arcs, which are formed by the subduction of the Philippine Sea plate along the Ryukyu trench and the Nankai trough, respectively. The tectonics of the island gained attention by the occurrence of the 2016 Kumamoto earthquake (Mw 7.1). To understand why this earthquake was triggered and assess the risk of future crustal earthquakes in this region, it is necessary to model stress loading on the source faults due to the dominant subduction system, which can be well constrained by the regional GPS data. Several studies obtained slip-rate deficit under the Nankai Trough. However, little attention has been given to the retreat of the Ryukyu trench.

In the present study, we developed a 3D finite element model (FEM) to quantify the evolution of plate stresses from the Ryukyu trench to the Nankai trough based on our previous model. The slip region along the Ryukyu trench–Nankai trough is divided into 8 x 27 subfaults where unit slip responses are calculated for input into an inversion analysis. Since the interseismic deformation includes the effect of the concurrent viscous relaxation in the asthenosphere, we used responses after complete relaxation of unit slips. For crustal deformation data, we used 10-year time series before the 2011 Tohoku-oki earthquake at 453 stations from the daily coordinates by GSI of Japan. We revised the source fault model by the Headquarters for Earthquake Research Promotion based on recent geophysical and geological data and added new faults especially in the Sea of Japan.

Our interseismic inversion suggests a 4-8 cm/year slip-rate deficit along the Nankai trough and ~4 cm/year slip-rate excess along the Ryukyu trench. While the slip-rate deficit along the Nankai trough is similar to the previous studies, the slip-rate excess along the Ryukyu trench is consistent with slab rollback at the Ryukyu trench and necessary to explain the characteristic anti-clockwise motion on the Kyushu island. Using the slip distribution, we can also calculate the evolution of the crustal stress field. Coulomb stress is positive in the western part of the EW trending Median Tectonic Line, the source faults in the Sea of Japan, and those in Kyushu associated with historic earthquakes. In particular, positive Coulomb stress on the source faults of the 2016 Kumamoto earthquake and the other M7 earthquakes is consistent with their occurrence.

Assessing kinematic compatibility of fault geometry and slip rates along the southern San Andreas fault system in the San Gorgonio Pass region, Jennifer L Hatch, and Michele L Cooke (Poster Presentation 165)

Assessment of seismic hazards in southern California may be improved with more accurate characterization of geometry and slip rates along the active San Andreas fault strands within the San Gorgonio Pass region. On-going debate centers on the activity level and active geometry of the Mill Creek and Mission Creek strands. Crustal deformation models with alternative three-dimensional active geometries of the Mill Creek and Mission Creek strands produce fault slip rates that match some, but not all, of the available geologic strike-slip rates at sites along both the San Andreas and San Jacinto faults. Sites with disagreement between the model and geologic slip rates indicate where the model geometry is incompatible with the interpreted geologic slip rate. We test the kinematic compatibility of slip rates and fault geometry by investigating mechanical models that prescribe geologically determined strike-slip rates within the model at positions corresponding to the sites of the geologic investigations. The faults outside of these regions slip freely in response to tectonic loading, fault interaction and the influence of the sites of prescribed slip. We assess the kinematic incompatibility of the models by calculating the off-fault distortion, here defined as the sum of the curl and the divergence of the surface velocity field.

Here, we investigate the kinematic incompatibility of the San Gorgonio Pass region using a suite of models. Because most geologic investigations provide ranges for slip rates, one model prescribes the mean geologic slip rates at investigated sites and a second one prescribes the slip rate limit that minimizes the misfit to the freely slipping model. Off-fault distortion maps of the model results reveal regions of kinematic incompatibility at the branch of the San Andreas fault near Indio Hills, as well as along the San

Bernardino strand near Cajon Pass. These same regions have freely slipping model slip rates that over- or under-estimated the geologic slip rates, indicating that the prescribed fault slip rates are not effectively accommodated along the simulated fault surfaces. These incompatibilities at Indio Hills and Cajon Pass suggest that we have incorporated inaccurate fault configuration at these branches or included incorrect slip rates.

Characteristics of Three Small (Mw < 4.5) Urban Area Sequences in the Walker Lane: Earthquake Interaction, Fault Structure, and Source Properties, Rachel L Hatch, Rachel E Abercrombie, Christine J Ruhl, and Ken D Smith (Poster Presentation 076)

We analyze three well-recorded small earthquake sequences (2015 Thomas Creek; 2017 Truckee; 2014 Virginia City) within urban areas in the Walker Lane region. Using absolute and relative relocation along with source parameter analysis, we detect fault structures, stress drop, directivity, and observe distinct event migration, including fluid and aseismic rates.

In the 2017 Truckee sequence, two events (Mw 3.65 foreshock and Mw 3.85 mainshock), occurred north of Truckee, California, on 27 June 2017. We relocate 50 out of 52 earthquakes within the sequence, which define a single structure between 5 and 6 km depth, trending ~N45°E and dipping ~70°–80° to the northwest. The structure matches the northeast-striking plane from two moment tensor solutions and computed first-motion focal mechanisms, indicating sinistral strike-slip motion. We observe stress drops averaging ~5 MPa and spatial variation related to the rupture areas of the foreshock and mainshock. We are able to detect components of directivity toward the northeast for the foreshock, and directivity toward the southwest for the mainshock, both aligning with the fault plane.

The Virginia City, Nevada earthquake sequence (ML ≤ 3.2) began in early 2014, with the main part of the sequence occurring over a ~10 day period in late January. We are able to relocate 366 of the 429 catalog events, which reveal three well-defined planar structures spanning ~1 km, ranging from 8-10 km in depth. Observations show a clear migration of seismicity, from east to west, with each structure activating in turn. Stress drops for 12 of the events average ~3.5 MPa. Key observations of event migration and stress drop suggest that fluids and aseismic movement play a role within this sequence.
The 2015 Thomas Creek occurred in south Reno, NV on 22 Dec, 2015 with a period of foreshocks lasting nearly 30 minutes prior to the Mw 4.3 mainshock. We relocate 156 or the 202 detected events in the sequence, which give evidence for a west-dipping structure, interpreted to project to the surface on the west side of the Virginia Range along the eastern boundary of the Reno basin. Average stress drop for 14 events in the sequence is ~8 MPa, and we detect directivity for several events.

This analysis demonstrates the ability to extract details in fault and source properties, and rupture propagation for small sequences. These data can provide a more informed seismic hazard assessment for these urban areas.

Paleoearthquake record of the Conway segment of the Hope fault: Implications for patterns of earthquake occurrence in northern South Island and southern North Island, New Zealand, Alexandra E Hatem, James F Dolan, Robert M Langridge, Robert W Zinke, Russ J Van Dissen, Christopher P McGuire, and Ed J Rhodes (Poster Presentation 221)

Paleoseismic trenches excavated at two sites reveal the ages of late Holocene earthquakes along the Conway segment of the Hope fault, the fastest-slipping fault within the Marlborough fault system in northern South Island, New Zealand. At the Green Burn East site (GBE), a fault-perpendicular trench exposed gravel colluvial wedges, fissure fills, and upward fault terminations associated with five, and possibly six, paleo-surface ruptures. Radiocarbon age constraints indicate that these six earthquakes have occurred during the past 2,000 years, with the three most recent surface ruptures occurring during a relatively brief (< 350 year) period between c. 1500 CE and the beginning of the historical earthquake record c.1840 CE. Additional trenches excavated at the Green Burn West site (GBW) site 1.4 km to the west reveal four coseismically generated landslides that occurred at approximately the same times as the four most recent GBE paleoearthquakes. Combining age constraints from both trench sites reduces dating uncertainties and provides independent age ranges for all events. These new data facilitate comparisons with similar paleoearthquake records from other faults within the Alpine-Hope-Jordan-Kekerengu-Needles-Wairarapa (Al-Hp-JKN-Wr) fault system of through-going, fast slip rate dextral and oblique reverse-dextral faults that accommodate the majority of Pacific-Australia relative plate boundary motion. These comparisons indicate that, although the faults of the Al-Hp-JKN-Wr system commonly rupture in brief sequences that encompass large sections of the system, system-wide “wall-to-wall” rupture sequences involving all faults in the system are rare

Sudden Surges of Seismicity within Natural Slow Growing and Long Duration Seismicity Swarms near Cahuilla Valley in the Central Peninsular Ranges, Southern California, Egill Hauksson, Zachary E Ross, and Elizabeth S Cochran (Poster Presentation 069)

The most recent Cahuilla swarm that started back in mid 2016 has grown steadily in number of events (~10,000 of M>0.3) and presently extends over an almost north-south linear trend of ~7 km. Since late on 11 August 2018 the seismicity accelerated with a ~120 event foreshock sequence, which culminated with a mainshock of Mw4.4 on 15 August 2018. The mainshock was followed by more than 200 aftershocks of M>0.3 over a period of 12 hours. This new activity extends the spatial distribution of the sequence ~1 km to the southwest. The b-value decreased from ~0.94 to ~0.74 during this most recent activity, suggesting that a new region, possibly of higher state of stress, was being activated.

Three major Cahuilla Valley swarms occurred in 1980-1981, 1983-1984, and 2016/6-2018, with the latest swarm still ongoing. The first two swarms had no clear mainshock, with the largest events of M3.6 and M3.7. They had similar moment release with about 100 events of M≥1.5, but the ongoing swarm now has a Mw4.4 mainshock and has generated more than 180 events of M≥1.5. These swarms are prolific in generating small earthquakes down to M0.3 or less suggesting abundant availability of trigger ignitions along the joints or foliations of the plutonic Mesozoic rock. Successive seismicity surges, which appear to originate at the swarm initiation focus, lengthen the spatial extent of the swarm lineament, thus providing a mechanism for how natural swarms increase in spatial extent. The style of faulting that is predominantly strike-slip with a small normal component is consistent with possible counter-clockwise block rotation of smaller crustal blocks. Such rotation could be driven by geometrically complex plate-boundary stress loading along the two nearby major late Quaternary strike-slip faults, Elsinore and San Jacinto faults.

Progress toward a Community Rheology Model of Southern California, Elizabeth H Hearn, Michael E Oskin, Wayne R Thatcher, Greg Hirth, Whitney M Behr, and Mark R Legg (Poster Presentation 152)

The principal goal of the SCEC Community Rheology Model (CRM) TAG for SCEC5 is to develop a three-dimensional description of the rheology of southern California's lithosphere. Though the CRM is intended as a resource for developing realistic and internally consistent model-based products for SCEC5, synthesizing constraints on temperature, composition and rheology from diverse fields has led to new insights and targets for continuing research. Since our 2017 workshop, which focused on developing a pilot CRM for the Mojave region, our TAG has made significant advances toward its next goal: delivering a preliminary CRM for all of southern California and adjacent regions.

The CRM comprises the Community Thermal Model (CTM), a Geologic Framework (GF), and a set of rheologies for the main GF rock types (including both low-strain rocks and shear zones). The CTM, which is also a stand-alone SCEC community model, will soon be available in draft form. It is currently being refined (1) using constraints from P/T conditions of erupted lavas and xenoliths sourced in the upper mantle, and (2) by accounting for transient thermal processes such as slab-free window effects and lower lithosphere foundering. The preliminary GF comprises 21 lithotectonic provinces, with boundaries registered to the CFM, and each represented with a 1D lithologic column. Whole-rock ductile flow laws for common GF rock types are being developed using mixing laws together with modal mineralogy, where available, such as from the exhumed crustal section of the Southern Sierra Nevada. These will be complimented by independent estimates of rheology based on seismic velocity data. Guidance on how to represent the geometry and rheology of viscous shear zones will also be a feature of the interim CRM. Efforts are underway to develop a web interface for sharing the model.

Nucleation and propagation of slow slip pulses on rate-strengthening faults, Elias R Heimisson, Eric M Dunham, and Martin Almquist (Poster Presentation 187)

Slow slip instabilities and transient aseismic slip have been observed in many settings, including the San Andreas system and subduction zones. Most theories for slow slip events postulate that instabilities initiate under rate-weakening friction, but are limited in rupture and slip speed by heterogeneities or additional stabilizing processes like dilatancy or a transition to rate-strengthening friction with increasing slip rate. However, slow slip occurs in regions where rate-strengthening friction is expected, based on experiments involving clay-rich minerals and temperature controls on the rate weakening-to-strengthening transition. Using linear stability analysis of perturbations about steady sliding with rate-and-state friction, we show that for two distinct destabilizing mechanisms, both involving coupling of slip and effective normal stress, perturbations can be unstable for sufficiently mild rate-strengthening friction. The destabilizing reductions in effective normal stress occur through poroelastic or elastic bimaterial effects. In contrast to the classic instability with rate-weakening friction, for which all wavelengths greater than a critical length are unstable, our instability occurs only for a range of wavelengths centered around a preferential wavelength of maximum growth rate. We derive expressions for the preferential wavelength, phase velocity, and growth rate that demonstrate that these instabilities are fundamentally different from earthquake-inducing instabilities. For example, the nucleation dimension is typically a hundred times larger than for earthquakes and instabilities develop over slip distances much larger than the state evolution distance. We augment our stability analysis with numerical simulations that couple quasi-static Biot poroelasticity and (nonlinear) rate-and-state friction. The simulations, initialized with small random perturbations about steady sliding, show emergence of a slip pulse that shares many characteristics of slow slip in nature, such as large slip patch dimension, rupture speeds much lower than elastic wave speeds, and low stress drop and total slip. The linear stability analysis provides insight into the parameter combinations controlling slip pulse length and propagation speed.

Multicomponent Model of Crustal Stress at Cajon Pass with Implications for Stress Field Heterogeneity, Elliott C Helgans, Karen M Luttrell, and Bridget R Smith-Konter (Poster Presentation 259)

Cajon Pass (CP) marks the primary junction between the San Andreas and San Jacinto fault networks. Highly segmented faulting in the region encourages investigation into whether the junction acts as a behavioral boundary on multi-fault ruptures. Stress maps, inverted from nearby focal mechanisms, feature a rotation in the stress field south of the junction. Identifying the causes of this rotation will help determine how stress modulation in CP affects future rupture behavior. We model the CP in situ stress field as the superposition of stress from three tectonic processes: the accumulation of stress on locked faults over variable loading times, the load of topography, and the far field geodynamic driving stress. Our model serves to quantify which processes dominate in CP over which length scales, and to identify potential heterogeneities in the geodynamic driving stress. Existing models for stress from locked faults and topography are used with loading times drawn from paleoseismic slip histories to derive a set of simple driving stress fields. We constrain the magnitude and orientation of the geodynamic stress field by comparing the forward model to the "modern in situ¬" stress field, inverted from a catalog of ~180,000 regional focal mechanisms. We find that individually neither stress from topography nor locked faults capture the heterogeneity or large-scale features present in the in situ field. To fully understand stress state across the region we consider contributions from locked faults, topography, and far field plate driving stresses together. We first examine the simple scenario of a series of homogenous regional geodynamic stress fields with a single set of load times at each fault segment. For each segment, as the orientation of the geodynamic stress field trends further east larger load times are required to best fit the model to the in situ field. Fit improves as the magnitude of the geodynamic stress increases until a threshold differential stress of ~30 MPa after which fit only marginally improves for all segments. We find that it is not geologically feasible to fit the stress orientations at each fault segment with a single load time. It is apparent that variably loaded fault segments, a heterogeneous geodynamic stress field, or likely both are required to fit the data. Ultimately, understanding the sources of stress heterogeneity in CP will aid in evaluating how stress variations across the pass affect through-going rupture probabilities.

The Development of 3-D Software to Assist the Visualization of Large and Concurrent Earthquake Data, Brandon T Ho, Shalani R Weerasooriya, Alejandro G Narvaez-Colon, Tiffany Streitenberger, Dian Zhu, Trent L Jones, Bill Addo, John Yu, Kevin R Milner, Gabriela R Noriega, Jozi K Pearson, and Thomas H Jordan (Poster Presentation 314)

SCEC-VDO or the Southern California Earthquake Center Visual Display of Objects, is a software that assists in visualizing seismic and geological information for publication, education, and animation. A software created, developed, and annually improved by USEIT interns, each iteration of VDO is in support of researchers and students alike. In addition to the main goal of visualizing Rate-State earthQuake Simulator (RSQSim) catalogs, we set out to improve various facets of VDO in order to improve the overall quality and experience of the software. To best manage the changes we hope to see, we divide ourselves into sub-groups that best fit our skills and various goals. Our main points of focus included creating and integrating a dual-window for earthquake catalog loading, further implementing statefulness, reinstating the earthquake shakemaps plugin, enhancing VDO's menus, improving loading time, making a web-based VDO project viewer, and conceptualizing mockups for future VDO features and alterations. A demo of dual-window loading of earthquake catalogs provides a glimpse of users being able to compare and contrast separate visuals side by side in VDO's 3D environment. Statefulness now captures the various plugins and parameters that were activated during a user's prior session with the software. VDO menus have been made more intuitive and uniform across the application. Loading time upon launching the software has been reduced by several seconds. The shake-map plugin has now been made functional and less visually obstructive. Using VTK/VTP, a web based application allows SCEC VDO models to be more accessible to the public. Lastly, based on collected observations of using the program, visual mock-ups of future alterations were created and can be implemented throughout upcoming years of interns.

Investigating and validating surface rupture characteristics with rupture dynamics on faults with shallow complexities, Sebastien Hok, Rihab Sassi, and Yann Klinger (Poster Presentation 203)

Earthquake surface rupture style can take many forms, ranging from a sharp cut in the landscape to a wide distribution of cracks. This complexity is related to several physical parameters (either average or local parameters of the rupture) that we can investigate with rupture dynamics: e.g. focal mechanism, number and geometry of existing faults, local variations of stresses and stress drop at depth and along strike, as well as local subsurface properties.

Surface rupture hazard for critical facilities is currently estimated from empirical datasets by averaging and mixing available data and controlling parameters. Therefore physics-based rupture models can help to better compute site-specific estimations, taking into account the local properties that control the final surface slip. For instance, prior knowledge of the fault network and geometries can be used to evaluate the secondary rupture probabilities and amount of slip.

Before being used for hazard assessment, the physics-based rupture models need a careful validation step. For that reason, within the recently funded research project DISRUPT, we are starting implementing dynamic surface rupture models to compare their results with observations of surface rupture and deformation. With its exceptional dataset covering a 200km-long rupture trace, the 2013 Baluchistan earthquake exhibits several interesting configurations of surface rupture patterns to validate models and provide new insights on surface rupture mechanisms (segmentation, partitioning, off-fault deformation). We have started studying the impact of fault geometrical complexities on the distributed slip occurrence around the main fault, and specifically fault dip angle change close to the surface. We will also investigate the link between dynamic stresses and surface rupture partitioning.

A Proposal for an Industry-Scale Seismic Survey in the Los Angeles Basin, Daniel D Hollis, and Robert W Clayton (Poster Presentation 097)

We are proposing a large-scale seismic survey for the Los Angeles sedimentary basin for the purpose of determining the structure of the basin and the underlying crust. We believe the survey will be valuable for creating densely sampled micro-zonation maps for seismic hazard and for providing better velocity models for strong motion modeling. The survey may reveal structures that show some hydrocarbon potential as well has image the aquifer system in the basin.

We are planning on a survey that will sample the basin at 10 sensors per square kilometer, which is about an order of magnitude less dense that a standard industry 3D survey, but which should provide adequate coverage for determining the basin structure and the 3D velocity variations. The survey will have about 18,000 receiver positions that will be occupied by a rolling get of 5000 sensors, each occupying a given position for 30 days of passive recording. It will take 4 months for this array to traverse the basin. We plan to have a fixed array of 200 three-component nodes that will record for the entire duration of the survey. In addition, we are planning on 60-70 deep hole (50m +/-) explosive charges to help determine the shallow P-wave velocities, and to look for possible reflections.

We are planning to fund this project with an industry consortium that will be composed of primarily oil companies that have production activity in the basin, and potentially water districts and city that are in the basin. The survey will be carried out by a geophysical contractor that has experience operating in urban areas. The estimated cost is $5-6M. We are in the process of requesting industry sponsorship for this project.

Lithosphere Viscosity Variations in Southern California, William E Holt, Laurent G Montesi, and Alireza Bahadori (Poster Presentation 162)

We combine stress estimates from geodynamic models and predictions of lithosphere rheology based on various SCEC community models to generate an integrated view of the strength of the lithosphere at regional scale. We use RHEOL to calculate the vertically-integrated strength of the lithosphere on a grid covering Southern California based on crustal thickness (Shen and Ritzwoller, 2016). Models assume either dry or wet rheologies for the lower crust and the mantle. In alternative model realizations, grain size is either fixed to 1cm or adjusted to satisfied piezometric relations (Twiss, 1977; van der Wal, 1993). The thermal structure is based on an analysis of shear wave velocity in the mantle and extrapolated into the crust. We compare these models with viscosity estimates obtained from geodynamic models constrained by lithosphere structure and topography along with mantle flow (Flesch et al., 2007; Klein et al., 2009; Ghosh and Holt, 2012). Our goal is to use discrepancies between the two models to guide refinements in the rheological model and include, for example, reduced strength shear zones. In this way, the refined view of lithospheric-scale rheology, using depth-dependent viscosity and heterogeneity, will be useful to understand the characteristics of long-term loading of faults in Southern California.

Development of monitoring and forecasting methods for crustal activity utilizing large-scale high-fidelity finite element simulations with 3D heterogeneous medium, Takane Hori, Tsuyoshi Ichimura, Kohei Fujita, Takuma Yamaguchi, Takeshi Iinuma, and Ryoichiro Agata (Poster Presentation 030)

To analyse crustal activity in the Earth's interior, such as spatio-temporal variation in slip velocity on the plate/fault interfaces including ordinary and slow earthquakes, we need to use the data observed mostly on the Earth's surface. If the data are limited far from the deformation sources, it would be enough to use simple model as elastic half space. However, it is becoming intrinsic to consider 3D heterogeneous structure of the interior, especially in subduction zone, since we can obtain dense surface deformation data on land and partly on the sea floor, just above the sources. Thus, to fully utilize such fruitful data, it is necessary to develop physics-based data analysis methods including (1) a structural model with the 3D geometry of the plate/fault interfaces and the material property such as elasticity and viscosity, (2) calculation codes for crustal deformation and seismic wave propagation using (1), (3) inverse analysis codes both for structure and fault slip using (1) and (2). To accomplish these, it is at least necessary to develop highly reliable large-scale simulation codes to calculate crustal deformation and seismic wave propagation for 3D heterogeneous structure. Unstructured finite element (FE) non-linear seismic wave simulation code has been developed (Ichimura et al. [2015]). A high-fidelity FE simulation code with mesh generator has also been developed to calculate crustal deformation in and around Japan with complicated surface topography and subducting plate geometry for 1km mesh (Ichimura et al. [2016]). This code has been improved for higher resolution in calculation of crustal deformation and achieved 2.05 T-DOF with 45m resolution on the plate interface (Fujita et al. [2016]). This high-resolution analysis enables evaluation of stress change acting on the plate interface. For inverse analyses, waveform inversion code for modeling 3D crustal structure has been developed (Ichimura et al. [2017]). Furthermore, such large-scale simulation codes have been implemented on the GPU clusters and analysis tools have been developed to estimate fault slip distribution with considering uncertainty in structural models (Yamaguchi et al. [2017a,b]). Utilizing them, we are developing the data assimilation method for monitoring and forecasting the slip velocity variation on the plate/fault interfaces with 3D heterogeneous structure. We have been modeled subduction zones in Japan and are planning to model southern California fault systems.

The 1933 Long Beach, California, Earthquake, Susan E Hough, and Robert W Graves (Poster Presentation 302)

We present a first-ever synoptic characterization of the distribution of ground motions from the 11 March 1933 Mw6.5 Long Beach, California, earthquake, using available macroseismic and instrumental data. The detailed shaking intensity pattern supports the conventional association of the earthquake with the Newport-Inglewood fault; it further reveals a concentration of especially severe damage centered in the town of Compton, where several credible accounts suggest vertical ground motions exceeding 1g, and intensities as high as Modified Mercalli Intensity 9. We use the broadband simulation approach of Graves and Pitarka (2010) to develop a rupture scenario for the earthquake, informed by the detailed damage distribution. Overall, the predicted shaking matches the observed intensities well using a 25-km long by 12-km wide rupture model with a hypocenter at 11 km depth near the southern end of the rupture, and a high-slip-patch near the northern end of the rupture. The modeling predicts high peak ground velocities in some near-field regions where liquefaction was documented but observed shaking intensities were relatively low, suggesting that high-frequency (≈2-8 Hz) energy was de-amplified by nonlinear site response. The concentration of damage near Compton can be explained by a combination of local site amplification, source-controlled directivity, and three-dimensional basin effects whereby energy was channeled towards the central Los Angeles Basin. In contrast with other inferred high-strain regions, it appears that high frequency energy was not de-amplified in this area. The overall success of the modeling in matching observed intensities provides a measure of confidence that the same modeling approach can be used to predict shaking from future earthquakes, with the caveat that, where the response is strongly nonlinear, ground motions may be lower than predicted using a simple Vs30-based model for non-linear site response, as used in our modeling.

Kinematic Source Models for Earthquake Simulations with Fault-zone Plasticity, Zhifeng Hu, Daniel Roten, Kim B Olsen, and Steven M Day (Poster Presentation 018)

Fault slip and surface deformation patterns are essential factors in seismic hazard assessment. However, slip inversions reveal a widely observed shallow slip deficit (SSD) which has not yet been clearly explained. One possible cause of the SSD is distributed plastic deformation in the fault damage zone near the surface. Roten et al. (2017) performed 3D dynamic rupture simulations of the 1992 M7.3 Landers earthquake in a medium governed by Drucker-Prager plasticity. The study showed that while linear simulations tend to underpredict SSD and off-fault deformation (OFD), nonlinear simulations with moderately fractured rock mass can properly reproduce results that are consistent with the 30-60% SSD and around 46% OFD reported in geodetic observations. Analysis of the Roten et al. (2017) results shows that discrepancies between linear and nonlinear simulations are only significant in the top hundreds of meters of the surface-rupturing fault. Although inelastic responses in the fault damage zone provide more realistic representations of earthquake physics, it can be computationally expensive or numerically unfeasible (e.g., in adjoint methods) to include nonlinear effects in ground motion simulations. One solution proposed here is to use an equivalent kinematic source (EKS) model that mimics the fault-zone plastic effects. This method generates source-time-functions by modifying the slip rate time histories based on comparisons of linear and non-linear dynamic rupture models, which are then used as input to kinematic simulations. The EKS model is able to reproduce the reduction of ground motions observed in dynamic simulations with fault-zone plasticity compared against linear simulations. In spite of its simple formula, the EKS model is robust in the presence different stress drop, rock strength and rupture directions for a M7.8 earthquake scenario on the San Andreas Fault. Further verification of the method and comparison with the output from kinematic rupture generators are needed before the anticipated use in practical applications such as the SCEC CyberShake and Broadband platforms.

Comprehensive Study on Reservoir-induced Seismicity in the Xiaowan Reservoir, Yunnan Province, China, Wei Hua, Naichen Ke, and YAQIONG DAI (Poster Presentation 071)

The Xiaowan reservoir is located in the middle section of the Lancang River in the west of Yunnan province, China, and the Xiaowan Reservoir Digital Seismic Station Network (XRDSSN) had been in operation since 21 May 2005. Its filling operations took place in

five phases, starting on December 16, 2008. The seismicity in the Xiaowan reservoir area after the impoundment has changed obviously with respect to the pre-impoundment. A notable increase in seismicity was only observed during the third filling phase, starting on July 15, 2010. Seismicity increase was mostly localized within two clusters, located to the northwest and west of the dam. Seismicity rates in these clusters showed a significant correlation with the water level increase, with the seismicity starting to increase when the water level reached the area covered by the two clusters, which additionally support they were induced by the reservoir impoundment. 3-D shear wave velocity images, measured by the local earthquake tomography method SIMUL2000, show that low-Vs anomalies after the impoundment can be found beneath and around the Lancang River and the Heihui River in the reservoir area, where the two clusters are located. It may be related to the water loading and unloading and water permeation. We further investigate source parameters for 44 pre-impoundment earthquakes and 164 post-impoundment earthquakes with ML≥2.0. Corner frequencies, seismic moments, and stress drops are obtained based on the spectral analysis of regional data, upon corrections for geometrical spreading, frequency-dependent Q, and site effects. Our results show that during the post-impoundment phase reservoir-induced seismicity (RIS) inside the two clusters have systematically lower stress drops with respect to those occurring at further distance, and surrounding natural tectonic earthquakes, by a factor of about two to three times, suggesting a possible source characteristic that differentiate reservoir-induced seismicity from natural tectonic earthquakes.

Matched-filter Detection of Microseismicity Around the Eruption of the 2018 Kilauea Volcano, Hawaii, Hui Huang, and Lingsen Meng (Poster Presentation 060)

The eruption of the Kilauea volcano started on April 30th, 2018, followed by widespread lava flows along the Southwest and East rift zones. Micro-seismicity analysis is important for identifying underground magma movement before the eruption. Here, we employ a template matching method to detect the small seismic events that are missing in the local Hawaiian Volcano Observatory (HVO) catalog. The template events are relocated using the double-difference method. We detect additional 3294 M >= 1 events within ~30 days before the eruption, ~10 times more than the HVO catalog. The result highlights the different temporal evolution between shallow (< 4 km) and deep (~4-12 km) seismicity. The total number of deep seismicity is about twice that of the shallow seismicity. But the deep seismicity is characterized by two major episodes starting ~18.5 and ~13 days before the eruption, both lasting less than 1 day. The deep cluster became almost quiet after the second episode while the shallow seismicity started to accelerate at ~8.5 days before the eruption, with a duration of ~6.5 days. The deep events are located below the Kilauea crater while the shallow events are aligned with the Upper Southwest and Upper East rift zones. The episodic activation of deep seismicity may be indicators of movement of pressurized magma, feeding the shallow reservoir and triggering prolonged shallow seismicity. This observed spatio-temporal pattern of deep and shallow seismicity may be an early precursor of the volcanic eruption.

Geomorphic evidence for the geometry and slip rate of the Southern San Cayetano fault: Implications for hazard assessment and fault interaction in complex tectonic environments, Alex Hughes, Dylan H Rood, Alexander Whittaker, Rebecca Bell, Thomas K Rockwell, Yuval Levy, Klaus Wilcken, Lee Corbett, Paul Bierman, Duane E DeVecchio, Scott T Marshall, Larry D Gurrola, and Craig Nicholson (Poster Presentation 253)

We present surface evidence and displacement rates for an active, low-angle (~20°) thrust fault in close proximity to major population centers in southern California (U.S.A.), the Southern San Cayetano fault (SSCF). Active faulting along the northern flank of the Santa Clara River Valley displaces young landforms, such as late Quaternary river terraces and alluvial fans. Geomorphic strain markers are examined using field mapping, high-resolution lidar topographic data, 10Be surface exposure dating, and subsurface well data to provide evidence for a young, active, low-angle SSCF along the northern flank of the Santa Clara River Valley. Displacement rates for the SSCF are calculated over thousand to ten thousand year timescales with maximum slip rates for the central SSCF of 1.9 +1.0/-0.5 mm/yr between ~19-7 ka and minimum slip rates of 1.3 +0.5/-0.3 mm/yr since ~7 ka. Uplift rates for the central SSCF have not varied significantly over the last ~58 ka, with maximum values of 1.6 +0.6/-0.4 mm/yr since ~58 ka, down to 1.2 +/- 0.3 mm/yr since ~7 ka. The SSCF is interpreted as a young, active, low-angle range-front structure with onset of activity at some point after ~58 ka. The geometry for the SSCF presented here, with a ~20° north-dip, is the first interpretation of the SSCF based on geological field data and is significantly different from the previously proposed model-derived geometry, which dips more steeply at 45-60° and outcrops in the Santa Clara River Valley. We suggest that the SSCF may rupture in tandem with the main San Cayetano fault. Additionally, the SSCF could potentially act as a rupture pathway between the Ventura fault and the San Cayetano fault in large-magnitude, multi-fault earthquakes in southern California. However, given structural complexities, including significant changes in dip and varying Holocene displacement rates and slip histories along strike, further work is required to examine the possible mechanism, likelihood, and frequency of potential thorough-going ruptures between the Ventura and San Cayetano fault systems.

Persistent effects of low-velocity fault zones on earthquake rupture after multiple earthquake cycles, Benjamin Idini, and Jean-Paul Ampuero (Poster Presentation 196)

Faults are usually embedded in a damaged zone characterized in field observations by distributed fractures and micro-cracks and in seismological and geodetic observations by reduced wave velocities relative to the wall rock. Recent dynamic rupture simulations show that the presence of a damaged zone around a fault can induce complex rupture modes that depart from a classical crack under a simple slip-weakening friction law (i.e. pulse-like rupture or super-shear rupture speed under relatively low background stresses). However, the efficiency of the mechanism promoting such complexity is strongly dependent on the prescribed initial level of stress. Here we investigate the effects of damaged fault zones on the promotion of rupture complexity throughout multiple earthquake cycles, in which the stress at the onset of rupture is a consequence of self-organization along the cycles. We consider a simple tabular model where a fault is bisecting a homogeneous low-rigidity layer (the damaged zone) embedded in an intact medium (the wall rock). The model is described by two parameters: damage level, D = 1 – G_d/G, and damage zone thickness, h. We conduct simulations based on the conventional Dieterich-Ruina rate-and-state friction and the quasi-dynamic approximation. Our numerical results show the development of complex rupture patterns at a critical damage-zone thickness defined between two end members in which h is large or small compared to the fault size. The complex rupture behavior involves secondary fronts emerging from the main rupture front and propagating in the opposite direction. Moreover, it involves shorter rise-times, flatter slip profiles, and

lower stress drops than in intact homogeneous media, the first two being signatures of pulse-like rupture. The back-propagating pulses tend to nucleate and arrest at localized stress heterogeneities left by previous ruptures. To test the hypothesis that damage zones are a viable mechanism for Rapid Tremor Reversals (RTR) observed during Episodic Tremor and Slip in Cascadia and Japan, we model slow slip by introducing a linear velocity-strengthening. Results show that our model is capable of reproducing RTRs qualitatively, and motivate further work to examine how damage zones quantitatively affect tremor migration patterns.

Quaternary slip history of the Santa Susana fault, western Transverse Ranges: Insights from U-Pb detrital zircon geochronology, Jonathan Ingram, Reed J Burgette, and Brian A Hampton (Poster Presentation 256)

The Santa Susana fault (SSF) is the western extension of the Sierra Madre reverse fault system, an east-west trending reverse fault system in the western Transverse Ranges. The SSF has the highest possible slip rate of any Sierra Madre fault segment but a wide uncertainty in slip rate in the UCERF-3 model. This ranges from negligible to significant (0.5-10 mm/yr). Slip on the SSF and related faults was associated with growth of the Santa Susana Mountains, which form the southern boundary of the Ventura basin. The Saugus Fm. in the footwall of the SSF is comprised of poorly lithified Pleistocene strata and was cut off from source areas to the north by slip on the SSF and uplift of the mountains. The upper range of the UCERF-3 slip rate is derived from previous studies that estimated initiation of uplift between 2.3-0.7 Ma through paleomagnetic dating and upsection changes in clast provenance, yielding a geologic slip rate of 5.9 ±3.9 mm/yr. Our study utilizes detrital zircon geochronology and sandstone modal compositions to build upon previous cobble provenance studies to examine the provenance of the Saugus Fm. and refine the timing of uplift of the Santa Susana Mountains.

Samples were collected from the Saugus Formation along stratigraphic transects in the SSF footwall and from Neogene units exposed in the hanging wall. Sandstone modal compositions and U-Pb detrital zircon ages are consistent with sediment derived from crystalline basement in the San Gabriel Mtns. Distinctive upsection trends in the detrital zircon spectra of the samples reveal changes in provenance over time. Across the transition from the lower marine to the middle non-marine members of the Saugus Fm. there is a disappearance of the 1.2 Ga anorthosite complex signature from the north in the San Gabriel Mtns. and a shift to similar provenance with the upper Neogene units in the SSF hanging wall. This indicates that the SSF hanging wall was a local source of sediment by ~1.1 Ma based on sedimentation rates and sample locations.
Preliminary models for the structural growth of the SSF and balanced cross sections are used to estimate slip for two portions of the Quaternary that can be tied to provenance changes. The cross sections were balanced to the top of the Neogene Pico Fm., which we infer to pre-date the reverse activation of the SSF. This refined slip record for the SSF will be used to assess slip variation over the Quaternary history of the SSF.

Late Holocene Rupture History of the South-Central San Andreas Fault at the Van Matre Ranch site, Carrizo Plain, California, Nick J Inserra, and Sinan O Akciz (Poster Presentation 266)

Characterizing long-term rupture patterns for the South-Central San Andreas Fault (SAF) is integral in evaluating seismic hazard in southern California. Recent paleoseismic data from both Bidart Fan and Frazier Mountain sites indicate recurrence intervals of ~100 yrs between large surface-rupturing earthquakes in the Carrizo Plain and Big Bend sections of the SAF during the past 800 years. Paleoseismic data from a site in-between is necessary to provide new timing constraints to the correlation of earthquake events between the two sites. Two connected fault-perpendicular trenches, both 3.5 m deep and 30 m long, were excavated at the new Van Matre Ranch (VMR) paleoseismic site, located ~20 km SE of Bidart Fan and ~80 km NW of Frazier Mountain. These trenches were excavated across a single, linear fault scarp from the active portion of the SAF. The primary fault zone in the trenches is 5 m wide and located below a prominent, linear fault scarp observed at the surface. This featureless fault zone juxtaposes the distal sediments of the VMR fan to the east against deposits of a more proximal fan to the west. The VMR fan deposits consist of layers of upward-fining fine sand-to-silt with no evidence of bioturbation or erosion. West of the fault zone are several distinct stratigraphic packages separated by >0.5 m thick bioturbated zones, suggesting that the earthquake record is incomplete. Evidences like fissures, upward termination of faults, apparent vertical offset, and lateral unit thickness changes were used to identify as many as five surface-rupturing earthquakes. Preliminary interpretation of the 32 detrital charcoal radiocarbon ages indicates that four of the five earthquakes recognized in the two trench walls occurred out of sequence during the last 9000 years. The penultimate earthquake is identified by evidence including mole track, truncations, and apparent vertical offsets, and has occurred sometime after 360±20 b.p. (uncalibrated C14 age). Focused deformation across the 5m-wide fault zone, discontinuous deposition, and long periods (>100 years) of bioturbation within the last 1000 years limit the potential of the VMR site to be further developed to correlate paleoearthquake records between Bidart Fan and Frasier Mountain sites.

Shallow Velocity Structure of Los Angeles Basin from ambient noise correlations with dense seismic arrays, Zhe Jia, Robert W Clayton, and Jorge A Castillo Castellanos (Poster Presentation 098)

It is important to understand the lateral variations in sediment structure of the Los Angeles (LA) Basin, since its shallow velocity structure can amplify strong ground motions. Existing sediment models of the LA Basin are generally derived from sonic logs and industry reflection profiles, but these models are limited by spatial coverage of well sites and seismic lines. There have been several dense seismic arrays that can be used to determine the shallow velocity structure. In this study, we show cross-correlations between five dense arrays and 21 continuous broadband stations of the Southern California Seismic Network (SCSN) in LA Basin. Each SCSN station is regarded as a virtual source, and all dense array stations are receivers. We observed clear fundamental and higher mode Rayleigh waves of 0.2~2.0 Hz from the noise correlation functions. These surface waves are sensitive to structure of depth less than 2 km, and their rays cover a large portion of LA Basin, and thus can provide improved resolution of the shallow LA Basin structure. However, Rayleigh wave dispersion curves show modal complexity and make automatic identification of particular mode branches challenging. We measured Rayleigh wave group velocities by fitting the peaks in frequency-time analysis, and use seismic tomography analysis for the shear-wave velocity structure.

Probing mechanisms of unsteady shallow creep on major crustal faults, Junle Jiang, and Yuri Fialko (Poster Presentation 188)

A number of major crustal faults exhibit geodetically detectable shallow creep that involves both spontaneous and triggered slip events along tens of kilometers-long fault sections. Notable examples include the Ismetpasa segment of the North Anatolian Fault (NAF) in Turkey and the Superstition Hills (SHF) and the Southern San Andreas (SSAF) faults in Southern California. Various mechanisms such as conditionally stable friction and dilatant strengthening of fault zones have been proposed to explain the slow slip phenomena, but how aseismic slow slip relates to fault slip during earthquakes is unclear in these interpretations. Using observations of the co-, post-, and inter-seismic slip on NAF, SHF, and SSAF, we explore consistent mechanisms of the associated slow slip and the rheology and seismic potential of shallow crustal faults. We consider 2D models of faults governed by depth-dependent effective stresses and standard rate-and-state frictional properties, with a velocity-neutral layer sandwiched between the surface layer with velocity-strengthening frictional properties and a deeper velocity-weakening zone, and potentially subject to pore compaction and dilatancy. For the interseismic period, we find that models with different rheologies can reasonably well produce slow slip events with displacements on the order of millimeters and periods of months, similar to observations. However, during seismic ruptures, the behavior of the shallow fault parts in these models is significantly different. In purely frictional models, shallow fault areas cannot arrest earthquakes efficiently while simultaneously promoting large-scale creep events that can propagate to the surface in the interseismic period. In models with dilatancy, the extent of coseismic shallow rupture is reduced due to dynamic fault strengthening, leading to small coseismic slip and robust postseismic slip at the surface, in a better agreement with available observations. By combining model ingredients tailored for each seismic-cycle phase, we reproduce the overall behavior for the NAF, SHF, and SSAF. Our results suggest that fluid-related, dynamic frictional processes may play a critical role in controlling the seismic potential of these shallow fault zones.

Advancing Simulations of Sequences of Earthquakes and Aseismic Slip [SEAS], Junle Jiang, and Brittany A Erickson (Oral Presentation Mon 14:00)

Robust predictive models of earthquake source processes have fundamental importance in earthquake science. Numerical simulations of dynamic earthquake ruptures have excelled in reproducing detailed processes during individual events. To bridge the shorter and longer time scales, it is important to consider earthquake source processes that interact with slow tectonic deformation, through the simulation of Sequences of Earthquakes and Aseismic Slip (SEAS). In SEAS models, the interplay of aseismic periods and dynamic events gives rise to a wide range of geophysical observables such as aseismic deformation, microseismicity, and ground shaking during dynamic ruptures, providing an avenue to connect earthquake behavior to geological, paleoseismic, and geodetic observations from a fault zone. SEAS modeling can also determine which physics at what scales dominates the resulting fault behavior, aiding the interpretation of long-term seismicity patterns in large-scale models of fault systems that require various simplifications.

Understanding how earthquakes nucleate, propagate, and terminate necessitates the development of SEAS models capable of simulating pre-, inter- and postseismic slip and loading between earthquakes. Multiscale faulting processes and multiple physical factors involved lead to the complexity of SEAS models, posing significant challenges for numerical simulations. This reality requires collaborations of researchers to compare and verify simulation results. Over the past year we have initiated a community code-verification effort, with the goals to further advance our computational capabilities, promote robust and reproducible earthquake science, and develop best practices and tools for the broader community. During the first SEAS workshop this spring, we brought together ~20 modelers to participate in our first benchmark problem, a 2D quasi-dynamic crustal faulting problem that serves as the first step to ensuring that different methodologies can produce closely matching results. The initial success of this benchmark prepares us to consider models with further complexities, including irregular earthquake patterns, nonvertical faults, 3D problems, and additional physics such as inelasticity and full dynamic effects, as we move forward. This community exercise will foster the development of a new generation of accurate SEAS models, towards a long-term goal to validate and integrate these models with geophysical observations.

Exploration of Prompt Elastogravity Signal for the 2004 M9.0 Sumatra and 2010 M8.8 Maule Earthquakes, Xinyu Jiang, and Lingsen Meng (Poster Presentation 087)

A rapid detection is of great importance to earthquake and tsunamis early warning. Generated by the change of gravitational field, instantaneous signals which travels at the speed of light and are much faster than elastic waves such as P wave, have a potential for quick detection and accurate size estimation of earthquake events. However, researchers haven't taken wide use of them because of the small magnitude of these signals and lack of big earthquakes with short durations. With the data of 2011 Mw 9.0 Tohoku earthquake, progress has recently been made in statistical (Montagner et al. 2016) or observational (Vallée et al. 2017) studies. But there are still not many observations of other events because of the noise and incomplete coverage of stations. Here we show our exploration to detect the gravity perturbation signal between event time and P arrival time for the 2004 Mw 9.0 Sumatra earthquake and the 2010 Mw 8.8 Maule earthquake. We apply methods previously used in the Tohoku earthquakes to the broadband seismograms of the Sumatra and Maule earthquake. Seismic array analysis is also included to boost the signal to noise ratios of station clusters. For the Sumatra earthquake, there exists an obvious trend using simple stacking of waveforms recorded by the XF array in Tibet. The statistical significance of a signal before P arrival, which exceeds the background noise, is more than 97%. While limited by the data quality of the Maule earthquake, the observation of the gravity signal is not certain given the strong background noise. In the future work, we plan to adopt more advanced seismic array processing to improve the signal-to-noise ratio of the prompt gravity signal and try to provide a theoretical value for comparison.

Characteristics of ground motion generated by interaction of wind gusts with trees, structures and other obstacles above the surface, Christopher W Johnson, Haoran Meng, Frank L Vernon, Nori Nakata, and Yehuda Ben-Zion (Poster Presentation 305)

Detection of small seismic events requires the ability to separate them from other sources of weak ground motion. Toward this goal we deployed 42 Fairfield ZLand geophones from 9 February to 17 March 2018 at the SGB site on the San Jacinto fault near Anza, CA. The instruments were arranged in a 350 x 300 m area and configured to target interactions of wind with obstacles above the surface producing ground motion. Located on the property is the PBO borehole seismometer B946 installed at a depth of 147 m and

an anemometer was installed to record the wind velocity. Temperature data was obtained from a weather station located 3 km to the north. The analysis is performed using 1 minute intervals of seismic data by estimating the spectra to produce spectrograms and group the waveforms by the reported wind velocity using a 1 m/s interval from 0 to 4 m/s. We select two days as a low and high wind day and compare the spectra during different wind conditions using a transect of geophones extending from a structure on the property. The results show a decrease in the spectral amplitude correlating with the wind velocity, where the maximum amplitude is observed during the strongest winds. The peak amplitudes decay three orders of magnitude over the 125 m spacing to the farthest geophone. The spectra indicate a peak in amplitude between 35-45 Hz, regardless of wind velocity, that shifts to higher frequencies as the distance increases. Daily spectrograms also indicate an increase in amplitude in the 35-45 Hz band that is present even in low wind conditions. During periods of elevated temperature, the peak amplitude shifts to higher frequencies with overtones observed clearly on days with sustained wind velocity >2m/s. The spectrogram for a geophone covered from direct sunlight does not display the same spectral shift. The geophone results indicate both the wind and temperature modify the instrument noise, which is not constant in time, and the noise amplitude is dependent on the distance to a local source as well as site specific conditions. Additionally, the borehole station B946 shows increased energy in the 1-5 Hz band that corresponds to increased wind speed and is not anthropogenic since one observation occurs at 2 am local time. The results indicate that wind produced ground shaking is observable to depths of 147 m and show an increase in energy in the bandwidth of interest for earthquake monitoring and detection.

Stress-glut representation by orthogonal moment-tensor fields, Thomas H Jordan, and Alan Juarez (Poster Presentation 281)

Seismic radiation from indigenous sources of arbitrary complexity can be represented by a second-order tensor field that Backus named the stress glut. We prove a new representation theorem that exactly and uniquely decomposes any stress-glut density into a set of orthogonal tensor fields of increasing degree, up to six in number, ordered by their first nonzero polynomial moments. The 0th-degree field is the projection of the stress-glut density onto its 0th polynomial moment, which defines the seismic moment tensor, Aki seismic moment M0, and centroid-moment tensor (CMT) point source. Our representation theorem generalizes the point-source approximation to a sum of multipoles that features the CMT monopole as its leading term. The 1st-degree field contributes a dipole, the 2nd-degree field contributes a quadrupole, and so on. We define the total scalar moment MT to be the integral of the scalar moment density, and we use the representation theorem to partition this total moment into a sum of moments for each degree. These moments are based on energy averaging, rather than the linear averaging that yields the Aki moment. If the faulting is simple enough, MT = M0 and the higher-degree terms will be small; however, when the faulting is more complex, MT > M0 and radiation from the higher-degree fields becomes sensible, especially at higher frequencies. We decompose various fault-rupture models to illustrate how the higher-degree terms characterize the source complexities, and we compute synthetic seismograms to characterize the radiation. Application to simple planar faulting shows that out-of-plane variations in slip-vector orientation reduce M0/MT more than in-plane variations of similar magnitude. We decompose stress-glut realizations from the Graves & Pitarka (2016) rupture simulator. Typical values of M0/MT are 0.8-0.9, consistent with analytical results. The higher-degree fields of the GP-16 sources typically produce substantial radiation up to degree 4; only the isotropic term is zero. We describe new inverse problems posed by the representation theorem, and we speculate on methods for their solution. Source models for the 2016 Kaikoura earthquake (Mw 7.8) indicate that the higher-degree radiation fields were large enough (M0/MT = 0.7) that it may possible to invert global datasets for at least some of the higher-degree multipoles.

Optimization of Data Functionals for Full-3D Tomography, Alan Juarez, and Thomas H Jordan (Poster Presentation 147)

Full three-dimensional tomography (F3DT) is an imaging technique for refining estimates of Earth structure by iteratively assimilating waveform data into 3D models of seismic wave propagation. We present a technique for systematically separating seismic phases using time-frequency spectra computed by the S-transform, which is based on Gaussian wavelets. Iterative waveform stripping decomposes seismograms into a finite set of waveforms, and subsets are then recomposed in an optimization process that localizes the seismic energy in the temporal domain and the structural sensitivity kernel in the spatial domain. The localization process reduces the high-wavenumber components of the structural kernel and improves the resolution to specific geologic structures. By increasing the coherent structural information that is derived from a single seismogram, this algorithm allows the identification of seismic phases that are not predicted by 1D structural models, such as basin-edge conversions. We show examples of seismogram decomposition and tomographic kernels computed for both synthetic models and recorded earthquakes in Southern California.

Simulating Millions of Years of Earthquakes in California using HPC, Varduhi Kababjyan, Shril P Panchigar, Anthony G Lopez, Tomoe Mizutani, Anthony A Guerra, Scott Callaghan, Jacquelyn J Gilchrist, Jozi K Pearson, Gabriela R Noriega, and Thomas H Jordan (Poster Presentation 312)

As part of the 2018 Undergraduate Studies in Earthquake Information Technology (USEIT) internship program, interns worked on a Grand Challenge to evaluate how well the Third Uniform California Earthquake Rupture Forecast (UCERF3) can predict long-term rates of M ≥ 7 ruptures on the Southern San Andreas Fault. The High Performance Computing (HPC) team was tasked with simulating long catalogs of earthquakes using the Rate-State Earthquake Simulator (RSQSim), a physics-based model that simulates long catalogs of seismicity from complex fault models. The HPC team worked on the Blue Waters supercomputer at NCSA using an education allocation of 25,000 node hours.

To configure an RSQSim simulation, one must specify a series of physical parameters, including: the rate- and state-friction coefficients, the initial value of normal stress (MPa), and the earthquake slip rate (m/s). Starting with a base catalog with default parameters, each member of the HPC team generated a short test catalog (50,000-75,000 simulated years) varying different input parameters to study their effects. Using the R programming language, the team conducted analysis on the simulated data with a focus on the recurrence interval and the magnitude frequency distribution of earthquakes on several sections on the San Andreas Fault. In cooperation with the Probabilities team, the HPC team concluded that increasing slip speed by 33% and the normal stress by 25% produced the best fit with the UCERF3 model for most fault sections chosen for the study. The team then used these parameters to simulate two million years of earthquakes, the longest catalog ever simulated using RSQSim. The simulated catalogs

were used by the Probabilities team to forecast earthquakes and by the Hazards and Risks Visualization team to analyze the casualties and risks of M ≥ 7 events

Borehole Breakout Determined Stress Regime in the Southern Los Angeles Basin, California, Justin O Kain, Patricia Persaud, and Edward H Pritchard (Poster Presentation 154)

The Los Angeles basin began its principal phase of opening with subsidence between the Palos Verde and Whittier fault zones and the Santa Monica fault systems. The basin then underwent early Pliocene NW-directed extension followed by transpression, which allowed for the complex structural setting of the Wilmington oil field in the basin's southwestern margin. The Wilmington oil field has little or no surface expression. Its general structure is that of an asymmetrical anticline crosscut by normal and oblique normal faults. The oil field has a complex history of multiple destructive earthquakes that caused millions of dollars in damage as a result of shifting boreholes and lost holes. These movements are frequently thought to result from compressive forces as a result of subsidence of the field and of the state. The Wilmington field is bounded to the south by two major fault systems, the THUMS-Huntington Beach fault and the right-oblique Palos Verdes fault. The THUMS-Huntington Beach fault parallels the southwest portion of the anticline and various interpretations of its dip and sense of slip exist.

As part of the effort to provide direct constraints on the in-situ stress field in Southern California, we use oriented 4-arm and 6-arm caliper data obtained from industry to determine the orientations of borehole breakouts or compressive shear failures along wellbore walls. The 36 wells in the Wilmington field are distributed in a ~12 x 3 km2 area and sample a depth up to ~3140 m. Wells were assigned a group of I-V based on their bottom hole locations and breakouts were used to determine a best estimate of SHmax orientations and the in-situ stress regime. We present preliminary results that are based on breakouts obtained in 14 wells. Further analysis of the stress data will allow for the estimation of slip potential on local faults.

Mechanics of Fault-Tip Deformation in Brittle and Ductile Faults: Laboratory Test of Off-Fault Yield Models & Fracture Energy Budget, Taka Kanaya, and Greg Hirth (Poster Presentation 178)

Off-fault damage was characterized for propagating fault tips in experimentally deformed granular rocks, in conjunction with fracture mechanics analyses of fault-tip stress fields. (1) Tip regions of dynamic brittle faults formed at 20°C show microcrack damage consistent with compressional yielding through Hertzian cracking. Microcracks increase in density towards the fault, with higher densities and fault-parallel fabrics on the compressional side, in agreement with those expected for faults stressed at low angles. In contrast, quasistatic ductile fault-tips formed at 900°C display anastomosing shear bands emanating from the tip with limited Hertzian cracking. (2) For dynamic faulting, the observed damage zones are orders of magnitude thinner than predicted using a Mohr-Coulomb yield criterion. We propose that strengthening mechanisms, such as rate-dependence, may be considered for the formation of damage zones involving extreme loading rates. Conversely, for quasistatic faulting, the observed extent of shear damage agrees with that expected for shear yielding using a yield criterion constrained from our high-temperature tests. (3) Energetic analyses of fault tips suggest that, for brittle faulting, microcracking accounts for almost all fracture energy, in which dissipation occurs mostly within the central gouge layer, but little outside. In contrast, the large fracture energy associated with ductile faulting results from frictional dissipation along anastomosing shear bands. We conclude that increasing temperature induces a transition in fault rupture mode from dynamic to quasistatic, because the activation of major fault-tip yielding results in an increase in the fracture energy. Furthermore, our findings - the temperature dependence of damage zone dissipation - have an important implication for whether fracture energy increases with fault size. For brittle faulting, the negligible damage zone dissipation observed suggests that, with increasing fault length, fracture energy does not increase as fast as energy release rate, resulting in earthquake runaway. In contrast, for ductile faulting, the significant damage zone dissipation observed suggests that, with increasing fault length, fracture energy increases as damage zone expands, leading to rupture self-arrest and slow slip.

Paleoseismology and Neotectonics of the Southern Sierra El Mayor, Baja California, Mexico, Keene W Karlsson, Thomas K Rockwell, John M Fletcher, Allen M Gontz, Paula M Figueiredo, and Lewis A Owen (Poster Presentation 240)

We present the results of detailed mapping and paleoseismic investigation along the southwestern flank of the Sierra El Mayor, a NW-SE trending mountain range in Baja California, Mexico, situated in a transtensive oblique rift boundary between the East Pacific Rise to the south, and the San Andreas fault system to the north. Complex fault scarp arrays associated with the Cañada David detachment, a low-angle oblique normal fault, as well as a soil chronosequence developed for a sequence of seven alluvial fans comprising a bajada that flanks the southwestern range front, were mapped in detail using high-resolution drone imagery. Soil pits were excavated, and soil characteristics were described using the USDA soil taxonomy in order to estimate their relative ages with soil development index (SDI) values. Three paleoseismic trenches were excavated across active surface faults that root into the Cañada David detachment at depth. Stratigraphic units in the trenches were described in detail, and samples were collected for optically stimulated luminescence (OSL) dating. The three trenches in this study show strong evidence for four Holocene earthquakes at about 1.5-2 ka, 4-5 ka, 6.5-7 ka and 8-8.5 ka, as well as weak to moderate evidence for three additional earthquakes between ~8.5 ka and ~16 ka. The results of this study were compared to other nearby studies in terms of rate of soil development, complexity and other characteristics of scarp arrays, and timing of past earthquakes.

Paleoseismology of the northern San Jacinto fault, San Bernardino County, Katherine J Kendrick, and Thomas E Fumal (Poster Presentation 218)

The Colton paleoseismic site is located 5 km south of San Bernardino, along the Claremont segment of the San Jacinto Fault, in southern California. The excavations, two parallel trenches oriented orthogonal to the fault strike, exposed a broad, complex fault zone, including a zone of compressional uplift closely juxtaposed with an extensional graben. Sedimentary deposits at this site are characterized by interbedded peat, clay and sand. Radiocarbon dating of detrital charcoal, seeds and other plant parts contained in the peat layers shows that most of the units were deposited between approximately 4000 – 6000 14C yr BP. We found evidence for at least 6 earthquakes in this older part of the stratigraphic section, including filled fissures, deformation, growth strata, upward terminations of faults, and cross-cutting fault relations. The youngest part of the section is within the extensional graben and contains evidence for three additional, younger earthquakes, but datable material in this part of the stratigraphic section is scarce.

Radiocarbon dating of a single detrital charcoal sample constrains the most recent rupture to be less than 170 14C yr BP. There is no record of ground rupture associated with historical earthquakes in this area; in this San Bernardino region, the fault system ruptured in 1907 (M 5.8; all magnitudes based on historical reports, after Toppozada, 2002) and 1923 (M 6.2), although there were no reports of ground rupture in the region. The northern San Jacinto Fault system experienced earthquakes in 1899 (M 6.7) and 1918 (M 6.8), but the maximum damage in both of these was much further to the SE, and no damage was reported in the area of the paleoseismic site. A nearby paleoseismic site on the Claremont fault, at Mystic Lake (Onderdonk et al., 2013), located ~ 28 km to the SE, also has evidence suggesting an earthquake within ~150 yr BP, but this feature is instead attributed to subsidence, compaction, liquefaction or creep rather than co-seismic rupture. Here we present evidence for and radiocarbon age constraints for each of the paleoearthquakes.

Periodic Slow Slip Events and Their Interactions with Megathrust Earthquakes on Northeast Japan Subduction Zone, Mostafa Khoshmanesh, Jennifer M Weston, Manoochehr Shirzaei, and Naoki Uchida (Poster Presentation 119)

Slow-slip event (SSE), a temporarily accelerated aseismic slip lasting hours to months, changes the stress regime on the fault itself and surrounding areas. On northeast Japan subduction zone (NJSZ), SSEs on the shallow locked zone, which is characterized by velocity-weakening (VW) properties, are suggested to induce major seismic events, including the 2011 Mw9.0 Tohoku earthquake. Moreover, periodic SSEs on the northern area of the 2011 earthquake rupture zone are collocated with elevated seismicity. Here, we model the daily evolution of creep distribution on the NJSZ during the interseismic period of 1996-2003 using GPS and repeating earthquake observations. Our results indicate that episodic SSEs occur annually on the velocity-strengthening area, located downdip of the shallow locked segment, which is confined to depths between 30 and 50 km. We show that the time series of the total seismic moment on the shallow VW segment is correlated with the timing of the downdip periodic SSEs. Also, the majority of Mw5+ earthquakes on this VW segment occurred during the peak Coulomb stress caused by the downdip SSEs. This suggests a causal relationship between the transient and seismic events. Also, the SSEs are accompanied by an increase in the ratio of smaller to larger earthquakes on the VW zone, apparent in the increasing trend of Gutenberg-Richter b-value time series. We suggest that the VW zone of NJSZ is paved with individual asperities, which form localized high frictional strength contact areas of different size, embedded in the low strength creeping areas that often act as seismic barriers. Elevated shear stress on the VW zone imparted by the downdip SSEs may result in two partially coupled processes; 1) failure of smaller asperities, leading to the observed increase in the number of small earthquakes, 2) domino effect due to the efficient interaction between microearthquake ruptures, leading to much bigger seismic events. To further support this hypothesis, we extended the b-value analysis to the year 2011, and show that b-value has an increasing trend before the majority of Mw6+ earthquakes. Our observations and models provide new insight into triggering mechanism of megathrust earthquakes that can improve forecast models.

Monitoring Seasonally-Driven Stress Changes on Faults within the Plate Boundary Zone in California using cGPS Observations, Jeonghyeop Kim, Alireza Bahadori, and William E Holt (Poster Presentation 156)

Using horizontal continuous GPS data between 2007 and 2018, we have quantified time-dependent horizontal transient strains within the Plate Boundary Zone in California. We also determine associated Coulomb stress changes on existing fault structures through time. These long-wavelength anomalies highlight remarkable seasonal periodic motions throughout much of the entire Great Valley and Sierra Nevada over the eleven-year time interval. We have detected a seasonal positive dilatational strain and Coulomb stress transient along the San Andreas fault zone that occurs between 34° N – 37° N during most summers. The Great Valley and Sierra Nevada also experience dilatational strains during most summers and displace a total of 1-2 mm toward the Great Basin. During winter, the dilatational strain patterns typically reverse. The Great Valley and Sierra Nevada enter compression and move 1 – 2 mm westward and a zone of dilatational compression develops along much of the San Andreas fault. Negative Coulomb stress changes are also shown on much of the San Andreas fault during most winters. To investigate our hypothesis that these horizontal long-wavelength anomaly patterns are related to seasonal hydrologic loading, we analyze the UNAVCO surface-loading displacement models derived from NLDAS-Noah (Puskas et al, 2017). We produce the strain and displacement patterns predicted by the hydrologic predictions. Comparisons of predictions from this model show similar spatial and temporal correlations with the long-wavelength anomaly patterns inferred from cGPS. However, evident disagreements appear during the severe drought (2012-2016). The solution inferred from cGPS shows significantly diminished winter signals and augmented summer patterns. We infer that these patterns are due to the lower amounts of precipitation during the drought winter and more loss of water during the drought summer. The solution inferred from UNAVCO hydrologic model fails to predict the effect of drought because the model only represents the variation in loading near the surface. This implies that either ground water or deep soil moistures are mainly affected by the drought. We also analyze a model of variations in water storage inferred from the vertical GPS displacements (Argus et al, 2017) and we compare the horizontal field predicted by this model with our horizontal long-wavelength anomaly patterns.

2017 Mw 5.4 Pohang earthquake, South Korea and poroelastic stress change associated with fluid injection, YoungHee Kim, Hobin Lim, Kai Deng, Jin-Han Ree, and Teh-Ru Song (Poster Presentation 091)

We compute the spatiotemporal change in Coulomb stress using a fault failure model under various conditions to better understand the nature of 2017 Mw 5.4 earthquake (2017-11-15, 05:29) that occurred near the geothermal power plant in Pohang, South Korea. This Mw 5.4 earthquake is the second largest earthquake in South Korea during the instrumental period, and the space-time variation of seismicity before this event is well correlated with fluid injection history from January 2016 (Kim et al., 2018). We compute the stress and pore pressure perturbed by fluid injection at the geothermal site in the framework of linear poroelasticity. Shear modulus, drained Poisson s ratio, Skempton s coefficient, the viscosity of the fluid, and frictional coefficient are assumed to be 30 GPa, 0.25, 0.75, 10-16 m2, 0.4x10-3 Pa·s, and 0.6. respectively, and these values are previously used in the modeling for understanding earthquakes induced by hydraulic fracturing in Central Alberta, Canada (Deng et al., 2016). We define our fault geometry with a strike of N36°E, a dip of

Probabilistic Seismic Hazard Analysis for Harrat Madinah, Saudi Arabia Using Regional Ground Motion Prediction Equations, Ryota Kiuchi, Walter D Mooney, and Hani M Zahran (Poster Presentation 027)

We present Probabilistic Seismic Hazard Analysis (PSHA) associated with future volcanic activity in Harrat (volcanic lava field) Madinah, Saudi Arabia using region-specific GMPEs. Harrat Madinah, which located in northwestern part of the Arabian Peninsula, has experienced two known seismic episodes: (1) a precursor seismic swarm to a historical eruption in 1256 CE, and (2) a 1999 seismic swarm in the subsurface (20-40 km). We evaluated three different scenarios M 6, 6.5, 7 as the maximum magnitude of the future event to accompanied any future volcanic eruption. The location of the largest event is assumed to correspond to the calculated spatial probability of vent opening (Dietterich et al., 2017). The background seismicity related to this mainshock is also taken into account for PSHA by applying Gutenberg-Richter (G-R) magnitude-frequency relation. The new region-specific GMPEs used in this analysis developed by revising the model of Boore et al. (2014) as reference GMPEs. This revision was accomplished using selected records of PGA and PGV from 177 earthquakes with magnitude 3.0 – 5.4 that have occurred in Saudi Arabia. In this revision of the reference GMPEs, smaller magnitude scaling and lower anelastic attenuation are incorporated to yield the updated region-specific GMPEs. The PSHA derived by the region-specific GMPEs, assuming M 6.5 as the largest event, indicate ground motions of up to 0.25 g of PGA for 2 % probability of exceedance in 50 years.

Earthquake damage patterns resolve complex rupture processes. The 2016 M7.8 Kaikoura earthquake, Yann Klinger, Kurama Okubo, Amaury Vallage, Johann Champenois, Arthur Delorme, Esteban Rougier, Zhei Lei, Earl Knight, Antonio Munjiza, Claudio Satriano, Stephane Baize, Robert M Langridge, and Harsha S Bhat (Poster Presentation 124)

Fracture damage patterns around faults induced by dynamic earthquake rupture are an invaluable record to clarify the rupture process on complex fault networks. The 2016 Mw 7.8 Kaikōura earthquake in New Zealand has been reported as one of the most complex earthquakes ever documented that ruptured at least 15 crustal faults. High-resolution optical satellite image displacement maps provide distinctive profiles of displacement across the faults, and helps visualize the off-fault damage pattern. They are combined with field observation and coupled with a numerical tool that captures the dynamics of the rupture and simultaneous activation of off-fault damage, to allow the determination of the most likely rupture scenario. This study demonstrates that complex rupture processes can be explained in a rather simple way via a synergetic combination of state-of-the-art observation and first principle physics-based numerical modeling of off-fault damage

Shallow fault mapping in the Sacramento-San Joaquin Delta, Shannon A Klotsko, Jillian M Maloney, and Janet Watt (Poster Presentation 246)

In fall 2017, a chirp and sidescan survey was conducted in the Sacramento-San Joaquin Delta (Delta) to map and characterize shallow fault locations and geometries. The most prominent fault observed in the data is the Kirby Hills Fault, located at the western extent of the Delta. The new chirp coupled with legacy, lower frequency USGS data reveal the fault's deep structure as well as the shallow deformation. The fault offsets the Delta floor, suggesting relatively recent activity. The Midland Fault is the main fault that traverses the central Delta. Only one crossing of the Midland Fault images near-surface deformation, with acoustic reflectors dipping down into the fault on the west side and flat-lying reflectors on the eastern side. This same stratigraphic pattern is observed in a deep penetration, onshore seismic line from the region. Very slight deformation is also observed along minor faults that were first described from well data in the Rio Vista and River Island gas fields. Well data indicate that there has not been any recent activity on these faults, so the shallow deformation observed may be solely from fluvial processes.

3D insights into active deformation, stratigraphic architecture, and submarine slope failure in the Santa Barbara Channel, southern California, Jared W Kluesner, Daniel S Brothers, Alexis Wright, and Samuel Johnson (Poster Presentation 248)

Multiple submarine landslides, including the Gaviota (0.01 – 0.02 km3) and Goleta landslide complexes (3 – 4 km3) have been documented along the slope of the seismically active Santa Barbara Basin, however the preconditioning factors leading to slope failure are still poorly understood in this region. Past studies utilized 2D seismic reflection datasets to analyze the regional framework geology, however these datasets were insufficient to characterize the complex nature of active faulting and folding that is possible with 3D seismic data. In this study, we integrate 3D multichannel seismic (MCS) reflection volumes and newly–collected high-resolution 2D MCS, CHIRP, and multibeam bathymetry datasets to analyze the relationships between deep structure, near-surface deformation, stratigraphic architecture, fluid-flow pathways and submarine slope failure. The 3D seismic volumes show that the Pitas Point Fault Complex (PPFC) controls the shallow deformation observed beneath the Gaviota and Goleta landslide complexes, and a seafloor fissure (incipient failure) located between the two landslides. A series of steeply dipping thrusts within the PPFC underlies the Goleta landslide complex, where the faults extends to within a few hundred meters of the seafloor near the shelf break and headwall scarp. To the west near the Gaviota landslide, high-resolution MCS data show that the shallow portion of the PPFC is composed of a previously undocumented network of en echelon faults striking ~25° counterclockwise to the dominant structural grain of the region. Within this system of shallow faults is a locally uplifted zone of fault-propagation folding beneath the Gaviota slide headwall. Analogous patterns of deformation are identified beneath adjacent sections of intact slope, suggesting these areas may be preconditioned for failure. We present a preliminary model for differential compaction between the slope and basin that induces a lateral pressure gradient and updip migration of fluids, which creates a mid-slope zone of reduced shear strength. The model explains the positioning of the Gaviota slide and adjacent incipient failures (tension fissures), and suggests that sections of the adjacent intact slope are likely to destabilize during seismic shaking.

An Efficient Numerical Method for the Simulation of Earthquake Cycles in Complex Geometries, Jeremy E Kozdon, and Brittany A Erickson (Poster Presentation 291)

The aim of this project is to develop a more complete understanding of the earthquake cycle by accounting for remote tectonic loading, material heterogeneity, and complex fault geometries. To do this we plan to couple interseismic cycle models with dynamic rupture simulations. One of the challenges that we have been facing in this endeavor is determining the right numerical method to use in the interseismic phase that is efficient and capable of handling the necessary complexity.

Here, we present a new finite difference method which significantly reduces the number of degrees of freedom needed for finite difference based earthquake cycle simulation. The scheme uses a multi-block decomposition of the computational domain which allows us to handle quite general complex geometries. When then discretize each "block" using summation-by-parts finite difference methods. All of the block interior degrees of freedom are then eliminated using the Schur complement method, so that the only degrees of freedom remaining are those on the mesh skeleton (block edges). Results are given here for the method applied to the two-dimensional antiplane problem demonstrating the accuracy, stability, and flexibility of the method.

3D Ruptures Simulations Across Stepping Faults; Comparing the Slip Weakening and Rate-State Friction, Kayla A Kroll, James H Dieterich, Keith B Richards-Dinger, and David D Oglesby (Poster Presentation 197)

Large earthquakes commonly involve the rupture of two or more faults sections including cases where the ruptures jump across gaps between disconnected sections. Several large earthquakes including the 3 November 2002 Mw7.9 Denali, Alaska, the 4 April 2010 Mw7.2 El Mayor-Cucapah, Mexico, and the 14 November 2016 Mw7.8 Kaikoura, New Zealand events all ruptured numerous fault sections, including disconnected sections. Because the total rupture length is a primary determinant of earthquake magnitude, understanding how earthquake ruptures are able to jump across fault gaps is of critical importance for estimates of seismic hazard. For example, to develop a catalog of possible earthquake rupture events in the system of active faults in California, the UCERF3 forecasts employ a set of parametric rules to define the type of gaps earthquake rupture might jump. Here, we explore the effect of RSF on the rupture of parallel fault stepovers using homogeneous initial stress conditions. We compare our results to more traditional dynamic rupture models that employ SWF. Results are evaluated in terms of the slip distribution, re-nucleation location, and maximum jump distance. In this context, we also investigate the effect the normal stress change on the evolution of the state variable and effect of time-dependent nucleation on delayed rupture jumps. We perform this analysis for fault systems classified by high (S=0.49) and low (S=1.25) initial stress states. We show that results from RSQSim compare favorably with those from FaultMod. We find that the average slip is inversely related to offset in both simulations. Average source and receiver fault stress drops vary considerably with larger offsets. Receiver fault re-nucleation locations lie within lobes of increased static stress for extensional and compressional offsets. For models with low stresses, the maximum jump distance is ~0.5 km for both simulation methods. For models with high stresses, FaultMod simulations jump larger offsets (~3km) than those produced with RSQSim (~2 km).

Prepared by LLNL under Contract DE-AC52-07NA27344.

Probabilistic Seismic Hazard Analysis in California Using Non-Ergodic Ground-Motion Prediction Equations, Nicolas M Kuehn, Norman A Abrahamson, and Melanie Walling (Poster Presentation 025)

With an increasing number of strong-motion records over the last decade, it has become clear that there are significant differences in ground-motion scaling even within relatively small regions such as California. Since GMPEs are typically based on the so-called ergodic assumption, these differences are usually not modeled. Hence, PSHA results are biased because they do not include systematic source, path and site effects. By including the systematic source, path and site effects in fully non-ergodic GMPEs it is possible to reduce the value of the aleatory variability by about 30-40%. This requires the estimation of the systematic effects for every possible source/site combination, together with their epistemic uncertainty. If a non-ergodic GMPE is used in seismic hazard analysis, it is very important to propagate the epistemic uncertainty of the systematic effects to obtain the full hazard distribution. We build a non-ergodic GMPE for California, based on the assumption that the systematic source, path and site effects are spatially correlated. We calculate hazard for three sites in California and show the impact of incorporating the non-ergodic GMPE into seismic hazard analysis. For sites that have abundant data in their vicinity, the non-ergodic hazard changes compared to the ergodic on, while for sites with sparse date the mean hazard stays the same, but there is a large increase in the epistemic uncertainty range of the hazard.

Combining 3D printing and virtual reality goggles in outreach and communication events , Christodoulos Kyriakopoulos, and David D Oglesby (Poster Presentation 316)

Earthquake scientists face a significant challenge in explaining their work to non-experts and the general public. For most non-experts the physical processes behind the generation of earthquakes remain something mysterious and difficult to visualize. Here we present a number of outreach and educational activities performed using a collection of 3D printed physical displays specifically generated to better elucidate the complexity of earthquake faults. The centerpiece of our collection is a 5-foot-long 3D printed model of the most major California faults based on UCERF3 (Field et al., 2013). The activities include the 2017 Great California ShakeOut drill, a variety of departmental visits and lab tours, and a field hearing of the house of representatives discussing the reauthorization of NEHRP. Finally, we are also working towards the extension of our outreach and educational activities to include the use of Virtual Reality (VR) goggles, adding a new technological dimension to our work.

Long Shaking Durations within the Los Angeles Basin from Shallow Earthquakes, Voon Hui Lai, Zhongwen Zhan, Robert W Graves, and Donald V Helmberger (Poster Presentation 001)

Shaking duration is a critical factor in assessing seismic hazards and building collapse risk, potentially as important as peak ground motion in large earthquake scenarios. The depths of earthquakes are often overlooked in ground motion studies, yet we observed that that earthquake depth strongly modulates waveform amplitude and ground motion duration in the Los Angeles basin. Shallow earthquakes excite particularly long durations of shaking within the Los Angeles basin, rising concerns over future large earthquakes with extensive surface ruptures. Current SCEC community velocity models (CVMs) can predict well the waveforms up to 2s period, but not the late coda waves, which contribute to the long shaking durations. 3D simulations of the two similar magnitude Fontana events of different depths using the latest CVM-H15.1.1 and CVM-S4.26-M01 models reveals several promising results to accurately model ground motion at higher frequency (up to 0.5 Hz). Overall, the CVM-S4.26-M01 model fits the waveforms better for both events, including the first several tens of seconds at period up to 2 seconds and can also capture well the unusually large ground motions at Whittier Narrows region. For the shallow event, which is not used in the inversion for the velocity model, the model captures most of the initial ground motions well but do not capture the long duration even at the period of 5 seconds. Given the small

earthquakes can be modeled as point source at our targeted frequency, the discrepancy between the model and the synthetics suggests that the shallow crustal layer in the CVMs may not be fully described. In addition, beam-forming analysis of a shallow earthquake event recorded by temporary dense arrays shows several packets of coherent energy with different slowness, and in particular at 80 – 110 seconds arriving from off-great circle azimuths, indicative of strong scattering behavior within basin. A better understanding of the shallow structures in basin can help explain the long shaking duration and overall stronger ground motions observed for shallow earthquakes.

Earthquake Sequences in Rate-and-State Fault Models with Thermal Pressurization, Valere R Lambert, Stephen M Perry, and Nadia Lapusta (Poster Presentation 194)

Theoretical studies and laboratory experiments indicate that dynamic weakening, such as thermal pressurization of pore fluids, likely acts during earthquakes on mature natural faults. At first glance, this seems incompatible with the fact that stress drops are inferred to be magnitude-invariant, since larger events may experience greater weakening, with lower final shear stresses. Through studies of long-term earthquake sequences in fault models that include standard rate-and-state friction and thermal pressurization, we show that such models do reproduce observationally inferred stress drop invariance for events that do not span the entire seismogenic segment, due to the averaged initial shear stress being lower for larger events. Stress drops for segment-spanning events depend on the properties of the arresting velocity-strengthening region at the segment edges. Furthermore, such models (1) also reproduce the inferred values of the radiation efficiency and the inferred increase of breakdown energy with event magnitude, and (2) result in ruptures with seismological estimates of fracture energy and radiation efficiency similar to values inferred directly based on the on-fault properties, making comparison to the values inferred for natural earthquakes self-consistent. However, the resulting ruptures, for the model parameters investigated, are either crack-like or mildly pulse-like, and not sharply pulse-like as suggested by some observations. Our current work is directed towards investigating parameter regimes that produce more pulse-like ruptures.

Gravity and aeromagnetic maps of the San Gorgonio Pass region, California: Potential insights from potential-field data on fault and basin geometry in a restraining bend, Victoria E Langenheim, and Jonathan C Matti (Poster Presentation 272)

Gravity and aeromagnetic maps superposed on detailed geologic mapping in San Gorgonio Pass (SGP) reveal details of fault and basin geometry where the southern San Andreas fault (SAF) breaks up into multiple strands as it curves into a restraining bend. Prominent gravity lows reflect basins beneath Coachella Valley, the Beaumont area south of the Banning fault, and San Jacinto Valley. Smaller gravity lows are strung out east-west along the SGP south of the Banning fault and beneath Morongo Valley. Gravity data indicate that the northern part of Coachella Valley is underlain by an asymmetric basin that deepens NE towards the Mission Creek strand of the SAF. The fault dips steeply NE based on the position of the steepest horizontal gravity gradient at the base of the gradient and modeling of magnetic data that inform on the downward projection of the fault dip into basement. The SW basin margin, in contrast to the linear NE basin margin, appears to be stepped. Along the SW basin margin, the SE-most alignment of density boundaries coincides with the Banning strand of the SAF. North of Garnet Hill, the maximum horizontal gradient steps ~2 km to the left (SW) for a distance of 5 km, before stepping again to the SW onto the Garnet Hill fault near the mouth of Whitewater Canyon, where the boundaries curve to a N trend. Within SGP, basin deposits are generally less than 1 km deep east of the Beaumont area. The late Miocene Banning fault forms the northern margin of the exposed basin deposits, but the presence of this fault at the base of a gentle gravity gradient indicates the basement-bounding fault dips shallowly to the north, with basin deposits extending as far as 5 km north of the fault at the surface. The gentle gradient bounding the northern part of the SGP contrasts with steep, irregular gradients that mark the south side of the SGP and that delineate buried prongs of basement that extend northward into the Pass--mirroring the sawtooth pattern of Quaternary thrust and tear faults in the SGP fault zone. These prongs may reflect undulations on the West Salton Detachment, a low-angle normal-fault complex that evolved coevally with the southern SAF. In this scenario, the late Miocene marine Imperial Formation and non-marine strata at Garnet Hill and similar-aged deposits in SGP represent deposits that formed in the hanging wall of the detachment. We speculate that the earlier extensional faulting influenced later compressional deformation.

On the present and future of physics-based earthquake source modeling, Nadia Lapusta (Oral Presentation Tue 11:00)

Accelerating streams of field observations, lab studies, and numerical modeling have significantly improved our understanding of earthquakes and physical factors that affect them. The main suspects have been known for a while. Tectonic loading, static and wave-mediated stress transfers, aseismic slip, rate-and-state friction, fault geometry and roughness, visco-plastic deformation at depth, shear heating during rapid slip, variations in pore fluid pressure, and off-fault damage/healing have all been shown to significantly affect, and in some cases dominate, the stress/strength evolution on faults and hence the earthquake patterns that result. Through combined field, lab, and numerical studies, our research community is well on the way to systematically quantifying the physical factors and evaluating their relative importance for different faults/phenomena/scales. A number of earthquake source models are being developed, focusing on different combinations of the physical factors and scales, to aggregate the available knowledge and identify crucial gaps. Together, the modeling efforts are advancing towards interpreting field observations in terms of tractable models with physically meaningful fault and bulk properties that can be evaluated, at least in principle, through lab, field, and smaller-scale numerical studies.

Earthquake simulators have taken on a necessary and formidable task of investigating earthquake patterns on realistic fault networks, which is presently tractable only with simplifications and omissions of the other physical factors. They have been successful in finding sets of parameters, some physical and some ad-hoc, that allow the models to match known statistical properties of regional earthquake sequences. The simulators are valuable research tools for studying fault system dynamics. However, their simplifications necessitate careful considerations about which conclusions they allow us to draw. For example, why would we expect the simulators to provide realistic probabilities of jumps over step-overs if they ignore the potentially dominating physics - dynamic stress changes brought by seismic waves? Including the simulators in hazard assessment requires clear communication of their limitations, verification through comparisons with smaller-scale models that more accurately capture relevant

physics, and community consensus of what criteria and observations the models need to satisfy. We are not there yet, but we are on the right track.

Numerical Modeling of a Fluid-Induced Aseismic-Seismic Slip Sequence on a Rate-and-State Fault, Stacy Larochelle, Nadia Lapusta, Jean-Paul Ampuero, and Frederic Cappa (Poster Presentation 186)

Numerous activities in the geo-energy industry (e.g., hydraulic fracking, wastewater disposal, CO2 sequestration and enhanced geothermal systems) involve fluid injections into the shallow crust (~1 to 5 km depth). That these fluid injections can induce fault slip (either seismic or aseismic) is now well recognized from surface and borehole observations. When injected directly into a fault system, fluids decrease fault strength by increasing pore pressure. This strength drop may in turn result in seismic or aseismic slip. However, what conditions promote stable versus unstable failure, and the exact physical mechanisms at play are still poorly understood. For example, the fluid-injection field experiment described by Guglielmi et al. (Science, 2015) resulted in aseismic slip first, followed by a sequence of 80 seismic events (i.e. microearthquakes), with the initial aseismic slip attributed to velocity-strengthening rate-and-state properties based on a spring-slider model. In this study, we seek to determine the range of frictional regimes consistent with the experimental observations through numerical simulations of slip on a fault in a continuum medium. Specifically, we simulate slip on a rate-and-state fault embedded in a homogeneous elastic medium and subjected to increasing pore pressure at the injection site, with the fault and pore pressure parameters informed by the Guglielmi et al.'s study. We use an elastodynamic boundary-integral code supplemented with fluid pressure diffusion along the fault. We find that fault models with velocity-weakening friction can explain the initial aseismic slip as well as the velocity-strengthening ones. Constraining the frictional parameters further would require more experimental studies with simultaneous measurements of fluid pressure, fault-normal and fault-parallel displacements, and seismicity, both at the injection site and in its surroundings.

Complex faulting structures in Eureka Valley, Death Valley National Park, CA, Michael J Lawson, Steven G Okubo, Tyanna M Schlom, Ed J Rhodes, Jeff Knott, and An Yin (Poster Presentation 235)

Eureka valley is a large basin in the northwest corner of Death Valley National Park. In 1993, a moment magnitude 6.1 earthquake occurred within the valley but due to its remoteness limited mapping has occurred in the area. As part of my dissertation work, we mapped faults within the valley with the goal of understanding the potential for modern slip. Luminescent dating was utilized to derive a new scarp diffusivity constant (1.79 m2ka-1) that was applied to scarps where sampling was not possible. Fast static GPS mapping was subsequently used to model offset on scarp profiles at two locations in the field area representing two distinct fault systems: oblique- normal in the west and mostly normal in the east. In Hanging Rock Canyon, six scarps representing five strands of an oblique normal fault system were mapped and modeling suggests vertical slip rate of ~0.7 mm/yr. Thirty kilometers to the south at the Dedeckera Canyon site, eleven scarp profiles representing four fault strands were found to have ~ 2 mm/yr vertical slip. Within the main valley, a previously unmapped fault (proposed to be named the "Frankel fault" in memory of Dr. Kurt Frankel) will also be presented.

Toward Hybrid Broadband Ground Motion Simulation Validation for Mw>3.5 New Zealand Earthquakes, Robin L Lee, Brendon A Bradley, and Xavier Bellagamba (Poster Presentation 016)

Recent advances in computational performance and physics-based ground motion simulation methodologies are making physics-based seismic hazard analysis a reality. Extensive validation of physics-based ground motion simulations against observations are needed to both understand their predictive performance (and hence their degree-of-belief weighting in a logic tree for prediction), and efficiently identify areas for their iterative improvement. Recent ground motion simulation validation efforts in New Zealand have mostly been focused on the Canterbury region where the 2010-2011 Canterbury Earthquake Sequence occurred, and we have begun to extend our focus to New Zealand in its entirety. This poster presents preliminary ground motion simulation validation results considering small-to-moderate magnitude (3.5<Mw<5.0) earthquake events across New Zealand, with clusters of earthquakes generally located along the tectonic plate boundary. Source characteristics are obtained from centroid moment tensor solutions provided by GeoNet and a unified New Zealand Velocity Model provides crustal seismic velocities. A total of 638 earthquake ruptures, modelled as point sources, are considered with over 5000 quality-assured ground motions recorded at 382 recording stations. In order to scale our analyses to a large number of ground motions we have also developed a neural network for ground motion quality classification, and introduced event-specific computational mesh determination to optimize total compute core hour requirements. The performance of the simulations, and conventional empirical ground motion models (for benchmarking purposes), are quantified using a mixed-effects analysis framework where the biases and uncertainties associated with the simulation methodology and systematic source, site and paths effects are explicitly determined.

Offshore Geology Framework for the Community Rheology Model, Mark R Legg, and Michael E Oskin (Poster Presentation 151)

The California Continental Borderland comprises the 250-km wide offshore part of the Pacific-North America transform plate boundary in southern California. The Offshore Geologic Framework (GF) for the SCEC Community Rheology Model (CRM) is based on the large-scale crustal blocks represented by the tectono-stratigraphic terranes (Howell and Vedder, 1981). These terranes represent basement lithology and structure derived from the Farallon-North America subduction zone and dismembered and rearranged during the continental margin transform plate boundary evolution. Four blocks south of the Transverse Ranges are included in the simple model. The Inner Borderland is represented by the offshore Catalina oblique-rift terrane and the coastal Santa Ana (Peninsular Ranges) terrane. The Outer Borderland is represented by the Nicolas forearc and Patton accretionary wedge terranes. A fifth terrane consists of the Pacific oceanic lithosphere adjacent to the Patton Escarpment. Published geological and geophysical cross-sections of the California Continental Borderland provide data for creating the simple 1-D lithospheric columns. The block boundaries for the simple model were originally envisioned as high-angle strike-slip fault zones (Vedder, 1987). Borderland GF block boundaries are derived from major faults that exist in the SCEC Community Fault Model (CFM). Most faults are high-angle, strike-slip in character. However, known major low-angle faults (detachments) are important components of a 3-D block boundary definition. The low-angle faults imaged by reflection seismology and mapped throughout the Inner Borderland Rift include

the Thirtymile Bank and Oceanside/Coronado Bank structures. In the Outer Borderland terranes, one major low-angle fault is represented by the former subduction megashear that dips eastward from the base of the Patton Escarpment. Low-angle faults exist in the CFM, and these will be updated as needed to define significant block boundaries in the GF. Outer Borderland faults missing from the CFM are being compiled and prepared for loading into the updated Community Models. We consider upgraded GF models to include important sub-terranes that describe more complex structure within each of the simple blocks. Four sub-terranes within the Inner Borderland Rift include: 1) Catalina core complex; 2) Santa Monica-San Diego Trough, adjacent rift basins; 3) coastal rifted continental crust (Coronado Bank); 4) San Clemente Basin, a highly extended rhombochasm.

Structural Architecture of the Western Transverse Ranges and Potential for Large Earthquakes - New Results of Trishear Forward Models , Yuval Levy, Thomas K Rockwell, John H Shaw, Andreas Plesch, Neal W Driscoll, and Hector Parea (Poster Presentation 252)

Fold-and-thrust belts usually evolve over time, can produce large-scale faults and potentially accommodate large magnitude earthquakes. The thrust fronts of these structures typically form large fold structures in their hanging walls, and they tend to propagate forward (in sequence) over time to form new thrust fronts. In the Santa Barbara and Ventura region of the Western Transverse Ranges (WTR) of southern California, the Pitas Point-Ventura fault is interpreted as the current frontal thrust structure of this system, with spatially stable back thrusts accommodating deformation in the hanging wall block of the thrust sheet (More Ranch fault, Rincon Creek fault, other faults). We interpret the nearly continuous, overturned Tertiary stratigraphy of the Santa Ynez Mountains as a large anticlinorium that formed as the first thrust front over the (mostly) blind San Cayetano fault, and that the thrust front propagated south with time to the Red Mountain fault and eventually to the currently active, southward-verging Pitas Point-Ventura fault. Offshore Summerland, the Red Mountain fault is currently also active and may have been the dominant structure in the Holocene after sea level rise; the Red Mountain fault does not extend west of Santa Barbara. Our interpretation of the deep structure of the WTR is based on a combination of various data sources and previously published models. To test our interpretations of the evolution and structure of the WTR, we used Trishear forward modeling. The Trishear models are a good first-order match to published geologic maps and well data. While our solution is non-unique, it is consistent with all of the currently available observations. For this poster, we present new cross-sections westward to Point Conception and show that the amount of slip required to reproduce these structures is lower than the amount of slip required across the major structures to the east in Ventura Basin. This result is expected due to the location of the different faults relatively to the big bend of the San Andreas fault and is consistent with the geodetic signal. Further, modeling of multiple cross-sections argues that all of the observed deformation can be explained by an evolving fold and thrust belt, which includes a regionally extensive decollement underlying the observed thrusts and folds. In addition, our fault model supports the contention that the WTR are capable of generating large magnitude earthquakes, based on scaling relations.

Delayed Triggering of small Local Earthquakes near the San Jacinto Fault after the 2014 Mw 7.2 Papanoa Earthquake, Bo Li, and Abhijit Ghosh (Poster Presentation 070)

We find evidence of delayed triggering of small earthquakes off San Jacinto Fault (SJF) near the Anza Gap. We develop a move max matched-filter method to analyze seismicity that occurred near the SJF one month before and after the 2014 Mw 7.2 Papanoa earthquake. During this period, there are 880 local events in this area recorded by the Advanced National Seismic System (ANSS) and the Southern California Seismic Network (SCSN) catalog. Using the catalog events as templates, the move max matched-filter method detects 5.4 times of catalog earthquakes, while the matched-filter method only distinguishes 3.2 times of catalog events using the same detection threshold. The seismicity rate increases significantly few hours after the passage of the seismic waves of the Papanoa earthquake and the high seismic rate persists for about one week. Interestingly, the most heightened seismicity is located west to the SJF (off SJF) and city Anza, on an apparently unmapped blind fault that strikes nearly perpendicular to the SJF and steeply dips to the northwest. We speculate that more than one mechanisms may be responsible for this delayed triggering. The transient dynamic stresses may have triggered a slow slip or fault creep, and lead to the increased and protracted seismicity along the San Jacinto Fault (SJF). Alternatively, a time-dependent acceleration to failure process initiated by the dynamic stress change may result in the enhanced seismicity on the blind fault. The newly discovered fault points out existence of additional fault structure (off SJF), which may be capable of producing damaging earthquakes near or within the Anza seismic gap.

Fault Continuity and Rupture Branching of the 2014 Mw 6.0 South Napa Earthquake Viewed by Fault-Zone Trapped Waves, Yong-Gang Li (Poster Presentation 284)

We present fault-zone trapped waves (FZTWs) generated by aftershocks and explosions detonated within the rupture zones of the 2014 Mw 6.0 South Napa earthquake, and use them to characterize the fault continuity and rupture branch structure along the West Napa Fault and Franklin Fault (WNF-FF) at depth. We analyzed waveforms of these FZTWs in both time and frequency. Observation and 3D finite-difference simulation of the FZTWs generated by aftershocks suggest a 400–500 m wide subsurface rupture zone with the 14-km-long mapped surface breaks along the main trace of the West Napa Fault Zone (WNFZ), within which wave velocities reduced by 40%–50%. Post-S coda durations of FZTWs increase with focal depths and epicentral distances from the recording arrays, suggesting that the low-velocity waveguide along the WNFZ extend to 5–7 km depth and further southward with a moderate reduction of %30-35% to FF. The combined WNF/FF zone is at least 50 km long. The FZTWs generated by explosions show the branch structure of rupture zones along multiple fault strands of the WNFZ associated with the 2014 M6 mainshock. To the east of the main surface rupture, there exist two ~4-6-km-long surface rupture zones along subordinate fault strands of the WNFZ. The east rupture zones show slightly smaller wave velocity reductions than that within the main rupture zone, and they likely merge at 2-3-km depth, showing a tree-shape rupture structure beneath the surface. FZTWs also show a waveguide with velocity reduction of ~35% along the Carneros Fault (CF) that lies ~1-km west of the main WNF and connects the south WNF-FF, but did not rupture in the 2014 M6 earthquake. 3-D finite-difference simulations of recorded FZTWs infer the branching structure along multiple fault strands associated with the South Napa earthquake in 2014. Our observations and simulations of recorded FZTWs show large amplitudes and long wavetrains at stations located within the fault zone, illuminating that a great amount of seismic energy is localized within the damage zones along multiple strands of the WNFZ due to the trapping effect of

low-velocity waveguides. The longer and more continuous WNF-FF zone and multiple rupture branches in a broader range may pose significant regional hazards from localized amplification, extended ground shaking, and increase damage along the fault-zone waveguides, even if the surface rupture is limited to only a portion of the overall fault zone.

Present day interseismic slip rates of the Xianshuihe Fault observed by InSAR, Yuexin Li, and Roland Bürgmann (Poster Presentation 121)

Located at the southeastern boundary of the Tibetan Plateau, the Xianshuihe Fault is one of the most active major faults in China. It serves as one of the main structures accommodating the collision between the Indian and Eurasia plates. Historically, more than 20 M>6 earthquakes ruptured the fault since 1700. With the recent launch of ESA Sentinal-1 and JAXA ALOS-2, large spatial coverage and short recurrence intervals make the study of spatial and temporal features of fault slip rates with InSAR possible.

In our study, we use more than 3 years of Sentinel-1A data to obtain the interseismic surface velocity field along the Xianshuihe Fault. The Small Baseline Subset method (SBAS, Berardino et al., 2002) is used to process time series from more than 170 interferograms. The turbulent component of atmospheric delay is corrected iteratively using a common point stacking method (Tymofyeyeva and Fialko, 2015). Then tropospheric delay is further mitigated by fitting a linear trend between line of sight deformation and the topography. Remaining unwrapping errors are excluded by throwing away data points with large residuals.

To complement the InSAR results, GPS velocities from Zheng et al. (2017) are also used for slip rate inversions and forward modeling. We aim to extract a full 3D deformation field with the combination of Sentinal-1, ALOS-2 and GPS data. The GPS velocities will help document InSAR satellites' capability of capturing subtle long-wavelength interseismic signals in a limited time span. With the InSAR results, we also seek to resolve slip rates, locking depth, and partially coupled or creeping sections on the Xianshuihe Fault, which will help us better evaluate the earthquake potential in this area.

Checking Data Quality of Co-located Broadband and Strong-motion Sensors in Southern California Seismic Network, Zefeng Li, Egill Hauksson, Thomas H Heaton, Luis Rivera, and Jennifer R Andrews (Poster Presentation 055)

Differences in waveforms recorded by broadband and strong motion sensors at the same site can be caused by sensor failure, mis-orientation in deployment, wrong instrument response parameters etc. Deployed instruments can malfunction and produce unreal seismic records, which may mess up real-time seismic processing and eventually cause wrong estimates of source and structure parameters. Thus, it is important to check sensor health regularly for rapid detection of sensor failures, which is essential for earthquake early warning systems that operate in real time. Here, we detect instrument malfunctions in Southern California Seismic Network (SCSN), by taking advantage of co-located broadband and strong-motion seismometers. We assume that healthy co-located broadband and strong-motion sensors should provide almost identical instrumental corrected waveforms, when the signal is within their common resolution range. Specifically, we remove the instrument response of both records and compare the waveforms of small local earthquakes. We examine two metrics, amplitude ratio and cross-correlation, both of which should be ~1 in normal state. Deviation from 1 in either metric suggests inconsistency between the broadband and strong-motion data. We calculate the two metrics for the year of 2017 and identify several problematic sites. For example, the site WMF has wrong instrument gain on one sensor: the broadband amplitude tends to be twice of the strong-motion amplitude. In addition, in the site SBPX, the strong-motion records are consistently different from the broadband motion records in both amplitude and shape, suggesting one of the two sensors being faulty. Our final goal is to develop an automatic workflow to monitor the sensor health near real-time. Besides local earthquakes, we are in the process of exploring the usefulness of microseism and teleseismic signals for this real-time diagnostic task. Updates will be reported in the meeting.

A Dynamic Earthquake Simulator for Geometrically Complex Faults Governed by Rate- and State- Friction, Dunyu Liu, Benchun Duan, and Bin Luo (Poster Presentation 205)

We develop a dynamic earthquake simulator based on finite element methods (FEM) to model dynamics of geometrically complex faults governed by the rate- and state- friction (RSF) over multiple earthquake cycles. The simulator combines a dynamic FEM code EQdyna and a newly developed static FEM code EQquasi to model quasi-static phases of earthquake nucleation, post-seismic and inter-seismic processes. Both FEM codes are parallelized through MPI to speed up computations. EQdyna and EQquasi exchange on-fault physical quantities including shear and normal stresses, slip-rates and state variables. The two-code scheme shows advantages to reconcile the computational challenges from different deformation phases of an earthquake cycle, which are mainly related to 1) handling time steps ranging from hundredths of a second to a few years based on the variable time stepping scheme and 2) the element size small enough to resolve the cohesive zone at the rupture front of dynamic ruptures. The dynamic earthquake simulator is different from most existing earthquake simulators in the community in the sense that it includes fully dynamic rupture propagation and can handle complex fault geometry.

Earthquake cycles on a 3D strike-slip fault with a bend are simulated. The sizes of nucleation patches depend on the normal stress resolved from the regional stress field and stress heterogeneities induced by previous ruptures near the bend. The bend tends to stop dynamic ruptures and accumulates very limited amount of slip over the long-term. Complex earthquake event patterns are identified in the fault system. Earthquakes on the two segments interact. Some earthquakes breaking consecutively the two fault segments can be separated by tens of days, a few days, or even several minutes. The relation between the ratio of the shear stress to the normal stress and the reference friction coefficient in the RSF affects the creeping rate of velocity strengthening regions of the two fault segments. A reduced critical slip distance in the RSF results in faster rupture speed and stronger stress heterogeneity around the bend.

The dynamic earthquake simulator is capable of studying rupture behaviors at the Cajon Pass earthquake gate after further parallelization development of the quasi-static component EQquasi for better scaling.

A 6000-Year-Long Paleoseismologic Record of Earthquakes along the Xorkoli Section of the Altyn Tagh Fault, China, Jing Liu, Zhaode Yuan, Wei Wang, Ray J Weldon, Michael E Oskin, and Yanxiu Shao (Poster Presentation 217)

Long records of paleoearthquakes are essential for understanding earthquake recurrence behavior of active faults and for evaluating regional seismic hazard. However, paleoseismic data on the Altyn Tagh fault (ATF), one of the longest strike-slip fault in Asia, are scarce. We document a long paleoseismic record along the Xorkoli section of the central ATF. Eight and probably nine earthquakes are identified based on event evidence in the form of open fissures, folds, unconformities, and upward fault terminations, with modeled mean (95% confidence) ages of A.D. 1598 (1491-1741) yr (event A), A.D. 797 (676-926) yr (B), B.C. 668 (732-589) yr (C), B.C. 956 (1206-715) yr (D), B.C. 1301 (1369-1235) yr (E), B.C. 2105 (2233-1987) yr (F, probable), B.C. 2663 (2731-2601) yr (G), B.C. 2818 (2878-2742) yr (H), B.C. 3396 (3522-3205) yr (I). The mean recurrence interval is 620±410 years with a coefficient of variation (COV) of 0.67, indicating that earthquake recurrence is weakly periodic, with individual intervals ranging from as short as 150 years to as long as 1460 years. A global compilation of 35 strike-slip paleoseismic sites yields a similar average COV of 0.69. Synthesis of paleoseismic sites from the central ATF indicates that not all earthquakes ruptured to the eastern end of the Xorkoli section, within the Aksay restraining bend. Given that the 420-year elapsed time since the most recent event, well within a COV of mean interval, a large surface-rupturing earthquake could occur at any time along the central ATF.

Finite Frequency Sensitivity Kernel for the Correlation of Ambient Noise Correlations: Theory and Numerical Tests, Xin Liu, and Gregory C Beroza (Poster Presentation 108)

Full waveform adjoint tomography has achieved great success in applications from global structure using earthquakes to exploration seismology using active sources. When combined with ambient seismic noise interferometry, however, the shape of the sensitivity kernel can be distorted with significant sensitivity outside the inter-station region due to non-isotropic distribution of far field noise sources. We compute the sensitivity kernel for ambient noise cross-correlation differently from existing approaches by introducing an additional station to the classic two-station setting. We cross-correlate the two noise cross-correlations from two station pairs and use the resulting cross-correlation (C2) to compute synthetic and data waveform misfit function. This differential sensitivity kernel based on C2 shows prospect for canceling the overlapping part of the original kernels for two pairs of stations in interferometry, thus reducing the effect of non-isotropically distributed noise sources. We derive analytically and calculate numerically the differential sensitivity kernel for seismic interferometry and show examples based on 2D membrane waves.

The earthquake rates they are a-changin': Improving forecasts during earthquake swarms, Andrea L Llenos, Andrew J Michael, Morgan T Page, Nicholas J van der Elst, and Sara K McBride (Poster Presentation 051)

Earthquake swarms present challenges for operational earthquake forecasting (OEF), because they are often modeled as time-varying changes in background seismicity that are driven by external processes such as fluid flow or aseismic creep, in addition to inter-earthquake triggering based on aftershock statistics. While the time decay of aftershock sequences can be modeled with the modified Omori law, it is difficult to forecast how long a swarm is likely to last or how seismicity rates may vary without being able to forecast the behavior of the external processes. The 2016 Bombay Beach, CA swarm highlighted the need to improve OEF for swarms. Because of its proximity to the southern San Andreas fault, the swarm caused concern that a larger earthquake could be triggered on that fault. However, computing that likelihood was not a trivial task, because current forecast methodologies typically do not account for changes in background rate.

Here we summarize some ways to improve OEF during swarms that we have developed and tested on the 2016 Bombay Beach and 2015 San Ramon, CA swarms. We make forecast models using the Epidemic-Type Aftershock Sequence (ETAS) model (Ogata, JASA, 1988), which can account for background rate changes during a swarm. Additional improvements include: 1) developing a regional swarm model based on fitting previous swarms to capture higher background rates; 2) creating a duration model to estimate how long a swarm is likely to last based on actuarial statistics of previous swarms; 3) updating background rates periodically during a swarm using a number of different lookback windows over which to estimate the background rate; and 4) constructing ensemble forecasts, which enables us to combine different models weighted according to their performance and avoid making arbitrary decisions at the outset of a swarm as to which single model will perform the best. We also briefly explore how forecasts for the 2016 Bombay Beach swarm were communicated and lessons learned from that experience to inform future communication about swarm forecasts.

Building Earthquake Early Warning Networks With Low Cost, Off-the-Shelf Components, Ryan Logsdon, Robert L Walker, and Sean Gibbons (Poster Presentation 052)

We seek to demonstrate the ability to use minimal cost, off-the-shelf components to create disparate networks for earthquake detection. These networks seek to draw a balance between fully crowd-sourced data gathering, such as that generated through smartphones, and dedicated, scientific operations, as exemplified by conventional seismometer networks. The resulting system is intended to provide at least a significant fraction of the continuity afforded by traditional seismometer networks, at a fraction of the price, and orders of magnitude increase in the number of streaming data sources.

Individual sensors are built around open standards and previous projects that have demonstrated an optimal balance between data quality, flexibility of use, and cost. While our individual "stations" are designed in a manner as to minimize cost, they are similarly intended to allow for easy expansion with more advanced and robust tools as they become available, allowing for an agile development lifecycle. At present, data gathering is focused around MEMS accelerometers which are ubiquitous in today's hardware designs, especially in the Internet of Things (IOT) space. Utilizing these sensors comes with the drawback of having much less reliable input data. However, since drift and noise filtering are largely well-understood problems, these drawbacks are easily combated. The main benefits of using IOT components are that we can warn the public without reliance on telephony, and the cost to produce our seismic sensors is so low, whole metropolises such as Los Angeles and San Diego can be fully protected.

Data gathered is treated initially using standard signal processing and seismological techniques, allowing for meaningful detections of P and S wave arrivals from what would otherwise be largely noisy and unreliable data. By employing a novel recurrent neural

network (RNN), we may further analyze the live data by assigning each seismic sensor ephemeral probabilities of accuracy and signal confidence. The resultant data is used to identify and locate earthquakes in real time, allowing us to warn members of the public prior to the arrival of damaging effects in their geographic location. The learning model begins as an isotropic velocity model. It is augmented with a localized model of peak ground acceleration. It is then updated aposteriori with the velocities measured by our sensors during times of seismic activity.

Soil moisture effects on InSAR time series in arid regions, Rowena B Lohman, Teresa Jordan, and Junle Jiang (Poster Presentation 141)

We examine the effects of soil moisture variations on InSAR time series analysis in arid and hyperarid regions, including the impact on phase and amplitude. We demonstrate that amplitude variations alone do not correlate well with precipitation except for in a subset of surface types, and that phase coherence time series can be a much better proxy for soil moisture variations and the associated effects on phase. We apply our approach to data from ESA's Sentinel-1a/b platform covering desert regions in Chile and Saudi Arabia, where infrequent rain events allow clear separation of time periods with and without a soil moisture perturbation. We also present initial results of our analysis in the Imperial Valley, California. We quantify the effects on line-of-sight displacement time histories and the potential to correct these effects.

The Effect of Along-Strike Variation in Dip on Rupture Propagation on Strike-Slip Faults, Julian C Lozos (Poster Presentation 207)

Strike-slip faults are nonplanar structures. Most large strike-slip faults have mapped complexities and discontinuities along strike, but seismological and geodetic inversions, as well as field geophysical studies, suggest dip can also vary substantially along the length of these faults. The southern San Andreas Fault, which twists from a northwest dip in the Carrizo Plain to vertical in the Mojave Desert to a southeast dip through San Gorgonio Pass, is a particularly notable example. A large body of observational and modeling research on the effects of along-strike geometrical complexity on rupture propagation already exists. However, I know of no previous existing modeling studies addressing the effect of an along-strike change in dip on rupture propagation on strike-slip faults. In this geometrical parameter study, I conduct 3D dynamic models of rupture propagation on strike-slip faults with a planar strike but a change in dip midway along the fault, in order to see how far rupture is able to propagate beyond the dip inflection point. I test a variety of compressional and extensional dip angles, and I vary the abruptness at which the dip change occurs. I explore this parameter space for several initial stress amplitudes and orientations. This study may help assess possible rupture segmentation and endpoints for strike-slip faults with variable dip, as well as providing potential explanations for rupture endpoints along apparently planar fault segments.

Nowcasting Induced Seismicity at the Groningen gas field in the Netherlands , Molly Luginbuhl, John B Rundle, and Donald L Turcotte (Poster Presentation 034)

The Groningen gas field in the Netherlands is one of the most productive gas fields in Europe. Production began in 1963 and in 1991 the area experienced their first induced earthquake. Since then there has been a significant level of induced seismicity; this seismicity is attributed to fluid withdrawal not fluid injection. The largest induced earthquake was a magnitude 3.6 in 2012, which caused thousands of damage claims and led to a reduction in gas production in January 2014. In this project, we utilize truncated Gutenberg-Richter frequency-magnitude scaling to introduce a possible maximum earthquake with M = 3.85. We also demonstrate an almost complete absence of aftershocks following the largest induced earthquakes. To quantify the temporal evolution of the induced seismicity we perform our nowcasting method. Nowcasting uses the catalog of seismicity in the region. The method utilizes the number of small earthquakes that occur between pairs of large earthquakes. A major advantage of nowcasting is that it relies on "natural time", earthquake counts, between events rather than clock time. Thus, the results are applicable to induced seismicity that varies in time. We count the rate of occurrence of small induced earthquakes to nowcast the probability of occurrence of larger earthquakes.

Estimates of Shallow Crustal Stress Heterogeneity Length Scale from Borehole Breakouts and Local Earthquake Focal Mechanism Inversions in the Los Angeles Basin, Karen M Luttrell, and Jeanne L Hardebeck (Poster Presentation 143)

Many contributions to the SCEC Community Stress Model rely heavily on the observations of stress field orientation provided by earthquake focal mechanisms and borehole breakouts to constrain their estimates. However, earthquake focal mechanisms and borehole breakouts necessarily sample different locations within the 3-D crust, and it is unclear how these observations should be jointly interpreted and incorporated into ongoing modeling efforts. Previous comparisons between existing borehole breakout observations and local earthquake focal mechanism inversions indicate strong disagreement between the two, even when considering only shallow earthquakes. The goal of this research is to constrain the length scale over which borehole breakouts and earthquake focal mechanisms indicate consistent stress field orientations. We consider 60 published observations of SHmax from borehole breakouts throughout the Los Angeles basin area. We identified subsets of earthquakes nearby each borehole, using a range of maximum depth criteria and maximum distance criteria, and inverted each subset of earthquake focal mechanisms for the orientation of the local stress state. Focal mechanisms in each subset are derived from the

A Moving Mud Pot Threatening Railroad Tracks and a Highway, Imperial County, California, David K Lynch, Travis Deane, Carolina Zamora, Dean G Francuch, James S Bailey, Christopher W Allen, Justin D Rogers, and Cassandra Gouger (Poster Presentation 277)

INTRODUCTION The Salton Trough is a sag in stepover regions between the San Andreas, Imperial and Cerro Prieto Faults in southern California and northern Baja, Mexico. Due to a high geothermal gradient in the Colorado River sediments, the trough contains many CO2-driven geothermal features like gryphons and mud pots, and is home to several geothermal generating plants.

DEVELOPMENTS In 2016 an ambient temperature CO2-driven “mud spring” appeared near a long lived mound spring and began moving southwest toward the Union Pacific railroad tracks and SR111 at about 20 ft per year. It is less than a mile NE of the Wister Fault (SE extension of the San Andreas Fault) and moved as though along a cross fault. As it advanced, the mud spring carved a

~24,000 sq ft basin about 18 ft deep and 75 ft wide (400,000 cf). The spring moved in a fairly straight line and remained a small, discrete, roughly circular structure and did not develop into a linear source, as might be expected if moving along a fault. To our knowledge, such movement and behavior of a mud spring (mudpot, etc.) has not been seen before. Since pumping began in June 2018, the water discharge rate was roughly constant (45,000 gallons per day).

MITIGATION In early 2018 the Union Pacific Railroad (UPR) began taking steps to prevent the spring from undermining their tracks. A number of acoustic imaging studies were carried out, rip-rap was dumped into the mud spring, a 75 ft deep sheet pile wall 120 ft long was built between the spring and tracks and the basin was drained. A well was dug and pumped with the hope of depressurizing the aquifer that is driving the spring. The well encountered highly pressurized artesian conditions at the upper most part of the aquifer at a depth of about 300 ft but did not appear to affect the mud spring. The spring continued its SW movement and eventually met the sheet piles (40 ft from the tracks) where it began to expose them.

CURRENT STATUS In August, as a contingency, UPR began construction of a shoofly (track detour). Two more depressurization wells are being drilled and additional subsurface imaging is being completed. At the time of this writing (mid Aug 2018), the mud spring is stationary because it is being confined by the sheet piles, though it seems likely that the underground source is still moving southwest and will eventually surface in the next few years, possibly undermining the existing railroad tracks or possibly further west under State Route 111.

Inelastic Wedge Failure and Along-Strike Variations of Tsunami Generation in the Shallow Subduction Zone, Shuo Ma, and Shiying Nie (Poster Presentation 280)

One remaining and important puzzle about the 2011 Tohoku tsunami is that the largest tsunami heights were observed along the Sanriku coast (between 39.5 and 40.25°N), ~100 km north of where the largest slip (>50 m) occurred in the trench, with tsunami more than a factor of two larger in the north than the south (Mori et al., 2011). Most seismic and geodetic slip models have no or little slip to the north of 39°N and can not explain the large tsunami heights in Sanriku. Tsunami inversions suggest that near-trench slip needs extend further to the north of 39°N (e.g., Satake et al., 2013; Yamazaki et al., 2017). However, bathymetry surveys to the north of 39°N before and after the 2011 Tohoku earthquake indicate no large slip at the trench (Fujiwara et al., 2017). Here we show that inelastic wedge failure can provide a good explanation to this puzzle. In the Japan subduction zone the amount of sediments in the overriding wedge increases from south to north (Tsuru et al., 2002), which suggests that coseismic wedge failure can occur more easily in the north. We construct a simple 3D shallow subduction earthquake model allowing wedge failure, with a closeness-to-failure (CF) parameter larger in the north motivated by the above observation. Our simulations show that large slip at the trench occurs in the south due to the wedge far from failure (small CF), which causes large horizontal seafloor displacement and small uplift due to shallow fault dip. However, in the north, due to large presence of sediments (large CF) the inelastic deformation in the wedge diminishes the fault slip at the trench, but causes uplift efficiently landward from the trench, similar to our previous 2D results (Ma, 2012; Ma and Hirakawa, 2013). The uplift in the north can be well more than twice larger than in the south. This along-strike seafloor uplift pattern is consistent with the tsunami height observations of Mori et al. (2011) and bathymetry surveys of Fujiwara et al. (2017). The resulting tsunami from large inelastic uplift in the north is expected to be shorter-wavelength and more dispersive than that from the slip on the fault, also consistent with tsunami observations along the Sanriku coast. Thus we propose that the largest tsunami heights during the 2011 Tohoku earthquake are likely due to inelastic wedge failure to the north of 39°N, not large slip at the trench.

Modeling Dynamic Ruptures with High Resolution Fault Zone Physics, Xiao Ma, and Ahmed E Elbanna (Poster Presentation 200)

Earthquakes are among the costliest natural hazards on earth. The dynamical instabilities responsible for the onset and propagation of these events are linked to fundamental physics- friction, fracture, heating, and compaction- of fluid filled granular materials and rocks in the subsurface subjected to extreme geophysical conditions.

Here, we present a new hybrid computational algorithm for modeling earthquake ruptures in complex fault zone structures. The hybrid method combines Finite element method (FEM) and Spectral boundary integral (SBI) equation through the consistent exchange of displacement and traction boundary conditions, thereby benefiting from the flexibility of FEM in handling problems with nonlinearities or small-scale heterogeneities and from the superior performance and accuracy of SBI. We validate the hybrid method using a benchmark problem from SCEC dynamic rupture simulation validation exercises. We further demonstrate the capability and computational efficiency of the hybrid scheme for resolving off-fault complexities using a first-of-its kind model of a fault zone with explicit representation of small scale secondary faults and branches enabling new insights into earthquake rupture dynamics that may not be realizable in homogenized isotropic plasticity or damage model. For example, we have observed that, for a range of parameters, when the secondary faults are activated they not only act as energy sinks but also as energy source by dynamically loading the main fault enhancing the rupture speed and slip rate of the main fault rupture. Furthermore, the interaction of the emitted waves with the explicitly represented secondary faults and branches lead to interference patterns that complexify the wave field and enhance high frequency generation. These observations enabled by our novel developments in computational dynamic fracture open new opportunities for multiscale modeling of earthquake physics for next generation seismic hazard models.

The SCEC Software Ecosystem for Earthquake System Science Research, Philip J Maechling, Jacobo Bielak, Scott Callaghan, Yifeng Cui, Edward H Field, Christine A Goulet, Robert W Graves, Thomas H Jordan, Kevin R Milner, Kim B Olsen, Daniel Roten, William H Savran, Fabio Silva, Mei-Hui Su, Ricardo Taborda, and John E Vidale (Poster Presentation 296)

The Southern California Earthquake Center Community Modeling Environment (SCEC/CME) collaboration has developed a collection of independent, but inter-related, scientific software systems designed to support earthquake system science research. We describe this collection as a software ecosystem to emphasize that these codes are developed and co-evolve in a shared collaborative scientific and open-science computing environment. The SCEC software ecosystem includes the Unified Community Velocity Model (UCVM) to deliver several California crustal velocity models (CVM-S, CVM-H, UCVM), advanced Probabilistic Seismic Hazard Analysis (PSHA) methods (OpenSHA), broadband ground motion methods (Broadband Platform), deterministic

wave propagation codes (AWP-ODC, Hercules), a physics-based PSHA platform (CyberShake), and a forecast testing center (CSEP). SCEC scientific software distributions are provided to the research community as open-source scientific software that can be compiled and run in standard Linux environments on multiple computer architectures. The SCEC scientific applications are usually developed as stand-alone codes that input and output standardized data formats. Selected computationally intensive codes have been parallelized, and in some cases, accelerated on many-core systems, to support large-scale ground motion simulations. Scientific codes in the ecosystem can often be combined into complex workflows to automate multi-stage research calculations, with the interfaces between programs using file-based data exchange formats, or database queries. In some cases, such as with the AWP-ODC and Hercules earthquake wave propagation software, the SCEC software ecosystem supports multiple scientific applications that perform equivalent calculations using alternative methods, helping to verify computational results for complex problems where theoretical and/or analytical solutions are not available. As individual programs, and through the combined capabilities of multiple codes, the SCEC software ecosystem has enabled significant scientific and computing advances and groundbreaking earthquake system science research.

Can we hide an active fault within a geodetic network? Yes, we can., Maria Beatrice Magnani (Poster Presentation 130)

Comparison of deformation rates around the New Madrid seismic zone (NMSZ), central U.S., indicates an apparent inconsistency between geologic and geodetic rates. In intraplate regions such as the central U.S., geologic rates, inherently longer-term, might be better indicators for future seismic activity than GPS data, which sample a shorter timeframe. Here I show how a Holocene active fault might go undetected within the geodetic network monitoring the central U.S. seismically active area. High resolution marine seismic reflection data acquired along the Mississippi river image a previously unknown NW-SE striking north-dipping fault displacing the base of the Quaternary alluvium by 15m with reverse sense of movement, and consistently deforming the Tertiary, Cretaceous and Paleozoic formations. The fault crosses the river south of the NMSZ, between Caruthersville, MO and Osceola, AR. Although the fault appears aseismic, geomorphological evidence from river channel sinuosity suggests that the latest slip occurred in the last 200 years. Here I explore whether movement along this fault can be detected by the GNSS Array for Mid-America (GAMA) network, which is specifically designed for tectonic studies in and around the NMSZ. GAMA stations straddle the fault with the closest stations located ~30 km to the north and ~50 km to the south. I model the amount and extent of surface displacement due to a shear fault in an isotropic half-space (Okada, 1992) and compare the results against the GAMA data as processed by Boyd et al., 2015. The model is applied to a 20 km-long fault that dips to the north ~60º, strikes N125º, and extends to 10 km depth. Both dip slip and strike slip dislocations are tested. Results show that a dislocation rate of 4 mm/yr is required to produce a detectable surface signal. Based on recent coring of the floodplain alluvium south of the study area, the age of the oldest Quaternary deposit along the most recent meander belt is 14.3ka±0.5ka. If fault slip has been steady state during the Holocene, then a slip rate of 1mm/yr is reasonable for the imaged fault, resulting in undetectable displacement rates at the nearest geodetic stations. My results indicate that it is possible for a fault of substantial dimension (~200 km2 area) with a Holocene slip rate exceeding 1mm/yr to hide within the geodetic network. Undetected by the GPS stations and currently aseismic, such fault could therefore represent an unrecognized seismic hazard.

Two Moho-Depth Earthquake Swarms along the Sierra Microplate Basin and Range Boundary Region, Emily L Maher, Ken D Smith, Rachel L Hatch, Kent M Graham, Neal W Driscoll, and Noah Conway (Poster Presentation 068)

Two unprecedented near Moho-depth earthquake sequences, 2003-04 and 2011-12, occurred along the eastern Sierra Microplate northern Walker Lane boundary at ~30 km depth separated by ~50 km. Whereas typical seismogenic depths in this tectonic setting between 15-18 km, depths for the two sequence are well constrained and range between ~25-35 km. The N. Tahoe, California, sequence occurred over a 6 month time period in 2003-2004 and consisted of over 1600 located events with a largest ML 2.2. The second swarm occurred in 2011 over a 9 month period below Sierraville, California. For this sequence, 2235 deep events were located beneath Sierra Valley with the largest at magnitude ML 1.9. Initial relocations for both swarms (Smith et al, 2004; Smith et al., 2006) indicate that they occur along structures with a nearly identical strike (~N45°W) and dip (~50°NE). In addition each sequence defines a planar structure, 7x7 in extent. On 29 September 2011, a single deep earthquake occurred at the midpoint of the two sequences further implying that the swarms occurred along the same deep geologic structure. Potential causes for the two deep swarms relate to deep basaltic injection or fluid injection at near Moho depths. However there is currently no evidence for volcanic type earthquake sources. We review phase picks for the sequences to improve available first motions for focal mechanisms, stress inversions and 'GrowClust' (Trugman and Shearer, 2017) relocations. Here we present results of a continuing analysis of these unique earthquakes for a better understanding the interaction between the Sierra Microplate and the Basin and Range boundary region at these latitudes.

Active Tectonics across the Indo-Burma Range, Patcharaporn Maneerat (Poster Presentation 243)

The potentially active tectonics of the oblique subduction zone across the Indo-Burman Range (IBR), which formed due to India-Eurasia continent-continent collision in the Paleogene (Mitchell, 1993), remains controversial. To address the poorly understood kinematics of faulting and associated deformation, we study evidence of active tectonics by investigating the geomorphology, active crustal deformation and seismicity of the IBR. Geomorphic indices, such as the steepness index and hypsometric integral, geodetic measurements, and focal mechanism of the earthquakes occurred across IBR are used to investigate evidence for active surface uplift, crustal deformation, and stress orientations. We calculated geomorphic indices, and used GPS data from Steckler et al. (2016) and Kreemer et al. (2014) to generate strain-rate maps across our study region. We determined stress orientation and stress ratio using an inversion from the focal mechanisms of the events which occurred across the IBR. The geomorphic data suggest that the higher uplift rates are distributed across the IBR, especially in areas between the Kabaw and Churachanpur Mao Faults. Moreover, the geodetic strain maps indicate a significant component of contraction across the study region. Despite this, a lack of full GPS station coverage, specifically in the southern IBR, means we cannot conclude that oblique subduction is active. Furthermore, the principal stress directions obtained from stress inversion of the earthquake focal mechnism suggest strike-slip motion across IBR. The shortening direction is likely orientated in NW-SE. Further analysis is required in this area, and we will work more on the geomorphology at stream scales, including stream profiles, valley-width-height ratio of channels,

and knickpoints since these channels likely capture tectonic perturbations. We will also continue working on improving the GPS strain maps by including elastic block models in the analysis. We are planning to investigate changes in angles between maximum principal stress and the slab interface, and compare our results with other subduction regions (Hardebeck, 2015). By investigating both long- and short-term processes, we hope to apply these observations and measurements to constrain a conceptual model of the active tectonics of the IBR and improve our understanding of the associated seismic hazard from the subduction thrust and crustal faults.

Fault linkage through the Imperial Valley, California is required to match current slip rate estimates, Scott T Marshall, Elizabeth H Madden, Jacob H Dorsett, and Michele L Cooke (Poster Presentation 166)

The Imperial Valley hosts a seismically active network of strike-slip faults that comprise the southern San Andreas and San Jacinto fault systems and together accommodate the majority of relative Pacific-North American plate motion in southern California. In order to better understand how these faults link and accommodate plate motions, we use a suite of mechanical models to simulate the long-term fault mechanics of four fault networks with different degrees of connectivity through the Imperial Valley. The full three-dimensional distribution of fault slip rates is solved for based on a far-field Pacific-North American plate rate of 45-50 mm/yr at an azimuth of 320-325 degrees. We evaluate model results against average fault slip rates from the Uniform California Earthquake Rupture Model version 3 (UCERF3) and geologic slip rate estimates made at individual points along the regional faults. A model incorporating faults from the SCEC Community Fault Model version 5.0 (CFM5.0) fits 8 of 12 UCERF3 slip rates and 5 of 19 geologic estimates and the Imperial fault has a modeled average slip rate of 3.5-6.6 mm/yr, in disagreement with the minimum UCERF3 estimate of 15.0 mm/yr and far below the UCERF3 preferred rate of 35 mm/yr. A model with continuous linkage from the Coachella segment of the southern San Andreas fault to the Imperial fault through the western Brawley Seismic Zone to the Cerro Prieto fault matches 11 of 12 average slip rates and 8 of 19 geologic slip rates. With a modeled rate of 13.6-15.1 mm/yr, this is the only model that matches the UCERF3 rate on the Imperial Fault. The Elmore Ranch fault slips left-laterally at geologically compatible rates only in models with continuous linkage. The El Centro fault slips less than 1 mm/yr in all models. Analysis of model-calculated strain energy density patterns suggests that models with continuous linkage produce less off-fault strain compared to the raw and less connected CFM5.0 geometry.

Crustal seismogenic layer at active faults inferred by background seismicity and temperature data in Japan, Makoto Matsubara, and Tomoko E Yano (Poster Presentation 067)

The lower limit of seismogenic layer within the crust relates to the maximum size of earthquakes caused by the active fault. We used the index “D95”, the depth above which 95 % of the whole crustal earthquakes occurred from the surface, to define the lower limits of the crustal seismogenic layer. We verify D95 for particular earthquakes after 2001 with magnitude larger than 6.5 by comparison with several parameters such as, the actual main shock hypocenter depth, their aftershocks, main slip region on the fault, and depth of the temperature as 250, 300, and 450 degrees in Celsius.

We estimated D95 with the catalog in which we relocated hypocenters between 2001 and 2012 from the NIED Hi-net catalog with Double-Difference method (Waldhauser and Ellsworth, 2000) for high resolved hypocenter locations (Depth <40 km, M>0.0) (JUICE catalog, Yano et al. 2017). Events with M>1.5 were chosen to satisfacty the Gutenberg-Richter magnitude-frequency relation. To calculate D95 was the same as Matsubara and Sato (2015). We estimated depths where the crustal temperature reaches 250, 300, and 450 degrees from heat flux (Matsumoto, 2007; Sakagawa et al., 2005) by using the steady-state, one-dimensional, heat conduction equation with an exponential decrease in the radioactivity heat generation introduced in Tanaka (2004).

Our result, D95, located under the deepest boundary of majority of aftershocks and main coseismic slip regions for many large. Except the deep aftershocks of the 2016 Kumamoto earthquake penetrated about 5 km deeper than the D95. We concluded that they occurred within the brittle-ductile transition zoon owing to too high Vp as 7.4 km/s for crustal brittle layer with temperature between 300 and 400 degrees. We also looked at the temperature around the volcanic zone such as Iwate-Miyagi Inland earthquake since the D95 is 10 km in spite of the D400 as 5 km.

Late Quaternary Deformation in the Inverted Santa Maria Basin, CA: Documenting and Quantifying Active Folding from Syn-Tectonic Deposits, Ian McGregor, and Nate W Onderdonk (Poster Presentation 247)

The Santa Maria area is an inverted basin in southern California with several kilometers of shortening deforming and uplifting deep-water basin rocks. Abundant subsurface data from active oil fields document total shortening and near-surface structures, but does not include the Late Quaternary history and whether these structures are still active. Minimal constraints on the amount and rate of Quaternary shortening prevents accurate estimates of regional seismic hazards for the local population and the Diablo Canyon Nuclear Power Plant 40 km to the north. Conflicting structural models have been proposed for the deformation present and a quantitative description of fold growth is needed to determine which structural models best describe recent deformation. Careful documentation of late Quaternary deformation within the Santa Maria basin, in terms of amount, timing, and style of fold growth, would provide information imperative for evaluating earthquake risk and regional tectonic models.

Quantifying uncertainty in cumulative surface slip along the Cucamonga Fault, a crustal thrust fault in southern California, Devin McPhillips, and Katherine M Scharer (Poster Presentation 255)

Studies of historic earthquake surface ruptures show that displacements along strike are spatially variable. As a result, latest Quaternary slip rates developed from a spatially restricted set of cumulative displacement measurements may not accurately represent fault velocity. Moreover, dispersion that persists over multiple ruptures may stem from complex deformation processes, including fault segmentation, distributed deformation, blind faulting, and rupture nucleation and propagation. Here, we undertake a detailed examination of the dispersion of slip along the Cucamonga Fault. The Cucamonga Fault is part of a network of faults that have generated damaging historical earthquakes in the Los Angeles, California region, and numerous scarps along its ~25 km length are well expressed on alluvial fans. These fans were deposited with conical geomorphic surfaces at intervals throughout late Quaternary time and periodically broken by surface-rupturing earthquakes. We make 310 measurements of vertical separations

across the scarps using lidar data. We also re-interpret cosmogenic radionuclide data in order to better understand the alluvial fan surface ages. We show that the along-strike dispersion of the vertical separations cannot be explained by our best estimates of analytical uncertainties alone. Additional, epistemic uncertainties are required. We find that the magnitude of the required epistemic uncertainty is typically larger than analytical uncertainty by a factor of 3 and typically about 20% of the maximum vertical separation. This result holds at several spatial scales, from the full fault length (25 km) to ~2 km sections. We examine three potential sources of epistemic uncertainty and find that neither surface age uncertainty, fault dip, nor anthropogenic landscape alteration are likely sufficient to explain the over-dispersion of the data. As a result, we infer that deformation processes are responsible for a significant fraction of the over-dispersion. We calculate a range of plausible dip-slip rates between 0.4 and 2.6 mm/yr. In light of our results, we suggest that future thrust-fault slip-rate studies adopt an epistemic uncertainty of ~20% for vertical separation measurements, unless there are sufficient data to demonstrate otherwise. Whenever possible, slip rate studies will benefit from additional reporting of the spatial distribution of strain.

Reliable Real-Time Signal/Noise Discrimination with Deep and Shallow Machine Learning Classifiers, Men-Andrin Meier, Zachary E Ross, Anshul Ramachandran, Ashwin Balakrishna, Peter Kundzicz, Suraj Nair, Zefeng Li, Egill Hauksson, and Thomas H Heaton (Poster Presentation 064)

In Earthquake Early Warning (EEW), every sufficiently impulsive signal is potentially the first evidence for an unfolding large earthquake. More often than not, however, impulsive signals are mere nuisance signals, e.g. from a nearby airport or from an instrument malfunction. One of the most fundamental - and difficult - tasks in EEW is to rapidly and reliably discriminate between real local earthquake signals, and any kind of other signal. This discrimination is necessarily based on very little information, typically a few seconds worth of seismic waveforms from a small number of stations. As a result, current EEW systems struggle to avoid discrimination errors, and suffer from false and missed alerts. In this study we show how modern machine learning classifiers can strongly improve real-time signal/noise discrimination. We develop and compare a series of non-linear classifiers with variable architecture depths, including random forests, fully connected, convolutional (CNN) and recurrent neural networks, and a generative adversarial network (GAN). We train all classifiers on the same waveform data set that includes 374k 3-component local earthquake records with magnitudes M3.0-9.1, and 946k impulsive noise signals. We find that all classifiers outperform existing simple linear classifiers, and that the deep architectures significantly outperform the more simple ones. Using 3s long waveform snippets, the CNN and the GAN classifiers both reach 99.5% precision and 99.3% recall on an independent validation data set. Most misclassifications stem from impulsive teleseismic records, and from falsely labeled records in the data set. We show that, in turn, 95.5% of the false triggers on teleseismic waveforms can be avoided with a simple secondary random forest classifier. Our results suggest that machine learning classifiers can strongly improve the reliability and speed of EEW alerts.

Coral microatolls as a tool for subduction zone paleoseismology: Identifying rare events along the Sunda megathrust and the Manila trench, Aron J Meltzner (Poster Presentation 242)

Over the course of a seismic cycle, the land and seafloor above a subduction zone rise and fall. These land-level changes are recorded by coral microatolls, coral colonies living near the base of the intertidal zone whose upper level of growth is tightly limited by exposure during low water. As these microatolls grow, their growth patterns reflect changes in relative sea level. Their skeletons allow us to infer a history of land-level changes, caused by gradual strain accumulation between earthquakes and sudden strain release during earthquakes. This, in turn, provides insight into subduction zone fault processes and allows us to recognize paleoseismic events that have occurred in past centuries.

In 2004, an unexpected Mw 9.2 rupture of the northern Sunda megathrust triggered a tsunami that took >230,000 lives across the Indian Ocean. Subsequently, our studies of microatolls in Sumatra, along with colleagues' paleotsunami investigations, revealed that predecessors of the 2004 earthquake and tsunami had occurred ~600 and ~1000 years earlier. If these results had been known earlier, the 2004 catastrophe might have been anticipated.

Farther south, along the Mentawai section of the Sunda megathrust, microatolls have revealed that clusters of large earthquakes occur periodically, every ~200 years. Large (Mw ~8.8) ruptures occurred in 1797 and 1833, and the most recent cluster began in 2007. Patterns of uplift and subsidence recorded by microatolls suggest that another large earthquake, approaching the size of 2004, may occur in the Mentawai region in the decades ahead.

Along the Manila trench west of Luzon, no earthquakes of Ms >7.6 are known from the historical record, but is this fault capable of rare, much larger earthquakes? We have begun a microatoll study along the west coast of Luzon, and our findings should provide insight into the earthquake and tsunami potential along the Manila trench and in the South China Sea.

Capturing Frictional Asperities along the Complex Structure of the Main Himalayan Thrust in Nepal after the 2015 Mw 7.8 Gorkha Earthquake, Manuel M Mendoza, Bo Li, Abhijit Ghosh, Marianne S Karplus, John Nabelek, Soma N Sapkota, Lok B Adhikari, Simon L Klemperer, and Aaron A Velasco (Poster Presentation 092)

The 2015 Mw 7.8 Gorkha earthquake produced 4 m of peak co-seismic slip as the Main Himalaya Thrust (MHT) ruptured eastward under the dense population centers, such as Kathmandu. The aftermath of destruction left over 9,000 people killed, and more than 2 million displaced from their homes due to both infrastructure failure and seismically triggered landslides throughout the High Himalaya. There is concern that since the MHT did not fully release much of its strain by rupturing to the surface, that another large damaging earthquake could occur. Our group, in collaboration with other institutions, rapidly assessed the evolving state of stress in the region via the deployment of "NAMASTE", a 45-station seismic network composed of a mix of broadband, short-period, and strong motion sensors, that operated from June 2015 to May 2016. Blanketing the 27,650 km2 rupture area, and beyond, we obtain a catalog containing over 7,000 precisely located earthquakes that range in local magnitude from 0.3 to 6.5. A result of particular interest from these locations, is the illumination of both a shallow dipping MHT, and a set of high-angle faults that we infer to be components for a duplex structure. The investigation presented here aims to understand the frictional properties of the duplex structure with relation to the MHT, through analyses of b-value mapping and repeating earthquakes. The b-value has been observed to vary laterally and with depth in this area; in particular, we observe a significantly low b-value area in the easternmost end of the

network where the duplex structure is illuminated, which could be reflecting the presence of asperities, or stress concentrations. In addition, using the catalog events, we find many repeating earthquakes. Repeating earthquakes are inferred to occur as a result of repeated failure of small asperities that are surrounded by a stable and continuous sliding area along the fault. By reconciling a relationship in both space and time between areas of low b-value and where repeating earthquakes occur, our goal is to gain valuable insights into the frictional properties along the MHT that may control the recurrence of the next large event in Nepal, Himalaya.

Pre-seismic and co-seismic deformation of the 2017 Mw 6.5 Jiuzhaigou, eastern Tibet earthquake constrained by GPS and InSAR data, Guojie Meng, Xiaoning Su, Shunying Hong, Xin Zhou, Yanfang Dong, and Chengtao Li (Poster Presentation 127)

We investigate pre-seismic and co-seismic crustal deformation of the 2017 Mw 6.5 Jiuzhaigou, which occurred in the eastern boundary of Bayan Har block, Tibet Plateau, using geodetic data. Pre-seismic deformation is in the epicentral area is realized from continuous and campaign GPS data acquired during the 2009-2017 period. The left-lateral strike and extensional rates are 3.0 mm/yr and 3.1 mm/yr, respectively, for the northern extension of the Huaya Fault, where no co-seismic rupture identified along the hidden segment. Strain tensor components show an evident localized strain accumulation in the vicinity of epicenter zone. Co-seismic deformation field is derived by GPS and InSAR data in multiple SAR viewing geometries. The fault geometry models retrieved with multiple inversion methods are highly consistent, showing a source model with a strike of ~154° and a dip angle of ~ 77°. Based on the optimal fault geometry model, the fault slip distribution jointly inverted from InSAR and GPS data shows the slip is mainly concentrated in the depth of 1 - 15 km, and only one slip center appears in the depth of 5 - 9 km with a maximum slip of about 1.06 m. Taking the shear modulus of μ = 32 GPa, the seismic moment derived from the distributed slip model is about 7.85 ×1018 Nm, equivalent to an earthquake of Mw 6.5. Most of the aftershocks with magnitude < M 3 happened in stress shadow area with depth between 5-15 km; whereas, the aftershocks with magnitude ≥ M 3 predominately happened in an area with positive Coulomb stress changes in a depth more than 15 km. The static Column stress triggered by the mainshock significantly increased at the Tazang fault northwest to the epicenter, the hidden North Huya fault and partial segments of Minjiang fault west of the epicenter.

Towards Quasi-Automated Estimates of Source Properties of Small to Moderate Southern California Earthquakes with Second Seismic Moments , Haoran Meng, Jeff J McGuire, and Yehuda Ben-Zion (Poster Presentation 072)

We develop a method for quasi-automated estimation of directivity, rupture area, duration, and centroid velocity of earthquakes with second seismic moments. The method is applied to small to moderate earthquakes in southern California. The P and S phase picks are given by a 1-D ray tracing algorithm and cataloged event locations. These are refined for deconvolution by using a grid search on zero-crossings within a short time window around the automated P, S picks. Source Time Functions (STFs) of target events are derived using deconvolution with 3 stacked empirical Green's function (seGf). The use of seGf suppresses non-generic source effects such as directivity in individual eGf's. The seGf for each target event is based on stacking individual eGfs (normalized by seismic potencies) selected by spatial and magnitude criteria as well as performances in the projected Landweber deconvolution. The weighted stack of eGfs, with coefficients determined by grid search and waveform fits, helps further to correct inaccuracies of focal mechanisms. For stations near the source we allow using only 2 individual eGfs to increase the take-off angle coverage. Compared with a single eGf, analysis with a weighted stack can significantly improve waveform fit and typically allows getting 5 to 15 more STFs. The method is suitable for analysis of large seismic datasets and it works for target events in southern California with magnitudes as small as 3.5. We analyzed 40 small to moderate earthquakes from 2009 to 2016 in southern California and get stable results for 25 events. Most analyzed events have significant directivities. We also estimate the optimized, minimum and maximum values of the rupture area that are consistent with a particular dataset at the 95% confidence level. This is used to estimate stress drops. Most of the stress drops are well constrained and the optimized stress drops vary in the range 20-100 MPa.

Tsunami Source Inversions Using Adjoint-state Methods, Lingsen Meng, Tong Zhou, Xie Yuqing, and Jiayuan Han (Poster Presentation 279)

Traditional source inversion using tsunamis waves is based on either the finite-fault slip modeling or the time-reversal imaging. Such inversion methods suffer from the uncertainty of fault parameters or crustal rigidity. Moreover, the heavy computational burden of calculating Green's functions result in limited spatial resolution and hinders the real-time applicability of the traditional methods to tsunami early warning. In this work, we transplant the state-of-art adjoint-state full-waveform inversion method from exploration seismology to tsunami source imaging. The adjoint-state method solves the initial-water-elevation pattern with less computational cost, which potentially improves the speed of the tsunami early warning and reduces the blind zone. Our new method does not rely on pre-defined fault parameters and is suitable for tsunami-generating earthquakes with unknown fault geometry. This method also efficiently handles dense mesh grid and is capable of resolving small-scale secondary tsunami sources, such as the seafloor landslide or secondary ruptures on splay faults. We valid this approach with synthetic tsunami sources, and apply it to the 2014 Mw 8.1 Iquique tsunami event, and the 2017 Mw 8.1 Oaxaca tsunami event. Our preliminary results show that the adjoint-state method is of high resolution and produces little artifacts, outperforming the traditional tsunami source inversions. Our new adjoint-state tsunami inversion will advance tsunami science and earthquake source dynamics and set the stage to improve real-time applications such as tsunami early warning.

Preliminary Results on Fully Nonergodic Ground Motion Models in Central California Using NGA-West2 and SCEC CyberShake Datasets, Xiaofeng Meng, Christine A Goulet, Kevin R Milner, and Scott Callaghan (Poster Presentation 024)

A key input to probabilistic seismic hazard analyses (PSHA) is the total standard deviation of the misfits between ground motion observations and the median ground motion models (GMMs, a.k.a GMPEs), commonly known as σtot. The most promising way to reduce hazard is to reduce σtot through the removal of the ergodic assumption. Although the strong motion networks has been rapidly growing in recent decades, in most cases the empirical data are still too sparse to establish a fully nonergodic model. In comparison, numerical simulations can generate large ground motion datasets at any desired site, which are optimal to reduce σtot by identifying and removing repeatable effects in a fully nonergodic model. However, before the simulation-based σtot can be adopted by engineers in PSHA applications, it is crucial to validate the simulated ground motions against empirical data and models.

In this study, we evaluate the ability of the Southern California Earthquake Center (SCEC) physics-based CyberShake platform to capture the repeatable source, site and path effects from the empirical data. CyberShake Study 17.3 was computed for central California and generated over 285 million ground motion seismograms at 334 sites. We estimate the source, site and path effects by applying the mixed effects regression model to the CyberShake dataset at 3s period and compare them with results from a subset of NGA-West2 dataset in the same area. Preliminary results suggest that the correlation of site effects between CyberShake and NGA-West2 is relatively stable, while the path effects show a wide range of correlation coefficients, indicating a potential mismatch between the simulations and the recorded. We also found good agreement between the source effects obtained from the CyberShake model and stress drop maps for California. This presentation will summarize these results from our analyses.

High Resolution Geodetic Measurements of Co-seismic Fault-zone Deformation for Probabilistic Fault Displacement Hazard Assesment and Confidence Intervals on Geologic Slip Rates, Chris W Milliner, and Andrea Donnellan (Poster Presentation 228)

Understanding how co-seismic shear strain changes with distance from the primary fault rupture, has importance for characterizing the hazard it poses to critical infrastructure and reliably estimating geologic slip rates from offset geomorphic features. Probabilistic Fault Displacement Hazard Analysis (PFDHA), defines the probability of distributed faulting with distance from the primary fault strand, and has so far been constrained solely from field observations of recent surface ruptures. Here we assess how measurements of near-field surface deformation (< 2 km) of several large magnitude earthquakes (Mw > 7), derived from different geodetic imaging techniques (e.g., optical image and radar amplitude correlation), can be used to better constrain the fall-off of inelastic, co-seismic shear strain away from the primary fault. From the resulting displacement maps we can measure the full across-fault co-seismic surface strain at multiple points along-strike of the surface rupture (n>1500), providing the probability of occurrence of distributed inelastic deformation. Although the field mapping accuracy of expected rupture occurrence dominates the PFDHA hazard, we find geodetic-based measurements can still help reduce the epistemic uncertainty associated with the probability of near-field distributed displacement (< 500 m) for different types of geologic material and macroscopic fault-zone complexity. Assuming fault strain release is an ergodic process, we also discuss how these probabilistic estimates of fault-zone width could characterize the probability a geologic slip rate measurement, taken over some fault perpendicular distance, captures the full, across-fault geologic strain release. High-resolution measurements of near-field deformation from surface ruptures can help reduce the epistemic uncertainty in PFDHA models, providing more precise information to structural engineers, and place confidence limits on geologic slip rates that would be useful input for PSHA.

Fully physics-based PSHA: coupling RSQSim with deterministic ground motion simulations, Kevin R Milner, Bruce E Shaw, Thomas H Jordan, Scott Callaghan, and Christine A Goulet (Poster Presentation 032)

Probabilistic seismic hazard analysis (PSHA) is typically performed by combining an earthquake rupture forecast (ERF) with a set of empirical ground motion prediction equations (GMPEs). ERFs have typically relied on observed fault slip rates, scaling relationships, and regional magnitude-frequency distributions to estimate the rate of large earthquakes on pre-defined fault segments. GMPEs, which regress against recorded ground motions, often lack data at short site-rupture distances and for large, complex ruptures. The CyberShake platform (Graves et al., 2011) replaces GMPEs with deterministic three-dimensional ground motion simulations, characterizing the effects of basin response and other path effects which are parameterized or treated as aleatory variability in GMPEs. We replace traditional ERFs with a multi-cycle physics-based earthquake simulator, the Rate-State Earthquake Simulator (RSQSim), developed by Dieterich & Richards-Dinger (2010). RSQSim simulations on the Uniform California Earthquake Rupture Forecast, Version 3 (UCERF3) fault system produce seismicity catalogs that match long term rates on major faults and yield remarkable agreement with UCERF3 when carried through to GMPE-based PSHA calculations. Unlike traditional ERFs, RSQSim produces full slip-time histories for all simulated ruptures which can be used directly as input to deterministic wave propagation simulations. We couple the RSQSim model with CyberShake to create the first fully physics-based PSHA model. Resultant ground motions match GMPE estimates of mean and variability of shaking well over magnitudes and distances for which GMPEs are well constrained. Aggregated over many sources and sites, variability is similar to ergodic GMPE predictions. Variability is reduced for individual pairs of sources and sites, which sample a single path. This is expected in a non-ergodic model, and reduces exceedance probabilities for extreme ground motions at many sites. We will present these comparisons and preliminary fully physics-based RSQSim/CyberShake hazard curves.

Fluid-enhanced grain boundary sliding in pseudotachylyte survivor clasts: does creep cavitation lead to earthquake rupture?, Elena Miranda, and Alberto Perez-Huerta (Poster Presentation 172)

Viscous shearing in the middle and lower crust is observed to localize within pseudotachylyte veins hosted in coeval mylonite, but it is unclear what role hydrous fluids play in enhancing strain localization in pseudotachylyte. We investigate coeval pseudotachylytes and granodiorite mylonites from the footwall of the South Mountains core complex, Arizona, where strain localization in pseudotachylyte was achieved by linear viscous flow accommodated by grain boundary sliding (GBS). We use both electron backscatter diffraction (EBSD) and atom probe tomography analyses to evaluate the role of hydrous fluids during linear viscous flow by targeting polycrystalline quartz survivor clasts for analysis. EBSD analyses reveal the presence of ubiquitous four-grain junctions, small grain diameters (<5 um), and weak CPO patterns, confirming deformation by GBS. We selected a transect across an EBSD-analyzed survivor clast for subsequent atom probe tomography analysis to characterize the presence and spatial distribution of hydrous fluids. Atom probe tomography analyses on 6 prepared tips extracted from grains along the transect reveal the presence of structural water (OH) within the interiors of all grains. The OH content appears spatially uniform within the volumes of the analyzed tips. In addition, atomic density profiles of Si, OH, SiO and O2 in one of the tips reveal a tube-like structure that bears resemblance to a partially-healed fracture. The apparent partially-healed fracture may be indirect evidence for creep cavitation during GBS, where creep cavities coalesce along grain boundaries to make macroscopic cracks. The partially-healed fracture may indicate self-healing of creep cavitation damage, which may help explain how deformation was sustained within zones of GBS. This

implies that in the absence of this self-healing mechanism, creep cavitation damage may go unmitigated, leading to macroscopic failure and possibly earthquake rupture, consistent with the presence of these survivor clast microstructures within pseudotachylyte.

Using GeoGateway Data to Explore Deformation in the Cajon Pass Region, Megan A Mirkhanian, Lisa Grant Ludwig, Andrea Donnellan, Jay W Parker, and Robert A Granat (Poster Presentation 258)

GeoGateway (http://geo-gateway.org) is a web map-based science gateway supported by NASA's ACCESS program. A goal of GeoGateway is to expand the utility of NASA's geodetic imaging data products by making them easy to access, analyze, and interpret. The objective of this project is to use GeoGateway to explore tectonic deformation associated with recent seismic activity in the Cajon Pass region. The area can be investigated using the Line-of-Sight (LOS) tool which allows us to easily select UAVSAR (Uninhabited Aerial Vehicle Synthetic Aperture Radar) Interferometry data and Global Positioning Satellite (GPS) data via GeoGateway. The Cajon Pass, a fault junction between the San Andreas Fault and San Jacinto Fault (SJF), contains many critical lifeline facilities, and is bounded by the San Bernardino and San Gabriel mountain ranges in southern California. The Cajon Pass is being investigated as a possible "Earthquake Gate", where areas of fault complexity halt earthquake ruptures depending on if the gate is "opened" or "closed." Identification of interseismic strain accumulation and co-seismic slip on faults near Cajon Pass is important for understanding fault system behavior and mitigating damage from earthquakes. We used GeoGateway to search for deformation associated with the 29 December 2015 Mw4.4 Devore earthquake (epicenter 34.191°N 117.413°W) which occurred at depth of ~7.0 km on the SJF, to assess if such deformation can be identified. Using LOS tool for UAVSAR interferometric data display, we found measurable change, but the anthropogenic and hydrologic signals appears to be larger than the tectonic signal, making it difficult to identify tectonic deformation. However, there might be a slight persistent uplift of about 1 mm a year in the Cajon Pass. An elastic forward model of the earthquake shows that the event is too small and far from the Cajon Pass to produce measurable surface deformation, however the observed regional uplift deformation and the occurrence of the earthquake may be reflective of the state of stress of the crust in that region and long-term tectonic motion.

RHEOL_GUI: A Matlab-based graphical user interface for the interactive investigation of strength profiles, Laurent G Montesi, and William Leete (Poster Presentation 150)

As a contribution to the Community Rheology Model we developed an intuitive tool for the exploration and study of strength profile. Built as a Matlab Graphical User Interface, this tool, called RHEOL_GUI, allows the user to define a stratigraphic column, associate to it a temperature profile, taken for example from the CTM, select for each stratigraphic layer rheologies and assumption on pore fluid pressure and grain size, and compute a strength profile. The tool also allows the user to compute an effective rheology (relation between strain rate and integrated strength) for the lithosphere as a whole, which can used for further modeling.

RHEOL_GUI v1.0 is open source and publicly available under the MIT license at https://github.com/montesi/RHEOL_GUI, doi:10.5281/zenodo.1341844. The package contains a database of rheologies, both brittle and ductile, for several rock types, taken from the literature. Grain size can be specified a priori or allowed to adjust to obey one of several available piezometric relationships to address the possibility of weakening the lithosphere at shear zones through grain size reduction.

As a demonstration, we consider an idealized structure of the Mojave tectonic block, composed of a 30 km thick crust (10 km quartzite and 20 km feldspar) over a 70 km thick lithospheric mantle. Brittle failure obeys Byerlee's law, with a maximum strength of 300 MPa, and hydrostatic fluid pressure in the crust. Pore fluid pressure is 20% of lithostatic in the mantle. Diffusion and dislocation creep flow laws are taken from Hirth et al. (2001) for quartzite, Rybacki et al. (2006) for feldspar, and Hirth and Kohlstedt (2004) for olivine. Wet or dry rheologies are used in feldspar and wet rheology (fluid-saturated) for the olivine.

Integrated strength (average viscosity) is highly nonlinear, with an effective stress exponent in excess of 10. That is because, although ductile rheologies have n smaller than ~5, at least half of the stress is supported in the brittle regime. This implies that, with regards to long-term tectonics, even a small change of stress can have a dramatic effect on strain rate. Changing grain size can increase strain rate by about two orders of magnitude, but, especially at low strain rate, the largest effect comes from changing the lower crust rheology from dry to wet, implying that details of mineralogy and hydration state are very important for lithospheric strength.

Modal mineralogy of the continental crust and implications for fault-zone rheology: Data mining the Southern Sierra Nevada exhumed crustal section, Alex E Morelan, and Michael E Oskin (Poster Presentation 149)

We examine the exhumed section from the southern Sierra Nevada to constrain modal mineralogy of batholithic crust as a function of depth, from 6 km to 35 km, for inclusion into the Community Rheology Model. We combine mineralogy data collected by Ross (1987) and paleobarometry data compiled by Chapman et al. (2012) to quantify mineral content with depth and across an east-west compositional gradient. Modal mineralogy of approximately 1500 samples from across the southern Sierra Nevada batholith are reported in the form of small, hand-drawn maps of each pluton body with corresponding handwritten tables listing the modal mineralogy of each sample. In order to mine this dataset, we georeferenced 62 maps of individual plutonic bodies to locate the samples and digitized the associated data tables. We predict paleo-depth for each sample by interpolating paleobarometric data using a kriging algorithm. By integrating these datasets we have a clearer picture of how modal mineralogy changes with depth in the crust over areas of intact batholithic crust, including the Peninsular Ranges batholith where crossed by the Elsinore and San Jacinto faults. We confirm that mineralogy of the batholith changes little over most of its depth extent, consisting of 54 to 59% feldspar, primarily plagioclase (averages reported over 5 km intervals). Rheologically weak quartz and biotite are present throughout the crust, at 21-24% and 9-11% average abundance above 30 km, declining to 14% and 7%, respectively, averaged from 30 to 35 km depth. Rheologically strong hornblende increases in abundance with depth, from 7% to 22%. This unique dataset will be used to test bulk and shear-zone models for the crustal strength.

Rupture Model of the 2016 M5.8 Pawnee Induced Earthquake, Morgan P Moschetti, Stephen Hartzell, and Robert B Herrmann (Poster Presentation 088)

The 2016 M5.8 earthquake near Pawnee, Oklahoma is the largest induced earthquake in Oklahoma and is the largest wastewater-injection-induced earthquake the in the U.S. We invert regional and teleseismic waveforms to produce a rupture model of the time-evolution of coseismic slip. Use of empirical Green's functions for modeling the regional wave propagation allows us to invert waveforms to higher frequencies (0.5-3 Hz) than previous slip models, providing additional information about the evolution of the earthquake rupture and its potential interaction with injection related pore pressure perturbations. The rupture model indicates that slip was largely confined to two-shallow and deep-slip patches. Rupture initiated near 5 km depth, with initial rupture towards the surface and confined within the shallow slip patch. About 1 s into the rupture, our model indicates that slip initiated at a greater depth (z>8 km). About one third of the moment of the earthquake rupture occurred at this greater depth. The relation of coseismic slip to the region of pore pressure perturbation is of great interest for understanding the magnitudes of induced-earthquakes. In particular, some models of maximum magnitude for induced earthquakes assume that earthquakes will be limited to the region where pore pressures are perturbed by industrial activities. The observation that rupture can initiate and propagate outside of regions of pore-pressure perturbation implies that the magnitude of an induced earthquake is not controlled by injection operations. Comparison of the slip model with inferred distributions of pore pressure (from previous coupled hydrologic-geomechanical modeling efforts; Barbour et al., 2017) and with aftershock distributions suggests that the Pawnee earthquake ruptured beyond the zone of perturbed pore pressure influenced by wastewater injection. This observation is consistent with recent numerical modeling work and has important consequences for forecasting the size of and hazards associated with injection-induced earthquakes.

Geometric and Level Set Tomography for Interface Detection in the Near Surface, Jack B Muir, and Victor C Tsai (Poster Presentation 105)

Seismic travel time tomography is a key component of geophysicists' basic toolbox for the characterization of the near surface. Traditional seismic travel time tomography seeks to optimize a field of velocity parameters to fit observed data; this is fundamentally an ill-posed infinite dimensional inverse problem, necessitating smoothing regularization to ensure stability of the inversion. In many instances however, a priori geological knowledge suggests that the subsurface would be better parametrized by subhorizontal (e.g. layered media) or subvertical (e.g. buried fault scarps) interfaces delineating discrete geologic units. Introducing these features into a formal seismic inverse problem in 2 or 3 dimensions requires a flexible and expressive parametrization of the Earth that can incorporate our geologic knowledge, as well as inversion algorithms that can handle this parametrization. We present results using an ensemble Kalman inversion scheme to invert for sharp interfaces in a typical near-surface seismic refraction tomography geometry. We use a mixture of geometric primitives (fault offsets) and the level sets of anisotropic Gaussian fields (undulating layer interfaces) to parametrize the material properties of the subsurface. Synthetic tests on geometries similar to cross-sections perpendicular to the Landers fault show that recovery of sharp interfaces is improved compared to traditional tomographic modeling, without recourse to explicit forward refraction modeling.

Recent spatiotemporal evolution of deformation in the Los Angeles Basin and southern Central Valley of California in the context of anthropogenic activity, Kyle D Murray, and Rowena B Lohman (Poster Presentation 136)

Southern California experiences ongoing crustal deformation associated with tectonic processes such as interseismic fault creep. However, anthropogenic activities, including subsurface fluid extraction, can result in widespread and even larger magnitude deformation signals. We analyze the recent spatiotemporal evolution of deformation in the southern Central Valley and Los Angeles Basin using GPS and Sentinel-1a/b SAR imagery (November 2014 - August 2018). In the southern Central Valley, subsidence associated with large-scale groundwater extraction for agricultural irrigation and municipal use reaches rates as high as 45 cm/yr projected into the the satellite line-of-sight (LOS) during the recent drought (2012 - 2017), with a pause or slowdown in some areas associated with the heavy precipitation in Spring, 2017. We find distinct modulation in seasonal and secular trends that correspond to a complex combination of anthropogenic and natural components of the water cycle. In the Los Angeles Basin, there are numerous fault-bounded and off-fault subsidence features related to fluid extraction reaching rates over 30 cm/yr in the satellite line-of-sight, as well as tectonic fault creep on the San Andreas, San Jacinto, and Elsinore faults with LOS rates of up to ~1 cm/yr.

Characterization of high-wavenumber subsurface random heterogeneity using a very dense array at Diablo Canyon, California, Nori Nakata (Poster Presentation 298)

Characterization of the subsurface random heterogeneity for higher wavenumber is key for high-frequency ground motion prediction. Recent technologies of portable user-friendly geophone arrays are useful for imaging much smaller heterogeneities as velocity perturbations than what regional arrays can do, and we can use such heterogeneities to characterize the randomness of the heterogeneities. At Diablo Canyon, Central California, about 7200 geophones were deployed within a 20x20 km2 area for six weeks in 2011. Here, we apply correlation-based methods to this dataset to extract coherent surface waves in the 0.5--4.0 Hz frequency range and use them for imaging subsurface structure. Note that this frequency range is much higher than previous studies for ambient seismic wavefields. Because of the dense array, we can spatially average seismic data over several sensors to improve the signal-to-noise ratio and extract multiple wave types including P and both fundamental and higher-mode Rayleigh waves. We show that the subsurface velocity model imaged by this array has much higher spatial resolution than that developed from regional arrays with receiver spacing of about 10~20 km, and the heterogeneities are following a von Karman model as similar to what we found in the Long Beach.

Enhancements, Updates, and Improved Access to the Community Fault Model, Craig Nicholson, Andreas Plesch, John H Shaw, and Scott T Marshall (Poster Presentation 145)

Although the Community Fault Model (CFM) is one of the most mature modeling efforts within SCEC and has seen widespread use in many aspects of our science (e.g., UCERF3, ground motion studies, earthquake simulators, rupture modeling, hazard assessment, etc.), it remains critical that the CFM be validated, updated and improved to more effectively support a wide range of community modeling activities targeted by SCEC5. For 2018, we continue to focus on expanding access to the current model and

improving its database component, while developing additional CFM enhancements. This includes completing a formal release of CFM version 5.2, an updated and expanded fault metadata spreadsheet, GIS map trace representations of CFM fault surface traces and blind fault tip-lines, remeshed versions of CFM-v.5.2 fault surfaces at regular-gridded 100 & 500-m intervals, an expanded CFM 3D fault set, and a new formal SCEC CFM webpage available at: https://www.scec.org/research/cfm. The CFM webpage now provides links to the v.5.2 original and remeshed triangulated surfaces, previously reviewed and ranked CFM versions 3.0 and 4.0, as well as a suite of community tools to help evaluate and view the CFM. The expanded CFM database includes linkages between CFM fault geometry and UCERF3 slip rate information, which together with the remeshed CFM surfaces helps support earthquake simulator modeling efforts. The expanded 3D fault set for CFM includes an updated Lytle Creek fault in the Cajon Pass Earthquake Gate Area, an alternative, low-angle Southern San Cayetano fault in the Ventura Special Fault Study Area, down-dip extensions of the east-dipping Thirtymile Bank and Coronado Bank detachments (and potential interaction with the Newport-Inglewood-Rose Canyon fault system), and an updated Santa Susana fault. We are also working on developing additional web-based tools for viewing and evaluating CFM in preparation for a formal community review of CFM-v.5.2. Currently, CFM-v.5.0 is available for 3D viewing by accessing links to the latest version of SCEC-VDO (v.17.8) and an associated README instruction file from the CFM webpage.

Testing the Amplitude of Ambient-field Green's Function by Simulated Scattered Waves in a 3D Sedimentary Basin , Shiying Nie, and Shuo Ma (Poster Presentation 107)

We numerically simulate the scattered waves in a 3D sedimentary basin by using small-scale heterogeneities with 4421 point sources, uniformly distributed surrounding the basin. The simulated scattered wave fields make an ideal environment to test different methods of extracting the amplitude of Green's functions from the random field, as the deterministic station-to-station Green's functions can be computed in the known velocity structure. Our results show that both raw correlation- and deconvolution-based Green's functions extracted from the scattered wave fields match well with the deterministic Green's functions in terms of amplitude and phase, i.e., clear basin amplification is reproduced from either the correlation or deconvolution approach. The data processing methods of the cross-correlation approach—mainly one-bit and whitening—generally worsen the fit between retrieved and simulated Green's function. In a realistic setting where the noise source distribution is non-uniform, however, we expect that both approaches may lead to possible biases in the amplitude of ambient-field Green's functions.

Towards topography in AWP-ODC, Ossian O'Reilly, Alexander N Breuer, Yifeng Cui, Christine A Goulet, and Kim B Olsen (Poster Presentation 293)

A central component for reliable seismic hazard assessment is that models produce good agreements with observations. To match observations at high frequencies (> 1 Hz) it becomes increasingly important to capture the interaction of seismic waves with topography. Therefore, we aim to bring topography support into future seismic hazard computations by adding new capabilities to the fourth-order finite-difference wave propagation solver AWP-ODC (Anelastic Wave Propagation, Olsen-Day-Cui). The AWP-ODC solver is extensively used for seismic hazard assessment within SCEC's Cybershake and High-F projects. The main difficulty that must be addressed here is how to ensure compatibility between the topography support and the AWP internal solver for practical purposes. That is, how to 1) roughly maintain the computational efficiency of the code, 2) limit geometric treatment to only cover the first few km of the upper part of the computational domain 3) deliver accurate computations at a tractable number of grid points per wavelengths (PPW, targeting ~ less than 15 PPW), 4) ensure stability, including at long simulation times, and 5) enable placement of point forces on the free surface (needed for reciprocity computations).

While there are many ways to incorporate topography in FD-based methods, such as immersed boundary methods, vacuum formulation methods, hybrid methods, we have chosen to focus on curvilinear coordinate transforms. Here, topography, in the form of elevation map data, is mapped to a curved grid by applying a 1D coordinate transform in the vertical direction. Our method is based on summation-by-parts (SBP) and is energy conserving. We have derived novel SBP interpolation operators for staggered grids. We investigate how the different formulations perform (e.g., solutions using covariant basis decomposition versus Cartesian), and how the coordinate transform influences accuracy (how deep the transform must reach before it can be coupled to a regular Cartesian grid block).

In a 2D point source simulation of the acoustic wave equation, featuring a Gaussian hill and canyon geometry, we find excellent agreement compared to EDGE (Breuer et. al 2017) at 10 PPW. We also demonstrate that the method is capable of simulating elastic waves in a challenging 2D geometry that samples a cross-section of the San Jacinto Mountains.

Breuer A., Heinecke A., Cui Y. (2017) EDGE: Extreme Scale Fused Seismic Simulations with the Discontinuous Galerkin Method. In: Kunkel J., Yokota R., Balaji P., Keyes D. (eds) High Performance Computing. ISC 2017. Lecture Notes in Computer Science, vol 10266. Springer, Cham

3D models of seismicity beneath the Greater Tokyo Area, Yosihiko Ogata, Koichi Katsura, Hiroshi Tsuruoka, and Naoshi Hirata (Poster Presentation 036)

We consider a 3D models for the short-term forecast beneath the Metropolitan area (Kanto region) by extending the epidemic-type aftershock sequence (ETAS) models, taking account of the induced effect from the 2011 Tohoku-Oki earthquake of M9. Especially, owing to the configuration of the three tectonic plates beneath the Kanto region, location-dependent space-time ETAS model for the seismicity in 3D space (longitude, latitude and depth) down to 100km depth is required. Moreover, we also consider 3D location-dependent b-value for Gutenberg-Richter (GR) law of magnitude frequency. We use the 3D Delaunay-based piecewise linear functions to estimate such parameter functions. Then, based on the long-term hypocenter data beneath the focal Kanto Region, we simultaneously solve the background rates, the aftershock productivity rates, alpha-value of magnitude effects, p-value for the decay rates, b-value of the GR law, and the induced factor from the Tohoku-Oki Earthquake of M9. The optimally inverted 3D spatial image of each of such characteristic parameters represents quite interestingly different characteristics among the volume in shallow crust, and surface boundaries of subducting Pacific Plate and Philippine Sea Plates. Furthermore, the location-dependent

external triggering factor shows how strong or weak the induced effect from the M9 earthquake resulted in and on each zone beneath Kanto Region.

Dynamic rupture and cross-fault activation: the effect of high pre-stress contrast, David D Oglesby, Christodoulos Kyriakopoulos, Thomas K Rockwell, Aron J Meltzner, Michael Barall, and Jon Fletcher (Poster Presentation 206)

The Brawley Seismic Zone (BSZ) is postulated to consist of several cross-faults that are roughly perpendicular to the main fault structures in the area, including the Southern San Andreas (SSAF) and Imperial (IF) fault systems. This geometric configuration provides a natural laboratory to test potential dynamic interactions between cross-faults and adjacent main structures. In particular, we are interested in whether rupture of the main fault segments facilitates rupture of the cross-faults, and vice versa. We run 3D dynamic rupture models of the above system in the BSZ. Under constant traction assumptions, the perpendicularity of the cross faults to the SSAF and IF somewhat limits the dynamic interaction between them, and tends to hinder propagation of rupture from the main structures to the cross-faults. This is true whether the initial shear stress is low or high on the entire system. However, we find out that such interaction is more likely when there is a pre-stress contrast between the SSAF-IF system and the CFs, with the cross-faults pre-stressed at a significantly higher shear stress level than the main segments. This arrangement is plausible because the cross faults are more favorably oriented with the regional stress. With higher slip tendency, they should be closer to a critical stress threshold compared to the SSAF and IF structures. Importantly, it is the contrast in stress that facilitates such cross-fault rupture, not the absolute stress level. Furthermore, activation of the cross-faults can have a significant effect on rupture propagation on the main structures: slip on the cross faults can dynamically clamp one of the main structures, hindering rupture on it. An additional result is that if one of the main structures (the SSAF or IF) is constrained against slipping, rupture of the cross-faults is also facilitated, regardless of stress level. The resulting complex faulting patterns are reminiscent of other geometrically complex earthquakes, such as the Mw7.8 2016 Kaikoura, NZ event.

California Transverse Mercator projection (CATM) for Building Gridded Seismic Velocity Volumes for Seismic Wave Propagation Simulations, David A Okaya, Yao-Yi Chiang, Philip J Maechling, and Mei-Hui Su (Poster Presentation 288)

Numerical computation of seismic wave propagation is a major tool within SCEC community research. From CME's high-end CyberShake and Broadband Platforms down to individual researcher needs for synthetic seismograms, all of these require inputs of 3D seismic velocity earth volumes representing regions within California. A standard procedure to create a gridded velocity volume is to use UTM-based coordinates to define uniformly-spaced rectilinear points. This grid is then used to extract from latitude/longitude-based community velocity models such as SCEC's CVM for southern California. A UTM zone is an independent metric rectilinear coordinate frame that is only 6 longitude degrees wide due to transverse Mercator (TM) projection stretch. Zone 11 (centered at -117W longitude) and Zone 10 (-123W) are widely used for southern and northern CA gridding, respectively.

Central California straddles Zones 10 and 11, and statewide California at -114W to -124W spans both zones. In practice, gridding of these cases is performed using one zone's coordinate frame with results subject to projection stretch. We describe a modified, California-centric TM zone that offers gridding that minimizes projection stretch. Defining a local TM zone needs just four parameters: the centering longitude (central meridian, mandatory) and optional reference latitude and false easting/northing. The simplest version of the California zone ("CATM") is to re-center the zone at -120W (zone "10.5"). An advanced version is to move the central meridian and reference latitude to inside California, such as to -120W, 37N ("CATM-Madera"). Other variations are possible. Other regions that straddle UTM zones and have implemented their own zones include Wisconsin (WTM), Idaho (IDTM83), New Zealand (MZTM2000), and Taiwan (TM2).

In our presentation, we review the selection of UTM zones used in recent key SCEC velocity studies in California, provide background information on the UTM system, and determine projection stretch outside normal zone boundaries. We describe how to define the above CATM versions and how it reduces projection distortion compared to using Zones 10 or 11 for central California and state-wide volumes. We show how to easily implement this projection using Proj, a widely-used projection software library. Community discussion can decide if to use a CATM and if so its specific definition. Alternative projection methods exist such as California Albers and may be equivalent or superior.

Faulty Intuition about b-values and Aftershock Productivity within a Fault Network, Morgan T Page, and Nicholas J van der Elst (Poster Presentation 044)

When it comes to smaller earthquakes, are major faults special? Page et al. (2011) showed that earthquakes near the faults that compose version 3.0 of the SCEC Community Fault Model (CFM) have a lower Gutenberg-Richter b-value than earthquakes elsewhere in Southern California. Here we revisit their result, using newer earthquake data recorded after version 3.0 of the CFM was completed. We find that the correlation between earthquake size and proximity to major faults is not present in the newer seismicity data. This indicates that to some degree the CFM is over-tuned to past seismicity, with some structures related to transient features in seismicity rather than persistent geologic features. We also search for differences in aftershock productivity and foreshock statistics near faults, and find that they are insensitive to distance from major faults as well. Our results suggest that the fault system in Southern California is highly connected, since the chance of an earthquake nucleating on or near a major fault versus on a secondary structure is independent of its final size.

Salton Trough Deformation in GeoGateway Tools, UAVSAR and GeoFEST, Jay W Parker, Gregory A Lyzenga, Andrea Donnellan, Margaret T Glasscoe, Marlon E Pierce, Jun Wang, Magali Barba, and Kristy F Tiampo (Poster Presentation 142)

The southern Salton Trough is the best observed high-deformation zone on the western North American Plate boundary. The GeoGateway toolset and data portal allows access to several measures of deformation as customized layers in a Google Maps environment. Of particular interest for the Salton Trough are UCERF faults, USGS catalog seismicity, UAVSAR repeat-pass interferograms, GNSS station jumps, trends, and series, experimental forecast contours, nowcasting metrics including local Gutenberg Richter plots, and (imported via KML) interferogram-based surface fractures. Analysis of these data shows a possible Cerro Prieto fault precursor to the EMC 2010 Mw7.2 earthquake, distributed EMC-induced deformation in the Imperial Valley,

triggered slip on major regional faults including the far-south San Andreas, a rich network of 1-10 cm slipping faults in the Yuha Desert, long-term afterslip in the Ocotillo region, and measure of seismic and aseismic faults slipping in the Brawley Swarm. Finite element modeling of the main faults is carried out with the GeoFEST modeling system, to be expanded for Green's function inversions of slip.

The Hidden Past of the Alai Valley: Understanding the Seismic History and Behavior of the Central Pamir Frontal Thrust System through Paleoseismology., Magda Patyniak, Angela Landgraf, Ramon Arrowsmith, Atyrgul Dzhumabaeva , Alana M Williams, Kanatbek Abdrakhmatov , and Manfred Strecker (Poster Presentation 241)

The Pamir–Tien Shan convergence zone represents a major tectonic part of the Indian-Eurasian collision zone by accommodating nearly one-third of the total 44 mm/yr total shortening in the greater Pamir region. These high deformation rates across relatively short distances compared to other intracontinental orogenic settings drive strain release with resulting large-magnitude earthquakes of up to M7 or higher. In comparable intraplate settings, deformation patterns are expected to be complex and distributed in space and time, the earthquake recurrence intervals are long, and rupture behavior often associated with reactivation of pre-existing crustal anisotropies.

In the Pamir mountains, however, GPS data show that the highest shortening rates across the greater Pamir-Tien Shan collision zone are observed along the northward-propagating Pamir Frontal Thrust system (PFT), the northern most arc-shaped boundary of the Pamir orogen with an intermontane basin – the Alai Valley - separating it from the Tien Shan mountains to the north. Extensive studies of temporary seismic networks across the PFT underline the recent seismic activity and distribution of shallow and intermediate-depth earthquakes. However, modern seismicity patterns do not fully explain the relation between seismicity and surface rupture behavior, nor the detailed rupture zone geometry and might thus not reflect the long-term deformation history.

Our paleoseismological study presents preliminary data and new slip rate estimates for different late Quaternary timescales from trenches along the central segment that is characterized by the geomorphological youngest thrust zone of the PFT. This fairly straight sector of the mountain front comprises several uplifted fluvial terraces in the hanging wall, and hosts fault scarps with colluvial wedges suggesting multiple seismic events in the recent past. We combined high-resolution structure-from-motion analysis of offset stratigraphic horizons in the trenches with UAV-based DEM analysis and dGPS profiling of displaced landforms. Our earthquake chronology is supported by representative radiocarbon and luminescence dating of distinct event horizons.
We were able to define at least 4 seismic events that offset alluvial-fan strata of the Pamir mountain front. These new data provide new insights into the late Quaternary earthquake history and ultimately help to refine the earthquake recurrence times along the central segment of the PFT.

Developing Software to Support SCEC Research Collaborations and Data Dissemination: A Case Study of the Committee for the Utilization of Ground Motion Simulations (UGMS) Project, Edric Pauk, Tran T Huynh, Kevin R Milner, Scott Callaghan, David Gill, Christine A Goulet, and C.B. Crouse (Poster Presentation 297)

Extremely large and complex datasets can be generated as a result of scientific research investigations. However, making these datasets easily accessible and usable for a wider community remains a challenging goal. The SCEC Committee for the Utilization of Ground Motion Simulations (UGMS) provides a useful case study on how such challenges can be overcome when researchers and software programmers collaborate to build tools that prioritize the end-user's needs. The result can be the dissemination of curated datasets for use by a broader community who can benefit from access to such peer-reviewed data for varied purposes, rather than only the researchers working on the project.

In 2013, the SCEC UGMS Committee was tasked to develop long-period response spectral acceleration maps for inclusion in revisions of the Los Angeles City building codes. The maps would be based on ground motions computed using 3D numerical ground-motion simulations (SCEC CyberShake) and latest empirical ground-motion prediction equations (PEER NGA). The Committee identified the need for a web-based data access tool to allow engineers to obtain site-specific data without the need to engage with esoteric software or to interact directly with extremely large datasets. The Committee worked with end-users and research programmers (1) to establish a methodology for developing response spectral acceleration maps that integrates numerical and empirical methods, (2) to determine target sites and datasets, (3) to perform post-processing calculations and analyses, and (4) to define what data would be outputted and how it should be displayed. Clearly defined data formats and input/output parameters ensured data delivered through the software was valuable to the engineers using the datasets. The data access tool was released in 2018 and is available through https://www.scec.org/research/ugms. This site documents the UGMS Committee process and the data access tool, and provides information on the project team, meetings, and publications.

The lessons learned from developing the SCEC UGMS data access tool can be applied to support research data dissemination for other SCEC projects. The close collaboration between scientists, research programmers, and end-users are critical to the software project success. When large datasets are well curated, and the use cases clearly defined, software can be better developed to support a broader community access to research data and information.

Paleoseismology of the central Garlock Fault in Searles Valley, California., Kyle Peña, Sally F McGill, Ed J Rhodes, James F Dolan, Robert Zinke, Alexandra E Hatem, and Nathan D Brown (Poster Presentation 239)

In this study, a paleoseismic trench that was previously excavated by McGill, [1992] across the central Garlock Fault near Christmas Canyon, in Searles Valley, California, was reopened to investigate potential temporal variability in earthquake recurrence on the Garlock fault. In a trench near El Paso Peaks, ~ 33 km west of Christmas Canyon, Dawson et al., [2003] observed four closely spaced earthquakes in the past 2 ka, preceded by a 3,000-year gap in which there were no earthquakes recorded in the paleoseismic record. We seek to discover whether a similar pattern of earthquake occurrence is recorded at Christmas Canyon. The original trench at Christmas Canyon provided a record of at least four prehistoric earthquakes, but contained only one sample suitable for radiocarbon dating methods. To provide age constraints on the paleo-surface-rupturing events from the new trench, we collected 54 luminescence samples and will employ the single-grain luminescence dating technique post-IR_50-IRSL_225. The

re-excavated trench at Christmas Canyon was 32 m long and 3.5 m deep. The trench exposed interbedded alluvial sand and pebble-gravels, with well sorted, rounded, lacustrine sand present at the base of the trench. The lacustrine sand is inferred to have been deposited during the latest highstand of pluvial Lake Searles at c. 10 ka. Preliminary findings suggest eight to thirteen surface rupturing earthquake events occurred since the deposition of these lacustrine sands. Event ages from this trench will be compared to published earthquake ages from other trenches and to ages from geomorphic features offset in recent prehistoric earthquakes along the central segment of the Garlock fault. Comparison of earthquake ages from the Christmas Canyon trench to ages of these locally offset geomorphic features will enable us to infer the number of earthquakes associated with the offset of each of those features and to calculate incremental slip rate estimates.

Urban Nodal Array Maps Structure of the Northern Los Angeles Basins with Teleseismic Receiver Functions, Patricia Persaud, Guibao Liu, and Robert W Clayton (Poster Presentation 276)

Earthquake ground motions in the greater Los Angeles area are known to be affected by basin amplification and the channeling and focusing of seismic energy as it passes through the San Gabriel and San Bernardino basins in the northern part of this region. Accurate representations of basin shape and depth are therefore key for providing realistic estimates of basin amplification. Various studies have provided improvements to the shape of the northern basins, e.g., using gravity modeling, through finite difference simulations of ground motion and with active source seismic profiles across the San Bernardino basin. However, the current Southern California Earthquake Center velocity model, CVM-S4.26, still lacks sufficient detail on the structure of these basins.

To help increase the accuracy of ground shaking models for the Los Angeles area, we use an urban array of 384 nodal geophones. Our data set is comprised of teleseismic events recorded along three transects in the greater Los Angeles area in 2017 and three additional transects collected in 2018. In each year, the instruments recorded for ~35 days. We have computed receiver functions along the three 2017 profiles to map the depth and shape of the sediment-basement interface and to identify possible deep fault offsets (Liu et al., 2018). The results show the Moho discontinuity, the bottom of the basement, and intermediary sedimentary layers. There are also indications of mid-crustal offsets along strike of the Red Hill and Raymond Faults. The results are compared to receiver functions from nearby permanent broadband stations and the 1993 LARSE experiment. The images show that dense deployments of node-type sensors can be used to investigate structure at the basin scale in a noisy urban environment, and therefore have potential value for seismic hazard studies

Liu, G., P. Persaud and R. W. Clayton (2018), Structure of the Northern Los Angeles Basins Revealed in Teleseismic Receiver Functions from Short−Term Nodal Seismic Arrays. Seismological Research Letters. http://dx.doi.org/10.1785/0220180071

Dynamic rupture modeling to investigate the role of fault geometry in jumping rupture between parallel-trace thrust faults, Paul L Peshette, Julian C Lozos, Doug Yule, and Eileen L Evans (Poster Presentation 209)

Fold and thrust belts (such as those found in the Himalaya or California Transverse Ranges) consist of many neighboring thrust faults in a variety of geometries. Active thrusts within these areas individually contribute to regional seismic hazard, but there is also possibility of multi-fault rupture in a single event. Investigations of historic thrust surface traces suggest that within a single event rupture can jump from one fault to a separate fault up to 8 km away. There is also observational data of jumps occurring between thrust faults ~50 km apart. In contrast, previous modeling studies of thrust faults find a maximum jumping rupture distance of merely 0.2 km. Here, we present a new dynamic rupture modeling parameter study that attempts to reconcile these differences and determine which geometric and stress conditions promote jumping rupture. We use a community-verified 3D finite element method to model rupture on pairs of thrust faults with parallel surface traces and opposite dip orientations. We vary stress drop and the dimensionless strength ratio to determine which conditions produce jumping rupture at different dip angles and different minimum distance between faults. We find that geometry plays an essential role in determining whether or not rupture will jump to a neighboring thrust fault. Rupture is more likely to jump in faults oriented dipping toward one another at steeper angles, and the behavior tapers down to no rupture jump in shallow dip cases. Our variations of stress parameters emphasize these toward-orientation results. Rupture jump in faults dipping away from one another is complicated by variations of stress conditions, but the most prominent consistency is that for mid-dip angle faults rupture rarely jumps. In most of our models, rupture does not jump beyond 3 km, while some reach 5 km, and in one unique dipping away case rupture jumps beyond 20 km (potentially much farther). If initial stress conditions are such that they are already close to failure the possibility of a long distance jump increases. Our models call attention to specific geometric and stress conditions where the dynamic rupture front is most important to potential for jump. However, our models also highlight the importance of near-field stress changes due to slip. According to our modeling, the potential for rupture to jump is strongly dependent on both dip angle and orientation of faults.

Causes of deaths and injuries in the 2015 Gorkha (Nepal) earthquake , Marla A Petal (Poster Presentation 317)

The Mw7.8 April 25, 2015 Gorkha Earthquake took place on a Saturday, at 11:56am and reached maximum intensity of IX (MMS). The earthquake and its aftershocks killed more than 8,800 people and injured more than 22,000. There is urgent need to better understand protective actions for earthquakes in Nepal and elsewhere. Future earthquakes in Nepal are expected to have more devastating impacts, in the absence of more robust, extensive, and well-coordinated programs of public awareness, and facilitation of risk mitigation. The purpose of this study was to identify the causes of injuries and deaths, to provide a scientific basis for education and training of the public, and to add to the global body of knowledge about earthquake epidemiology.

The survey was conducted 11 months after the earthquake, among 500 households in 10 of the hardest-hit villages located in 5 of the 14 hardest-hit districts. The households surveyed had 1,855 members present at the time of the earthquake: 88% were uninjured, 10% were injured, and 2% died. Most of the households sampled were stone and brick masonry construction, referred to as gārowālā (as distinguished from pillarwālā construction which is typically reinforced concrete or masonry and has a frame or columns).

Research questions were:

- What specific risk factors are associated with injuries of different severity?

- What hazards in the built environment and building typologies have specific risks for human casualties?
- What specific risk mitigation efforts will decrease deaths and injuries?
- What specific behavior during and after an earthquake may decrease deaths and injuries?
- How important is rapid search and rescue and medical treatment to injury outcomes?
- What disaster preparedness measures are identified by earthquake survivors as both feasible and effective?

Significant findings are organized around:

- The hazard (shaking frequency, ground acceleration, and ground displacement)
- Individuals and behavior
- The buildings
- The injuries
- Protective action
- Mitigation and preparedness measures

Based on the findings, key recommendations were developed for individuals and households covering: situational risk awareness, assessment and planning, risk reduction, and response preparedness as well as recommendations for the scientific and advocacy community for public discussion and consensus-building.

SCFM 3.1: Updates, maps and modeling support, Andreas Plesch, John H Shaw, . SCFM Working Group, and Craig Nicholson (Poster Presentation 144)

We present an updated and enhanced version of the northern California Statewide Community Fault Model (SCFM-V.3.1). The updated model includes improved 3d fault representations, a new GIS trace map fully consistent with the 3d model, and a set of triangular meshes of fault surfaces more suitable for numerical modeling applications.

Based on generous feedback resulting from an earlier workshop on evaluating and ranking the SCFM, we could improve on a series of fault models focused on the offshore Hosgri-San Simeon fault zone, the offshore San Gregorio fault zone and parts of the San Andreas fault zone. Notable additions include the offshore eastern Monterey Bay and Gualala faults, both tens of kilometers in length and in close proximity to the coast.

To allow for convenient map access to the 3D model, we extracted the fault surface traces and blind fault tip-lines from the 3d fault representations and made those available in GIS compatible formats. The expected use allows for layering these maps on existing maps for evaluation and comparison purposes, as for example to assess the degree of model generalizations for a given fault, or its proximity to a large urban population.

The native tsurf 3d representations of the fault geometry are based on the availability and resolution of the data used to evaluate and eventually construct a given triangular mesh. Therefore, the native meshes reflect these conditions and are often not directly suitable for numerical modeling applications which have conflicting requirements on the properties of a triangular mesh. It is possible to retriangulate with high fidelity the native tsurf representations using various methods. Thus, in addition to the native 3D fault models and in an effort to support efforts seeking to utilize the SCFM in a variety of numerical modeling environments, we also provide a set of remeshed 3D fault surfaces with higher quality, regular-gridded triangular elements of ~1-km dimension. In further modeling support, we demonstrate use of Extensible Markup Language (XML) to encode fault geometry and fault meta-data into the general purpose, ISO-defined, 3d graphics format X3D.

New Constraints on Stress Heterogeneity along High Risk Fault Systems in the Santa Barbara Channel, California from Borehole Breakouts, Edward H Pritchard, Patricia Persaud, and Joann M Stock (Poster Presentation 153)

The Santa Barbara Channel represents the offshore portion of the Ventura Basin in Southern California. Miocene extension and ongoing transpression related to a regional left step in the San Andreas Fault have led to the formation of highly complex, active structures beneath the channel. Recent studies have suggested that faults within the northern region of the channel could be capable of a multisegment rupture and producing a Mw 7.7–8.1, tsunamigenic earthquake. However, the level of structural complexity and stress heterogeneity that would limit earthquake rupture in this region are still undetermined.

We use oriented 4-arm caliper data from 18 deviated wells (depths < 1800 m) obtained from industry to identify borehole breakouts beneath the Holly and Gail oil platforms in the Channel. A misfit-based forward modeling technique is used to determine the best fit stress regime and provides quantitative constraints on the orientations and relative magnitudes of the three principal stresses beneath the platforms. At platform Gail, we determine a thrust faulting stress regime with an SHmax trending N44°E. Our results are consistent with local structures, which reflect deeper regional scale trends, and with similar studies onshore nearby. We also determine a thrust faulting stress regime at platform Holly, located in the structurally complex north channel region. Our SHmax orientation of N55°W differs from previous studies onshore and offshore to the west. But, both our results and those of previous studies are consistent with the complex changes in fault strike within the Pitas Point-North Channel-Red Mountain fault systems. One important finding from our study is that borehole breakouts may record stress on a localized scale, allowing stress heterogeneity to be recognized where other methods may fall short. Our results also provide ground truth for future modeling efforts seeking to test the influence of in-situ stress variability on estimates of maximum earthquake size.

Dear Prudence: how many surface clasts are required to yield an accurate exposure date?, Veronica B Prush, and Michael E Oskin (Poster Presentation 231)

Prush and Oskin (submitted) propose a new statistical model for determining the exposure age of offset fluvially deposited surfaces dated using surface clasts. Our model requires fitting a generalized Pareto distribution (GPD) to these datasets, rather than the commonly assumed Gaussian distribution, to model the inherited component of exposure age. In our study we use a Monte Carlo Markov Chain algorithm to fit the GPD model to published Beryllium-10 datasets that include 8 or more surface clasts. Such small sample size reflects current sampling practices and allows us to analyze 64 published sites. Unfortunately, such small sample sizes

are inadequate to recover the true distribution of inheritance, and thus limits prediction of surface age. To determine the number of clasts required to adequately sample the GPD, we use our algorithm to recover the age and other fit parameters from populations of clast ages randomly drawn from a known distribution. Our results suggest that approximately 20 clasts are required for the expected value from 50% of the synthetic tests to fall within 1 kyr of the true surface age. Out of all published datasets surveyed, only 6 10Be surface clast datasets meet this rigorous requirement, two of which are from California. However, only ~15 clasts are required to determine the surface age with 95% confidence. Though it is preferable to sample and date as many clasts as possible depending on the unique time and financial constraints of a study, we show that there are diminishing returns to including additional samples, and that statistically meaningfully ages can be determined with ~15 clasts.

Multi-scale study of ground motion coherence in Piñon Flats Observatory, Lei Qin, Christopher W Johnson, Frank L Vernon, and Yehuda Ben-Zion (Poster Presentation 299)

Characterizing ground motions between closely spaced broadband stations can reveal new insight on variations in the crustal response to earthquake, seasonal and ambient sources of seismic energy. We study the coherence using three years (2015-2017) of continuous waveforms from the Piñon Flats Observatory Array (PY). The array includes 13 broadband sensors arranged on three circles with station separated by about 65m, 330m, and 780m. The examined data include ambient noise and earthquake signals from local and teleseismic sources recorded by PY sensors. The coherence values are sensitive to signal source properties, local structures and sensor performance. The ambient noise coherence remains high in the 0.1-1.0 Hz band if the interstation distance is small (<65 m), and decreases quickly outside the dominant frequency band with increasing station distances. The horizontal coherences are reduced to ~0.2 at frequencies <0.1 Hz likely due to interstation ground tilt. The noise coherence in 1-10 Hz band is affected by incoherent high frequency signals including anthropogenic activities and local earthquakes. The local earthquake signals exhibit high coherence up to 50 Hz, while the teleseismic waves increase the coherence in the low frequency band (<0.1 Hz). In addition, high-coherence (>0.95) frequency bands in the two horizontal components exhibit seasonal variations likely related to strains associated with ocean loading and thermoelastic deformation. The coherence signals at PY contain anomalies in ~2-4 Hz band starting 30 days before the 2016 Mw5.2 Borrego Springs earthquake; however, careful analysis indicates that they result from anthropogenic activities and not precursory earthquake signals.

Eikonal Tomography of the Southern California Plate Boundary Region , Hongrui Qiu, Yehuda Ben-Zion, and Fan-Chi Lin (Poster Presentation 100)

We use eikonal tomography to derive directionally-dependent phase and group velocities of surface waves for the plate boundary region in southern CA sensitive to the approximate depth range 1-20 km. Seismic noise data recorded by 346 stations in the area provide a spatial coverage with ~5-25 km typical station spacing and period range of 1-20 s. Noise cross-correlations are calculated for all 9 components data recorded in year 2014. Rayleigh wave and Love wave group and phase travel times are derived for each station pair using frequency-time analysis. For each common station, all available phase and group travel time measurements with sufficient signal to noise ratio and envelope peak amplitude are used to construct a travel time map for a virtual source at the common station location, respectively. By solving the eikonal equation, the propagation direction is evaluated as the normal vector at each location for each virtual source in the phase travel time map, and then phase and group velocities are estimated along the propagation direction. Isotropic phase and group velocities and 2- psi azimuthal anisotropy and their uncertainties for periods in the range 2-16 sec are determined statistically using measurements from different virtual sources. By using the CVM-S4.26 constructed in Lee et al. (2014) as starting model, the obtained phase and group dispersions of Rayleigh and Love waves are then jointly inverted on a 0.05° x 0.05° grid for local 1D piecewise shear wave velocity structures with the algorithm of Hermann (2014). The results are consistent with previous observations of Zigone et al. (2015) and other tomography results in the overlapping area. Compared with the CVM-S4.26, our final model is able to resolve structure above 5 km with better resolution and shows lower shear wave velocity in the top 5 km, particularly in areas such as basins and fault zones. The results also show clear velocity contrasts across the major faults, such as the San Andreas, San Jacinto, Elsinore and Garlock faults, and suggest that the San Andreas Fault southeast of San Gorgonio Pass is dipping to the northeast.

Multi-physical couplings and microstructure size effects on the localization of deformation in a fault core, Hadrien Rattez, Ioannis Stefanou, Jean Sulem, Manolis Veveakis, and Thomas Poulet (Poster Presentation 204)

Seismic slip in the brittle part of the lithosphere is often accompanied by extreme shear strain localization into a narrow, thin zone, which is called Principal Slip Zone (PSZ). According to field observations, the PSZ has a finite thickness and varies from hundreds of microns to few centimeters. The size of this zone plays a major role in the mechanism of earthquakes as it affects the energy budget of the fault core and its stability.

We model here the creation of shear bands inside fault gouges considering the effect of microstructure by resorting to elastoplastic Cosserat continua and Thermo-Hydro-Chemo-Mechanical couplings. The use of Cosserat theory not only enables to regularize the problem of localization by introducing an internal length into the constitutive equations, but at the same time it introduces information about the size of the microstructure.

The results obtained with numerical simulations are compared with experimental and in situ observations for the shear band thickness and the fracture energy. It enables us to understand the role of various phenomena on the behavior of a fault, such as thermal pressurization, flash heating and the size of the microstructure, among others on the thickness of the band but also on the stability of the system.

Geomorphic and structural mapping in pursuit of a slip rate for the Santa Susana Fault, Southern California, Michael P Reed, Reed J Burgette, Katherine M Scharer, Nathaniel Lifton, and Devin McPhillips (Poster Presentation 257)

The Santa Susana Fault (SSF) is a 38-km-long thrust fault that connects active faults along the margins of the Ventura and San Fernando basins within the Western Transverse Ranges of southern California. Despite proximity of the SSF to metropolitan areas, the slip rate on the SSF remains very uncertain; the highest rate (10 mm/yr) comes from structural reconstructions and the lowest

rate (0.5 mm/yr) is an estimate based on the lack of fresh geomorphic offsets along its trace. Working towards a more robust late Quaternary slip rate, we have characterized the geology and topography of the SSF utilizing lidar datasets, photogrammetrically-derived DEMs from 1920-30s pre-development aerial photographs, and field surveying and mapping. We focused on an area along the west-central SSF north of Simi Valley where a set of alluvial fans is offset by the fault. Vertical separations are ~24 m for the fan surfaces, and a minimum of ~22 m for the underlying alluvium/bedrock contact. Age results from 36Cl cosmogenic nuclide depth profile samples of the offset fan surfaces will assist in correlating alluvial fan surfaces and yield the first late Quaternary slip rate for the SSF derived from modern chronologic techniques. The geomorphology of the footwall valley indicates a period of widespread incision followed by aggradation, producing flat-bottomed valleys inset into the alluvial fan margins. This history suggests a complex interaction between local tectonics and/or climatic changes, which we examine through quantitative analysis of stream channel geometry. Preliminary analysis indicates a modest decrease in normalized channel steepness along the western half of the fault, which may reflect interactions with other faults to the south. Better understanding the tectonic regime, as well as constraining the slip rate for the SSF, will assist earthquake hazard forecasting for southern California and reveal the spatio-temporal patterns of sedimentation and erosion associated with tectonism for the Western Transverse Ranges.

Are offset channels accurate representations of strike-slip fault displacement? Implications from landscape evolution modeling, Nadine Reitman, Karl J Mueller, Gregory E Tucker, and Katherine R Barnhart (Poster Presentation 227)

Strike-slip fault slip rates are commonly determined by correlating offset channels and dating the incised deposits. This approach is complicated by large uncertainties in pre-faulted channel morphology and temporal variation of stream incision, stream capture, and channel abandonment. In this study, we use landscape evolution modeling to investigate how slip frequency, fault zone width, and oblique slip influence fault zone geomorphology and the apparent channel offset distance. We model evolution of a theoretical channelized landscape in response to progressive lateral shear in a variety of strike-slip tectonic settings. Models are run for 100 ka, accumulating 300 m of lateral displacement. The explored parameter space includes slip frequency (continuous small displacement events vs. infrequent large displacement events), fault zone width (0–1000 m), and oblique slip (uplift by 0-50% of lateral slip). We evaluate the differences between final topography by comparing channel pixel aspects (fault-parallel vs. fault-perpendicular) and ridge connectivity across the fault zone and model domain. Preliminary results suggest that fault zone width plays a larger role in determining fault zone geomorphology than slip frequency. Diagnostic patterns of fault zone width are readily preserved in the landscape, whereas indicators of slip frequency are subtler. Modeled offset channels were then measured and compared to the prescribed slip amount as a test on our ability to accurately correlate and measure offset channels from digital elevation data. We find that offset channels are rarely reconstructed to within error of the total or per-event slip amounts, especially for fault zone widths > 100 m. This study provides insight into how slip frequency and fault zone width are recorded in the landscape within 1-2 km of a strike-slip fault, and highlights how these complexities can affect our ability to accurately measure channel offsets. In the future, these models can be modified by varying soil transport and channel incision parameters to investigate the roles that lithology and climate play in modulating channel preservation and fault zone morphology.

Fast moment acceleration in the development phase of an earthquake derived from a large catalog of Source Time Functions, Julien Renou, and Martin Vallée (Poster Presentation 074)

The earthquake source physics giving rise to events of very different magnitudes remains debated. Features in the initiation phase carrying information on the final magnitude have been proposed. Conversely, in the cascade model, the rupture grows in a magnitude-independent way, implying that the final seismic moment M_0 is controlled by the earthquake duration. The characteristics of the accelerating phase of the rupture process (hereafter mentioned as ``development phase'') provides insights on these competing hypotheses and can help to constrain the rupture dynamics.

Our study aims at observing the development phase using the SCARDEC database, a global catalog containing more than 3000 Source Time Functions (STFs) of earthquakes with magnitude $M_w > 5.7$. The method consists in computing the STFs slope, i.e. the moment acceleration, at several prescribed moment rates. In order to ensure that the chosen moment rates intersect the development phase of the STF, we select in all STFs the window in which the signal is both not too low and not too close from the peak. This approach does not use any rupture time information, which is interesting as (1) the exact hypocentral time can be uncertain and (2) the main rupture expansion can be delayed compared to origin time. Thus, even if the times at which rupture strongly develops vary a lot, the method always isolates the development phase.

First results do not exhibit variations of the slope with magnitude. However, our method clearly points out that slope values fastly increase with the moment rate, which leads to a moment in the development phase growing quicker than cubically with time. The existence of such a local fast-growing phase, together with other time windows of the STF where the rupture is less efficient, are qualitatively consistent with the classical scaling $M_{0} \propto T^3$ observed for the whole rupture duration T. We finally create a synthetic STF catalog integrating the properties of the development phase and reproducing the real SCARDEC catalog diversity. Consistently with previous studies, our median of synthetic STFs tends to have a linear growth. As none of the individual synthetic STFs develop linearly, this observation is understood to result from the large diversity of the STFs shapes, and its physical interpretation has therefore to be done with care.

Towards Structural Imaging Using Scattering Artifacts Detected in Ambient Field Correlations, Lise Retailleau, and Gregory C Beroza (Poster Presentation 304)

Correlations of the ambient seismic field have been used successfully for tomographic imaging of the Earth on a wide range of scales. This is based on the theoretical and experimental observations that correlation functions computed between the signals recorded by two stations contain an approximation of the impulse response (Green’s function) between these stations.

The waves that comprise the ambient field are subject to scattering due to the heterogeneous earth which can generate supplementary arrivals on the correlations functions. It is possible to use these effects of scattering that do not correspond to the propagation between the two stations considered, to locate potential external sources of signal.

or this analysis, we use correlation functions computed from continuous signals recorded between 2001 and 2017 by seismic stations in Central California. We identify supplementary arrivals in the correlation functions and use array analysis to map the source of scattering effects linked to strong structural variations.

We are particularly interested in imaging scatters that result in coupling between the P-SV and SH systems because they are a consequence of lateral heterogeneities in Earth structure. For that reason, we particularly focus on components of the correlation tensor, different from the Vertical-Vertical component, and we expect the Radial/Vertical to Transverse components to be particularly helpful.

Improved medium-term earthquake forecasting: Compensating for incomplete contributions of precursory earthquakes, David A Rhoades, and Annemarie Christophersen (Poster Presentation 050)

The EEPAS earthquake forecasting model treats Every Earthquake as a Precursor, According to Scale, of larger earthquakes to follow it in the medium term. It applies empirical predictive relations derived from examples of the precursory scale increase phenomenon to estimate the contribution of an individual precursory earthquake to the future earthquake occurrence rate density at any future time, magnitude and location. The contributions of precursory earthquakes are complete, for a given target earthquake magnitude and future time, if all earthquakes that could contribute to the earthquake occurrence rate density at the target time and magnitude are included in the catalog. If there is a time-lag between the time of the forecast and the target time, then contributions from precursory earthquakes will be incomplete because earthquakes expected to occur during the time-lag will be missing from the catalog. The EEPAS model will therefore tend to under-predict the rate density of earthquakes unless the forecast is compensated for the incompleteness of precursory earthquake contributions. We estimate the completeness of the precursory earthquake contributions at a given target magnitude when forecasting with a given time lag. We also consider two end-members for compensating for incompleteness, by augmenting (1) only the time-varying component, and (2) only the time-varying background component, of the EEPAS model. Using the New Zealand earthquake catalog, we derive an optimal combination of these two end-members for each target magnitude and time lag, and illustrate the effect on forecasts of major earthquakes in central New Zealand using the earthquake catalog up to 2018 to make forecasts with time-horizons out to 2030.

Envelope-Based Early Warning Algorithm Using Nested Grid Search, Becky Roh, Thomas H Heaton, and Zachary E Ross (Poster Presentation 065)

We present an envelope-based algorithm that implements a nested grid search. This algorithm is a direct solution that is simple to implement in parallel execution. The goal is to predict the magnitude, location, and origin time of an event using a probabilistic approach, based on Cua-Heaton ground motion prediction equations. A unique aspect of this algorithm is that it will be valuable for complex sequences, such as foreshocks and mainshocks that are closely spaced in time.

Grids in consideration are magnitude, latitude, longitude, and origin time. These grids depend highly on the information given by the first-triggered station (for it is assumed to be the nearest to the epicenter). At each grid point, observed and predicted envelopes are calculated and compared in a goodness-of-fit test. The predicted envelopes we use are the Cua-Heaton ground motion envelopes. They are combinations of noise, P-, and S-wave envelopes as a function of magnitude, epicentral distance, and soil conditions. Nested within this grid search is another search of previous recorded events from the catalog. These envelopes are also considered in the goodness-of-fit test.

Likelihoods are quantified to find the parameters that give the best fitting envelopes. We look at results for each station, intensity measure, and component. We also examine the sensitivity of the grid search predictions to different conditions, such as station density and discriminant for P- and S-waves.

A long-term-average estimate of earthquake likelihoods and the largest earthquake in central Los Angeles, Chris Rollins, and Jean-Philippe Avouac (Poster Presentation 134)

Thrust earthquakes present a substantial hazard to Los Angeles, and geodetic data suggest that major thrust faults underlying the city are accruing elastic strain that may be released in future earthquakes. To quantify this hazard, we express this strain accumulation as the buildup rate of a deficit of seismic moment, 1.6 +1.3/-0.5 x 10^17 Nm/yr in total, and assume that on the long-term average, 1) this is also the total rate at which seismic moment is released in earthquakes and 2) those earthquakes obey a log-linear magnitude-frequency distribution up to a maximum magnitude that they do not exceed. We generate a comprehensive suite of long-term-average earthquake rate models satisfying these criteria, vet each model by evaluating how likely it would be to have produced the magnitude-frequency distribution of earthquakes in the 1932-2016 instrumental catalog in Los Angeles, and use these likelihoods to estimate the probability density functions of long-term-average earthquake likelihoods and the maximum earthquake. We estimate a maximum magnitude of Mw=6.8 +1.05/-0.4 or Mw=7.05 +0.95/-0.4 depending on the nature of the assumed magnitude-frequency distribution. The occurrence rates of small and moderate earthquakes in the best-fitting models are similar to the instrumental catalog. We show how these models can be used for probabilistic seismic hazard assessment to estimate, for example, the probability of observing an earthquake of or exceeding a given magnitude within a given timespan.

Detecting millions of earthquakes in southern California with template matching, Zachary E Ross, Egill Hauksson, Daniel T Trugman, and Peter M Shearer (Oral Presentation Tue 14:00)

Over the last twenty years, earthquake detection rates in southern California have improved dramatically, resulting in the minimum magnitude of completeness decreasing from M~2.5 to M~1.5 today. It is believed, however, that these events still constitute less than 10% of all activity that is being recorded by the seismic network on a regular basis. To address these shortcomings, we applied a matched filter (template matching) algorithm to the entire continuous waveform archive of the Southern California Seismic Network using the seismograms of ~300,000 past events as templates. This GPU supercomputing effort resulted in a catalog of ~2.4 million earthquakes for the period 2008-2017, which is ~13 times as many events as the standard regional catalog, and has a completeness magnitude of ~0.5. The recent double-difference GrowClust algorithm was applied to the entire dataset and its 1.3 billion differential times, resulting in state-of-the-art hypocenter precision for the whole of southern California. I will first discuss basic

summary information about the catalog and new regional-scale observations. Then, I will focus on the most active sequences that occurred during the period and use the seismicity to investigate connections between properties of fault zones and the earthquake rupture process. The unprecedented level of detail in this next-generation seismicity catalog is expected to facilitate important new analyses of earthquakes and faults in southern California.

Implementation of Iwan-type Plasticity Model in AWP-ODC, Daniel Roten, Kim B Olsen, Steven M Day, and Yifeng Cui (Poster Presentation 019)

Strong ground motions recorded on vertical arrays indicate that site response formalism (decoupled from source and path effects) fails to reproduce empirical surface-to-borehole transfer functions in the majority of cases due to the presence of lateral heterogeneities. These observations motivated one of SCEC5's research priorities and the creation of a Technical Activity Group, with the goal of understanding ground motions as the coupled response of inelastic off-fault and shallow nonlinear behavior.

We have implemented an Iwan-type nonlinear model in the CPU version of the 3D finite difference (FD) wave propagation code AWP-ODC (AWP-Iwan) which captures the stress-strain relationship of shallow crustal material (weathered rock and sedimentary deposits) more accurately than a single Drucker-Prager yield surface used in past scenario simulations. The code reproduces Masing re-loading and unloading behavior by tracking an overlay of individual von Mises yield surfaces arranged in a parallel-series configuration. Because AWP-Iwan needs to store the stress tensor, the Lamé parameters and the yield stress pertaining to each surface, the implementation requires major changes in the code's computation and communication routines, and results in significantly increased computational and memory costs compared to simulations using a single yield surface.

To verify the method against established 1D and 2D nonlinear codes we perform 1D simulations for the KiK-net site KSRH10 using plane strain and periodic boundary conditions, as well as 2D P-SV simulations for a generic sediment-filled basin. Synthetic ground motions computed using AWP-Iwan with ~20 yield surfaces are able to reproduce the nonlinear response (i.e., reduced amplification and shift in resonance frequency) predicted by the codes Noah and Noah2D, but the quality of the solution decreases notably if too few ($\lessapprox$10) yield surfaces are used.

The Iwan model will be further optimized and integrated in the highly efficient and scalable GPU version of AWP which supports simulations on a discontinuous FD mesh.

Full waveform ambient noise inversion, Korbinian Sager, Christian Boehm, Laura Ermert, Lion Krischer, and Andreas Fichtner (Poster Presentation 106)

We develop and apply a novel full waveform ambient noise inversion that jointly constrains 3D Earth structure and heterogeneous noise sources at the global scale. Modern tomographic techniques aim to exploit details in waveforms for the benefit of improved resolution. Their application is so far mostly limited to transient point sources, e.g. active sources or earthquakes. Despite the widely-used assumption that the inter-station correlation of noise recordings is equal to a scaled version of the Green function between both receivers, a transfer to ambient noise tomography is not readily feasible. The required assumptions of Green function retrieval, e.g. wavefield diffusivity and equipartitioning, or equivalently the isotropic distribution of both mono- and dipolar uncorrelated noise sources, are typically not satisfied on Earth. Heterogeneous and non-stationary noise source distributions inevitably leave an imprint on correlation waveforms. To exploit their full waveform information regarding noise generation and Earth structure, we develop a method – referred to as full waveform ambient noise inversion – that is valid for arbitrary noise source distributions in both space and frequency, and which accounts for the full seismic wave propagation physics in 3D heterogeneous and attenuating media.

The forward problem of modeling correlation functions and the computation of sensitivity kernels for noise sources and Earth structure are implemented based on the spectral-element solver Salvus. Many studies, which were previously impossible or complicated to conduct, are now rendered feasible. For a first use case, we investigate the emergence of signals in correlation functions in general and in particular of body waves. In contrast to surface waves, body waves likely emerge from very localized sources and their interpretation as pure body waves is prone to misinterpretation due to significant cross-terms. In addition, we present a first application of full waveform ambient noise inversion with real data, a global data set focusing on the Earth's hum period band. We jointly invert for the distribution of noise sources and Earth structure.

Nonlinear Modeling of High-Rise Buildings Subject to Long-Period Ground Motion, Lauren M Santullo, Ahmed E Elbanna, and Setare Hajarolasvadi (Poster Presentation 005)

High rise buildings are particularly susceptible to long-period earthquake ground motion since the maximum displacement of the structure may approach or even exceed the peak ground displacement. Much of the currently used accelerometer data is of relatively lower magnitude earthquakes, with magnitudes of around 6 to 7 on the MMS. In contrast, large-magnitude earthquakes are expected in major metropolitan areas based on paleo-seismic records as well as numerical simulations. Areas such as Los Angeles, San Francisco, and Seattle have numerous high-rise buildings that might be affected. For an M8 earthquake, expected for example on San Andreas fault, the ground displacements may reach several meters. The response of tall structures, and in particular their structural stability, may be compromised in these cases due to complex nonlinear and second-order effects.

To simulate the effect of a large seismic event on a high-rise structure, time history analyses are performed on a 100-story, four-bay structure. The structure considered is a multi-story multi-bay steel frame with vertical loads computed based on representative concrete floors. The structure has a first natural period of about 6.7 seconds- above the common threshold for long-period structures- and used proportional damping values of 2% and 5% for a realistic scenario. A static pushover and elastic time history analyses were carried out. For the pushover, the top of the structure was displaced 6 meters to simulate a larger earthquake. Accelerometer data for the 1994 Northridge and 1992 Landers earthquakes were scaled so that the peak ground displacement was around 6 meters, a magnitude of displacement which is expected in a future San-Andreas earthquake. Preliminary results based on the elastic scaled time history analyses suggest an increase in the maximum top displacement, above the peak ground displacement, and a significant increase in the base moment pointing towards a possible loss of stability if the foundation is not

properly designed. Preliminary results from the inelastic analysis suggest pervasive development of plastic hinges in the superstructure. Future work will focus on generating proper ground motion scenarios based on kinematic or dynamic earthquake models and nonlinear site response analysis. A variety of structural systems and layouts will also be considered to investigate the structural vulnerability landscape in a future mega-earthquake.

Simulated ground motions for induced seismicity at a 12-story structure in Oklahoma using the SCEC Broadband Platform, Jessie K Saunders, Frankie Martinez, Jennifer S Haase, and Mohamed Soliman (Poster Presentation 014)

Oklahoma has been experiencing an increase in seismicity due to wastewater injection related to oil and natural gas production. As many buildings in Oklahoma were constructed before this increase, it is imperative to determine the response of these buildings to significant ground motion. We use a multi-instrument approach to monitor a 12-story reinforced concrete building at Oklahoma State University (OSU), where several campus buildings experienced damage from the 2016 M5.8 Pawnee earthquake. A strong-motion accelerometer collocated with a GPS receiver were installed on the roof of the building, and an additional accelerometer was installed on the ground floor. Combined GPS/seismic monitoring on the roof can provide a broadband view of the shaking, particularly low-frequency motion and static offset information necessary for determining damage. Since the instrument installation in July 2017, we have recorded over 10 M4+ earthquakes. In a preliminary data assessment, we find shaking amplification ratios of the roof relative to the ground floor are 2.1 and 2.5 in the E-W and N-S directions, respectively, consistent with the structure's rectangular shape and orientation.

The maximum magnitude of induced earthquakes is not known and remains controversial, however estimates of acceleration levels with a given probability of exceedance are now calculated annually using methodology consistent with the National Probabilistic Seismic Hazard Assessment maps. These are useful tools that are made available to the engineering community. To build on that effort, we are calculating scenario ground motions for the OSU study site to be made available for estimating the expected building response to larger earthquakes. We will generate synthetic waveforms from a suite of ruptures using the frequency-wavenumber approach to compute Green's functions for frequencies <1 Hz, combined with stochastic high-frequency waveform components generated using the SCEC Broadband Platform. We first generate synthetic ruptures along the Sooner Lake Fault, which ruptured in the 2016 Pawnee earthquake. We compare our synthetic waveforms with observations from the 2016 Pawnee earthquake to verify the approach. We are using a M4.6 earthquake from April 2018 to assess the consistency of the simulations with new observed data at the study site. For the future scenario calculations, the ruptures are based on two known faults near OSU, the Stillwater and Lake Carl Blackwell faults.

Gouge Development in the San Andreas Fault from Lake Elizabeth core samples, Heather M Savage, Randolph Williams, and Christie D Rowe (Poster Presentation 171)

Fault gouge is produced through a variety of processes, including pulverization, fracturing, grinding, weathering reactions, hydrothermal alteration, precipitation of cements, compaction, dilation, and possibly flash heating. We seek to quantify the meaning of fault rock 'maturity' by relating mineralogical and textural characteristics of gouge at different stages of evolution to frictional properties through triaxial shearing experiments. Using core samples from the shallow San Andreas Fault near the Elizabeth Tunnel in the Sierra Pelona Mountains, we track the evolution of fault gouge using grain size, bulk chemistry, microstructure and mineralogy to document the evolution from wall rock to fault core. We have selected samples adjacent to, and genetically related to, the most abundant North American wall rock to the SAF, which is a Mesozoic tonalite-granodiorite, a relatively simple rock characteristic of continental crust. Laser diffraction grain size analyses (n=60) reveal bimodal grain size distribution in most samples, tracking cataclasis of framework silicates (quartz and feldspar) in the coarser population (>5-10 μm) and authigenic clay appearance in the finer fraction (1-2 μm). Bulk chemistry of fault gouges (n=90) roughly co-varies with changes in grain size distribution, indicating that fluid-rock interaction and precipitation of authigenic clays and zeolites (principally smectite and laumontite) is accompanied by hydration of the rock and preferential enrichment in Ca and Mg. X-ray diffraction analysis (n=100) of bulk gouge samples and clay separates demonstrate that phyllosilicate enrichment in damaged wall rock predates significant cataclasis, as chlorite and illite / illite-smectite are present in mechanically 'intact' samples, and abundant components added to fault gouge through cataclasis. Authigenic Ca-rich smectites increase to 10-20% or more of clay gouge samples. Our preliminary results show that grain size evolution depends on both cataclastic grain size reduction of detrital grains and also on the rate and style of authigenic gouge mineral development. Cataclasis and mineral transformations are inter-dependent and drive incredible diversity in the style of fabric/foliation in the gouge, which we predict will have significant effects on strength and frictional behavior.

The Collaboratory for the Study of Earthquake Predictability version 2.0 (CSEP2.0): New Capabilities in Earthquake Forecasting and Testing , William H Savran, Philip J Maechling, Maximilian J Werner, Thomas H Jordan, Danijel Schorlemmer, David A Rhoades, Warner Marzocchi, John Yu, and John E Vidale (Poster Presentation 033)

The Collaboratory for the Study of Earthquake Predictability (CSEP) supports an international effort to rigorously conduct earthquake forecasting experiments. CSEP testing centers now operate in California, New Zealand, Japan, China, and Europe, with 442 models under prospective evaluation. CSEP supports retrospective forecast evaluations (testing forecasts on existing data) and prospective experiments (testing forecasts on data to be collected in the future). Current CSEP experiments evaluate forecasts that are expressed as expected rates in small space-magnitude bins and updated at regular intervals (e.g., daily or yearly). This experiment design is simple and allows a wide range of models to participate. However, recent forecast models, including candidate models for Operational Earthquake Forecasting (OEF), involve simulation of thousands of synthetic seismicity catalogs (stochastic event sets), which express important dependency structures between triggered earthquakes. In addition, some models, such as the third version of the Uniform California Earthquake Rupture Forecast (UCERF3), forecast spatially extensive ruptures on specified faults. As part of CSEP's second phase (CSEP2.0), we are redesigning CSEP's software to support the testing of such models. Requirements include access to high-performance computing, distributed processing of forecasts and evaluations, and streamlined data management, as well as adhering to CSEP's goals of transparency and reproducibility within a controlled, open-source software environment. This redesign is being implemented through a modularization of CSEP's codes to allow for tailored

experiments that do not fit into the current framework allowing for easy recombination of modules for new types of experiments should greatly expand CSEP's model and experiment space. Experiments will be described using directed-acyclic graphs (DAGs) that allow us to execute the computation using workflow tools. This allows for introducing high-performance computing resources while still maintaining the core values of CSEP testing centers. The improved capabilities of the CSEP software will be made available to the earthquake forecast research community. We follow best-practices of open-source software, which include continuous integration of the scientific and utilities codes, a collection of unit and acceptance tests, and thorough documentation that includes example forecasts and evaluations.

Paleoearthquakes within 100 km and 1000 years of modern Cajon Pass, California, Katherine M Scharer (Poster Presentation 263)

Cajon Pass, located at the juncture of the San Andreas Fault (SAF) and the San Jacinto Fault (SJF), is an area of significant risk due to its dense network of energy, communication, and transportation infrastructure that connects the greater Los Angeles region with the rest of the nation. To examine the hazards posed by earthquakes in Cajon Pass, I compiled available paleoearthquake data from the region within a 100 km radius of the Pass. I examine hazards from fault displacement using on a rupture model based on age correlation of paleoearthquakes on the SAF and SJF. Within the restricted region examined, at least 13 ground-rupturing earthquakes have occurred on these faults last 1000 years. Rupture lengths in the model vary from the northern ~10 km of the Mw6.9 SJF earthquake in 1918 to maximum rupture lengths that could span the 200 km diameter such as a ca. 1330 AD event on the SAF and a ca. 980 AD earthquake that could have ruptured both the SAF and the SJF. Apart from the SAF and SAF, other faults pose shaking hazards to the Pass. The most active source within the 100 km radius is the Elsinore Fault (Glen Ivy section), with 6 earthquakes in the last 1000 years but calculated average displacement less than 50 cm given the slip rate on the fault. More typical for the region is the Newport Inglewood fault, or the Cucamonga and Sierra Madre thrust faults, which have repeat times on the order of 500-1000 years and displacements of multiple meters. Closer to Cajon Pass, the most notable data gap exists along the boundaries of the San Bernardino basin, where a ~40-km-long swath along both the SAF and SJF have sparse earthquake age and slip per event data, and no paleoearthquake data is available for the NE-trending extensional Crafton Hills Fault complex. Overall, the dataset for understanding earthquake hazards in Cajon Pass is quite rich; however, further work around the San Bernardino basin is needed to better characterize the earthquake hazard near the junction of the SAF and SJF.

Dipping fault structures near the brittle-ductile transition and deep foliation fabric in southern California, Vera Schulte-Pelkum, Zachary E Ross, Karl J Mueller, and Yehuda Ben-Zion (Poster Presentation 159)

We investigate fault structure and shear zone fabric across the brittle-ductile transition zone in Southern California using the earthquake catalog of Hauksson et al. (2012) and seismic anisotropy results from receiver functions. Depth profiles of seismicity across major transform faults in the area of the Elsinore Fault and major branches of the San Jacinto and San Andreas Faults show seismicity on consistently NE-dipping planes with a listric appearance, with dip shallowing from subvertical near the surface down to ~45° near the brittle-ductile transition. A possible regional trend is from steeper dips (80-85°) near the coast (along the Elsinore Fault) to shallower dips going inland towards the Northeast (San Jacinto and San Andreas faults). Another striking observation are dipping planar seismicity features at mid-crustal levels that do not connect to seismicity or mapped fault traces at the surface, appearing as blind dipping faults in a strike-slip regime within the recorded time span. Generally much younger damage zones accompanying the major faults are also located on the northeastern side of each major surface trace.

An independent constraint on fabric near and below the brittle-ductile transition is given by anisotropic receiver functions. We use azimuthally varying conversions from anisotropy contrasts, not splitting of a converted shear phase. First-order observables are strikes of dipping foliation contrasts and dominance of dipping versus vertical or horizontal foliation. In Southern California, the anisotropic signal in the upper seismogenic and deeper ductile crust is from dipping foliation contrasts despite subvertical fault traces mapped at the surface and presumed subhorizontal schists emplaced in the lower crust during the Laramide, and is consistent with the listric patterns seen in seismicity.

Strike-slip motion on dipping faults is not optimally oriented relative to the current state of stress in Southern California, nor are the transform-orthogonal seismicity planes and shear fabric seen in our observations. Our initial interpretation is that inherited structures thus exert control on present-day deformation. This is supported by geological interpretations of the development of transform faults that dip at depth where they have reactivated older east-dipping extensional faults, such as the Western Salton Detachment influencing the present-day geometry of the Elsinore and San Jacinto faults.

Creep Along the Central San Andreas Fault Measured from Surface Cracks, 3D Topographic Differencing, and UAVSAR imagery, Chelsea P Scott, Nathan A Toke, Michael Bunds, and Manoochehr Shirzaei (Poster Presentation 116)

Along and near-fault observations of surface deformation on the central creeping segment of the San Andreas fault constrain on-fault slip rate, distributed deformation, and the physical mechanisms that accommodate shallow aseismic deformation. Here, we integrate observations of on- and off-fault surface deformation at the Dry Lake Valley paleoseismic site at different spatial scales including surface cracks within the fault zone's surface trace, topographic differencing over a 1 km aperture, and UAVSAR range-change over a 40 km aperture. We quantify rates of on-fault and distributed creep as well as fault zone width along fault segments with varying geometric complexity. We examine these observations for evidence of permanent deformation.

We use three types of observations to constrain surface deformation at the Dry Lake Valley site and surrounding portions of the central San Andreas Fault. (1) Left-stepping en-echelon cracks accommodate brittle creep across a 3-7 m width along the primary fault trace. They open during drought periods are inferred to be Mode 1 cracks with opening parallel to the extension direction of the San Andreas Fault. (2) We calculate three-dimensional surface creep using topographic differencing methods. We difference the 2007 EarthScope Northern California lidar imagery with a 2017 structure-from-motion (SfM) point cloud covering 2.75 km2 constructed with a Sensefly eBee Plus, a local GNSS base, on-board geolocation, and ground control points. We calculate 30 m resolution 3D displacements using the Iterative Closest Point (ICP) algorithm. We explore approaches for mitigating noise due to the varying sensitivity of lidar and SfM imagery to vegetation. The results show 25-30 cm of right-lateral slip and ~8 cm of NE side-up

vertical motion localized to a 40 m width over the ~10 year period. The right-lateral displacement rate is consistent with other geodetic observations. Vertical uplift on the NE side of the fault is consistent with the regional topography, but the magnitude of the rate measured here may reflect significant noise. (3) We measure deformation over a 40 km aperture using a time-series analysis of UAVSAR L-Band (wavelength=23.8 cm) imagery from three flight paths with acquisitions from 2009-2017. This imagery reveals localized deformation and remains coherent adjacent to the fault, despite the vegetation and high topographic relief.

Detailed mapping of normal fault array geometry using dm-scale high resolution topographic imagery from the Volcanic Tablelands, Bishop, California, Tyler R Scott, Ramon Arrowsmith, Chelsea P Scott, and Daniel Lao Davila (Poster Presentation 170)

The Volcanic Tablelands in northern Owens Valley California offer an unusual exposure of well-preserved and discontinuous meter to kilometer long normal faults formed by regional E-W extension. The region is one of the best natural laboratories to study normal fault growth evolution. Our goals are to capture fault zone structure and geomorphology at very fine scales to identify geometric patterns and eventually forecast normal fault evolution in the Volcanic Tablelands and apply the results to normal faults from other geographic regions. Understanding growth of normal faults will help predict and develop reliable models for rupture dynamics and potentially mitigate seismic hazard.

Our research team acquired 13,912 aerial photographs using 2 unmanned aerial vehicles covering ~20 km2. We mapped normal fault traces, relay ramps, and fracture patterns from the 10 cm resolution Structure from Motion digital elevation models and orthoimagery derived from the aerial photographs. We began our multi-resolution detailed geomorphologic and structural mapping at a 1:5000 scale and progressively moved to finer scales. We assumed that more evolved faults are narrower and have a straighter trace than less evolved faults. We focused on two N-S trending, normal fault strands at 37.449N, 118.441W.

The northern most fault (FZ1) is ~1.5 km long, has a maximum height of 20 m, and dips to the west. The southern strand (FZ2) is 1.5 km long, has a maximum height of 30 m, and dips to the east. The two faults are deflected away from each other at their intersection. This results in a topographic low broken by inward facing scarps on each side. FZ1 shows few additional splays, breaks, and changes in fault trend confined to within 50 m of the fault. FZ2 is similar to FZ1 along the fault tips, but in the central 1.3 km portion is dominated by rhythmic and partially segmented with ridges and troughs.

We interpret that this fault geometry represents a preserved relay ramp formed by growing en echelon faults and relay ramp breach processes. Because FZ2 is geometrically more complex than FZ1, we infer that FZ1 is structurally more evolved.

When do San Andreas Fault ruptures diverge on to other faults?, Gordon G Seitz, and David P Schwartz (Poster Presentation 265)

Increasingly, multi-fault ruptures have been recognized and hazard models have evolved to consider fault network behavior rather than that of individual faults. The San Andreas Fault (SAF) has major fault branches with the San Jacinto (SJF) and San Gregorio (SGF) faults. The SAF-SJF step-over has experienced two large historical ruptures in 1812 (Mw 7.5) and 1857 (Mw 7.8). The SAF-SGF intersection experienced the 1906 (Mw 7.9) earthquake. The Mw 7.9 2002 Denali Fault rupture (DFR) with similar geometric and geologic characteristics provides an analog. The DFR propagated onto the Totschunda Fault (TF), which has a direct connection. Although various models tried to explain this rupture divergence, we found that the higher accumulated stress path, as defined by the elapse time and slip rate on each fault branch, was favored. Applying this reasoning to the San Andreas Fault we find:

The surface traces of the SAF and the SJF do not intersect; rather, the SJF terminates with a parallel reach separated by a distance of 2 km. Paleoseismology places the 1812 rupture on the Mojave and San Bernardino (SB) SAF sections and provides an initial accumulated stress state based on the elapse times. 1812 displacements along the SB section may have played a role in the location of the 1857 rupture termination, which stopped north of the SAF-SJF step-over. A lack of seismicity along the SB SAF may indicate the 1812 rupture path. Through-going SB SAF ruptures are supported by matching paleoseismic event series at the north (Pitman Canyon; 7 events/1100 yrs) and south (Burro Flats; 7 events/1200 yrs) ends. Although individual event dates on the SJF (Mystic Lake:7/1600 yrs) may correlate with SAF events, the overall event series does not match.

The SAF-SGF intersection is a direct connection. Paleoseismic records on the Peninsula SAF and the SGF indicate the estimated accumulated slip prior to 1906 was 3x greater on the SAF than on the SGF and thus a SAF rupture was favored.

Matching paleoseismic event series along faults with nearly identical average recurrence intervals provides strong support for continuous ruptures. Although fault geometry has generally been recognized as a factor controlling rupture paths at fault branches, stress conditions are of similar importance. What may most strongly control ruptures at fault branches is stress resulting from prior earthquakes, hence we expect improvements in models when such an initial stress field is used.

Seismic Radiation During Slip Along a Bimaterial Fault: An Experimental Investigation, Tanner Shadoan, Brett M Carpenter, Ze'ev Reches, Xiaofeng Chen, and Simon Zu (Poster Presentation 175)

Large slip along faults is likely to place crustal blocks of different lithological and mechanical properties against one another to form bimaterial-faults. For example, the Punchbowl fault in southern California is a bimaterial fault with igneous and metamorphic basement in contact with the Punchbowl Formation Sandstone. To explore frictional behavior and seismic radiation of such faults, we conducted shear experiments on bimaterial-faults composed of two blocks of either gabbro, limestone, or sandstone, with nine block combinations. The blocks were in contact along a ring-shaped surface, approximately 24 cm2 in area, and were loaded in a rotary shear apparatus (ROGA) at the University of Oklahoma. Shear rates and normal stresses ranged from 1μm/s to 1cm/s and 0.5 to 5 MPa, respectively. We performed constant velocity experiments and monitored the shear stress and seismic radiation along the fault. Seismic radiation was recorded at a rate of 1 MHz via four 3D accelerometers mounted ~2 cm away from the experimental fault.

The frequency spectrum data of the laboratory seismic events revealed differences in seismic behavior associated with rupture processes and ray path characteristics. For example, for an experimental fault composed of gabbro and limestone, the recorded events on the more compliant side (limestone) of the fault have high intensities at lower frequencies. We deduce that the ray path, which is controlled by the rock block properties, is responsible for this difference. When keeping the ray path constant (i.e. accelerometers mounted on gabbro) while changing the other fault block, to either gabbro, sandstone, or limestone, also indicate differences in the frequency content, this time due to rupture characteristics along the fault. By taking the spectral ratio of two events, we found that experimental faults with a compliant rock, e.g., sandstone, have lower energy at higher frequencies. This suggests that compliant rocks attenuate higher frequencies more than less compliant rocks, e.g. gabbro. In summary, the experiments show distinct dependence of both friction and seismic radiation on the mechanical properties of the three lithologies used here, and it is anticipated that related effects would occur along natural bimaterial faults.

The Similarity Matrix Profile, an efficient method for detecting both low and high signal to noise ratio seismic events in very long time series, Nader Shakibay Senobari, Gareth Funning, Zachary Zimmerman, Yan Zhu, and Eamonn Keogh (Poster Presentation 063)

We propose here an alternative, efficient method for seismic event detection for continuous data– the similarity Matrix Profile (MP). The MP is essentially a report of the index (i.e. location in the time series) and correlation coefficient (CC) value of the nearest neighbor for any subwindow of continuous data. Several algorithms for computing the MP efficiently on GPU cards and/or clusters have been developed in recent years so that it is now possible to calculate the MP for time series containing up to 1 billion data points (equivalent to 579 days of waveform data at 20 Hz). The MP is an efficient way of detecting both low and high signal to noise ratio events, as the nearest neighbor CC values for background noise tend to be relatively low. Therefore, the MP approach, with an appropriate threshold, can be used to detect earthquake swarms, aftershocks and foreshocks, low-frequency earthquakes (LFEs), repeating events and more.

We demonstrate the MP approach for two data sets, 580 days each of continuous recorded seismic data. Our first test is centered on the 2004 Mw 6.0 Parkfield earthquake using a nearby borehole station, We detect ~16 times more Parkfield aftershocks using the MP approach with a conservative detection criterion (CC>0.9); the number of detected events per day fits the Omori-Utsu law almost perfectly. Individual LFEs and non-volcanic tremor (NVT) are also detectable in the MP as their CC values are 0.8-0.9, compared with background noise (~0.6).we also find multiple new repeating families of seismic events that were activated 2-3 weeks prior to the mainshock. For our second test, we use data from a USArray station located near Mapleton, OR that is affected by NVT. Most events here with CC>0.9 are LFEs, based on their shapes, durations and frequency contents. We observe two periods of increased LFE activity in August to November 2006 and June to October 2007, broadly in agreement with the published literature. However our detection shows a more gradual increase in detected LFEs, rather than a sharp onset, as seen in that earlier studies. In all cases we observe abrupt changes in MP values associated with P-wave arrivals, suggesting that the method could be used to facilitate automated phase picking.

Seismic imaging of the Southern California plate boundary around the South-Central Transverse Ranges using double-difference tomography and fault zone head waves, Pieter-Ewald Share, Hao Guo, Clifford H Thurber, Haijiang Zhang, and Yehuda Ben-Zion (Poster Presentation 101)

We image seismic velocity structures within the South-Central Transverse Ranges using fault zone head waves (FZHW) and a new double-difference tomography algorithm incorporating both event and station pairs. The tomography provides information on velocity structure at scales >4 km, whereas FZHW give direct evidence for the existence and continuity of bimaterial fault interfaces. Tomographic images of velocities within a 222 km x 164 km region are obtained using >1,000,000 P and S arrival times (picked with an automatic detection algorithm) and differential times associated with >10,000 local events from 1/1/2010 to 30/6/2015 recorded by >250 stations. Early P waveforms from the same dataset (augmented by events from earlier years) are analyzed for the presence of FZHW.

he resulting tomography models include low velocities along major fault segments and across-fault velocity contrasts. Analyses of FZHW reveal bimaterial interfaces at the core of several of these fault segments. Extensive faulting and Pelona schist manifest as low velocities throughout the San Bernardino basin. High velocity granitic rocks are juxtaposed in this basin to the SW and NE, forming continuous bimaterial interfaces in the northern San Jacinto fault zone (SJFZ) and the San Andreas Fault (SAF) NW of San Gorgonio Pass (SGP). The bimaterial interface along the northern SJFZ extends through and perhaps slightly beyond Cajon Pass. The results also show a bimaterial interface across the SAF SE of SGP that is offset from the fault surface trace to the NE at depth. We interpret this to be a dipping section of the southern SAF (estimated dip=57°), which separates granitic rocks in the SW from gneisses and schists in the NE. The flip in velocity contrast polarity across the SAF through SGP imaged with FZHW, complemented by abrupt west-to-east changes in elastic properties observed in the tomography models, have implications for large earthquake ruptures in this area.

Similarly large P and S datasets employed in the inversion lead to high quality VP/VS estimates for the region. These models show very high VP/VS anomalies near shallow damaged rock, whereas fault zones exhibit either low (<1.73) or high (>1.73) VP/VS characteristics at greater depth. Regional-scale low and high VP/VS values are related to relative abundances of igneous or metamorphic rocks. Near-fault VP/VS anomalies at depth are likely associated with variations of crack densities and fluid content.

Earthquake Simulators are Ready for Prime Time, Bruce E Shaw (Oral Presentation Tue 10:30)

A major leap has been made in the last year where earthquake simulators have been shown to replicate seismic hazard statistics across California, matching remarkably well the results from UCERF3. What this means, how to take advantage of it, why it has worked, and where we are pushing further forward will all be discussed. This application of earthquake simulators will also be deployed as an example to address the more general question of how to use, and how not to use simulators, and the importance of robustness.

Testing and Reconciling EGF Methods for Estimating Corner Frequency and Stress Drop from P-wave Spectra, Peter M Shearer, Rachel E Abercrombie, Daniel T Trugman, and Wei Wang (Poster Presentation 075)

Researchers have long used empirical Green's function (EGF) approaches to correct body-wave spectra for attenuation and estimate corner frequencies and Brune-type stress drops. Recently, however, it has become clear that there are strong tradeoffs among parameters in the model fits, which may explain why stress-drop estimates of specific earthquakes show relatively poor agreement between different studies. We examine this issue by analyzing a tight 6-km-wide cluster of over 3000 M 0.5–5.5 aftershocks of the 1992 Landers earthquake, recorded by many SCSN stations. Because the cluster dimension is small compared to the station distances, we assume that attenuation and path effects are constant for each station, thus simplifying the analysis. We begin by computing P-wave spectra from unclipped vertical-component data using the multi-taper approach of Trugman and Shearer (2017) and retain spectra with good signal-to-noise between 2.5 and 25 Hz. We then apply and compare two different analysis and modeling methods: (1) the spectral decomposition and global EGF fitting approach (e.g., Shearer et al., 2006; Trugman and Shearer, 2017), and (2) the more traditional EGF method of estimating target-event corner frequencies (fc) using spectral ratios with smaller nearby events (e.g., Abercrombie et al., 2016). We find that spectral decomposition yields event terms that are consistent with stacks of spectral ratios for individual events. The main source of fc differences between the two methods comes from the modeling approach to estimate the EGF. The global EGF-fitting approach suffers from parameter tradeoffs among the absolute stress drop, the stress-drop scaling with moment, and the high-frequency falloff rate, but has the advantage that the relative stress drops among the different events in the cluster are well-resolved even if their absolute levels are not. Because the spectral-ratio approach solves for a different EGF for each target event and does not impose any constraint on the corner frequencies of the smaller events, it can produce biased results for target-event corner frequencies. For the Landers cluster, the performance of the spectral-ratio method can be improved by constraining the average small-event fc to a fixed value, in which case the two methods yield very similar results. We plan to apply these insights to devise optimal strategies for spectral analysis and stress-drop estimation for large datasets of distributed seismicity.

Illuminating faulting complexity of the 2017 Yellowstone (Maple Creek) earthquake swarm, David R Shelly, and Jeanne L Hardebeck (Poster Presentation 062)

The 2017 Maple Creek earthquake swarm was one of the most prolific swarms to occur in the Yellowstone region in the past decades, with more than 2000 earthquakes up to Mw 4.4 cataloged by University of Utah Seismograph Stations (UUSS) between June and September 2017. The swarm occurred just east of Hebgen Lake, within a zone of high seismicity (and previous swarms) extending northwest from the caldera. To gain insight into the mechanics and underlying mechanisms of this swarm, we performed a high resolution seismic analysis. Using the routinely cataloged earthquakes as waveform templates, we detected and precisely located nearly 16,000 earthquakes, about 6 times the number included in the routine catalog. We further utilized the cross-correlation measurements derived from this processing to determine relatively polarities for event pairs and to estimate focal mechanisms for this large population of events, following the technique proposed by Shelly et al. [2016].

The results illuminate a complex network of faults activated progressively during the swarm. The dominant set of faults strikes ENE, with a secondary set striking toward the NW, potentially forming a conjugate fault set. Short-term migration of hypocenters primary expands along ENE-striking faults, and longer-term migration activates new ENE-striking faults toward the NW and SE. Focal mechanisms indicate primarily strike-slip motion with a contribution of normal faulting. Based on these patterns and comparisons with past swarm activity in the area, we hypothesize that this complexity may arise from the diffusion of fluid pressure through a complex network of pre-existing, relatively permeable faults. Thus, fluid-driven earthquake sequences may naturally generate more complex faulting geometries compared to earthquake sequences dominated by stress transfer.

Decadal variation of crustal deformation in California inferred from EDM and GPS and its implication to seismic hazard, Zheng-Kang Shen, and Yuehua Zeng (Poster Presentation 132)

Prior to GPS, the Electronic Distance Meter (EDM, or Trilateration) technique was used from the 1960s to early 1990s to measure crustal deformation across major faults in California. Although the data may not be as accurate as GPS (relative uncertainties of 10e-7 vs 10e-8), inclusion and careful analysis of the EDM data can still effectively extend the observation time span from the last 2-3 decades to the last half century. This provides a unique opportunity to examine the temporal evolution of the deformation field in California, particularly along the San Andreas fault. A preliminary analysis of the EDM data has indeed shown signs of such a deformation rate change, with the overall relative motion determined by EDM measurements in the 1970s-1980s a couple of millimeters per year slower than that measured by GPS in recent years across the Mojave and Coachella sections of the San Andreas fault. This change of deformation rate is consistent with our recent study of seismicity and geodetic strain patterns, which demonstrated that earthquakes of M≥4.0 in California and Nevada became significantly more concentrated along the San Andreas fault system for the period of 1990 to 2013 than for the period of 1933 to late 1980s. It also showed that the seismicity rate for events of M>6.5 was more than doubled for the later period than for the earlier period (Zeng et al., 2018). The geodetic and seismic results seem to lend support to a model of accelerated seismicity late into the earthquake cycle, suggesting increased seismic risk in California.

Modeling low-frequency earthquakes on a rate-and-state fault, Zhichao Shen, and Nadia Lapusta (Poster Presentation 191)

Benefitting from the dense seismic networks deployed over the past two decades, the discovery of low-frequency earthquakes (LFEs) has enhanced our vision of the fault slip behavior. Compared to regular earthquakes of the same magnitude, LFEs are depleted in high frequency signals but are inferred to still represent shear slip. Seismologically, LFEs are characterized as events with small magnitudes (Mw0.3 ~ Mw2.6), long durations (0.2 s ~ 0.5 s), and low stress drops (1 kPa ~ 30 kPa). Given these observations, two views are possible regarding the origin of LFEs. One is that the sources of LFEs are regular earthquakes, but their seismic measurements are biased by strong near-source attenuation. The other is that the source process of the LFEs is conceptually different. In this work, we show that LFE-like events can be produced on rate-and-state faults with sub-critical velocity-weakening (VW) patches and typical rate-and-state properties, supporting the second view. For the sizes d of the VW patch

that are 0.7-0.95 of the theoretical estimate h* of the nucleation size, the slip on the patch accelerates significantly, but to peak slip rates that 1-3 orders of magnitude below the slip rates of 0.1-1 m/s typical for traditional earthquakes. The seismological analysis of the synthetic seismograms produced by such sources results in source parameters similar to those inferred for the natural LFEs, for the models with certain parameter selections, e.g. the effective normal stress of 25 MPa, steady-state velocity weakening of 0.002, characteristic distance of 160 microns, and d/h* = 0.93-0.96. Our current work is directed towards exploring the range of fault properties that would result in observable LFEs.

Inferring crustal viscosity from seismic velocity: Application to the lower crust of Southern California, William Shinevar, Mark Behn, Greg Hirth, and Oliver Jagoutz (Poster Presentation 148)

We investigate the role of composition on the viscosity of the lower crust through a joint inversion of seismic P-wave (Vp) and S-wave (Vs) velocities. We determine the efficacy of using seismic velocity to constrain viscosity, extending previous research demonstrating robust relationships between seismic velocity and crustal composition, as well as crustal composition and viscosity. First, we calculate equilibrium mineral assemblages and seismic velocities for a global compilation of crustal rocks at relevant pressures and temperatures. Second, we use a rheological mixing model that incorporates single-phase flow laws for major crust-forming minerals to calculate aggregate viscosity from predicted mineral assemblages. We find a robust correlation between crustal viscosity and Vp together with Vs in the α-quartz regime. Using seismic data, geodetic surface strain rates, and heat flow measurements from Southern California, our method predicts that lower crustal viscosity varies regionally by four orders of magnitude, and lower crustal stress varies by three orders of magnitude at 25 km depth. At least half of the total variability in stress can be attributed to composition, implying that regional lithology has a significant effect on lower crustal geodynamics. Finally, we use our method to predict the depth of the brittle–ductile transition and compare this to regional variations of the seismic–aseismic transition. The variations in the seismic–aseismic transition are not explained by the variations in our model rheology inferred from the geophysical observations. Thus, we conclude that fabric development, in conjunction with compositional variations (i.e., quartz and mica content), is required to explain the regional changes in the seismic–aseismic transition.

The SCEC Broadband Platform: Open-Source Software for Strong Ground Motion Simulation and Validation, Fabio Silva, Philip J Maechling, Christine A Goulet, and John E Vidale (Poster Presentation 015)

The Southern California Earthquake Center (SCEC) Broadband Platform (BBP) is a carefully integrated and validated collection of modular open-source scientific software programs that can simulate broadband (0-20+ Hz) ground motions for earthquakes at regional scales. The BBP uses earthquake rupture and wave propagation modeling software to simulate ground motions from earthquakes. Users input an earthquake location, fault plane geometry and moment magnitude, along with a list of station locations, and then the BBP software calculates ground motions for the specified stations. The BBP simulations are based on 1D layered velocity models, which are provided with Green's functions for a suite of pre-defined regions. The platform also includes validation tools to be used for cases in which the simulated historical events have recordings, which also allows for the refinement of simulation techniques and the development of new simulation methods that are consistent with data.

The BBP scientific software modules implement kinematic rupture generation, low- and high-frequency seismogram synthesis using wave propagation through 1D layered velocity structures, a site-effects module, several ground motion intensity measure calculations, and various ground motion goodness-of-fit tools. These modules are integrated into a software system that provides user-defined, repeatable calculation of ground-motion seismograms, using alternative simulation methods, and software utilities to generate tables, plots, and maps. The BBP has been developed over the last eight years in an international collaborative project involving geoscientists, earthquake engineers, graduate students, and SCEC software developers.

The BBP is continuously evolving and new versions are released periodically on GitHub. The latest SCEC BBP software can be compiled and run on recent Linux systems with GNU compilers. It includes eight simulation methods, nine simulation regions covering California, Japan, Central and Eastern North America, and the ability to compare simulation results against empirical ground motion models. The current release also includes updated ground motion simulation methods, and the ability to simulate multi-segment ruptures.

Sequence of cascading earthquakes on the Newport-Inglewood-Rose Canyon Fault zone from paleoseismic observations, Drake M Singleton, Thomas K Rockwell, and Jillian M Maloney (Poster Presentation 219)

Approximately 10-20% of the estimated 50 mm/yr plate boundary deformation in southern California is accommodated by the offshore faults that comprise the Inner Continental Borderlands (ICB). The precise distribution of slip and earthquake history in the ICB is poorly constrained due to a combination of observational limitations and a lack of geophysical and geological data integration. The Newport-Inglewood-Rose Canyon fault (NIRC) is the easternmost fault in the ICB and is composed of both onshore and offshore segments, offering the opportunity to resolve the earthquake history for a fault within the ICB. We present the results of two paleoseismic trenches opened in Holocene stratigraphy across the Rose Canyon fault (RCF), the southern onshore section of the NIRC in San Diego, CA. From the stratigraphic record in the trenches, there is evidence for six surface ruptures in the past ~3,300 years. Based on the width and amount of faulting, four of the paleo-earthquakes are interpreted to represent larger-magnitude events (M ~6.5-7). Furthermore, these events correlate well in time with paleo-earthquakes reported at locations farther north along the onshore NIRC, indicating the possible occurrence of either end-to-end ruptures or a sequence of cascading earthquakes. The apparent timing of these earthquakes suggests a late-Holocene recurrence interval of ~700-800 years for the NIRC, several hundred years shorter than previous estimates, and raises important questions regarding the slip rate and slip per event for the southern NIRC. Furthermore, an apparent lack of documented young earthquakes along the northern most section on the NIRC strengthens previous ideas that this section of the fault is likely closer to a failure threshold than the central and southern sections, or that the slip rate has substantially decreased towards the northern terminus of the fault zone.

Characterizing seismogenic fault structures in Oklahoma, Rob Skoumal, and J. Ole Kaven (Poster Presentation 090)

Oklahoma is now one of the most seismically active places in the United States as a result of industry activities. A principal challenge in investigating induced seismicity is the identification and characterization of seismogenic faults. Earthquake locations can illuminate dense fault fabrics previously unbeknownst to seismologists and provide insight into the rupture process. In order to characterize these fault networks in Oklahoma, we created a catalog of over 200,000 earthquakes identified using large-scale template matching and relocated the events using GrowClust. To make the process of identifying fault segments more easily accessible and objective, we developed an algorithm that 1) identifies clusters of seismicity and 2) distinguishes linear/planar features within each cluster. With this approach, we are able to rapidly characterize a wide variety of fault features, such as strike, dip, and depth, and also identify conjugate faults within the improved earthquake catalog. We investigate the largest magnitude earthquake sequences in greater detail, including the 2011 M 5.7 Prague and 2016 M 5.8 Pawnee earthquakes, in addition to characterizing numerous faults throughout the state that have not been previously identified. The improved catalog also allows hydraulic fracturing induced seismicity to be characterized with greater confidence, and we find that these earthquakes have strong spatiotemporal correlations with the relatively short-duration hydraulic stimulations. The vast majority of seismogenic faults identified are optimally oriented relative to in-situ maximum principal horizontal stress measurements and are in agreement with moment-tensor solutions, where available. Using the cross-correlation coefficients between event pairs, moment tensors of smaller magnitude events can also be estimated, providing deeper insight into the rupture processes.

Searching for Spot-Fire Earthquakes Triggered During the 2004 Parkfield Mainshock, Norman H Sleep (Poster Presentation 212)

Strong P waves have the potential to trigger earthquakes ahead of the main rupture front. The triggered daughter event may grow large and merge with the parent event as a supershear rupture. Alternatively, a daughter nucleation may die quickly, just as most ordinary earthquakes do. The kinematics of failed daughter events are similar to those of spot fires set by wind-blown firebrands ahead of the main fire line. We seek to determine whether such spot fire earthquakes are common by analyzing recordings on the SAFOD Pilot Hole array of the 2004 Parkfield mainshock. The array is situated just off the north end of the rupture in the forward directivity direction for this earthquake. The interval between initial P wave and direct S wave on the array could contain both P and S waves from suitably located spot-fire earthquakes. For the Parkfield mainshock, almost all of the waves in this interval are P waves. We detected two transverse S wave arrivals 2 s before the direct S arrival that are plausibly from spot fire earthquakes of Mw ~3.5. However, data from small aftershocks near the mainshock hypocenter show that strong mainshock coda arrived between initial P and direct S on both the radial and transverse horizontal components. Transverse coda would tend to mimic S waves from spot fire earthquakes. In addition, the short 240 m length of the array at the time of the mainshock was too small to migrate arrivals back to apparent sources. That is, we could not clearly distinguish converted transverse phases derived from the mainshock P wave from those of true spot fire earthquakes. In general, detecting modest earthquakes triggered by mainshock P waves would help quantify the reality of stress concentrations that may accommodate supershear rupture and rupture jumps between fault segments.

InSAR/GPS time series deformation of the 2018 Kilauea event: Preparation for a large Southern California event, Bridget R Smith-Konter, Xiaohua Xu, Lauren Ward, Liliane Burkhard, and David T Sandwell (Poster Presentation 138)

In preparation for the next major earthquake in Southern California, a key task of SCEC5 is to develop methods to integrate dense spatiotemporal geodetic datasets for post-earthquake rapid response. Events like the 2018 Kīauea Volcano eruption, observed every three days since May 2nd by ESA's Sentinel-1 satellites, provide an unprecedented opportunity to refine our GPS/InSAR time series integration capabilities in preparation for future Southern California events. Using open source software GMTSAR, we processed all ascending and descending Sentinel-1A/B InSAR line-of-sight (LOS) data for the Big Island of Hawai'i since the start of the eruption, and have been actively providing these data to the scientific community as they become available (http://pgf.soest.hawaii.edu/Kilauea_insar/). Here we present a crustal deformation time-series for the 2018 Kilauea event (April 30 - August 9) using integrated GPS/InSAR measurements. We geometrically align all Sentinel-1 acquisitions using precise orbital information and select interferograms based on a 150-m perpendicular baseline and 60-day temporal baseline. Interferograms are masked with a universal stacked coherence, nearest-neighbor interpolator and then unwrapped with SNAPHU. Lastly, the time-series is constructed using a common-scene stacking technique to absorb turbulent atmospheric noise and coherence-based SBAS to recover ground deformation. These data provide critical modeling constraints of the ~90-day deformation event at Kīlauea from several sources: (1) the April 30th collapse of Pu'u 'Ō'ō crater, (2) the May 1st dike intrusion, propagation, and subsequent contraction of the lower East Rift Zone, (3) sprawling deformation from the May 4th Mw6.9 Leilani Estates thrust earthquake along the south flank region (subsidence and southeast-directed displacement in excess of 0.3 m and 0.8 m, respectively), and (4) continuous deflation of Kīlauea's summit region as large volumes of magma are withdrawn. Moreover, the continual near-real-time geodetic observations spanning the last three months of the 2018 Kīlauea eruption provide a exceptional testbed for rapid hazard response and a unique opportunity to further refine our time series integration methods in preparation for post-earthquake rapid response in Southern California.

ShakeAlert v. 2.0 Testing and Certification, Deborah E Smith, Monica D Kohler, Jennifer R Andrews, Angela I Chung, Renate Hartog, Ivan Henson, Douglas D Given, and Stephen Guiwits (Poster Presentation 053)

Earthquake early warning algorithms have to undergo rigorous real-time and offline testing before being accepted into the ShakeAlert production system. In anticipation of the scheduled ShakeAlert v. 2.0 phase 1 rollout in late 2018, multiple algorithms and associated configurations were tested using the ShakeAlert Testing and Certification platform procedure. The testing system attempts to simulate how the production system will perform by deploying the proposed algorithms, configurations, earthworm rings/modules, and ActiveMQ messaging on separate, nearly identical hardware. For the real-time testing, the test servers are fed the same West Coast input waveform data, and the algorithms' performance is compared between the test and existing production systems after a minimum of two weeks. For the offline testing, four simultaneous instances of the algorithms are run on one machine with a historic test suite of earthworm tankplayer files (format used for replaying data into an earthworm ring with realistic

timing). These tankplayer files include data from West Coast earthquakes (M4.1 to M7.2), teleseisms, regional events, and problematic data sets (recenterings, calibrations, noisy data, etc.). The algorithms included in the ShakeAlert v 2.0 test are: 1) EPIC (Earthquake Point-source Integrated Code), 2) FinDer (Finite Fault Detector), 3) EqInfo2GM (Earthquake Information to Ground Motion), 4) SA (Solution Aggregator), and 5) DM (Decision Module).

Tectonic and geometric constraints for the Wind Canyon fault block on the western Garlock fault: an apatite fission track analysis, Iris Smith (Poster Presentation 236)

New apatite fission track analyses from the southeastern side of the Garlock fault near Mojave, CA were obtained in order to better understand the fault evolution and tectonics of the region. Apatite fission track analyses are commonly used to date the timing of exhumation of fault blocks, and in this case, can help us constrain fault geometries. The study area appears to include a fault block, referred to here as the Wind Canyon fault block. The fault block is ~13 km in length parallel and ~5 km in width perpendicular to the Garlock fault. The convex shape of the southeastern margin of the Wind Canyon block suggests that it is bounded on that side by either a southeast-vergent thrust fault or normal fault. Our initial apatite fission track ages from granitoids within the fault block are 51 to 31 Ma. These ages are intermediate between the youngest and oldest apatite fission track ages from the Tehachapi mountains (Blythe and Longetti, 2013) immediately to the north of the Wind Canyon fault block. Our initial interpretation is that Wind Canyon fission track ages are consistent with partial resetting by exhumation along the Wind Canyon fault during Miocene time. Different tectonic scenarios will be further evaluated with these new data.

Investigating the Ground Motion Characteristics of the 2016 Mw 5.5 Gyeongju, South Korea, Earthquake Using the SCEC Broadband Platform, Seok Goo Song, Kwan-Hee Yun, and Sangmin Kwak (Poster Presentation 301)

The 2016 Mw 5.5 Gyeongju, South Korea, earthquake is the largest instrumentally recorded seismic event in the country. This event provided a valuable set of recorded strong ground motion data in the Korean Peninsula. We investigated the ground motion characteristics of the event through a physics-based approach using the SCEC BBP. The recorded ground motions for the Gyeongju event show patterns consistent with simulated ground motions for a stable continental region. High stress drop and low attenuation, commonly observed in the stable continental region, may control ground motion characteristics in the Korean Peninsula, which could be an important factor to consider in seismic hazard assessment of the region. Physics-based ground motion modeling may be a useful tool to obtain ground motion characteristics from the recorded ground motion data and may play an important role in advanced seismic hazard assessment and mitigation

Investigation of Adaptive Time-Stepping Algorithms for Simulating Sequences of Earthquakes and Aseismic Slip (SEAS), Yanke Song, Valere R Lambert, and Nadia Lapusta (Poster Presentation 193)

Modeling earthquake behavior involves resolving the complex interaction of processes active across timescales ranging from hundreds to thousands of years of tectonic loading, down to milliseconds during the dynamic rupture process. To make such problems computationally feasible, simulations of sequences of earthquakes and aseismic slip (SEAS) employ adaptive time-stepping algorithms in order to optimally sample the temporal evolution of fault behavior. The choice of time steps during the dynamic and quasi-static phases of fault slip can impact the accuracy and long-term evolution of the computed quantities (e.g. fault slip, slip rates, and stresses) as well as the computational cost of such simulations. In order to explore the trade-offs for an optimal time-step selection, we study the simulations of SEAS with various adaptive time-stepping algorithms, comparing long-term fault behavior as well as the computational costs in terms of the total number of simulated time steps. We begin with a quasi-dynamic formulation of a 2D antiplane problem based on the first benchmark simulation from the SEAS code comparison exercise supported by the Southern California Earthquake Center. We plan to expand this study to explore the optimal adaptive time-stepping methods for simulations that include fully dynamic stress interactions and enhanced dynamic weakening mechanisms, such as the thermal pressurization of pore fluids.

Assessing the Deep Geometry of the Los Angeles Basin Using Full H/V Spectral Ratio and Multimode Surface Waves , Zack Spica, Mathieu Perton, Robert W Clayton, and Gregory C Beroza (Poster Presentation 146)

The H/V spectral ratio (HVSR) of the auto-correlated signal at a seismic station is proportional to the ratio of the imaginary parts of the Green's function. Observations of H/V can be compared to their theoretical counterpart for a locally layered elastic media to constrain the velocity structure. We use broadband stations of the “Los Angeles Syncline Seismic Interferometry Experiment” (LASSIE) to perform a combined inversion of multiple HVSR measurements and multimode dispersion curves for Rayleigh and Love waves along the dense line of sensors. The presence of low frequency peaks (~0.1 Hz) in the HVSR allow us to constrain the deep structure of the basin. Our modeling differs substantially in approach from previous measurements of crustal velocity structure in southern California; however, the velocity models we obtain are for some position in good agreement with the SCEC community velocity model. Our results confirm both the utility of the diffuse field HVSR measurements for deep structural characterization and the predictive value of the SCEC community velocity model in the Los Angeles region.

Strong ground motions simulations for Dunedin city, New Zealand: First steps using the SCEC Broadband Simulation Platform, Mark W Stirling (Poster Presentation 009)

Our poster will present on-going QuakeCoRE-funded work (quakecore.nz) on developing strong motion simulations for the greater Dunedin city area. The city has never experienced strong ground motions in the entire 179 year historical record, and has an aging built environment. Source modelling and ground motion simulations are being carried out for the city center using the SCEC Broadband Simulation Platform (SCEC BBSP). The BBSP computes broadband (0-10 Hz) seismograms from modeled earthquake sources. The Akatore Fault, the most active fault in Otago and closest major fault to Dunedin, is focused on in the present study. Simulations for various Akatore Fault source scenarios will be presented in the poster.

Path and site effects are key components considered in the simulation process. A 1D shear wave velocity profile is required by the SCEC BBSP to represent the Akatore-to-CBD path and site, and we have chosen the BBSP’s Mojave profile for representing Dunedin conditions. The choice was based on comparison of the available BBSP 1D profiles to our profile developed from seismic

reflection lines acquired in the city in 2017-8. A 3D shear wave velocity model is currently under development for Dunedin, and this will be applied to future ground motion simulations for the city.

Preliminary Results of a Study to Identify Archaeological Artifacts from San Salvador in Colton, CA, Using Ground Penetrating Radar, Chloe S Sutkowski, Oscar Prado, Veronica Hernandez, and Jascha Polet (Poster Presentation 320)

We will present the preliminary results of an ongoing archaeo-geophysical survey at Pellissier Ranch in Colton, CA. Historical archives suggest that the 200-acre vacant lot was home to a significant portion of San Salvador, the largest non-native settlement in the mid-1800s along the Old Spanish Trail between New Mexico and Los Angeles. An overwhelmed Santa Ana River led to the Great Flood of 1862, which either washed away or buried beneath a thick layer of sandy river deposits, all adobe structures and settlers' belongings. Artifacts are anticipated to be buried at a shallow depth of 1.5 – 3 meters, making them a good target for several different types of geophysical surveys.

round Penetrating Radar (GPR), Electro-Magnetic induction (EM), and ground-based magnetic gradiometry have proven successful in non-invasively identifying archaeological artifacts in a variety of different environments. In dry, southwestern sites, the most successful of these has historically been GPR. Much work has been accomplished by researchers at other sites in identifying buried adobe structural remains by their "adobe melt" signature in GPR profiles of adobe walls in the subsurface. We employ GPR using a 400 MHz antenna across this site and have imaged several anomalies that have a high probability of being related to San Salvador. The most noteworthy are a north-south trending canal signature buried at a depth of ~1.5 meters, an "adobe melt" signature at a depth of ~2.5 meters, and a feature that resembles a collapsed structure that is ~30 meters long in profile view. Significant hyperbolic signatures exist in the profiles that image the potential collapsed structure, located just below the strong reflector interface at a depth of 1 – 3 meters. We hypothesize that the strong reflections are caused by the significant difference in dielectric properties between the sandy river deposits and the adobe walls which would have dissolved quickly in the flood and been redeposited. As GPR continues to locate potential San Salvador artifacts, concentrated surveys using magnetic gradiometry and EM are being planned for confirmation. Our goal is to aid the Spanish Town Heritage Foundation in proving the cultural importance of this site before the city of Colton's plans to develop the land are implemented.

Monitoring Fault Creep on the Hayward Fault using Structure from Motion, Jerlyn L Swiatlowski, and Gareth J Funning (Poster Presentation 117)

Fault creep is an ongoing process that can be a problem for urban areas that lie along the fault trace. A prime example is Fremont, CA, on the creeping Hayward Fault, where the mean creep rate is ~6 mm/yr. Expressions of fault creep can be seen through offsets in man-made features such as fences, sidewalks, and buildings. Of these features, sidewalk offsets become more visible over the years due to fault movement. Since most sidewalk offsets are along public streets, they can be recorded photographically for years. Monitoring sidewalk offsets allows us a to measure the local creep rate of the Hayward fault and monitor how it is affecting the surrounding urban areas. Here we present creep rate results using photogrammetry to observe and measure creep from multiple sidewalks along the Hayward fault in Fremont.

Since 2009, we have been measuring the creep rate in Fremont, using digital cameras. Originally, we took photos with the camera set up horizontally on a tripod at a fixed height above, and centered over, the offset feature. In 2015, we moved to using Structure from Motion (SfM), a photogrammetric technique that uses multiple 2D images to create 3D point clouds. The main requirements for this technique is to have a fixed focal length camera, take an even distribution of photos around the sidewalk, and have a known reference scale within each photo. Using the Agisoft PhotoScan software, we produce 3D point clouds of each offset sidewalk, using a reference object photographed along with the sidewalk for scale. This newer approach eliminates the need to align and level the camera, and reduces the total time to take photos at each site.

We have 3 years of photographs, and point clouds derived from them, for 36 sidewalk sites in Fremont. We use the Iterative Closest Point (ICP) method to compare point clouds from the same sidewalk from different years. First, we roughly align the sidewalks and crop out the same are. Then we align the point clouds using only points from one side of the offset, by identifying as many features as possible that are the same between each set of photographs and marking them as anchors to fine tune the alignment. The final step is then to estimate the displacement between the two point clouds on the side that was not aligned – the result of creep during the time interval. Preliminary results show that measuring displacement using SfM and ICP is possible, and we can resolve creep at rates as low as 3 mm/yr using the method.

Evaluating and Improving Ground Motion Predictions for Scenario Earthquakes in The San Francisco East Bay by Integrating Earthquake Ground-Motion Simulations and Noise-Derived Empirical Green's Functions , Taka'aki Taira, and Arthur J Rodgers (Poster Presentation 003)

Simulations of scenario earthquake ground motions play an increasingly important role in improving seismic hazard assessment. In the San Francisco Bay Area (SFBA) the USGS has developed a 3D geologic/seismic model. Simulations of large magnitude (M) 7 Hayward Fault scenario earthquakes show dramatic differences in peak ground motions across the fault, arising from wavespeed differences, which introduce the uncertainty in ground motion estimation. Preliminary comparison of observed and simulated waveforms from M 4 earthquakes reveals bias in the travel times of direct S-waves for paths crossing the East Bay Hills, east of Hayward Fault. To reduce the uncertainty in ground motion prediction for scenario earthquakes, we systematically evaluate bias in the current USGS 3D velocity model of the SFBA with emphasis on the East Bay Hills where strong ground motions are predicted. Our work involves performing earthquake ground motion simulations incorporating the USGS 3D velocity model for moderate Bay Area local earthquakes (M 3.5-4.5) including the recent 2018 Mw 4.4 Berkeley earthquake to quantify the accuracy of 3D model predictions by comparing observed and simulated waveforms. We also retrieve noise-based empirical Green's functions (NEGFs) from ambient noise cross-correlation and earthquake coda waves to illuminate path-specific bias in the USGS 3D velocity model. We will report resultant path-specific bias to update the current 3D velocity model. Results from our work will provide the groundwork for the USGS 3D velocity model improvement and will result in improved accuracy of scenario ground-motion maps at the SFBA.

Evolution of frictional shear resistance in response to rapid variations of normal stress, Yuval Tal, Vito Rubino, Nadia Lapusta, and Ares J Rosakis (Poster Presentation 174)

A proper formulation of the shear-resistance evolution during rupture is essential for many earthquake source problems, including simulations of the ground motion. While the shear resistance is typically assumed to be proportional to normal stress, several studies have shown a gradual, slip-dependent, response of the frictional shear resistance to rapid variations in the normal stress. Here we use laboratory experiments to quantify normal stress variations and the corresponding evolution of the frictional shear resistance produced by the interaction of dynamic ruptures with the free surface, similarly to what occurs in natural thrust events. The experiments also enable studying the potential fault opening and ground motion of the simulated thrust faults. In order to image and quantify the full-field behavior of the ruptures near the free surface, we use an experimental technique (Rubino et al., 2017) that combines ultra-high speed photography and digital image correlation to produce maps of dynamic displacements, velocities, strains, and stresses at intervals of less than a microsecond. It allows us to image the evolution of fault-normal stress and fault-parallel shear stress, and thus to study how friction evolves under the conditions of rapid normal stress variations. We enhance the experiments with dynamic simulations, using a self-developed finite element simulator (Tal and Hager, 2017). The simulations help us to design the experiments, explore a wider range of geometries and loading conditions, constraint parameters and conditions that cannot be constraint solely by the experiment, and study how the ground motion would be affected by different assumptions about the friction evolution on the fault near the free surface.

Lower-crustal rheology and thermal gradient in the Taiwan orogenic belt illuminated by the 1999 Chi-Chi earthquake, Chi-Hsien Tang, Ya-Ju Hsu, Sylvain D Barbot, James Moore, and Wu-Lung Chang (Poster Presentation 129)

The strength of the lithosphere controls tectonic processes and seismic cycles. Laboratory rock experiments provide fundamental insights into rock rheology under various conditions, but an extrapolation to the strain-rate and length scale relevant to the lithosphere is still required. The response of the lithosphere to the stress perturbation generated by large earthquakes can be treated as a large-scale creep experiment, but so far this approach has been limited to testing simplified assumptions. Here, we exploit the stress change following the 1999 Mw 7.6 Chi-Chi earthquake and 14 years of postseismic GPS observations to directly image the spatio-temporal viscoelastic transient beneath the Taiwan orogenic belt and to constrain its physical properties. We show that the evolution of stress and strain-rate beneath the middle section of the Central Range is best explained by a power-law Burgers rheology, suggesting that rocks exhibit nonlinear transient creep shortly after the mainshock before reaching steady-state dislocation creep. This evolution is compatible with the flow laws for quartz and feldspar and thermal gradients of 35 °C/km and 20 °C/km beneath the Central Range and Coastal Plain, respectively. The effective viscosity rapidly increases from ~10^17 to ~10^19 Pa s in the first year, and to 2x10^19 Pa s after a decade. Our study demonstrates the potential for geodesy to constrain in situ rheological properties of lithosphere rocks, bridging the gap between laboratory and fault-system scales of creep behaviors.

Evaluation of CyberShake ground motions for engineering practice, Ganyu Teng, and Jack W Baker (Poster Presentation 006)

This poster presents the results from evaluation of CyberShake ground motions for high-rise building design in the Los Angeles region. The feasibility of CyberShake is studied by comparing simulated ground motions against recordings from past earthquakes as well as empirical models. This study considers two sites with different underlying soil conditions in the Los Angeles region, and selects comparable suites of ground motion records from CyberShake and NGA-West2 according to the ASCE 7-16 requirements. In particular, intensity measures, shaking duration, directional polarization and consistency of the selected ground motions' properties with hazard deaggregation are analyzed. This poster highlights major evaluation results: 1) Selected ground motions from CyberShake and NGA-West2 share similar features; 2) During CyberShake ground motion selection, it is easy to choose records with specific sources to match the hazard deaggregation; 3) CyberShake durations on soil match well with empirical models, whereas those on rock are consistently shorter; 4) Some ground motions generated by San Andreas fault ruptures produce excessive polarization, but they can be usually excluded after the ground motion selection process. This study serves as a preliminary evaluation of CyberShake and results suggest that CyberShake ground motions are suitable for engineering practice.

Heat Flow Data and Seismic Imaging Reveal Both Transient and Steady-State Thermo-Mechanical Processes at Work Beneath Southern California, Wayne R Thatcher, and David S Chapman (Oral Presentation Mon 10:30)

Analysis of heat flow and seismic data provides glimpses of the dynamical processes shaping the thermal evolution of southern California. The present day thermal field bears an imprint of long-lived subduction prior to 30 Ma and subsequent growth of a continental transform boundary. Post 30 Ma processes include (1) a continental analog of seafloor spreading beneath the Salton Trough, (2) thermal pulses due to slab window effects, (3) mantle lithosphere detachment and sinking beneath late Cretaceous batholiths, and (4) extension and formation of metamorphic core complexes (MCC) in the offshore Inner Borderland.

Over 200 high quality surface heat flow (SHF) measurements define 14 distinct southern California heat flow regions (HFRs) where SHF is relatively constant. Assuming seismic estimates of lithosphere-asthenosphere boundary depth (sLAB) coincide with thermal LAB, two remarkable features are revealed. First, for 11 HFRs with SHF 40-83 mW/m2, sLAB depth is a surprisingly constant 70 ± 5 km. These data points naturally separate into 2 clusters, the first with average SHF of 40-58 mW/m2 (Cluster 1), the second with SHF of 68-83 mW/m2 (Cluster 2).

Simple 1D steady-state thermal conduction models can match the six Cluster 2 HFRs. P/T constraints from mantle xenoliths and erupted lavas considerably narrow the range of acceptable geotherms, with Moho at 700˚- 800˚C and LAB 1200˚- 1300˚C. However, such simple models are inconsistent with the low SHF of Cluster 1. In each of these 5 HFRs there is geologic and/or seismic evidence for Late Cenozoic detachment and sinking of mantle lithosphere. A transient 1D conduction model is used that includes an initially 30 to 50 km thick lithosphere exposed to hot asthenosphere 3-10 Ma BP conductively cooled and thickened by mafic underplating. Current temperatures are warm in the lower crust, ~850˚C at the Moho, and ~1200˚C at the LAB.

Salton Trough has the highest SHF (100-140 mW/m2) and thinnest lithosphere (45-55 km) in southern California. A model with steady state crustal thickness of 24 km, constant rates of stretching and sedimentation into the Trough and basaltic under-plating at the Moho matches the data, with a hot lower crust and ~1400˚C asthenosphere at the Moho.

Finally, the Inner Borderland HFR has an unusually thin lithosphere of 49±6 km and SHF of 77±6 mW/m2, consistent with its origin as a Miocene MCC subsequently unroofed and depleted of its upper crustal heat producing elements.

Sensitivities and Uncertainties in Probabilistic Fault Displacement Hazard Analysis in Southern California, Hong Kie Thio, and Jeff R Bayless (Poster Presentation 303)

As applications of Probabilistic Fault Displacement Hazard Analysis (PFDHA) become more prevalent in California, it is of interest to understand the sensitivities and uncertainties in the models used, both for the source characterization as well as the empirical displacement prediction equations. In California, UCERF3 is the standard recurrence model for seismic hazard applications. In order to explore the effect of epistemic uncertainties on the uncertainties in the final hazard results we have used the full logic tree of UCERF3 in a PFHDA for a generic sites on the Newport-Inglewood strike-slip fault. For the displacement equations, we used the six relations from the Petersen et al. (2011) study, which is specifically geared towards strike-slip faults as well as the Takao et al. (2014) relations for all mechanisms for Japanese earthquakes.

The UCERF3 logic tree comprises of 2 geometrical alternatives (UCERF3.1 and UCERF3.2) each with 720 branches. Additional branches are 8 for the displacement relations and 2 more for alternative models for the probability of surface rupture. We will present the hazard results as maps of the hazard for an area around the fault, mean and fractile hazard curves to illustrate the range of uncertainty and tornado plots, which demonstrate the sensitivity of the final results to specific branches of the logic tree.

Unraveling a tectonic knot: structural domains, voluminous fault zones, creep, and dispersed strain between the San Andreas Fault and Brawley Seismic Zone, Clara Thomann, Susanne U Jänecke, Daniel Markowski, James P Evans, and Robert Quinn (Poster Presentation 274)

We report preliminary results from an ongoing analysis of the southern tip of the San Andreas fault (SAF) and northern Brawley seismic zone (BSZ). The SAF consists of the compressional Durmid ladder structure (DLS) along the northeast shore of the Salton Sea, and it progressively transitions into the only exposed part of the extensional BSZ north of Bombay Beach (Jänecke et al. 2018). We name this region between two dispersed and voluminous fault zones the Pope transition zone (PTZ) for a railroad stop within it. The PTZ has well exposed faults and folds, illustrating the complex boundary between major fault zones along the edge of the North America plate. The geometric pattern emerging from our field- and image-based research shows that the single main strand of the SAF loses its identity southward, and structural domains replace one another along strike and laterally. From NW to SE, the main strand of the SAF changes from a single, NW-striking trace with intense damage to a southward-widening zone of small-offset faults that span >1-km near Bombay Beach. A western fault zone abuts the DLS southeast-plunging anticline with folded 0.76 Ma Bishop Ash, and trends NNW overall with right-stepping mini-ladders and faults. On the NE side, an eastern fault zone separates the mostly NW-striking structures and significant Holocene cover of the PTZ from the exhuming structures of the Hidden Springs ladder structure. Deformation between the east and west belts is variable, including many N-, NE-, ENE-, and ESE-striking cross faults. Subsidence and Holocene sediment within the PTZ progressively increase moving southward, and therefore we identify active fault traces using creep-related fractures, sinks and erosional features. NNE- to NNW-striking normal-oblique faults in the PTZ cut modern sediment, a pattern consistent with the transtensional BSZ to the south. Plate boundary strain appears to be distributed across the entire volume of the dispersed PTZ and adjacent DLS regions. Long trenches will be necessary to assess the latest Holocene earthquakes given creep and recent fracturing is distributed across the PTZ. Trenching by Lindvall (1989) showed that 123-m long trenches were too short to capture all the active faults in the fault zone. These findings have clear implications for models and paleoseismic studies in a region overdue for a large earthquake, and whether large ruptures have passed through or been inhibited by the knot of structures within the PTZ.

The New Zealand Velocity Model (NZVM) Version 2.0 and ground motion simulations of Hope Fault earthquakes, Ethan M Thomson, Brendon A Bradley, and Robin L Lee (Poster Presentation 287)

This poster presents recent updates to the New Zealand Velocity Model (NZVM) for use in physics-based broadband ground motion simulation and scenario simulations of ruptures on the Hope Fault. The NZVM is based on the concept of embedding high-resolution regional models in a modular fashion within a lower-resolution 3D tomography-based velocity model for the shallow crust. This flexible and extensible approach allows new regional models to be incorporated within the NZVM as they become available. The NZVM Version 2.0 builds on Version 1.0 by incorporating seven recently developed regional sedimentary basin models, distributed throughout New Zealand, to supplement the existing Canterbury region model implemented in Version 1.0. Additionally, a Vs30-based near-surface geotechnical layer and a new basin-edge smoothing regime have been implemented.

Broadband ground motion simulations for scenario ruptures of the Hope Fault are presented as a test case to assess the new basin models. The Hope Fault is a strike-slip fault in the South Island that transects the Hanmer and Kaikoura Basins, which are explicitly modelled in NZVM Version 2.0. It is a major contributor to the seismic hazard in the region and has the second highest slip rate (~20mm/yr) of any South Island fault. Results of ground motion simulations for historic small to moderate magnitude (4.0<Mw<5.0) earthquakes are used to validate the velocity structure within the new basins characterised in NZVM Version 2.0. Numerous scenario source geometries involving multiple fault segments spanning from the Kelly Fault (a splay fault off the Alpine fault) through to the Jordan Thrust were considered. The scenarios varied from Mw 7.1 to a maximum magnitude of 7.7. Simulation results for the Hope Fault scenarios are compared with 14th November 2016 Kaikoura Mw 7.8 earthquake to compare their relative regional impacts.

The Thousand Lake Fault: Earthquake Geology of a Long Recurrence Normal Fault at the Eastern Edge of the Basin and Range, Nathan A Toke, David W Marchetti, Christopher M Bailey, Robert Biek, Joseph Phillips, Hanna Bartram, and Clayton Forster (Poster Presentation 223)

The Thousand Lake fault (TLF) is 50-kilometer-long normal fault and a prominent structural boundary between the Basin and Range and the Colorado Plateau in southern Utah. Many of the most active faults in the Basin and Range (those with slip rates > 0.5 mm/a) are located along the margins of the physiographic province such as the Wasatch, East Cache, Great Salt Lake, and Oquirrh faults in northern and central Utah. However, faulting along this margin in southern Utah becomes distributed across an array of less active faults. Determining the relative rates of activity within this array is important for understanding how deformation has been accommodated across the Basin and Range and for characterizing the earthquake hazard. The easternmost fault in this array is the TLF, which trends north-south and dips steeply to the west. Here, we present a preliminary assessment of the TLF earthquake geology based upon bedrock mapping, cross sections, geomorphology, and paleoseismic investigation. Geologic mapping and cross sections reveal that the cumulative throw across the TLF is defined by a Tertiary volcanic tableland which has been displaced by 700-1500 m in the central portion of the fault zone. This indicates that the slip rate has ranged from 0.05-0.15 mm/a since Basin and Range initiation during the mid-Miocene. Surface age dating of terraces along the nearby Fremont River, which flows to the east, cross-cutting the central TLF, indicates that the river is incising at ~0.5 mm/a since about 200 kya, clearly outpacing the fault. In 2018 we conducted a paleoseismic investigation across a ~4m high fault scarp developed within an abandoned alluvial fan surface near Bicknell, Utah. Helium-3 exposure age dating of the large andesite boulders (> 1 m in diameter) which are strewn across the surface indicate that the fan was abandoned during the Late Pleistocene (from 81-246 kya). Paleoseismic trenching revealed good evidence for one ground-rupturing earthquake that displaces a stage III soil carbonate horizon by 0.8-1.2 m. These data indicate that the late Pleistocene slip rate could be less than 0.05 mm/a and that the hazards-relevant recurrence rate along the TFL is likely within the range of 50,000 to 125,000 years per event.

Updating GPS site positions and velocities and improving GPS coverage in southern California for the Community Geodetic Model, Eneas Torres Andrade, Gareth Funning, and Jerlyn L Swiatlowski (Poster Presentation 137)

We have conducted a GPS resurvey of geodetic benchmarks in the Inland Empire of southern California, with the goal of more precisely determining the rates of movement of the major strike slip faults in the region – the San Andreas, San Jacinto and Elsinore faults. The gathering and processing of the acquired GPS data from these geodetic benchmarks will ultimately provide updated and more precise GPS velocities, which will in turn lead to better constraints on modeled fault slip rates. In addition, new campaign GPS surveys provide the opportunity to add additional campaign sites that can, with time and with additional measurements, yield new velocity estimates. Finally, GPS resurveys can help to maintain memory of locations of GPS benchmarks, and hence improve our ability to respond promptly to earthquakes.

To conduct the survey we used three high precision GNSS receivers and antennas (Trimble R7 receivers and Trimble Zephyr Geodetic antennas) to log GPS satellite measurements. Benchmarks were typically occupied overnight, yielding observations spanning 15 hours or longer. The resulting raw data were preprocessed into the RINEX file format using the runpkr00 and teqc software. Next, the resulting RINEX files were processed using the GAMIT processing suite to update or estimate new GPS positions of the surveyed benchmarks, and also to check the quality of the data. In total, we occupied 26 benchmarks over a 10 week period. We added a total of six new benchmarks – two in the Cajon Pass area and three in Whitewater Canyon near the San Andreas fault, and an additional one near the San Jacinto fault, improving the density of GPS coverage in the region. We also surveyed sites measured for the first time by past SCEC interns and updated the positions from these sites, adding a total of three new velocities.

Visualization of Hazards Associated with Simulated Earthquakes in Southern California, Ashlee Trotter, Ramon Mei, Paige R Given, Christina Polcino, Elvis Carrillo, Jordan Wolz, Resherle Verna, Jozi K Pearson, Gabriela R Noriega, and Thomas H Jordan (Poster Presentation 315)

The 2018 Undergraduate Studies in Earthquake Information Technology (USEIT) internship program challenged the Hazard and Risk Visualization (HaRVi) Team to analyze and visualize threatening earthquake scenarios on the southern section of the San Andreas Fault system based on economic loss and location. The scenarios were selected from a 1-million year catalog of earthquake simulations generated by the USEIT High Performance Computing Team using the Rate-State earthQuake Simulator. We utilized the Open Seismic Hazard Analysis (OpenSHA) software and Javascript to manipulate seismic data into ShakeMap files that display ground motion along a fault rupture. These ShakeMaps were then converted to XML files and uploaded into FEMA's Hazus (hazard analysis software application) to calculate the impact of ground motion within different affected areas. Based on magnitude and location, scenarios were selected to calculate economic losses and to estimate average annualized losses to serve as an indicator of high-risk events. The data was narrowed and categorized by constructing various different earthquake "classes" based on the faults ruptured, percentage of fault rupture, and event magnitude. This allowed us to conduct thrust fault analyses of the Greater Los Angeles Area. Over 100 simulated scenarios were analyzed using this process. The HaRVi team worked closely with the SCEC-VDO (Visual Display of Objects), Probabilistic Forecasting, and the HPC teams in order to achieve their research goals. We utilized visualization tools such as ESRI's ArcGIS program and SCEC-VDO to illustrate the results based on Hazus' calculations.

Progress Report 2 on Addition of a High-Speed Drive to High-Pressure, Rotary-Shear Apparatus, Terry E Tullis (Poster Presentation 177)

Rotation of the sample in my rotary-shear, high-pressure machine is driven by two systems. The first uses an electrohydraulic stepping motor providing unlimited displacement at >7 orders of magnitude in speed from 0.001 microns/s to 10 mm/s. The second system rides piggy-back on the rotating table driven by the first system, and is a hydraulic rotary servo with 9 degrees of rotation, allowing effective stiffening of the loading system.

This project involves adding a high-speed servo motor drive to the apparatus to allow rotation of samples at slip speeds up to ~4.5 m/s. This will allow study of high-speed friction weakening mechanisms at effective normal stresses similar to those at which crustal earthquakes occur. The motor will be positioned on the table rotated by the electrohydraulic stepping motor, replacing the present hydraulic rotary servo. This will allow continuous changes in speed of over 9.5 orders of magnitude.

Since our last report 2 years ago we have turned the motor design into a functional motor by fabricating and assembling a large number of fixtures, bearings, etc. We have also assembled and connected several components needed for the motor to function, including a Haskris chiller, a Siemens Simanic S120 motor controller, and a control system that allows LabVIEW control of programed slip speed and displacement sequences. We have built a 27-bit Heidenhain absolute optical encoder into the motor as the feedback device for the Siemens motor controller, allowing tight motor control to a precision corresponding to a nominal sample slip of 1 nanometer; in practice, noise degrades this by a factor of about 8. The controller can use the existing 24-bit resolver in a secondary feedback loop, allowing electronic stiffening of the apparatus as at present, but at higher speeds.

The motor is currently being tested on the bench prior to installing it in the deformation apparatus. Although its performance is impressive, additional tuning of the motor control parameters is needed to attain the precision of speed and displacement control and the accelerations that the system is nominally capable of. A video showing a sequence of motor speed steps will be shown at the poster.

Once the motor is installed and operational, jacketing of the samples at high slip speeds is the next challenge. Elevated temperatures due to frictional heating of the samples will require use of more refractory materials than the present Teflon rings and Viton O-rings.

Preliminary Site Response Results across the San Gabriel and San Bernardino Basins Utilizing the Ambient Noise Spectral Ratio Method, Anisha D Tyagi, Margaret Grenier, Rachel Kreuziger, Jacob S Kays, and Jascha Polet (Poster Presentation 111)

Sedimentary basins, such as the San Gabriel and San Bernardino Basins, are known to amplify earthquake ground motions; therefore, it is important to characterize these Basins and determine site response parameters across these structures to mitigate seismic hazard. One of the effects causing ground motion amplification in basins is resonance. Basins have a specific resonance period that depends on their geometry and material properties. If this resonance period is the same as that of a building, the resulting double resonance effect will further increase the potential for damage. The San Gabriel and San Bernardino Basins are densely populated regions that are surrounded by a network of faults, which have the capacity to produce significant earthquakes. Additionally, the energy from a potential major rupture on the southern San Andreas Fault could be funneled through the San Gabriel and San Bernardino Basins, acting as a waveguide, into the Los Angeles Basin (Denolle et al., 2014).

inear seismic arrays consisting of hundreds of nodes were deployed across the San Gabriel and San Bernardino Basins in 2017 and nearly one month of three-component waveform data was collected. The ambient noise waveform data was processed using the Geopsy software to determine Horizontal-to-Vertical Spectral Ratio (HVSR) curves, which inform us about the resonance frequency and ground motion amplification at each site. Site Effects Assessment Using Ambient Excitations (SESAME) guidelines are applied to the HVSR curves to determine reliability and clarity for all processed data. The analysis of the spectral ratio curves shows a significant variation in both resonance periods and amplification factors across both Basins. Results for the Western San Gabriel Basin line indicate peak frequencies above 1 Hz for nodes situated to the north of the Raymond Fault and peak frequencies that range from 0.2-0.3 Hz for nodes south of the Raymond Fault. Higher peak frequencies along the Central Basin line suggest a shallower basin. Nodes in the southern portion of the San Bernardino Basin, specifically in the southern half of the Chino Basin, indicate peak frequencies around 0.4 Hz. The peak HVSR amplitudes range from 2.0-4.5, indicating potential for significant ground motion amplification. Future work includes comparison of our resonance periods with those predicted by structural models of the Basins to help improve our understanding of their deep subsurface structure.

Geodetic and geologic observations of creep on the Southern San Andreas Fault triggered by the 2017 Chiapas (Mexico) earthquake, Ekaterina Tymofyeyeva, Yuri Fialko, Junle Jiang, Roger Bilham, David T Sandwell, Thomas K Rockwell, Chelsea M Blanton, and Allen M Gontz (Poster Presentation 114)

Observations of shallow fault creep reveal increasingly complex time-dependent slip histories that include quasi-steady creep and triggered as well as spontaneous accelerated slip events. We report a recent slow slip event on the southern San Andreas fault (SSAF) triggered by the 2017 Mw 8.2 Chiapas (Mexico) earthquake that occurred approximately 3000 km away. Geodetic and geologic measurements indicate that 4-12 mm of surface slip that occurred on a 40-km-long section of the SSAF between the Mecca Hills and Bombay Beach over 6 months following the Chiapas earthquake. Both the magnitude and the depth extent of creep vary along strike. We derive a high-resolution map of surface displacements by combining Sentinel-1 Interferometric Synthetic Aperture (InSAR) acquisitions from different lines of sight. InSAR-derived displacements are in good agreement with the creepmeter data and field mapping of surface offsets. In addition, we calculate InSAR time series at selected locations along the fault. Although InSAR acquisitions are too infrequent to pinpoint the exact timing of the event, we are able to capture the temporal history of the transient surface deformation due to triggered creep. Inversions of surface displacement data using dislocation models indicate that the highest amplitudes of surface slip are associated with shallow (<1 km) depth extent of transient slip.

Surface Displacement and Ground Motion from Dynamic Rupture Models of Thrust Faults with Variable Dip Angles and Burial Depths, Sirena Ulloa, and Julian C Lozos (Poster Presentation 210)

Historic earthquakes and empirical studies show that thrust fault ruptures produce stronger ground motion than normal or strike-slip events of the same size. This is due to a combination of hanging wall effects, vertical asymmetry and higher stress drop due to compression. Surface displacement occurs with blind thrust ruptures in addition to those with surface expression. This poses a hazard since surface displacement can potentially break lifelines, such as water pipes and gas lines. Our 3D dynamic rupture modeling parameter study focuses on planar thrust faults of varying dip angles and burial depth, in order to establish a physics-based understanding of how these geometrical parameters affect surface displacement and ground motion. We vary dip

angles from 20º to 70º, and burial depths from 0 km down to 5 km, and we conduct rupture models on these geometries under several different initial stress conditions. We analyze how systematic variation of these parameters affects peak particle velocity and surface displacement over the fault, with a particular focus on hanging wall versus footwall effects. Due to the simple geometry of a planar fault, our results can be applied to understanding basic behavior of specific real-world thrusts. The results of this study can also be used to aid in global hazard calculation.

New software for computing time dependent seismic hazard during aftershock sequences using the OpenSHA platform, Nicholas J van der Elst, Kevin R Milner, Edward H Field, Sara K McBride, and Morgan T Page (Poster Presentation 045)

The chaos caused by a major earthquake does not end when the shaking stops. Search and rescue, damage assessment, and lifeline repairs all need to be carried out under the constant threat of damaging aftershocks. In some cases, aftershocks can be even more destructive than the initial event, as was the case in Christchurch, New Zealand in the 2010-11 earthquake sequence. While it may never be possible to predict the exact time, place, and magnitude of an impending earthquake, it is nonetheless possible to make probabilistic assessments of aftershock hazard based on past regional sequences and the specifics of an ongoing sequence. Forecasts, and in particular forecast maps, can provide situational awareness, increase public resilience, and help prioritize response and recovery operations. During times of crisis, quick production and release of these forecasts can help fill the vacuum of information and assist a variety of people in making informed decisions.

The USGS, with support of USAID-Office of U.S. Foreign Disaster Assistance, is developing several lines of aftershock forecasting products with the goal of providing rapid quantitative aftershock information to emergency managers and affected communities. Here we introduce software designed to streamline the process of analyzing and forecasting aftershock sequences within a modified Epidemic-Type Aftershock Sequence framework. Forecasts are a Bayesian combination of a regionalized generic model and a specific model tuned to the ongoing sequence as reported by ComCat. The software translates spatio-temporal rate forecasts into time-dependent probabilistic hazard estimates using standard ground-motion prediction equations. Graphical forecast summaries and hazard maps supplement standard magnitude-probability tables. This presentation will describe modifications to the ETAS model that allow for efficient and stable generation of aftershock forecasts, and discuss expected applications of the software.

Sequential Data Assimilation for Seismicity: Probabilistic Estimation and Forecasting of Fault Stresses, Ylona van Dinther, Hans Rudolf Künsch, and Andreas Fichtner (Poster Presentation 042)

Our physical understanding and forecasting ability of earthquakes is significantly hampered by limited indications on the evolving state of stress and strength on faults. Integrating observations and physics-based numerical modeling to quantitatively estimate this evolution of a fault's state is crucial. However, systematic attempts are limited and tenuous, especially in light of the scarcity and uncertainty of natural data and the difficulty of modelling the physics governing earthquakes. We adopt the statistical framework of sequential data assimilation - extensively developed for weather forecasting - to efficiently integrate observations and prior knowledge in a forward model, while acknowledging errors in both.

To prove this concept we perform a perfect model test in a simplified subduction zone setup, where we assimilate synthetic noised data on velocities and stresses from a single location. Using an Ensemble Kalman Filter, these data and their errors are assimilated to update 150 ensemble members from a Partial Differential Equation-driven seismic cycle model.

Probabilistic estimates of fault stress and dynamic strength evolution capture the truth exceptionally well. This is possible, because the sampled error covariance matrix contains prior information from the physics that relates velocities, stresses and pressure at the surface to those at the fault. During the analysis step, stress and strength distributions are thus reconstructed such that fault coupling can be updated to either inhibit or trigger events. In the subsequent forecast step the physical equations are solved to propagate the updated states forward in time and thus provide probabilistic information on the occurrence of the next event. At subsequent assimilation steps, the system’s forecasting ability turns out to be significantly better than that of a periodic recurrence model (requiring an alarm ~17% vs. ~68% of the time). This thus provides distinct added value with respect to using observations or numerical models separately. Although several challenges for applications to a natural setting remain, these first results indicate the large potential of data assimilation techniques for probabilistic seismic hazard assessment and other challenges in dynamic solid earth systems.

On the Role of Temperature and Rheology in Seismicity in Convergent Margins, Ylona van Dinther, Luca Dal Zilio, Mario D'Aquisto, Robert Herrendörfer, and Taras Gerya (Oral Presentation Mon 11:00)

Earthquake nucleation, propagation and arrest are governed by fault stress and strength. Thus understanding how these are regulated by long-term processes involving temperature, rheology and tectonic forcing - in combination with short-term earthquake interactions - is important. To decipher and extend our too limited and indirect observational record, we developed the first quantitative model able to simulate the dynamics governing both tectonic processes over millions of years and the family of fault slip processes down to milliseconds. We utilize this seismo-thermo-mechanical modeling framework to show how stress evolution, temperature, and crustal and lithospheric rheology interact to shape convergent margins, seismic cycle observations and seismicity behavior. Through quantifying their feedback in a self-consistent manner, we establish how convergence rate across continental collision zones affects temperature and viscosity distribution. This determines stress and strength distributions, which govern earthquake maximum magnitude, recurrence patterns, and Gutenberg-Richter statistics. In a more observationally constrained approach, temperature, geometry and forcing can be predefined using geological and geophysical constraints to improve our understanding of seismicity in particular regions. Such tectonically realistic models of the Nepal Himalaya demonstrate the Main Himalayan Thrust geometry facilitates a bi-modal seismicity regime with M>=8 surface ruptures following a series of deeper, ~M7 megathrust earthquakes. In the Northern Apennines (Italy), such models show that slab delamination and retreat along with a high temperatures and a ductile lower crustal rheology are necessary to match both long- and short-term observations. These self-consistent and regionally-constrained examples illustrate the importance of thermal and rheological models for understanding seismicity.

Enhancing 0.4-1.0 Hz seismic signals in Green's functions through judicious selection of time intervals, Ian Vandevert, Aaron K Anderson, Taro Okamoto, and Toshiro Tanimoto (Poster Presentation 112)

When we compute cross-correlation of seismic noise, we typically see dominant signals in the microseism frequency band, approximately 0.05-0.3 Hz. Cross-correlations have been done for higher frequency ranges, say up to 2 Hz, but if we do not pay attention to details, the Green's functions tend to be dominated by the signals below 0.3 Hz. In this study, we attempt to obtain reliable high-frequency signals in cross-correlated waveforms by choosing time intervals when the Los Angeles Basin is filled with high frequency signals; this should lead to an improved shallow seismic velocity structure in the Los Angeles Basin.

We have noted that there are days when the Los Angeles Basin is filled with high frequency noise about 0.4-1.0 Hz in addition to noise in the microseism frequency band. They last a few days each time but they appear only a few times per month. We propose to choose such days, based on time-frequency plots from various stations, and then apply the cross-correlation Green's function method. We typically find good signals in Green's functions for frequencies about 0.4-1.0 Hz.

In order to understand the nature of these waves, we numerically computed the kernels by the finite difference method for a pair of stations for the range 0.4-1.0 Hz and examined depth sensitivity of waves to the SCEC CVM models. The kernels indicate high sensitivity to depths shallower than 2 km and suggest that we can improve LA Basin structure through collections of such Green's functions. Group velocity measurements of the maximum amplitude phases in such Green's functions show regional variations and seem to match surface geological features.

Assessing off-fault damage during development of a dismembered flower structure, Emma J Vierra, Bonnie A Flynn, Mario S Bermudez, Heather N Webb, Gary H Girty, and Thomas K Rockwell (Poster Presentation 158)

As part of our ongoing study of off-fault damage along the San Jacinto fault (SJF), southern California, we here document the physical and chemical properties controlling damage intensity NW of Hog Lake and compare these results to those published from the Wellman Ranch locality, ~19 km to the SE. The two sites represent portions of a dismembered flower structure that is offset along the Clark fault segment. At both sites, damage in sandstones of the Pleistocene Bautista Fm is defined by intragranular fractured quartz grains with jig-saw puzzle texture, representing pulverization at the grain scale.

At the site NW of Hog Lake, the number of quartz grains containing >10 fractures/grain was greatest in sandstones within 5 meters of the fault core. Also, within this 5 m interval, porosity, in general, decreases, and damage intensity varies as a function of the proportion of matrix. In addition, textural analysis of damaged samples at Hog Lake reveal two crudely developed directions of foliation that are not apparent in samples outside the damage zone and may record NE-SW contraction associated with thrusting. Mass balance calculations derived from chemical analysis of Hog Lake samples indicate a statistically significant loss of 31% (+30/-21) Si and 29% (+23/-17) K mass, and an overall loss of ~23% (+/- 20) bulk mass and ~33% (+/- 18) volume. In contrast, at Wellman Ranch, the number of quartz grains containing >10 fractures/grain were greatest in sandstones with <18% matrix, and damage is heterogeneously developed at distances of at least 25 m. In addition, changes in bulk mass and volumetric strain are not statistically significant.

Based on data from both locations, the site NW of Hog Lake has a more well defined ~5 m thick damage zone where pulverization falls within the limits imposed by published experimental and theoretical experiments. Our data imply that pulverization within the damage zone at this site likely occurred during the development of the flower structure and over-thrusting along the boundary thrust fault. Moreover, there is evidence that highly acidic solutions migrated through the damage zone. Hence, there may have been cycles of fragmentation followed by focused fluid flow within damaged zones during the overall development of the flower structure.

The slow slip of viscous faults, Robert C Viesca, and Pierre Dublanchet (Poster Presentation 189)

We examine a simple mechanism for the spatiotemporal evolution of transient, slow slip. We consider the problem of in-plane or anti-plane slip on a fault that lies within an elastic continuum and whose strength is proportional to sliding rate. This rate dependence may correspond to a viscously deforming shear zone or the linearization of a non-linear, rate-dependent fault strength. We examine the response of such a fault to external forcing, such as local increases in shear stress or pore fluid pressure. We show that the slip and slip rate are governed by a type of diffusion equation, the solution of which may be found by using a Green's function approach. We derive the appropriate long-time, self-similar asymptotic expansion for slip or slip rate, which depend on both time t and a similarity coordinate eta = x/t, where x denotes fault position. The similarity coordinate shows a departure from classical diffusion and is owed to the non-local nature of elastic interaction among points on an interface between elastic half-spaces. We demonstrate the solution and asymptotic analysis of several example problems. Following sudden impositions of loading, we show that slip rate ultimately decays as 1/t while spreading proportionally to t, implying both a logarithmic accumulation of displacement as well as a constant moment rate. We discuss the implication for models of post-seismic slip as well as spontaneously emerging slow slip events.

Geologic and Structural Characterization of The Rock Volume Imaged by the Dense Nodal Seismic Array Along the San Jacinto Fault at Sage Brush Flat, Southern California, Adam Wade (Poster Presentation 229)

Characterization of fault zones is critical to understanding earthquake mechanics and seismic hazard evaluations. Investigations of fault zones often involve detailed surface mapping, and/or subsurface imaging through seismic waves and other geophysical data. Direct comparison of these different data sets are often difficult due to their differing scales and depth ranges. This study composites detailed mapping and local morphology, along with a previous study's 3D seismic shear wave tomography from a dense nodal array, to evaluate shallow (<1 km depth) properties of the San Jacinto fault zone (SJFZ). Previous mapping of the SJFZ at Sage Brush Flat (SGB) near Anza, CA, traces multiple fault strands into a single fault along the metamorphic-plutonic contact. We've revised both the fault trace and geologic mapping using high resolution topography. Previous unmapped geologic units, include a subunit within the metamorphic rock, and the Plio-Quaternary Bautista Beds, which both help define the fault zone via rock deformation extents and displacement. Topographic profiles reveal a general asymmetry of basin bounding gully widths and spur/ridge slopes. Spatial distribution of rock damage within SGB and Alkali Wash are seemingly asymmetric with pulverization dominantly between fault

strands or in the NE fault block. 3D shear wave tomography illuminates up to three low velocity troughs in the upper 700 m depth. Southwest of SGB the fault is not isolated to a single strand along the main geologic boundary, but remains bifurcated with the second strand NE of the main trace. Slow shear wave velocity troughs are attributed to both active and older fault structures, traced at the surface, and illustrated in our 3D fault zone model. Asymmetric morphology of the SGB basin is partially attributed to structural growth and fault zone damage. Geologic models from both 3D shear wave tomography, and geologic mapping, indicate surface observations and shallow seismic data compare well. Theoretical models of earthquake ruptures along a bi-material interface result in asymmetric damage from a preferred rupture direction. Asymmetric rock damage in outcrops appear similar to those from seismic wave interpretations at SGB, and findings elsewhere along the SJFZ, suggesting a preferred NW rupture propagation. This study highlights the utility of a dense seismic array paired with detailed surface observation in evaluating shallow fault zone depths to capture complete 3D structure.

Understanding Injection-induced Seismicity Effects on Fault Damage Zones: Beyond Poroelastic Models, Robert L Walker, Mahshad Samnejad, and Fred Aminzadeh (Poster Presentation 184)

A rise in earthquake activity attributed to anthropogenic causes has stressed the the need for physics based hazard mitigation, based on robust predictive models. Recent efforts have addressed the problem of modeling injection-induced fault slip using poroelastic coupled computations. Current models commonly represent faults as frictional planes of a dimension lower than the overall model, necessarily neglecting the existence and/or the evolution of fault damage zones. Despite this, near-fault regions have been demonstrated to be critical to the complete picture of fault stress change and rupture, and thus accurate modeling of fluid migration and pore pressure change in these off-fault areas represent important factors in the analysis of fault stability.

We go beyond conventional poroelastic simulations by addressing the varying physical characteristics of material with progression from the linear fault plane in a discrete fashion. We differentiate between fault rupture planes, fault damage zone, and host rock by means of differing physical models. As it has been shown that the inelastic deformation of fault damage zone material can drastically couple with pore pressure evolution in the subsurface, we also include material nonlinearity for the fault damage zone in our model, which is critical to understanding fault hydromechanics.

Our multiphysics modeling toolset allows for the assignment of heterogeneous characteristic hydromechanical properties to damaged zone elements. Similarly, nonlinear material properties may be solved for as auxiliary variables, dependent on the resultant primary variables (e.g. displacement and pore fluid pressure) of a given iteration, or in a manner fully coupled with the primary variables, should it be deemed necessary.

We analyze pore pressure and stress state changes spatiotemporally by applying a continuum damage mechanics workflow to our computational simulation framework, which allows the integration of multi-scale physical processes, such as flow, deformation, and crack growth. We will conclude with safe injection design implications with respect to well placement and flow rate for various representative cases.

The Network of the Americas (NOTA) GNSS Network in California - Providing Reliable Data Streams for Early Warning Applications, Christian Walls, Doerte Mann, Ryan C Turner, Shawn Lawrence, Ken Austin, Glen S Mattioli, Tim Dittman, and Karl Feaux (Poster Presentation 133)

The Network of the Americas (NOTA) GNSS Network in California, funded by the NSF and operated by UNAVCO, is comprised of 599 permanent GPS and GNSS stations spanning three principal tectonic regimes. The Plate Boundary Observatory (PBO) is being federated with other NSF-funded cGNSS networks (TLALOCNet in Mexico and COCONet spanning the Caribbean) into the hemisphere-scale multi-platform Network of the Americas (NOTA). While NOTA was originally designed for tectonic and volcanic analysis using 24-hr daily files, it has proven to be of significant value to stakeholders who use real-time data streams for early warning systems (i.e. earthquake, tsunami, meteorological). 497 of NOTA stations in CA are currently streaming GPS (n=376) or GNSS (n=121) data in real-time with the majority of stations located along plate boundaries of the Cascadia subduction zone and the San Andreas Fault system. Of these stations, 44 real-time GNSS sites are located within 15 km of the west coast and benefit ionospheric studies for tsunami wave height detection and 49 stations also stream meteorological data. The 1 Hz real-time data is available from UNAVCO in BINEX and RTCM3 formats along with PPP position estimates generated for each site and broadcast in the NMEA format.

Providing complete, low-latency GNSS real-time streams from the site to the processing center hinges critically on operational equipment and reliable data telemetry. These in turn rely on a comprehensive state-of-health monitoring system that allows us to optimize station maintenance activities and equipment upgrades, prevent data loss and telemetry outages, and optimize data quality. We present an overview of the types of telemetry used in the network and performance metrics as well as the tools we use for GNSS state-of-health monitoring.

Robust GPS/GNSS real-time streams are essential for any type of GNSS-supported early warning application. For Earthquake Early Warning, high data completeness is needed to estimate peak ground displacement, depth and magnitude of an event, whereas low data latencies facilitate a rapid warning for a larger area. We present an update on our activities of incorporating NOTA GNSS stations into the Shake Alert Earthquake Early Warning System that is being developed for California, Oregon, and Washington.

Mapping Near-Surface Rigidity Structure using Co-located Pressure and Seismic Sensors from the EarthScope Transportable Array, Jiong Wang, and Toshiro Tanimoto (Poster Presentation 102)

For frequencies below 0.05 Hz, Sorrells (1971) and Sorrells et al. (1971) proposed a promising model in which moving pressure waves on the surface of the Earth generate low-frequency seismic signals. By using Sorrells model, we can study the pressure-ground interaction via co-located pressure and seismic sensors. Taking advantage of the EarthScope Transportable Array (TA) stations, which have pressure sensors attached since 2011 (Tytell et al. (2016)), we analyze surface-pressure induced ground motions recorded at frequencies 0.01 and 0.02 Hz. Adopting the homogeneous half-space model, we estimate the near-surface rigidity within 50-100 meters from the surface at 458 TA stations, by taking ratios of horizontal seismic PSDs and pressure PSDs.

We compare our calculated rigidity with the USGS Global Vs30 model, where we find good regional agreement with the surface geology at unique locations, for example, in the Appalachian Mountains and the Mississippi Alluvial Plain. Co-located stations in TA provide new data to retrieve near-surface structure information, which is important for ground-motion prediction studies.

There are 9 stations located in Piñon Flats Observatory Array (PY) that have co-located barometers since late 2015. We have computed rigidity from data of frequencies that range from 0.01 to 0.05 Hz with an increment of 0.005 Hz for 9 PY stations. Different frequencies correspond to different depths that seismic motions can extend; thus making it possible to study layered structure. Tanimoto and Wang (2018) showed that retrieved rigidities tend to be a bit higher for 0.01 Hz results comparing to 0.02 Hz results, which suggests an increase of rigidity with depth. We also show the relationship between the observed seismic noise and the structure property of the underlying medium. Station with higher near-surface rigidity will require larger surface pressure to generate significant seismic signals, especially vertical signals, that could be separated visually from other sources such as ocean waves.

Earthquake catalog reconstruction from analog seismograms: Application to the Rangely Experiment microfilms, Kaiwen Wang, William L Ellsworth, Gregory C Beroza, Gordon Williams, Miao Zhang, Dustin Schroeder, and Justin L Rubinstein (Poster Presentation 058)

Before the digital era of seismic recordings, decades of seismic data were recorded in analog form and read manually by analysts. Despite the abundance of analog recordings, surprisingly few recent efforts have been made to analyze them. One common format is the 16 mm Develocorder film which recorded up to 20 channels. As the channels are closely spaced, signals commonly overlap with the adjacent channels making it difficult to convert the images into vector time series, especially for earthquakes. In this study, we discard the idea of converting analog data to vector time series, and instead build a set of image-based methods for detection, location and characterization. We validate the automatic processing workflow on one month of Develocorder films from the Rangely earthquake control experiment run by the U. S. Geological Survey from 1969 to 1975 in an oil field in western Colorado. Each day-long microfilm is scanned into ~700 images that total about 10GB in size. To detect events in this large and unlabeled image dataset, we first apply an unsupervised learning algorithm, Principle component analysis (PCA), to represent image features in lower dimensions and then use a Support vector machine (SVM) classifier to separate out earthquake events in the feature space defined by PCA. We next apply a STA/LTA picker which runs on the scaled image and its horizontal gradient to generate P-wave picks. The picks are fed into a grid-search associator to form individual earthquakes that are input to a location program. We also apply 2-D image correlation around the pick time to measure differential arrival times for double-difference relocation and estimate similarity between event pairs for clustering purpose. By running the workflow described above, we build a catalog of ~200 events based on the Develocorder films. Among them ~40 local events cluster at the injection wells, which is consistent with the original analysis of Raleigh et al. (1976). To locate these events, we also use 2-D image correlation to read the time code, correct for the film misalignment, and recover station locations from the original map. A distinct advantage over other approaches is that we do not need to convert the analog data to time series, but can work directly with the image itself. Our processing techniques have the potential for wide application to the decades of historical data before the digital era in seismology.

Probing fault frictional properties during afterslip up- and down-dip of the 2017 Mw 7.3 Iran-Iraq earthquake, Kang Wang, and Roland Bürgmann (Poster Presentation 126)

On November 12th, 2017, an earthquake of Mw 7.3 occurred near the Iran-Iraq border, causing hundreds of deaths in both countries. The earthquake occurred along the Zagros mountain range, a broad and complex zone of continental collision between the Arabian and Eurasian plates. We use Interferometric Synthetic Aperture Radar (InSAR) data collected by the Sentinel-1 mission to study the co- and postseismic deformation of this earthquake. We derive the fault geometry of the mainshock in a Bayesian inversion framework, assuming a single rectangular slip patch. We find that the strike of the rupture that yields the highest value of PDF of posterior data fitting is ~ 355 deg., which is at least 20-30° larger than the average strike of the structures in this region, but in good agreement with the focal mechanism solution (~ 351 deg.) determined for the east-dipping nodal plane from seismic data. The amount of dextral slip is comparable to the thrust component, although the dip angle of the fault is found to be small (~16 deg.). Most of the coseismic moment release is found to be at a depth range between 15 and 21 km, well beneath the boundary between the sedimentary cover and underlying basement. Data from all four tracks also reveal robust postseismic deformation during ~ 8 month after the mainshock (from November 2017 to July 2018). Kinematic inversions show that the observed postseismic InSAR LOS displacements are well explained by oblique (thrust + dextral) afterslip both updip and downdip of the coseismic peak slip area. The dip angle of the shallow afterslip fault plane is found to be significantly smaller than that of the coseismic rupture, corresponding to a shallowly dipping detachment located near the base of the sediments. Aftershocks during the same time period exhibit a similar temporal evolution as the InSAR time series, with most of the aftershocks being located within and around the area of maximum surface deformation. We also observe prominent coseismic and postseismic surface deformation along several secondary fold-like structures. The postseismic deformation data are consistent with stress-driven afterslip models, assuming that the afterslip evolution is governed by rate-and-state friction. Under the assumption that the effective normal stress on the fault is hydrostatic and depth dependent, the average (a-b) is estimated to be ~ 7*10^-3, consistent with previous laboratory results and in situ measurements from geodetic data.

Implementing Inter-Frequency Correlations into the SDSU Broadband Ground Motion Method, Nan Wang, Rumi Takedatsu, Kim B Olsen, and Steven M Day (Poster Presentation 010)

Earthquake ground motion records reveal frequency-dependent correlations, which has implication for seismic risk (Bayless and Abrahamson, 2017). The empirical inter-frequency correlation model of within-event residual for the Effective Amplitude Spectrum (EAS) computed from the PEER NGA-West2 database shows correlation of ground motions between nearby frequencies. We attempt to incorporate such correlation as a post-processing method into the current San Diego State University (SDSU) Broadband (BB) ground motion generator module, which combines deterministic (low-frequency) and stochastic (high-frequency) components. We first apply Cholesky decomposition of the regressed inter-frequency covariance model (C) and multiply it with an uncorrelated normal random variable with zero mean to generate a correlated random variable (zero mean, covariance is proportional to C) for

different realizations, which are then multiplied with the Fourier amplitude of the high-frequency ground motion synthetics calculated using Zeng et al. (1991)'s scattering theory. Using our improved method, the BB results for 7 western U.S. events with Mw5.0-7.2 show that the empirical inter-frequency correlations of EAS are well predicted in the SDSU module for a large number of realizations from a single event with unbiased goodness-of-fit of the spectral accelerations in the presence of correlated synthetics. This post-processing method can also be extended to improve frequency-dependent spatial correlations.

Comparison of Brune-type Stress Drops Estimated from Direct P, S, and Coda Waves, Wei Wang, and Peter M Shearer (Poster Presentation 082)

Analysis of seismograms recorded by local networks provides fundamental information on earthquake source spectra and site effects. Previous studies have used different parts of the seismograms, e.g., direct P, S, and coda waves, to study these parameters. Site effects and stress drops derived from source spectra have practical implications for strong ground motion prediction. In this study, our aim is to comprehensively compare the source spectra and site effects derived from direct waves and coda waves separately and to constrain the degree of self-similar scaling of earthquake source properties. We analyze about 1500 earthquakes with local magnitude (ML) from 1.2 to 3.5 within a compact cluster in the San Jacinto Fault region of California. We apply the spectral decomposition method (e.g., Shearer et al., 2006; Trugman & Shearer, 2017) to estimate source spectra and use both self-similar and non-self-similar Brune-type models to fit the spectra. We first explore the parameter tradeoffs among the absolute stress drop, the stress-drop scaling with moment, and the high-frequency falloff rate. We also study the time-dependent evolution from direct to coda-wave spectra by analyzing spectra from consecutive time windows following the direct S wave and comparing the results with traditional direct S and coda wave analysis. We estimate uncertainties by applying a bootstrap resampling approach. Our goal is to eventually apply these methods in a comprehensive analysis of earthquake source spectra and site effects across southern California.

Post-seismic deformation mechanism of the Mw 9.0 Tohoku-Oki earthquake detected by GPS and GRACE observations, Wuxing Wang, Xiaodong Zhang, Ming Liang, and Jing Zhang (Poster Presentation 128)

Post-seismic deformation characteristics of the Mw 9.0 Tohoku-Oki earthquake are studied by using GPS and GRACE observations. GPS continuous observations show that the regional post-seismic displacements are characterized by exponential function, and the rate of change accords with the attenuation characteristic of the Omori formula. Significant post-seismic gravity changes are detected by GRACE also, which shows that gravity rises on both sides of the seismic rupture. However, the rate of gravity change is faster on the ocean side. Here we combine the theories of afterslip and viscoelastic dislocation to simulate the post-seismic deformations and explore the comprehensive application of GPS and GRACE observations. The results demonstrate the combination of afterslip and viscoelastic relaxation theories can make a reasonable explanation for the post-seismic deformations of the Mw 9.0 Tohoku-Oki. The contribution of afterslip plays a major role in the initial stage, and it gradually weakens one or two years later, while the contribution of viscoelastic relaxation increases with time. The method of combining GPS and GRACE observations to infer regional viscous structure is formed. Firstly, inverse a preliminary regional viscous structure by post-seismic GPS observation, then modify the viscosity of the deepest layer by GRACE observation, and fine tune the viscosity of the shallower layer by synthetically using GPS and GRACE observations. Finally, determine the regional viscous structure. Based on this method, we estimated the mantle viscous structure in the region of the Mw 9.0 Tohoku-Oki earthquake by GPS and GRACE observations.

Deducing Crustal-scale Reverse-Fault Slip Distribution from Folded River Terraces, Qilian Shan, China, Yiran Wang, Michael E Oskin, and Youli Li (Poster Presentation 244)

Studies have shown that for many compressional orogens, such as the Andes, the North Los Angeles fault system, and the Longmenshan fault, rates of shortening from geodesy are faster than geologically determined rates. Lack of documented faulting or other processes that absorb this missing convergence limits our ability to understand of the evolution of compressional orogens and their seismic hazard potential. The Qilian Shan ('Shan' as mountains in Chinese) of northwest China is an actively shortening orogen developed along the northern margin of the Tibetan Plateau. Two generations of fill terraces (T1 and T2) are well preserved along Beida River from the foreland basin to at least 45 km within the Qilian Shan hinterland. Both terraces are offset by the North Qilian fault along the range front. Preservation of these terraces across the mountain range presents a unique opportunity to quantify additional fault slip absorbed by folding of the range interior. We mapped and surveyed fluvial terraces for a distance of 45 km upstream of the mountain front. Using the deformed terrace profiles and field observation of fault dip, we constrained forward and inverse elastic modelling of the North Qilian fault to deduce its geometry and estimate its slip distribution at depth. The T2 terrace profile reveals a long wavelength fold (~30km) with a largest vertical deformation of ~130m relative to T1. Elastic modelling indicates that this folding of North Qilian Shan is a result of a thick-skinned fault that dips at a high angle near the surface (~50o) and soles into a decollement at ~25km depth. Estimated slip at depth is ~10 times of the fault slip at the surface, indicating that the majority of slip is absorbed by folding of the range interior. This study indicates that for orogens like the Qilian Shan, most of the shortening is accommodated within the mountain range by folding, and surface displacement by reverse fault slip at the mountain front reveals only a fraction of the total shortening. This suggests a need to pay more attention to long-wavelength folding when estimating fault activity and evaluating earthquake hazard.

A Physical Interpretation for Anomalous Source Spectra with a Deficit at Intermediate Frequencies, Yongfei Wang, Steven M Day, and Peter M Shearer (Poster Presentation 216)

Many small crustal events in the northern Ibaraki prefecture and the Fukushima prefecture Hamadori area of Japan deviate systematically from the standard omega-square model, with an intermediate-frequency deficit (concavity) in the spectra and low- and high-frequency bumps in residual spectra that may reflect source complexity (Uchide and Imanishi, 2016). This anomaly may result from propagation effects (e.g., multipathing or attenuation) or source complexity (e.g., asperity or barrier models). We investigate the multipathing hypothesis by testing if the anomaly is specific to certain stations or paths, but find that the anomaly is broadly distributed over station location, azimuth, and source depth. With respect to attenuation, we find that a frequency-dependent Q model (e.g., power-law Q) can theoretically explain the spectral concavity if the falloff of inverse Q at high

frequency is close to predictions of a Debye peak, but the required falloff rate (-1) is much steeper than permitted from Q studies and observations of source spectra. Thus, source effects are a more likely explanation for the anomalous spectra and we find that a composite source model (an outer big circle filled with smaller subevents) can account for the concavity in spectra. Compared with asperity models with varying stress drop, a model with appreciable acceleration/deacceleration in rupture velocity and variant subevent sizes appears a viable candidate. By simulating dynamic rupture scenarios and performing analytical derivations, we discover such a model has: (1) a high frequency decay with omega-square asymptote that is mainly controlled by outer marginal stopping phases, (2) spectral concavity that is related to the spatial density and the maximum/minimum radius of the subevents, and (3) seismic moment in this composite source is self-similarly proportional to the cube of the outer radius. Thus, based on spectra from our dynamic simulations, we can construct a physical link between stress drop and apparent corner frequency for our composite source model, similar to that described for simpler models in Madariaga (1976), Kaneko and Shearer (2014, 2015), and Wang and Day (2017). In the future, we would like to generalize a spectral model to deal with composite sources to better characterize source complexities and stress regimes.

Strain rate dependence on crustal rheology for the Cajon Pass, California, Lauren Ward, Bridget R Smith-Konter, Xiaohua Xu, and David Sandwell (Poster Presentation 260)

While the dependency of fault strain rates on locking depth and slip rate variations are reasonably well-understood, our understanding of the sensitivity of fault loading to rheologic controls is still developing. Furthermore, how strain rates evolve throughout earthquake cycles and whether they are inclined to promote or inhibit earthquake gate behavior of conditionally opening or halting ruptures of neighboring segments likely depends on several factors, including lithosphere rheology and fault zone strength. The Cajon Pass, uniquely positioned between the junction of the southern San Andreas and San Jacinto fault segments, has been hypothesized as an earthquake gate; the Cajon Pass is also situated within a region of modest, but potentially important, crustal structure variation that may influence strain accumulation rate of key faults. Using the growing archive of GPS and InSAR measurements spanning the North American-Pacific plate boundary, we provide updated estimates of present-day surface strain rates using a new physical model (Sandwell and Smith-Konter, 2018) that extends our modeling capabilities to include the effects of spatial heterogeneities in crustal rigidity. For this work, we adopt a simplified representation of crustal rigidity derived from preliminary heat flow estimates and LAB depths. Incorporating reasonable uncertainties in these estimates, we explore the sensitivity of strain rate along the Mojave, North San Bernardino and San Jacinto Valley fault segments from a suite of crustal rigidities. For example, crustal rigidities along the Mojave segment (~30 GPa) may increase by ~25% south of the Cajon Pass, which may lower strain rates by 10-15% along the San Andreas San Bernardino segment and the San Jacinto Claremont segment. Moreover, the implication of an evident change in crustal rigidity south of the Cajon Pass lends support for the idea that strain rate reductions impede through-going ruptures in some cases. Future integration of rheology and crustal structure models provided by the CRM and CTM will help to refine simulations of earthquake cycle strain accumulation, as well as our understanding of the probability of large, multi-segment and multi-fault ruptures of the southern San Andreas Fault System.

Shear wave velocity structure of a remnant slab beneath the western Transverse Ranges offshore southern California, Dayanthie S Weeraratne, Kaitlyn Amodeo, Sampath Rathnayaka, Escobar Lennin, Carlos D Gomez, and Monica D Kohler (Poster Presentation 110)

Data from the amphibious ALBACORE (Asthenospheric and Lithospheric Broadband Architecture from the California Offshore Region Experiment) seismic array across the southern California continental margin allows us to simultaneously study oceanic and continental lithosphere in one seismic study. The complexity of this region allows us to study limits in the rigidity and strength of the lithosphere, as it has undergone spreading center subduction, translation through the mantle, and block rotation. We invert Rayleigh wave phase velocity data for shear velocity structure. Our study area is divided into oceanic regions ranging from 35-10 Ma, the Borderlands, and fault bounded continental regions. A unique starting shear wave velocity (Vs) model is used for each region with detailed crust and mantle velocities based on previous studies in each area. Phase velocities predicted from these Vs models are compared to observed phase velocities from the ALBACORE array to solve for the best fit Vs in a least square sense. Combined data from 100 marine and land based seismometers with good earthquake distribution produce excellent resolution from 20 - 200 km depth. These results are then used to create 1D velocity profiles and integrated into 3D tomographic cross sections. High velocities associated with the lithosphere-asthenosphere boundary (LAB) are clearly observed beneath oceanic lithosphere at 75 km depth +/-15 km and beneath continental lithosphere west of the San Andreas Fault (SAF) at 65 km depth. The continental LAB is deeper east of the SAF at 75 km. In the Borderlands between 33.5 N and 34.5 N (Western Transverse Ranges, WTR) demonstrate anomalous velocities with a horizontal orientation that are 11% higher than ambient mantle at 100-130 km depth. This high velocity anomaly bends sharply dipping northeastward towards the continental margin at an angle of 65o +/- 25o extending to depths of at least 250 km. We suggest this dipping high velocity structure may indicate a remnant slab fragment beneath the WTR left behind from complexities in the subduction of the East Pacific Rise spreading center 10-25 Ma and later rotation of the Transverse Ranges. Azimuthal anisotropy at sublithospheric depths below 90 km is consistent with NW Pacific plate motion direction everywhere except beneath the WTR where fast directions are oriented in a NE-SW direction consistent with a remnant slab fragment oriented in the direction of the ancient Farallon plate subduction.

How Much Farther? Estimating Rupture Length Probabilities After a Rupture Has Started, Steven G Wesnousky, and Glenn P Biasi (Poster Presentation 041)

The USGS ShakeAlert Earthquake Early Warning (EEW) system is designed to detect and alert within a few seconds of earthquake initiation. We investigate the probability that the rupture will grow, and develop estimates for eventual rupture length and magnitude. The condition that the rupture is under way distinguishes our estimates from a-priori rupture probabilities such as the Uniform California Earthquake Rupture Forecast v.3 (UCERF3) or that one might infer from a Gutenberg-Richter (GR) relationship. We investigate on three primary lines. For all models, we assume a UCERF3-like fault discretization with subsections of a few km in length, and that the EEW earthquake that has started roughly fills one subsection. A reference model that assumes equal probability ruptures of any length (2, 3, 4, … subsections) is appealing for its simplicity, but does not scale well with fault length.

Applying a GR relation makes relative probabilities of length and magnitude look more realistic, but Field et al., SRL, 2017 question application of the GR on faults, and there are no fault physics inherent to the GR. We consider using UCERF3 time-independent probabilities of length and magnitude as proxies for the conditional probability case given an EEW initiation. If used directly, median predicted lengths for examples on the San Andreas and San Jacinto faults are unrealistically long (>350 km, M 7.8+). An ad hoc reduction by the number of subsections in the rupture improves the prediction, but still results in unrealistic probabilities of a long rupture. Bends and steps in rupture provide a physical basis for relative probabilities among fault ruptures, with support in empirical observation and fault dynamical modeling. We present probabilities for these physical "challenges" to rupture and show that they can be applied to produce conditional EEW length and magnitude predictions without ad hoc applications of GR or UCERF3.

Detailed seismic catalog for the San Jacinto fault zone region (2008-2016) from automated processing of raw waveform data, Malcolm C White, Yehuda Ben-Zion, and Frank L Vernon (Poster Presentation 054)

We develop an automated processing procedure and apply it to eight years of raw waveform data, amalgamated from five seismic networks operating in the San Jacinto Fault Zone region, to derive an earthquake catalog containing >119, 000 events with approximate magnitude range –1.5 to 5.5. Earthquake locations are determined using separate P and S-wave phase detectors, a probabilistic, global-search 3D location method (NonLinLoc), and a waveform cross-correlation based double-difference relocation method (GrowClust). Local magnitudes are calculated using amplitude measurements from simulated Wood-Anderson instruments. The magnitude of completeness is estimated by the 99th percentile of the Gaussian CDF component of an exponentially-modified Gaussian distribution fit to the entire observed magnitude range using maximum likelihood estimation, and it varies from about 0.9 in a rectangle with dimensions 55 km and 95 km centered on the San Jacinto fault zone, to about 2.0 toward the edges of the study area. The results complement existing catalogs (the Southern California Seismic Network's standard catalog and its derivatives) with >1.6 times as many events in the focus of the study area. The new detected events are a consequence of increased station density relative to SCSN's routine processing. The additional seismicity in the new catalog illuminates different seismicity structures with greater detail, compared with other catalogs for the area. Using the catalog earthquakes as templates can increase further significantly the number of events, but the additional events will mainly increase the density of seismicity structures already in the catalog rather than reveal new ones.

Refining the earthquake chronology of the last millennium along the Cholame segment of the San Andreas fault, Alana M Williams, Ramon Arrowsmith, Thomas K Rockwell, Sinan O Akciz, and Lisa Grant Ludwig (Poster Presentation 267)

The Cholame section of the San Andreas Fault (SAF) is positioned between the Parkfield and Carrizo sections to the NW and SE, respectively. Motivated by its critical position along the SAF, we have developed the Annette site (20 km SE of Highway 46). In 2017, we studied 2 fault perpendicular excavations connected by a small fault parallel trench. We returned in 2018 and excavated 2 more perpendicular trenches to densify our dataset. Earthquake evidence spans a 5m-wide fault zone displaying horst and graben structures, colluvial wedges, and decreasing vertical offsets upsection. Stratigraphy consists of finely bedded sand, silt, gravel and bioturbated paleosols. We found evidence for 5 earthquakes (4 with good quality) and post-1857 deformation. We have numbered these events from youngest to oldest to correlate with the previous Annette trenches from 2017, in which we found 6 possible ruptures. E0 is a post-1857 ground shaking event and E1-E6 are interpreted as rupture events. Based on vertical offset, graben scale and stratigraphy, but without radiocarbon dates, the rupture evidence from 2018 can likely be correlated to E1, E2/3, E4, E5, and E6 from 2017 trenches. Post-1857 deformation is similar to evidence at the previous Annette trenches and the LY4 site 38 km southeast. Events with the most confidence overall are E1, E4, E5 and E6. Charcoal dates from 2017 excavations indicate that events E6-E1 occurred between 1300 A.D. and 1857, allowing for correlation of this earthquake sequence with the high-quality records of 6 ruptures at Bidart and Frazier Mountain (70 and 180 km SE, respectively) within a similar time period. OxCal derived dates of rupture sequences compared with southern San Andreas Fault paleoearthquakes from Scharer et al., 2014, show 4 of the 6 possible events could be attributed to Carrizo segment ruptures (E1, E2, E3, and E4/E5).

Dense mapping of shallow velocity structure in the Raymond Basin using the Pasadena Distributed Acoustic Sensing Array, Ethan F Williams, Zhongwen Zhan, Martin Karrenbach, Steve Cole, and Lisa LaFlame (Poster Presentation 023)

With the increasing ability of ground-motion simulations to accurately model earthquake wavefields at high frequencies and the dependence of the earthquake engineering community on site characterization metrics like Vs-30, the resolution of existing maps of shallow velocity structure in Southern California, such as the SCEC CVM geotechnical layer (GTL), is inadequate. Here, we combine information from active-source surface waves, teleseismic and regional earthquakes, and noise correlation functions to map near-surface shear wave velocity and site response in the Raymond Basin (northern San Gabriel Valley) using the Pasadena Array. The Pasadena Array employs distributed acoustic sensing (DAS) technology to convert a >25-km fiber-optic telecommunications cable into an array of horizontal, single-component linear strainmeters, which can record dynamic strains with spatial resolution as fine as 1 m and instrument noise levels comparable to a geophone. Exciting the resonant modes of Caltech's Millikan Library using a torsional shaker installed on the roof of the nine-story building, we measure surface wave dispersion between 1 and 5 Hz along the Pasadena Array and observe variations in Rayleigh wave speed as significant as 200 m/s across spatial distances of less than 100 m. Above 5 Hz we compute ambient noise correlation functions which further constrain the spatial scale of shallow velocity variations. We supplement our velocity study with a preliminary map of site amplification using the standard spectral ratio method for a small catalog of teleseismic and regional earthquakes. As a case study, our results demonstrate the tremendous value of dense DAS strainmeter arrays leveraging existing telecommunications infrastructure to address the current and future needs of Southern California earthquake science.

Broadband Ground Motion and Variability from 3D Dynamic Rupture Simulations along the Wasatch Fault, Utah, incorporating both Stochastic Fault Roughness and Deterministic Long-wavelength Geometry, Kyle B Withers, Morgan P Moschetti, and Kenneth Duru (Poster Presentation 004)

We numerically model earthquake rupture on a fault surface that includes long-wavelength geometry matching that of the Salt Lake City segment of the Wasatch fault, Utah, in addition to superimposed stochastic fault roughness. We seek to better understand the

rupture process and assess broadband ground motion and variability along dipping faults by extending deterministic ground motion prediction to higher frequencies (>1 Hz). Our approach utilizes dynamic rupture simulations using a summation by parts method with the recently developed finite difference code, Waveqlab3d. We generate a suite of ruptures ~Mw 7.0 (40 x 20 km along strike and width, respectively), with varying hypocenter locations and initial stress conditions. The fault roughness generates ground motion with flat acceleration spectra across a wide frequency bandwidth (from 0.1 up to 5-10 Hz). Long-wavelength geometry affects the initial stress distribution on the fault (along both strike and dip), creating regions where rupture is either inhibited or promoted. We also investigate the significance of features such as free-surface topography and off-fault plasticity (via a Drucker-Prager approach) and their influence on the features specific to dipping faults. For example, a dipping fault plane is known to cause asymmetries in the rupture across the hanging wall/footwall boundary. We find that plastic strain accumulation is mainly generated on the hanging wall, in agreement with previous studies, and that there are minimal effects of the free-surface topography to the rupture process. However, both of these features significantly affect the level of ground motion, by reducing peak amplitudes from shallow near-surface scattering. Our synthetically generated ground motion is near that of a median event and the level of intra-event variability slightly lower than that of recent GMPE relations. We expect that the use of a 3D seismic velocity model in future simulations, in place of a 1D velocity profile, will contribute to increasing the simulation-derived variability to values closer to what is observed in recorded ground motions.

The Wilmington Blind-Thrust Fault: An active, concealed earthquake source beneath Los Angeles, CA, Franklin D Wolfe, John H Shaw, Andreas Plesch, Daniel J Ponti, James F Dolan, and Mark R Legg (Poster Presentation 250)

Analysis of 2D and 3D offshore seismic reflection profiles, petroleum and water wells, and recent mapping of groundwater aquifers in the southwestern Los Angeles basin indicate that the Wilmington blind-thrust fault is tectonically active and capable of generating large, damaging earthquakes. This overturns the long-held view that the fault became dormant in the Late Pliocene, barring its inclusion in state-of-the-art regional earthquake hazard assessments. The size of the fault suggests that it is capable of generating moderate-magnitude earthquakes (M 6.2-6.3), while potential linkages with other nearby faults (e.g., Huntington Beach, Torrance, Compton) pose the threat of larger, multi-segment events (M > 7). These earthquakes would directly impact the Ports of Los Angeles and Long Beach, as well as the broader Los Angeles metropolitan area.

Landers 1992 "reloaded": an integrative dynamic earthquake rupture model, Stephanie Wollherr, Alice-Agnes Gabriel, and Paul M Mai (Poster Presentation 211)

The 1992 Mw 7.3 Landers earthquake raised awareness of unexpectedly large magnitude earthquakes caused by rupture of fault networks that were previously considered unconnected. While the overall kinematics of the event are thought to be well understood, many observations regarding its complicated rupture dynamics are still unresolved.

Here, we present 3D spontaneous dynamic rupture simulations that improve our understanding of the earthquake source and ground motions of the multi-segment Landers event. The model incorporates a new degree of realism by incorporating the interplay of fault geometry, topography, 3D rheology, off-fault plasticity and viscoelastic attenuation. These model complexities are enabled by the software package SeisSol (www.seissol.org) specifically suited for handling complex geometries and for the efficient use on modern high-performance computing infrastructure.

We find that fault geometry, as well as amplitude and orientation of initial fault stresses primary control sustained rupture along all fault segments. The resulting complex source dynamics include reverse slip, direct branching, and dynamic triggering over large distances. Fault slip terminates spontaneously on most of the principal fault segments due to the underlying fault geometry.

The model reproduces a broad range of observations, including seismic moment-rate, seismic waveform characteristics and peak ground velocities. Despite the complex rupture evolution, ground motion variability is close to what is commonly assumed in Ground Motion Prediction Equations. Our simulation results suggest that an along-strike variability of the shallow slip deficit of up to 20% is possible, even for laterally constant rock cohesion and bulk friction. These variations can be attributed to different principal stress directions and complex fault geometry. Further, we observe dramatically increased off-fault deformation in the vicinity of fault bends and intersections, in excellent agreement with recent maps of fault-zone width (Milliner et al., 2015, Geochemistry, Geophysics, Geosystems).

Finally, we examine the effects of variations in modeling parameterization, e.g. purely elastic setups or models neglecting viscoelastic attenuation, in comparison to our preferred model.

GMPE specific average velocity profiles for developing spatially-varying path coefficients, Kathryn E Wooddell, Linda Al Atik, and Norman A Abrahamson (Poster Presentation 026)

CyberShake simulations are being run to develop spatially-varying path coefficients in regions of sparse coverage that lack sufficient recorded earthquake ground motion data. The methodology for calculating the coefficients requires both 3D and 1D CyberShake simulations to remove the ergodic portion of the path effect and center the model on the GMPE following the approach of Wooddell and Abrahamson (2017). A preliminary attempt was made at this using a 1D velocity model that was a smoothed version of the available 3D velocity model. The idea was to use this model along with a correction factor to center it on the GMPE. However, an analysis of the currently available 1D simulations revealed that the 1D velocity model is insufficient for this application because it contains non-ergodic features that are not present in the GMPEs. Therefore, we develop a GMPE-specific 1D velocity model using the ASK14 model to allow us to proceed with this approach. The empirical Fourier Amplitude Spectrum (FAS) model (Bayless and Abrahamson, 2018) is used to compute the frequency-dependent linear site amplification factors for different Vs30 ranges. These factors are then used to remove the average kappa scaling and inverted to develop an average 1D velocity model for ASK14. This 1D velocity model is a representative of the average velocity profiles in the ASK14 dataset and will be run on the CyberShake platform and used to develop spatially-varying path coefficients.

Modeling Crust of Columbia River Basalts Using Ambient Noise Recordings, Mackenzie R Wooten, Jorge A Castillo Castellanos, and Robert W Clayton (Poster Presentation 104)

Flood-basalt eruptions are the Earth's largest volcanic events and are thought to have caused massive extinction events. These events take part in the formation of hotspots and produce lavas that have covered much of the Earth's surface. The dynamics of these events have yet to be resolved however. One of the most recent flood basalt eruption, the Columbia River Basalts (CRB), is the site of volcanic propagation from the Yellowstone hotspot. The CRB shows evidence of a reconstructed crust and large crustal magma chamber, possibly due to the foundering and sinking of large portions of the lithosphere into the asthenosphere, which controlled the flow and distribution of volcanism in the area. In this study, we use two years of ambient noise recordings from a 60-station line array stretching from northern Oregon to southern Washington to solve for the shear wave velocity structure beneath this region. In addition, we use the difference between horizontally and vertically polarized shear wave velocities along this experiment to quantify radial anisotropy and illuminate any structural fabric that might be related with the areal extent of a large magma chamber in the lithosphere and the existence of a descending pluton beneath it.

Using Kinematic models to Evaluate the Back Projection Results, Baoning Wu, Bo Li, David D Oglesby, and Abhijit Ghosh (Poster Presentation 085)

Back projection is a useful method for imaging the rupture process of large earthquakes. Despite great success in practice, there are still many questions on how to correctly interpret back projection results. First, the fundamental result of back-projection is the amplitude and location of maximum high-frequency seismic radiation; however, the seismic energy radiation mechanism is complicated for a large earthquake. The seismic energy received by a teleseismic station is generated not only from slip acceleration and deceleration, but also from rupture front acceleration and deceleration (Madariaga, 1977). Therefore, the physical meaning behind the beam energy and the location of maximum beam energy remain enigmatic. In addition, rupture can propagate on multiple locations on a fault system, including different segments simultaneously during a large earthquake, while the back projection method can only pick one location of maximum beam energy. How the back projection method works under this situation is still unclear. In this study, we generate synthetic earthquakes with kinematic model, and calculate the corresponding far field ground motion with the propagator matrix method. The back projection method will be performed using the synthetic seismograms, and the results will be compared with the known rupture history. Such comparisons using multiple models and their back projection results using multiple arrays demonstrate some similar characteristics. First, the back projection results show generally slower rupture velocity than the dynamic models. Second, depending on the rupture directions and array locations, the arrays on different azimuths can show different rupture propagations, especially when the events rupture in different directions or have branch ruptures. Third, rupture velocity changes will result in a higher amplitude in the seismograms, which will lead to stronger beam power in the back projection results. More dynamic and kinematic models will be designed to help us better understand the physical meaning of the back projection results and better interpret the back projection results.

Characteristics of earthquake source complexity in the San Jacinto Fault Zone, Qimin Wu, and Xiaowei Chen (Poster Presentation 077)

We systematically analyze the source complexity of earthquakes in the trifurcation area of the San Jacinto Fault zone (SJFZ), which represents a right-lateral strike-slip system that is of high structural and geometric complexity and most seismically active in southern California. We combine both frequency and time domain analysis based on the empirical Green's function (EGF) technique to investigate the characteristics of source complexity for earthquakes with a range of magnitudes (~M 2.5-5) to better understand the underlying earthquake physics and the associated seismic hazard of these earthquakes. In time domain, we apply an iterative deconvolution method to retrieve relative source time functions (RSTFs) for our target events using smaller nearby events as EGFs. The RSTFs obtained from multiple EGFs are stacked at each station to stabilize the results by removing random noise. Preliminary results for moderate earthquakes (~M 4-5) reveal clear directivity effects and the existence of multiple subevents. In frequency domain, we apply the multiple spectral ratio method (e.g., Uchide and Imanishi, 2016; Abercrombie et al., 2017), in which various EGF events are used to obtain spectral ratios for our target events. We explore the complexity of the stacked spectral ratios by examining their azimuthal variations and quantifying their deviation from simple omega-square source model. Preliminary results demonstrate that the spectral ratios of some events as small as ~M 3 deviate significantly from the simple omega-square source model. Further analysis will combine the time and frequency domain results to identify any dependence of apparent source complexity on magnitude or structural complexity.

Pre-seismic and Co-seismic Deformations in the Seismogenic zone of the Lushan MS7.0 earthquake, Yanqiang Wu (Poster Presentation 122)

The spatiotemporal deformation response of a seismogenic fault to a large earthquake is of great significance to understanding the nucleation and occurrence of the next strong earthquake. The Longmeshan fault, where the 2008 Wenchuan MS 8.0 earthquake and 2013 Lushan MS 7.0 earthquake occurred, provides an opportunity for us to study this important issue. The results are as follows: 1) during the co-seismic and post-seismic processes of the Wenchuan earthquake, the deformation is dominated by a continuous pattern in the Southern Segment of the Longmenshan Fault (SSLMF), which is different from the dislocation pattern in the middle-northern segment of the LMF. Quantitatively, the compressive strain present between 2008 and 2013 was equal to the strain accumulation of 69 years during the interseismic period in the SSLMF; 2) After the Wenchuan earthquake, the deformation adjustment (especially the shear deformation) in the region that crosses the Maoxian-Wenchuan Fault (MWF) and Beichuan-Yingxiu Fault (BYF) is significantly greater than that the eastern region of the Anxian-Guanxian Fault (AGF). Furthermore, the azimuth angles of the principal compressive strain rate in both regions change fast in the first year of the observation period and then turn into the stable state.

The co-seismic displacement GPS results indicate the thrust rupture is dominant and the laevorotation movement is secondary in the strain release of the Lushan earthquake. Some detailed results are obtainable. 1) The co-seismic displacements reflected by GPS data are mainly located in a region that is 230 km (NW direction) × 100 km (SW direction). 2) On a large scale, the co-seismic

displacement shows thrust characteristics, but the associated values are remarkably small in the near field (within 70 km) of the earthquake fault. Meanwhile, the thrust movement in this 70-km region does not correspond with the attenuation characteristics of the strain release, indicating that the rupture of this earthquake does not reach the earth's surface. 3) The laevorotation movements are remarkable in the 50-km region, which is located in the hanging wall that is close to the earthquake fault, and the corresponding values in this case correlate with the attenuation characteristics of the strain release.
In general, the deformation features of the SSLMF reveal that the Wenchuan earthquake promotes the occurrence of the Lushan earthquake.

Effect of source rupture directivity on the ground shaking from strike-slip earthquakes and its implication for directivity models, Junju Xie, Paolo Zimmaro, Xiaojun Li, and Zengping Wen (Poster Presentation 002)

We investigate spatial variability of observed ground motions, apparent period-dependence, and azimuthal variation, as well as narrow-banded effects on various intensity measures. We develop a simplified ground motion model that includes both geometric and anelastic attenuation terms. We also perform a log-linear regression of the residuals, using a new directivity predictor. Our results show that rupture directivity produces significant amplifications in the rupture forward direction, while strong deamplification effects are observed in the rupture backward region, which has generally been omitted in directivity models of NGA-West2 project. Directivity effects are particularly relevant for PGV and long-period spectral acceleration (i.e. SA at periods ≥ 2.0 s). Such effects do not have systematic influence on PGA and short period ground motions (i.e. SA at periods < 1.0 s). Rupture directivity during larger earthquakes tend to affect ground motion in the longer periods. We anticipate that results from this study will be useful for future ground motion models development.

Compressional branching during the 2012 Mw 8.6 Off-Sumatra Earthquake: Implications from Earthquake Cycle Simulations , Yuqing Xie, and Lingsen Meng (Poster Presentation 215)

The 2012 Mw 8.6 Off-Sumatra earthquake is the largest strike-slip intraplate earthquake ever recorded by modern seismology. Previous Back-projection studies of this earthquake suggests two episodes of rupture branching into compressional fault segments with elevated dynamic normal stress, leaving the dilatational segments unbroken or broken with a delay. Understanding the mechanism of such counter-intuitive rupture scenario could provide a physical basis to assess the maximum earthquake size in complex fault system. The compressive branching may involve many factors, among which the stress state is considered an essential one and has large uncertainties. The variation of stress state caused by previous earthquakes may create favorable condition of rupture propagation on the compressional branch. One possible scenario is that the stress is low on the dilatational branch due to a recent event and high on the compressional branch due to seismic quiescence. To investigate the details about the development of stress state on such a complicated fault system, we conduct the quasi-dynamic simulations of earthquake cycles on a T-shaped fault system using a rate- and state-dependent friction law. The preliminary results show that irregular earthquake sequences including compressional branching can be generated in such fault systems. We plan to use more realistic geometry and parameters in our subsequent research work. Particularly, we will explore how the normal stress σ, the steady slip rate Vslip in deep region of the faults and the characteristic slip distance Dc, affect the interactions between fault segments.

Surface Creep Rate of the Southern San Andreas Fault Modulated by Stress Perturbations from Nearby Large Events, Xiaohua Xu, Lauren Ward, Junle Jiang, Bridget R Smith-Konter, Ekaterina Tymofyeyeva, Eric O Lindsey, Arthur G Sylvester, and David T Sandwell (Poster Presentation 113)

Shallow surface creep, observed along a few seismically active strike-slip faults, is broadly understood to result from velocity strengthening materials in the uppermost (1-2 km) fault zone atop the velocity weakening materials at seismogenic depths. Creep sometimes occurs in discrete events, spontaneously or triggered by shaking from nearby large earthquakes. A major challenge for understanding the physics of shallow creep has been to observe and model the long-term effect of stress changes on creep rate. Here we investigate the surface creep along the southern San Andreas fault (SSAF) using data from interferometric synthetic aperture radar (InSAR) spanning over 25 years (ERS 1992-1999, ENVISAT 2003-2010, and Sentinel-1 2014-present). To resolve fault creep unperturbed by passing seismic waves, we exclude interferograms spanning three major regional earthquakes for which dynamically triggered creep is well documented: the 1992 Mw 7.3 Landers, the 1999 Mw 7.1 Hector Mine and the 2010 Mw 7.2 El Mayor-Cucapah earthquakes. The main result of this analysis is that the average surface creep rate increased after the Landers event and then decreased by a factor of 2-7 over the past few decades. To further understand these pronounced variations in average creep rate, we consider quasi-static and dynamic Coulomb stress changes caused by these three major events and their effect on fault creep. The dynamic Coulomb stress changes are similar for all three events, contributing to triggered creep on the SSAF. In contrast, the static Coulomb stress changes on the SSAF are positive after the Landers and negative after the Hector Mine and El Major Cucapah, coinciding with the higher average creep rate after the Landers event and lower rates after the other two events. The elevated creep rates after the Landers can only be explained by static stress changes, indicating that even in the presence of dynamically triggered creep, static stress change has a long-lasting effect on SSAF creep rates. These results suggest time-scale-dependent complexity of shallow fault creep under stress perturbations from regional earthquakes.

Detecting the Earth's Interior Structure Using Reverse-Time Migration Based on Wavefield Normalized Cross-Correlation Imaging Condition, Lei Yang, Gregory C Beroza, and Liang Zhao (Poster Presentation 109)

Increasingly dense arrays are being deployed globally and new imaging methods are being developed to constrain the fine details of the earth's interior structure. In this study, we apply reverse-time migration (RTM), which is the most accurate migration method in exploration geophysics, to the detection of the earth's interior. RTM is based on the two-way wave equations, and it directly exploits the full waveform information from the seismic data without phase picking. It doesn't assume horizontal interfaces, and has potentially good resolution for interfaces with large dips. Thus, RTM provides more accurate imaging results than the traditional ray-based seismic imaging and receiver function methods. To implement RTM, we perform forward modeling, backward modeling and use the source wavefield normalized cross-correlation imaging condition to obtain the imaging results. For teleseismic events, hybrid method is adopted for an efficient forward wavefield modeling by combining generalized ray theory for far-field seismic wave

propagation and finite difference for local numerical simulation. Additionally, imaging results from different earthquake events are stacked together to improve the signal noise ratio. Compared with the existing passive RTM method based on the converted wave imaging condition, the new RTM method can better determine the stacking weighting coefficients for different seismic events, and it does not need a separation of P and S wave. Synthetic experiments demonstrate the capacity of the new method for imaging the fine details of the complex structure in the deep earth.

Effect of fault architecture and permeability evolution on response to fluid injection, Zhuo Yang, Alissar Yehya, and James R Rice (Poster Presentation 182)

Injection-induced seismicity is thought to be due primarily to increase in fluid pore pressure along existing faults and fractures, which reduces their frictional strength. We address the modeling and prediction of the hydro-mechanical response due to fluid injection, mainly as wastewater injection from the oil and gas industry. We consider the full poroelastic effects and also the changes in porosity and permeability of the rock matrix due to changes in local volumetric strains. Our results reveal the importance of using a realistic fault permeability structure, which includes a low permeability fault core and associated anisotropic high permeability damage zones, while considering permeability evolution due to the elastic deformation. Moreover, we apply our poroelastic model, with spatially and temporally varying permeability, to the Arkansas Guy-Greenbrier wastewater injection case. The overall trend of the Guy-Greenbrier earthquake sequence is consistent with our assumption of an anisotropic permeability structure of fault damage zones, such that they can act as barriers to flow across faults, and as conduits to diffuse pore pressure changes to deeper levels and greater distances. (supported by NSF-EAR 91315447 and NSF-DMR 90820484)

Re-evaluation of the late-Pleistocene slip rate of the Haiyuan fault near Songshan, Gansu province, China, WENQIAN YAO, Jing Liu, Michael E Oskin, Veronica B Prush, Wei Wang, and Zhanfei LI (Poster Presentation 220)

Well-constrained fault slip rates are important for understanding strain partitioning within a fault system and the associated seismic hazard. The Haiyuan fault is an ~1000 km-long active strike-slip fault in the northeast margin of the Tibetan Plateau with ongoing controversy over its late Pleistocene slip rate. Previous work by Lasserre et al. (1999) suggested a slip rate of 12+/-4 mm/yr, which is higher than recent geodetically determined rates on adjacent fault sections. In this paper, we reanalyze and re-evaluate the slip rates at their two sites, located north of the Songshan village, using airborne LiDAR data, field mapping, and Quaternary geochronology. A suite of loess-capped terraces document the slip history of this fault. At the Majia Wan site, using microtopographic analysis of these offset terraces, we document a sinistral displacement of 124 ± 15 m of the upper edge and 95 ± 15 of the lower edge of T1/T2 terrace riser, respectively, on the left bank of the channel. On the right bank, T1/T4 terrace riser indicates a 129 ± 15 m offset, similar to that previously documented. Combining optically stimulated luminescence, cosmogenic 10Be, and carbon-14 dates, we assess the abandonment age of T2 as 20.0 ± 2.8 ky and T1 as 9445 ± 30 yr. An upper terrace reconstruction of displacement yields a slip rate of 6.5 ± 1.6 mm/yr since ~ 20 ka, whereas the lower terrace reconstruction indicates a rate of ~10 mm/yr since ~ 9,500 ka at the site. The configuration of offset channels favors an upper terrace reconstruction of displacement accumulation. Our results, in conjunction with other geologic, paleoseismic, and geodetic slip rates along the Haiyuan fault, indicate an average slip rate of ~6 mm/yr, compatible with geodetic data and with no secular variation. Our re-evaluation supports that apparent slip rate discrepancies in northern Tibet share a common bias due to lower-terrace reconstruction used in interpreting the age of offset. The ephemeral channels of semi-arid northern Tibet do not vigorously refresh terrace risers to obliterate offset accumulated during channel downcutting.

Relating teleseismic backprojection images to earthquake kinematics, Jiuxun Yin, and Marine A Denolle (Poster Presentation 083)

Backprojection (BP) of teleseismic P waves is a powerful tool to study the evolution of seismic radiation of large earthquakes. The common interpretations on the BP results are qualitative comparisons with earthquake kinematic observations, such as the evolution of slip on the fault and rupture velocity. However, the direct relation between the BP images and physical properties of the earthquake rupture process remains unclear and is needed for further application of this technique. In this study, we start from a theoretical formulation of the BP images, which is linear in the frequency domain, and carry on a synthetic exercise with kinematic source representations and virtual receivers embedded in a homogeneous fullspace. We find that the fundamental linear formulation of the BP method is most correlated with the true kinematic source properties: the images from linear BP are a snapshot of the slip motion on the fault surface, after a spatial smoothing with a frequency-dependent resolution matrix F. We define a resolvability parameter for the resolution matrix F that quantifies the data resolution of the BP method. The direct comparison between the synthetic BP images and the kinematic models validates that the BP image can be directly used to track the spatio-temporal propagation of rupture front. However, because F is not strictly an identity matrix due to limited station coverage in space (azimuth and distance) and to the limited frequency bands of the seismograms, it remains difficult to recover the details in the rupture fronts from BP images. Since the resolution matrix F mostly depends on source mechanism and source-receiver geometry, we further calculate the resolvability and the corresponding resolvable source area/length for most tectonically active source regions and the commonly used seismic arrays. Based on this global resolvability analysis, we propose an empirical relation between the seismic frequency, resolvable area, and earthquake magnitude. It provides guidelines to properly choose the frequency band in seismic waveform and to interpret the BP image in terms of source slip rate. In general, this work attempts to provide a clear interpretation of the BP images in light of the real earthquake rupture process and give a systematic evaluation of seismic data limitations.

An Updated Compilation of VS30 in the United States, Alan Yong, Devin McPhillips, Julie Herrick, and Jessica Dozal (Poster Presentation 021)

VS30, the time-averaged shear-wave velocity (VS) to a depth of 30 meters, is a key index adopted by the earthquake engineering community to account for seismic site conditions. VS30 is typically based on geophysical measurements of VS derived from invasive and noninvasive techniques at sites of interest. Owing to cost considerations, as well as logistical and environmental concerns, VS30 data are sparse or not readily available for most areas. Where data are available, VS30 values are often assembled in assorted formats that are accessible from disparate and (or) impermanent Websites. To help remedy this situation, we compiled

VS30 measurements obtained by studies funded by the U.S. Geological Survey (USGS) and other governmental agencies. Thus far, we have compiled VS30 values for 4,371 sites in the United States, along with metadata for each measurement from government-sponsored reports, online databases, and scientific and engineering journals. Most of the data in our VS30 compilation originated from publications directly reporting the work of field investigators. A subset consisting of 20 percent of VS30 values was previously compiled by the USGS and other research institutions. VS30 originating from these earlier compilations were crosschecked against published reports when clarification was needed. Both downhole and surface-based VS30 estimates are represented in our VS30 compilation. Most of the VS30 data are for sites in the western contiguous United States (3,130 sites); 682 VS30 values are for sites in the Central United States; 267 VS30 values are for sites in the Eastern United States and Puerto Rico; 15 VS30 values are for sites in Alaska; 30 VS30 values are for sites in Hawaii. The remaining 247 sites are in the vicinity of Vancouver, Canada.

Holocene slip rates along the Mojave Section of the San Andreas fault, Elaine K Young, Eric S Cowgill, and Katherine M Scharer (Poster Presentation 269)

The ζ100-km long Mojave section of the San Andreas fault is positioned within a double restraining bend of the fault in southern California. The Holocene slip rate on the Mojave San Andreas Fault (MSAF) is not well known, despite its importance for understanding earthquake hazard, apparent discrepancies between geologic and geodetic slip rates along this fault section, and potential long-term fault interactions in southern California. Here we use detailed surficial geologic mapping, stratigraphic analysis, and radiocarbon dating of charcoal to characterize and determine ages of landforms offset by the MSAF at two slip-rate sites. To bracket the age of the offset landform, we date deposits emplaced before and after the feature formed. At site X-12, a beheaded channel that formed between ζ1700 and ζ550 calBP is offset ζ50 to ζ60 m. At site Ranch Center, a channel that formed between ~4200 and ~3700 calBP is deflected ~70 to ~100 m behind a shutter ridge. Data from Ritter Ranch suggests an absolute minimum rate of 21 mm/yr [1] since ~3 ka. In combination, the results at these MSAF sites suggest an increase in average slip rate from 17-27 mm/yr since ~4 ka (Ranch Center), to ≥29 mm/yr over the last ~1.7 ka (X-12). Our MSAF results may support a kinematic model for southern California faults [2] that predicts a shared slip history for the San Andreas fault, the Garlock fault, and faults in the Los Angeles basin that is anticorrelated with periods of increased slip in the Eastern California Shear Zone. The increase in average slip rate at ~1.7 ka is similar to the slip history for the Garlock fault [3]. The rate of 17-27 mm/yr since ~4 ka is lower than the long term (413 ka) average slip rate of 30-37 mm/yr [4], but the post ~1.7 ka rate of ≥29 mm/yr is in agreement or higher, suggesting variations in slip rate over time. The Holocene slip rates for the MSAF reported here are compatible with geodetic slip rates modeled using a viscoelastic crust [5] but are still generally higher than those modeled with an elastic crust.

[1] Weldon, 2009, USGS/NEHRP #G09AP00012 (UO #238610) Report

[2] Dolan et al., 2007, Geology. v.35, p. 855

[3] Dolan et al., 2016, EPSL. v. 446, p. 123

[4] Matmon et al., 2005, GSAB. V. 117 p. 795

[5] Chuang and Johnson, 2011, Geology. v. 39, p.627

Absolute and relative focal depth determination of moderate-sized earthquakes: An example from the 2010 El Mayor-Cucapah earthquake sequence, Chunquan Yu, Egill Hauksson, Zhongwen Zhan, Elizabeth S Cochran, and Donald V Helmberger (Poster Presentation 056)

Earthquake focal depth is a key parameter for understanding the geometry of fault zones, the rheology of the lithosphere and the tectonics of the continents. It is also crucial for seismic hazard assessment. Routine determination of earthquake focal depth relies on travel times of major body-wave phases. It works well in the presence of a dense nearby seismic network, but the uncertainty greatly increases as the distance to the nearby station increases. Precise focal depth can be determined, however, if regional depth phases are identified along with their reference phases. The differential travel time between the depth phase and its reference phase, which is most sensitive to the focal depth, can be determined with regional waveform modeling. We demonstrate our procedure using data from the 2010 Mw 7.2 El Mayor-Cucapah earthquake sequence (M>4.0). The focal depths for this earthquake sequence were poorly determined in the Southern California catalog as they are located near the edge of, or outside, the Southern California Seismic Network. We determine the absolute depth of ~30% of all M>4.0 earthquakes (122) in this sequence using regional waveform modeling. For other events with weak or complicated depth phases, we further develop a relative relocation method using Pn differential travel times in addition to Pg and Sg differential travel times. The incorporation of Pn differential travel times greatly reduces the uncertainty of relative depth estimation. In total, we are able to determine the focal depth of about ~75% of the 122 M>4.0 events. Our results show tight depth distribution of the 2010 El Mayor-Cucapah earthquake sequence, with the majority located between 3-10 km. The depth distribution of these earthquakes is similar to focal depths determined using a temporary seismic network. The relatively shallow depth range is consistent with the expectation from high surface heat flows.

Cloud Computing and Big Data – Using the Southern California Earthquake Data Center (SCEDC) and the Southern California Seismic Network (SCSN) Products and Services for Earthquake Research, Ellen Yu, Prabha Acharya, Aparna Bhaskaran, Shang-Lin Chen, Jennifer R Andrews, Valerie Thomas, Egill Hauksson, and Robert W Clayton (Poster Presentation 057)

Improved Data Access:

Looking for beta testers! The SCEDC is planning to store one month of continuous and triggered data in Amazon Web Services (s3) in preparation to store the SCEDC waveform archive as an Amazon Open Data Set. We are looking for users who will provide feedback and use cases on what development is needed. The potential benefits of hosting the archive in the cloud include:

1. Improved data access speed
2. Direct access to the archive as a mounted file system (may benefit large dataset analysis)

3. Leveraging AWS technologies and services.

The SCEDC has been determining ways to improve performance of the dataselect webservice. Reorganization of data into contiguous segments of a seismic channel improves download rates by a factor of 4.

The SCEDC is developing a data availability service. Users will be able to determine the time ranges for which triggered and continuous waveform time series are available for download. This service is compliant with the IRIS data availability service.

New data holdings:

The SCEDC data holdings now include a double difference catalog (Hauksson et. al 2011) spanning 1981 through 2017 available via STP and FDSN Event web service, and a focal mechanism catalog (Yang et al. 2011).

The SCEDC website now hosts training and validation datasets that are for deep learning research. (Ross et al. 2018)

To maximize data completeness, the SCEDC has implemented an automated gap detection and data retrieval mechanism for stations digitized by Basalt loggers with an onsite data store. This is effective when data could not be telemetered in real time due to a telemetry outage and service is later resumed.

Uncertainties in Probabilistic Seismic Hazard Analysis for a Poisson Earthquake Occurrence Model, Yuehua Zeng, and Mark D Petersen (Poster Presentation 049)

We revisit the theory for the probabilistic seismic hazard analysis (PHSA) and solve for the standard errors of the rate and probability of exceedance. We show that the PSHA defined by the probability of one or more ground motion exceedances over a time period is equivalent to the mean probability of exceedance for a Poisson earthquake occurrence model. We apply a California seismic hazard model to evaluate the standard errors of the rate and probability of exceedances. We find that the range of values between the lower and upper limits are very high for the following cases: (1) rate/probability of exceedance for fixed ground motion and (2) ground motions with a fixed probability of exceedance. These uncertainties for probability/rate of exceedance and ground motions are both correlated with the relative earthquakes rate uncertainties on faults across the region. For example, at a fixed 2% in 50-year PGA probability of exceedance, the uncertainties in probability caused by the Poisson rate calculation are highest over less active faults and lower over the San Andreas Fault (SAF). Overall the standard error of the probability of exceedances are often higher than the mean and can span a factor of 2 to 10. On the other hand, the uncertainties in probability of exceedance for fixed ground motions is highest over the SAF and lower near the less active faults. The results also show that the average ground motion uncertainties across the state are about 70%. In general, the uncertainties in the rate/probability of exceedance are much higher than many people have assessed in previous analyses and are comparable in size to the uncertainties in ground motions, often a factor of two or more. The results suggest that in places where seismic hazards are low, the risk could be higher because of the high uncertainties.

Induced Earthquake Forecasting in Oklahoma Using Models of Fluid Diffusion and Earthquake Nucleation, Guang Zhai, and Manoochehr Shirzaei (Poster Presentation 035)

There is a growing body of evidence suggesting that the recent 900-fold increase in the number of earthquakes in the eastern and central USA is linked to deep waste fluid disposal, co-produced with oil and gas productions. The current efforts to evaluate and mitigate induced seismic hazard are often informed by the empirical relation established between seismic response and injection volume and rates. Therefore, it is not a surprise that such efforts yield a limited success, as the empirical relations do not capture the entire physics governing processes of induced earthquake due to fluid injection. To this end, we devise a physics-based forecasting scheme considering the underlying process governing fluid diffusion and a rate-and-state earthquake nucleation model. This method evaluates the changes in the crustal stress and seismicity due to fluid diffusion, which, in combination with a statistical framework, can be used for assessment of induced earthquake hazard. Here, we investigate the seismic, hydrogeologic, and injection data spanning the period of 1995 2017 in northern-central Oklahoma. The magnitude-time distribution of the observed M3+ earthquakes for the period of 2008 2017 is accurately reproducible. In response to injection rate reduction in 2016, Western Oklahoma shows larger decrease in the earthquake magnitude exceedance probability than that of Central Oklahoma, primarily due to faster fluid diffusion rate and larger injection reduction in Western Oklahoma. Our model predicts that the earthquake probability will approach to its historical background level by 2025 at both Central and Western Oklahoma af

Coupled interactions of fluid-pressure and earthquake cycles: Numerical simulations of fault-valve behaviour, Weiqiang Zhu, Kali L Allison, and Eric M Dunham (Poster Presentation 195)

Fluids are well known to play an essential role in controlling effective normal stress and hence fault strength. While most models of earthquake behavior assume a fixed pore pressure distribution, geologists have documented cyclic changes in fluid pressure and migration of fluids along fault zones. In particular, the fault-valve model (e.g., Sibson, 1990) posits the development of fluid overpressure during the interseismic period, when fault zone permeability is reduced by solution transfer and related healing processes, which is then released immediately after earthquakes when permeability has been enhanced by shearing of the fault zone. Despite this evidence for fluid overpressure development and fault valving, quantitative modeling studies of fault-valve behaviour are still missing. In this study, we extend our 2D antiplane shear earthquake cycle code to simultaneously model fluid flow along faults and permeability evolution. The fault is governed by rate-and-state friction, and we assume Darcy flow along the fault zone with no fluid loss to the adjacent medium. We introduce a simple, linear permeability evolution model that captures two physical processes: a rapid permeability increase accompanying earthquake slip and a gradual permeability recovery with time. The evolution equation has a minimal number of parameters (e.g., minimum and maximum permeability and healing time scale), making it ideally suited for parameter-space exploring of fault valving. We use this fully coupled model to quantify conditions under which fluid overpressure can reach sufficiently high levels that the earthquake process is altered. We identify several relevant length and time scales, which are combined to form the dimensionless parameters that control system behavior. The simulation methodology

could be extended to utilize more realistic permeability evolution laws and, as in other work by our group (Allison and Dunham, 2017), to account for viscous flow in the lower crust and mantle.

3D surface deformation in the 2016 MW 7.8 Kaikōura, New Zealand earthquake from optical image correlation: Implications for strain localization and tectonic evolution of the Pacific-Australian plate boundary, Robert Zinke, James Hollingsworth, James F Dolan, and Russ J Van Dissen (Poster Presentation 123)

We measure high-resolution, 3D surface deformation patterns resulting from the 2016 MW 7.8 Kaikoura, New Zealand earthquake using stereo WorldView satellite imagery, with an advanced workflow based on COSI-Corr subpixel optical image correlation. This workflow triangulates 3D displacement vectors directly from different combinations of stereo pre- and post-earthquake image correlations, providing highly detailed maps of 3D surface deformation without the need to combine multiple sensors, or generate separate DEMs to orthorectify imagery. From these high-resolution correlation maps, we extract measurements of horizontal and vertical fault slip at 500 m intervals along 19 mapped fault strands. We use these measurements to refine interpretations of fault rupture kinematics in the Kaikoura earthquake, which in turn provide new insights into the role of the 2016 earthquake in accommodating relative tectonic plate motions. Comparison of our correlation measurements with published field measurements along the Kekerengu fault indicates a significant amount of coseismic surface deformation was expressed as distributed, off-fault deformation (OFD), which occurs over zones of variable width (typically within ~100 m of the primary fault). Specifically, comparison of traditional, short-aperture (< 5 m) field offsets shows that ~35% of surface deformation is expressed as OFD. In contrast, comparison of our correlation measurements with field offsets for which previously linear features (e.g., fence lines) are projected into the fault demonstrates that field measurements capture nearly all (~90 %) surface deformation when projected > 5-100 m from the fault.

Meeting Participants

Aagaard Brad, USGS, talk Wed 08:30, poster 295
Abdelmeguid Mohamed, UIUC, poster 198, 199
Abdrakhmatov Kanatbek, poster 241
Abercrombie Rachel, Boston U, poster 075, 076, 081
Abolfathian Niloufar, USC, poster 155
Abrahams Lauren, Stanford, poster 192, 202
Abrahamson Norman, PG&E, poster 011, 025, 026, 232
Acharya Prabha, Caltech, poster 057
Addo Bill, Cornell, poster 314
Adhikari Lok, poster 092
Afshari Kioumars, Karen Clark & Co
Agata Ryoichiro, poster 030
Ahdi Sean, UCLA, poster 022
Aho Marissa, Office LA Mayor, talk Wed 09:00
Ajala Rasheed, LSU, poster 103
Akciz Sinan, CSU Fullerton, poster 266
Al Atik Linda, poster 026
Albertini Gabriele, poster 199
Allam Amir, U Utah, poster 233
Allen Christopher, poster 277
Allevato Andrew, CSUN, poster 096
Allison Kali, Stanford, poster 161, 192, 195, 202
Almond Peter, poster 225
Almquist Martin, Stanford, poster 187
Alongi Travis, UCSC
Aminzadeh Fred, USC, poster 184
Amodeo Kaitlyn, UC Davis, poster 110
Ampuero Jean-Paul, Caltech, poster 186, 192, 196
Anderson Aaron, UCSB, poster 112
Anderson John, UNR
Anderson Kent, IRIS
Andrews Jennifer, Caltech, poster 053, 055, 057
Arba Ryan, Cal OES
Archuleta Ralph, UCSB, poster 017
Arduino Pedro, U Washington
Armstrong Alysha, poster 233
Arrowsmith Ramon, ASU, poster 170, 241
Ascencio Katia, LA Harbor College, poster 313
Asimaki Domniki, Caltech, poster 012, 020
Aslam Khurram, U Memphis, poster 201
Aso Miki, U Tokyo, poster 275
Aso Naofumi, Caltech, poster 275
Aster Richard, Colorado State
Astiz Luciana, NSF
Ault Alexis, Utah State, poster 173, 176
Austin Ken, poster 133
Avouac Jean-Philippe, Caltech, poster 118, 134, 286
Bachhuber Jeffrey, PG&E, poster 225
Baden Curtis, Stanford, poster 271
Badt Nir, Brown, poster 181
Bae Sung, QuakeCoRE-Canterbury, poster 008
Bahadori Alireza, Stony Brook, poster 156, 162, 163
Bailey Christopher, poster 223
Bailey James, poster 277
Baize Stephane, poster 124
Baker Jack, Stanford, poster 006, 007
Balakrishna Ashwin, poster 064
Ballmann Jason, USC
Bao Han, UCLA, poster 084
Barall Michael, Invisible Software, poster 192, 206
Barba Magali, UC Boulder, poster 142
Barbot Sylvain, USC, poster 129, 192
Barnhart Katherine, poster 227
Barnhart William, U Iowa, poster 125
Barth Nicolas, UCR, poster 038
Bartram Hanna, poster 223
Bayless Jeff, AECOM/UC Davis, poster 011, 303
Beas Guillermo, ELAC, poster 311, 313
Beaudoin Bruce, IRIS
Beck Susan, U Arizona
Becker Thorsten, UT Austin, poster 120, 157
Bedford John, U Liverpool, talk Tue08:30, poster 179
Beeler N., USGS
Behn Mark, WHOI, poster 148
Behr Whitney, ETH Zurich, poster 152, 157
Bell Rebecca, Imperial College, poster 253
Bellagamba Xavier, poster 016
Bellana Naresh, HAI
Ben-Zion Yehuda, USC, poster 054, 066, 072, 100, 101, 155, 159, 299, 305
Bennett Richard, U Arizona, poster 238
Bennett Scott, USGS, poster 224
Benoit Margaret, NSF
Benthien Mark, USC
Bermudez Mario, SDSU, poster 158
Beroza Gregory, Stanford, poster 058, 078, 108, 109, 146, 304
Beyer Jennifer, poster 208
Bhaskaran Aparna, Caltech, poster 057
Bhat Harsha, ENS Paris, poster 124
Bhattacharya Pathikrit, Tufts, poster 185
Bianco Michael, UCSD, poster 094
Biasi Glenn, USGS, poster 038, 041, 264
Biek Robert, poster 223
Bielak Jacobo, CMU, poster 296
Bierman Paul, poster 253
Bilham Roger, UC Boulder, poster 114
Bird Peter, UCLA
Blanpied Michael, USGS
Blanton Chelsea, SDSU, poster 114, 226, 278
Blisniuk Kimberly, SJSU, poster 238
Bluemle Felix, poster 039
Bochicchio Regina, Miramar College
Boehm Christian, poster 106
Bohnhoff Marco, GFZ Potsdam, poster 039
Bormann Jayne, CSULB, poster 249, 251
Boulton C, talk Tue08:30
Boyd Dan, CSULB, poster 249
Bozorgnia Yousef, UCLA, poster 022
Bradbury Kelly, Utah State, poster 169
Bradley Brendon, QuakeCoRE-Canterbury, poster 008, 016, 287
Branum Dave, CGS
Bray Jonathan, UC Berkeley, talk Tue09:00
Breuer Alexander, SDSC, poster 093, 289, 293, 294
Briggs Rich, USGS, poster 125, 224
Brocher Thomas, USGS, poster 043
Brodsky Emily, UCSC, poster 046, 089, 183
Brooks Benjamin, USGS
Brothers Daniel, USGS, poster 160, 248
Brown Jack, SDSU
Brown Nathan, UCLA, poster 234, 239
Bryan Jared, Utah State, poster 093
Bunds Michael, Utah State, poster 116
Burgette Reed, NMSU, poster 254, 256, 257
Burgi Paula, Cornell, poster 140
Bürgmann Roland, UC Berkeley, poster 121, 126
Burkhard Liliane, U Hawaii, poster 138, 262
Burns James, CSUSB, poster 234
Caccamise Dana, NOAA
Cadena Ana, Cadena Consulting
Caklais Anna, Imperial College, poster 232
Callaghan Scott, USC, poster 024, 032, 295, 296, 297, 312
Calzolari Gabriele, Utah State, poster 176
Cappa Frederic, U NSA France, poster 186
Carlson Grace, ASU, poster 135
Carlson Jean, UCSB
Carpenter Brett, U Oklahoma, poster 175
Carrillo Elvis, CSU Dominguez Hills, poster 315
Castillo Bryan, CSUSB, poster 268
Castillo Castellanos Jorge, Caltech, poster 095, 098, 104
Cato Kerry, CSUSB
Cattania Camilla, Stanford, poster 190, 192
Celebi Mehmet, USGS, poster 300
Champenois Johann, poster 124
Chang Wu-Lung, U Utah, poster 129

SCEC Institutions

The Southern California Earthquake Center (SCEC) is an institutionally based organization that recognizes both **core institutions**, which make a major, sustained commitment to SCEC objectives, and a larger number of **participating institutions**, which are self-nominated through the involvement of individual scientists or groups in SCEC activities and confirmed by the Board of Directors. Membership continues to evolve because SCEC is an open consortium, available to any individual or institution seeking to collaborate on earthquake science in Southern California.

Core Institutions and Representatives

Core institutions are designated academic and government research organizations with major research programs in earthquake science. Each core is expected to contribute a significant level of effort (both in personnel and activities) to SCEC programs, including Communication, Education and Outreach Program. Core institutions are obligated to contribute a yearly minimum of $35K of institutional resources (spent in-house on SCEC activities) as matching funds to Center activities. Each core institution appoints an Institutional Director to the Board of Directors.

USC, Lead
John Vidale

Caltech
Jean-Phillippe Avouac

CGS
Tim Dawson

Columbia
Bruce Shaw

Harvard
John Shaw

MIT
Tom Herring

SDSU
Tom Rockwell

Stanford
Paul Segall

Texas A&M
Patrick Fulton

UC Los Angeles
Peter Bird

UC Riverside
David Oglesby

UC San Diego
Yuri Fialko

UC Santa Barbara
Toshiro Tanimoto

UC Santa Cruz
Emily Brodsky

UNR
Graham Kent

USGS Golden
Nico Luco

USGS Menlo Park
R. Harris, S. Hickman

USGS Pasadena
Kate Scharer

Domestic Participating Institutions and Representatives

SCEC membership is open to participating institutions upon application. Eligible institutions may include any organization (including profit, non-profit, domestic, or foreign) involved in a Center-related research, education, or outreach activity. Participating institutions do not necessarily receive direct support from the Center. Each participating institution (through appropriate official) appoints a qualified Institutional Representative to facilitate communication with the Center. The interests of the participating institutions are represented on the Board of Directors by two Directors At-Large.

AECOM
Paul Somerville

Appalachian State
Scott Marshall

Arizona State
J Ramon Arrowsmith

Boston University
Rachel Abercrombie

Brown
Terry Tullis

CalPoly Pomona
Jascha Polet

CSU Fullerton
Dave Bowman

CSU Long Beach
Nate Onderdonk

CSU Northridge
Doug Yule

CSU Sacramento
Steve Skinner

CSU San Bernardino
Sally McGill

Carnegie Mellon
Jacobo Bielak

Colorado Sch. Mines
Edwin Nissen

Cornell
Rowena Lohman

Georgia Tech
Zhigang Peng

Indiana
Kaj Johnson

JPL
Andrea Donnellan

LLNL
Arben Pitarka

Marquette U
Ting Lin

Oregon State
Andrew Meigs

Penn State
Eric Kirby

Portland State
Brittany Erickson

Purdue
Andrew Freed

Smith
John Loveless

SMU
M. Beatrice Magnani

SUNY at Stony Brook
William Holt

Tufts
Robert Viesca

U Alaska Fairbanks
Carl Tape

UC Berkeley
Roland Bürgmann

UC Davis
Michael Oskin

UC Irvine
Lisa Grant Ludwig

U Cincinnati
Lewis Owen

U Illinois
Karin Dahmen

U Kentucky
Sean Bemis

U Massachusetts
Michele Cooke

U Michigan Ann Arbor
Eric Hetland

U New Hampshire
Margaret Boettcher

U Oregon
Ray Weldon

U Texas El Paso
Bridget Smith-Konter

U Texas Austin
Whitney Behr

U Wisconsin Madison
Clifford Thurber

Utah State
Susanne Janecke

Utah Valley
Nathan Toke

WHOI
Jeff McGuire

International Participating Institutions

Academia Sinica (Taiwan)

CEA (China)

CICESE (Mexico)

CRUST (Italy)

ERI Tokyo (Japan)

ETH Zürich (Switzerland)

GNS (New Zealand)

KIGAM (Korea)
Seok Goo Song

Nat'l Central U (Taiwan)

Nat'l Taiwan U (Taiwan)

Univ of Bristol (UK)
Max Werner

Univ of Canterbury (NZ)
Brendon Bradley

Univ of Otago (NZ)
Mark Stirling

Western Univ (Canada)